frontiers | Research Topics

# Ecology of marine zooplankton and micronekton in polar and sub-polar areas

**Edited by**
Letterio Guglielmo, Alessandro Bergamasco, Guang Yang and Antonia Granata

**Published in**
Frontiers in Marine Science

ISSN 1664-8714
ISBN 978-2-8325-5628-3
DOI 10.3389/978-2-8325-5628-3

## About Frontiers

Frontiers is more than just an open access publisher of scholarly articles: it is a pioneering approach to the world of academia, radically improving the way scholarly research is managed. The grand vision of Frontiers is a world where all people have an equal opportunity to seek, share and generate knowledge. Frontiers provides immediate and permanent online open access to all its publications, but this alone is not enough to realize our grand goals.

## Frontiers journal series

The Frontiers journal series is a multi-tier and interdisciplinary set of open-access, online journals, promising a paradigm shift from the current review, selection and dissemination processes in academic publishing. All Frontiers journals are driven by researchers for researchers; therefore, they constitute a service to the scholarly community. At the same time, the *Frontiers journal series* operates on a revolutionary invention, the tiered publishing system, initially addressing specific communities of scholars, and gradually climbing up to broader public understanding, thus serving the interests of the lay society, too.

## Dedication to quality

Each Frontiers article is a landmark of the highest quality, thanks to genuinely collaborative interactions between authors and review editors, who include some of the world's best academicians. Research must be certified by peers before entering a stream of knowledge that may eventually reach the public - and shape society; therefore, Frontiers only applies the most rigorous and unbiased reviews. Frontiers revolutionizes research publishing by freely delivering the most outstanding research, evaluated with no bias from both the academic and social point of view. By applying the most advanced information technologies, Frontiers is catapulting scholarly publishing into a new generation.

## What are Frontiers Research Topics?

Frontiers Research Topics are very popular trademarks of the *Frontiers journals series*: they are collections of at least ten articles, all centered on a particular subject. With their unique mix of varied contributions from Original Research to Review Articles, Frontiers Research Topics unify the most influential researchers, the latest key findings and historical advances in a hot research area.

Find out more on how to host your own Frontiers Research Topic or contribute to one as an author by contacting the Frontiers editorial office: frontiersin.org/about/contact

# Ecology of marine zooplankton and micronekton in polar and sub-polar areas

**Topic editors**

Letterio Guglielmo — Anton Dohrn Zoological Station Naples, Italy

Alessandro Bergamasco — Institute of Marine Science, National Research Council (CNR), Italy

Guang Yang — Institute of Oceanology, Chinese Academy of Sciences (CAS), China

Antonia Granata — University of Messina, Italy

**Citation**

Guglielmo, L., Bergamasco, A., Yang, G., Granata, A., eds. (2024). *Ecology of marine zooplankton and micronekton in polar and sub-polar areas*. Lausanne: Frontiers Media SA. doi: 10.3389/978-2-8325-5628-3

# Table of contents

frontiers | Frontiers in Marine Science

TYPE Editorial
PUBLISHED 21 October 2024
DOI 10.3389/fmars.2024.1487229



OPEN ACCESS

EDITED AND REVIEWED BY
Jonathan Cohen,
University of Delaware, United States

*CORRESPONDENCE
Alessandro Bergamasco
alessandro.bergamasco@ve.ismar.cnr.it

RECEIVED 27 August 2024
ACCEPTED 08 October 2024
PUBLISHED 21 October 2024

CITATION
Guglielmo L, Bergamasco A, Yang G and Granata A (2024) Editorial: Ecology of marine zooplankton and micronekton in polar and sub-polar areas.
*Front. Mar. Sci.* 11:1487229.
doi: 10.3389/fmars.2024.1487229



# Editorial: Ecology of marine zooplankton and micronekton in polar and sub-polar areas

Letterio Guglielmo[1,2,3], Alessandro Bergamasco[4]*, Guang Yang[5] and Antonia Granata[3,6]

[1]Institute of Polar Sciences, National Research Council (CNR), Messina, Italy, [2]CONISMA Local Research Unit (LRU) Messina, Department of Chemical, Biological, Pharmaceutical and Environmental, Sciences, University of Messina, Messina, Italy, [3]Integrative Marine Ecology Department, Zoological Station "Anton Dohrn", Naples, Italy, [4]Institute of Marine Sciences, National Research Council (CNR), Venice, Italy, [5]Key Laboratory of Marine Ecology and Environmental Sciences, Institute of Oceanology, Chinese Academy of Sciences, Qingdao, China, [6]Institute for Marine Biological Resources and Biotechnology (IRBIM), National Research Council (CNR), Messina, Italy

KEYWORDS

**zooplankton, krill, editorial, climate change, vertical migration, predator-prey interactions**

Editorial on the Research Topic
Ecology of marine zooplankton and micronekton in polar and sub-polar areas

## Introduction

As reported by Azam et al. (2017) the polar and subpolar regions are characterized by ecosystems with high biodiversity and species richness. Hunt et al. (2016) highlighted that the variability among polar ecosystems, such as sea ice cover and thickness, population structure, abundance, diversity and food web, from phytoplankton to marine mammals, is due to the different circulation patterns of water masses between north and south. Huge environmental changes have been induced in those areas by a high climate dynamic, which has generated loss of biodiversity and consequent reduction of ecosystem services provided to the entire planet (Laffoley and Baxter, 2016). In this context, much attention was paid to the effects of these environmental changes on zooplankton structure and dynamics, and consequently on the matter and energy cycling in polar ecosystems, as also demonstrated by the results of La et al. (2019) on how climate changes can alter the zooplankton vertical migration (DVM) in the Southern Ocean. The high vulnerability of these ecosystems, in the presence of pressures such as climate change and overfishing, jeopardizes the essential ecosystem services they provide, e.g. in terms of carbon storage and suitable habitats for nursing and feeding (Azam et al., 2017; Johnston et al., 2022). The polar ecosystem presents high spatial variability in terms of the rate and direction of change in temperature and sea ice, but little is known about the mechanisms through which the spatial distribution of planktonic species is influenced (Yang et al., 2021). These changes appear to impact circumpolar food webs involving krill and other zooplankton. It follows that knowledge of the density and distribution of zooplankton is crucial to correctly estimate the energy transfer within the food web of the continental shelf and its response to climate change (Minutoli et al., 2024). In turn, ocean warming can have a significant impact on the structure and functioning of zooplankton (Fraser et al., 2023; Swadling et al., 2023).

## Summary of the topic papers

With this Research Topic, many researchers involved in the study of zooplankton and micronekton ecology have had the opportunity to provide updated data on their latest research in polar and subpolar environments. Therefore, their results will certainly contribute to improving the state of knowledge on polar ecology in these still poorly understood areas, which require urgent and significant operations to prevent and to mitigate, as soon as possible, the effects of climate change on ecosystems.

In this Research Topic, 11 papers by 74 authors collaboratively address issues related to the zooplankton and micronekton spatial distribution, biomass, production, diel vertical migration, trophic relationships, and effects of climate change both in Antarctica (5 papers) and in the Arctic (6 papers). Two papers carried out by echosurvey in the Ross Sea concerned the spatial distribution of the biomass both in the crystal (*E. crystallorophias*) and Antarctic krill (*E. superba*). In particular, the authors focused their study on the possible impact of water masses on the vertical krill structure in different sectors of the Ross Sea, from Terra Nova Bay to Cape Adare. Barra et al. also emphasized the need to carry out multidisciplinary research campaigns for a better and more complete interpretation of the results, while De Felice et al. gave significant importance to salinity and the predator-prey relationship. Attention to the water mass structure and to biotic and abiotic variables in determining the composition of zooplankton communities characterized the study by Liu et al. The authors compared the abundance and biodiversity data from the surface down to 1500 m among samples collected in the East Pacific and the Indian sectors of the Southern Ocean. The study on phytoplankton carried out by Liu et al. on a grid of stations located around the South Shetland Islands, along the Antarctic Peninsula, highlighted the importance of some environmental factors such as temperature and ice concentration, in determining the structure of phytoplankton communities. A direct relationship between pennate diatoms and krill was highlighted by multivariate analysis. The study by Chen et al. on the composition and diversity of heterotrophic flagellates in the western Cosmonaut Sea highlighted the remarkable abundance of this community in the euphotic zone and a strong correlation between environmental factors and taxonomic distribution. Most studies carried out in different areas of the Arctic have highlighted the effects of climate change on zooplankton, and in particular on copepods. Espinel-Velasco et al. focused on the potential implications that ocean acidification and warming may have on Arctic populations of calanoid copepods, with possible consequences on the entire food-web. The results of Gawinski et al. added among the climate variables also the reduction of Arctic sea ice as an effect on small-sized copepods, with cascading consequences on secondary production. Hop et al. studied the abundance of zooplankton communities at four glacier fronts in Kongsfjorden, Svalbard and concluded that under current conditions of global warming these glaciers could act as an "elevator effect" of prey (zooplankton) thus facilitating the feeding of predators, and particularly seabirds. The results of Ishihara et al. on the ecology, trophodynamics, and fatty acid composition of the copepod *C. glacialis/marshallae* in the Eastern and Northeastern Chukchi and Canadian basins, highlighted the adaptation of this species to climate changes in the Pacific Arctic Ocean. Kumagai et al., examining the zooplankton size spectra demonstrate that in the northern Bering Sea an optimal and efficient predator-prey relationship is established between zooplankton and fish larvae/juveniles. Kim et al. note the uncommon presence of ichthyoplankton species into the Chukchi Sea, attributing this "anomaly" to several climatic factors including freshwater inflow from the East Siberian Sea and the intrusion of warm Atlantic and Pacific waters.

## Gaps and perspectives

The global importance of the rich, unique and valuable biodiversity in the polar and subpolar ecosystems on which it depends has been recognized internationally. Unfortunately, it has been established that these ecosystems have already been affected by the physical and chemical impacts due to global change. For this reason, the international scientific community has recently recognized that an integrated multidisciplinary approach is needed to better understand the functioning of these vulnerable ecosystems, with particular interest in the carbon cycle to clarify the response of zooplankton to climate change (e.g. Everett et al., 2017; Hill et al., 2024; Ratnarajah et al., 2023).The importance of considering biological interactions in planktonic studies has been highlighted, employing open access and machine learning for measurable and repeatable distribution modeling and providing crucial ecological insights for informed conservation strategies in the face of environmental change (Grillo et al., 2022, 2024).

## Author contributions

LG: Writing – review & editing, Writing – original draft. AB: Writing – review & editing, Writing – original draft. GY: Writing – review & editing, Writing – original draft. AG: Writing – review & editing, Writing – original draft.

## Acknowledgments

Special thanks are due to the editors, reviewers and all the staff who patiently and competently followed the entire process for the publication of this Research Topic.

## Conflict of interest

The authors declare that the research was conducted in the absence of any commercial or financial relationships that could be construed as a potential conflict of interest.

The author(s) declared that they were an editorial board member of Frontiers, at the time of submission. This had no impact on the peer review process and the final decision.

## Publisher's note



## References

Azam, C.-S., Marteau, C., Piton, V., Borot, C., and Tixier, P. (2017). Regional ecosystem profile – Polar and Sub-polar Region. 2017. EU Outermost Regions and Overseas Countries and Territories, Terres australes et antarctiques françaises (TAAF). BEST, Service contract 07.0307.2013/666363/SER/B2, European Commission, 225 p + 31 Annexes.

Everett, J. D., Baird, M. E., Buchanan, P., Bulman, C., Davies, C., Downie, R., et al. (2017). Modeling what we sample and sampling what we model: challenges for zooplankton model assessment. *Front. Mar. Sci.* 4. doi: 10.3389/fmars.2017.00077

Fraser, A. D., Wongpan, P., Langhorne, P. J., Klekociuk, A. R., Kusahara, K., Lannuzel, D., et al. (2023). Antarctic landfast sea ice: a review of its physics, biogeochemistry and ecology. *Rev. Geophys.* 61, e2022RG000770. doi: 10.1029/2022RG000770

Grillo, M., Huettmann, F., Guglielmo, L., and Schiaparelli, S. (2022). Three-dimensional quantification of copepods predictive distributions in the Ross Sea: first data based on a machine learning model approach and open access (FAIR) data. *Diversity* 14, 355. doi: 10.3390/d14050355

Grillo, M., Schiaparelli, S., Durazzano, T., Guglielmo, L., Granata, A., and Huettmann, F. (2024). Machine learning applied to species occurrence and interactions: the missing link in biodiversity assessment and modelling of Antarctic plankton distribution. *Ecol. Processes* 13, 56. doi: 10.1186/s13717-024-00532-6

Hill, S. L., Atkinsoin, A., Arata, J. A., Belcher, A., Nash, S. B., Bernard, K. S., et al. (2024). Observing change in pelagic animals as sampling methods shift: the case of Antarctic krill. *Front. Mar. Sci.* 11, 1307402. doi: 10.3389/fmars.2024.1307402

Hunt, J. G. L., Drinkwater, K. F., Arrigo, K., Berge, J., Daly, K. L., Danielson, S., et al. (2016). Advection in polar and sub-polar environments: Impacts on high latitude marine ecosystems. *Prog. Oceanography* 149, 40–81. doi: 10.1016/j.pocean.2016.10.004

Johnston, N. M., Murphy, E. J., Atkinson, A., Constable, A. J., Cotté, C., Cox, M., et al. (2022). Status, change, and futures of zooplankton in the southern ocean. *Front. Ecol. Evol.* 9. doi: 10.3389/fevo.2021.624692

La, H. S., Park, K., Wåhlin, A., Arrigo, K. R., Kim, D. S., Yang, E. J., et al. (2019). Zooplankton and micronekton respond to climate fuctuations in the Amundsen Sea polynya, Antarctica. *Sci. Rep.* 9, 10087. doi: 10.1038/s41598-019-46423-1

D. Laffoley and J. M. Baxter (Eds.) (2016). *Explaining ocean warming: Causes, scale, effects and consequences. Full report* (Gland, Switzerland: IUCN), 456 pp, ISBN: . doi: 10.2305/IUCN.CH.2016.08.en

Minutoli, R., Bonanno, A., Guglielmo, L., Bergamasco, A., Grillo, M. , Schiaparelli, S., et al. (2024). Biodiversity and functioning of mesozooplankton in a changing Ross Sea. *Deep–Sea Res. II* 217(2024), 105401. doi: 10.1016/j.dsr2.2024.105401

Ratnarajah, L., Abu-Alhaija, R., Atkinson, A., Batten, S., Bax, N. J., Bernard, K. S., et al. (2023). Monitoring and modelling marine zooplankton in a changing climate. *Nat. Commun.* 14, 564. doi: 10.1038/s41467-023-36241-5

Swadling, K. M., Constable, A. J., Fraser, A. D., Massom, R. A., Borup, M. D., Ghigliotti, L., et al. (2023). Biological responses to change in Antarctic sea ice habitats. *Front. Ecol. Evol.* 10. doi: 10.3389/fevo.2022.1073823

Yang, G., Atkinson, A., Hill, S. L., Guglielmo, L., Granata, A., and Li, C. (2021). Changing circumpolar distributions and isoscapes of Antarctic krill: indo–Pacific habitat refuges counter long-term degradation of the Atlantic sector. *Limnol. Oceanogr.* 66, 272–287. doi: 10.1002/lno.11603

frontiers | Frontiers in Marine Science

TYPE Original Research
PUBLISHED 30 June 2023
DOI 10.3389/fmars.2023.1161912



OPEN ACCESS

EDITED BY
Antonia Granata,
University of Messina, Italy

REVIEWED BY
Daria Martynova,
Zoological Institute (RAS), Russia
Lech Stempniewicz,
University of Gdansk, Poland
Ivan Pérez-Santos,
University of Los Lagos, Chile

*CORRESPONDENCE
Haakon Hop
Haakon.Hop@npolar.no

RECEIVED 08 February 2023
ACCEPTED 19 May 2023
PUBLISHED 30 June 2023

CITATION
Hop H, Wold A, Vihtakari M, Assmy P, Kuklinski P, Kwasniewski S, Griffith GP, Pavlova O, Duarte P and Steen H (2023) Tidewater glaciers as "climate refugia" for zooplankton-dependent food web in Kongsfjorden, Svalbard.
*Front. Mar. Sci.* 10:1161912.
doi: 10.3389/fmars.2023.1161912



# Tidewater glaciers as "climate refugia" for zooplankton-dependent food web in Kongsfjorden, Svalbard

Haakon Hop[1]*, Anette Wold[1], Mikko Vihtakari[2], Philipp Assmy[1], Piotr Kuklinski[3], Slawomir Kwasniewski[3], Gary P. Griffith[1,4], Olga Pavlova[1], Pedro Duarte[1] and Harald Steen[1]

[1]Norwegian Polar Institute, Fram Centre, Tromsø, Norway, [2]Institute of Marine Research, Fram Centre, Tromsø, Norway, [3]Institute of Oceanology, Polish Academy of Sciences, Sopot, Poland, [4]High Meadows Environmental Institute, Princeton University, Princeton, NJ, United States

With climate warming, many tidewater glaciers are retreating. Fresh, sediment-rich sub-glacial meltwater is discharged at the glacier grounding line, where it mixes with deep marine water resulting in an upwelling of a plume visible in front of the glacial wall. Zooplankton may suffer increased mortality within the plume due to osmotic shock when brought in contact with the rising meltwater. The constant replenishment of zooplankton and juvenile fish to the surface areas attracts surface-foraging seabirds. Because access to other feeding areas, such as the marginal ice zone, has become energetically costly due to reduced sea-ice extent, glacial plumes may become increasingly important as "climate refugia" providing enhanced prey availability. Here, we investigated zooplankton concentrations within the plume and adjacent waters of four tidewater glaciers in Kongsfjorden, Svalbard, in early August 2016 and late July 2017. Our aim was to compare the zooplankton composition, abundance, and isotopic signatures within the plumes to those in adjacent fjord and shelf waters. Our hypothesis was that the plumes resulted in increased zooplankton mortality through osmotic shock and increased prey availability to predators. The mortality due to osmotic shock in the glacial plume was low (<5% dead organisms in samples), although slightly higher than in surrounding waters. This indicates that plumes are inefficient "death traps" for zooplankton. However, the high abundance and biomass of zooplankton within plume areas suggest that the "elevator effect" of rising glacial water supplies zooplankton to the sea surface, thereby enhancing prey availability for surface-feeding seabirds. Thus, our study provides evidence that glacial plumes are important as "climate refugia" for foraging seabirds. Stable isotope signatures showed that the glacial bay zooplankton and fish community represent a distinct isotopic niche. Additionally, zooplankton mortality associated with the plume estimated over 100-days of melt season supports a flux of 12.8 tonnes of organic carbon to benthic communities in the glacial bays. Benthic scavengers, such as *Onisimus*

*caricus* and *Anonyx nugax*, were abundant in the glacial bay, where they feed on sinking organic matter.

KEYWORDS

zooplankton, death trap, meltwater, tidewater glaciers, Kongsfjorden, Arctic

# Introduction

Glacial plumes in front of tidewater glaciers may play an increasingly important role as "climate refugia" and foraging areas for seabirds in a warmer climate. Knowledge of tidewater glaciers has increased in recent years, showing their importance for fjord biological production and nutrient dynamics (Meire et al., 2016; Calleja et al., 2017; Meire et al., 2017; Hopwood et al., 2018; Szeligowska et al., 2021). With climate warming, glaciers in Svalbard have been retreating and thinning since the beginning of the 20$^{th}$ century (e.g., Hagen et al., 2005; Kohler et al., 2007; Geyman et al., 2022), and some glaciers have already retreated onto land (Østby et al., 2017; Halbach et al., 2019). Glacial retreat and diminishing impact of meltwater discharge will result in less upwelling of nutrient-rich water and less productivity in glacial fjords (Meire et al., 2017). This could also affect the foraging areas for seabirds and marine mammals in the glacial bays (Urbanski et al., 2017; Everett et al., 2018).

The turbid plumes in front of the tidewater glaciers and in the glacial bays are recognised as foraging "hotspots" for seabirds such as black-legged kittiwake (*Rissa tridactyla*), northern fulmar (*Fulmarus glacialis*), black guillemot (*Cepphus grylle*), and Arctic tern (*Sterna paradisaea*) (Stempniewicz et al., 2017; Urbanski et al., 2017; Nishizawa et al., 2020; Stempniewicz et al., 2021). Because the marginal ice zone is retreating northwards (Barber et al., 2015), flying longer distances becomes energetically costly and seabirds may use glacial bays and fronts in Svalbard to a greater extent (Lydersen et al., 2014; Varpe and Gabrielsen, 2022). However, a recent study found a complex relationship, rather than an apparent pattern, between annual use of the glacial fronts by black-legged kittiwakes in Kongsfjorden and glacial discharge volume or zooplankton prey abundance in the fjord (Bertrand et al., 2021a). The subglacial discharge in front of glaciers fluctuates in time and space, which implies that the feeding "hotspots" for seabirds vary in time (Urbanski et al., 2017). Kittiwakes from different colonies around the inner fjord basin feed in the glacial bays including the glacier fronts, but also elsewhere in the fjord system (Bertrand et al., 2021b). Thus, the best foraging areas will change in time and space depending on prey availability as well as the distance to the colony.

Some marine mammals, particularly ringed seals (*Pusa hispida*) and white whales (*Delphinapterus leucas*) also forage close to glacial fronts (Lydersen et al., 2001; Everett et al., 2018). In Kongsfjorden, they are likely targeting the aggregations of fish feeding on zooplankton in the glacial bays, such as polar cod (*Boreogadus saida*), Atlantic cod (*Gadus morhua*) and haddock (*Melanogrammus aeglefinus*), all of which were caught in the glacial bay during our investigations.

Glacial plumes can act as a "death trap" for zooplankton if caught in rising freshwater from a glacial outflow near the bottom of a glacier (Weslawski and Legezynska, 1998; Lydersen et al., 2014). Several studies have proposed or estimated increased mortality of zooplankton in the vicinity of glacial outflow due to osmotic shock (Weslawski and Legezynska, 1998; Zajaczkowski and Legezynska, 2001; Urbanski et al., 2017). Abrupt exposure of *Calanus* spp. in simple bottle experiments to salinity <24 caused 100% mortality within 1 h, whereas exposure to salinity <9 shortened this to 15 min (Zajaczkowski and Legezynska, 2001). These authors estimated a mortality rate in the inner fjord basin (20 km$^2$) of 6 mg C m$^{-2}$ d$^{-1}$, or 85 tonnes wet weight over the melt season (100 days). Thus, 15% of the estimated standing stock of zooplankton in the fjord would then be removed because of mortality due to osmotic shocks. If not preyed upon by seabirds and marine mammals, dead zooplankton will sink to the bottom, where they are utilized by benthic necrophagic amphipods and other soft-bottom fauna (Legeżyńska et al., 2000; Legeżyńska, 2001).

Despite our increased knowledge of zooplankton within glacial plumes, many questions remain. Our aim was to focus on three key questions. 1) Is a glacial plume a "death trap" for zooplankton resulting in enhanced prey availability? 2) Do the mixing and circulation of the glacial meltwater and deep water result in an "elevator" effect with enhanced surface or near-surface prey availability? 3) How important are the inner, partially isolated bays of a glacier fjord for zooplankton aggregation? To answer these questions on the importance of glacial plumes as "climate refugia" by maintaining prey availability to foraging seabirds, we carried out two intensive glacial front sampling campaigns in Kongsfjorden on Spitsbergen, Svalbard.

# Materials and methods

## Area description

Our study was conducted in a sub-Arctic fjord (Kongsfjorden), located on the west coast of Spitsbergen in the Svalbard archipelago (79°N, 11–12°E), which extends over a length of 20 km and a width ranging from 4 to 10 km (Svendsen et al., 2002; Figures 1A, B). The fjord is about 350 m deep at the mouth and becomes gradually narrower and shallower towards the inner basin. The fjord has no distinct sill at its mouth allowing exchange of intermediate and deep

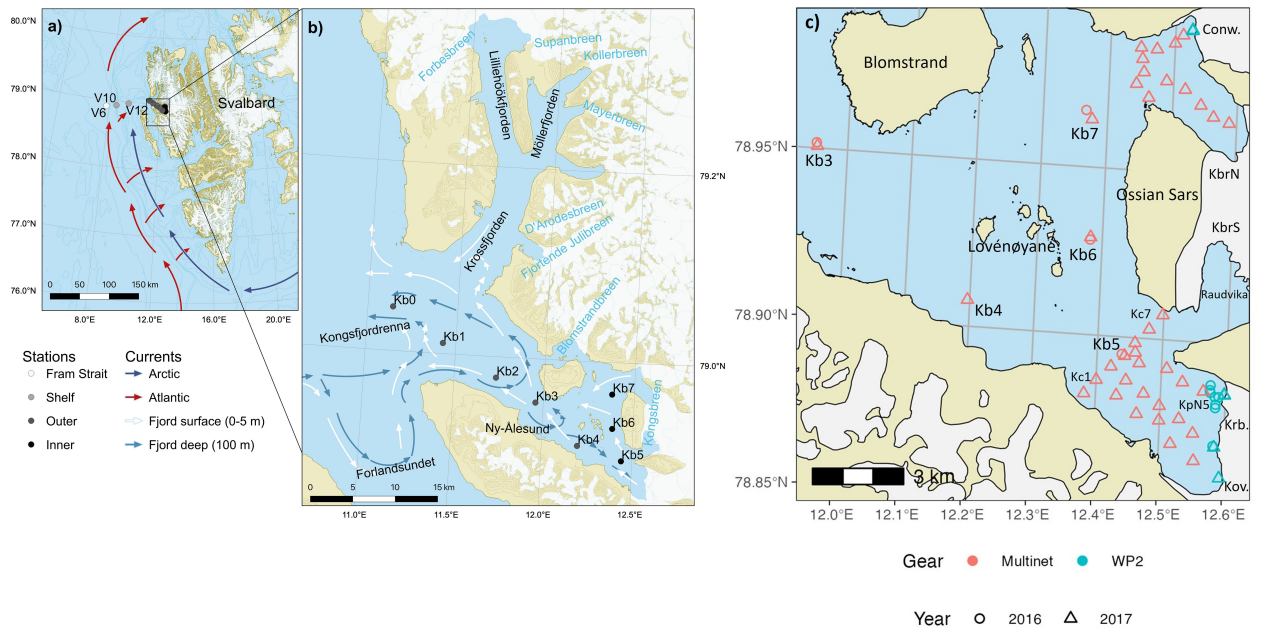


FIGURE 1
Kongsfjorden transect stations in **(A)** Shelf and shelf slope to Fram Strait (V6, V10, V12) with Atlantic and Arctic currents, **(B)** fjord stations with main circulation patterns indicated outside and inside the fjord (Modified from Hop et al., 2019), **(C)** Sampling stations with RV *Lance* and a helicopter in front of Kongsfjorden tidewater glaciers on 1-3 August 2016 and 25-28 July 2017. Red rings/triangles are *Lance* stations in 2016/2017 sampled with MultiNet, whereas cyan equivalents indicate helicopter sampling stations with WP-2 and WP-3 in the respective years. The sampling was more extensive in 2017 than in 2016, and the northern stations were only sampled in 2017. Glaciers are Conwaybreen (Conw.), Kongsbreen North and South (KbrN, KbrS), Kronebreen (Krb.) and Kongsvegen (Kov.). The location of main sampling stations (Kb4-Kb7) is referred to as inner fjord basin, whereas sampling near the glaciers are in the respective glacial bays (outer bay, mid bay and at the glacial front).

fjord waters with offshore water masses comprising warm, saline Atlantic Water (AW) of the West Spitsbergen Current and cold, less saline Arctic waters flowing northwards along the Spitsbergen shelf (Cottier et al., 2005; Tverberg et al., 2019). These water masses mix on the shelf and are advected into the fjord as AW (T>3.0 °C, S>34.65) and Transformed Atlantic Water (TAW: T 1.0-3.0 °C , S >34.65; Svendsen et al., 2002). During the summer, AW and TAW typically dominate the hydrography of Kongsfjorden (Hop et al., 2006; Assmy et al., 2023; Santos-García et al., 2023), which is the main reason for referring to it as sub-Arctic when compared to the Arctic fjords in northern Svalbard (Hop et al., 2002; Santos-García et al., 2023).

In the inner part of the fjord, the islands of Lovénøyane and the associated rising seabed, with a shallow sill (about 20 m deep) to the south and a deeper sill (50 m) to the north, form the inner basin of Kongsfjorden. There are four tidewater glaciers in the inner part of Kongsfjorden: Kongsvegen, Kronebreen, Kongsbreen, and Conwaybreen (Figure 1C). The inner fjord basin can be further divided into a northern glacial bay (max depth 125 m) and southern glacial bay (max depth 95 m), north and south of the Ossian Sars Mountain (Figure 1C). In the southern glacial bay, Kronebreen and Kongsvegen drain through a shared terminus which reaches around 50-60 m depth (Supplementary Figure S1). Kronebreen currently occupies about 70% of the glacier width at the terminus (Sund et al., 2011), and together these glaciers form the largest tidewater glacier terminus in Kongsfjorden. The main outflow from the glaciers was situated in front of Kronebreen at the time of the study. The part of Kongsbreen located south of the Ossian Sars Mountain (Kongsbreen South) is more influenced by the runoff from the Kronebreen-Kongsvegen system, which involves erosion of red sandstone into the glacial bay named Raudvika (red bay). Kongsbreen south and Raudvika were not included in our survey, but have been previously studied (Urbanski et al., 2017). The deepest parts of the bays surveyed in our study are located in the northern glacial bay, in front of Kongsbreen North, which sits partly on land. Conwaybreen rests largely (<70%) on bedrock above the water line. The northern glacial bay receives less run-off with sediments because Conwaybreen and Kongsbreen North erode hard rocks of marble, gneiss and granite (Dallmann, 2015).

The water temperature in the inner fjord basin is typically lower, or more Arctic, than further down fjord and offshore (Santos-García et al., 2023). It is suggested that such cold and saline waters are remnants of winter-cooled waters resulting from heat loss to the atmosphere and contact with glacial fronts (Torsvik et al., 2019). However, in summer, the mixing of meltwater from the glaciers with ambient seawater results in lower salinity (Torsvik et al., 2019). The water column in inner Kongsfjorden has warmed by 0.13 °C $y^{-1}$ at 35 m and 0.06 °C $y^{-1}$ at 85 m depth from 2010 to 2020, while salinity has increased by 0.3 (De Rovere et al., 2022). Depth-averaged temperatures have increased by 0.21°C $y^{-1}$ in the warmest months of the year, whereas they appear relatively stable in the coldest months (De Rovere et al., 2022).

## Sampling by vessels and helicopter

The along-fjord transect in Kongsfjorden was taken with RV *Lance* both years, 25-28 July 2016 and 30 July-2 August 2017, from the inner fjord basin out to station V6 in Fram Strait at 1000 m depth (Hop et al., 2019; Figures 1A, B). The inner fjord with glacial bays was subject to more intensive sampling both years, because of the focus of the study on investigating the small-scale patterns and the potential effect of glacial run off on zooplankton survival.

Samples in front of tidewater glaciers were collected by helicopter and RV *Lance* in the glacial bays on 1-3 August 2016 and 26-31 July 2017 (Figure 1B). In 2016, four stations were sampled from RV *Lance* and eight stations were sampled by a helicopter in front of Kronebreen. The sampling was conducted around the North plume of Kronebreen. In 2017, the sampling campaign in the glacial bays was more extensive and included the bays in front of several glaciers around the inner basin. Sampling stations were clustered based on their similar hydrography and distance to glacier fronts in the southern and northern part of the glacial bays: Kronebreen-Kongsvegen (South) and Conwaybreen-Kongsbreen (North). The inner part of Kongsfjorden was surveyed with the research vessel for hydrography in 2017 from the inner transect station Kb5, with one transect across the outer glacial bay and one from Kb5 towards the glacial front of Kronebreen. Sampling closest to the glacial fronts was performed by helicopter also in 2017. In addition, a small surface net was pulled across the brown glacial plume in front of Kronebreen with a small vessel (AKVA Polarcirkel RBB) at a safe distance from a stable section of the glacial front. The hydrography was also surveyed outside Conwaybreen and Kronebreen North, as presented in Halbach et al. (2019).

Biogeochemical environmental variables such as nutrients, chlorophyll *a* (Chl *a*), phytoplankton and suspended matter were sampled both from RV *Lance* and by helicopter in close proximity to the glacier fronts. On board the ship, water samples were collected with 8L Niskin bottles mounted on a rosette sampler equipped with a CTD (conductivity-temperature-depth, Sea-Bird Electronics SBE911, Bellevue, WA, USA), photosynthetically active radiation (400-700 nm, PAR: Spherical underwater Quantum Sensor Li-193, LI-COR Biosciences) and fluorescence (WETStar, Sea-Bird Electronics) sensors.

From helicopter, sampling was done by means of a CTD rosette at 33-m distance to the Kronebreen front and 93-m distance to the Conwaybreen front. The Hydro-Bios Multi Water Sampler SlimLine 6 rosette equipped with an integrated CTD and 6×3.5 L Niskin bottles was attached 5 m above a 500 kg counterweight (cement drum), which was connected to a wire of 100 m length. Sampling was conducted by lowering the counterweight to the bottom, causing notable slack on the wire, and then pulling up slowly (1 m $s^{-1}$) with the ascending helicopter which was hovering well above the glacier. Thus, water samples were taken from the entire water column from 5 m above the bottom.

## Zooplankton

Zooplankton sampling from RV *Lance* was done with a Multiple Plankton Sampler (MultiNet type Midi, Hydro-Bios Kiel), consisting of five nets with 0.25 $m^2$ opening and 200 µm mesh size, hauled at a speed of about 0.5 m $s^{-1}$ and closed in sequence. Depth strata sampled were bottom-200 m, 200-100 m, 100-50 m, 50-20 m, 20-0 m. For the shallow stations, the depth intervals were reduced (bottom-50 m, 50-20 m, 20-0 m). Zooplankton sampling from Polarcirkel was done in 2017 with a surface net (0.4 × 0.7 m opening, with 200 µm mesh) towed slowly at about 1 m $s^{-1}$ for estimated (GPS) distances of 244-1317 m (mean 617 m) in five tows.

For zooplankton sampling by helicopter, the CTD rosette was replaced by plankton nets: WP-2 (0.25 $m^2$ opening, 200 µm mesh) or WP-3 (1 $m^2$ opening, 1000 µm mesh). These were operated similarly, at same locations, sampling the entire water column from 5 m above the bottom (towing speed ca. 1 m $s^{-1}$), and samples were retrieved by a ground team.

The plankton nets used are known to sample mesozooplankton representatively, but tend to undersample both microzooplankton and macrozooplankton (Hop et al., 2019). The nets will collect some macrozooplankton, such as *Themisto* spp. and *Thysanoessa* spp., but predominately the smaller size classes. Logistically, in the glacial bays with icebergs and by sampling from helicopter, it was impossible to use larger nets, such as MIK and Tucker trawl, which would have sampled macrozooplankton and fish larvae-juveniles more efficiently (Hop et al., 2019).

Samples for taxonomical analyses were preserved with a hexamethylenetetramine-buffered formalin solution at a final concentration of 4% immediately after collection. For determining non-consumptive dead vs. live zooplankton in and around the glacial plume, samples from 2016 were subjected to neutral red staining. The stock solution was made according to Elliott and Tang (2009) and applied to zooplankton samples immediately after collections. After staining for 15 min, the sample was rinsed on 200 µm mesh and preserved with formalin at a final concentration of 4%. Subsequent analyses involved counts of stained (live) vs. not-stained (dead) organisms.

For taxonomic determination, organisms were identified and counted under a stereomicroscope equipped with an ocular micrometre, according to standard procedures, including morphology and prosome length for *Calanus* spp. (Postel et al., 2000; Kwasniewski et al., 2003). Other zooplankters were identified to the lowest possible taxonomic level based on available literature and web descriptions. The zooplankton were separated into groups for presentation in figures: small copepods (< 2.5 mm total length as adults), large copepods as *Calanus* species (*C. finmarchicus, C. glacialis, C. hyperboreus*), other large copepods (e.g., *Metridia longa* and *Paraeuchaeta* spp.), meroplankton (e.g., Bivalvia, Echinodermata, and Polychaeta), other zooplankton (e.g., *Fritillaria borealis*, *Limacina helicina*, *Parasagitta elegans*). The dry mass conversion factors from Hop et al. (2019) with subsequent updates (Assmy et al., 2023) were applied for calculating zooplankton biomass.

The abundances (ind. $m^{-3}$) or biomasses (mg dry mass (DM) $m^{-3}$) for each species or a group of species were summed up by stage, size group and/or species and averaged over depth strata for each station using the following equation:

$$D^{-1}\sum_{i=1}^{n} a_i d_i$$

where $a_i$ is the abundance or biomass of species $a$ at depth stratum $i$, $d_i$ is the sampled distance for depth stratum $i$ in meters, D is the total depth of net haul, and $n$ is the number of depth strata at a station. In order to compare all stations of the fjord and shelf transect to V6, only data from the upper 200 m were included or bottom if shallower (inner part). Abundances were expressed as ind. $m^{-3}$ to be able to compare with earlier studies (e.g., Kwasniewski et al., 2003; Walkusz et al., 2009; Kwasniewski et al., 2013; Hop et al., 2019). Since samples from the inner part of the fjord were taken shallower (40-50 m) than mid-fjord samples (upper 200 m), we also presented the number of zooplankton as ind. $m^{-2}$, which expresses the total number of organisms at a site (Circle plots in Supplementary Figures S1–S3; Supplementary Tables S1, S2).

## Benthic amphipods

Benthic amphipods were caught in baited traps, in strings of five traps each deployed overnight from Polarcirkel at different locations in the glacial bay outside Kronebreen in 2017. The baited traps consisted of plastic pipe (20 cm long, 10 cm in diameter) with a funnel attached to one end and a removable net (mesh size: 1 mm) on the other. Bait was raw chicken meat packed in fine-mesh bags to prevent the amphipods from getting access to it (Nygård et al., 2009). The collected scavenging species were identified under a stereomicroscope.

## Stable isotope analysis

Samples for stable isotopes were obtained from MIK and WP-3 net hauls from the entire water column performed at the sampling stations (Table S7). Some of the fish were caught in those nets, whereas larger specimens of Atlantic cod (*Gadus morhua*) and haddock (*Melanogrammus aeglefinus*) were caught by jigging from the research vessel. Samples for stable isotopes $\delta^{15}N$ and $\delta^{13}C$ were prepared according to the method described by Søreide et al. (2006a) and Søreide et al. (2006b), with removal of lipids and carbonates from samples in order to reduce variability. They were analysed at the Institute for Energy Technology, Kjeller, after the same procedure as described in Søreide et al. (2006b).

Stable isotope data provide quantitative information on the resources that a community uses (bionomic) and its bioclimatic habitat (scenopoetic). This information can be used to define the community's ecological niche (Newsome et al., 2007). A difference in ecological niche would indicate a difference in primary carbon sources and the background bioclimatic conditions (Jackson et al., 2011). An ecological niche can be represented as an $n$-dimensional hyperspace that can be partitioned into scenopoetic axes, representing environmental components of niche space, and bionomic axes, which refer to the trophic components of niche space (Hutchinson, 1978). Location on these axes can be quantified using stable isotopic ratios (Jackson et al., 2011) and formalized in the concept of the 'isotopic niche' (Newsome et al., 2007). It is important to note that 'isotopic niche' does not explicitly define an 'ecological niche' as it does not typically provide species or taxon information on resource use. Instead, within the broad domain of 'ecological niche', it can provide a useful summary of ecological characteristics such as primary carbon sources of each area (glacial bay, inner and outer fjord).

Various metrics have been proposed to analyse the spread of data points within the $n$-dimensional hyperspace defined by the bionomic and scenopoetic axes to quantify the 'isotopic niche' (Jackson et al., 2011). To date, the most useful has been to calculate the convex hull area (TA) encompassing the data points (Supplementary Figure S5), providing an indication of the niche width of each community in question (Layman et al., 2007; Jackson et al., 2011). A significant shortcoming of this approach, relevant to our study is high sensitivity to sample size and composition (Jackson et al., 2011). Instead of convex hulls, we have used an alternative approach based on standard ellipses (Batschelet, 1981), reformulated in a Bayesian framework (Jackson et al., 2011). This allows robust comparison between data sets (Supplementary Table S9) comprising different sample sizes accounting for uncertainty. The computational code to calculate the metrics is available in the free-to-download package Stable Isotope Analysis for R (SIBER).

## Data analysis

Positions of glacier fronts were estimated by vectorising the fronts from a Sentinel-2 satellite photograph taken on 31 July 2017 (see Halbach et al., 2019). Euclidian distance of each station to the closest front was then calculated using a UTM projection (epsg:32633) and the st_distance function from the sf package (Pebesma, 2018) for R (R Core Team, 2022).

The relation of total zooplankton biomass and abundance to the distance from the closest glacier front was examined using log-linear [lm(log(total) ~ log(dist)] and general additive [gam(log (total) ~ s(log(dist))] models. We performed a principal component analysis (PCA) on a square root transformed proportion species composition matrix [i.e., "Hellinger transformation" in Legendre and Gallagher (2001)]. The analysis was performed using the rda function, and the transformation using the decostand function from the vegan package (Oksanen et al., 2022) for R.

# Results

Oceanographic conditions for Kongsfjorden and the shelf were characteristic for the summer situation in late July, with rather similar conditions in 2016 and 2017 (Figures 2A–D). Relatively

10.3389/fmars.2023.1161912

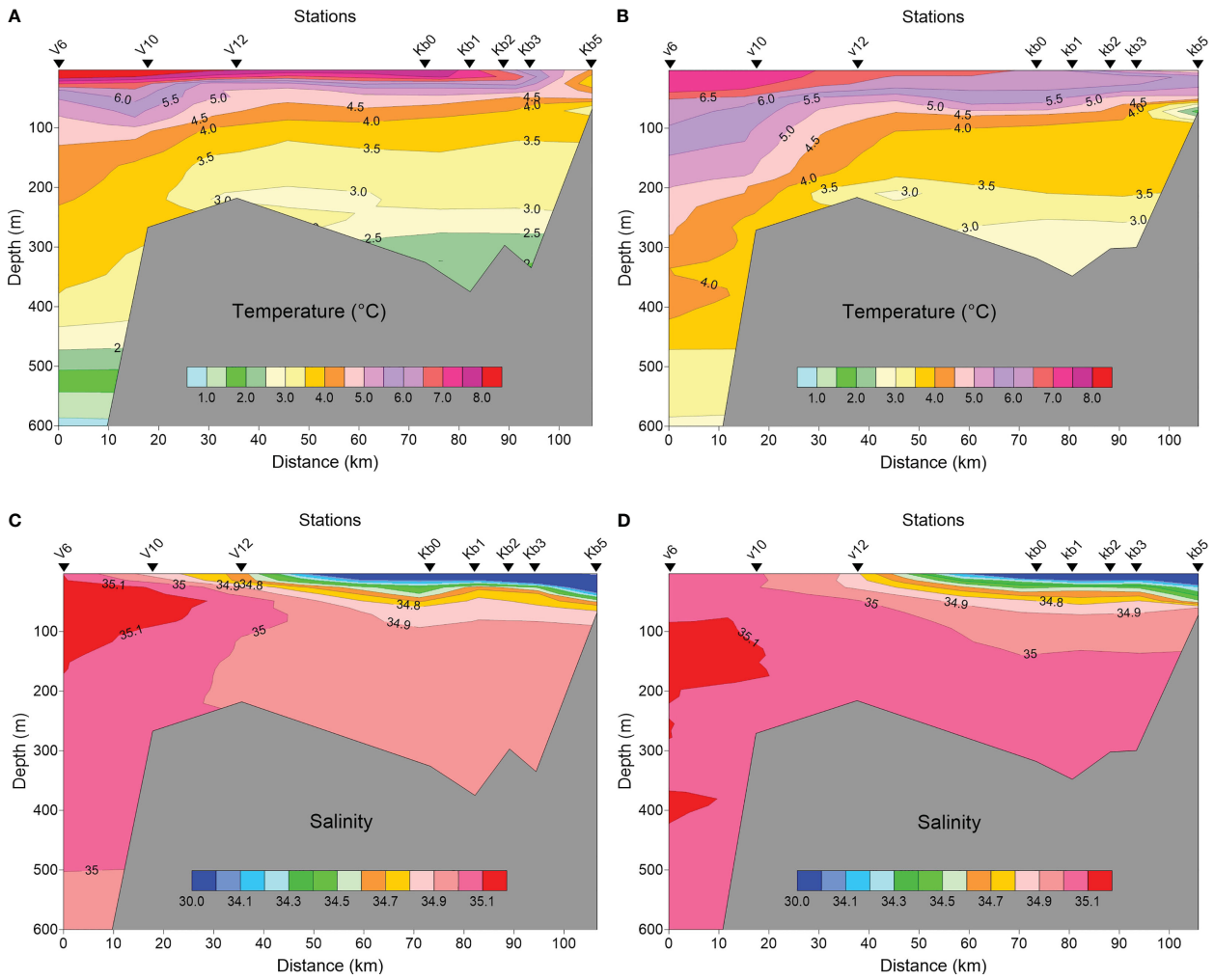


FIGURE 2
Temperature **(A, B)** and salinity **(C, D)** profiles along Kongsfjorden from V6 in Fram Strait to station Kb5 in the inner basin in late July 2016 **(A, C)**, and late July-early August 2017 **(B, D)**.

warm (6-8°C) surface waters with reduced salinity (<30), increased in vertical extent towards the inner fjord basin. Transformed Atlantic Water constituted most of the water mass in the fjord. In both years, TAW with temperatures 2.5-3.0°C extended to the bottom.

The water column in the inner part of Kongsfjorden, based on measurements from 2017, was stratified, even behind the inner sill of 50 m depth (Figures 3A–D). The temperature varied from 5.5°C in surface waters to 1.5°C near the bottom at 70 m depth. The glacial effect, including both glacial river discharge and direct ice melting, caused some freshening of the surface layers to <30, but no salinity values below 26 (Figure 4). The glacial effect was not very strong even at the innermost station sampled (KpN5), which was about 1 km from the main glacial water outlet at Kronebreen. The fresher surface water only comprised the upper 5 m of the water column and became further reduced outside the sill. Atlantic water and TAW prevailed in the deeper parts (>50 m depth) in the fjord, and extended to the inner fjord basin and glacial bays (Figure 4).

Zooplankton distribution (in terms of abundance and biomass) at stations along the main fjord transect) is described below, and zooplankton distribution at stations in the inner fjord basin and glacial bays then follows.

The three *Calanus* species showed variable abundance in the upper 200 m along the transect, with generally higher abundance and biomass in early August 2016 than in late July 2017 (Tables 1A, 1B; Supplementary Figure S1A. One exception was the high abundance (1330 ind. $m^{-3}$) of *Calanus finmarchicus* in the inner fjord station Kb5 in 2017. The biomass of *C. finmarchicus* was generally high (> 150 ind. $m^{-3}$) in 2016 and 2017 both in the inner fjord and at the outer shelf break (V6), where Atlantic water masses prevailed. The Arctic *C. glacialis* showed variable lower abundance, but higher contribution to biomass within Kongsfjorden, with highest abundance values in the inner fjord basin (140 ind. $m^{-3}$) in August 2016, and lower abundance (50-60 ind. $m^{-3}$) in the inner fjord in 2017. *Calanus hyperboreus* was present but contributed little to abundance (generally <10 ind. $m^{-3}$) or biomass (Tables 1A, 1B).

The distribution of zooplankton biomass in relation to the distance from the glacier did not show any well-defined statistical trend; it was relatively even (lm log(dist) $p = 0.17$, gam s(log(dist))

10.3389/fmars.2023.1161912

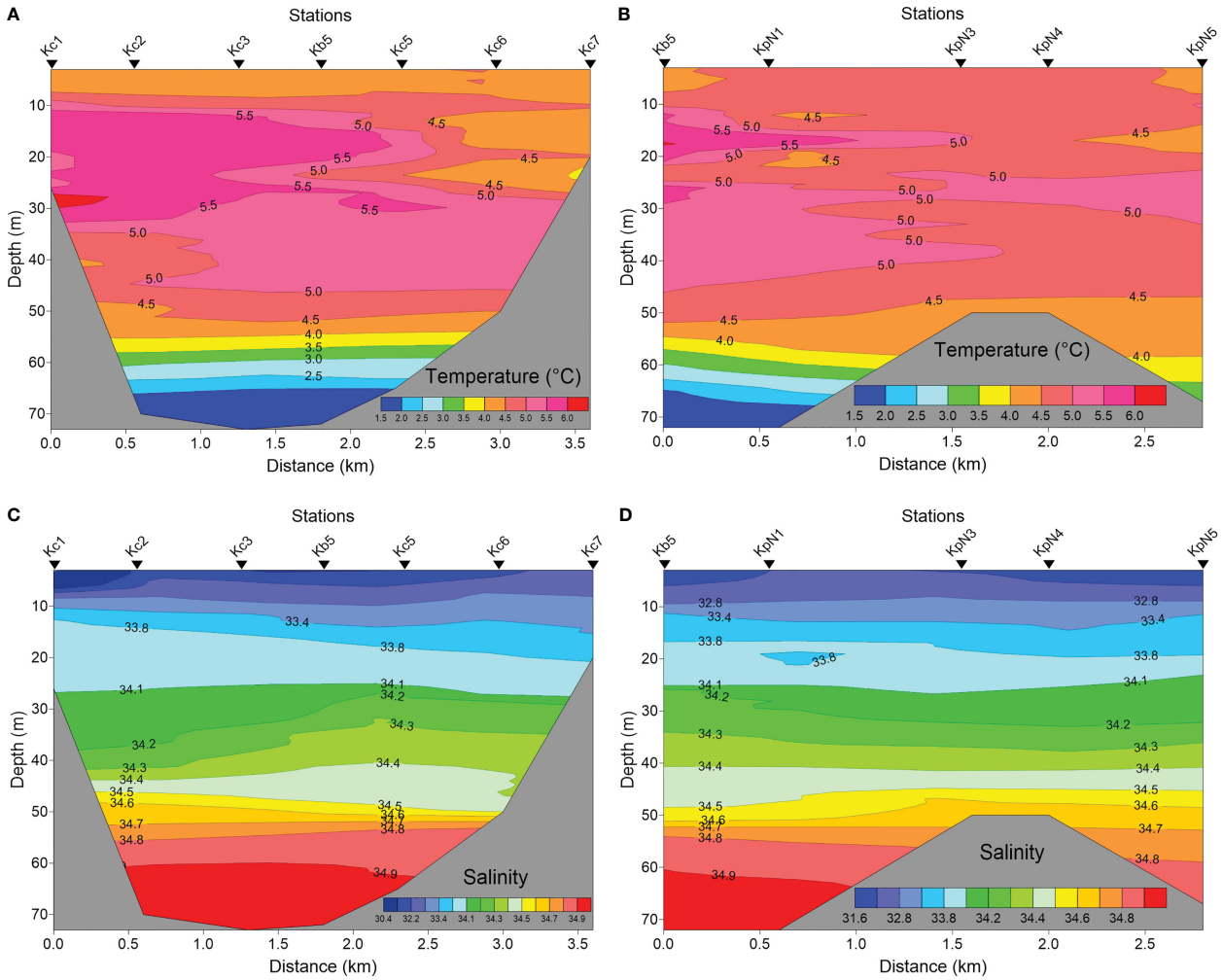


FIGURE 3
Temperature **(A, B)** and salinity **(C, D)** in the glacial bay of Kongsfjorden in late July 2017 across the southern glacier bay (Kc1 via Kb5 to Kc7) **(A, C)**, and from station Kb5 (Figure 1) to the glacial front of Kongsvegen/Kronebreen (station KpN5) **(B, D)**.

$p$ = 0.33). Despite this, the community differed with the distance showing spatial and annual variation (Figure 5). MultiNet covered a wider range in the PCA space (i.e. contained more species) than WP-2, mainly because there were more MultiNet casts in the dataset (Figure 5B). The results show that in 2017 there were more *C. finmarchicus* than in 2016, but this was mostly because high biomass of *C. finmarchicus* was found in samples from Conway- and Kronebreen stations (Table 2A; Supplementary Table S4B), which were collected only in 2017 (Figures 5C, D). As a result, *C. finmarchicus* showed generally a negative correlation with distance from closest glacier front (Figure 5E). Also *C. glacialis* demonstrated negative correlation with distance from the closest glacier front. The mean biomass of *C. glacialis* appeared uniform within Kongsfjorden and decreased on the continental shelf. *Calanus hyperboreus* showed to some degree negative biomass trends with distance from the closest glacier front. On the contrary, the chaetognath *Eukrohnia hamata* demonstrated the opposite correlation being more abundant on the shelf than in the fjord and glacial bays, although it also had a high biomass in some Kronebreen front stations (Figures 5D, E).

Small zooplankton was dominated by *Oithona similis* at all stations, with abundance values in the 400-1500 ind. $m^{-3}$ range in 2016 (Table 1A; Supplementary Figure S1B). The abundance of this species was generally higher in 2017, increasing towards the inner fjord basin (10,000 ind. $m^{-3}$ at station Kb5; Table 2A). *Pseudocalanus* spp. were the second-most abundant small copepods, both years, with highest density (400-550 ind. $m^{-3}$) at the inner basin station Kb5, and <300 ind. $m^{-3}$ in the middle and outer reaches of the fjord, with highest abundance in 2016. Copepoda nauplii showed variable abundance, and could be high both at the outer stations (200-400 ind. $m^{-3}$) and in the middle to inner part of the fjord (200-260 ind. $m^{-3}$). *Microcalanus* spp. were less abundant (30-120 ind. $m^{-3}$) with no clear pattern. The biomass contribution generally reflected the abundance pattern, although with larger contributions of *Pseudocalanus* spp., particularly at Kb5 in the inner fjord basin in 2016.

Other large copepods were mainly represented by *Metridia longa* and *Paraeuchaeta* spp., but also included less abundant species of the genera *Aetideopsis* and *Scaphocalanus* present at stations outside the main fjord basin. This group as a whole,

10.3389/fmars.2023.1161912

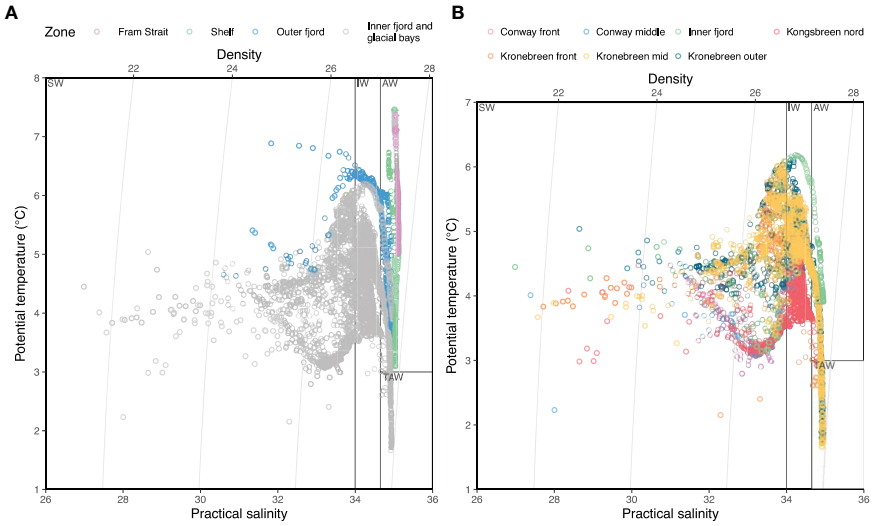


FIGURE 4
Temperature-salinity plots showing water masses in the upper 200 m in the entire study area **(A)** and only the inner fjord and glacial bays **(B)** in 2017. Ten observations with salinity < 5 from Conway-front and Kronebreen-front have been removed to make the plots readable. Water mass classifications follow those of Cottier et al. (2005): SW, surface water; IW, intermediate water; AW, Atlantic water; TAW, transformed Atlantic water.

however, was most abundant at Kb5 in the inner basin during both years, with 16-25 ind. $m^{-3}$ for *M. longa* and <1 ind. $m^{-3}$ for *Paraeuchaeta* spp. (Supplementary Figure S1C). Other large copepods had considerable biomass in the outer shelf region out to V6, but the highest was recorded for station Kb1 and Kb0 in the outer deep part of Kongsfjorden, and the main contributor to biomass was *Metridia longa*. Biomass of large copepods was generally higher in 2016 than in 2017.

Meroplankton included mainly larvae of Bivalvia and Echinodermata (Tables 1A, B; Supplementary Figure S1D). Bivalvia veligers and juveniles reached high abundance values (>1600 ind. $m^{-3}$) in the glacial bay in 2016 and occasionally also

TABLE 1A Zooplankton abundance (ind. $m^{-3}$) at stations in Kongsfjorden, from inner fjord basin to outer fjord in July 2016.

| Station | | V6 | V12 | V10 | Kb0 | Kb1 | Kb2 | Kb3 | Kb5 |
|---|---|---|---|---|---|---|---|---|---|
| Date (2016) | | 28 July | 27 July | 27 July | 27 July | 26 July | 26 July | 26 July | 26 July |
| Depth (m) | | 200-0 | 200-0 | 200-0 | 200-0 | 200-0 | 200-0 | 200-0 | 60-0 |
| | | (ind. $m^{-3}$) | (ind. $m^{-3}$) | (ind. $m^{-3}$) | (ind. $m^{-3}$) | (ind. $m^{-3}$) | (ind. $m^{-3}$) | (ind. $m^{-3}$) | (ind. $m^{-3}$) |
| Copepoda | | | | | | | | | |
| Calanoida | *Calanus finmarchicus* | 841.48 | 251.96 | 153.59 | 488.40 | 320.40 | 300.21 | 631.79 | 697.00 |
| | *Calanus glacialis* | 1.38 | 53.09 | 17.22 | 86.03 | 64.49 | 106.53 | 133.88 | 143.16 |
| | *Calanus hyperboreus* | 0.30 | 1.05 | 0.16 | 0.90 | 3.85 | 0.95 | 3.93 | 5.40 |
| | *Metridia longa* | 9.35 | 10.20 | 5.65 | 5.42 | 5.42 | 6.63 | 8.69 | 25.05 |
| | *Microcalanus* spp. | 30.95 | 91.16 | 53.51 | 141.56 | 91.50 | 53.92 | 79.62 | 121.05 |
| | *Pseudocalanus* spp. | 54.94 | 55.14 | 45.81 | 230.18 | 210.11 | 174.63 | 286.45 | 559.39 |
| | *Paraeuchaeta* spp. | 0.19 | 0.30 | 0.24 | 0.15 | 0.10 | 0.53 | 0.02 | 0.99 |
| | Other Calanoida | 1.70 | 0.32 | 0.17 | 1.62 | 3.81 | 3.17 | 6.89 | 30.54 |
| Cyclopoida | *Oithona similis* | 1110.03 | 409.10 | 612.86 | 1091.52 | 952.62 | 1053.23 | 1363.91 | 1441.26 |
| | *Triconia borealis* | 61.71 | 37.31 | 21.96 | 40.19 | 21.26 | 17.10 | 15.30 | 43.72 |
| | Other Cyclopoida | 24.41 | 21.88 | 25.68 | 19.96 | 11.76 | 27.81 | 15.44 | 6.30 |
| Harpacticoida | Harpacticoida | 0.00 | 0.00 | 0.25 | 0.37 | 1.88 | 0.79 | 0.00 | 1.67 |

*(Continued)*

10.3389/fmars.2023.1161912

TABLE 1A Continued

| Station | | V6 | V12 | V10 | Kb0 | Kb1 | Kb2 | Kb3 | Kb5 |
|---|---|---|---|---|---|---|---|---|---|
| Date (2016) | | 28 July | 27 July | 27 July | 27 July | 26 July | 26 July | 26 July | 26 July |
| Depth (m) | | 200-0 | 200-0 | 200-0 | 200-0 | 200-0 | 200-0 | 200-0 | 60-0 |
| | | (ind. $m^{-3}$) | (ind. $m^{-3}$) | (ind. $m^{-3}$) | (ind. $m^{-3}$) | (ind. $m^{-3}$) | (ind. $m^{-3}$) | (ind. $m^{-3}$) | (ind. $m^{-3}$) |
| | Copepoda nauplii | 383.98 | 92.25 | 179.36 | 121.46 | 54.57 | 182.50 | 257.56 | 260.91 |
| Malacostraca | | | | | | | | | |
| Amphipoda | *Themisto abyssorum* | 6.11 | 0.28 | 0.10 | 0.35 | 0.76 | 2.04 | 1.42 | 6.44 |
| | *Themisto libellula* | 0.31 | 0.25 | 0.02 | | 0.05 | 0.06 | 0.14 | 0.91 |
| Decapoda | *Hyas* & *Pagurus* larvae | 0.00 | 0.03 | 0.00 | 0.02 | 0.03 | 0.03 | 0.08 | 0.12 |
| Euphausiacea | *Thysanoessa* spp. | 6.37 | 0.32 | 1.06 | 1.13 | 0.43 | 0.31 | 0.00 | 1.75 |
| Isopoda | Bopyridae | 0.15 | 0.48 | 0.24 | 0.13 | 0.21 | 0.63 | 0.27 | 2.33 |
| Other phyla/classes | | | | | | | | | |
| Appendicularia | *Fritillaria borealis* | 14.08 | 81.23 | 49.79 | 19.00 | 36.73 | 23.51 | 15.98 | 35.92 |
| | *Oikopleura* spp. | 6.35 | 131.17 | 67.28 | 20.40 | 27.67 | 12.89 | 10.61 | 29.23 |
| Bivalvia | Bivalvia larvae | 7.97 | 89.03 | 48.36 | 2733.07 | 593.47 | 438.38 | 373.61 | 1658.89 |
| Bryozoa | Bryozoa larvae | | | | 0.13 | | | | 2.06 |
| Chaetognatha | *Parasagitta elegans* | 0.19 | 2.11 | 2.14 | 10.82 | 11.69 | 9.90 | 12.02 | 42.87 |
| | *Eukrohnia hamata* | 34.83 | 5.60 | 5.04 | 3.90 | 2.29 | 1.40 | 2.13 | 7.02 |
| Cirripedia | Cirripedia nauplii | | 0.55 | 0.08 | 2.77 | 0.85 | 0.82 | 3.37 | 1.67 |
| Ctenophora | *Mertensia ovum* | | 0.02 | | 0.09 | | 0.02 | 0.05 | 0.31 |
| Echinodermata | Echinodermata larvae | 1.51 | 16.88 | 2.57 | 225.20 | 71.25 | 74.97 | 89.03 | 128.77 |
| Gastropoda | *Clione limacina* | | 0.15 | | 0.04 | | | 0.04 | |
| | *Limacina helicina* | 18.35 | 646.46 | 152.69 | 1401.06 | 897.79 | 319.75 | 927.03 | 2277.20 |
| | *Limacina retroversa* | 0.63 | 0.38 | 0.32 | 3.75 | 0.70 | | | |
| Hydrozoa | Hydrozoa larvae | | | | 0.98 | | 0.02 | | 0.66 |
| | *Aglantha digitale* | 0.92 | 0.56 | 3.00 | 1.02 | 3.89 | 2.30 | 0.80 | 0.69 |
| Ostracoda | Ostracoda | 13.04 | 0.46 | 0.86 | | 0.08 | | | 2.96 |
| Polychaeta | Polychaeta larvae | 0.24 | 1.09 | 1.10 | 4.72 | 3.17 | 1.05 | 2.00 | 5.35 |

Polychaeta larvae: *Myrianida* sp. (formerly *Autolytus* sp.), *Pelagobia* sp., Typhloscolecidae.
Decapoda zoea & megalopa: *Pagurus* (c.f. *P. pubescens*) zoea & megalopa, *Hyas* (c.f. *H. araneus*) megalopa, *Pandalus borealis* zoea.
Depth range has been limited to 200 m or the bottom of the fjord.

TABLE 1B Zooplankton abundance (ind. $m^{-3}$) at stations in Kongsfjorden, from inner fjord basin to outer fjord in July-August 2017.

| Station | | V6 | V12 | V10 | Kb0 | Kb1 | Kb2 | Kb3 | Kb4 | Kb5 |
|---|---|---|---|---|---|---|---|---|---|---|
| Date (2017) | | 1 Aug. | 1 Aug. | 1 Aug. | 31 July | 31 July | 30 July | 30 July | 29 July | 27 July |
| Depth (m) | | 200-0 | 200-0 | 200-0 | 200-0 | 200-0 | 200-0 | 200-0 | 100-0 | 50-0 |
| | | (ind. $m^{-3}$) | (ind. $m^{-3}$) | (ind. $m^{-3}$) | (ind. $m^{-3}$) | (ind. $m^{-3}$) | (ind. $m^{-3}$) | (ind. $m^{-3}$) | (ind. $m^{-3}$) | (ind. $m^{-3}$) |
| Copepoda | | | | | | | | | | |
| Calanoida | *Calanus finmarchicus* | 136.90 | 195.73 | 54.16 | 240.90 | 201.11 | 217.48 | 109.10 | 115.75 | 1331.60 |
| | *Calanus glacialis* | 3.64 | 32.78 | 5.79 | 92.45 | 37.06 | 49.51 | 51.79 | 47.90 | 61.38 |

*(Continued)*

TABLE 1B Continued

| Station | | V6 | V12 | V10 | Kb0 | Kb1 | Kb2 | Kb3 | Kb4 | Kb5 |
|---|---|---|---|---|---|---|---|---|---|---|
| Date (2017) | | 1 Aug. | 1 Aug. | 1 Aug. | 31 July | 31 July | 30 July | 30 July | 29 July | 27 July |
| Depth (m) | | 200-0 | 200-0 | 200-0 | 200-0 | 200-0 | 200-0 | 200-0 | 100-0 | 50-0 |
| | | (ind. $m^{-3}$) | (ind. $m^{-3}$) | (ind. $m^{-3}$) | (ind. $m^{-3}$) | (ind. $m^{-3}$) | (ind. $m^{-3}$) | (ind. $m^{-3}$) | (ind. $m^{-3}$) | (ind. $m^{-3}$) |
| | *Calanus hyperboreus* | 0.55 | 1.58 | | 0.80 | 0.69 | 0.31 | 0.67 | 2.44 | 10.57 |
| | *Metridia longa* | 5.89 | 12.69 | 2.94 | 15.91 | 7.31 | 5.61 | 10.20 | 1.17 | 15.99 |
| | *Microcalanus* spp. | 61.12 | 98.54 | 85.52 | 53.57 | 50.05 | 121.67 | 72.88 | 54.62 | 27.31 |
| | *Pseudocalanus* spp. | 9.06 | 37.70 | 8.51 | 166.37 | 63.94 | 106.15 | 93.01 | 93.71 | 406.26 |
| | *Paraeuchaeta* spp. | 1.67 | 0.08 | 0.31 | | | | 0.03 | | |
| | Other Calanoida | 1.22 | 1.88 | 0.50 | 0.92 | 0.56 | 1.39 | 1.76 | 1.06 | 14.59 |
| Cyclopoida | *Oithona similis* | 960.07 | 1629.92 | 1307.27 | 1107.80 | 901.36 | 1185.04 | 1882.79 | 4293.71 | 10189.52 |
| | *Triconia borealis* | 23.13 | 13.63 | 27.71 | 9.35 | 9.08 | 3.27 | 5.65 | 8.22 | 81.97 |
| | Other Cyclopoida | 33.57 | 24.11 | 48.53 | 5.24 | 6.94 | 10.82 | 11.45 | 12.17 | 30.12 |
| Harpacticoida | Harpacticoida | 1.22 | 0.92 | 0.68 | 0.29 | 0.22 | 0.65 | 1.06 | 2.35 | 2.98 |
| | Copepoda nauplii | 368.19 | 188.93 | 186.37 | 37.86 | 66.14 | 11.57 | 7.76 | 0.94 | 53.91 |
| Malacostraca | | | | | | | | | | |
| Amphipoda | *Themisto abyssorum* | 0.61 | 14.21 | 0.36 | 0.60 | 0.78 | 2.49 | 1.37 | 2.27 | 3.15 |
| | *Themisto libellula* | 0.02 | 0.24 | | 0.02 | 0.02 | 0.19 | 0.02 | 0.08 | 0.68 |
| | *Hyperoche medusarum* | | | | | 0.02 | | | | |
| Decapoda | *Hyas* & *Pagurus* larvae | 0.00 | 0.02 | 0.02 | 0.00 | 0.02 | 0.05 | 0.03 | 0.25 | 0.92 |
| | *Pandalus borealis* | | | | | 0.02 | 0.02 | | | |
| Euphausiacea | *Thysanoessa* spp. | 1.70 | 1.03 | 0.93 | 0.24 | 0.05 | 0.12 | 0.03 | 0.37 | 3.96 |
| Isopoda | Bopyridae | 0.96 | 0.77 | 0.43 | 0.44 | 0.30 | 0.28 | 0.14 | 0.29 | 2.98 |
| | Isopoda | 0.12 | | | | | | 0.11 | | |
| Other phyla/classes | | | | | | | | | | |
| Appendicularia | *Fritillaria borealis* | 205.33 | 218.76 | 57.35 | 12.19 | 16.77 | 11.26 | 5.07 | 0.19 | 5.96 |
| | *Oikopleura* spp. | 129.67 | 441.77 | 93.50 | 41.30 | 21.66 | 14.84 | 14.57 | 3.60 | 47.66 |
| Bivalvia | Bivalvia larvae | 3.73 | 57.67 | 1.94 | 137.39 | 69.99 | 64.71 | 40.72 | 7.75 | 57.43 |
| Bryozoa | Bryozoa larvae | 0.98 | 0.26 | | | 0.08 | 0.13 | 0.13 | 0.20 | |
| Chaetognatha | *Parasagitta elegans* | 0.52 | 4.46 | 1.12 | 10.25 | 6.97 | 5.78 | 10.05 | 7.60 | 17.26 |
| | *Eukrohnia hamata* | 29.65 | 4.51 | 4.37 | 1.66 | 1.47 | 0.45 | 0.20 | | 1.96 |
| Cirripedia | Cirripedia nauplii | 1.35 | | 0.07 | 0.88 | 0.64 | 0.94 | 0.84 | 1.06 | |
| Ctenophora | *Mertensia ovum* | | | | | | | | | 0.26 |
| Echinodermata | Echinodermata larvae | 9.05 | 259.04 | 17.38 | 119.58 | 42.99 | 10.65 | 15.73 | 2.23 | 402.63 |
| Gastropoda | *Clione limacina* | 2.06 | 0.54 | 1.35 | | 0.20 | | 42.57 | | 1.91 |
| | *Limacina helicina* | 45.54 | 87.93 | 19.22 | 191.76 | 104.36 | 32.82 | 31.71 | 26.29 | 203.95 |
| | *Limacina retroversa* | 0.88 | 0.26 | 0.55 | | | | | | |
| Hydrozoa | *Bougainvillia superciliaris* | | | | 0.02 | | | | | |
| | *Aglantha digitale* | 0.27 | 0.30 | 0.07 | 0.61 | 0.58 | 0.20 | 0.02 | | |

*(Continued)*

TABLE 1B Continued

| Station | | V6 | V12 | V10 | Kb0 | Kb1 | Kb2 | Kb3 | Kb4 | Kb5 |
|---|---|---|---|---|---|---|---|---|---|---|
| Date (2017) | | 1 Aug. | 1 Aug. | 1 Aug. | 31 July | 31 July | 30 July | 30 July | 29 July | 27 July |
| Depth (m) | | 200-0 | 200-0 | 200-0 | 200-0 | 200-0 | 200-0 | 200-0 | 100-0 | 50-0 |
| | | (ind. $m^{-3}$) | (ind. $m^{-3}$) | (ind. $m^{-3}$) | (ind. $m^{-3}$) | (ind. $m^{-3}$) | (ind. $m^{-3}$) | (ind. $m^{-3}$) | (ind. $m^{-3}$) | (ind. $m^{-3}$) |
| Ostracoda | Ostracoda | 2.92 | 0.41 | 0.87 | | | | | | |
| Polychaeta | Polychaeta larvae | 0.76 | | 0.90 | 1.22 | 0.62 | 0.69 | 0.26 | 0.09 | 1.91 |

Hydrozoa medusae: *Botrynema ellinorae*, *Bougainvillia superciliaris*, Siphonophora: *Dimophyes arctica*.
Polychaeta larvae: *Myrianida* sp. (formerly *Autolytus* sp.), *Pelagobia* sp., Typhloscolecidae.
Decapoda zoea & megalopa: *Pagurus* (c.f. *P. pubescens*) zoea & megalopa, *Hyas* (c.f. *H. araneus*) megalopa, *Pandalus borealis* zoea.
Depth range has been limited to 200 m or the bottom of the fjord.

further out in the fjord (2700 ind. $m^{-3}$ at station Kb0). A similar pattern can be seen for 2017, although the abundance was much lower (Supplementary Figure S1D). Echinodermata larvae were less abundant with high values in the glacial bay (130-400 ind. $m^{-3}$) both years, and also highest abundance (260 ind. $m^{-3}$) outside Kongsfjorden on the shelf (station. V12) in 2017.

Other zooplankton were mainly represented by the pteropod *Limacina helicina*, the appendicularian *Oikopleura* spp. and the chaetognath *Parasagitta elegans* (Tables 1A, B; Supplementary Figure S1E). Particularly *L. helicina* was abundant as veligers in the inner fjord basin (2300 ind. $m^{-3}$ at Kb5) and also in the outer reaches of Kongsfjorden and Kongsfjordrenna (1400 ind. $m^{-3}$) in 2016. In 2017, the abundance of *L. helicina* was generally low (<90 ind. $m^{-3}$), except for at the inner fjord basin and outer fjord, also for veligers (200 ind. $m^{-3}$). *Oikopleura* spp. were only occasionally abundant at single stations (e.g., 440 ind. $m^{-3}$ at V12 in 2017; Table 2A). *Parasagitta elegans* was generally not abundant, but with some elevated abundance (17-43 ind. $m^{-3}$) at the inner station in both years, and lower abundance (10 ind. $m^{-3}$) in the outer part of the fjord in 2017. Because of its size, however, its contribution to biomass at the inner basin (Kb5) was relatively large. Less abundant species included *Clione limacina*, *Themisto* spp., *Thysanoessa* spp., and *Meganyctiphanes norvegica*, but because of their large size, their contribution to biomass could be considerable (Supplementary Figure S1E).

The inner fjord basin and glacial bays near the tidewater glaciers were subject to the most intensive sampling both years. The abundance of both *Calanus finmarchicus* and *C. glacialis* was high both near the glacial front and further out into the inner fjord basin (Table 2B; Supplementary Figure S2A). However, *C. hyperboreus* was mainly present at low abundance away from the glacial front. Of other large copepods, the abundance of small copepods in 2016 was generally high, particularly of *Oithona similis* and *Pseudocalanus* spp. (Table 2B; Supplementary Figure S2B). The abundance and biomass were variable, but with similarly high values close to the glacial front and further out into the inner basin. Copepoda nauplii also showed variable abundance, with highest densities in the outer part of the glacial bays. *Metridia longa* was abundant at the glacial front as well as further out in the glacial bay, but lower in the central part of the inner fjord basin (Supplementary Figure S2C). Meroplankton, represented by Bivalvia and Echinodermata, was abundant in the glacial bay and further out in the fjord basin, but nearly absent at the glacial front (Supplementary Figure S2D). Bivalvia constituted most of the biomass. *Limacina helicina* showed a similar distribution pattern, with highest abundance away from the glaciers (Supplementary Figure S2E). Other taxa, such as amphipods (e.g., *Themisto* spp.), were more abundant close to the glacial front.

In 2017, the three *Calanus* species. were homogenously distributed within the glacial bays, with *C. finmarchicus* and *C. glacialis* as the most abundant species. *Calanus glacialis* was more abundant in the glacial front areas than in the outer and central locations, although this was less apparent for biomass (Table 2A; Supplementary Figure S3A). As in 2016, small copepods were omnipresent in 2017, but with no clear pattern regarding the location in glacial bays or distances from the glacial front (Table 2A; Supplementary Figure S3B). As before, the biomass followed the abundance values of these small copepods, with larger contribution of *Pseudocalanus* spp. Other large copepods, such as *Metridia longa,* were also more abundant and with higher biomass in the glacial front areas of Kronebreen than further out in the glacial bays and the central part of the inner fjord basin (Supplementary Figure S3C). However, *Paraeuchaeta* spp. were only found in the middle glacial bay and were not present at the fronts. The meroplankton was variable, with high abundance of Bivalvia at the Conwaybreen front and high abundance of Echinodermata at the Kronebreen front (Supplementary Figure S3D). The biomasses showed the same split for Bivalvia and Echinodermata, but within each location the taxa were more evenly distributed from bay to the glacial front. Other meroplankton, such as polychaetes and gastropod veligers, were occasionally abundant in the glacial bays, with polychaetes contributing with the largest biomass (Supplementary Figure S3D). *Limacina helicina* and *Parasagitta elegans* were rather evenly distributed within the glacial bays, with *L. helicina* as the most abundant species contributing largely to the biomass at the glacial front of Kronebreen (Supplementary Figure S3E). Because of their larger sizes, *Parasagitta elegans* and other taxa contributed most to the biomasses at the glacial fronts (Supplementary Figure S3E).

In the close vicinity of the glacial front, zooplankton abundance was variable between years (Tables 2A, B). In 2016, the abundance of zooplankton was generally lower close to the glacial front than further out in the glacial bay and in the central basin. The opposite was true

10.3389/fmars.2023.1161912

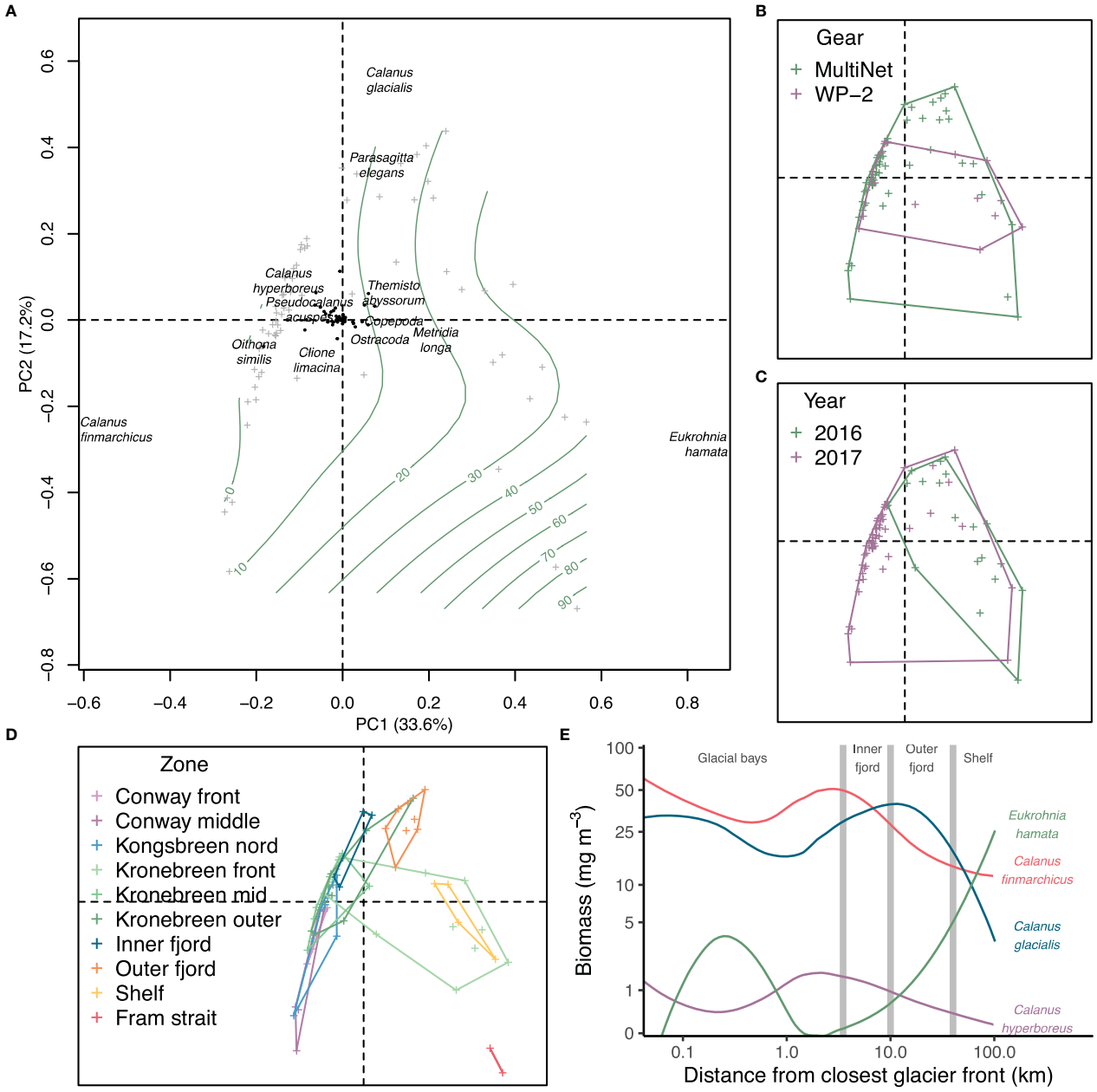


FIGURE 5
Principal component analysis of Hellinger transformed zooplankton biomass in Kongsfjorden. **(A)** Main species contributing to variation in biomass. Grey crosses indicate stations and green contour lines distance from the closest glacier front. Envelopes for **(B)** gear, **(C)** year and **(D)** zone in the fjord. Colours refer to the variable. **(E)** LOESS averages of biomass of most contributing species in **(A)** related to distance from the closest glacier front. Grey lines give approximate locations in Kongsfjorden. Both axes are logarithmic.

for 2017, when there were higher abundances inside the plume close to the glacial front, particularly for *Calanus finmarchicus*, *C. glacialis*, *Metridia longa* and *Pseudocalanus* spp. The abundance was higher outside of Kronebreen/Kongsvegen and lower outside Conwaybreen/Kongsbreen in 2017. Close to the surface, based on the surface net tow performed close to the glacial front of Kongsbreen, the zooplankton abundance was, nonetheless, not higher than the average for the water column within the plume (Table 2A). It also needs to be remembered that the mean abundance values (ind. $m^{-3}$) for the glacial bay stations are based on sampling within shallower depths (40-60 m) than for the mid-fjord stations (upper 200 m). Abundances expressed as ind. $m^{-2}$ (Circle plots in Supplementary Figures S1–S3; Supplementary Tables S1, S2) show that some dilution effects are apparent for the deeper samples. Biomass values (mg $m^{-3}$) tend upgrade large organisms such as *Calanus* spp., chaetognaths and other large zooplankton, and downplay smaller forms, such as cyclopoid and harpacticoid copepods, and meroplankton (Supplementary Tables S3, S4).

Neutral Red staining, applied to samples in 2016, showed that most zooplankton were alive both inside and outside the plume

TABLE 2A Zooplankton abundance (ind. $m^{-3}$) in the inner central basin and glacial bay near Kronebreen, early August 2016.

| Area (2016) | | Central | | | Kronebreen-outer | Kronebreen-front | | |
|---|---|---|---|---|---|---|---|---|
| Replicates | | n=2 | | | n=1 | n=8 | | |
| Depth (m) | | 50-0 | | | 60-0 | 48-0 | | |
| | | (ind. $m^{-3}$) | | | (ind. $m^{-3}$) | (ind. $m^{-3}$) | | |
| | | mean | | SD | | mean | | SD |
| Copepoda | | | | | | | | |
| Calanoida | *Calanus finmarchicus* | 465.75 | ± | 21.50 | 697.00 | 257.50 | ± | 151.52 |
| | *Calanus glacialis* | 159.68 | ± | 101.99 | 143.16 | 148.22 | ± | 117.59 |
| | *Calanus hyperboreus* | 2.45 | ± | 0.75 | 5.40 | | | |
| | *Metridia longa* | 3.63 | ± | 3.01 | 25.05 | 132.56 | ± | 119.81 |
| | *Microcalanus* spp. | 44.97 | ± | 5.54 | 116.09 | 44.02 | ± | 48.33 |
| | *Pseudocalanus* spp. | 315.04 | ± | 23.70 | 564.35 | 185.41 | ± | 92.35 |
| | *Paraeuchaeta* spp. | | | | 0.99 | | | |
| | Other Calanoida | 8.27 | ± | 0.67 | 30.54 | 0.89 | ± | 1.34 |
| Cyclopoida | *Oithona similis* | 652.51 | ± | 115.73 | 1441.26 | 400.78 | ± | 407.44 |
| | *Triconia borealis* | 10.83 | ± | 2.93 | 43.72 | 7.59 | ± | 16.27 |
| | Other Cyclopoida | 2.25 | ± | 0.22 | 6.30 | | | |
| Harpacticoida | Harpacticoida | 1.96 | ± | 0.27 | 1.67 | | | |
| | Copepoda nauplii | 63.45 | ± | 8.14 | 260.91 | | | |
| Malacostraca | | | | | | | | |
| Amphipoda | *Themisto abyssorum* | 4.10 | ± | 4.60 | 6.44 | 5.77 | ± | 5.86 |
| | *Themisto libellula* | 0.26 | ± | 0.37 | 0.91 | 0.22 | ± | 0.53 |
| Decapoda | *Pandalus borealis* | 0.03 | ± | 0.04 | | 0.00 | ± | 0.01 |
| Euphausiacea | *Thysanoessa* spp. | 0.75 | ± | 0.20 | 1.75 | 0.69 | ± | 0.56 |
| Isopoda | Bopyridae | 1.52 | ± | 0.56 | 2.33 | | | |
| | Isopoda | 0.59 | ± | 0.83 | | | | |
| Other phyla/classes | | | | | | | | |
| Appendicularia | *Fritillaria borealis* | 1.52 | ± | 1.70 | 35.92 | | | |
| | *Oikopleura* spp. | 1.55 | ± | 2.19 | 29.23 | | | |
| Bivalvia | Bivalvia larvae | 563.41 | ± | 228.47 | 1658.89 | 3.20 | ± | 6.80 |
| Bryozoa | Bryozoa larvae | | | | 2.06 | | | |
| Chaetognatha | *Parasagitta elegans* | 4.56 | ± | 0.32 | 10.72 | | | |
| | *Eukrohnia hamata* | 0.69 | ± | 0.08 | 5.53 | 18.93 | ± | 18.49 |
| Ctenophora | *Mertensia ovum* | 0.04 | ± | 0.06 | 0.31 | | | |
| | *Beroe cucumis* | | | | | | | |
| Cirripedia | Cirripedia nauplii | 2.15 | ± | 0.80 | 1.67 | | | |
| Echinodermata | Echinodermata larvae | 21.15 | ± | 6.59 | 128.77 | | | |
| Gastropoda | *Limacina helicina* | 430.61 | ± | 175.72 | 2277.20 | | | |
| Hydrozoa | Hydrozoa larvae | | | | 0.66 | | | |

*(Continued)*

10.3389/fmars.2023.1161912

TABLE 2A Continued

| Area (2016) | | Central | | | Kronebreen-outer | Kronebreen-front | | |
|---|---|---|---|---|---|---|---|---|
| Replicates | | n=2 | | | n=1 | n=8 | | |
| Depth (m) | | 50-0 | | | 60-0 | 48-0 | | |
| | | (ind. $m^{-3}$) | | | (ind. $m^{-3}$) | (ind. $m^{-3}$) | | |
| | | mean | | SD | | mean | | SD |
| | *Aglantha digitale* | | | | 0.69 | | | |
| Ostracoda | Ostracoda indet. | 0.51 | ± | 0.19 | 0.99 | 3.13 | ± | 8.84 |
| Polychaeta | Polychaeta larvae | 0.53 | ± | 0.31 | 5.35 | | | |

Lacking data of Copepoda nauplii from Kronebreen front in 2016 are due to taxonomic reporting.

(Figure 6). Only a small percentage (< 5%) of dead zooplankton was recorded inside the plume, and none outside. WP-2 catches consisted mainly of *Calanus* copepods. *Calanus glacialis* comprised the bulk of biomass both in WP-2 and WP-3 nets, seconded by *C. finmarchicus* and *M. longa*. Of other zooplankton, chaetognaths and *Themisto* spp. contributed with largest biomasses in both nets.

The composition of dead zooplankton was dominated by *Calanus* copepods and chaetognaths, whereas amphipods *Themisto* spp. and *Onisimus litoralis*, krill *Thysanoessa* spp., and shrimp *Pandalus borealis* were less affected (Figure 7). Of copepods, *Calanus finmarchicus* was more abundant than *C. glacialis* in the dead zooplankton fraction. Dead zooplankton concentrations were up to 6 mg DM $m^{-3}$ in front of Kronebreen, but typically outside the centre of the plume, which had the lowest salinity (Figures 8A, B). The salinity in the upper meter was brackish, but never<30 in the upper meter (Figure 8B). In surface samples taken with a bucket in 2017, the salinity varied between 22.0 and 30.3.

Three probable distinct isotopic niches were identified using our Bayesian inference approach. We classified these as the glacial bay, mid-fjord and shelf isotopic niche communities (Figure 9). The glacial bay community showed the widest isotopic niche suggesting a wider source of primary carbon sources to zooplankton compared to the other niches and a different scenopoetic environment. The composition of zooplankton and fish in our samples were also different (Supplementary Table S5).

Benthic scavengers, *Onisimus caricus* and *Anonyx nugax*, caught in baited traps were present and relatively abundant at and near the brown plume with daily catches of 10 animals per trap (Figure 10). However, the highest abundance was further out in the glacial bay, with up to 50 animals per trap per day, with 75% share of *Anonyx* spp. and 25% or less *O. caricus*.

## Discussion

We found that zooplankton mortality in the "death trap", indicated by Weslawski and Legezynska (1998), was not high as measured by neutral red staining of dead zooplankton. Thus, the studied glacial run offs did not appear to induce high zooplankton mortality, at least based on our snapshot-observations. Zooplankton is supposedly killed or stunned by osmotic shock, but our transect towards the glacier did not indicate very low salinity levels at the surface, certainly not at the brackish levels (salinity 9) used in experiments by Zajaczkowski and Legezynska (2001). The surface water salinity we observed in the glacial bay in front of Kronebreen was 30-33 in the upper 5 m, which is similar to seal-collected CTD data from the terminus of Kronebreen (Everett et al., 2018). Thus, the salinity near the surface in the inner glacial bay was not close to that causing zooplankton mortality in low-salinity experiments (Zajaczkowski and Legezynska, 2001), and the duration of exposure to fresher water deeper in the plume was likely short. The study by Everett et al. (2018) suggests continued mixing of glacial discharge water with ocean water between 40 and 0 m, which brings the water at the surface back to near-marine salinity conditions. The mixing during summer with dispersion of salinity is further elaborated by Torsvik et al. (2019). The prevailing down-fjord katabatic winds enhance this vertical mixing of the glacier discharge and fjord waters near the glacier front and contribute to the outflow of fresher surface water along the northern shore.

Seasonally, the mortality of zooplankton is much greater during the winter than in summer, when our study was conducted. Even if non-consumptive mortality in zooplankton is rarely reported, a few studies have detected high percentages of dead zooplankton in samples from the winter season. Daase et al. (2014) caught zooplankton in the southern Nansen Basin north of Svalbard in January 2012, of which 94% were dead. A wider study with seasonal sampling at several locations in Svalbard, found 11-35% dead copepods during winter, and 2-12% during spring and summer (Daase and Søreide, 2021). The spring/summer estimates are comparable to the 0-6% found in this study. *Calanus* spp. contributed most to this mortality, particularly during winter. Mortality was also observed in smaller copepods, such as *Pseudocalanus* spp., *Microcalanus* spp. and *Oithona similis*, whereas other zooplankton contributed little. Daase and Søreide (2021) did not sample close to glacier fronts and could not link mortality to osmotic shock. They rather suggested that insufficient energy stores to sustain activities throughout winter contributed mostly to the non-consumptive mortality.

TABLE 2B Zooplankton abundance (ind. $m^{-3}$) in the inner central basin and glacial bays, late July 2017.

| Area (2017) | | Central | | | Kronebreen-outer | | | Kronebreen-mid | | | Kronebreen-front | | | Kongsbreen North | | | Conway-middle | | | Conway-front | | | Kronebreen (surface) | | |
|---|---|---|---|---|---|---|---|---|---|---|---|---|---|---|---|---|---|---|---|---|---|---|---|---|---|
| Replicates | | n= 2 | | | n=8 | | | n=14 | | | n=4 | | | n=8 | | | n=5 | | | n=3 | | | n=4 | | |
| Depth (m) | | 45-0 | | | 45-0 | | | 57-0 | | | 52-0 | | | 95-0 | | | 34-0 | | | 43-0 | | | 1-0 | | |
| | | (ind. $m^{-3}$) | | | (ind. $m^{-3}$) | | | (ind. $m^{-3}$) | | | (ind. $m^{-3}$) | | | (ind. $m^{-3}$) | | | (ind. $m^{-3}$) | | | (ind. $m^{-3}$) | | | (ind. $m^{-3}$) | | |
| | | mean | | SD | mean | | SD | mean | | SD | mean | | SD | mean | | SD | mean | | SD | mean | | SD | mean | | SD |
| **Copepoda** | | | | | | | | | | | | | | | | | | | | | | | | | |
| Calanoida | *Calanus finmarchicus* | 247.72 | ± | 63.13 | 952.81 | ± | 361.75 | 935.94 | ± | 284.68 | 1211.78 | ± | 403.22 | 351.13 | ± | 206.11 | 590.89 | ± | 120.35 | 988.72 | ± | 477.68 | 166.3 | ± | 120.8 |
| | *Calanus glacialis* | 25.95 | ± | 4.01 | 67.66 | ± | 38.32 | 61.13 | ± | 34.46 | 112.07 | ± | 43.41 | 39.58 | ± | 21.56 | 27.47 | ± | 24.68 | 93.58 | ± | 66.43 | 5.9 | ± | 6.9 |
| | *Calanus hyperboreus* | 2.30 | ± | 0.24 | 6.70 | ± | 3.50 | 8.78 | ± | 8.58 | 5.55 | ± | 3.27 | 2.56 | ± | 1.66 | 4.70 | ± | 5.27 | 2.03 | ± | 1.49 | 1.0 | ± | 1.2 |
| | *Metridia longa* | 1.26 | ± | 1.31 | 4.42 | ± | 5.34 | 4.69 | ± | 2.79 | 6.56 | ± | 2.85 | 1.09 | ± | 0.85 | 1.32 | ± | 0.70 | 2.21 | ± | 1.46 | 1.1 | ± | 1.2 |
| | *Microcalanus* spp. | 18.29 | ± | 1.31 | 19.57 | ± | 9.79 | 23.26 | ± | 19.17 | 42.94 | ± | 13.79 | 29.45 | ± | 26.68 | 17.70 | ± | 13.60 | 17.38 | ± | 11.46 | 0.8 | ± | 1.4 |
| | *Pseudocalanus acuspes* | 11.28 | ± | 0.29 | 25.25 | ± | 14.83 | 35.44 | ± | 14.69 | 71.15 | ± | 57.41 | 12.15 | ± | 6.24 | 13.42 | ± | 8.01 | 15.77 | ± | 4.97 | | | |
| | *Pseudocalanus minutus* | 13.39 | ± | 2.70 | 6.41 | ± | 3.57 | 11.62 | ± | 21.75 | 74.24 | ± | 59.51 | 14.47 | ± | 7.27 | 15.22 | ± | 6.14 | 18.30 | ± | 6.22 | | | |
| | *Pseudocalanus* spp. | 141.20 | ± | 59.51 | 404.27 | ± | 144.53 | 476.91 | ± | 190.37 | 805.24 | ± | 511.99 | 145.00 | ± | 155.70 | 178.45 | ± | 81.86 | 210.14 | ± | 117.00 | 71.7 | ± | 53.4 |
| | Other Calanoida | 0.00 | ± | 0.00 | 5.43 | ± | 0.93 | 6.63 | ± | 1.04 | 4.48 | ± | 0.57 | 8.06 | ± | 0.79 | 20.85 | ± | 3.72 | 11.28 | ± | 1.27 | 0.5 | ± | 0.4 |
| Cyclopoida | *Oithona similis* | 3159.45 | ± | 1037.60 | 5937.70 | ± | 2110.46 | 4218.03 | ± | 1928.65 | 4489.79 | ± | 2039.91 | 3122.48 | ± | 3666.88 | 2830.42 | ± | 900.27 | 1465.92 | ± | 906.51 | 110.4 | ± | 115.9 |
| | *Triconia borealis* | 15.50 | ± | 3.87 | 64.24 | ± | 21.68 | 76.82 | ± | 50.66 | 98.37 | ± | 31.29 | 20.68 | ± | 11.75 | 21.83 | ± | 11.22 | 8.54 | ± | 10.06 | 1.3 | ± | 1.5 |
| | Other Cyclopoida | 8.05 | ± | 1.07 | 27.86 | ± | 4.73 | 353.29 | ± | 427.20 | 8.74 | ± | 2.39 | 11.62 | ± | 5.23 | 7.88 | ± | 2.26 | 7.59 | ± | 1.81 | 2.7 | ± | 2.4 |
| Harpacticoida | Harpacticoida | 1.01 | ± | 0.57 | 2.50 | ± | 1.18 | 4.55 | ± | 4.17 | 4.55 | ± | 2.33 | 4.26 | ± | 4.16 | 7.12 | ± | 2.68 | 7.91 | ± | 3.02 | | | |
| | Copepoda nauplii | 11.35 | ± | 12.16 | 59.47 | ± | 41.86 | 73.47 | ± | 47.90 | 64.95 | ± | 17.68 | 16.99 | ± | 19.52 | 52.46 | ± | 43.31 | 18.67 | ± | 14.62 | 0.3 | ± | 0.5 |
| **Malacostraca** | | | | | | | | | | | | | | | | | | | | | | | | | |
| Amphipoda | *Themisto abyssorum* | 3.86 | ± | 4.93 | 1.20 | ± | 0.98 | 1.11 | ± | 0.46 | 2.19 | ± | 0.48 | 0.43 | ± | 0.25 | 0.64 | ± | 0.41 | 0.06 | ± | 0.05 | 0.4 | ± | 0.4 |
| | *Themisto libellula* | 0.85 | ± | 1.20 | 0.70 | ± | 0.42 | 0.61 | ± | 0.33 | 1.46 | ± | 0.98 | 0.05 | ± | 0.10 | 0.28 | ± | 0.00 | 0.09 | ± | 0.09 | 0.01 | ± | 0.0 |
| | Amphipoda indet. | | | | | | | 0.13 | ± | 0.41 | 0.02 | ± | 0.04 | | | | | | | | | | | | |
| Decapoda | *Hyas* & *Pagurus* larvae | 0.32 | ± | 0.17 | 0.35 | ± | 0.17 | 0.28 | ± | 0.12 | 0.86 | ± | 0.11 | 0.21 | ± | 0.06 | 0.27 | ± | 0.06 | 0.09 | ± | 0.08 | 0.05 | ± | 0.1 |
| | *Pandalus borealis* | | | | 0.01 | ± | 0.02 | 0.09 | ± | 0.11 | 0.16 | ± | 0.25 | 0.04 | ± | 0.03 | 0.02 | ± | 0.03 | | | | 0.01 | ± | 0.01 |
| Euphausiacea | *Thysanoessa* spp. | 1.25 | ± | 0.32 | 3.04 | ± | 0.74 | 1.09 | ± | 0.15 | 3.56 | ± | 1.15 | 0.32 | ± | 0.10 | 0.94 | ± | 0.13 | 2.31 | ± | 0.76 | 0.02 | ± | 0.0 |
| Isopoda | Bopyridae indet. | 0.53 | ± | 0.05 | 1.44 | ± | 1.03 | 1.35 | ± | 1.22 | 1.00 | ± | 0.53 | 0.92 | ± | 0.74 | 0.90 | ± | 0.84 | 0.63 | ± | 0.54 | 0.3 | ± | 0.5 |
| | Isopoda indet. | 0.42 | ± | 0.60 | | | | 0.29 | ± | 0.45 | 0.00 | ± | 0.00 | 0.34 | ± | 0.37 | 0.15 | ± | 0.21 | | | | | | |

*(Continued)*





10.3389/fmars.2023.1161912

TABLE 2B Continued

| Area (2017) | | Central | | | Kronebreen-outer | | | Kronebreen-mid | | | Kronebreen-front | | | Kongsbreen North | | | Conway-middle | | | Conway-front | | | Kronebreen (surface) | | |
|---|---|---|---|---|---|---|---|---|---|---|---|---|---|---|---|---|---|---|---|---|---|---|---|---|---|
| Replicates | | n= 2 | | | n=8 | | | n=14 | | | n=4 | | | n=8 | | | n=5 | | | n=3 | | | n=4 | | |
| Depth (m) | | 45-0 | | | 45-0 | | | 57-0 | | | 52-0 | | | 95-0 | | | 34-0 | | | 43-0 | | | 1-0 | | |
| | | (ind. $m^{-3}$) | | | (ind. $m^{-3}$) | | | (ind. $m^{-3}$) | | | (ind. $m^{-3}$) | | | (ind. $m^{-3}$) | | | (ind. $m^{-3}$) | | | (ind. $m^{-3}$) | | | (ind. $m^{-3}$) | | |
| | | mean | | SD | mean | | SD | mean | | SD | mean | | SD | mean | | SD | mean | | SD | mean | | SD | mean | | SD |
| **Other phyla/classes** | | | | | | | | | | | | | | | | | | | | | | | | | |
| Appendicularia | *Fritillaria borealis* | 0.92 | ± | 0.37 | 9.29 | ± | 9.75 | 7.10 | ± | 6.72 | 1.13 | ± | 2.26 | 5.06 | ± | 10.84 | 3.12 | ± | 2.37 | 0.63 | ± | 0.55 | | | |
| | *Oikopleura* spp. | 0.66 | ± | 0.93 | 19.58 | ± | 17.35 | 5.40 | ± | 5.38 | 2.05 | ± | 2.42 | 5.12 | ± | 3.97 | 7.17 | ± | 5.80 | 1.90 | ± | 3.29 | 0.1 | ± | 0.2 |
| Bivalvia | Bivalvia larvae | 41.52 | ± | 37.75 | 79.69 | ± | 70.70 | 54.43 | ± | 33.96 | 37.18 | ± | 35.34 | 252.99 | ± | 437.62 | 555.56 | ± | 413.47 | 536.73 | ± | 388.44 | 0.7 | ± | 0.9 |
| Bryozoa | Bryozoa larvae | | | | | | | 0.09 | ± | 0.24 | 0.87 | ± | 1.74 | 0.68 | ± | 1.21 | 1.36 | ± | 2.35 | | | | | | |
| Chaetognatha | *Parasagitta elegans* | 11.66 | ± | 10.39 | 7.42 | ± | 2.81 | 9.62 | ± | 4.18 | 6.46 | ± | 4.14 | 1.17 | ± | 1.02 | 1.30 | ± | 1.13 | 4.54 | ± | 2.93 | 1.2 | ± | 0.7 |
| | *Eukrohnia hamata* | 0.09 | ± | 0.13 | 1.53 | ± | 2.68 | 0.16 | ± | 0.33 | | | | 0.005 | ± | 0.01 | | | | | | | | | |
| Ctenophora | *Mertensia ovum* | 0.05 | ± | 0.07 | 0.10 | ± | 0.11 | 0.23 | ± | 0.18 | 0.39 | ± | 0.22 | 0.01 | ± | 0.02 | | | | | | | 0.02 | ± | 0.02 |
| | *Beroe cucumis* | | | | 0.05 | ± | 0.11 | 0.21 | ± | 0.50 | 0.03 | ± | 0.06 | 0.06 | ± | 0.07 | 0.03 | ± | 0.05 | | | | | | |
| Cirripedia | Cirripedia nauplii | 0.28 | ± | 0.40 | 0.29 | ± | 0.78 | 1.19 | ± | 1.63 | 1.37 | ± | 2.75 | 1.07 | ± | 0.79 | 0.48 | ± | 0.68 | | | | 0.1 | ± | 0.2 |
| Echinodermata | Echinodermata larvae | 42.52 | ± | 33.96 | 245.24 | ± | 107.64 | 615.21 | ± | 675.56 | 967.45 | ± | 156.90 | 11.80 | ± | 7.28 | 7.36 | ± | 5.59 | 0.32 | ± | 0.55 | 21.8 | ± | 28.0 |
| Gastropoda | *Clione limacina* | | | | 12.13 | ± | 29.42 | 0.61 | ± | 0.90 | 1.82 | ± | 2.75 | 0.67 | ± | 0.36 | 1.76 | ± | 2.01 | 0.95 | ± | 1.65 | 0.1 | ± | 0.1 |
| | Gastropoda indet. | 0.08 | ± | 0.12 | 0.66 | ± | 1.15 | 6.55 | ± | 16.02 | | | | | | | | | | | | | | | |
| | *Limacina helicina* | 24.62 | ± | 13.98 | 148.99 | ± | 61.39 | 259.23 | ± | 429.72 | 103.24 | ± | 105.42 | 21.56 | ± | 12.14 | 50.08 | ± | 31.82 | 31.27 | ± | 14.95 | 4.8 | ± | 6.7 |
| Hydrozoa | Hydrozoa indet. | | | | 0.00 | ± | 0.00 | 0.32 | ± | 0.73 | | | | | | | | | | | | | | | |
| | *Aglantha digitale* | 0.04 | ± | 0.05 | 0.13 | ± | 0.34 | 0.04 | ± | 0.15 | | | | 0.02 | ± | 0.03 | 0.62 | ± | 0.52 | 0.03 | ± | 0.05 | 0.01 | ± | 0.01 |
| Ostracoda | Ostracoda indet. | | | | 0.07 | ± | 0.19 | 0.11 | ± | 0.28 | 0.13 | ± | 0.25 | 0.40 | ± | 0.86 | | | | | | | 0.1 | ± | 0.1 |
| Polychaeta | Polychaeta larvae | 0.91 | ± | 1.29 | 1.50 | ± | 2.06 | 48.62 | ± | 170.71 | 2.50 | ± | 4.62 | 0.95 | ± | 0.64 | 10.67 | ± | 15.49 | 0.63 | ± | 0.55 | 0.1 | ± | 0.2 |

Zooplankton abundance (ind. $m^{-3}$) by taxa taken at the central part of the inner fjord basin (stations Kb6, Kb7), outer parts of the glacial bays at the transects across the bays (4 km from the glacial front of Kronebreen, 2 km from the glacial front of Conwaybreen), middle glacial bays (i.e. areas between outer transects and glacial fronts), and glacial fronts at the immediate vicinity (< 100 m) of the glacial front. Sampling was done with Multi Plankton Sampler (MPS), WP-2 net, and Surface net. Glaciers are Kronebreen, Kongsbreen North, and Conwaybreen.





10.3389/fmars.2023.1161912

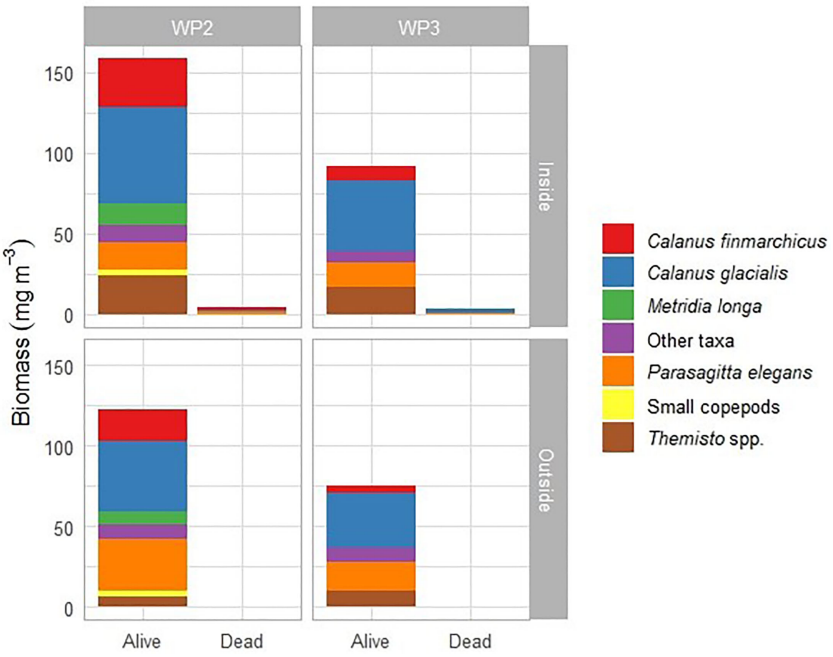


FIGURE 6
Biomass of alive and dead zooplankton sampled inside and outside the glacial plume from helicopter in July 2016 with WP-2 and WP-3 net.

Abundance and biomass of zooplankton generally increased in the inner fjord basin compared to most transect stations in middle and outer fjord. This particularly applied to Arctic species, such as *Calanus glacialis* and *Limacina helicina*, but also older life stages of Atlantic species, which showed high biomass in the basin and glacial bay. This is in line with previous work by Kwasniewski et al. (2003), who related the abundance and biomass to stage development of *Calanus* spp. and fjord circulation patterns. Some of the zooplankton species, such as *C. finmarchicus* and *Limacina helicina*, showed large variations between years, which may be reflected in their 2-year life cycles (Kwasniewski et al., 2003; Gannefors et al., 2005) or related to annual differences in water-mass advection to Kongsfjorden (Tverberg et al., 2019).

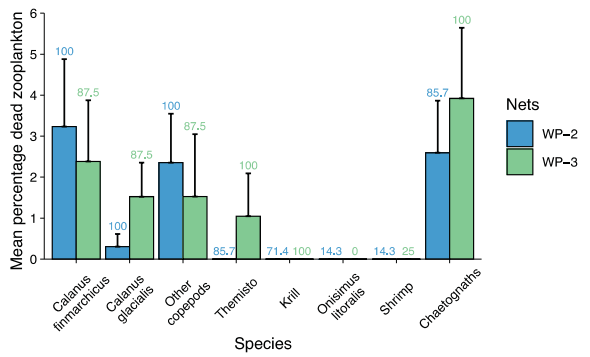


FIGURE 7
Composition of dead zooplankton as mean percentage (+SE). Numbers above bars are frequency of occurrence of a given group in all helicopter samples from early August 2016.

We suggest that advection is the dominant process for the observed pattern in zooplankton distribution. The sampling in 2016 and 2017 indicates similar spatial variations in zooplankton distribution, within the circulation pattern and upwelling of "deep" waters with high zooplankton abundance of older stages between the 20 m deep sill before the inner fjord basin and the 50 m deep sill before the glacial front. The largest zooplankton concentrations of *C. finmarchicus* in 2016 were recorded 1-3 km away from the glacial front, in the inner fjord basin (at Kb5), whereas in 2017 this species was more evenly distributed in the glacial bay. *Calanus glacialis* showed the opposite pattern in 2017 and was most concentrated close to the glacial front and in the bay near the glacier, but with lower concentrations in the inner fjord basin. The annual hydrographic conditions in Kongsfjorden seemed rather similar for 2016 and 2017, both on an increasing trend of temperature (0.13°C y$^{-1}$; Feldner et al., 2022). Thus, the years of sampling were not extremely warm or cold with resulting influence on the composition of Atlantic vs. Arctic zooplankton.

The younger zooplankton stages are mostly associated with surface waters and may have originated on the shelf outside the fjord. They are advected in surface and subsurface waters into the fjord and subsequently into the inner fjord basin as they develop (Basedow et al., 2004; Willis et al., 2006). Thus, a combination of ontogenetic growth and advection result in increased abundances of older stages (CIV-CV) and adult females in the inner basin. The oldest copepodid stages (CV) of *C. glacialis* were mostly deep in the inner basin whereas *C. finmarchicus* stages were more evenly distributed in the water column (Basedow et al., 2004). The advection of *C. finmarchicus* is higher than *C. glacialis*, which may be more locally produced (Basedow et al., 2004). By descending the zooplankton prevent being transported out of the

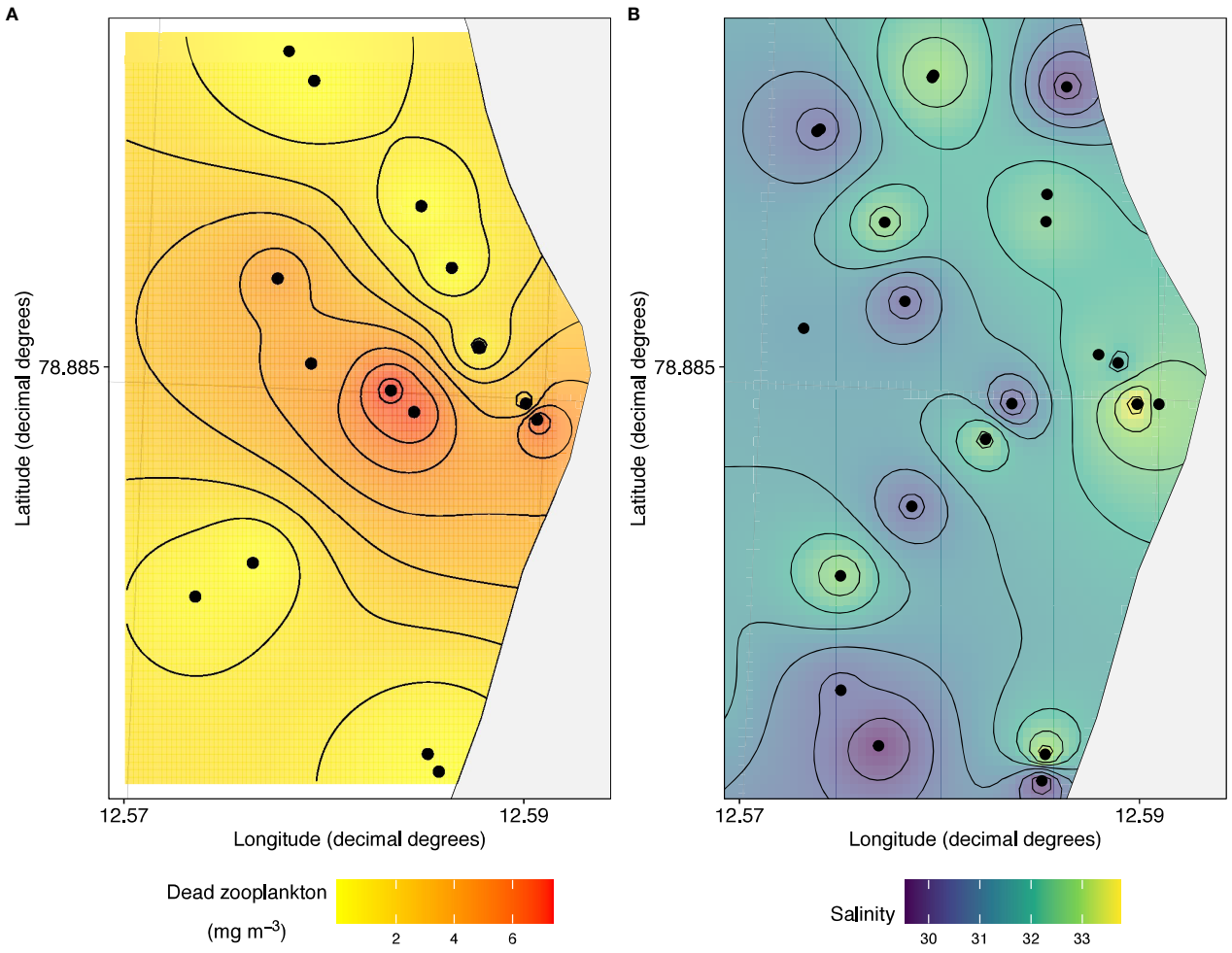


FIGURE 8
Interpolated distribution of **(A)** dead zooplankton (dry mass, mg $m^{-3}$), **(B)** salinity in the upper meter of the water column in front of Kronebreen, 1-3 August, 2016. The easternmost point marks the centre of the plume.

inner basin by the outgoing surface currents. Also, descending, especially in late summer by older, wintering life stages, may be a way to avoid increasing water temperature (Kosobokova, 1999; Kwasniewski et al., 2003). The entrance to the inner basin is mainly along the southern shore, whereas the exit is along the northern side of the glacial bay where subglacial discharges release freshwater and sediments in front of the tidewater glaciers (Halbach et al., 2019) and this flow continues further out into the fjord basin and the transitional zone of the main fjord (Hop et al., 2002).

The abundance and biomass of the zooplankton in the glacial bays may also be a consequence of the glacial run-off, which contributes nutrients to the inner glacial bays (Halbach et al., 2019). The seasonal run-off from glaciers, with associated nutrients, are expected to fuel the summer blooms of mixed communities, involving diatoms, the prymnesiophyte *Phaeocystis pouchetii* and particularly smaller flagellates (Piwosz et al., 2009; Calleja et al., 2017; Halbach et al., 2019; Assmy et al., 2023). Some studies have documented massive blooms near the glacier front, in the inner basin, prior to the main run-off season in spring (Calleja et al., 2017), whereas others have documented later blooms in the middle or outer fjord (Hegseth and Tverberg, 2013). Where and when blooms are occurring are important for feeding and development of zooplankton populations (Daase et al., 2013).

Our stable isotope analysis revealed that the glacial bay houses a separate and wider isotopic niche than communities outside the sill to the inner fjord basin. As the isotopic niche is defined by $\delta^{15}N$ and $\delta^{13}C$, this does imply different primary carbon and nitrogen sources for this zooplankton community (Santos-García et al., 2023). It is unknown to us at present if the community of zooplankton and fish represents a different trophic niche as isotopic niche is not necessarily correlated to the trophic niche (Jackson et al., 2011). More extensive sampling for stable isotopes than what was possible within the time frame of our study could help better interpreting such results. Thus, further work on the trophic structure of the glacial bays vs. the main parts of the fjord is required.

The physics of subglacial plumes with impact on fjord circulation is well established (e.g. Everett et al., 2018), and the entrainment of ambient water with subsequent transport of zooplankton to the surface is likely a direct consequence of these plumes. The glacial plumes in front of tidal glaciers are highly

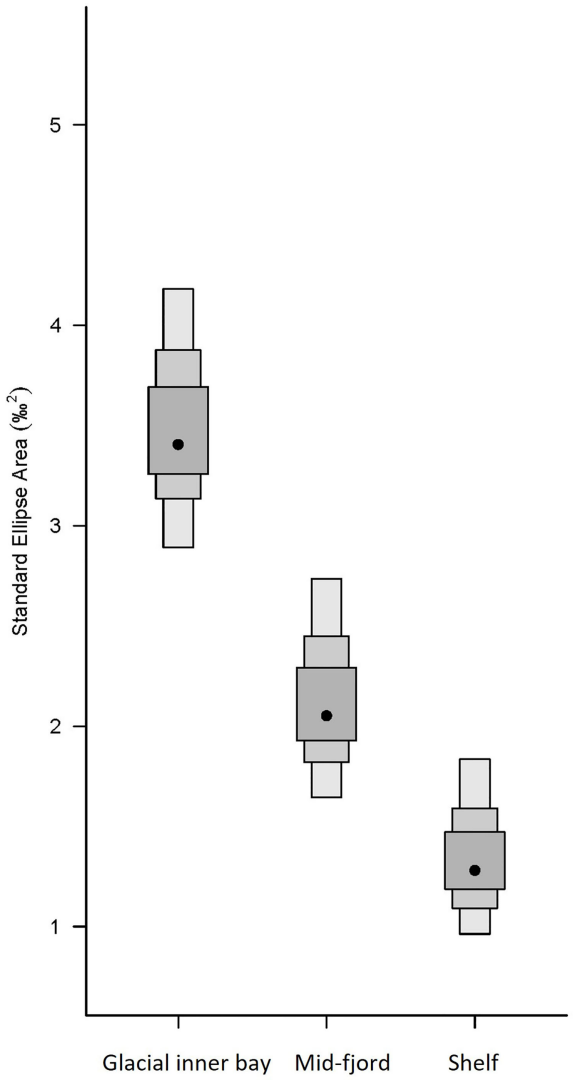


FIGURE 9
Isotopic niche width based on analyses with Bayesian inference. Shaded boxes represent the 25%, 75% and 95% confidence intervals (from dark to light grey) and black dots represent centre of mass of each community centroid. Isotope scatter plot of the raw data overlaid with ellipses the Bayesian Standard Eclipse Area for each community group (glacial bay, mid-fjord and shelf) is in Supplementary Figure S2.

buoyant, raising to the surface while entraining ambient water and its organisms (Cowton et al., 2015). This "elevator effect", combined with advection of later-stage zooplankton to the inner fjord basin, supports the potential increasing importance of the glacial plume and glacial bay as "climate refugia" for foraging seabirds. Some marine mammals, particularly ringed seals and white whales that forage close to glacial fronts, may also benefit from this effect (Lydersen et al., 2001; Everett et al., 2018). The direct evidence for this in our study was the higher biomass of zooplankton, particularly of *Calanus* spp. and *Themisto* spp., inside the plume near Kronebreen glacier in 2017.

With the "elevator effect" even a low mortality of zooplankton can become substantial when multiplied by daily entrainment rates during 100 days of melt season. The mortality rate can be estimated as follows:

$M = W * E * 0.05$, where M is the mortality rate in mg DM $d^{-1}$, W is the total zooplankton biomass concentration at the Kronebreen front in mg DM $m^{-3}$, E is the entrainment rate in $m^3$ $d^{-1}$ and 0.05 the measured fraction of dead zooplankton. We used a plume entrainment rate from late July 2017 of $33\times10^6$ $m^3$ $day^{-1}$ reported in Halbach et al. (2019).

Extrapolated over the 100-day melt season, this amounts to 21.3 tonnes of dead zooplankton DM or 12.8 tonnes of carbon based on conversion factors in Postel et al. (2000). Our estimate is similar to the 85 tonnes of dead zooplankton wet weight, equivalent to 10.2 tonnes carbon, estimated by Zajaczkowski and Legezynska (2001). Thus, the carbon input to the glacial bay in Kongsfjorden because of the seasonal "elevator effect" is likely substantial.

In addition, the glacial "elevator effect" brings the zooplankton to the surface in turbid waters, where they can be easily picked up by surface-feeding predators. Pelagic fishes are also present in the glacial plumes, since polar cod were caught in the plankton nets during helicopter sampling (Appendix Table S5). Predation of zooplankton by seabirds, particularly black-legged kittiwakes, northern fulmars and Arctic terns, can be substantial, and sometimes large aggregations of these seabirds are observed foraging in front of tidewater glaciers (Lydersen et al., 2014; Bertrand et al., 2021a). However, the availability of food in glacial bays is variable and dependent on the glacial outflow (Everett et al., 2018). There is not necessarily more food in the entire water body for the birds in the glacial bays, but it is periodically brought to the surface and thus readily available to large aggregations of surface-feeding birds foraging at the same time.

The surface-feeding seabirds prey on a variety of zooplankton as well as fish. In glacial bays with turbid water, they can only see prey that are brought to the surface and movements of live prey in murky water would presumably enhance foraging activity. Indeed, turbid waters can have a detrimental effect on surface feeding seabirds. An unusual bloom of the coccolithophore *Emiliania huxleyi* that turned waters into milky colour caused mass mortality in short-tailed shearwaters in Bering Strait in 1997 (Baduini et al., 2001). Black-legged kittiwakes often feed in flocks on organisms close to the water surface, where they feed on both invertebrates and fish (Vihtakari et al., 2018). Stomach samples may contain amphipods, euphausiids, polychaetes and polar cod or other pelagic fishes (Mehlum and Gabrielsen, 1993; Vihtakari et al., 2018). Northern fulmars also aggregate to feed on a variety of zooplankton, including amphipods, krill, copepods and pteropods, and also fish, squid and jellyfish (Hartley and Fisher, 1936; Camphuysen, 1993). They generally feed close to the surface, but can dive to a few metres to obtain fish they see from the surface (Hobson and Welch, 1992). Arctic terns are also surface feeders and often seen picking prey near glacial fronts. In Svalbard they feed on both crustaceans and fish, generally in shallow waters along the shore (Anker-Nilssen et al., 2000). Large aggregations of the black guillemot, which is a diving seabird, have also been observed in the inner glacial area of Kongsfjorden (Varpe and Gabrielsen, 2022). They mostly feed on fish, but amphipods and euphausiids can be an

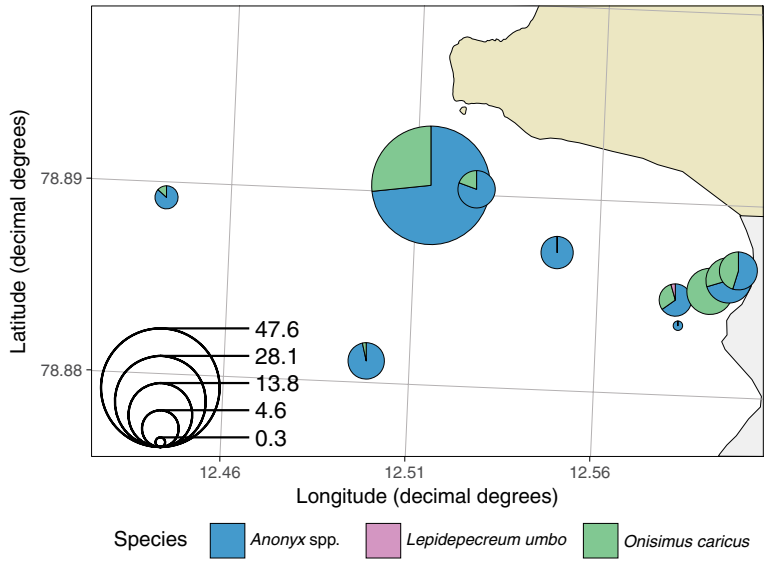


FIGURE 10
Amphipods caught in baited traps in the glacial bay in front of Kronebreen, 2017. Pie size indicates catch per unit of effort (CPUE as ind. per trap day), and the colours in pies indicate shares of different scavengers in the unit catch, their relative abundance.

important part of the diet in coastal areas (Mehlum and Gabrielsen, 1993).

If not preyed upon by seabirds and marine mammals, zooplankton and organic matter from seabird feeding activities, including prey damage, regurgitates, and faecal matter, will sink to the bottom, where they are utilized by benthic necrophagic amphipods and other soft-bottom fauna (Legeżyńska et al., 2000; Legeżyńska, 2001). This is supported by the relatively high abundances of the benthic scavenging amphipods *Onisimus caricus* and *Anonyx nugax* in the glacial bay. These amphipods likely represent a food source for diving seals, e.g. ringed seals (Labansen et al., 2007).

With "climate warming", we suggest that while the front of tidewater glaciers may not be a "biological hotspot", its importance lies in advection and "elevator effect" of prey to foraging seabirds, which sometimes may be very efficient. In that context, they do represent potentially important "climate refugia" for zooplankton-dependant food webs, especially with regard to surface feeders.

## Conclusions and outlook

In conclusion our study provided evidence that glacial plumes may be important as "climate refugia" for prey availability due to the continuous "elevator effect" of supplying near-surface zooplankton to foraging seabirds during the glacial meltwater season. Even though the zooplankton "death trap" by osmotic shock was rather inefficient, causing <5% direct mortality, the "elevator effect" during 100 days was substantial with 12.8 tonnes of zooplankton carbon, which was similar to the estimate by Zajaczkowski and Legezynska (2001). The zooplankton mortality associated with the rising plume, glacially-released stored carbon and seabird feeding activities also support a continuous flux of organic matter into the glacial bays, supporting benthic scavengers. The contradictory results between 2016 and 2017 with higher/lower values outside/inside the plume near the glacial front and lower abundances in surface tow net samples suggest that the "elevator" in the plume is highly variable in space and time. Our data did not have the spatial and temporal resolution to properly detect the highly stochastic bursts of subglacial discharges arising at the surface, even though we observed the surface expressions of these in plumes from the helicopter. Thus, future studies should aim for longer sampling campaigns to address the temporal variability in the glacial discharge and its associated zooplankton concentrations. Seabirds feed when there is food to eat, otherwise they fly to other "hotspots" for feeding in the fjord system or on the shelf. A key question that remains is whether the carbon flux in glacial plumes with the associated supply of zooplankton would be sufficient to maintain a "climate refugium" for foraging seabirds in the future. Tidewater glaciers are currently retreating because of climate warming and their enhanced mixing effect on the marine system becomes reduced once they become land-terminated with freshwater discharge only at the surface. This climate-related transition will potentially cause negative effects on the production and energy transfer within the marine food web of glacial fjords.

## Data availability statement

The original contributions presented in the study are included in the article/Supplementary Materials. Data are available at the Norwegian Polar Data Centre: Oceanography (CTD): Doi: 10.21334/npolar.2023.62247dad Mesozooplankton diversity: Doi: 10.21334/npolar.2023.cb059b78 Stable isotope of zooplankton and fish: Doi: 10.21334/npolar.2023.e8d95fe0 Amphipods: Doi: 10.21334/npolar.2023.852a5138. Further inquiries can be directed to the corresponding author.

## Author contributions

The project design and sampling campaigns were led by HS, HH, PA and MV. Sampling campaigns by ship and helicopter in Kongsfjorden were carried out by HH, AW, MV, PA, PK, GG, OP, PD and HS. Zooplankton analyses at IO PAN was managed by SK. Data processing and figures were performed by AW, MV, GG, and OP. HH led the writing with input from all co-authors, all of which approved the final version of the manuscript. All authors contributed to the article and approved the submitted version.

## Funding

This study was supported by the former Centre of Ice, Climate and Ecosystems (ICE) at the Norwegian Polar Institute and the Research Council of Norway (TIGRIF project #243808 and Boom or Bust project #244646).

## Acknowledgments

We thank assistants and crews of RV *Lance* and helicopter that contributed to this research. Analyses of zooplankton taxonomy were performed by personnel at the Institute of Oceanology (IO PAN), Sopot, Poland.

## Conflict of interest

The authors declare that the research was conducted in the absence of any commercial or financial relationships that could be construed as a potential conflict of interest.

## Publisher's note



## Supplementary material

The Supplementary Material for this article can be found online at: https://www.frontiersin.org/articles/10.3389/fmars.2023.1161912/full#supplementary-material

SUPPLEMENTARY FIGURE 1
Abundance and biomass (mean, ± SD) of zooplankton in the upper 200 m along transect from the shelf break (V6) to inner basin (Kb5) in 2016 (upper panel) and 2017 (lower panel). **(A)** *Calanus* spp., **(B)** Small copepods, **(C)** Other large copepods, **(D)** Meroplankton, **(E)** Other zooplankton taxa. Note different scales on y-axes for abundance (ind. $m^{-3}$) and biomass (mg $m^{-3}$). Circle plots show locations of samples with abundance as ind. $m^{-2}$. Values of abundance and biomass are in Tables 1A, B and Supplementary Tables.

SUPPLEMENTARY FIGURE 2
Abundance and biomass (mean, +SD) of zooplankton at stations sampled in the inner basin and glacial bay of Kongsfjorden, early August 2016. **(A)** *Calanus* spp., **(B)** Small copepods, **(C)** Other large copepods, **(D)** Meroplankton, **(E)** Other zooplankton. Note different scales on y-axes for abundance (ind. $m^{-3}$) and biomass (mg $m^{-3}$). Circle plots show locations of samples with abundance as ind. $m^{-2}$. Values of abundance and biomass are in Tables 2A, B and Supplementary Tables.

SUPPLEMENTARY FIGURE 3
Abundance and biomass (mean, +SD) of zooplankton at stations sampled in the inner basin and glacial bays of Kongsfjorden, late July 2017. **(A)** *Calanus* spp., **(B)** Small copepods, **(C)** Other large copepods, **(D)** Meroplankton, **(E)** Other zooplankton. Note different scales on y-axes for abundance (ind. $m^{-3}$) and biomass (mg $m^{-3}$). Circle plots show locations of samples with abundances as ind. $m^{-2}$. Values of abundance and biomass are in Table 2 and Supplementary Tables.

SUPPLEMENTARY FIGURE 4
Depth (m) from fjord basin to glacial bay and fronts of Kronebreen and Kongsvegen.

SUPPLEMENTARY FIGURE 5
Isotope scatter plot of the raw data overlaid with ellipses the Bayesian Standard Eclipse Area (SEA) for each community for each community group (glacial bay, mid-fjord and shelf). The SEAs encompass the posterior estimates using 95% of the data points. The inner eclipses represent the 95% confidence interval of the bivariate mean.

## References

Anker-Nilssen, T., Bakken, V., Strøm, H., Golovkin, A. N., Bianki, V. V., and Tatarinkova, I. P. (2000). *The status of marine birds breeding in the Barents Sea Region* (Tromsø: Norwegian Polar Institute). Report No. 113.

Assmy, P., Kvernvik, A. C., Hop, H., Hoppe, C. J. M., Chierici, M., David T, D., et al. (2023). Plankton dynamics in Kongsfjorden during two years of contrasting environmental conditions. *Prog. Oceanogr.* 213, 102996. doi: 10.1016/j.pocean.2023.102996

Baduini, C. L., Hyrenbach, K. D., Coyle, K. O., Pinchuk, A., Mendenhall, V., and Hunt, Jr. G.L. (2001). Mass mortality of short-tailed shearwaters in the south-eastern Bering Sea during summer 1997. *Fish. Oceanogr.* 10, 117–130. doi: 10.1046/j.1365-2419.2001.00156.x

Barber, D. G., Hop, H., Mundy, C. J., Else, B., Dmitrenko, I. A., Tremblay, J. -É., et al. (2015). Selected physical, biological and biogeochemical implications of a rapidly changing Arctic marginal ice zone. *Prog. Oceanogr.* 139, 122–150. doi: 10.1016/j.pocean.2015.09.003

Basedow, S. L., Eiane, K., Tverberg, V., and Spindler, M. (2004). Advection of zooplankton in an Arctic fjord (Kongsfjord, Svalbard). *Estuar. Coast. Shelf Sci.* 60, 113–124. doi: 10.1016/j.ecss.2003.12.004

Batschelet, E. (1981). *Circular statistics in biology* (London: Academic Press).

Bertrand, P., Bêty, J., Yoccoz, N. G., Fortin, M., Strøm, H., Steen, H., et al. (2021b). Fine–scale spatial segregation in a pelagic seabird driven by differential use of tidewater glacier fronts. *Sci. Rep.* 11, 222109. doi: 10.1038/s41598-021-01404-1

Bertrand, P., Strøm, H., Bêty, J., Steen, H., Kohler, J., Vihtakari, M., et al. (2021a). Feeding at the front line: interannual variation in the use of glacier fronts by foraging black-legged kittiwakes. *Mar. Ecol. Prog. Ser.* 677, 197–208. doi: 10.3354/meps13869

Calleja, M. L., Kerhervé, P., Bourgeois, S., Kędra, M., Leynaert, A., Devred, E., et al. (2017). Effects of increase glacier discharge on phytoplankton bloom dynamics and pelagic geochemistry in a high Arctic fjord. *Prog. Oceanogr.* 159, 195–210. doi: 10.1016/j.pocean.2017.07.005

Camphuysen, C. J. (1993). Birds and mammals in Svalbard 1985-91. *Sula* 7, 3–44.

Cottier, F., Tverberg, V., Inall, M., Svendsen, H., Nilsen, F., and Griffiths, C. (2005). Water mass modification in an Arctic fjord through cross-shelf exchange: the seasonal hydrography of Kongsfjorden, Svalbard. *J. Geophys. Res.* 110, C12005. doi: 10.11029/12004JC002757

Cowton, T., Slater, D., Sole, A., Goldberg, D., and Nienow, P. (2015). Modeling the impact of glacial runoff on fjord circulation and submarine melt rate using a new subgrid-scale parameterization for glacial plumes. *J. Geophys. Res. Oceans* 120, 796–812. doi: 10.1002/2014JC010324

Daase, M., Falk-Petersen, S., Varpe, Ø., Darnis, G., Søreide, J. E., Wold, A., et al. (2013). Timing of reproductive events in the marine copepod *Calanus glacialis*: a pan-Arctic perspective. *Can. J. Fish. Aquat. Sci.* 70, 871–884. doi: 10.1139/cjfas-2012-0401

Daase, M., and Søreide, J. E. (2021). Seasonal variability in non-consumptive mortality of Arctic zooplankton. *J. Plankton Res.* 43, 565–585. doi: 10.1093/plankt/fbab042

Daase, M., Varpe, Ø., and Falk-Petersen, S. (2014). Non-consumptive mortality in copepods: occurrence of *Calanus* spp. carcasses in the Arctic Ocean during winter. *J. Plankton Res.* 36, 129–144. doi: 10.1093/plankt/fbt079

Dallmann, W. K. (2015). *Geoscience atlas of Svalbard* (Tromsø: Norwegian Polar Institute). Report 148.

De Rovere, F., Langone, L., Schroeder, K., Miserocchi, S., Giglio, F., Aliani, S., et al. (2022). Water masses variability in inner Kongsfjorden (Svalbard) during 2010–2020, front. *Mar. Sci.* 9. doi: 10.3389/FMARS.2022.741075

Elliott, D. T., and Tang, K. W. (2009). Simple staining method for differentiating live and dead marine zooplankton in field samples. *Limnol. Oceanogr. Methods* 7, 585–594. doi: 10.4319/lom.2009.7.585

Everett, A., Kohler, J., Sundfjord, A., Kovacs, K. M., Torsvik, T., Pramanik, A., et al. (2018). Subglacial discharge plume behaviour revealed by CTD instrumented ringed seals. *Sci. Rep.* 8, 13467. doi: 10.1038/s41598-018-31875-8

Feldner, J., Hübner, C., Lihavainen, H., Neuber, R., and Zaborska, A. (2022). "SESS report 2021," in *The State of Environmental Science in Svalbard - and annual Report* (Svalbard Integrated Arctic Earth Observing System (SIOS) Longyearbyen).

Gannefors, C., Böer, M., Kattner, G., Graeve, M., Eiane, K., Gulliksen, B., et al. (2005). The Arctic sea butterfly *Limacina helicina*; lipids and life strategy. *Mar. Biol.* 147, 169–177. doi: 10.1007/s00227-004-1544-y

Geyman, E. C., van Pelt, W. J. J., Maloof, A. C., Aas, H. F., and Kohler, J. (2022). Historical glacier change on Svalbard predicts doubling of mass loss by 2100. *Nature* 601, 374–379. doi: 10.1038/s41586-021-04314-4

Hagen, J. O., Eiken, T., Kohler, J., and Melvold, K. (2005). Geometry changes on Svalbard glaciers: mass-balance or dynamic response? *Annal. Glaciol.* 42, 255–261. doi: 10.3189/172756405781812763

Halbach, L., Vihtakari, M., Duarte, P., Everett, A., Granskog, M. A., Hop, H., et al. (2019). Tidewater glaciers and bedrock characteristics control the phytoplankton growth environment in a fjord in the Arctic. *Front. Mar. Sci.* 6. doi: 10.3389/fmars.2019.00254

Hartley, C. H., and Fisher, J. (1936). The marine food of birds in an inland fjord region in West Spitsbergen. *J. Anim. Ecol.* 5, 370–389.

Hegseth, E. N., and Tverberg, V. (2013). Effect of Atlantic water inflow on timing of the phytoplankton spring bloom in a high Arctic fjord (Kongsfjorden, Svalbard). *J. Mar. Syst.* 113, 94–105. doi: 10.1016/j.jmarsys.2013.01.003

Hobson, K. A., and Welch, H. E. (1992). Determination of trophic relationships within a high Arctic marine food web using $\delta^{13}$C and $\delta^{15}$N.analysis. *Mar. Ecol. Prog. Ser.* 84, 9–18.

Hop, H., Falk-Petersen, S., Svendsen, H., Kwasniewski, S., Pavlov, V., Pavlova, O., et al. (2006). Physical and biological characteristics of the pelagic system across Fram Strait to Kongsfjorden. *Prog. Oceanogr.* 71, 182–231. doi: 10.1016/j.pocean.2006.09.007

Hop, H., Pearson, T., Hegseth, E. N., Kovacs, K. M., Wiencke, C., Kwasniewski, S., et al. (2002). The marine ecosystem of Kongsfjorden, Svalbard. *Polar Res.* 21, 167–208.

Hop, H., Wold, A., Vihtakari, M., Daase, M., Kwasniewski, S., Gluchowska, M., et al. (2019). "Zooplankton in Kongsfjorden, (1996–2016) in relation to climate change," in *The ecosystem of Kongsfjorden, Svalbard*. Eds. H. Hop and C. Wiencke, C. (Cham: Springer). *Adv. Polar Ecol.* 2, 229–300. doi: 10.1007/978-3-319-46425-1_7

Hopwood, M. J., Carroll, D., Browning, T. J., Meire, L., Mortensen, J., Krisch, S., and Achterberg, E. P. (2018). Non-linear response of summertime marine productivity to increased meltwater discharge around Greenland. *Nat. Commun.* 9, 3256. doi: 10.1038/s41467-018-05488-8

Hutchinson, G. E. (1978). *An introduction to population biology* (New Haven: Yale University Press).

Jackson, A. L., Inger, R., Parnell, A. C., and Bearhop, S. (2011). Comparing isotopic niche widths among and within communities: SIBER-stable isotope Bayesian ellipses in r. *J. Anim. Ecol.* 80, 595–602. doi: 10.1111/j.1365-2656.2011.01806.x

Kohler, J., James, T. D., Murray, T., Nuth, C., Brandt, O., Barrand, N. E., et al. (2007). Acceleration in thinning rate on western Svalbard glaciers. *Geophys. Res. Lett.* 34, L1850210. doi: 10.1029/2007GL030681

Kosobokova, K. N. (1999). The reproductive cycle and life history of the Arctic copepod *Calanus glacialis* in the White Sea. *Polar Biol.* 22, 254–263. doi: 10.1007/s003000050418

Kwasniewski, S., Hop, H., Falk-Petersen, S., and Pedersen, G. (2003). Distribution of *Calanus* species in Kongsfjorden, a glacial fjord in Svalbard. *J. Plankton Res.* 25, 1–20. doi: 10.1093/plankt/25.1.1

Kwasniewski, S., Walkusz, W., Cottier, F. R., and Leu, E. (2013). Mesozooplankton dynamics in relation to food availability during spring and early summer in a high latitude glaciated fjord (Kongsfjorden), with focus on *Calanus*. *J. Mar. Syst.* 111-112, 83–96. doi: 10.1016/j.jmarsys.2012.09.012

Labansen, A. L., Lydersen, C., Haug, T., and Kovacs, K. M. (2007). Spring diet of ringed seals (*Phoca hispida*) from northwestern Spitsbergen, Norway. *ICES J. Mar. Sci.* 64, 1246–1256. doi: 10.1093/icesjms/fsm090

Layman, C. A., Arrington, D. A., Montana, C. G., and Post, D. M. (2007). Can stable isotope ratios provide for community-wide measures of trophic structure? *Ecology* 88, 42–48. doi: 10.1890/0012-9658(2007)88

Legeżyńska, J. (2001). Distribution patterns and feeding strategies of lysianassoid amphipods in shallow waters of an Arctic fjord. *Polish Polar Res.* 22, 173–186.

Legeżyńska, J., Węsławski, J. M., and Presler, P. (2000). Benthic scavengers collected by baited traps in the high Arctic. *Polar Biol.* 23, 539–544. doi: 10.1007/s003000000118

Legendre, P., and Gallagher, E. D. (2001). Ecologically meaningful transformations for ordination of species data. *Oecologia* 129, 271–280. doi: 10.1007/s004420100716

Lydersen, C., Assmy, P., Falk-Petersen, S., Kohler, J., Kovacs, K. M., Reigstad, M., et al. (2014). The importance of tidewater glaciers for marine mammals and seabirds in Svalbard, Norway. *J. Mar. Syst.* 129, 452–471. doi: 10.1016/j.jmarsys.2013.09.006

Lydersen, C., Martin, A. R., Kovacs, K. M., and Gjertz, I. (2001). Summer and autumn movements of white whales *Delphinapterus leucas* in Svalbard, Norway. *Mar. Ecol. Prog. Ser.* 219, 265–274.

Mehlum, F., and Gabrielsen, G. W. (1993). The diet of high-arctic seabirds in coastal and ice-covered, pelagic areas near the Svalbard archipelago. *Polar Res.* 12, 1–20. doi: 10.1111/j.1751-8369.1993.tb00417.x

Meire, L., Mortensen, J., Meire, P., Juul-Pedersen, T., Sejr, M. K., Rysgaard, S., et al. (2017). Marine-terminating glaciers sustain high productivity in Greenland fjords. *Global Change Biol.* 23, 5344–5357. doi: 10.1111/gcb.13801

Meire, L., Mortensen, J., Rysgaard, S., Bendtsen, J., Boone, W., Meire, P., et al. (2016). Spring bloom dynamics in a subarctic fjord influenced by tidewater outlet glaciers (Godthåbsfjord, SW Greenland). *J. Geophys. Res. Biogeosci.* 121, 1581–1592. doi: 10.1002/2015JG003240

Newsome, S. D., Martınez del Rio, C., Bearhop, S., and Phillips, D. L. (2007). A niche for isotopic ecology. *Front. Ecol. Environ.* 5, 429–436. doi: 10.1890/060150.01

Nishizawa, B., Kanna, N., Ohashi, Y., Sakakibara, D., Asaji, I., Abe, Y., et al. (2020). Contrasting assemblages of seabirds in the subglacial meltwater plume and oceanic water of Bowdoin Fjord, northwestern Greenland. *ICES. J. Mar. Sci.* 77, 711–720. doi: 10.1093/icesjms/fsz213

Nygård, H., Vihtakari, M., and Berge, J. (2009). Life history of *Onisimus caricus* (Amphipoda: Lysianassoidea) in a high Arctic fjord. *Mar. Ecol. Prog. Ser.* 5, 63–74. doi: 10.3354/ab00142

Oksanen, J., Simpson, G. L., Blanchet, F. G., Kindt, R., Legendre, P., Minchin, P. R., et al. (2022) *Vegan: community ecology package*. Available at: https://CRAN.R-project.org/package=vegan.

Østby, T. I., Vikhamar Schuler, T., Hagen, J. O., Hock, R., Kohler, J., and Reijmer, C. H. (2017). Diagnosing the decline in climatic mass balance of glaciers in Svalbard over 1957-2014. *Cryosphere* 11, 191–215. doi: 10.5194/tc-11-191-2017

Pebesma, E. (2018). Simple features for r: standardized support for spatial vector data. *R J.* 10, 439. doi: 10.32614/RJ-2018-009

Piwosz, K., Walkusz, W., Hapter, R., Wieczorek, P., Hop, H., and Wiktor, J. (2009). Comparison of productivity and phytoplankton in a warm (Kongsfjorden) and a cold (Hornsund) Spitsbergen fjord in mid-summer 2002. *Polar Biol.* 32, 549–559. doi: 10.1007/s00300-008-0549-2

Postel, L., Fock, H., and Hagen, W. (2000). "Biomass and abundance," in *ICES zooplankton methodology manual*. Eds. R. Harris, P. Wiebe, J. Lens, H. R. Skjoldal and M. Huntley (San Diego: Academic Press), 83–192.

R Core Team. (2022). "R: a language and environment for statistical computing," in *Version 4.2* (Vienna, Austria: R Foundation for Statistical Computing). Available at: http://www.r-project.org.

Santos-García, M., Ganeshram, R. S., Tuerena, R. E., Debyser, M. C. F., Husum, K., Assmy, P., et al. (2023). Stable nitrogen isotopic studies reveal future impacts of climate change on nitrogen inputs and cycling in Arctic fjords: Kongsfjorden and Rijpfjorden (Svalbard). *Biogeosci.* 19, 5973–6002. doi: 10.5194/bg-19-5973-2022

Søreide, J. E., Hop, H., Carroll, M. L., Falk-Petersen, S., and Hegseth, E. N. (2006a). Seasonal food web structures and sympagic-pelagic coupling in the European Arctic revealed by stable isotopes and a two-source food web model. *Prog. Oceanogr.* 71, 59–87. doi: 10.1016/j.pocean.2006.06.001

Søreide, J. E., Tamelander, T., Hop, H., Hobson, K. A., and Johansen, I. (2006b). Sample preparation effects on stable C and N isotope values: a comparison of methods in Arctic marine food web studies. *Mar. Ecol. Prog. Ser.* 328, 17–28.

Stempniewicz, L., Goc, M., Gluchowska, M., Kidawa, D., and Weslawski, J. M. (2021). Abundance, habitat use and food consumption of seabirds in the high–Arctic fjord ecosystem. *Polar Biol.* 44, 739–750. doi: 10.1007/s00300-021-02833-4

Stempniewicz, L., Goc, M., Kidawa, D., Urbanski, J., Hadwiczak, M., and Zwolicki, A. (2017). Marine birds and mammals foraging in the rapidly deglaciating Arctic fjord - numbers, distribution and habitat preferences. *Clim. Change* 140, 533–548. doi: 10.1007/s10584-016-1853-4

Sund, M., Eiken, T., and Rolstad Denby, C. (2011). Velocity structure, front position changes and calving of the tidewater glacier Kronebreen, Svalbard. *Cryosph. Disc.* 5, 41–73. doi: 10.5194/tcd-5-41-2011

Svendsen, H., Beszczynska-Møller, A., Hagen, J. O., Lefauconnier, B., Tverberg, V., Gerland, S., et al. (2002). The physical environment of Kongsfjorden–Krossfjorden an Arctic fjord system in Svalbard. *Polar Res.* 21, 133–166.

Szeligowska, M., Trudnowska, E., Boehnke, R., Dąbrowska, A. M., Dragańska-Deja, K., Deja, K., et al. (2021). The interplay between plankton and particles in the Isfjorden waters influenced by marine- and land-terminating glaciers. *Sci. Tot. Environ.* 780, 146491. doi: 10.1016/j.scitotenv.2021.146491

Torsvik, T., Albretsen, J., Sundfjord, A., Kohler, J., Sandvik, A. D., Skarðhamar, J., et al. (2019). Impact of tidewater glacier retreat on the fjord system: modeling present and future circulation in Kongsfjorden, Svalbard. *Estuar. Coast. Shelf Sci.* 220, 152–165. doi: 10.1016/J.ECSS.2019.02.005

Tverberg, V., Skogseth, R., Cottier, F., Sundfjord, A., Walczowski, W., Inall, M., et al. (2019). "The Kongsfjorden transect: seasonal and inter-annual variability in hydrography," in *The ecosystem of Kongsfjorden, Svalbard*. Eds. \H. Hop and C. Wiencke (Cham: Springer). *Adv. Polar Ecol.* 2, 49–104. doi: 10.1007/978-3-319-46425-1_3

Urbanski, J. A., Stempniewicz, L., Węsławski, J. M., Dragańska-Deja, K., Wochna, A., Goc, M., et al. (2017). Subglacial discharges create fluctuating foraging hotspots for sea birds in tidewater glacier bays. *Sci. Rep.* 7, 43999. doi: 10.1038/srep43999

Varpe, Ø., and Gabrielsen, G. W. (2022). Aggregations of foraging black guillemots (*Cepphus grylle*) at a sea-ice edge in front of a tidewater glacier. *Polar Res.* 41, 7141. doi: 10.33265/polar.v41.7141

Vihtakari, M., Welcker, J., Moe, B., Chastel, O., Tartu, S., Hop, H., et al. (2018). Black-legged kittiwakes as messengers of Atlantification in the Arctic. *Sci. Rep.* 8, 1178.1233–1240 doi: 10.1038/s41598-017-19118-8.

Walkusz, W., Kwasniewski, S., Falk-Petersen, S., Hop, H., Tverberg, V., Wieczorek, P., et al. (2009). Seasonal and spatial changes in the zooplankton community in Kongsfjorden, Svalbard. *Polar Res.* 28, 254–281. doi: 10.1111/j.1751-8369.2009.00107.x

Weslawski, J. M., and Legezynska, J. (1998). Glaciers caused zooplankton mortality? *J. Plankton Res* 29, 1233–1240.

Willis, K., Cottier, F., Kwasniewski, S., Wold, A., and Falk-Petersen, S. (2006). The influence of advection on zooplankton community composition in an Arctic fjord (Kongsfjorden, Svalbard). *J. Mar. Syst.* 61, 39–54. doi: 10.1016/j.jmarsys.2005.11.013

Zajaczkowski, M., and Legezynska, J. (2001). Estimation of zooplankton mortality caused by an Arctic glacial outflow. *Oceanologia* 43, 341–351.

frontiers | Frontiers in Marine Science

TYPE Original Research
PUBLISHED 20 September 2023
DOI 10.3389/fmars.2023.1168015



OPEN ACCESS

EDITED BY
Guang Yang,
Chinese Academy of Sciences (CAS), China

REVIEWED BY
Daria Martynova,
Zoological Institute (RAS), Russia
Elizaveta Ershova,
UiT The Arctic University of Norway, Norway
Vladimir G. Dvoretsky,
Murmansk Marine Biological Institute, Russia
Emilia Trudnowska,
Polish Academy of Sciences, Poland

*CORRESPONDENCE
Minami Ishihara
minami0525konakichi@eis.hokudai.ac.jp

RECEIVED 17 February 2023
ACCEPTED 23 August 2023
PUBLISHED 20 September 2023

CITATION
Ishihara M, Matsuno K, Tokuhiro K, Ando Y, Sato K and Yamaguchi A (2023) Geographic variation in population structure and grazing features of *Calanus glacialis/marshallae* in the Pacific Arctic Ocean.
*Front. Mar. Sci.* 10:1168015.
doi: 10.3389/fmars.2023.1168015



# Geographic variation in population structure and grazing features of *Calanus glacialis/marshallae* in the Pacific Arctic Ocean

Minami Ishihara[1]*, Kohei Matsuno[1,2], Koki Tokuhiro[3], Yasuhiro Ando[1], Kazutoshi Sato[4] and Atsushi Yamaguchi[1,2]

[1]Faculty/Graduate School of Fisheries Sciences, Hokkaido University, Hakodate, Hokkaido, Japan, [2]Arctic Research Center, Hokkaido University, Sapporo, Hokkaido, Japan, [3]Demonstration Laboratory, Marine Ecology Research Institute, Kashiwazaki, Niigata, Japan, [4]Arctic Environment Research Center, National Institute of Polar Research, Tachikawa, Tokyo, Japan

*Calanus glacialis/marshallae* is a dominant zooplankton species in the Pacific Arctic Ocean that is widely distributed in shelf areas, and it plays a vital role in connecting primary production to higher trophic levels. Its phenology is well adapted to hydrography, but there is little available information about regional and diel changes in population structure and grazing features. In this study, we investigated *C. glacialis/marshallae* during autumn 2019 in the Eastern and Northeastern Chukchi and Canadian basins to reveal geographic and diel variations in population structure, body size, grazing activity, and fatty acid composition. The abundance of *C. glacialis/marshallae* was found to be high on the slopes and low on the shelves. Body size (prosome length) was well described by the Bělehrádek equation combined with *in-situ* temperature throughout the sampling region. Cluster analyses based on hydrographic parameters were divided into four regions: southern shelf, northern shelf, slope, and basin. The southern shelf was dominated by copepodite stage five (C5) transported from the Bering Sea by Pacific waters. C4 and C5 were dominant on the northern shelf, suggesting that they grew slower than those on the southern shelf, and the populations also exhibited higher concentrations of fatty acids originating from dinoflagellates than those originating from the pan-Arctic Ocean, indicating low productivity in the region. The population on the slope had the highest abundance, C4 was dominant, and large amounts of diatom-derived eicosapentaenoic acid (EPA). These features are attributed to the upwelling of populations and nutrients that support diatom growth. In the basin, the early copepodite stages of composition were distinctly higher than those recorded in previous studies, because larger amounts of organisms flow into the region, resulting in more extended reproduction periods. In the basin, small and large forms of C5 were simultaneously found, and the small form exhibited a diel grazing activity pattern, but the large forms did not. These findings suggest their well adaptation in changing of the Pacific Arctic Ocean.

KEYWORDS

***Calanus glacialis/marshallae*, Pacific Arctic Ocean, population structure, body size, fatty acid, gut pigment**

# 1 Introduction

*Calanus* Leach, 1816 is the dominant copepod genus in the zooplankton biomass within the Pacific Arctic Ocean (Kosobokova and Hirche, 2009). Three *Calanus* species have been identified in different areas of the Pacific Arctic Ocean: *Calanus hyperboreus* in the basin (Conover, 1988), *Calanus glacialis* on the shelf (Kosobokova and Hirche, 2009; Kosobokova and Hopcroft, 2010), and *Calanus marshallae* in the southeastern Bering Sea (Frost, 1974; Vidal and Smith, 1986). Of these, *C. hyperboreus* has the largest body size and can be easily distinguished from the other two species. *Calanus glacialis* and *C. marshallae* are morphologically similar and difficult to distinguish (Frost, 1974), although they have been distinguished by genetic analysis (haplotype-based on 18S rRNA), and results have indicated that *C. marshallae* is transported to the shelf by the Pacific waters (Nelson et al., 2009; Ashjian et al., 2021). However, a genetic analysis was not conducted in the current study, and the *C. glacialis/marshallae* species complex is therefore referred to as *C. glacialis* in this work. *Calanus glacialis* has two populations (the Bering Sea and Arctic Basin populations that can also be distinguished using haplotype analyses (Nelson et al., 2009; Ashjian et al., 2017; Pinchuk and Eisner, 2017; Ashjian et al., 2021). Although these populations are believed to be morphologically indistinguishable, haplotype analysis indicates that the Bering Sea population is distributed on the Chukchi Sea shelf, and the Arctic Basin population is distributed north of the Beaufort Sea slope/Basin (Nelson et al., 2009). In addition, these populations appear to differ in their copepodid stage composition during the same season (Ershova et al., 2015; Pinchuk and Eisner, 2017), suggesting that the life cycles differ between populations.

*Calanus glacialis* is the dominant biomass species on the shelf of the Pacific Arctic Ocean (Kosobokova and Hirche, 2009; Kosobokova and Hopcroft, 2010), and it plays an essential role in connecting primary production to higher trophic levels in fish, birds, and mammals (Dickson and Gilchrist, 2002; Bengtson et al., 2005; Falk-Petersen et al., 2009; Crawford et al., 2012; Choquet et al., 2018). The population peaks near the shelf border (the shelf break) and declines sharply in the basin (Kosobokova and Hirche, 2009; Wassmann et al., 2015; Ershova et al., 2021). *Calanus glacialis* has a generation length of 1–3 years (Kosobokova, 1999; Ashjian et al., 2003; Falk-Petersen et al., 2009), and it grows from an egg to C3 and C4 within one year (Scott et al., 2000). The species has mixed reproductive strategies depending on food conditions (Plourde et al., 2005; Daase et al., 2013): capital breeding (based on internal energy storage before the onset of the spring bloom) and income breeding (utilizing ice algal or pelagic blooms) (Varpe et al., 2009). Due to this flexibility, their reproduction is initiated under sea ice and continues for one to two months using ice algae and pelagic phytoplankton blooms (Tourangeau and Runge, 1991; Campbell et al., 2009; Daase et al., 2013). However, if individuals reproduce in the late season, they cannot grow to the diapause stage in a short period (Falk-Petersen et al., 2009; Daase et al., 2013). As the developmental time between the stages is negatively related to temperature under sufficient food conditions (Corkett et al., 1986; McLaren et al., 1988), it is acknowledged that the life cycle of this species exhibits plasticity in response to environmental conditions that are reflected in the biological features of the species, such as body size, grazing activity, and the accumulation of fatty acids.

The body size of copepods varies depending on the temperature and prey conditions (Digby, 1954; Viitasalo et al., 1995; Kobari et al., 2003). Low temperatures and high food availability stabilize the growth of copepods (Vidal, 1980), which increases the body size (Viitasalo et al., 1995). Geographic variations in the body size of this species have been reported in the Atlantic sector of the Arctic Ocean when conducting interspecific comparisons with *Calanus finmarchicus* (Kosobokova, 1999; Choquet et al., 2018), but little information is available for the Pacific Arctic Ocean (Ashjian et al., 2003).

*Calanus glacialis* is omnivorous, feeds mainly on diatoms and dinoflagellates (Søreide et al., 2008; Yeh et al., 2020), and adapts flexibly to changes in its prey composition (Stevens et al., 2004a; Banas et al., 2016; Freese et al., 2016). With respect to feeding, the fatty acid composition has been well analyzed, mainly in the Atlantic sector of the Arctic Ocean (Stevens et al., 2004a; El-Sabaawi et al., 2009; Falk-Petersen et al., 2009; Trudnowska et al., 2020). The fatty acid composition of zooplankton varies with diet (Stevens et al., 2004b). Zooplankton contains unique fatty acids that are taken up and preserved without chemical changes in the body; fatty acids can be analyzed to obtain an index of their feeding records (El-Sabaawi et al., 2009). For example, diatoms are rich in eicosapentaenoic acid (EPA), and dinoflagellates are rich in docosahexaenoic acid (DHA; Budge and Parrish, 1998). The gut pigment is another index of the feeding activity of copepods, and it is useful for evaluating diel changes in grazing activity (Conover and Huntley, 1991); however, it has also not been well studied in the Pacific Arctic Ocean (Matsuno et al., 2015). Therefore, the regional differences in body size, feeding activity (fatty acid composition), and diel grazing patterns during autumn remain unknown. In this study, therefore, we investigated the population structure and ecological features (body size, feeding activity, and fatty acid composition) of *C. glacialis* to assess its current state in the changing Arctic Ocean.

# 2 Materials and methods

## 2.1 Field survey and onboard analysis

Zooplankton sampling was conducted via the R/V *Mirai* in the Pacific Arctic Ocean (66.50–78.04°N, 145.00–168.75°W) from October 8 to 27, 2019. Zooplankton samples were collected using vertical tows and a ring net (mouth diameter: 80 cm, mesh size: 335 μm) and a quad-NORPAC (North Pacific) net (mouth diameter: 45 cm, mesh sizes: 150 μm and 63 μm; Hama et al., 2019) at 10 m above the bottom or 150 m to the surface at 40 stations (Figure 1; Supplementary Table 1). The volume of the water filtered through the NORPAC net with the 150-μm mesh was estimated using a one-way flow meter (Rigosha CO., Ltd., Bunkyo-ku, Tokyo, Japan) mounted in the mouth of the net for quantitative collection of all copepodite stages in *C. glacialis*. Temperature, salinity, dissolved

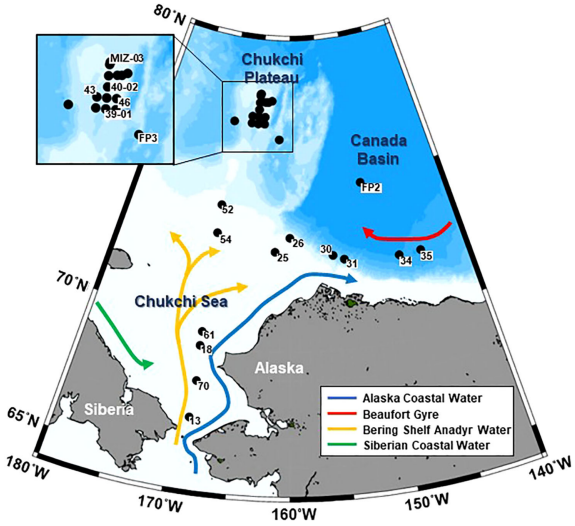


FIGURE 1
Location of sampling stations in the Pacific sector of the Arctic Ocean. Solid circles indicate where NORPAC net (150-μm mesh) sampling of *Calanus glacialis/marshallae* occurred in October 2019. The currents were adapted from Grebmeier et al. (2006).

oxygen, and turbidity were simultaneously measured using vertical casts from a conductivity temperature depth (CTD) sensor (Sea-Bird Electronics Inc., SBE 911plus).

NORPAC net samples (mesh size: 150 μm) were immediately preserved in 5% v/v borax-buffered formalin to analyze the abundance and population structure of *C. glacialis*. The remaining samples collected by the ring net and the NORPAC net (mesh size: 63 μm) were used to conduct gut pigment and fatty acid composition analyses. Gut pigment analyses were conducted in samples from 11 stations on the Chukchi Plateau (77°N) obtained during October 21–24, and fatty acid analyses were conducted in samples from throughout the study area.

With respect to the gut pigment analysis, 10% v/v soda (saturated with $CO_2$ in water) was immediately added to the fresh samples after sample collection to avoid copepod grazing, gut evacuation, and the decomposition of gut pigments (cf. Matsuno et al., 2015). Fresh specimens of *C. glacialis* copepodite stage five (C5) were sorted using a stereomicroscope (M165C-Ergo/MCI-HH/1; Leica Inc., Wetzlar, Germany). All specimens were sorted under low-temperature and dim-light conditions within 1 h, and the prosome length (PL) was measured using an eyepiece micrometer attached to a stereomicroscope with an accuracy of 0.001 mm. The sorted specimens (two to five specimens, average: three) were margined in small (2.5–3.3 mm) or large (3.4–3.8 mm) categories and transferred into cuvette tubes filled with 6 mL of N, N-dimethylformamide. One to four duplicates were obtained at each station, resulting in a total of 31 and 28 gut piments samples for the small and large categories, respectively. All samples were kept under cool and dark conditions for at least 24 h to extract chlorophyll and phaeopigments. After extraction, chlorophyll and phaeopigments were analyzed using a fluorometer (10-AU-005; Turner Designs Inc., California, United States), and the results were combined and expressed as the digestive tract pigment content (μg pigment ind.$^{-1}$; cf. Mackas and Bohrer, 1976).

The remaining sorted fresh samples were desalted using Milli-Q (Millipore Inc.), stored in 3-mL ointment bottles, and frozen at -80° C until the fatty acid composition was analyzed.

## 2.2 Sample analysis

In the laboratory, 19 zooplankton samples (Supplementary Table 1) collected by the NORPAC net with a 150-μm mesh size were split using a Motoda box splitter (Motoda, 1959). *Calanus glacialis* was identified at the copepodid stage level based on Brodsky (1967) in the aliquots and counted under a dissecting microscope (SMZ1000, C-BD115, Nikon Corporation, Japan). To calculate the total species abundance (ind. m$^{-3}$), the count at each stage was summarized and divided by the filtered volume (m$^3$) of the net. *Calanus marshallae* is potentially distributed in the northern Bering Sea and Chukchi Sea (Frost, 1974), but many zooplankton studies have treated this species as *C. glacialis/marshallae* owing to difficulties in their identification. Therefore, as mentioned in the Introduction, we refer to specimens from the *C. glacialis/marshallae* species complex as *C. glacialis* hereafter.

To determine geographical differences in the body size of *C. glacialis*, the PL of at least 10 *C. glacialis* C5 individuals at each station was measured using an eyepiece micrometer attached to a stereomicroscope with an accuracy of 0.001 mm. This measurement was performed for all zooplankton samples (Figure 1).

The length of lipid accumulation relative to the PL (lipid accumulation level) was measured at three levels: low, 0–4% of PL; medium, 4–40% of PL; and high, >40% of PL (Matsuno et al., 2016). To compare *C. glacialis* data, the abundance (ind. m$^{-2}$) was calculated by multiplying the population density (ind. m$^{-3}$) with the sampling depth to eliminate the influence of sampling depth differences at each station. The mean *C. glacialis* copepodid stage (MCS) was calculated using Eq (1).

$$MCS = \frac{\sum_{i=1}^{6} i \times Ai}{\sum_{i=1}^{6} Ai} \quad (1)$$

where $i$ (1–6 indicates C1–C6) indicates the copepodid stage for *C. glacialis*, and $Ai$ (ind. $m^{-2}$) is the abundance of a copepodid stage (cf. Marin, 1987). Similarly, the mean lipid stage (MLS) of *C. glacialis* C5 was calculated using Eq (2).

$$MLS = \sum_{j=1}^{3} j \times Bj \quad (2)$$

where $j$ (1, 2, and 3 indicates low, medium, and high, respectively) indicates the lipid accumulation level, and $Bj$ (ind. $m^{-2}$) is the ratio of the lipid accumulation level to the abundance.

Gonad maturation in adult females of the dominant copepod species was classified as stage I (immature), stage II (small oocytes in the ovary or oviduct), or stage III (large eggs or distended opacity in the oviduct) (cf. Miller et al., 1984; Niehoff, 1998).

## 2.3 Fatty acid analysis

Fatty acid analyses were performed using a simplified direct saponification/methylation method (Matsumoto et al., 2018) after necessary modifications were made for wax ester-containing samples. Each *C. glacialis* sample was transferred to a pre-weighed screw-capped glass vial and dried *in vacuo* until a constant weight was achieved. Methyl tricosanoate and 1-tricosanol in toluene (2 mg $mL^{-1}$ and 1 mg $mL^{-1}$, respectively; 1 µL) and 1 M KOH in 95% ethanol (50 µL) were added to the vial, and after being crushed with a stainless-steel rod, the sample was directly saponified overnight in the dark at 23°C. The reaction was stopped by adding 3 M HCl in methanol (33 µL; Sigma-Aldrich), and the solvents and excess HCl were evaporated under a stream of nitrogen and then *in vacuo*. The fatty acids released into the vial were methylated in 3 M HCl in methanol (100 µL) at 80°C for 10 min, and the reagent was evaporated under a stream of nitrogen. The fatty acid methyl esters were purified via column chromatography using silica gel 60 (Merck) and hexane/diethyl ether (95:5, v/v), and fatty alcohols were recovered from the same column by elution with hexane/diethyl ether (50:50, v/v) and stored.

The purified fatty acid methyl esters were analyzed via gas chromatography using a GC-4000 gas chromatograph (GL Sciences, Tokyo, Japan) and an InertCap Pure-WAX column (30 m × 0.32 mm i.d., 0.25 µm film thickness; GL Sciences, Tokyo, Japan). The column temperature was programmed to increase from 90°C to 170°C at 20°C $min^{-1}$, then to 240°C at 4°C $min^{-1}$, and to be finally maintained at 240°C for 25 min. The injector and detector temperatures were set at 240°C. The carrier gas was helium at a linear velocity of 29.3 cm $s^{-1}$ at 170°C. Methyl esters dissolved in hexane were injected into the column in the splitless injection mode, which was held for 1 min. A flame ionization detector (Shimadzu Corporation, Japan) and Shimadzu C-R3A integrator (Shimadzu Corporation, Japan) were used for detection and conducting peak area measurements. Peaks were identified by comparing their retention times with those of sardine oil fatty acids. The fatty acid content was calculated from the peak area ratios of methyl tricosanoate added to the initial *C. glacialis* samples.

## 2.4 Data analysis

To compare the biological parameters of *C. glacialis* C5 within the Pacific sector of the Arctic Ocean in 2019, a cluster analysis of environmental data was conducted. In this respect, water column (from the surface to 10 m above the bottom or 150 m above the bottom) averages of hydrographic data (temperature, salinity, dissolved oxygen, and turbidity) were calculated at each station. The water column data were then standardized, and similarities between stations were examined using the Euclidean distance. To group stations, similarity indices were coupled with hierarchical agglomerative clustering and the complete linkage method (unweighted pair group method with arithmetic mean, UPGMA) using the SIMPROF test. Based on the dendrogram, stations were separated to define regions with similar hydrographic conditions. A principal component analysis (PCA) was performed using standardized hydrographic data to evaluate hydrographic condition trends in each group. These analyses were conducted using Primer 7 software (PRIMER-E Ltd.).

Non-metric multi-dimensional scaling (NMDS) ordination was conducted using Primer 7 based on population structure, and Pearson's regressions of standardized hydrographic data were then conducted to delineate the relationship between population structure and hydrography. The abundance of each copepodid stage (ind. $m^{-2}$) was transformed into that of the $4^{th}$ root stage ($X^{-4}$). Similarities between samples were examined using the Bray-Curtis index according to differences in the stage composition.

To obtain the fatty acid composition, we calculated seven indices (docosahexaenoic acid (DHA)/eicosapentaenoic acid (EPA), 16 polyunsaturated fatty acids (PUFA)/18PUFA, 18:2n-6, 15:0 + 17:0, PUFA/saturated fatty acid [SFA], 18:1n-9/18:1n-7, and diatoms [D]/flagellates [F]) for the prey record of *C. glacialis* (Kaneda, 1991; Budge and Parrish, 1998; Dalsgaard et al., 2003; Stevens et al., 2004b; Alfaro et al., 2006).

Differences in biological parameters (abundance, MCS,PL, MLS, and fatty acid composition) of *C. glacialis* C5 among regions (identified by the cluster analysis based on hydrography) were tested using the max-t method with a heteroscedastic consistent covariance estimation (HC3) (Herberich et al., 2010). The tests were conducted using R software with the packages "multcomp" and "sandwich" (version 4.1.2, R Core Development Team, 2021). The relationship between the PL of C5 and temperature was regressed using the Bêlehrádek equation. A PCA based on normalized seven-index data was performed for fatty acids using Primer 7.

# 3 Results

## 3.1 Regions and water masses

The cluster analysis of biological parameters using hydrological data identified four regions in the Pacific sector of the Arctic Ocean (Figure 2A). As these regions were clearly divided geographically, they were named (from south to north) the southern shelf, northern shelf, slope, and basin (Figures 2A, C). The PCA results showed that

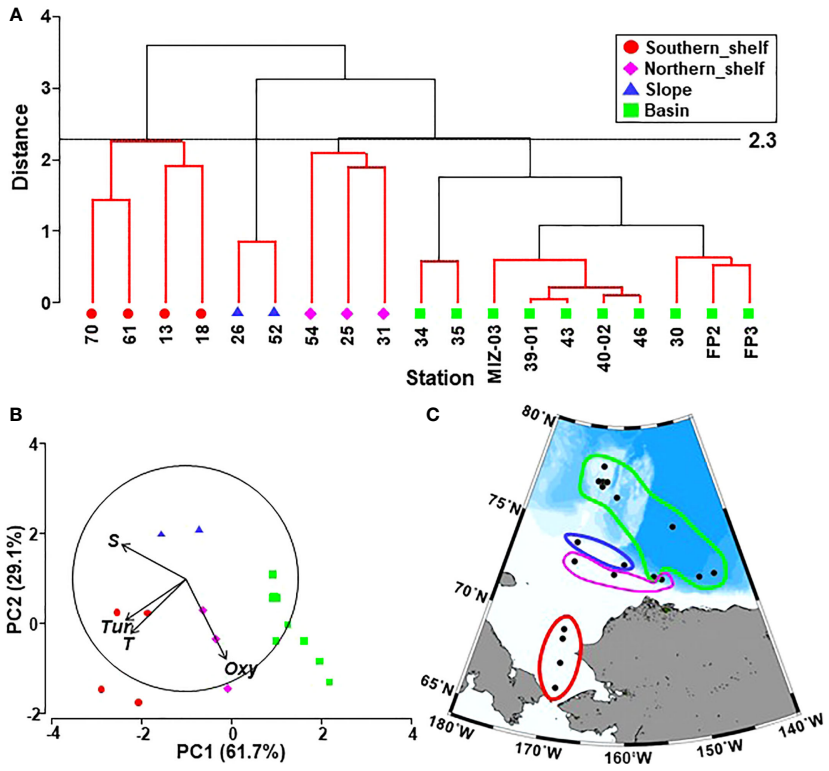


FIGURE 2
**(A)** Results of Q-mode clustering based on hydrographic variables by Euclidean distance connected with group average mode in the Pacific sector of the Arctic Ocean in October 2019. Red lines indicate non-significant station groupings, as tested by SIMPROF. Labels show sampling stations. **(B)** Principal component analysis with base variables showing four groups based on the cluster analysis. **(C)** Geographical distribution of the groups identified by the cluster analysis in the Pacific sector of the Arctic Ocean during October 2019.

temperature, salinity, and turbidity were higher on the southern shelf and lower in the basin (Figure 2B). Salinity was exceptionally high on the slope, and the dissolved oxygen level was high on the northern shelf and basin (Figure 2B).

Danielson et al. (2020) defined water masses based on temperature and salinity as follows: warm Coastal Water (wCW), warm Shelf Water (wSW), Ice Melt Water, cool Coastal Water (IMW cCW), cool Shelf Water (cSW), Anadyr Water (AnW), Modified Winter Water (MWW), Winter Water (WW), and Atlantic water and bearing basin water (AtlW and BBW) (Figure 3A). Within the 20 m depth on the southern shelf, wSW was dominant on October 8 but cSW occupied this depth range on October 27 (Figure 3B; Supplementary Table 1). A comparison of the temperature and salinity on these two dates showed that salinity was similar (32–32.49 vs. 31.99–32.36) but temperature was lower on October 27 (decreased from 3.77–5.85°C to 2.36–2.84°C). In the northern shelf region, the water masses differed because the stations and currents were widely distributed. AnW was observed below a depth of 25 m at St. 54, and AtlW and BBW were found below depths of 100 m and 125 m, respectively, on the slope. In the basin, a similar vertical distribution was observed among the stations; the surface layer (0–40 m or 0–60 m) comprised IMW cCW, while cSW, MWW, or WW existed at depths below these water masses.

## 3.2 Geographical abundance and body size of *C. glacialis*

The abundance of *C. glacialis* ranged from 126 to 2,968 ind. $m^{-2}$, with higher and lower abundances on the slope and shelf, respectively (Supplementary Figure 1). A comparison of the abundance and stage composition between the regions showed that the southern and northern shelves exhibited low abundance but had a high composition of C4 and C5 (Figure 4A). On the southern shelf, C5 was predominant in early October (St. 13 and 18), whereas adult females and males were predominant in late October (Sts. 61 and 70). The highest abundance of C3–C5 was observed on the slope. In the basin, the early stages (C1 or C2) occurred at 80% of stations (8/10), and the highest proportion of early stages was 44% (St. FP3; Figure 4). A few adult females were observed in each region, and almost all specimens showed stage I gonadal maturation (data not shown). NMDS based on the population structure showed relatively good separation with clustering by hydrography (Figure 4B). Among the hydrographic variables, temperature and turbidity had significant relationships with population structure. Of the basin group, Sts. 30, 34, and 35 were located slightly further from the main distribution of the basin community owing to the inflow of cSW at these stations (cf. Figure 3).

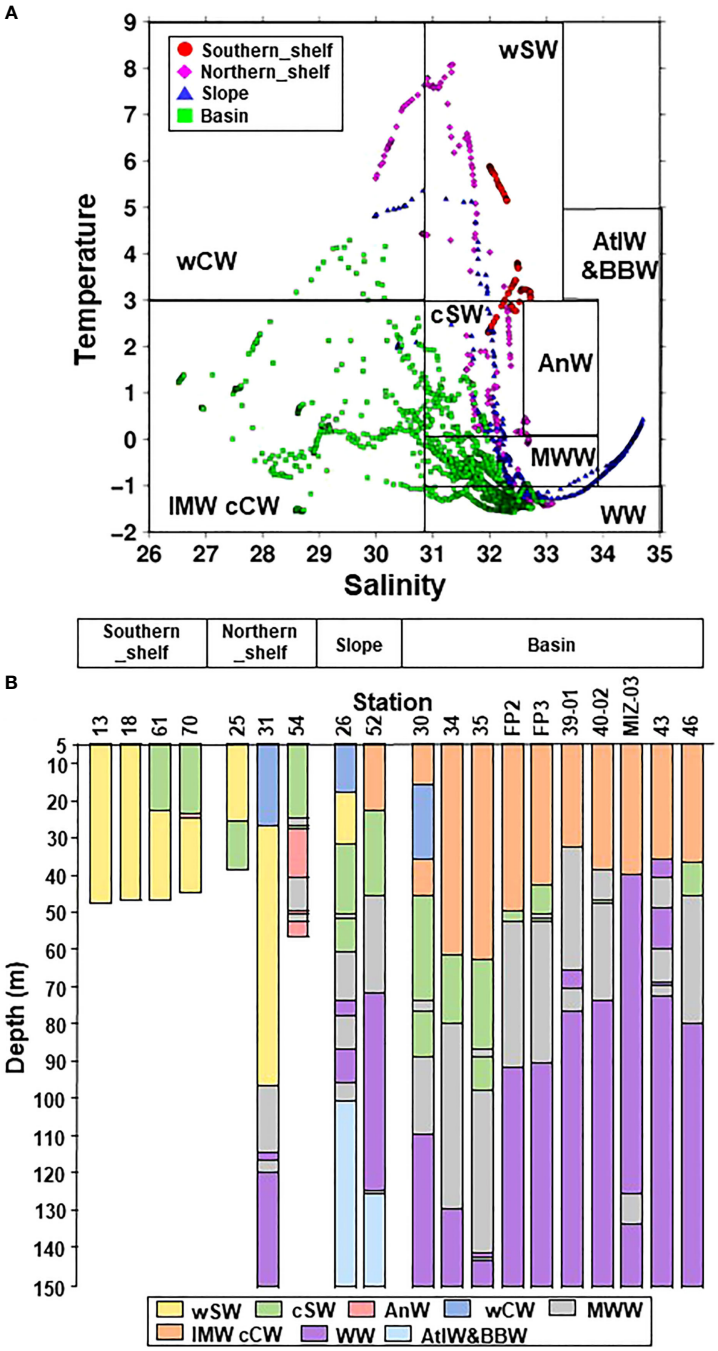


FIGURE 3
**(A)** T-S diagram in the Pacific sector of the Arctic Ocean in October 2019. The colored symbols indicate the four groups identified via cluster analysis (cf. Figure 2A): wCW, warm Coastal Water; wSW, warm Shelf Water; IMW cCW, Ice Melt Water and cool Coastal Water; cSW, cool Shelf Water; AnW, Anadyr Water; MWW, Modified Winter Water; WW, Winter Water; AtlW&BBW, Atlantic Water & Bering Basin Water (cf. Danielson et al., 2020). **(B)** Vertical distribution of water masses at each station in the Pacific sector of the Arctic Ocean in October 2019. The x-axis labels indicate groups identified by cluster analysis (cf. Figure 2A).

The body size (PL) of *C. glacialis* C5 ranged from 2.4–3.8 mm throughout the sampling region (Figure 5). The median PL value of each region showed an increasing trend from the Chukchi Sea toward the Arctic basin, in the order of the southern shelf, northern shelf, slope, and basin (Figure 5). Body size was well described by the Bêlehrádek equation ($PL=23594\ (T+76.17)^{-2.05}$; Figure 6).

## 3.3 Relationship between abundance, fatty acid index, gut pigment and geographical distribution

A comparison of the biological parameters of *C. glacialis* among regions showed significant differences in the abundance of C5, PL of C5,

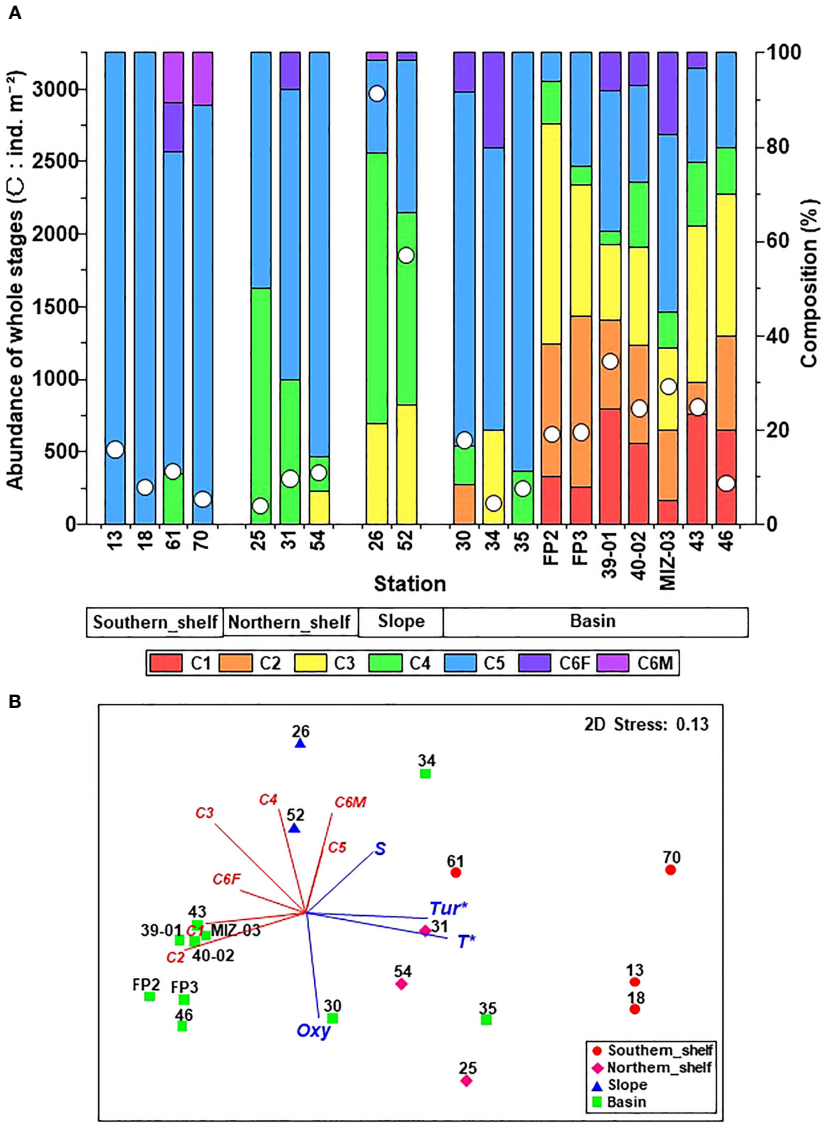


FIGURE 4
**(A)** Abundance and stage composition of *Calanus glacialis/marshallae* in the Pacific sector of the Arctic Ocean in October 2019. The x-axis labels indicate groups identified via cluster analysis (cf. Figure 2). **(B)** Non-metric multi-dimensional scaling (NMDS) ordination based on population structure with Pearson's regressions of hydrography. Symbols indicate clustering groups (cf. Figure 2A), and numbers with symbols are station IDs. Red lines indicate correlations between each copepodite stage. T, temperature; S, salinity; Tur, turbidity; Oxy, dissolved oxygen. *: $p < 0.05$.

total fatty acid content per individual, and fatty acid index (16PUFA/18PUFA, PUFA/SFA, and D/F; Table 1). The abundance of C5 was significantly higher on the slope than on the other regions. (Figure 4; Table 1). Significant differences in the MCS were detected, and it decreased from south to north (Figure 4; Table 1). There was no significant difference in MLS among regions; however, a minimum value was observed on the southern shelf (Table 1; Supplementary Figure 2). The total fatty acid content per individual in the basin was significantly higher than that on the southern shelf (Table 1). With respect to the fatty acid index, 16PUFA/18PUFA, PUFA/SFA, and D/F were significantly lower on the northern shelf, but DHA/EPA, 18:2n-6, and 15:0 + 17:0 were higher, although not significantly (Figure 7; Table 1). The results of the PCA based on the fatty acid indices showed that the northern shelf was distant from the distribution of the other groups (Figure 8). As shown in the regional comparison using the max-t test, the northern shelf had high 15:0 + 17:0, DHA/EPA, and 18:2n-6 values (Figure 8), and the other groups had relatively high 16PUFA/18PUFA, D/F, and PUFA/SFA ratios. There was no significant difference between the three groups (excluding the northern shelf), and the variabilities within the southern shelf and slope were within the basin variability.

In the basin, small (2.5–3.3 mm in PL) and large (3.4–3.8 mm in PL) forms occurred simultaneously (Figure 9). The cut off criteria between the forms is a length of 3.3 mm. Both small and large specimens were found in all 11 samples during October 21–24. The gut pigment showed a distinct diel pattern in the small forms, with high values during the night but low values during the daytime. However, the large forms did not exhibit a diel grazing activity pattern. The fatty acid indices were not significantly different between the small and large forms (data not shown).

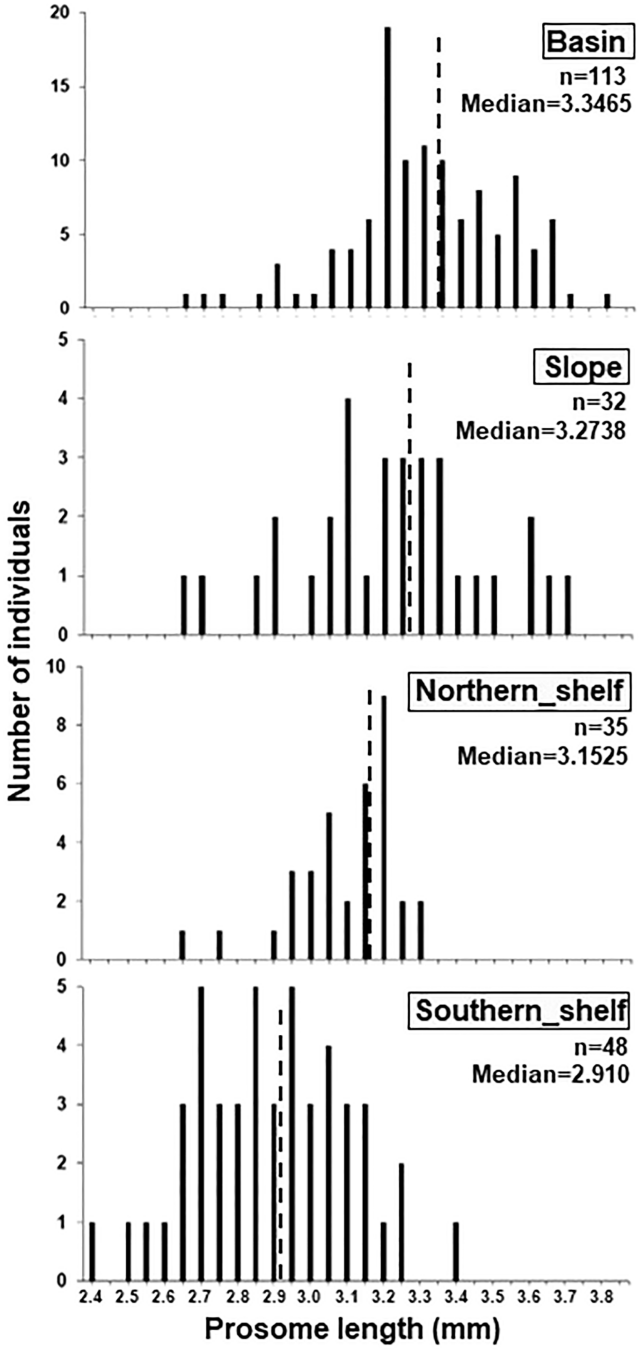


FIGURE 5
Size distribution of C5 *Calanus. glacialis/marshallae* in each clustering group (cf. Figure 2A) within the Pacific sector of the Arctic Ocean. Dashed lines indicate the median of the prosome length of the species in each region.

# 4 Discussion

## 4.1 Geographical variation in body size

The body size of copepods varies with the environment (temperature and food concentration; Deevey, 1960; Viitasalo et al., 1995; Kobari et al., 2003). In the Chukchi Sea in 2004, 2009, and 2012, the body size of *C. glacialis* C5 was found to be negatively correlated with temperature (Ershova et al., 2015). Similar results were detected in our study for the Chukchi Sea and Arctic Basin.

In the pan-Arctic Ocean, the size range of the PL of species from each region has been well reported: 2.9–3.8 mm in Kandalaksha Bay and the White Sea (Kosobokova, 1999), 2.55–3.55 mm near the Svalbard Islands (Choquet et al., 2018), 2.8–4.0 mm in Disko Bay (Nielsen et al., 2014), 2.4–3.6 mm in Kongsfjorden (Gabrielsen et al., 2012), and 2.4–3.7 mm in the Canadian Arctic and on the Atlantic coasts (Parent et al., 2011). Compared to those reports

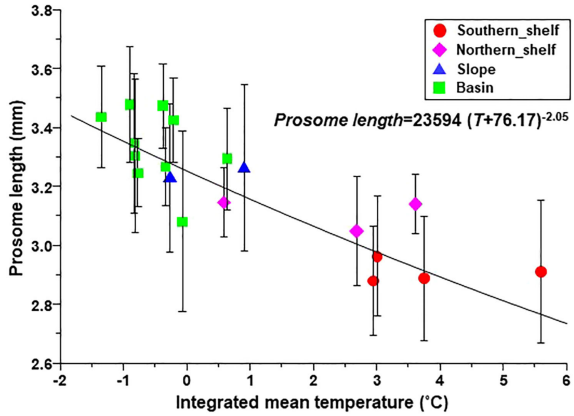


FIGURE 6
Relationship between prosome length of C5 *Calanus glacialis/marshallae* and integrated mean temperature in the Pacific sector of the Arctic Ocean. The symbols and error bars indicate the mean and standard deviation, respectively. The relationship was expressed using Bêlehrádek equations. The groups were identified via cluster analysis (cf. Figure 2A).

**TABLE 1** Regional comparison of biological parameters of *Calanus glacialis/marshallae* in different areas of the Pacific sector of the Arctic Ocean during October 2019.

| Parameters | Groups | | | | Max-t test + HC3 | | | |
|---|---|---|---|---|---|---|---|---|
| | South_shelf | North_shelf | Slope | Basin | | | | |
| Abundance of whole stages (ind. $m^{-2}$) | 328 ± 128 | 266 ± 100 | 2412 ± 556 | 619 ± 302 | NS | | | |
| Abundance of C5 (ind. $m^{-2}$) | 294 ± 135 | 187 ± 99.0 | 590 ± 6.88 | 200 ± 127 | North_shelf[2] | Basin[2] | South_shelf[2] | Slope[1] |
| MCS (Mean copepodid stage) | 5.05 ± 0.05 | 4.68 ± 0.13 | 4.06 ± 0.04 | 3.67 ± 0.83 | Basin[3] | Slope[3] | North_shelf[2] | South_shelf[1] |
| Prosome length of C5 (mm) | 2.91 ± 0.21 | 3.11 ± 0.15 | 3.24 ± 0.26 | 3.34 ± 0.23 | South_shelf[3] | North_shelf[2] | Slope[1] | Basin[1] |
| MLS (Mean Lipid Stage) | 2.07 ± 0.53 | 2.54 ± 0.03 | 2.42 ± 0.08 | 2.48 ± 0.27 | NS | | | |
| Fatty acid (μg $ind.^{-1}$) | 138 ± 30.7 | 230 ± 97.3 | 233 ± 77.8 | 305 ± 149 | South_shelf[2] | North_shelf[1,2] | Slope[1,2] | Basin[1] |
| DHA/EPA[a] | 0.47 ± 0.12 | 0.92 ± 0.24 | 0.30 ± 0.02 | 0.33 ± 0.10 | NS | | | |
| 16PUFA/18PUFA[b] | 0.65 ± 0.27 | 0.28 ± 0.02 | 0.89 ± 0.12 | 0.45 ± 0.23 | North_shelf[2] | Basin[1,2] | South_shelf[1,2] | Slope[1] |
| 18:2n-6[c] | 0.89 ± 0.14 | 2.30 ± 1.02 | 0.89 ± 0.20 | 0.92 ± 0.20 | NS | | | |
| 15:0 + 17:0[d] | 1.50 ± 0.16 | 2.31 ± 0.35 | 1.66 ± 0.37 | 1.23 ± 0.20 | NS | | | |
| PUFA/SFA[e] | 2.02 ± 0.29 | 0.92 ± 0.18 | 2.11 ± 0.53 | 1.92 ± 0.34 | North_shelf[2] | Basin[1] | South_shelf[1] | Slope[1] |
| 18:1n-9/18:1n-7[f] | 6.90 ± 1.82 | 6.66 ± 0.25 | 4.77 ± 1.63 | 6.02 ± 1.57 | NS | | | |
| D/F[g] | 1.98 ± 0.47 | 1.62 ± 0.23 | 3.06 ± 0.37 | 3.26 ± 0.95 | North_shelf[2] | South_shelf[2] | Slope[1,2] | Basin[1] |

Different superscript numbers in the Max-t test + HC3 column indicate significant differences between regions. NS, not significant.
[a:] Dinoflagellates/diatoms, carnivory (Budge and Parrish, 1998); [b:] Diatoms/flagellates (Budge and Parrish, 1998; Alfaro et al., 2006); [c:] Terrestrial detritus or green algae (Dalsgaard et al., 2003); [d:] Bacteria (Kaneda, 1991); [e:] Carnivory (Stevens et al., 2004a); [f:] Carnivory or omnivory (Stevens et al., 2004b); [g:] Diatoms (16 polyunsaturated fatty acids (PUFA), 16:1n-7 + 16:1n-9, 20:5n-3)/flagellates (22:6n-3, 18PUFA, 18:2n-6; Dalsgaard et al., 2003).

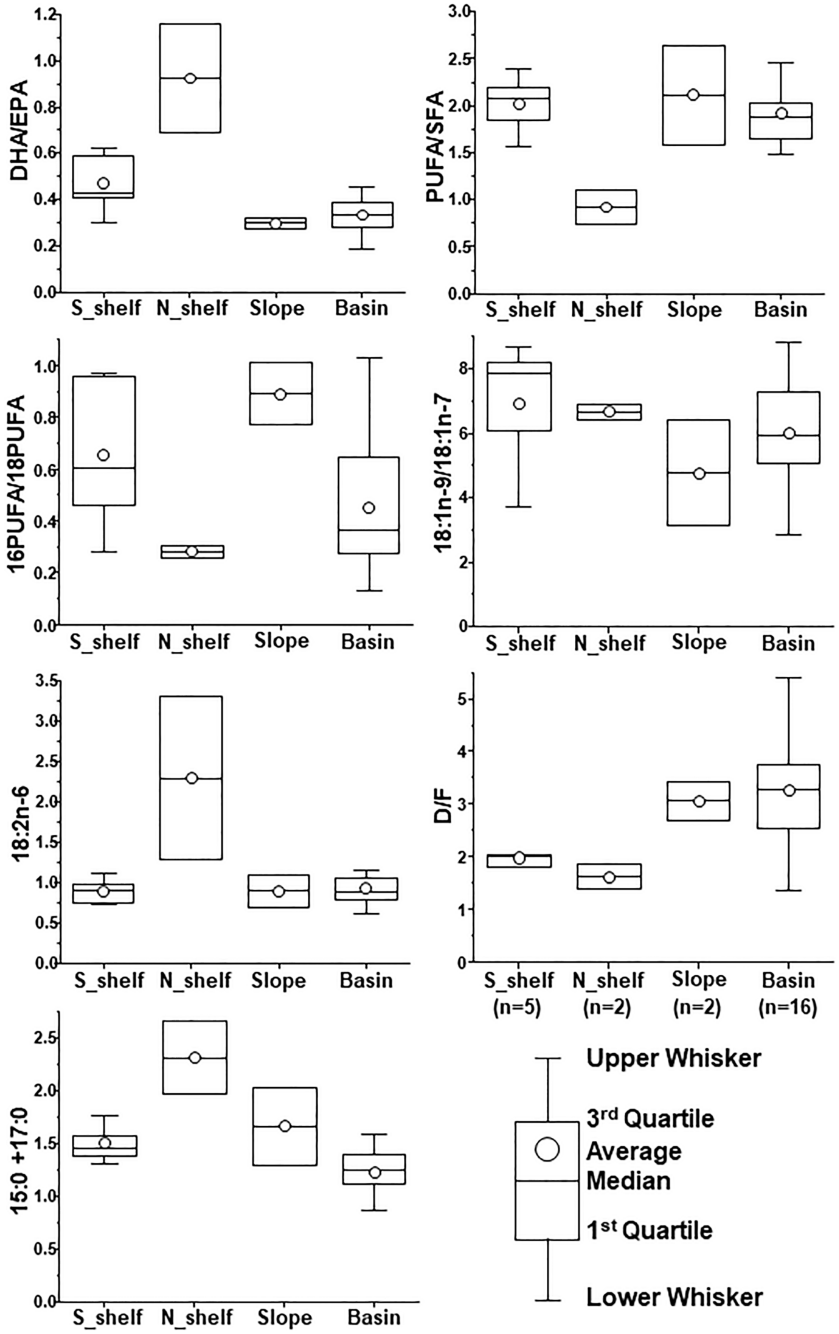


FIGURE 7
Regional comparison of biomarker indices in fatty acids of C5 *Calanus. glacialis/marshallae* in the Pacific sector of the Arctic Ocean in October 2019. The x-axis labels indicate groups identified via cluster analysis (cf. Figure 2A).

from other regions, the PL size range in our study (2.4–3.8 mm) was one of the largest, and this was because the border of the sampling region was situated in the Pacific sector of the Arctic Ocean. The body size of C5 in the Canada Basin in October 1997 was reported as 3.38 ± 0.03 mm (Ashjian et al., 2003), which is similar to our results (basin: 3.34 ± 0.23 mm; slope: 3.24 ± 0.26 mm; Beaufort Sea: 3.46 ± 0.20 mm). However, smaller body sizes were observed on the southern and northern shelves in our study (2.91 ± 0.21 mm, and 3.11 ± 0.15 mm, respectively). It is considered that the co-occurrence of *Calanus marshallae*, which is slightly smaller than *C. glacialis* is (Frost, 1974), may decrease the mean body size in both these regions.

Two *C. glacialis* haplotypes exist in the study area: Bering Sea and Arctic Basin populations (Nelson et al., 2009). The Bering Sea population extends from the Bering Strait to the northern Chukchi Sea owing to the inflow of Pacific Ocean water (Nelson et al., 2009; Ashjian et al., 2021). The inflow of Pacific water usually peaks from August to October (Woodgate, 2018) and is mainly composed of wSW (Danielson et al., 2020). As individuals in the Bering Sea population experience warmer conditions than do those in the

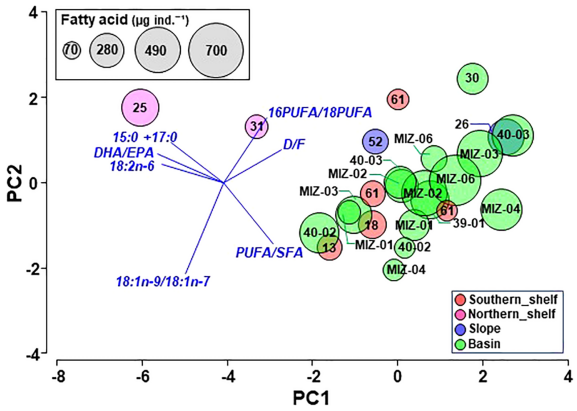


FIGURE 8
PCA based on biomarker indices in fatty acids of C5 *Calanus glacialis/marshallae* in the Pacific sector of the Arctic Ocean in October 2019. The size of the circle indicates the fatty acid content per individual.

Arctic Basin population, it is considered that the Bering Sea population would be smaller than would the Arctic Basin population be. However, a haplotype analysis could not be conducted in this study because ethanol samples were consumed for another scientific work, and the difference in the PL between the Bering Sea and Arctic Basin populations, therefore, remains unclear.

## 4.2 Reproduction and growth

*Calanus glacialis* is believed to undergo capital and income breeding depending on the food conditions (Plourde et al., 2005; Daase et al., 2013). Although our sampling was conducted in autumn, and our results do not, therefore, contain evidence of reproduction, the timing of reproduction in spring was back-calculated using the developmental time and embryonic duration (Corkett et al., 1986) (see Supplementary Figure 3, Supplementary Table 3). This type of back-calculation helps to remove the sampling time gap among regions (Kimura et al., 2022). The estimation showed that almost all individuals had been spawned in July and August.

In the Pacific sector of the Arctic Ocean, peaks in phytoplankton blooms have been observed during May in the Chukchi Sea, and in June and July in the Siberian and Beaufort Seas (Arrigo and van Dijken, 2011). In relation to this seasonality, early stages (C1 and C2) dominate within the southern Chukchi Sea (Ashjian et al., 2021). However, there was a timing gap between the phytoplankton blooms (May–July) and our estimated reproduction period (July–August), which could have been caused by the shorter development time for the back-calculation of reproduction timing (Supplementary Table 3). The developmental time was assessed using the temperature from our sampling period (October); however, they survived in colder conditions (Spring and Summer). Since warmer temperature induce shorter development time (Corkett et al., 1986), therefore, the estimated development time was shorter than the *in-situ* value. Another hypothesis is that northward currents flushed out individuals during May–July, and individuals transported from the Bering Sea could not be established in the Chukchi Sea because of their short flushing time (Ashjian et al., 2021).

Timing of phytoplankton blooms shifts from south to north in the Pacific Arctic Ocean (Arrigo and van Dijken, 2011), subsequent reproduction of *C. glacialis* is expected to be associated with that. However, interestingly, it was suggested that the earliest reproduction period occurred in June in the basin region. This was potentially caused by the longer residence time of C5 than that of the other stages: the developmental time from nauplius three to copepodite five is almost similar for each molting, but the period from C5 to molt adults is longer (Peterson, 1986). Alternatively, it is possible that another previous generation survived because of the low metabolic rate at cold temperatures and the low grazing pressure by fish (Mundy et al., 2017; Skjoldal, 2022).

## 4.3 Southern shelf

In early October, the entire water column was occupied by wSW, but the surface layer (0–20 m) changed to cSW in late October, possibly due to cooling by low air temperature, as other shelf water masses (e.g., AnW and wCW) were not observed. Regarding the population structure, C5 was predominant in early October, whereas adults were predominant in late October. Based on these results, the population of *C. glacialis* appeared to grow, with some adults developing in late October. Incubation experiments revealed that 50% of *C. glacialis* individuals develop from C5 to adulthood in 20 days at 10°C (Peterson, 1986). In our development time estimation based on Corkett et al. (1986), it would take 10 days to undergo this process at 10°C and 20 days at 3°C (Supplementary Figure 3); therefore, it was not surprising that some adults were observed in October. A high abundance of adult females was observed in the Arctic Basin in February, but only a few such individuals were found throughout the year (Ashjian et al., 2003). During its life cycle, *C. glacialis* is capable of diapause from C4 and C5 when it descends into the deep sea, and rich lipids are stored in its body during autumn and winter (Lane et al., 2008; Ershova et al., 2015; Pinchuk and Eisner, 2017). Because a sufficient

depth (> 200 m) is required for the diapause of this species (Hirche, 1991; Ashjian et al., 2003), the shallow bottom depth (approximately 50 m; Nelson et al., 2009; Ershova et al., 2015) and short residence time within the Chukchi Sea (Ashjian et al., 2021) imply that the population cannot be sustained/established.

The northward transportation of Pacific zooplankton has been reported in the Pacific Arctic Ocean during warm years (Matsuno et al., 2011; Ershova et al., 2015). *Calanus marshallae*, which was originally distributed in the Northern California Current system to the coastal Gulf of Alaska and the Bering Sea (Frost, 1974), should be included within the Pacific species; however, many studies have not distinguished it from *C. glacialis* owing to the morphological similarities between the species. Genetic approaches have shown that *C. marshallae* is present in the Chukchi Sea during the summer (Nelson et al., 2009 and Ashjian et al., 2021). In addition, the northward flow at the Bering Strait is increasing (0.01 Sv per year), and residence time in the Chukchi Sea has decreased by ~1.5 months (from 7.5 months to ~ 5 months) based on mooring results from 1990 to 2019 (Woodgate and Peralta-Ferriz, 2021), which subsequentially extend *C. marshallae* distribution. Therefore, the inflow of *C. marshallae* potentially distorts any changes identified in the *C. glacialis* population, especially in the shelf region during warm years. Genetic analyses are therefore required to avoid this distortion.

## 4.4 Northern shelf

The population structure of this area mainly comprises C4 and C5 *C. glacialis*. Assuming that this population on the shelf originates from water masses similar to those on the southern shelf (wSW and cSW) that occupy more than half of the water column, the population on the northern shelf (i.e., C4 and C5) is younger than that on the southern shelf (C5). This may be attributed to the shorter intermolt period at warmer temperatures (Corkett and McLaren, 1978; Supplementary Table 3). The effect of temperature on copepod growth has also been observed during warm and cold years in the Chukchi Sea (Matsuno et al., 2011).

High variability in hydrography and water masses was observed in this study, and the fatty acid composition of the specimens collected on the northern shelf was lower in terms of 16 PUFA/18PUFA, PUFA/SFA, D, and F than that of specimens from other areas. The fatty acid composition is a valuable index for prey records because the composition of predators reflects that of their prey (El-Sabaawi et al., 2009). This result implies that individuals on the northern shelf do not actively utilize diatoms or protozoans (Stevens et al., 2004a; Stevens et al., 2004b). In contrast, higher values of DHA/EPA, 18:2n-6, and 15:0 + 17:0 were observed in specimens on the northern shelf than in those from other areas. Docosahexaenoic acid is abundant in dinoflagellates, and EPA is abundant in diatoms (Budge and Parrish, 1998), and the high DHA/EPA ratio, therefore, suggests that this species grazes mostly on dinoflagellates within this area. However, this feature is considered to be rare in the Arctic Ocean compared with that in the well-studied Atlantic Arctic Ocean. A survey in the southern shelf area west of Spitsbergen in July 2018 showed a DHA/EPA of 0.67 (Trudnowska et al., 2020), which is lower than that observed in our study (0.92). In addition, a DHA/EPA value of 0.21 was observed in Kongsfjord in the Atlantic Arctic Ocean during autumn in 1997 (Falk-Petersen et al., 2009), 0.15 in the Fram Strait during autumn in 2003 (Søreide et al., 2008), and 0.22 in Northwater during the autumn of 1999 (Stevens et al., 2004a). It is evident that this species can change its diet depending on the time and location (Banas et al., 2016), and the results here show that the species on the northern shelf in the study area are highly dependent on dinoflagellates.

Considering the energy flow in lower ecosystems, eutrophic conditions induce the dominance of diatoms because their growth is rapid from ingesting rich nutrients; however, oligotrophic conditions stimulate microbial loop production (Pomeroy, 1974). In the oligotrophic state, bacteria act as primary producers using dissolved organic carbon, and several predator-prey interactions (bacteria vs. heterotrophic nanoflagellates, heterotrophic nanoflagellates vs. small ciliates) occur, reaching their production into heterotrophic dinoflagellates (Jakobsen and Hansen, 1997; Levinsen and Nielsen, 2002). Therefore, the number of transfers between trophic levels is much greater under oligotrophic conditions, resulting in a low transfer efficiency. This suggests that the *Calanus glacialis* can survive in a low-productivity ecosystem. In addition, although a high 18:2n-6 value indicates that the species grazes on green algae of a terrestrial origin (Dalsgaard et al., 2003), there have been no reports on the feeding on green algae by this species in the ocean; therefore, further research is required.

## 4.5 Slope

The highest abundance was observed on the slope, and these results are consistent with those obtained during studies conducted in August (Lane et al., 2008; Llinás et al., 2009) and September (Ershova et al., 2021). In this area, easterly winds stimulate upwelling along the shelf-break (Pickart et al., 2013), resulting in the occasional transport of diapause individuals (mainly C4 and C5) from the deep sea to the surface (Lane et al., 2008; Llinás et al., 2009). AtlW and BBW were only observed in this region below depths of 100 m or 125 m, which suggests the presence of upwelling (Carmack and Kulikov, 1998). A higher abundance was therefore observed on the slope because of the presence of individuals derived from the deep sea via upwelling (Pickart et al., 2013; Rutzen and Hopcroft, 2018). Another mechanism that increases abundance is anti-cyclonic, cold-core eddy formation from the boundary current flowing along the Chukchi Shelf (Pickart et al., 2005; Llinás et al., 2009). Although the accumulation of zooplankton by eddies is not very strong (Llinás et al., 2009), the formation rate of eddies is very high, with up to 1–2 eddies per day from early spring to early autumn (Pickart et al., 2005). As previously mentioned, although shelf populations are flushed out into the basin (Ashjian et al., 2021), a high abundance is frequently observed in this region, and this could potentially be related to the increased eddy formation rate.

The population structure derived in our study is considered to reflect population growth, and this has also been determined in other studies. In August, early stages (C1 and C2) are abundant (Lane et al., 2008), C1–C4 are dominant in September (Ershova et al., 2021), and C3–C5 are dominant in October (this study). The abundance alters between months, and it decreases from August (mean 18,910 ind. m$^{-}$

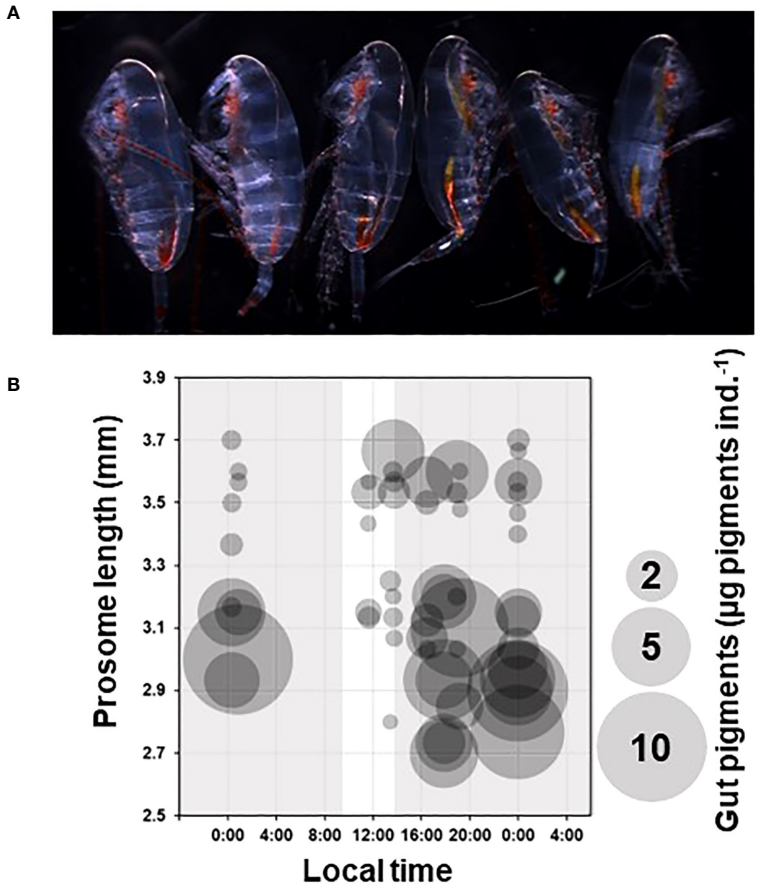


FIGURE 9
**(A)** Lateral view of small and large specimens taken at St. MIZ-07 (cf. Supplementary Table 1). The three on the right-hand side were small with rich gut pigments; the three specimens on the left-hand side were large with minimal gut pigment. **(B)** Comparison between grazing activity of small and large specimens in the basin region (cf. Figures 1, 2A) during October 21–24, 2023 (Supplementary Table 1). The local time is Alaska Standard Time (UTC: 9 h). The area of the circle represents the amount of gut pigment (µg pigments ind.$^{-1}$). The gray and white backgrounds represent nighttime and daytime, respectively. The prosome length was determined from the mean value of two-five specimens used in the gut pigment analysis (cf. Methods and Materials).

$^{2}$, Llinás et al., 2009) and September (mean 8,000 ind. m$^{-2}$, Ershova et al., 2021) to October (1,855-2,968 ind. m$^{-2}$). It is of note that all the abundance data were based on the samples collected using the 150 µm mesh. Assuming the mortality rate for broadcast spawner based on field measurements (Hirst and Kiørboe, 2002), a value of 0.0335 d$^{-1}$ was calculated at 0.27°C (Supplementary Table 3). Using this rate, the abundance in October was expected to be 2,448 ind. m$^{-2}$ (=18,910 ind. m$^{-2}$×(1-0.035)^(60 days)) from August and 2,878 ind. m$^{-2}$ (=8,000 ind. m$^{-2}$×(1-0.035)^(30 days)) from September. Predation mortality is independent of ambient temperature, and the ratio of predation mortality to total mortality increases to 3:4 in colder situations (Hirst and Kiørboe, 2002). This indicates that the decrease in abundance on the slope was mainly caused by predator feeding. A large biomass of polar cod has been observed in Atlantic Water along the slope (Crawford et al., 2012). Therefore, the high biomass of *C. glacialis* is due to physical processes, and the rich prey is grazed on by organisms in the higher trophic levels, such as fish, birds, and marine mammals (Dickson and Gilchrist, 2002; Bengtson et al., 2005; Crawford et al., 2012).

With respect to the fatty acid composition, this region had the lowest DHA/EPA ratio and the highest 16PUFA/18PUFA ratio among the four regions, which indicates that individuals in this area consume more diatoms than do dinoflagellates and flagellates. This area is prone to upwelling (Pickart et al., 2013), which supplies rich nutrients from deeper layers to the euphotic layer (Pickart et al., 2013; Rutzen and Hopcroft, 2018). Consequently, silicate concentrations in the northern Chukchi Sea increase, providing a suitable environment for diatom growth (Hill and Cota, 2005; Nishino et al., 2015). Therefore, geographical and physical features (i.e., upwelling) affect the *C. glacialis* population, and lipid accumulation relates to diatom grazing on the slope.

## 4.6 Basin

Based on the environmental data, Sts. 30, 34, and 35 were located in the basin, and the population structures at these stations differed considerably from those of the other stations on the Chukchi Plateau. This may be due to the transportation of shelf

individuals by cSW inflow to depths of 50–100 m (Lane et al., 2008; Llinás et al., 2009). Previous studies found that the C5 stage dominates the basin population in autumn (Ashjian et al., 2003; Hopcroft et al., 2005). However, in our study, C5 was not abundant. The early copepodite stages (C1 or C2) occurred at 80% of the basin stations, and the maximum population percentage composition was 44%. Similar results, such as the occurrence of early stages on the surface of the basin, have been reported in late summer (Hopcroft et al., 2005) and winter (Ashjian et al., 2003). However, the composition of the early stage was lower than 10% because this species is capable of diapause after C4 (Falk-Petersen et al., 2009; Daase et al., 2013), and it is likely that C1 and C2 cannot overwinter in the basin because of their short growth periods (Ji et al., 2012).

With respect to the population origin of the early stages, adult females were observed at some stations in the basin, but all specimens were immature. However, according to the developmental time (Supplementary Table 3), the early stages were spawned in August, and C5 was spawned in late June. This shows that long-term reproduction is supported by mixed reproductive strategies (Plourde et al., 2005; Daase et al., 2013). Primary production on the Chukchi Plateau is very low (Codispoti et al., 2013), but the region is greatly affected by the inflow of Pacific Summer Water (PSW), which transports heat and organisms via eddies (Watanabe et al., 2014; Muramatsu et al., 2021). The composition of PSW in the basin has increased in recent years compared to that during the 1990s and the 2000s (Bourgain and Gascard, 2012; Muramatsu et al., 2021). Therefore, more organisms are transported by PSW with eddies (Watanabe et al., 2014), and this extends the reproduction period of the species. Potentially due to the extended reproduction period, the early stages eventually become more abundant than those in the results of Ashjian et al. (2003) and Hopcroft et al. (2005). Field measurements of longevity have shown that adults are quickly removed 16 days after reproduction (Hirst and Kiørboe, 2002). These assumptions suggest that adult females reproduce over the long term using transported organisms (e.g., phytoplankton), then that are removed after reproduction. Similarly, overwintering individuals reproduce in the Chukchi Sea following sea ice retreat, and the early stages are transported to the basin (Ashjian et al., 2021). However, no genetic evidence is available to support this hypothesis, and a haplotype analysis of the early stages is required to reveal the extended distribution and establishment of the Bering Sea population in the basin (Ershova et al., 2021; Skjoldal, 2022),

Small and large forms co-occur on the Chukchi Plateau. On the Atlantic side of the Arctic Ocean, it is difficult to distinguish between *C. glacialis* and the smaller *Calanus finmarchicus* (Grainger, 1961). Choquet et al. (2018) investigated the possibility of identifying species based on PL, morphological characteristics (the 5$^{th}$ pair of swimming legs and mandible), antennules, genital somite pigmentation in live specimens, and genetic analyses. The represented PL helps to approximate the species composition, but no criteria for the species have been established; therefore, their size ranges overlap (Choquet et al., 2018). In our case, the small forms (2.5–3.3 mm) in C5 could be included as *C. finmarchicus* (Choquet et al., 2018), but this result was impossible to clarify because of a lack of genetic analysis.

An inter-form difference in the diel patterns of grazing activity was observed. Small forms show higher gut pigment levels at night than during the day, which is associated with diel vertical migration (DVM) (Conover and Huntley, 1991). The magnitude of DVM for *Calanus* spp. varies with season and copepodid stage, and the DVM intensity is greater during spring and autumn, when the diel changes in light penetration are large (Falkenhaug et al., 1997). During spring, *C. glacialis* responds sensibly to phytoplankton dynamics via DVM, reaching sea ice and exhibiting diel patterns in grazing activity (Runge and Ingram, 1991). In September, in the northern Chukchi Sea, diel changes in gut pigments have been reported during small autumn phytoplankton blooms (Matsuno et al., 2015). In contrast, DVM and active grazing ceases during the night for *Calanus* spp., as determined by the lipids accumulated in C5 (Falk-Petersen et al., 2008; Matsuno et al., 2015). Based on this knowledge, it is hypothesized that the small forms perform DVM and graze at night, while the large forms cease DVM and active grazing and stay in the deep layer. Although our sampling design could not corroborate this hypothesis, both forms were distributed within depths of 0–150 m due to their co-occurrence during the day and night (Falk-Petersen et al., 2008).

## 5 Conclusions

This study describes geographic variations in the population structure, body size, fatty acid composition, and diel changes in the grazing activity of *C. glacialis/marshallae* in the Pacific region of the Arctic Ocean during autumn. The body size of this species was found to be negatively correlated with the water temperature from the Chukchi Sea to the Arctic basin. The population developed from C5 was dominant on the southern shelf, and it was mostly transported from the Bering Sea. C4 and C5 were dominant on the northern shelf, suggesting that their growth was slower than the growth of those on the southern shelf. The fatty acid composition revealed that the rate of prey dependence on dinoflagellates was exceptionally high in the Arctic Ocean, indicating that the species existed in a low-productivity ecosystem. The highest abundance and composition of diatom-derived EPA among the fatty acids were found on the slope. This could be explained by the upwelling accompanying the inflow of this species from the deep sea, and the nutrient supply for the growth of diatoms. In the basin, early-stage individuals were more abundant than those reported in previous studies because a larger number of organisms had flowed into the region, resulting in extended reproduction. Small and large C5 forms were found, showing the different diel patterns of grazing activity. It appears that *C. glacialis/marshallae* have adapted to the flexibility in their life cycle caused by changes in the physical and chemical environments of the Pacific Arctic Ocean. However, vertically stratified sampling and haplotype analyses are required to monitor their biological features and reveal population origins.

## Data availability statement

The original contributions presented in the study are included in the article/Supplementary Material. Further inquiries can be directed to the corresponding author.

## Ethics statement

The manuscript presents research on animals that do not require ethical approval for their study.

## Author contributions

KM and AY designed the study. KT, KM, and KS performed field sampling. MI, KT, and YA analyzed the samples. MI and KM analyzed the data and MI and KM wrote the paper with contributions from all authors.

## Funding

This work was funded by the Arctic Challenge for Sustainability (ArCS; Program Grant Number JPMXD1300000000) and Arctic Challenge for Sustainability II (ArCS II; program grant number JPMXD1420318865) projects. This study was also supported by the Environment Research and Technology Development Fund (JPMEERF20214002) of the Environmental Restoration and Conservation Agency of Japan and partially supported by the Japan Society for the Promotion of Science (JSPS) KAKENHI (grant numbers JP22H00374 (A), JP21H02263 (B), JP20K20573 (Pioneering), JP20H03054 (B), JP20J20410 (B), JP19H03037 (B), JP18K14506 (Early Career Scientists), and JPJSBP120238801 (Bilateral program)).

## Acknowledgments

We thank the captain, officers, crew, and researchers onboard the R/V *Mirai*, the Canadian Coast Guard RV *Amundsen*, and IB *S.W. Laurier* for their outstanding efforts during field sampling.

## Conflict of interest

The authors declare that the research was conducted in the absence of any commercial or financial relationships that could be construed as a potential conflict of interest.

## Publisher's note



## Supplementary material

The Supplementary Material for this article can be found online at: https://www.frontiersin.org/articles/10.3389/fmars.2023.1168015/full#supplementary-material

## References

Alfaro, A. C., Thomas, F., Sergent, L., and Duxbury, M. (2006). Identification of trophic interactions within an estuarine food web (northern New Zealand) using fatty acid biomarkers and stable isotopes. *Estuar. Coast. Shelf. Sci.* 70, 271–286. doi: 10.1016/j.ecss.2006.06.017

Arrigo, K. R., and van Dijken, G. L. (2011). Secular trends in Arctic Ocean net primary production. *J. Geophys. Res.* 116, C09011. doi: 10.1029/2011JC007151

Ashjian, C. J., Campbell, R. G., Gelfman, C., Alatalo, P., and Elliott, S. M. (2017). Mesozooplankton abundance and distribution in association with hydrography in the Hanna Shoal on Hanna Shoal, NE Chukchi Sea, during August 2012 and 2013. *Deep. Sea. Res. II.* 144, 21–36. doi: 10.1016/j.dsr2.2017.08.012

Ashjian, C. J., Campbell, R. G., Welch, H. E., Butler, M., and Van Keuren, D. (2003). Annual cycle in abundance, distribution, and size in relation to hydrography of important copepod species in the western Arctic Ocean. *Deep. Sea. Res. I.* 50, 1235–1261. doi: 10.1016/S0967-0637(03)00129-8

Ashjian, C. J., Pickart, R. S., Campbell, R. G., Feng, Z., Gelfman, C., Alatalo, P., et al. (2021). Springtime renewal of zooplankton populations in the Chukchi Sea. *Prog. Oceanogr.* 197, 102635. doi: 10.1016/j.pocean.2021.102635

Banas, N. S., Møller, E. F., Nielsen, T. G., and Eisner, L. B. (2016). Copepod life strategy and population viability in response to prey timing and temperature: Testing a new model across latitude, time, and size spectrum. *Front. Mar. Sci.* 3. doi: 10.3389/fmars.2016.00225

Bengtson, J. L., Hiruki-Raring, L. M., Simpkins, M. A., and Boveng, P. L. (2005). Ringed and bearded seal densities in the eastern Chukchi Sea (1999–2000. *Polar. Biol.* 28, 833–845. doi: 10.1007/s00300-005-0009-1

Bourgain, P., and Gascard, J. C. (2012). The Atlantic and summer Pacific waters variability in the Arctic Ocean from 1997 to 2008. *Geophys. Res. Lett.* 39, L05603. doi: 10.1029/2012GL051045

Brodsky, K. A. (1967). Calanoida of the far eastern seas and polar basin of the USSR. *Keys. to Fauna. USSR.* 35, 1–442.

Budge, S. M., and Parrish, C. C. (1998). Lipid biogeochemistry of plankton, settling matter and sediments in Trinity Bay, Newfoundland. II. Fatty acids. *Org. Geochem.* 29, 1547–1559. doi: 10.1016/S0146-6380(98)00177-6

Campbell, R. G., Sherr, E. B., Ashjian, C. J., Plourde, S., Sherr, B. F., Hill, V., et al. (2009). Mesozooplankton prey preferences and grazing impact in the western Arctic Ocean. *Deep. Sea. Res. II.* 56, 1274–1289. doi: 10.1016/j.dsr2.2008.10.027

Carmack, E. C., and Kulikov, E. A. (1998). Wind-forced upwelling and internal Kelvin wave generation in Mackenzie Canyon, Beaufort Sea. *J. Geophys. Res.* 103, 18447–18458. doi: 10.1029/98JC00113

Choquet, M., Kosobokova, K. N., Kwaśniewski, S., Hatlebakk, M., Dhanasiri, A. K. S., Melle, W., et al. (2018). Can morphology reliably distinguish between the copepods *Calanus finmarchicus* and *C. glacialis*, or is DNA the only way? *Limnol. Oceanogr. Methods* 16, 237–252. doi: 10.1002/lom3.10240

Codispoti, L. A., Kelly, V., Thessen, A., Matrai, P., Suttles, S., Hill, V., et al. (2013). Synthesis of primary production in the Arctic Ocean: III. Nitrate and phosphate based estimates of the net community production. *Prog. Oceanogr.* 110, 126–150. doi: 10.1016/j.pocean.2012.11.006

Conover, R. J. (1988). Comparative life histories in the genera *Calanus* and *Neocalanus* in high latitudes of the northern hemisphere. *Hydrobiologia* 167–168, 127–142. doi: 10.1007/BF00026299

Conover, R. J., and Huntley, M. (1991). Copepods in ice-covered seas—Distribution, adaptations to seasonally limited food, metabolism, growth patterns and life cycle strategies in polar seas. *J. Mar. Syst.* 2, 1–41. doi: 10.1016/0924-7963(91)90011-I

Corkett, C. J., and McLaren, I. A. (1978). The biology of *Pseudocalanus*. *Adv. Mar. Biol.* 15, 1–231. doi: 10.1016/S0065-2881(08)60404-6

Corkett, C. J., McLaren, I. A., and Sevigny, J.-M. (1986). Rearing of the marine Calanoid Copepods *Calanus finmarchicus* (Gunnerus), *C. glacialis* Jaschnov, and *C. hyperboreus* Kroyer with comments on the equiproportional rule. *Syllogeus* 58, 539–546.

Crawford, R. E., Vagle, S., and Carmack, E. C. (2012). Water mass and bathymetric characteristics of polar cod habitat along the continental shelf and slope of the Beaufort and Chukchi seas. *Polar. Biol.* 35, 179–190. doi: 10.1007/s00300-011-1051-9

Daase, M., Falk-Petersen, S., Varpe, Ø., Darnis, G., Søreide, J. E., Wold, A., et al. (2013). Timing of reproductive events in the marine copepod *Calanus glacialis*: A pan-Arctic perspective. *Can. J. Fish. Aquat. Sci.* 70, 871–884. doi: 10.1139/cjfas-2012-0401

Dalsgaard, J., St John, M., Kattner, G., Müller-Navarra, D., and Hagen, W. (2003). Fatty acid trophic markers in the pelagic marine environment. *Adv. Mar. Biol.* 46, 225–340. doi: 10.1016/s0065-2881(03)46005-7

Danielson, S. L., Ahkinga, O., Ashjian, C., Basyuk, E., Cooper, L. W., Eisner, L., et al. (2020). Manifestation and consequences of warming and altered heat fluxes over the Bering and Chukchi Sea continental shelves. *Deep. Sea. Res. II.* 177, 104781. doi: 10.1016/j.dsr2.2020.104781

Deevey, G. B. (1960). Relative effects of temperature and food on seasonal variations in the lengths of marine copepods in eastern American and Western European waters. *Bull. Bing. Oceanogr. Coll.* 17, 54–86.

Dickson, D. L., and Gilchrist, H. G. (2002). Status of marine birds of the southeastern Beaufort Sea. *Arctic* 55, 46–58. doi: 10.14430/arctic734

Digby, P. S. B. (1954). Biology of marine planktonic copepods of Scores by Sound, east Greenland. *J. Anim. Ecol.* 23, 298–338. doi: 10.2307/1984

El-Sabaawi, R., Dower, J. F., Kainz, M., and Mazumder, A. (2009). Characterizing dietary variability and trophic positions of coastal calanoid copepods: Insight from stable isotopes and fatty acids. *Mar. Biol.* 156, 225–237. doi: 10.1007/s00227-008-1073-1

Ershova, E. A., Hopcroft, R. R., and Kosobokova, K. N. (2015). Inter-annual variability of summer mesozooplankton communities of the western Chukchi Sea: 2004–2012. *Polar. Biol.* 38, 1461–1481. doi: 10.1007/s00300-015-1709-9

Ershova, E. A., Kosobokova, K. N., Banas, N. S., Ellingsen, I., Niehoff, B., Hildebrandt, N., et al. (2021). Sea ice decline drives biogeographical shifts of key *Calanus* species in the central Arctic Ocean. *Glob. Change Biol.* 27, 2128–2143. doi: 10.1111/gcb.15562

Falkenhaug, T., Tande, K. S., and Semenova, T. (1997). Diel, seasonal and ontogenetic variations in the vertical distribution of four marine copepods. *Mar. Ecol. Prog. Ser.* 149, 105–119. doi: 10.3354/meps149105

Falk-Petersen, S., Leu, E., Berge, J., Kwasniewski, S., Nygård, H., Røstad, A., et al. (2008). Vertical migration in high Arctic waters during autumn 2004. *Deep. Sea. Res. II.* 55, 2275–2284. doi: 10.1016/j.dsr2.2008.05.010

Falk-Petersen, S., Mayzaud, P., Kattner, G., and Sargent, J. R. (2009). Lipids and life strategy of Arctic *Calanus*. *Mar. Biol. Res.* 5, 18–39. doi: 10.1080/17451000802512267

Freese, D., Søreide, J. E., and Niehoff, B. (2016). A year-round study on digestive enzymes in the Arctic copepod *Calanus glacialis*: Implications for its capability to adjust to changing environmental conditions. *Polar. Biol.* 39, 2241–2252. doi: 10.1007/s00300-016-1891-4

Frost, B. W. (1974). *Calanus marshallae*, a new species of calanoid copepod closely aligned to the sibling species *C. finmarchicus* and *C. glacialis*. *Mar. Biol.* 26, 77–99. doi: 10.1007/BF00389089

Gabrielsen, T. M., Merkel, B., Søreide, J. E., Johansson-Karlsson, E., Bailey, A., Vogedes, D., et al. (2012). Potential misidentifications of two climate indicator species of the marine arctic ecosystem: *Calanus glacialis* and *C. finmarchicus*. *Polar. Biol.* 35, 1621–1628. doi: 10.1007/s00300-012-1202-7

Grainger, E. H. (1961). The copepods *Calanus glacial* is Jaschnov and *Calanus finmarchicus* (Gunnerus) in Canadian Arctic-Subarctic Waters. *J. Fish. Res. Board. Can.* 18, 663–678. doi: 10.1139/f61-051

Grebmeier, J. M., Cooper, L. W., Feder, H. M., and Sirenko, B. I. (2006). Ecosystem dynamics of the pacific-influenced northern bering and chukchi seas in the amerasian arctic. *Prog. Oceanogr.* 71, 331–361. doi: 10.1016/j.pocean.2006.10.001

Hama, N., Abe, Y., Matsuno, K., and Yamaguchi, A. (2019). Effect of net mesh size on filtering efficiency and zooplankton sampling efficiency using quad-NORPAC net. *Bull. Fish. Sci. Hokkaido. Univ.* 69, 47–56. doi: 10.14943/bull.fish.69.1.47

Herberich, E., Sikorski, J., and Hothorn, T. (2010). A Robust procedure for comparing multiple means under heteroscedasticity in unbalanced designs. *PloS One* 5, e9788. doi: 10.1371/journal.pone.0009788

Hill, V., and Cota, G. (2005). Spatial patterns of primary production on the shelf, slope and basin of the western Arctic in 2002. *Deep. Sea. Res. II.* 52, 3344–3354. doi: 10.1016/j.dsr2.2005.10.001

Hirche, H.-J. (1991). Distribution of dominant calanoid copepod species in the Greenland Sea during late fall. *Polar. Biol.* 11, 351–362. doi: 10.1007/BF00239687

Hirst, A. G., and Kiørboe, T. (2002). Mortality of marine planktonic copepods: Global rates and patterns. *Mar. Ecol. Prog. Ser.* 230, 195–209. doi: 10.3354/meps230195

Hopcroft, R. R., Clarke, C., Nelson, R. J., and Raskoff, K. A. (2005). Zooplankton communities of the Arctic Canada Basin: The contribution by smaller taxa. *Polar. Biol.* 28, 198–206. doi: 10.1007/s00300-004-0680-7

Jakobsen, H. H., and Hansen, P. J. (1997). Prey size selection, grazing and growth response of the small heterotrophic dinoflagellate *Gymnodinium* sp. and ciliate *Balanion comatum*: A comparative study. *Mar. Ecol. Prog. Ser.* 158, 75–86. doi: 10.3354/meps158075

Ji, R., Ashjian, C. J., Campbell, R. G., Chen, C., Gao, G., Davis, C. S., et al. (2012). Life history and biogeography of Calanus copepods in the Arctic Ocean: An individual-based modeling study. *Prog. Oceanogr.* 96, 40–56. doi: 10.1016/j.pocean.2011.10.001

Kaneda, T. (1991). Iso- and anteiso-fatty acids in bacteria: Biosynthesis, function, and taxonomic significance. *Microbiol. Rev.* 55, 288–302. doi: 10.1128/mr.55.2.288-302.1991

Kimura, F., Matsuno, K., Abe, Y., and Yamaguchi, A. (2022). Effects of early sea-ice reduction on zooplankton and copepod population structures in the Northern Bering Sea during the summers of 2017 and 2018. *Front. Mar. Sci.* 9. doi: 10.3389/fmars.2022.808910

Kobari, T., Tadokoro, K., Shiomoto, A., and Hashimoto, S. (2003). Geographical variation in prosome length and body weight of *Neocalanus* copepods in the North Pacific. *J. Oceanogr.* 59, 3–10. doi: 10.1023/A:1022895802468

Kosobokova, K. N. (1999). The reproductive cycle and life history of the Arctic copepod *Calanus glacialis* in the White Sea. *Polar. Biol.* 22, 254–263. doi: 10.1007/s003000050418

Kosobokova, K. N., and Hirche, H.-J. (2009). Biomass of zooplankton in the eastern Arctic Ocean: A baseline study. *Prog. Oceanogr.* 82, 265–280. doi: 10.1016/j.pocean.2009.07.006

Kosobokova, K. N., and Hopcroft, R. R. (2010). Diversity and vertical distribution of mesozooplankton in the Arctic's Canada Basin. *Deep. Sea. Res. II.* 57, 96–110. doi: 10.1016/j.dsr2.2009.08.009

Lane, P. V. Z., Llinás, L., Smith, S. L., and Pilz, D. (2008). Zooplankton distribution in the western Arctic during summer 2002: Hydrographic habitats and implications for food chain dynamics. *J. Mar. Syst.* 70, 97–133. doi: 10.1016/j.jmarsys.2007.04.001

Levinsen, H., and Nielsen, T. G. (2002). The trophic role of marine pelagic ciliates and heterotrophic dinoflagellates in arctic and temperate coastal ecosystems: A cross-latitude comparison. *Limnol. Oceanogr.* 47, 427–439. doi: 10.4319/lo.2002.47.2.0427

Llinás, L., Pickart, R. S., Mathis, J. T., and Smith, S. L. (2009). Zooplankton inside an Arctic Ocean cold-core eddy: Probable origin and fate. *Deep. Sea. Res. II.* 56, 1290–1304. doi: 10.1016/j.dsr2.2008.10.020

Mackas, D., and Bohrer, R. (1976). Fluorescence analysis of zooplankton gut contents and an investigation of diel feeding patterns. *J. Exp. Mar. Biol. Ecol.* 25, 77–85. doi: 10.1016/0022-0981(76)90077-0

Marin, V. (1987). The oceanographic structure of the eastern Scotia sea—IV. Distribution of copepod species in relation to hydrography in 1981. *Deep. Sea. Res. Part A. Oceanographic. Res. Papers.* 34, 105–121. doi: 10.1016/0198-0149(87)90125-7

Matsumoto, Y., Ando, Y., Hiraoka, Y., Tawa, A., and Ohshimo, S. (2018). A simplified gas chromatographic fatty-acid analysis by the direct saponification/methylation procedure and its application on wild tuna larvae. *Lipids* 53, 919–929. doi: 10.1002/lipd.12098

Matsuno, K., Abe, Y., Yamaguchi, A., and Kikuchi, T. (2016). Regional patterns and controlling factors on summer population structure of *Calanus glacialis* in the western Arctic Ocean. *Polar. Sci.* 10, 503–510. doi: 10.1016/j.polar.2016.09.001

Matsuno, K., Yamaguchi, A., Hirawake, T., and Imai, I. (2011). Year-to-year changes of the mesozooplankton community in the Chukchi Sea during summers of 1991, 1992 and 2007, 2008. *Polar. Biol.* 34, 1349–1360. doi: 10.1007/s00300-011-0988-z

Matsuno, K., Yamaguchi, A., Nishino, S., Inoue, J., and Kikuchi, T. (2015). Short-term changes in the mesozooplankton community and copepod gut pigment in the Chukchi Sea in autumn: Reflections of a strong wind event. *Biogeosciences* 12, 4005–4015. doi: 10.5194/bg-12-4005-2015

McLaren, I. A., Sevigny, J.-M., and Corkett, J. (1988). Body size, development rate, and genome size of *Calanus* species in *Dev. Hydrobiol.*, eds G. A. Boxshall and H. K. Schminke. *Biol. Copepods.* 47, 275–284. doi: 10.1007/978-94-009-3103-9_27

Miller, C. B., Frost, B. W., Batchelder, H. P., Clemons, M. J., and Conway, R. E. (1984). Life histories of large, grazing copepods in a subarctic ocean gyre *Neocalanus plumchrus*, *Neocalanus cristatus*, and *Eucalanus bungii* in the northeast Pacific. *Prog. Oceanogr.* 13, 201–243. doi: 10.1016/0079-6611(84)90009-0

Motoda, S. (1959). Device for a simple plankton apparatus. *Mem. Fac. Fish. (Hokkaido. Univ.)* 7, 73–94.

Mundy, P. R., Ingvaldsen, R., and Sunnanå, K. (2017) *Synthesis of knowledge on fisheries science in the central Arctic Ocean and adjacent waters (ToR1) in Final report of the Fourth Meeting of Scientific Experts on Fish Stocks in the Central Arctic Ocean, FiSCAO*, (NOAA). 34–79.

Muramatsu, M., Ueno, H., Watanabe, E., Itoh, M., and Onodera, J. (2021). Transport and heat loss of the Pacific Summer Water in the Arctic Chukchi Sea northern slope: Mooring data analysis. *Polar. Sci.* 29, 100698. doi: 10.1016/j.polar.2021.100698

Nelson, R. J., Carmack, E. C., McLaughlin, F. A., and Cooper, G. A. (2009). Penetration of Pacific zooplankton into the western Arctic Ocean tracked with

molecular population genetics. *Mar. Ecol. Prog. Ser.* 381, 129–138. doi: 10.3354/meps07940

Niehoff, B. (1998). The gonad morphology and maturation in Arctic *Calanus* species. *J. Mar. Syst.* 15, 53–59. doi: 10.1016/S0924-7963(97)00048-1

Nielsen, T. G., Kjellerup, S., Smolina, I., Hoarau, G., and Lindeque, P. (2014). Live discrimination of *Calanus glacialis* and *C. finmarchicus* females: Can we trust phenological differences? *Mar. Biol.* 161, 1299–1306. doi: 10.1007/s00227-014-2419-5

Nishino, S., Kawaguchi, Y., Inoue, J., Hirawake, T., Fujiwara, A., Futsuki, R., et al. (2015). Nutrient supply and biological response to wind-induced mixing, inertial motion, internal waves, and currents in the northern Chukchi Sea. *J. Geophys. Res. Oceans.* 120, 1975–1992. doi: 10.1002/2014JC010407

Parent, G. J., Plourde, S., and Turgeon, J. (2011). Overlapping size ranges of *Calanus* spp. off the Canadian Arctic and Atlantic Coasts: Impact on species' abundances. *J. Plankton. Res.* 33, 1654–1665. doi: 10.1093/plankt/fbr072

Peterson, W. (1986). Development, growth, and survivorship of the copepod *Calanus marshallae* in the laboratory. *Mar. Ecol. Prog. Ser.* 29, 61–72. doi: 10.3354/meps029061

Pickart, R. S., Schulze, L. M., Moore, G. W. K., Charette, M. A., Arrigo, K. R., van Dijken, G., et al. (2013). Long-term trends of upwelling and their impacts on primary productivity in the Alaskan Beaufort Sea. *Deep. Sea. Res. I.* 79, 106–121. doi: 10.1016/j.dsr.2013.05.003

Pickart, R. S., Weingartner, T. J., Pratt, L. J., Zimmermann, S., and Torres, D. J. (2005). Flow of winter-transformed Pacific water into the western Arctic. *Deep. Sea. Res. II.* 52, 3175–3198. doi: 10.1016/j.dsr2.2005.10.009

Pinchuk, A. I., and Eisner, L. B. (2017). Spatial heterogeneity in zooplankton summer distribution in the eastern Chukchi Sea in 2012–2013 as a result of large-scale interactions of water masses. *Deep. Sea. Res. II.* 135, 27–39. doi: 10.1016/j.dsr2.2016.11.003

Plourde, S., Campbell, R. G., Ashjian, C. J., and Stockwell, D. A. (2005). Seasonal and regional patterns in egg production of *Calanus glacialis/marshallae* in the Chukchi and Beaufort Seas during spring and summe. *Deep. Sea. Res. II.* 52, 3411–3426. doi: 10.1016/j.dsr2.2005.10.013

Pomeroy, L. R. (1974). The ocean food web: A changing paradigm. *BioScience* 24, 499–504. doi: 10.2307/1296885

R Core Team (2021). *R: a language and environment for statistical computing*. Vienna, Austria: R Foundation for Statistical Computing. Available at: https://www.R-project.org/.

Runge, J. A., and Ingram, R. G. (1991). Under-ice feeding and diel migration by the planktonic copepods *Calanus glacialis* and *Pseudocalanus minutus* in relation to the ice algal production cycle in southeastern Hudson Bay, Canada. *Mar. Biol.* 108, 217–225. doi: 10.1007/BF01344336

Rutzen, I., and Hopcroft, R. R. (2018). Abundance, biomass and community structure of epipelagic zooplankton in the Canada Basin. *J. Plankton. Res.* 40, 486–499. doi: 10.1093/plankt/fby028

Scott, C. L., Kwasniewski, S., Falk-Petersen, S., and Sargent, J. R. (2000). Lipids and life strategies of *Calanus finmarchicus*, *Calanus glacialis* and *Calanus hyperboreus* in late autumn, Kongsfjorden, Svalbard. *Polar. Biol.* 23, 510–516. doi: 10.1007/s003000000114

Skjoldal, H. R. (Ed.) (2022). "Ecosystem assessment of the Central Arctic Ocean: Description of the ecosystem," in *ICES cooperative research reports*. 355, 341. doi: 10.17895/ices.pub.20191787

Søreide, J. E., Falk-Petersen, S., Hegseth, E. N., Hop, H., Carroll, M. L., Hobson, K. A., et al. (2008). Seasonal feeding strategies of *Calanus* in the high-Arctic Svalbard region. *Deep. Sea. Res. II.* 55, 2225–2244. doi: 10.1016/j.dsr2.2008.05.024

Stevens, C. J., Deibel, D., and Parrish, C. C. (2004a). Species-specific differences in lipid composition and omnivory indices in Arctic copepods collected in deep water during autumn (North water Polynya). *Mar. Biol.* 144, 905–915. doi: 10.1007/s00227-003-1259-5

Stevens, C. J., Deibel, D., and Parrish, C. C. (2004b). Incorporation of bacterial fatty acids and changes in a wax ester-based omnivory index during a long-term inCubation experiment with Calanus glacialis Jaschnov. *J. Exp. Mar. Biol. Ecol.* 303, 135–156. doi: 10.1016/j.jembe.2003.11.008

Tourangeau, S., and Runge, J. A. (1991). Reproduction of Calanus glacialis under ice in spring in southeastern Hudson Bay, Canada. *Mar. Biol.* 108, 227–233. doi: 10.1007/BF01344337

Trudnowska, E., Balazy, K., Stoń-Egiert, J., Smolina, I., Brown, T., and Gluchowska, M. (2020). In a comfort zone and beyond—Ecological plasticity of key marine mediators. *Ecol. Evol.* 10, 14067–14081. doi: 10.1002/ece3.6997

Varpe, Ø., Jørgensen, C., Tarling, G. A., and Fiksen, Ø. (2009). The adaptive value of energy storage and capital breeding in seasonal environments. *Oikos* 118, 363–370. doi: 10.1111/j.1600-0706.2008.17036.x

Vidal, J. (1980). Physioecology of zooplankton. II. Effects of phytoplankton concentration, temperature, and body size on the development and molting rates of *Calanus pacificus* and Pseudocalanus sp. *Mar. Biol.* 56, 135–146. doi: 10.1007/BF00397130

Vidal, J., and Smith, S. L. (1986). Biomass, growth, and development of populations of herbivorous zooplankton in the southeastern Bering Sea during spring. *Deep. Sea. Res. Part A. Oceanographic. Res. Papers.* 33, 523–556. doi: 10.1016/0198-0149(86)90129-9

Viitasalo, M., Koski, M., Pellikka, K., and Johansson, S. (1995). Seasonal and long-term variations in the body size of planktonic copepods in the northern Baltic Sea. *Mar. Biol.* 123, 241–250. doi: 10.1007/BF00353615

Wassmann, P., Kosobokova, K. N., Slagstad, D., Drinkwater, K. F., Hopcroft, R. R., Moore, S. E., et al. (2015). The Contiguous domains of Arctic Ocean advection: Trails of life and death. *Prog. Oceanogr.* 139, 42–65. doi: 10.1016/j.pocean.2015.06.011

Watanabe, E., Onodera, J., Harada, N., Honda, M. C., Kimoto, K., Kikuchi, T., et al. (2014). Enhanced role of eddies in the Arctic marine biological pump. *Nat. Commun.* 5, 3950. doi: 10.1038/ncomms4950

Woodgate, R. A. (2018). Increases in the Pacific inflow to the Arctic from 1990 to 2015, and insights into seasonal trends and driving mechanisms from year-round Bering Strait mooring data. *Prog. Oceanogr.* 160, 124–154. doi: 10.1016/j.pocean.2017.12.007

Woodgate, R., and Peralta-Ferriz, C. (2021). Warming and freshening of the Pacific inflow to the Arctic from 1990–2019 implying dramatic shoaling in Pacific winter water ventilation of the Arctic water column. *Geophys. Res. Lett.* 48, e2021GL092528. doi: 10.1029/2021GL092528

Yeh, H. D., Questel, J. M., Maas, K. R., and Bucklin, A. (2020). Metabarcoding analysis of regional variation in the gut contents of the copepod *Calanus finmarchicus* in the North Atlantic Ocean. *Deep. Sea. Res. II.* 180, 104738. doi: 10.1016/j.dsr2.2020.104738

frontiers | Frontiers in Marine Science

TYPE Brief Research Report
PUBLISHED 26 October 2023
DOI 10.3389/fmars.2023.1240673



OPEN ACCESS

EDITED BY
Guang Yang,
Chinese Academy of Sciences (CAS), China

REVIEWED BY
William Froneman,
Rhodes University, South Africa
Peter Thor,
Swedish University of Agricultural Sciences, Sweden

*CORRESPONDENCE
Nadjejda Espinel-Velasco
nadjejda.espinel@gu.se

†PRESENT ADDRESS
Nadjejda Espinel-Velasco,
Department of Marine Sciences, Tjärnö Marine Laboratory, University of Gothenburg, Strömstad, Sweden
Doreen Kohlbach,
Department of Arctic and Marine Biology, Faculty of Biosciences, Fisheries and Economics, UiT The Arctic University of Norway, Tromsø, Norway
Vanessa Pitusi,
The Arctic University Museum of Norway (UMAK), UiT The Arctic University of Norway, Tromsø, Norway

RECEIVED 15 June 2023
ACCEPTED 12 October 2023
PUBLISHED 26 October 2023

CITATION
Espinel-Velasco N, Gawinski C, Kohlbach D, Pitusi V, Graeve M and Hop H (2023) Interactive effects of ocean acidification and temperature on oxygen uptake rates in *Calanus hyperboreus* nauplii. *Front. Mar. Sci.* 10:1240673. doi: 10.3389/fmars.2023.1240673



# Interactive effects of ocean acidification and temperature on oxygen uptake rates in *Calanus hyperboreus* nauplii

Nadjejda Espinel-Velasco[1*†], Christine Gawinski[2], Doreen Kohlbach[1†], Vanessa Pitusi[3†], Martin Graeve[4] and Haakon Hop[1]

[1]Norwegian Polar Institute, Fram Centre, Tromsø, Norway, [2]Department of Arctic and Marine Biology, Faculty of Biosciences, Fisheries and Economics, UiT The Arctic University of Norway, Tromsø, Norway, [3]Department of Arctic Biology, The University Centre in Svalbard (UNIS), Longyearbyen, Norway, [4]Ecological Chemistry, Alfred-Wegener Institute Helmholtz Centre for Polar and Marine Research, Bremerhaven, Germany

The Arctic region is undergoing rapid and significant changes, characterized by high rates of acidification and warming. These transformations prompt critical questions about the resilience of marine communities in the face of environmental change. In the Arctic, marine zooplankton and in particular calanoid copepods play a vital role in the food web. Changes in environmental conditions could disrupt zooplankton communities, posing detrimental consequences for the entire ecosystem. Copepod early-life stages have been shown to be particularly sensitive to environmental stressors since they represent a bottleneck in the life cycle. Here, we investigated the responses of 4-day old *Calanus hyperboreus* nauplii when exposed to acidification (pH 7.5 and 8.1) and warming (0 and 3°C), both independently and in combination. Naupliar respiration rates increased when exposed to a combination of acidification and warming, but not when exposed to the stressors individually. Moreover, we found no discernible differences in lipid content and fatty acid (FA) composition of the nauplii across the different experimental treatments. Wax esters accounted for approximately 75% of the lipid reserves, and high amounts of long chain fatty acids 20:1 and 22:1, crucial for the reproduction cycle in copepods, were also detected. Our results indicate a sensitivity of these nauplii to a combination of acidification and warming, but not to the individual stressors, aligning with a growing body of evidence from related studies. This study sheds light on the potential implications of global change for Arctic copepod populations by elucidating the responses of early-life stages to these environmental stressors.

KEYWORDS

**Arctic copepods, early-life stages, metabolism, energy reserves, Barents Sea, environmental drivers, climate change, The Nansen Legacy**

# 1 Introduction

The Arctic region is rapidly changing, experiencing the highest rates of ocean acidification (OA) and warming on a global scale (AMAP, 2018). The occurrence of these environmental stressors frequently amplifies the impact of pre-existing pressures in the region, such as fluctuations in salinity or the discharge of environmental contaminants (Gunderson et al., 2016; AMAP, 2021). The physical changes resulting from acidification, solar radiation and warming can trigger changes in natural marine communities (e.g. changes in community composition, altered recruitment processes), potentially leading to cascading effects at the ecosystem level. In the Arctic region, many studies investigating the impact of climate change on ecosystem structure and functioning have focused on coastal ecosystems around Svalbard (Hop et al., 2019a, Hop et al., 2019b), as these areas experience the greatest variability in physical parameters. However, fewer studies have examined the responses of open-ocean organisms in Arctic waters to environmental changes (Ramondenc et al., 2022).

In the Arctic, marine zooplankton are a crucial element of the food web, connecting primary producers and predators, and any changes in their community composition and biology could have far-reaching consequences for the energy flow towards higher trophic levels (Falk-Petersen et al., 2007). Arctic copepods represent a critical food source for carnivorous zooplankton and fish, such as polar cod (*Boreogadus saida*), capelin (*Mallotus villosus*) and Arctic char (*Salvelinus alpinus*), and seabirds such as little auk (*Alle alle*)(Karnovsky et al., 2003; Falk-Petersen et al., 2007; Hop and Gjøsæter, 2013). The predominantly herbivorous copepods of the genus *Calanus* dominate the zooplankton biomass in the Arctic (Falk-Petersen et al., 2009; Daase et al., 2021). *Calanus hyperboreus* is the most important zooplankton species in terms of biomass in the Central Arctic Ocean (CAO, Ershova et al., 2021), although it is also present in marginal seas, such as the northern Barents Sea.

To endure the characteristic prolonged periods of food limitation associated with the Polar Night, Arctic copepods can undergo seasonal vertical migrations (diapause) and have multi-year life cycles (Daase et al., 2021). Successful reproduction of *C. hyperboreus* depends on energy reserves that the females pass onto their offspring via egg development. This species is a capital breeder, meaning that it relies entirely on its internal lipid reserves to fuel its reproduction (Falk-Petersen et al., 2009; Varpe, 2012). *Calanus hyperboreus* accumulates sufficient lipid stores to overwinter and can reproduce during winter, independent of the ice-algae and phytoplankton spring blooms (Hirche, 1997; Halvorsen, 2015; Daase et al., 2021). Egg production can occur from November to May (Halvorsen, 2015). At hatching, nauplii rely on stored lipid energy reserves to cover their metabolic costs during non-feeding stages (nauplii I to II) and will utilize the spring or summer blooms for growth and further development once these become available (Falk-Petersen et al., 2009; Jung-Madsen et al., 2013).

Early-life stages of marine invertebrates are known to be particularly vulnerable to environmental changes, and any impacts on these stages can have significant consequences for entire populations (Byrne, 2011). To fully comprehend the fate of marine ecosystems under future scenarios of change, it is crucial to understand how early-life stages respond to environmental stressors (Byrne, 2012). In the Arctic, changes in environmental parameters could alter the conditions that *C. hyperboreus* nauplii encounter after hatching, with potentially negative consequences for their survival. This could happen either directly, through changes in larval physiology or metabolism, or indirectly, through alterations in the timing and availability of their preferred food (Espinel-Velasco et al., 2018). This is especially important if changes in spring bloom phenology are expected in future scenarios (Falk-Petersen et al., 2007). Depletion of larval energy reserves prior to reaching feeding stages or before the food becomes available could change recruitment patterns, potentially leading to significant consequences for the ecology of the species. For example, *C. hyperboreus* nauplii from regions where the females overwinter at depths greater than 2000 m, such as the Fram Strait or the CAO, will need to actively swim upwards in order to reach the surface in time for the spring bloom (Jung-Madsen et al., 2013). Changes in metabolism or lipid energy reserves could compromise the timing of reaching the surface, potentially leading to adverse impacts on survival.

Arctic *Calanus* species have been the focus of numerous studies examining the effects of OA and warming on their physiology, including works by Lewis et al. (2013); Hildebrandt et al. (2014); Thor et al. (2016); Bailey et al. (2017a); Bailey et al. (2017b) and Thor et al. (2018). Although most research on calanoid copepods in the Arctic has focused on adult and late larval stages (CIV and CV), a few studies have explored the impacts of environmental stressors on naupliar stages and have indicated sensitivity to either acidification (Lewis et al., 2013) or warming (Jung-Madsen et al., 2013), individually, and only a handful of observations revealed interactive effects (e.g. warming and pyrene; Jortveit, 2022).

In this study, we conducted an exploratory assay to investigate the interactive effects of acidification, singularly and in combination with warming on 4-day old *C. hyperboreus* nauplii from females collected in the Barents Sea. We hypothesized that *C. hyperboreus* nauplii would be sensitive to both acidification and warming, and that this would be evident through altered respiration rates. To our knowledge, this is the first study investigating the responses of *C. hyperboreus* naupliar stages to multiple environmental stressors.

# 2 Materials and methods

## 2.1 Copepod collection and nauplii hatching

Mesozooplankton, including *C. hyperboreus*, was collected using a Bongo net (with opening 0.28 $m^2$ and mesh size 180 µm) equipped with a non-filtering cod end. During The Nansen Legacy seasonal cruise Q1 in March 2021, vertical net hauls were conducted at station P4 (79.75°N, 34.00°E) on the shelf (Figure 1), at a depth of ~300 m (bottom depth 332 m), as reported by Gerland et al. (2022). The collected samples were placed in a 60 L bucket filled with sea water acclimatized to the *in-situ* temperature. Gravid females of *C. hyperboreus* were carefully extracted from subsamples using tweezers and transferred into separate petri dishes filled with 15

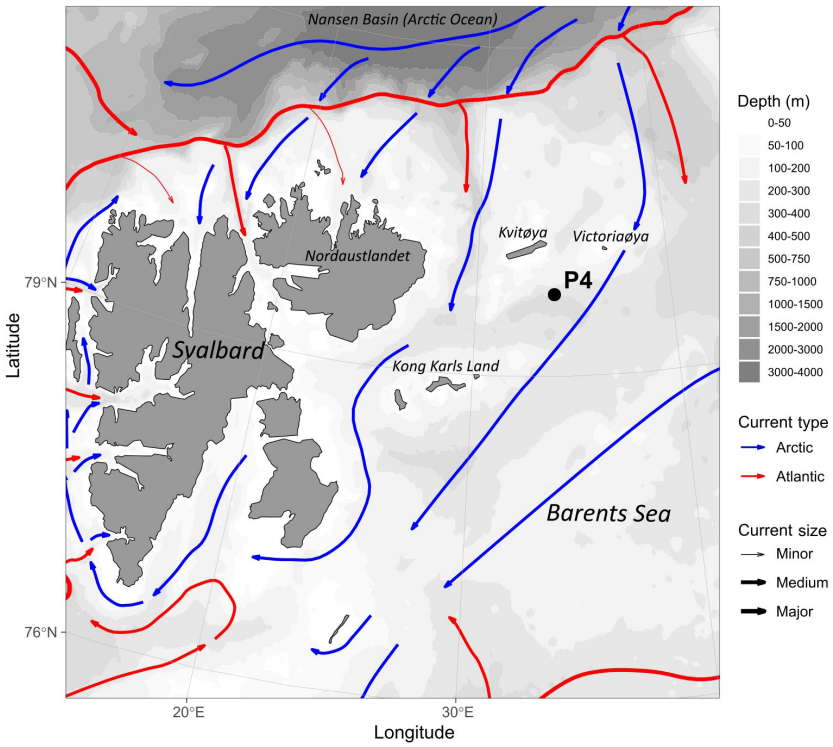


FIGURE 1
Location of the P4 station in the Barents Sea sampled during The Nansen Legacy seasonal cruise in March 2021, where *Calanus hyperboreus* females were collected for this study. The coloured lines indicate the type and direction of water masses (blue: Arctic; red: Atlantic), whereas the grey shadowing indicates depth. The current data were plotted in R using *GGOceanmaps* package and shapefiles from Natural Earth Data (Vihtakari et al., 2019; Vihtakari, 2022) and bathymetry data from NOAA (Amante and Eakins, 2009; NOAA, 2009).

mL of filtered seawater. These females were incubated in the dark for 10 days at 0°C. Every 48 h, half of the water in the petri dishes was replaced with filtered seawater at the same temperature. Eggs produced during the incubation period were counted every 24 h and transferred to new petri dishes until hatching (The Nansen Legacy, 2022). The nauplii hatched over a 4-day period were collected and pooled in a larger (2 L) glass jar with filtered seawater until the start of the incubation experiments. By that time, the nauplii were most likely N1 (with mean developmental time = 2.8 - 3.1 days, stage duration 2.3 - 2.5 days at 5°C; Jung-Madsen et al., 2013). The first two naupliar stages of *C. hyperboreus* do not feed, therefore no feeding took place prior to the start of the incubations. No abnormal nauplii were detected nor removed from the pool of larvae for the subsequent experiments.

## 2.2 Measurements of metabolic rates and closed-bottle incubations

Using the pool of hatched larvae, we conducted parallel measurements of metabolic rates as well as short-term bottle incubations to test the responses of the nauplii to acidification and warming. The experimental treatments consisted of a full factorial combination of pH and temperature as follows: i) low pH (7.5) + low/ambient temperature (0°C), ii) high/ambient pH (8.1) + low/ambient temperature (0°C), iii) low pH (7.5) + high temperature (3°C), iv) high/ambient pH (8.1) + high temperature (3°C). The pH treatments were achieved by manually introducing gaseous $CO_2$ into filtered seawater and corrected with filtered seawater at ambient pH until reaching the desired pH for each of the target temperatures, previously to introducing the larvae. Salinity, pH and temperature were manually checked with a handheld probe (Hanna pH meter HI98191).

To measure metabolic rates, 240 randomly-selected individuals were chosen from the pool of hatched nauplii. Respiration measurements were conducted using the Loligo® Microplate Respirometry System (MicroPlate™ software version 1.0.4) with 24 × 500 µL multiwell plates (Loligo Systems, Denmark). The plates were previously calibrated with filtered (0.2 µm) seawater at the target temperature and salinity 34. Calibration was carried out using water supersaturated in oxygen (100% $O_2$ air-saturation content) and water depleted of $O_2$ through the addition of sodium sulphite (0% air saturation). For the measurements, three nauplii were introduced into each well with water at the target treatment by means of a small pipette. Four wells in each plate served as a control, containing only filtered seawater, to calculate the background rate. The metabolic rate measurements were performed in the dark in incubators at a constant target temperature (0°C or 3°C) for 12 h. After measuring the metabolic rates, we visually inspected nauplii from each plate (treatment) for survival based on movement.

For the incubation assay we randomly selected 1440 nauplii from the pool of hatched individuals. Short-term incubations were conducted in triplicate using 200 mL brown glass bottles,

representing one of the four experimental treatments. Nauplii were added to each replicate at a density of ~0.6 ind. $mL^{-1}$. The bottles were kept in the dark in incubators at the target temperature for 24 h. After the incubation, all larvae from each treatment were extracted and checked for survival, and the remaining individuals were stored in Eppendorf tubes, freeze-dried, and kept at -80°C for lipid content analysis. To assess their body condition (*i.e.*, level of stored lipids), the lipid content and fatty acid composition of the copepod nauplii were analyzed at the Alfred Wegener Institute in Bremerhaven, Germany (see Supplementary Material and supporting data: 10.21334/npolar.2023.edc957ac; Espinel-Velasco et al., 2023a). The relative proportions of wax esters (main storage lipids of *Calanus* spp.) were estimated from the relation of fatty acids to fatty alcohols.

## 2.3 Statistical analyses

Data visualization and statistical analyses were performed with R v. 4.0.3. and RStudio v.1.4.1103 (R Core Team, 2021). The analysis and calculation of the metabolic rates were performed using the RespR package (Harianto et al., 2019). The main effects and interactions of pH and temperature on naupliar respiration were tested with a two-way ANOVA followed by a *post-hoc* Tukey's test ($p < 0.05$ was considered significant). The Levene's test was used to test for homogeneity of variances (conditions met).

# 3 Results

Individual naupliar respiration rates ranged from 0.055 $ngO_2$ $ind.^{-1}$ $h^{-1}$ (low pH and low temperature treatment) to 11.37 $ngO_2$ $ind.^{-1}$ $h^{-1}$ (low pH and high temperature treatment; Figure 2 and supporting data 10.21334/npolar.2023.ece3e9bb; Espinel-Velasco et al., 2023b).

Individual naupliar respiration rates were not significantly influenced by pH (F1 = 0.799, $p$ = 0.374) or temperature alone (F1 = 1.352, $p$ = 0.248). The statistical analyses point towards a significant effect of the interaction of both factors in the observed respiration rates (F1 = 8.784, $p$ = 0.004). Metabolic rates measured in nauplii kept at pH 7.5 and 3°C were significantly higher compared to their counterparts in 0°C ($p$ = 0.023) and their counterparts in pH 8.1 and 3°C ($p$ = 0.038).

# 4 Discussion

The results of our investigation indicated increased respiration rates of *C. hyperboreus* nauplii when exposed to a combination of warming and acidification, but not when exposed to the stressors individually. This suggests a sensitivity to the interactive effect while being more resilient to each of the stressors alone. To our knowledge, very few studies investigate the responses of early naupliar stages of Arctic *Calanus* copepods to multiple stressors. While there have been some investigations on the effects of acidification (Lewis et al., 2013; Bailey et al., 2017b) or temperature (Jung-Madsen et al., 2013) on nauplii, there is a scarcity of studies that look at the effect of multiple stressors on these nauplii.

The responses of calanoid copepods to ocean acidification appear to be dependent on the taxa and life-stage (Wang et al., 2018). For example, hatching rates in *Acartia steueri* and *Acartia erythraea* decrease following an exposure to OA (Kurihara et al.,

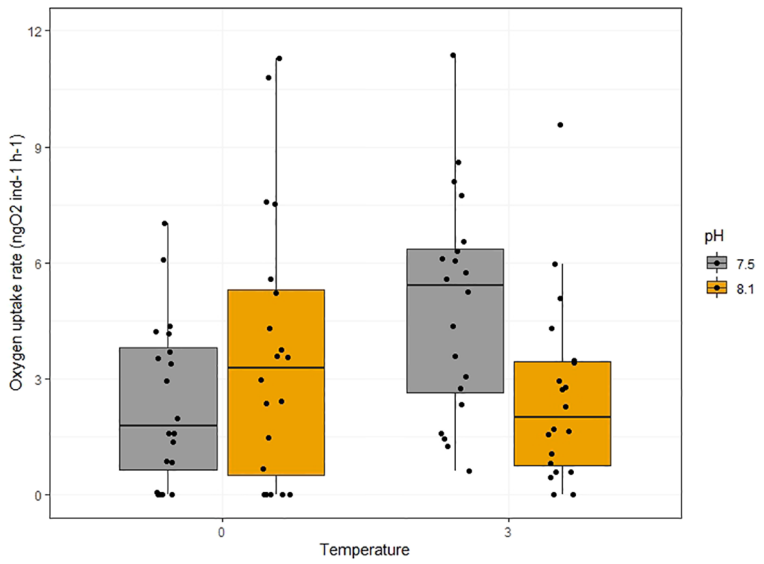


FIGURE 2
Individual oxygen uptake rates of *Calanus hyperboreus* nauplii (in $ngO_2$ $h^{-1}$) relative to the pH (colors) and water temperature (°C). The box-and-whisker plot displays the median (horizontal bar), interquartile range (box), and minimum/maximum values excluding outliers (whiskers). Outliers were defined as values beyond 1.5 times the interquartile range. The sample size was n = 240. The individual data points have been added on top of the boxplots and have been slightly offset for clarity.

2004), while vertically migrating adult *Calanus* spp. seem to be only marginally affected by high $pCO_2$ (Lewis et al., 2013). In *Calanus finmarchicus* females, OA did not affect egg production or cause biomass loss, but impacted naupliar hatching rate (Mayor et al., 2007). Studies focusing on *Calanus glacialis* have shown that ocean acidification increases metabolic rates and decreases ingestion rates in copepodite stage IV, but not in stage V (390 and 3000 µatm $pCO_2$, Hildebrandt et al., 2014; ~ 800 µatm $pCO_2$, Thor et al., 2016). In contrast, in *C. glacialis* females, no negative responses have been shown on metabolic rates, gonad maturation rate, or mortality after long term incubations (several months at 390 and 3000 µatm $pCO_2$; Hildebrandt et al., 2014). However, OA can cause delayed hatching and reduced overall hatching success, although egg production remains unchanged (pH ~ 6.9, Weydmann et al., 2012).

Increased temperatures can also have various effects on calanoid copepods, including altered fecundity (5 to 25°C; Hirst and Kiørboe, 2002; Bunker and Hirst, 2004), reduced grazing rates (10 and 14°C in female *C. finmarchicus*; Van Dinh et al., 2019), and increased oxygen consumption rates and sublethal stress (in diapausing *C. hyperboreus* females at 0, 5 and 10°C; Hildebrandt et al., 2014). These responses also seem to be taxa- and stage-specific. For example, increased temperature (5, 10 and 15°C) upregulates heat shock proteins in *C. finmarchicus* but not in *C. glacialis* (Smolina et al., 2015).

In contrast to the straightforward reactions to individual stressors, the way marine species respond to multiple stressors can be intricate and dependent on the specific taxon, on life stage and on the strength of the stressor itself (e.g. concentration level). Numerous studies have suggested that acidification and warming can produce synergistic effects, distinct from the additive responses observed in single-stressor situations. Multiple studies have explored the impacts of various stressors, such as warming, acidification, and increased pollution, on copepod survival, growth, development, fecundity, egg production rate, hatching success, and feeding (e.g. Zervoudaki et al., 2014; Garzke et al., 2016; Horn et al., 2016). Although a plethora of research has been conducted in this field, Arctic species have received relatively little attention. From the literature available, it is apparent that these stressors can have synergistic effects on copepod populations, resulting in negative impacts on reproduction and population growth rates. For instance, long-term investigations on adult *C. glacialis* and *C. hyperboreus* revealed a synergistic effect of ocean acidification (390 and 3000 µatm $pCO_2$) with ocean warming (0, 5 and 10°C), but no effect of acidification alone (Hildebrandt et al., 2014). Another study explored the combined effects of ocean warming and exposure to the oil compound pyrene on *C. finmarchicus* and found that the combined stressors negatively impacted the copepod's survival and growth (100 nM pyrene at 0 and 10°C, Grenvald et al., 2013).

Our observations showed no clear response to acidification, concurrent with previous studies on *Calanus* nauplii: Bailey et al. (2017b) studied naupliar development in wild populations of *C. glacialis* and found unaffected respiration rates under ocean acidification ($pCO_2$ 320 to 1700 µatm), as well as development and growth, although this was compensated by altered gene expression (Bailey et al., 2017a). However, Lewis et al. (2013) found lower survival and seemingly greater sensitivity to manipulated OA conditions ($pCO_2$ 1000 µatm) predicted for the year 2100 in *Calanus* spp. nauplii compared to the adults in a short-term exposure experiment. Similarly, exposure to acidification (over 5000 ppm $CO_2$) resulted in an increase in naupliar mortality in the copepods *Acartia steueri* and *A. erythraea* (Kurihara et al., 2004). Reasons behind these discrepancies include differences in experimental design, geographical variations (European *vs.* Canadian Arctic), and variations in the parameters used to measure responses.

Conversely, our observations of unchanged respiration as a response to warming contrast with a study on *C. hyperboreus* nauplii respiration under warming conditions, where authors found a clear sensitivity to warming alone in early-larval stages, which might affect future recruitment (Jung-Madsen et al., 2013). One explanation for these discrepancies could be differences in the experimental design (we tested 0°C and 3°C, while they tested 0, 5 and 10°C; we tested short-term exposure [24h] while they tested long-term exposure [40 days]), as well as geographical differences (we used *C. hyperboreus* collected in the northern Barents Sea, whereas they tested individuals collected in Eastern Greenland). Different populations of copepods may have varying degrees of tolerance to environmental stressors. For example, geographically-distinct populations of *C. glacialis* showed physiological differences in OA responses (Thor et al., 2018).

Our results indicated a sensitivity of the nauplii to the combined exposure to acidification and warming through a significant impact on the metabolic rate of the nauplii, as demonstrated by increased oxygen uptake. This could be due to increased energy requirements when exposed to warming, leading to less energy available to cope with acidification. These observations support the notion that responses to multiple stressors in marine invertebrates, particularly during early-life stages are more complex than just additive. For example, in a recent multiple-stressor study by Jortveit (2022), it was observed that temperature (5°C) increased the lethal sensitivity of *C. glacialis* nauplii to pyrene, while other exposure combinations did not significantly affect naupliar survival. However, since our study was focused on short-term exposure, we did not measure survival as an endpoint, and it is therefore not possible to compare both studies.

Negative impacts on physiological endpoints, such as changes in metabolic rates from exposure to stressors such as acidification, may be attributed to constraints in the energy budget (Pedersen et al., 2014). As a result, potential scenarios of environmental change may increase energy demands, which could affect the natural communities of *Calanus* copepods with potential negative effects on higher trophic levels.

As most of the copepod congeners, *C. hyperboreus* stores lipids primarily in the form of wax esters (Falk-Petersen et al., 2009; Supporting data 10.21334/npolar.2023.edc957ac; Espinel-Velasco et al., 2023a). Nauplii have large oil droplets at hatching, which sustain them during their non-feeding stages until the spring bloom. In contrast to other studies (e.g. pteropods: Lischka et al., 2022), our study found no differences in lipid content and fatty acid

(FA) composition of the nauplii between the different experimental treatments. This is expected since lipid-reserve mobilization in *Calanus* nauplii is slow after a long period of starvation (Daase et al., 2011), and our exposure duration was short. The FA composition observed in our nauplii is consistent with previous investigations on Arctic *C. hyperboreus*, with wax esters comprising ~75% of the lipid reserves. This observation concurs with analyses of *C. hyperboreus* nauplii collected east of Greenland (85-90% WE; Jung-Madsen et al., 2013). Moreover, we observed high relative proportions of long chained fatty acids 20:1 and 22:1, which are key elements for the reproduction cycle in copepods (see supporting data: 10.21334/npolar.2023.edc957ac; Espinel-Velasco et al., 2023a). Given that the decrease in lipid during the naupliar development is most likely due to the nauplii metabolizing the lipid reserves to cover their energy requirements, changes in the amount of lipids passed on from the mothers, or changes in energy requirements of the larvae, could have significant implications for the recruitment of the species. A warmer Arctic ocean with smaller mothers (Halvorsen, 2015) could lead to earlier spawning and smaller nauplii. Moreover, warmer temperatures alter the larval development and increase the metabolism (increasing carbon requirements), as well as decrease the duration of starvation that the nauplii can survive, potentially affecting the timing to reach the spring bloom. Therefore, a synergistic effect of warming and acidification could imply that nauplii may not survive a potential mismatch with the ice break-up and resulting phytoplankton bloom, which would have detrimental effects on the species recruitment (Søreide et al., 2010; Daase et al., 2013).

In recent years, molecular techniques such as metabolomics have emerged as a powerful tool to study the physiological mechanisms that organisms use to cope with environmental stressors. Combining these new techniques with traditional measurements can provide a more comprehensive understanding of the potential responses of Arctic zooplankton communities to future changes. For instance, a recent study by Thor et al. (2022) has demonstrated the usefulness of metabolomics in elucidating the metabolic pathways and responses of copepods to environmental stressors (through changes in cellular metabolism). Therefore, incorporating these molecular techniques into future experimental investigations could shed light on the underlying mechanisms that govern the physiological responses of Arctic organisms to multiple stressors.

While there is a growing body of literature on the responses of early life stages of Arctic zooplankton to combined stressors, many questions remain unanswered. The limited research on the effects of combined environmental stressors on Arctic copepods, including *C. hyperboreus*, highlights the need for further experimental investigations to fully comprehend their physiological responses in potential future Arctic scenarios. Future work should include long-term investigations that could help understand not only responses, but also discern resilience of the Arctic ecosystems (Griffith et al., 2019). Early-life stages remain an important element to consider, as they can act as a bottleneck for the development of the species. By furthering our understanding of how these organisms respond to environmental stressors, we may be better equipped to mitigate the effects of climate change on these vital ecosystems.

## Data availability statement

Supporting data for this study is available at 10.21334/npolar.2023.edc957ac (fatty acid data; Espinel-Velasco et al., 2023a) and 10.21334/npolar.2023.ece3e9bb (oxygen uptake rates; Espinel-Velasco et al., 2023b).

## Ethics statement

The manuscript presents research on animals that do not require ethical approval for their study.

## Author contributions

NE-V, CG and VP contributed to the conception and design of the study. NE-V, CG and VP carried out the experimental investigation. DK and MG carried out the lipid laboratory analyses. NE-V performed the analysis of the respiration data and the statistical analysis. NE-V wrote the first draft of the manuscript and subsequent versions. CG and DK wrote sections of the manuscript. All authors contributed to manuscript revision, read, and approved the submitted version.

## Funding

This work was funded by the Research Council of Norway through the project The Nansen Legacy (RCN # 276730).

## Acknowledgments

We thank Anette Wold, Norwegian Polar Institute, for her invaluable assistance during the sampling process, as well as the crew on board RV *Kronprins Haakon*.

## Conflict of interest

The authors declare that the research was conducted in the absence of any commercial or financial relationships that could be construed as a potential conflict of interest.

## Publisher's note



## Supplementary material

The Supplementary Material for this article can be found online at: https://www.frontiersin.org/articles/10.3389/fmars.2023.1240673/full#supplementary-material

# References


Amante, C., and Eakins, B. W. (2009). *ETOPO1 1 arc-minute global relief model: procedures, data sources and analysis. NOAA technical memorandum NESDIS NGDC-24* (National Geophysical Data Center, NOAA), p. 19. doi: 10.7289/V5C8276M

AMAP (2018). *AMAP assessment 2018: Arctic ocean acidification* (Tromsø, Norway: Arctic Monitoring and Assessment Programme (AMAP).

AMAP (2021). *Arctic climate change update 2021: key trends and impacts. Summary for policy-makers* (Tromsø, Norway: Arctic Monitoring and Assessment Programme (AMAP).

Bailey, A., De Wit, P., Thor, P., Browman, H. I., Bjelland, R., Shema, S., et al. (2017a). Regulation of gene expression is associated with tolerance of the Arctic copepod *Calanus glacialis* to $CO_2$-acidified sea water. *Ecol. Evol.* 7, 7145–7160. doi: 10.1002/ece3.3063

Bailey, A., Thor, P., Browman, H. I., Fields, D. M., Runge, J., Vermont, A., et al. (2017b). Early life stages of the Arctic copepod *Calanus glacialis* are unaffected by increased seawater $pCO_2$. *ICES J. Mar. Sci.* 74, 996–1004. doi: 10.1093/icesjms/fsw066

Bunker, A. J., and Hirst, A. G. (2004). Fecundity of marine planktonic copepods: global rates and patterns in relation to chlorophyll *a*, temperature and body weight. *Mar. Ecol. Prog. Ser.* 279, 161–181. doi: 10.3354/meps279161

Byrne, M. (2011). Impact of ocean warming and ocean acidification on marine invertebrate life history stages: vulnerabilities and potential for persistence in a changing ocean. *Oceanogr. Mar. Biol. Ann. Rev.* 49, 1–42. doi: 10.1016/j.marenvres.2011.10.00

Byrne, M. (2012). Global change ecotoxicology: Identification of early life history bottlenecks in marine invertebrates, variable species responses and variable experimental approaches. *Mar. Environ. Res.* 76, 3–15. doi: 10.1016/j.marenvres.2011.10.004

Daase, M., Berge, J., Søreide, J. E., and Falk-Petersen, S. (2021). "Ecology of Arctic pelagic communities," in *Arctic ecology*. Ed. D. N. Thomas, 231–259. doi: 10.1002/9781118846582.ch9

Daase, M., Falk-Petersen, S., Varpe, Ø., Darnis, G., Søreide, J. E., Wold, A., et al. (2013). Timing of reproductive events in the marine copepod *Calanus glacialis*: A pan-Arctic perspective. *Can. J. Fish. Aquat. Sci.* 70, 871–884. doi: 10.1139/cjfas-2012-0401

Daase, M., Søreide, J. E., and Martynova, D. (2011). Effects of food quality on naupliar development in *Calanus glacialis* at subzero temperatures. *Mar. Ecol. Prog. Ser.* 429, 111–124. doi: 10.3354/meps09075

Ershova, E. A., Kosobokova, K. N., Banas, N. S., Ellingsen, I., Niehoff, B., Hildebrandt, N., et al. (2021). Sea ice decline drives biogeographical shifts of key *Calanus* species in the central Arctic Ocean. *Glob. Change Biol.* 27, 2128–2143. doi: 10.1111/gcb.15562

Espinel-Velasco, N., Gawinski, C., Kohlbach, D., Pitusi, V., Graeve, M., and Hop, H. (2023a). *Fatty acid composition (relative proportions in %) of 4-day old Calanus hyperboreus nauplii from mothers collected in the Northern Barents Sea* (Norwegian Polar Institute). doi: 10.21334/npolar.2023.edc957ac

Espinel-Velasco, N., Gawinski, C., Kohlbach, D., Pitusi, V., Graeve, M., and Hop, H. (2023b). *Individual oxygen uptake rates of 4-day old Calanus hyperboreus nauplii when exposed to ocean acidification and warming (12 hour measurements)* (Norwegian Polar Institute). doi: 10.21334/npolar.2023.ece3e9bb

Espinel-Velasco, N., Hoffmann, L., Agüera, A., Byrne, M., Dupont, S., Uthicke, S., et al. (2018). Effects of ocean acidification on the settlement and metamorphosis of marine invertebrate and fish larvae: a review. *Mar. Ecol. Prog. Ser.* 606, 237–257. doi: 10.3354/meps12754

Falk-Petersen, S., Mayzaud, P., Kattner, G., and Sargent, J. R. (2009). Lipids and life strategy of Arctic *Calanus*. *Mar. Biol. Res.* 5, 18–39. doi: 10.1080/17451000802512267

Falk-Petersen, S., Pavlov, V., Timofeev, S., and Sargent, J. R. (2007). "Climate variability and possible effects on arctic food chains: The role of Calanus," in *Arctic alpine ecosystems and people in a changing environment*. Eds. J. B. Ørbæk, R. Kallenborn, I. Tombre, E. N. Hegseth, S. Falk-Petersen and A. H. Hoel (Berlin: Springer-Verlag), 147–166. doi: 10.1007/978-3-540-48514-8_9

Garzke, J., Hansen, T., Ismar, S. M. H., and Sommer, U. (2016). Combined effects of ocean warming and acidification on copepod abundance, body size and fatty acid content. *PloS One* 11, 1–22. doi: 10.1371/journal.pone.0155952

Gerland, S., Wold, A., Altuna, N. E., Anglada-Ortiz, G., Arumi, M. A., Bodur, Y., et al. (2022). "Seasonal cruise Q1 2021: Cruise report," in *The Nansen Legacy report series*. doi: 10.7557/nlrs.6464

Grenvald, J. C., Nielsen, T. G., and Hjorth, M. (2013). Effects of pyrene exposure and temperature on early development of two co-existing Arctic copepods. *Ecotoxicology* 22, 184–198. doi: 10.1007/s10646-012-1016-y

Griffith, G. P., Hop, H., Vihtakari, M., Wold, A., Kalhagen, K., and Gabrielsen, G. W. (2019). Ecological resilience of Arctic marine food webs to climate change. *Nat. Clim. Change* 9, 868–872. doi: 10.1038/s41558-019-0601-y

Gunderson, A. R., Armstrong, E. J., and Stillman, J. H. (2016). Multiple stressors in a changing world: The need for an improved perspective on physiological responses to the dynamic marine environment. *Ann. Rev. Mar. Sci.* 8, 357–378. doi: 10.1146/annurev-marine-122414-033953

Halvorsen, E. (2015). Significance of lipid storage levels for reproductive output in the Arctic copepod *Calanus hyperboreus*. *Mar. Ecol. Prog. Ser.* 540, 259–265. doi: 10.3354/meps11528

Harianto, J., Carey, N., and Byrne, M. (2019). respR—An R package for the manipulation and analysis of respirometry data. *Methods Ecol. Evol.* 10, 912–920. doi: 10.1111/2041-210X.13162

Hildebrandt, N., Niehoff, B., and Sartoris, F. J. (2014). Long-term effects of elevated $CO_2$ and temperature on the Arctic calanoid copepods *Calanus glacialis* and *C. hyperboreus*. *Mar. Pollut. Bull.* 80, 59–70. doi: 10.1016/j.marpolbul.2014.01.050

Hirche, J. (1997). Life cycle of the copepod *Calanus hyperboreus* in the Greenland Sea. *Mar. Biol.* 128, 607–618. doi: 10.1007/s002270050127

Hirst, A., and Kiørboe, T. (2002). Mortality of marine planktonic copepods: global rates and patterns. *Mar. Ecol. Prog. Ser.* 230, 195–209. doi: 10.3354/meps230195

Hop, H., Assmy, P., Wold, A., Sundfjord, A., Daase, M., Duarte, P., et al. (2019a). Pelagic ecosystem characteristics across the Atlantic Water Boundary Current from Rijpfjorden, Svalbard, to the Arctic ocean during summer, (2010-2014). *Front. Mar. Sci.* 6. doi: 10.3389/fmars.2019.00181

Hop, H., and Gjøsæter, H. (2013). Polar cod (*Boreogadus saida*) and capelin (*Mallotus villosus*) as key species in marine food webs of the Arctic and the Barents Sea. *Mar. Biol. Res.* 9, 878–894. doi: 10.1080/17451000.2013.775458

Hop, H., Wold, A., Vihtakari, M., Daase, M., Kwasniewski, S., Gluchowska, M., et al. (2019b). "Zooplankton in Kongsfjorden, (1996–2016) in relation to climate change," in *The ecosystem of Kongsfjorden, Svalbard*. Eds. H. Hop and C. Wiencke (Cham: Springer), 229–300. Adv. Polar Ecol. 2. doi: 10.1007/978-3-319-46425-1_7

Horn, H. G., Boersma, M., Garzke, J., Lo, M. G. J., Sommer, U., and Aberle, N. (2016). Effects of high $CO_2$ and warming on a Baltic Sea microzooplankton community. *ICES J. Mar. Sci.* 73, 772–782. doi: 10.1093/icesjms/fsv198

Jortveit, A. (2022). Interactive effects of temperature, ocean acidification, and pyrene on *Calanus glacialis* nauplii. master's thesis. (University of Oslo), 35.

Jung-Madsen, S., Nielsen, T. G., Grønkjær, P., Hansen, B. W., and Møller, E. F. (2013). Early development of *Calanus hyperboreus* nauplii: Response to a changing ocean. *Limnol. Oceanogr.* 58, 2109–2121. doi: 10.4319/lo.2013.58.6.2109

Karnovsky, N. J., Kwaśniewski, S., Węsławski, J. M., Walkusz, W., and Beszczyńska-Möller, A. (2003). Foraging behavior of little auks in a heterogeneous environment. *Mar. Ecol. Prog. Ser.* 253, 289–303. doi: 10.3354/meps253289

Kurihara, H., Shimode, S., and Shirayama, Y. (2004). Effects of raised $CO_2$ concentration on the egg production rate and early development of two marine copepods (*Acartia steueri* and *Acartia erythraea*). *Mar. Pollut. Bull.* 49, 721–727. doi: 10.1016/j.marpolbul.2004.05.005

Lewis, C. N., Brown, K. A., Edwards, L. A., Cooper, G., and Findlay, H. S. (2013). Sensitivity to ocean acidification parallels natural $pCO_2$ gradients experienced by Arctic copepods under winter sea ice. *Proc. Natl. Acad. Sci. U. S. A.* 110 (51), E4960-7. doi: 10.1073/pnas.1315162110

Lischka, S., Greenacre, M. J., Riebesell, U., and Graeve, M. (2022). Membrane lipid sensitivity to ocean warming and acidification poses a severe threat to Arctic pteropods. *Front. Mar. Sci.* 9. doi: 10.3389/fmars.2022.920163

Mayor, D. J., Matthews, C., Cook, K., Zuur, A. F., and Hay, S. (2007). $CO_2$-induced acidification affects hatching success in *Calanus finmarchicus*. *Mar. Ecol. Prog. Ser.* 350, 91–97. doi: 10.3354/meps07142

NOAA National Geophysical Data Center (2009) *ETOPO1 1 arc-minute global relief model* (NOAA National Centers for Environmental Information) (Accessed 05/06/2023).

Pedersen, S. A., Håkedal, O. J., Salaberria, I., Tagliati, A., Gustavson, L. M., Jenssen, B. M., et al. (2014). Multigenerational exposure to ocean acidification during food limitation reveals consequences for copepod scope for growth and vital rates. *Environ. Sci. Technol.* 48, 12275–12284. doi: 10.1021/es501581j

Ramondenc, S., Nöthig, E. M., Hufnagel, L., Bauerfeind, E., Busch, K., Knüppel, N., et al. (2022). Effects of Atlantification and changing sea-ice dynamics on zooplankton community structure and carbon flux between 2000 and 2016 in the eastern Fram Strait. *Limnol. Oceanogr.* 2012, 1–15. doi: 10.1002/lno.12192

R Core Team (2021) *R: A language and environment for statistical computing*. Available at: https://www.r-project.org/.

Smolina, I., Kollias, S., Møller, E. F., Lindeque, P., Sundaram, A. Y. M., Fernandes, J. M. O., et al. (2015). Contrasting transcriptome response to thermal stress in two key zooplankton species, *Calanus finmarchicus* and *C. glacialis*. *Mar. Ecol. Prog. Ser.* 534, 79–93. doi: 10.3354/meps11398

Søreide, J. E., Leu, E. V. A., Berge, J., Graeve, M., and Falk-Petersen, S. (2010). Timing of blooms, algal food quality and *Calanus glacialis* reproduction and growth in a changing Arctic. *Glob. Change Biol.* 16, 3154–3163. doi: 10.1111/j.1365-2486.2010.02175.x

The Nansen Legacy (2022). *Sampling protocols: version 10. The nansen legacy report series*. doi: 10.7557/nlrs.6684

Thor, P., Bailey, A., Dupont, S., Calosi, P., Søreide, J. E., De Wit, P., et al. (2018). Contrasting physiological responses to future ocean acidification among Arctic copepod populations. *Glob. Change Biol.* 24, 365–377. doi: 10.1111/gcb.13870

Thor, P., Bailey, A., Halsband, C., Guscelli, E., Gorokhova, E., and Fransson, A. (2016). Seawater pH predicted for the year 2100 affects the metabolic response to feeding in copepodites of the Arctic copepod *Calanus glacialis*. *PloS One* 11 (12), e0168735. doi: 10.1371/journal.pone.0168735

Thor, P., Vermandele, F., Bailey, A., Guscelli, E., Sartrou, L. L., Dupont, S., et al. (2022). Ocean acidification causes fundamental changes in the cellular metabolism of the Arctic copepod *Calanus glacialis* as detected by metabolomic analysis. *Sci. Rep.* 12, 1–14. doi: 10.1038/s41598-022-26480-9

Van Dinh, K., Olsen, M. W., Altin, D., Vismann, B., and Nielsen, T. G. (2019). Impact of temperature and pyrene exposure on the functional response of males and females of the copepod *Calanus finmarchicus*. *Environ. Sci. Pollut. Res.* 26, 29327–29333. doi: 10.1007/s11356-019-06078-x

Varpe, Ø. (2012). Fitness and phenology: Annual routines and zooplankton adaptations to seasonal cycles. *J. Plankton Res.* 34, 267–276. doi: 10.1093/plankt/fbr108

Vihtakari, M. (2022). *ggOceanMaps: Plot Data on Oceanographic Maps using 'ggplot2'* (R package version 1.3.7). Available at: https://mikkovihtakari.github.io/ggOceanMaps/ .

Vihtakari, M., Sundfjord, A., and de Steur, L. (2019). *Barents Sea ocean-current arrows modified from Eriksen et al., (2018)* (Norwegian Polar Institute and Institute of Marine Research). Available at: https://github.com/MikkoVihtakari/Barents-Sea-currents.

Wang, M., Jeong, C. B., Lee, Y. H., and Lee, J. S. (2018). Effects of ocean acidification on copepods. *Aquat. Toxicol.* 196, 17–24. doi: 10.1016/j.aquatox.2018.01.004

Weydmann, A., Søreide, J. E., Kwasniewski, S., and Widdicombe, S. (2012). Influence of $CO_2$-induced acidification on the reproduction of a key Arctic copepod *Calanus glacialis*. *J. Exp. Mar. Bio. Ecol.* 428, 39–42. doi: 10.1016/j.jembe.2012.06.002

Zervoudaki, S., Frangoulis, C., Giannoudi, L., and Krasakopoulou, E. (2014). Effects of low pH and raised temperature on egg production, hatching and metabolic rates of a Mediterranean copepod species (*Acartia clausi*) under oligotrophic conditions. *Mediterr. Mar. Sci.* 15, 74–83. doi: 10.12681/mms.553

frontiers | Frontiers in Marine Science

TYPE Original Research
PUBLISHED 13 November 2023
DOI 10.3389/fmars.2023.1254043



OPEN ACCESS

EDITED BY
Letterio Guglielmo,
Anton Dohrn Zoological Station Naples, Italy

REVIEWED BY
Martina Mascioni,
National University of La Plata, Argentina
Márcio Silva de Souza,
Federal University of Rio Grande, Brazil

*CORRESPONDENCE
Xinliang Wang
wangxl@ysfri.ac.cn

RECEIVED 06 July 2023
ACCEPTED 25 October 2023
PUBLISHED 13 November 2023

CITATION
Liu L, Zhang J, Zhao Y, Luan Q, Zhao X and Wang X (2023) Net-phytoplankton communities and influencing factors in the Antarctic Peninsula region in the late austral summer 2019/2020.
*Front. Mar. Sci.* 10:1254043.
doi: 10.3389/fmars.2023.1254043



# Net-phytoplankton communities and influencing factors in the Antarctic Peninsula region in the late austral summer 2019/2020

Lu Liu[1], Jichang Zhang[1,2], Yunxia Zhao[1], Qingshan Luan[1], Xianyong Zhao[1,2] and Xinliang Wang[1,2]*

[1]Key Laboratory of Sustainable Development of Polar Fisheries, Ministry of Agriculture and Rural Affairs, Yellow Sea Fisheries Research Institute, Chinese Academy of Fishery Science, Qingdao, Shandong, China, [2]Joint Laboratory for Open Sea Fishery Engineering, Qingdao Marine Science and Technology Center, Qingdao, Shandong, China

The waters near the Antarctic Peninsula are characterized with unique oceanographic conditions and rich krill resources. Based on samples collected around the South Shetland Islands (SSI) in austral summer of 2019/2020, the net-phytoplankton community structure and relevant major biotic and abiotic influencing factors were investigated. Eighty-one taxa were identified by light microscope, and diatoms were the most abundant group. The most abundant species were *Chaetoceros atlanticus*, *C. criophilus*, *C. dichaeta*, *Fragilariopsis kerguelensis* and *Pseudo–nitzschia lineola*. The abundance and Shannon-Weaver index of net-phytoplankton ranged from 100 to $2.64\times10^7$ cells/$m^3$ and 0.0747 to 4.0176 respectively, with significantly low values detected in the Bransfield Strait (BS) and high values in the west of the SSI. The dissimilarity was mainly caused by the differences in abundance of diatoms (including *Thalassiothrix antarctica* and the species in genus *Rhizosolenia*, *Chaetoceros*, *Fragilariophsis*). These diatoms and *Dictyocha speculum* were found in higher abundance in the west of the SSI, while *Corethron pennatum* and cryptophytes were found in higher abundance in the BS. Combined with acoustic density of krill and environmental data (Sea Surface Temperature and Sea Ice Concentration). The multivariate analysis suggested that phytoplankton community was positively affected by the SST, and the acoustic- derived krill density would be associated with the spatial distribution of pennate diatoms. This study enhances the knowledge about the selective feeding for krill and provides ecological implications for the Antarctic marine ecosystem.

KEYWORDS

**phytoplankton, community structure, sea surface temperature, sea ice concentration, Antarctic krill**

# 1 Introduction

The Southern Ocean is recognized as a key region in the modulation and global marine carbon cycle (Gonçalves-Araujo et al., 2015). There are complex water masses around the South Shetland Islands (SSI) especially in the waters of the Bransfield Strait (BS) which connect the Bellingshausen Sea and the Weddell Sea (Gonçalves-Araujo et al., 2015). The complexity of water masses and their diverse thermohaline structures makes the regions around the SSI be a hotspot for phytoplankton assemblages and high trophic predators.

Phytoplankton plays crucial roles in the marine ecosystem and they could respond sensitively to changes in the environment (Schloss and Estrada, 1994; Vernet et al., 2008; Liu et al., 2021). High values of phytoplankton biomass have been observed in particular regions, especially at oceanic fronts, marginal ice zones and near shore straits, bays, and lees of islands (Prézelin et al., 2000; Mendes et al., 2012). During the austral summer, the distribution of phytoplankton is patchy. The blooms in the Antarctic waters were dominated by nanoflagellates (Mascioni et al., 2019) or microphytoplankton (mainly diatoms) which were both occurred and recorded. The waters along the AP exhibits high value of phytoplankton abundance (Hewes et al., 2009). In contrast, waters in the BS have been dominated by nanoflagellates and characterized by low primary production away from the melting of sea ice (Holm-Hansen and Mitchell, 1991; Lancelot et al., 1993; Kang et al., 2001). In the west of the SSI, microphytoplankton community composition has been characterized by the genus of *Rhizosolenia* and *Chaetoceros* (Luan et al., 2013).

In the context of global climate change, there was a shift from micro-diatoms to nanoflagellates (Costa et al., 2020). When water heats up, stratification of water column caused by the sea-ice melting leads to the phytoplankton bloom (Rozema et al., 2017a). As sea ice receded, diatoms bloom to higher abundance and then, are replaced by cryptophytes (Ducklow et al., 2007). Besides abiotic factors, the distribution of phytoplankton may also be affected by the consumption of Antarctic krill (*Euphausia superba*, hereafter krill). Krill is a key species in the Antarctic marine ecosystem linking between phytoplankton and higher trophic predators. More than 50% total krill biomass are presumed to be located in the southwest Atlantic sector, in particularly in the waters around SSI (Atkinson et al., 2004; Hewitt et al., 2004; Watters et al., 2020). Krill is an important grazer on phytoplankton and a large krill aggregation can exert great pressure on phytoplankton biomass (Froneman et al., 2000; Bernard et al., 2012). Diatoms are the major food resources for krill and krill is mainly effective at grazing particles larger than 10 µm equivalent spherical diameter (ESD) (McClatchie and Boyd, 1983; Ishii et al., 1985; Haberman et al., 2003b).

As early as in the middle of the 20$^{th}$ century, there were surveys about microphytoplankton in Antarctic (Froneman et al., 1997). Due to the application of molecular and pigment analysis, composition of microphytoplankton by microscope is scarce. To supplement the lack of up-to-date knowledge about the microphytoplankton community, phytoplankton community around the SSI was investigated. In addition, regions near the SSI have suffered great impacts of climate change, so phytoplankton dynamics could reinforce the understanding about the response to the regional environment change including the sea surface temperature (SST), sea ice concentration (SIC) and krill density. The objective of this study is to clarify the distribution pattern and spatial difference of net- phytoplankton, identify the possible influencing factors, and then provide some indicators for krill selective grazing.

# 2 Materials and methods

## 2.1 Samples and data collection

The net-phytoplankton samples were collected during the Antarctic krill survey conducted by the Chinese krill fishing vessel *Fu Rong Hai* around the SSI from 8 to 12 in March 2020. Samples were collected at 40 stations with 21 stations in the west of SSI and 19 stations in the BS (Figure 1). Net-phytoplankton samples were collected with a standard net III (net area 0.1 m$^2$, mesh size 76 µm) by vertical hauling from 200 m depth or from the bottom to the surface when the depth was less than 200 m. The collected samples were preserved in 1 L bottles with 5% formaldehyde solution.

The krill density was estimated using acoustic data collected from a hull-mounted Simrad EK60 echosounder onboard F/V *Fu Rong Hai* along the transects survey as shown in Figure 1. Krill backscatters were identified using the swarm-based method (Krafft et al., 2021). The acoustic backscatter at 120 kHz attributed to krill were then integrated as nautical area scattering coefficient (NASC, m$^2$/n. mile$^2$) from the surface exclusion layer (15 m) to the lower limit (250 m), and exported at an elementary distance sampling unit (EDSU) of 1 n.mile. In the subsequent correlation analysis, the NASC values of each station were averaged by 6 n. miles (3 n. miles before and after of each station).

Environmental data, including the SST and SIC, were obtained from the Copernicus Marine Data Store (https://resources.marine.copernicus.eu/). The spatial resolution of the original data was 0.05° × 0.05°, and temporal resolution was daily mean.

## 2.2 Samples and data analysis

In the land-based laboratory, the phytoplankton samples were settled for more than 48 h, and the supernatant was aspirated off. The volume of the concentrated samples was about 100 ml, 0.5 mL of which was analyzed and counted under the Nikon Eclipse Ti2-U inverted microscope with 200× to 400× magnification. The taxa identification was based on species morphology referred to the books and literatures on phytoplankton classification and the website of www.algaebase.org.

The taxa abundance ($A$) was calculated as:

$$A = \frac{n_i}{V1}\frac{V2}{V}$$

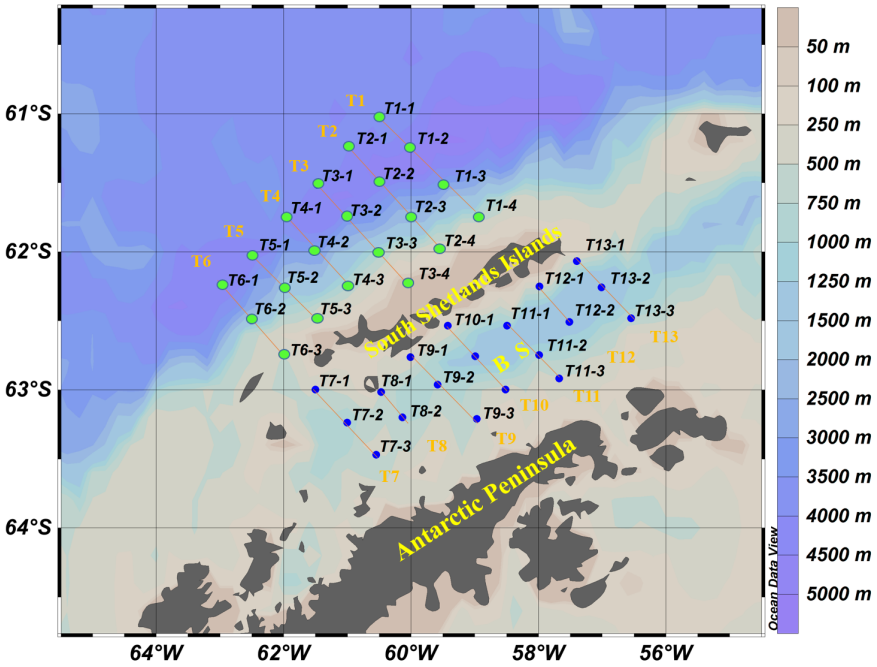


FIGURE 1
Map of sampling stations and transects (T1-T13) around the South Shetland Islands. BS- Bransfield Strait. The green dots were the stations in the west of SSI which defined as cluster 1, and the blue dots were the stations in the BS which defined as cluster 2.

where $n_i$ is the number of cells in species $i$, $V1$ is the analyzed volume 0.5 mL and $V2$ is the concentrated volume. $V$ is the filtration volume when hauling the net which was calculated as 200 m or the depth of water minus two meters and then multiply by the net area.

Shannon-Weaver index ($H'$) was used to evaluate the species diversity of phytoplankton community. $H'$ is calculated as (Shannon and Weaver, 1949):

$$H' = \sum_{i=1}^{s} P_i \log_2 P_i$$

Dominance ($Y$) was calculated as:

$$Y = \frac{n_i}{N} f_i$$

where $N$ is the total number of phytoplankton cells; $S$ is the number of species and $P_i$ is the ratio of the number of cells $i$ to the total numbers, $n_i$ is the number of cells in species $i$ and $f_i$ is the frequency of species $i$.

Phytoplankton community structure was examined by carrying out a multivariate analysis on abundance. Clustering was performed for each dataset based on the Bray- Curtis similarity matrix of log (x +1) transformed phytoplankton abundance and the average linkage group classification (Field et al., 1982; Shi et al., 2020) to distinguish the phytoplankton communities. In the process of analysis, stations in the west of SSI were defined as cluster 1, and the others were defined as cluster 2. ANOSIM (analysis of similarities) procedure was used to test the difference of phytoplankton community. To understand the circumstances of the dissimilar species that caused the difference between stratums, a similarity percentage analysis (SIMPER) was conducted. The species causing the difference between clusters were listed. The BIO-ENV analysis with Spearman rank correlation was carried out between the taxonomic and environmental data, to evaluate the best sets of environmental factors including SST, SIC and acoustic density of krill on phytoplankton communities.

# 3 Results

## 3.1 Net-phytoplankton community

Eighty-one taxa were identified in this study and the composition of phytoplankton was listed in Table 1. Diatoms were the dominant group with 67 species. Others groups including dinoflagellates, silicoflagellates and cryptophytes were less abundant. The most abundant species were all diatoms in chains including *Chaetoceros atlanticus*, *C. criophilus*, *C. dichaeta*, *Fragilariopsis kerguelensis*, and *Pseudo–nitzschia lineola*.

The distributions of different phytoplankton groups abundance were exhibited in Figure 2. Total phytoplankton abundance ranged from a minimum of 100 cells/$m^3$ at T13-2 station to a maximum of $2.64\times10^7$ cells/$m^3$ at T5-1 station. Phytoplankton abundance in the west of the SSI was apparently higher than that in the BS. The distribution patterns of different groups (diatoms, dinoflagellates and most abundant species) were similar to the total abundance. Compared with pennate diatoms, centric diatoms were more abundant in the BS.

The $H'$ ranged from 0.0747 to 4.0176 (Figure 3). In general, diversity indices were clearly higher in transects T1-T6 than those calculated in transects T7-T13. Interestingly, sampling stations with

10.3389/fmars.2023.1254043

TABLE 1 Taxa composition of net-phytoplankton around the South Shetland Islands during 8 to 12 March 2020.

| Taxa | $n_i/N$ | $f_i$ | $Y$ |
|---|---|---|---|
| **Bacillariophyta** | | | |
| *Actinocyclus actinochilus* (Ehrenberg) Simonsen | 0.0000 | 0.0250 | 0.0000 |
| *Actinocyclus* sp. | 0.0002 | 0.1500 | 0.0000 |
| *Asteromphalus parvulus* Karsten | 0.0003 | 0.0250 | 0.0000 |
| *Asteromphalus hookeri* Ehrenberg | 0.0001 | 0.0500 | 0.0000 |
| *Asteromphalus hyalinus* Karsten | 0.0005 | 0.0500 | 0.0000 |
| *Asteromphalus* spp. | 0.0000 | 0.0750 | 0.0000 |
| *Biddulphia* spp. | 0.0000 | 0.0250 | 0.0000 |
| *Chaetoceros atlanticus* Cleve* | 0.4118 | 0.6000 | 0.2471 |
| *Chaetoceros bulbosus* (Ehrenberg) Heiden | 0.0032 | 0.1750 | 0.0006 |
| *Chaetoceros castracanei* Karsten | 0.0187 | 0.2500 | 0.0047 |
| *Chaetoceros criophilus* Castracane* | 0.0288 | 0.7000 | 0.0201 |
| *Chaetoceros debilis* Cleve | 0.0003 | 0.0250 | 0.0000 |
| *Chaetoceros dichaeta* Ehrenberg* | 0.0683 | 0.3000 | 0.0205 |
| *Chaetoceros flexuosus* Mangin | 0.0002 | 0.0250 | 0.0000 |
| *Chaetoceros neglectus* Karsten | 0.0141 | 0.0500 | 0.0007 |
| *Chaetoceros neogracilis* VanLandingham | 0.0002 | 0.0250 | 0.0000 |
| *Chaetoceros pendulus* Karsten | 0.0107 | 0.3750 | 0.0040 |
| *Chaetoceros peruvianus* Brightwell | 0.0031 | 0.2250 | 0.0007 |
| *Chaetoceros simplex* Ostenfeld | 0.0038 | 0.2000 | 0.0008 |
| *Chaetoceros* spp.* | 0.0479 | 0.4250 | 0.0203 |
| *Cocconeis* sp. | 0.0003 | 0.4000 | 0.0001 |
| *Corethron pennatum* (Grunow) Ostenfeld | 0.0106 | 0.9750 | 0.0103 |
| *Coscinodiscus curvatulus* Grunow | 0.0000 | 0.1250 | 0.0000 |
| *Coscinodiscus oculus-iridis* (Ehrenberg) Ehrenberg | 0.0000 | 0.0250 | 0.0000 |
| *Coscinodiscus subtilis* Ehrenberg | 0.0001 | 0.0500 | 0.0000 |
| *Coscinodiscus radiatus* Ehrenberg | 0.0000 | 0.0250 | 0.0000 |
| *Coscinodiscus* spp. | 0.0000 | 0.2500 | 0.0000 |
| *Cyclotella* sp. | 0.0009 | 0.5250 | 0.0005 |
| *Cylindrotheca closterium* (Ehrenberg) Reimann & J.C. Lewin | 0.0000 | 0.0750 | 0.0000 |
| *Dactyliosolen antarcticus* Castracane | 0.0081 | 0.3500 | 0.0028 |
| *Dactyliosolen tenuijunctus* (Manguin) Hasle | 0.0164 | 0.4000 | 0.0066 |
| *Dactyliosolen* sp. | 0.0000 | 0.0250 | 0.0000 |
| *Diploneis* sp. | 0.0000 | 0.0250 | 0.0000 |
| *Eucampia antarctica* (Castracane) Mangin | 0.0015 | 0.0250 | 0.0000 |
| *Fragilariopsis curta* (Van Heurck) Hustedt | 0.0046 | 0.5750 | 0.0026 |
| *Fragilariopsis cylindrus* (Grunow ex Cleve) Helmcke & Krieger | 0.0029 | 0.4250 | 0.0012 |
| *Fragilariopsis kerguelensis* (O' Meara) Hustedt* | 0.0535 | 0.6000 | 0.0321 |
| *Fragilariopsis pseudonana* (Hasle) Hasle | 0.0073 | 0.3250 | 0.0017 |

*(Continued)*

10.3389/fmars.2023.1254043

TABLE 1 Continued

| Taxa | $n_i/N$ | $f_i$ | $Y$ |
|---|---|---|---|
| *Fragilariopsis ritscheri* Hustedt | 0.0000 | 0.0250 | 0.0000 |
| *Fragilariopsis rhombica* (O' Meara) Hustedt | 0.0009 | 0.3000 | 0.0003 |
| *Fragilariopsis* spp. | 0.0037 | 0.4000 | 0.0007 |
| *Leptocylindrus mediterraneus* (H.Peragallo) Hasle | 0.0001 | 0.0250 | 0.0000 |
| *Licmophora* spp. | 0.0000 | 0.2000 | 0.0000 |
| *Navicula* spp. | 0.0003 | 0.2250 | 0.0001 |
| *Nitzschia longissima* (Brébisson ex Kützing) Grunow | 0.0035 | 0.2250 | 0.0008 |
| *Nitzschia* spp. | 0.0000 | 0.0250 | 0.0000 |
| *Pleurosigma* spp. | 0.0000 | 0.0250 | 0.0000 |
| *Proboscia alata* (Brightwell) Sundström | 0.0121 | 0.5750 | 0.0070 |
| *Proboscia inermis* (Castracane) R.W.Jordan & Ligowski | 0.0042 | 0.4750 | 0.0020 |
| *Proboscia truncata* (G.Karsten) Nöthing & Ligowski | 0.0005 | 0.3000 | 0.0001 |
| *Pseudo-nitzschia heimii* Manguin | 0.0513 | 0.3500 | 0.0179 |
| *Pseudo-nitzschia lineola* (Cleve) Hasle* | 0.1277 | 0.7000 | 0.0894 |
| *Pseudo-nitzschia turgiduloides* G. R. Hasle | 0.0192 | 0.3500 | 0.0067 |
| *Pseudo-nitzschia* spp. | 0.0000 | 0.0500 | 0.0000 |
| *Rhizosolenia antennata* f. *semispina* Sundström | 0.0102 | 0.4750 | 0.0048 |
| *Rhizosolenia hebetata* f. *semispina* (Hensen) Gran | 0.0014 | 0.4250 | 0.0006 |
| *Rhizosolenia simplex* G. Karsten | 0.0000 | 0.0500 | 0.0000 |
| *Rhizosolenia styliformis* T. Brightwell | 0.0048 | 0.5000 | 0.0024 |
| *Rhizosolenia styliformis* var. *lattissima* Brightwell | 0.0000 | 0.0500 | 0.0000 |
| *Rhizosolenia styliformis* var. *longisipina* Hustedt | 0.0002 | 0.0250 | 0.0000 |
| *Rhizosolenia* spp. | 0.0130 | 0.6500 | 0.0085 |
| *Synedropsis* spp. | 0.0002 | 0.0500 | 0.0000 |
| *Thalassiosira* spp. | 0.0013 | 0.4750 | 0.0006 |
| *Thalassiothrix antarctica* Schimper ex Karsten | 0.0249 | 0.7000 | 0.0175 |
| *Trigonium antarcticum* Gogorev & Pushina | 0.0000 | 0.0500 | 0.0000 |
| Centricae | 0.0000 | 0.2000 | 0.0000 |
| Dinophyceae | | | |
| *Alexandrium* sp. | 0.0000 | 0.0500 | 0.0000 |
| *Cochlodinium* sp. | 0.0000 | 0.0250 | 0.0000 |
| *Dinophysis dens* Pavillard | 0.0000 | 0.0250 | 0.0000 |
| *Dinophysis* spp. | 0.0000 | 0.0500 | 0.0000 |
| *Diplopsalopsis* spp. | 0.0001 | 0.0750 | 0.0000 |
| *Gymnodinium* spp. | 0.0000 | 0.1250 | 0.0000 |
| *Gyrodinium* spp. | 0.0010 | 0.2250 | 0.0002 |
| *Heterocapsa* sp. | 0.0002 | 0.0250 | 0.0000 |
| *Lepidodinium* sp. | 0.0001 | 0.0500 | 0.0000 |
| *Prorocentrum antarcticum* (Hada) Balech | 0.0002 | 0.1750 | 0.0000 |

*(Continued)*

TABLE 1 Continued

| Taxa | $n_i/N$ | $f_i$ | $Y$ |
|---|---|---|---|
| *Protoperidinium antarcticum* (Schimper) Balech | 0.0000 | 0.0750 | 0.0000 |
| *Protoperidinium* spp. | 0.0000 | 0.0250 | 0.0000 |
| *Tripos pentagonus* (Gourret) F. Gómez | 0.0000 | 0.0500 | 0.0000 |
| dinoflagellates | 0.0005 | 0.3250 | 0.0001 |
| Ochrophyta | | | |
| *Dictyocha speculum* Ehrenberg | 0.0060 | 0.4000 | 0.0024 |
| Cryptophyta | | | |
| *Cryptophytes* sp. | 0.0000 | 0.1750 | 0.0000 |
| micro phytoplankton | 0.0000 | 0.0500 | 0.0000 |
| nano phytoplankton | 0.0075 | 0.5750 | 0.0043 |

*- the most abundant species.

extremely low species diversity were almost dominated by one species namely *Corethron pennatum*. For example, T11-3 was the station with the lowest diversity index, where *Corethron pennatum* accounted for 99.33% of the total abundance. And the second lowest index was found at the station T13-1, where *C. pennatum* accounted for 98.90% of the total abundance.

## 3.2 Spatial differences of phytoplankton community

Two clusters were classified at 25% of the similarity level shown in Figure 4, which were significant different between cluster 1 and 2 (ANOSIM: $R$=0.513, $p$=0.001). In summary, cluster 1 mainly assembled the stations in the west of the SSI whereas cluster 2 in the BS.

To understand the circumstances of the dissimilar species that caused the difference between two clusters, we then conducted a similarity percentage analysis (SIMPER). The average dissimilarity was 76.65% between two clusters. In view of the significant difference, the species that contribute more than 3% were listed in Table 2 and their accumulated contribution added to 37.13%. Some diatom species contributed more for the dissimilarity between the clusters at sampling stations (Table 2), mainly referred to centric diatoms (*Rhizosolenia styliformis*, *Chaetoceros criophilus*, *C. atlanticus*, *R. antennata* f. *semispina*, *Proboscia alata*, and *Corethron pennatum*).

## 3.3 Influencing factors on the net-phytoplankton community

The SST ranged from -0.35 to 3.88 °C. The SST in the BS was apparently lower than that in the west of the SSI (Figure 5). The distribution of SIC was totally different from the SST spatial distribution. The SIC values in most stations were mostly 0, namely there was no ice cover. Only several stations including T4-3, T8-1, T9-1, T10-1 near the SSI still had a few bits of ice floes.

Acoustic density of krill, ranged from 0 to 1194.4 $m^2$/n. $mile^2$, showed obvious spatial difference (Figure 6). In general, acoustic density was higher in the BS than on the west side of SSI and varied greatly between stations. More than half of stations had NASC values less than 10 $m^2$/n. $mile^2$, even the values in 13 stations were 0. And the high values occurred at transects T8, T9 and T10 in the BS (see Figure 1).

SST was the best environmental variable to explain the variance in the study area ($P$=0.01). Acoustic density was analyzed with the abundance of phytoplankton communities and abundant species respectively. It was found that the acoustic density was the best factor to explain the pennate diatoms ($P$=0.03).

# 4 Discussion

## 4.1 Characteristics of net- phytoplankton community and its dynamics around the northern tip of the Antarctic Peninsula

The phytoplankton communities in the study area were mainly composed of the micro-diatoms in chains like *Chaetoceros* spp., *Fragilariopsis* spp., *Pseudo–nitzschia* spp. and *Rhizosolenia* spp. Diatom assemblages in Antarctic waters exist transitional characteristics. Their ecological types included eurythermic species, cold-water species and endemic species in Antarctic. The abundant species were mainly endemic species in Antarctic and cold-water species, which reflected the survival strategy of phytoplankton in the Southern Ocean. Firstly, due to larger cells are more resistant to sinking, they can stay in the euphotic layer (Sun et al., 2003). Secondly, large diatoms in chains with high ratio of superficial and volume of cells are conductive to the absorption of nutrients, especially to the absorption of limiting nutrients such as iron (Sun et al., 2003; Luan et al., 2012). Finally, some larger cells would be less susceptible to ingestion, while some cells have thick cell wall that make digestion difficult for zooplankton. In addition, we missed the pico- and some nanophytoplankton cells to some

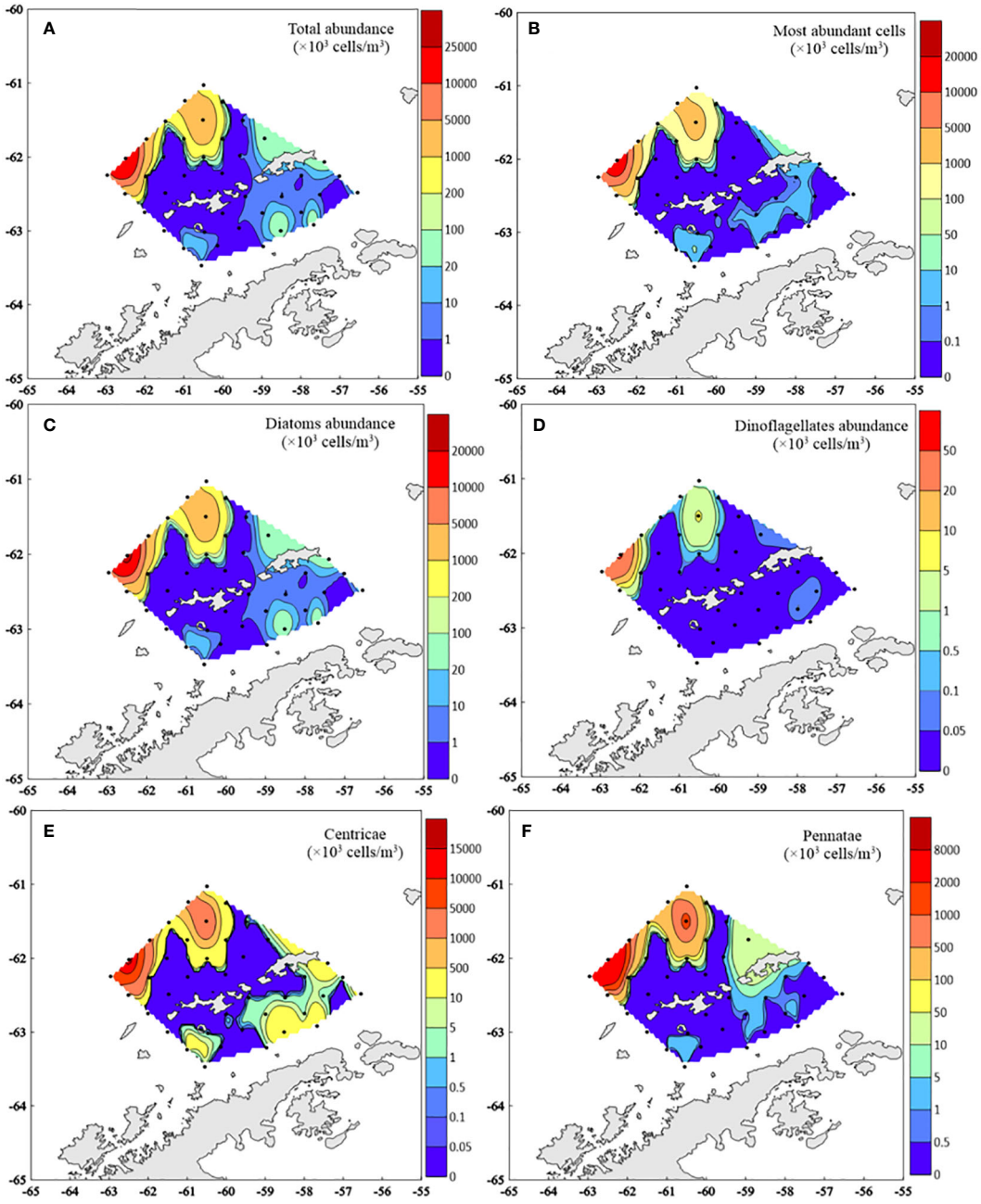


FIGURE 2
Distribution of different phytoplankton groups abundance (×10$^3$ cells/m$^3$) (**A**- Total abundance; **B**- Most abundant microphytoplankton cells abundance; **C**- Diatoms abundance; **D**- Dinoflagellates abundance; **E**- Centricae abundance; **F**- Pennatae abundance).

extent as we analyzed net-phytoplankton by the net sampling. These factors caused the net- phytoplankton communities to be dominated by larger cells or diatoms in chains (Sun et al., 2003).

In 1986-1987, dominant microphytoplankton were diatoms and the average cell density was 4.406×10$^6$ cells/m$^3$ in the BS and adjacent waters of EI (Zhu, 1993). Cefarelli et al. (2011) found diatoms were dominated in the mixed layer (1.06×10$^9$–2.09×10$^9$cells/m$^3$) and small centric diatoms were also highly abundant in the northwestern Weddell Sea between 10 March and 1 April 2009. Luan et al. (2012) used the same method we used to collect and analyze the phytoplankton community during austral summer 2010. Phytoplankton abundance varied from 387 to 1.04×10$^7$ cells/m$^3$ which was similar to our results. *Thalassiothrix antarctica*, *Gymnodinium* sp., *Chaetoceros* sp., *Pseudo-nitzschia lineola*, *Fragilariopsis kerguelensis*, *Chaetoceros criophilus*, *Corethron inerme and Fragilariopsis curta* were the most abundant species. These species were also occurred in our results. Compared with previous studies above, there was little difference in composition of phytoplankton community. The dominant species or genus were similar to our study. Due to the difference in survey area, season and sampling methods, the phytoplankton abundance are varied. Water samples were collected for HPLC/CHEMTAX

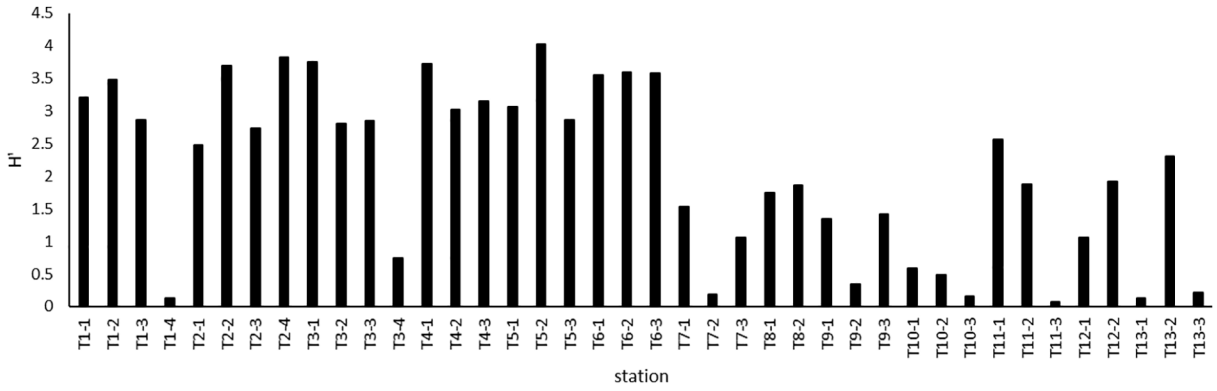


FIGURE 3
Histogram of Shannon-Weaver index (*H'*) across all sampling stations.

pigment and microscopic analysis around the tip of the AP during February/March 2008 and 2009. Phytoplankton assemblages were generally dominated by diatoms especially at coastal stations, while nanoflagellates replaced diatoms in open-ocean areas (Mendes et al., 2012). According to Mascioni et al. (2019), the highest phytoplankton abundance and biomass values were mainly represented by nanophytoflagellates, and the abundance of large bloom-forming diatoms was low in the relatively unexplored nearshore sites of the western AP during late summer of 2016 and during the spring-summer 2016-2017. As aforementioned, there are discrepancies among different results which might attribute to the conditions of sampling and methods of analyzing. So it seems to be necessary to have a long-term observation by same method at changeless location. Actually, rates of warming and sea ice loss are fastest in the southwest Atlantic sector with the impact of climate changes (Flores et al., 2012). Several studies have described a shift from large phytoplankton (diatoms) to smaller flagellated species (Moline et al., 2004; Monte-Hugo et al., 2009; Rozema et al., 2017b; Biggs et al., 2019). Therefore, long-term observation of the abundance of microphytoplankton is important to know more about size dynamics.

## 4.2 Relationships between environment features and net-phytoplankton community

As shown in the results, SST was the major environmental variable to explain the variance. In both laboratory (Eppley, 1972; Berges et al., 2002) and field investigations (Montagnes and Franklin, 2001; Hernando et al., 2018), temperature has been found to play an essential role in the growth of organisms, which can promote enzyme activity and metabolic processes. Higher temperature leads to accelerate phytoplankton growth and increase the matter accumulation (Winder and Sommer, 2012). With the increase of temperature, the biomass increased. In

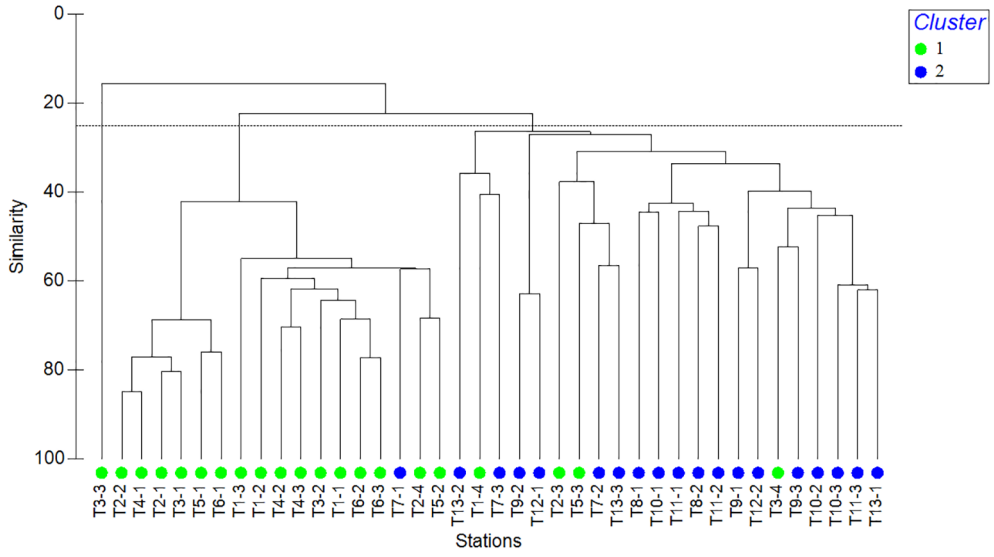


FIGURE 4
Cluster dendrogram of the phytoplankton community.

TABLE 2 Dissimilarity percentages-species contributions of phytoplankton community.

| Species | Av.Abund | | Av.Diss | Contrib% | Cum.% |
|---|---|---|---|---|---|
| | Cluster 1 | Cluster 2 | | | |
| *Rhizosolenia styliformis* | 5.94 | 0.31 | 2.87 | 3.75 | 3.75 |
| *Thalassiothrix antarctica* | 6.78 | 1.49 | 2.82 | 3.68 | 7.43 |
| *Chaetoceros criophilus* | 6.78 | 1.89 | 2.81 | 3.68 | 11.1 |
| *Fragilariopsis kerguelensis* | 6.49 | 0.92 | 2.73 | 3.56 | 14.67 |
| *Rhizosolenia* spp. | 6.39 | 1.15 | 2.72 | 3.55 | 18.22 |
| *Pseudo-nitzschia lineola* | 6.43 | 2.23 | 2.53 | 3.31 | 21.52 |
| *Chaetoceros atlanticus* | 6.33 | 1.28 | 2.48 | 3.24 | 24.76 |
| *Rhizosolenia antennata* f. *semispina* | 5.61 | 0.44 | 2.4 | 3.14 | 27.9 |
| *Proboscia alata* | 5.69 | 0.78 | 2.37 | 3.09 | 30.99 |
| *Fragilariopsis curta* | 5.29 | 0.79 | 2.35 | 3.07 | 34.07 |
| *Corethron pennatum* | 6.11 | 7.42 | 2.34 | 3.06 | 37.13 |

addition, Lionard et al. (2012) also found that high temperature was more favorable for the growth of large centric diatoms in phytoplankton assemblages in temperate environments. Therefore, SST might have promoted the growth of many net-phytoplankton taxa, which was highlighted by great contribution of microdiatoms.

The study area is hydrologically complex, with multiple water masses flowing from the Weddell Sea and the Bellingshausen Sea (Sangrà et al., 2011; Mendes et al., 2012). Within the surface layer of the BS, there are two major transitional waters being detected: Transitional Weddell Water (TWW) dominated by relatively cold and salty water mass flows north and west along the AP, and Transitional Bellingshausen Water (TBW) dominated by a relatively warm and fresh water mass, flows east (Gonçalves-Araujo et al., 2015). Thermohaline difference between TWW and TBW could be reflected in the phytoplankton communities. There is a well-mixed water column in the TWW where nanoplanktonic flagellates was dominant and exhibited lower chl *a*. On the contrary, microplanktonic diatoms were dominant and contributed higher chl *a* in the TBW because of the strong pycnocline and shallow upper mixed layers (Gonçalves-Araujo et al., 2015) within. In the west of the SSI, the high nutrients brought by Circumpolar Deep Water (CDW) and the deep water of subtropical Pacific Ocean accelerated the bloom of phytoplankton (Luan et al., 2012).

## 4.3 Grazing effect on phytoplankton by krill

Krill is a potential resource and their feeding behavior is complex, not only filtering phytoplankton and protozoa but also

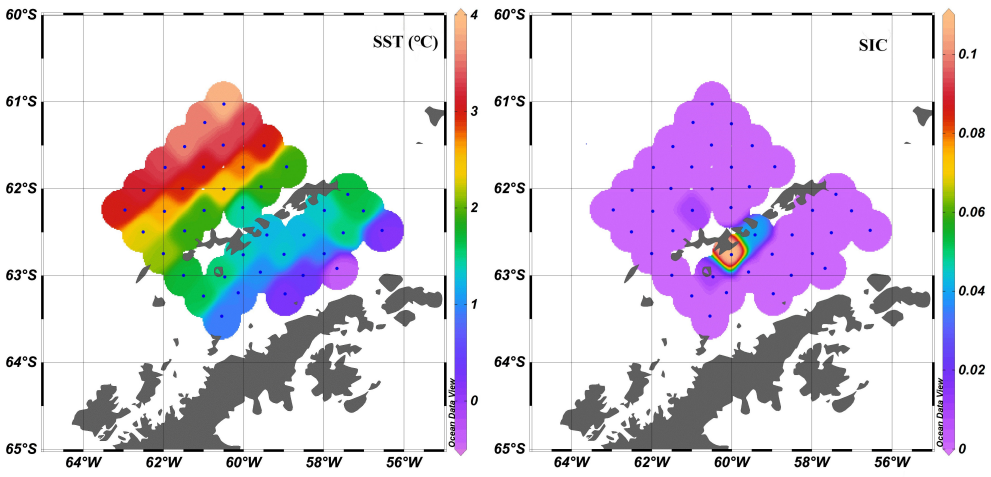


FIGURE 5
Distribution of sea surface temperature (left) and sea ice concentration (right). Data were obtained from the Copernicus Marine Data Store. The spatial resolution of the original data was 0.05° × 0.05°, and temporal resolution was daily mean.

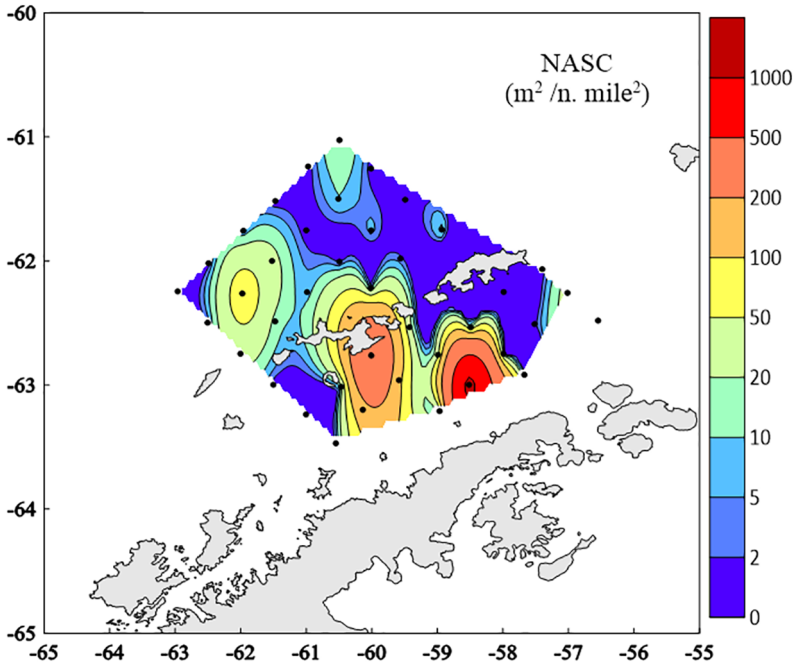


FIGURE 6
Krill acoustic density distribution around the South Shetland Islands during 8 to 12 March 2020. NASC- nautical area scattering coefficient.

preying on zooplankton (Cleary et al., 2018). In addition, krill feed on algae and detritus from sea ice and seabed (Price et al., 1988; Stretch et al., 1988; Clarke and Tyler, 2008; Schmidt et al., 2014). During the period of phytoplankton bloom, krill mainly feed on diatoms. While in the scarcity phase of phytoplankton, they also choose flagellates, copepods and detritus to sustain life (Schmidt and Atkinson, 2016). Analysis of stomach contents (Meyer and El-Sayed, 1983) and studies of the comparison of krill and phytoplankton distribution (Schmidt and Atkinson, 2016) suggested that krill feeding selective.

Early studies about krill gut content established the suitable phytoplankton species for feeding (Schmidt and Atkinson, 2016). In the South Georgia, microphytoplankton was the predominant component of gut contents. Solitary and colonial cells of *Nitzschia* spp., *Thalassiosira* spp. and *Fragilariopsis kerguelensis* were the most abundant (Pakhomov et al., 1997). It was also found that *Thalassiosira* spp. are preferred by krill feeding and some small pennate diatoms such as *Navicula* spp. and *Nitzschia* spp. are barely fed (Opaliński et al., 1997). In the stomach contents study of Cleary et al. (2018), krill have a diatom-based diet, while the occasional presence of copepod suggests carnivorous supplemented diet. Compared with cryptophytes or prymnesiophytes, diatoms are recognized as high quality food for zooplankton (Ross et al., 2000). Indeed, diatom bloom and gonad development of krill occurs simultaneously in spring (Cuzin-Roudy and Labat, 1992; Schmidt et al., 2012) and the accumulation of polyunsaturated fatty acids of krill by feeding on diatoms was more effective than that by feeding on copepods (Schmidt et al., 2014). In addition, krill were more likely to feed on chain-forming diatoms than solitary phytoplankton species (Stuart, 1989; Haberman et al., 2003a). This result should be mainly concerned with the cell size. For cells with large size greater than 70 µm, krill were incapable of ingestion, while the size was favored by krill at 20-40 µm (Meyer and El-Sayed, 1983; Drits and Pasternak, 1993; Maciewska and Opalinski, 1993 and Opaliński et al., 1997).

Compared with phytoplankton distribution, there was a negative correlation between krill abundance and primary production during the survey in the South Georgia (Pakhomov et al., 1997). And the abundance of phytoplankton community dominated by diatoms rapidly decreased due to the feeding of the krill swarm only in a few hours according to the observation of the scientific cruise in the Scotia-Weddell Sea (Smetacek and Veth, 1989). However, striking differences were observed between the stomach contents of krill collected in fjords and in adjacent open waters which could not be explained by differences in the surface water phytoplankton (Cleary et al., 2018). These findings are inconclusive. The distribution of krill is concentrated along the AP, and their spatial and temporal distribution is highly variable due to the ability of krill swarms migration (Ross et al., 1996; Moline et al., 2004). Large krill swarms may contain up to 10000–30000 individuals $m^{-3}$ (Hamner et al., 1983), and can rapidly clear phytoplankton up to a few litres per hour (Quetin et al., 1994). In fact, this phenomenon occurred mostly in local area. Spreading over larger areas, krill are difficult in grazing down phytoplankton (Atkinson et al., 2014). In the meanwhile, copepods were consistently part of krill diet (Schmidt et al., 2014). The distribution of zooplankton in waters also need to be considered, which may influence krill diet and increase the pressure on phytoplankton. In conclusion, it is hard to find the corresponding relationship between phytoplankton and krill density in the voyage survey even within the same region and season. This could explain why there was no correlation between phytoplankton abundance and krill density in our study.

Our research further analyzed the correlation between the distribution of pennate diatoms and the acoustic density of krill by BIO-ENV analysis. In the BS, krill density was high while the abundance of phytoplankton dominated by *Corethron pennatum* was low. In contrast, phytoplankton including pennate diatoms were abundant while the krill density was low in the west of SSI. Aforementioned findings were speculated that the phytoplankton assemblages were related to the krill grazing pressure. Biological processes, such as zooplankton grazing, superimposed to physical and chemical changes, can modify the abundance and dominance of different taxonomic assemblages (Cefarelli et al., 2011). Diatoms such as *Thalassiosira* spp., *Fragilariopsis* spp. and *Chaetoceros* spp. are feeding targets of krill, the low abundance of them and the dominance of *Corethron pennatum* in the BS may be the results of krill selective grazing, which seems to be the signal after krill grazing. *Corethron pennatum* may be the species krill refuses to eat. The structure of phytoplankton community is the result of consumption of higher trophic level including krill selective grazing. These conjectures may provide a new research direction for krill selective grazing and more evidence need to be explored.

## 5 Conclusion

In this study, we analyzed the structure and distribution of net-phytoplankton community near the SSI in the late austral summer 2019/2020. A total of 83 taxa (mostly at the species level) were recorded by light microscope, with diatoms being the most abundant group. There was significant difference between the BS and the west of the SSI. Combined with acoustic density of krill and environmental data including sea surface temperature and sea ice concentration, SST was the major environmental variable to explain the variance. It was also found that the acoustic density was the best factor to explain the pennate diatoms distribution. Our results clarified the composition and distribution of net-phytoplankton and provide some conjectures for selective feeding for krill. This study enhances the lack of up-to-date knowledge about the microphytoplankton community and give some conjectures about the selective feeding for krill and ecological implications for the Antarctic systems.

## Data availability statement

The datasets generated for this study are available on request to the corresponding author.

## Author contributions

LL conceived and led the study and writing of the manuscript. LQ, ZX and WX contributed substantially to writing the manuscript. ZJ collected the samples and provided data. ZY provided data. All authors read and approved the final manuscript.

## Funding

The author(s) declare financial support was received for the research, authorship, and/or publication of this article. This work was funded by the Marine S&T Fund of Shandong Province for Qingdao Marine Science and Technology Center (No. 2022QNLM030002-1); Central Public-interest Scientific Institution Basal Research Fund, Yellow Sea Fisheries Research Institute, CAFS, China (No. 20603022022013, 20603022021017); Qingdao Postdoctoral Applied Research Project; Central Public-interest Scientific Institution Basal Research Fund, CAFS, China (No. 2023TD02); the National Natural Science Foundation of China (No.42006194).

## Acknowledgments

We are grateful to the crew of the F/V Fu Rong Hai and the scientific observers onboard for helping with samples and data collection. We would also thank Professor Ruixiang Li for double checking the phytoplankton identification.

## Conflict of interest

The authors declare that the research was conducted in the absence of any commercial or financial relationships that could be construed as a potential conflict of interest.

## Publisher's note



## References

Atkinson, A., Hill, S. H., Barange, M., Pakhomov, E. A., Raubenheimer, D., Schmidt, K., et al. (2014). Sardine cycles, krill declines and locust plagues: revisiting "wasp-waist" food webs. *Trends. Ecol. Evol.* 29, 309–316. doi: 10.1016/j.tree.2014.03.011

Atkinson, A., Siegel, V., Pakhomov, E., and Rothery, P. (2004). Long-term decline in krill stock and increase in salps within the Southern Ocean. *Nat.* 432 (7013), 100–103. doi: 10.1038/nature02996

Berges, J. A., Varela, D. E., and Harrison, P. J. (2002). Effects of temperature on growth rate, composition and nitrogen metabolism in the marine diatom *Thalassiosira pseudonana* (Bacillariophyceae). *Mar. Ecol. Prog. Ser.* 225, 139–146. doi: 10.3354/meps225139

Bernard, K. S., Steinberg, D. K., and Schofield, O. M. E. (2012). Summertime grazing impact of the dominant macrozooplankton off the Western Antarctic

Peninsula. *Deep-Sea Res. Part I: Oceanogr. Res. Pap.* 62, 111–122. doi: 10.1016/j.dsr.2011.12.015

Biggs, T. E. G., Alvarez-Fernandez, S., Evans, C., Mojica, K. D. A., Rozema, P. D., Venables, H. J., et al. (2019). Antarctic phytoplankton community composition and size structure: importance of ice type and temperature as regulatory factors. *Pol. Biol.* 42, 1997–2015. doi: 10.1007/s00300-019-02576-3

Cefarelli, A. O., Vernet, M., and Ferrario, M. E. (2011). Phytoplankton composition and abundance in relation to free-floating Antarctic icebergs. *Deep. Res. Part II Top. Stud. Oceanogr.* 58, 11–12. doi: 10.1016/j.dsr2.2010.11.023

Clarke, A., and Tyler, P. A. (2008). Adult krill feeding at abyssal depths. *Curr. Biol.* 18, 282–285. doi: 10.1016/j.cub.2008.01.059

Cleary, A. C., Durbin, E. G., and Casas, M. C. (2018). Feeding by Antarctic krill *Euphausia superba* in the West Antarctic Peninsula: differences between fjord and open waters. *Mar. Ecol. Prog. Ser.* 595, 39–54. doi: 10.3354/meps12568

Costa, R. P., Mendes, C. R. B., Tavano, V. M., Dotto, T. S., Kerr, R., Monteiro, T., et al. (2020). Dynamics of an intense diatom bloom in the Northern Antarctic Peninsula, February 2016. *Limnol. Oceanogr.* 65, 2056–2075. doi: 10.1002/lno.11437

Cuzin-Roudy, J., and Labat, J. P. (1992). Early summer distribution of Antarctic krill sexual development in the Scotia Weddell region: a multivariate approach. *Polar Biol.* 12, 65–74. doi: 10.1007/BF00239966

Drits, A. V., and Pasternak, A. F. (1993). "Feeding of dominant species of the Antarctic herbivores zooplankton," in *Pelagic Ecosystems of the Southern Ocean*. Ed. N. M. Voronina (Moscow: Nauka Press), 250–259.

Drits, A. V., and Semenova, T. N. (1989). "Trophic characteristics of major planktonic phytophages from South Shetland Islands region during early spring," in *Complex Investigations of the Pelagic Zone of the Southern Ocean*. Ed. L. A. Ponomareva (Moscow: Shirshov Institute Oceanology Publishers), 66–78.

Ducklow, H. W., Baker, K., Martinson, D. G., Quetin, L. B., Ross, R. M., Smith, R. C., et al. (2007). Marine pelagic ecosystems: the West Antarctic Peninsula. *Phil. Trans. R. Soc B.* 362, 67–94. doi: 10.1098/rstb.2006.1955

Eppley, R. W. (1972). Temperature and phytoplankton growth in the sea. *Fish Bull. Nat. Ocean Atmos. Adm.* 70, 1063–1085.

Field, J. G., Clarke, K. R., and Warwick, R. M. (1982). A practical strategy for analysing multispecies distribution patterns. *Mar. Ecol. Prog. Ser.* 8, 37–52. doi: 10.3354/meps008037

Flores, H., Atkinson, A., Kawaguchi, S., Krafft, B. A., Milinevsky, G., Nicol, S., et al. (2012). Impact of climate change on Antarctic krill. *Mar. Ecol. Prog. Ser.* 458, 1–19. doi: 10.3354/meps09831

Froneman, P. W., Pakhomov, E. A., Perissinotto, R., and Laubscher, R. K. (1997). Microphytoplankton assemblages in the waters surrounding South Georgia, Antarctica during austral summer 1994. *Polar Bio.* 17, 515–522. doi: 10.1007/s003000050150

Froneman, P. W., Pakhomov, E. A., Perissinotto, R., and McQuaid, C. D. (2000). Zooplankton structure and grazing in the Atlantic sector of the Southern Ocean in late austral summer 1993. Part2. Biochemical zonation. *Deep-Sea Res. Part I: Oceanogr. Res. Pap.* 47, 1687–1702. doi: 10.1016/S0967-0637(99)00121-1

Gonçalves-Araujo, R., de Souza, M. S., Tavano, V. M., and Garcia, C. A. E. (2015). Influence of oceanographic features on spatial and interannual variability of phytoplankton in the Bransfield Strait, Antarctica. *J. Mar. Syst.* 142, 1–15. doi: 10.1016/j.jmarsys.2014.09.007

Haberman, K. L., Quetin, L. B., and Ross, R. M. (2003a). Diet of the Antarctic krill (*Euphausia superba* Dana): I. Comparisons of grazing on Phaeocystis Antarctica (Karsten) and *Thalassiosira Antarctica* (Comber). *J. Exp. Mar. Bio. Ecol.* 283 (1-2), 79–95. doi: 10.1016/s0022-0981(02)00466-5

Haberman, K. L., Ross, R. M., and Quetin, L. B. (2003b). Diet of the antarctic krill (*Euphausia Superba* Dana): II. selective grazing in mixed phytoplankton assemblages. *J. Exp. Mar. Biol. Ecol.* 283 (1-2), 97–113. doi: 10.1016/S0022-0981(02)00467-7

Hamner, W. M., Hamner, P. P., Strand, S. W., and Gilmer, R. W. (1983). Behavior of Antarctic krill, *Euphausia superba* – chemoreception, feeding, schooling and molting. *Science* 220, 433–435. doi: 10.1126/science.220.4595.433

Hernando, M., Schloss, I. R., Almandoz, G. O., Malanga, G., Varela, D. E., and De Troch, M. (2018). Combined effects of temperature and salinity on fatty acid content and lipid damage in Antarctic phytoplankton. *J. Exp. Mar. Biol. Ecol.* 503, 120–128. doi: 10.1016/j.jembe.2018.03.004

Hewes, C. D., Reiss, C. S., and Holm-Hansen, O. (2009). A quantitative analysis of sources for summertime phytoplankton variability over 18 years in the South Shetland Islands (Antarctica) region. *Deep-Sea Res. Part I: Oceanogr. Res. Pap.* 56 (8), 1230–1241. doi: 10.1016/j.dsr.2009.01.010

Hewitt, R. P., Watkins, J., Naganobu, M., Sushin, V., Brierley, A. S., Demer, D., et al. (2004). Biomass of Antarctic krill in the Scotia Sea in January/February 2000 and its use in revising an estimate of precautionary yield. *Deep. Res. Part II Top. Stud. Oceanogr.* 51, 1215–1236. doi: 10.1016/j.dsr2.2004.06.011

Holm-Hansen, O., and Mitchell, B. G. (1991). Spatial and temporal distribution of phytoplankton and primary production in the western Bransfield Strait region. *Deep-Sea Res. Part I: Oceanogr. Res. Pap.* 38, 961–980. doi: 10.1016/0198-0149(91)90092-T

Ishii, H., Omori, M., and Murano, M. (1985). Feeding behavior of the Antarctic krill *E. superba* Dana: I. Reaction to size and concentration of food particles. *Trans. Tokyo Univ. Fish.* 6, 117–124.

Kang, S. H., Kang, J. S., Lee, S., Chung, K. H., Kim, D., and Park, M. G. (2001). Antarctic phytoplankton assemblages in the marginal ice zone of the northwestern Weddell Sea. *J. Plankton Res.* 21 (4), 150–175. doi: 10.1163/9789004276796_008

Krafft, B. A., Macaulay, G. J., Skaret, G., Knutsen, T., Bergstad, O. A., Lowther, A., et al. (2021). Standing stock of Antarctic krill (*Euphausia superba* Dana 1850) (Euphausiacea) in the Southwest Atlantic sector of the southern ocean 2018–19. *J. Crustac. Biol.* 41 (3), 1–17. doi: 10.1093/jcbiol/ruab046

Lancelot, C., Mathot, S., Veth, C., and de Baar, H. (1993). Factors controlling phytoplankton ice-edge blooms in the marginal ice-zone of northwestern Weddell Sea during sea ice retreat 1988: field observations and mathematical modelling. *Polar Biol.* 13, 377–387. doi: 10.1007/BF01681979

Lionard, M., Roy, S., Tremblay-Létourneau, M., and Ferreyra, G. A. (2012). Combined effects of increased UV-B and temperature on the pigment-determined marine phytoplankton community of the St. Lawrence Estuary. *Mar. Ecol. Prog. Ser.* 445, 219–234. doi: 10.3354/meps09484

Liu, L., Fu, M., Sun, K., Xu, Q., Xu, Z., Zhang, X., et al. (2021). The distribution of phytoplankton size and major influencing factors in the surface waters near the northern end of the Antarctic Peninsula. *Acta Oceanol. Sin.* 40 (6), 92–99. doi: 10.1007/s13131-020-1611-3

Luan, Q., Sun, J., Wu, Q., and Wang, J. (2012). Phytoplankton community in adjoining water of the Antarctic Peninsula during austral summer 2010. *Adv. Mar. Sci.* 30 (4), 508–518.

Luan, Q., Wang, C., Wang, X., Sun, J., Niu, M., and Wang, J. (2013). Microphytoplankton communities off the Antarctic Peninsula region in austral summer 2010/2011. *Polish Polar. Res.* 34 (4), 413–428. doi: 10.2478/popore–2013–0025

Maciewska, K., and Opalinski, K. W. (1993). Spatial and temporal differentiation of food in Antarctic krill, *Euphausia superba*. *Pol. Arch. Hydrobiol.* 40, 291–311.

Mascioni, M., Almandoz, G. O., Cefarelli, A. O., Cusick, A., Ferrario, M. E., and Vernet, M. (2019). Phytoplankton composition and bloom formation in unexplored nearshore waters of the western Antarctic Peninsula. *Polar Biol.* 42, 1859–1872. doi: 10.1007/s00300-019-02564-7

McClatchie, S., and Boyd, C. M. (1983). Morphological study of sieve efficiencies and mandibular surfaces in the Antarctic krill, *Euphausia superba*. *Can. J. Fish. Aquat. Sci.* 40, 955–967. doi: 10.1139/f83-122

Mendes, C. R. B., Souza, M. S. D., Garcia, V. M. T., Leal, M. C., Brotas, V., and Garcia, C. A. E. (2012). Dynamics of phytoplankton communities during late summer around the tip of the antarctic peninsula. *Deep-Sea Res. Part I: Oceanogr. Res. Pap.* 65 (Jul.), 1–14. doi: 10.1016/j.dsr.2012.03.002

Meyer, M. A., and El-Sayed, S. Z. (1983). Grazing of *Euphausia superba* Dana on natural phytoplankton populations. *Polar Biol.* 1 (4), 193–197. doi: 10.1007/bf00443187

Moline, M. A., Claustre, H., Frazer, T. K., Schofield, O., and Vernet, M. (2004). Alteration of the food web along the Antarctic Peninsula in response to a regional warming trend. *Global Change Biol.* 10 (12), 1973–1980. doi: 10.1111/j.1365-2486.2004.00825.x

Montagnes, D. J. S., and Franklin, D. J. (2001). Effect of temperature on diatom volume, growth rate, and carbon and nitrogen content: reconsidering some paradigms. *Limnol. Oceanogr.* 46, 2008–2018. doi: 10.2307/3069070

Monte-Hugo, M., Doney, S. C., Ducklow, H. W., Fraser, W., Martinson, D., Stammerjohn, S. E., et al. (2009). Recent changes in phytoplankton communities associated with rapid regional climate change along the western Antarctic Peninsula. *Science* 323 (5920), 1470–1473. doi: 10.1126/science.1164533

Opaliński, K. W., Maciejewska, K., and Georgieva, L. V. (1997). Notes of food selection in the Antarctic krill, *Euphausia superba*. *Polar Biol.* 17 (4), 350–357. doi: 10.1007/pl00013376

Pakhomov, E. A., Perissinotto, R., Froneman, P. W., and Miller, D. G. M. (1997). Energetics and feeding dynamics of *Euphausia Superba* in the South Georgia region during the summer of 1994. *J. Plankton Res.* 4, 399–423. doi: 10.1093/plankt/19.4.399

Prézelin, B. B., Hofmann, E. E., Mengelt, C., and Klinck, J. M. (2000). The linkage between Upper Circumpolar Deep Water (UCDW) and phytoplankton assemblages on the west Antarctic Peninsula continental shelf. *J. Mar. Res.* 58, 165–202. doi: 10.1357/002224000321511133

Price, H. J., Boyd, K. R., and Boyd, C. M. (1988). Omnivorous feeding behavior of the Antarctic krill *Euphausia superba*. *Mar. Biol.* 97, 67–77. doi: 10.1007/BF00391246

Quetin, L. B., Ross, R. M., and Clarke, A. (1994). "Krill energetics: seasonal and environmental aspects of the physiology of *Euphausia superba*," in *(ed) Southern Ocean ecology: the BIOMASS perspective*. Ed. S. Z. El-Sayed (Cambridge: Cambridge University Press), 165–184.

Ross, R. M., Quetin, L. B., Baker, K. S., Vernet, M., and Smoth, R. C. (2000). Growth limitation in young *Euphausia superba* under field conditions. *Limnol. Oceanogr.* 45, 31–43. doi: 10.4319/lo.2000.45.1.0031

Ross, R. M., Quetin, L. B., and Lascara, C. M. (1996). "Distribution of Antarctic krill and dominant zooplankton west of the Antarctic Peninsula," in *Foundations for Ecosystem Research in the Western Antarctic Peninsula Region*. Eds. R. Ross, E. Hofmann and L. Quetin (Washington, DC: Antarctic Research Series, American Geophysical Union), 199–217.

Rozema, P. D., Biggs, T., Sprong, P. A. A., Buma, A. G. J., Venables, H. J., Evans, C., et al. (2017a). Summer microbial community composition governed by upper-

ocean stratification and nutrient availability in northern Marguerite Bay, Antarctica. *Deep. Res. Part II Top. Stud. Oceanogr.* 139, 151–166. doi: 10.1016/j.dsr2.2016.11.016

Rozema, P. D., Venables, H. J., van de Poll, W. H., Clarke, A., Meredith, M. P., and Buma, A. G. J. (2017b). Interannual variability in phytoplankton biomass and species composition in northern Marguerite Bay (West Antarctic Peninsula) is governed by both winter sea ice cover and summer stratification. *Limnol. Oceanogr.* 62, 235–252. doi: 10.1002/lno.10391|

Sangrà, P., Gordo, C., Hernández-Arencibia, M., Marrero-Díaz, A., Rodríguez-Santana, A., Stegner, A., et al. (2011). The Bransfield current system. *Deep-Sea Res. Part I: Oceanogr. Res. Pap.* 58, 390–402. doi: 10.1016/j.dsr.2011.01.011

Schloss, I., and Estrada, M. (1994). Phytoplankton composition in the Weddell-Scotia Confluence area during austral spring in relation to hydrography. *Pol. Biol.* 14 (2), 77–90. doi: 10.1007/bf00234969

Schmidt, K., and Atkinson, A. (2016). "Feeding and food processing in antarctic krill (*Euphausia superba* dana)," in *Biology and Ecology of Antarctic Krill, Advances in Polar Ecology*. Ed. V. Siegel, (Switzerland: Springer International Publishing) 175–224. doi: 10.1007/978-3-319-29279-3_5

Schmidt, K., Atkinson, A., Pond, D. W., and Ireland, L. C. (2014). Feeding and overwintering of Antarctic krill across its major habitats: the role of sea ice cover, water depth, and phytoplankton abundance. *Limnol. Oceanogr.* 59, 17–36. doi: 10.4319/lo.2014.59.1.0017

Schmidt, K., Atkinson, A., Venables, H. J., and Pond, D. W. (2012). Early spawning of Antarctic krill in the Scotia Sea is fuelled by "superfluous feeding" on non-ice-associated phytoplankton blooms. *Deep. Res. Part II Top. Stud. Oceanogr.* 59 (60), 159–172. doi: 10.1016/j.dsr2.2011.05.002

Shannon, C. E., and Weaver, W. (1949). *The mathematical theory of communication* (Urbana: University of Illinois Press), 1–117.

Shi, Y., Wang, J., Zuo, T., Shan, X., Jin, X., Sun, J., et al. (2020). Seasonal changes in zooplankton community structure and distribution pattern in the Yellow Sea, China. *Front. Mar. Sci.* 7. doi: 10.3389/fmars.2020.00391

Smetacek, V., and Veth, C. (1989). "Introduction," in *The expedition Antarktis VII/3 (EPOS Leg 2) of RV "Polarstern" in 1988/89*, vol. 65 . Eds. I. Hempel, P. H. Schalk and V. Smetacek (Bremerhaven: Berichte zur Polar for schung, Alfred-Wegener-Institut f€ur Polar- und Meeresforschung), 1–7.

Stretch, J. J., Hamner, P. P., Hamner, W. M., Michel, W. C., Cook, J., and Sullivan, C. W. (1988). Foraging behaviour of Antarctic krill *Euphausia superba* on sea ice microalgae. *Mar. Ecol. Prog. Ser.* 44, 131–139. doi: 10.3354/meps044131

Stuart, V. (1989). Observations on the feeding of *Euphausia lucens* on natural phytoplankton suspensions in the southern Benguela upwelling region. *Cont. Shelf Res.* 9 (11), 1017–1028. doi: 10.1016/0278-4343(89)90005-8

Sun, J., Liu, D. Y., Ning, X. R., and Liu, C. G. (2003). Phytoplankton in the Prydz Bay and the adjacent Indian sector of the Southern Ocean during the austral summer 2001/2002. *Oceanol. Limnol. Sinica.* 34 (5), 519–532.

Vernet, M., Martinson, D., Iannuzzi, R., Stammerjohn, S., Kozlowski, W., Sines, K., et al. (2008). Primary production within the sea-ice zone west of the Antarctic Peninsula: I. Sea ice, summer mixed layer, and irradiance. *Deep. Res. Part II Top. Stud. Oceanogr.* 55 (18–19), 2068–2085. doi: 10.1016/j.dsr2.2008.05.021

Watters, G. M., Hinke, J. T., and Reiss, C. S. (2020). Long-term observations from Antarctica demonstrate that mismatched scales of fisheries management and predator-prey interaction lead to erroneous conclusions about precaution. *Sci. Rep.* 10 (1), 2314. doi: 10.1038/s41598-020-59223-9

Winder, M., and Sommer, U. (2012). Phytoplankton response to a changing climate. *Hydrobiology*> 698, 5–16. doi: 10.1007/s10750-012-1149-2

Zhu, G. (1993). Study on distribution characteristics of microphytoplankton of the Bransfield Strait and adjacent waters of Elephant Island. *Donghai Mar. Sci.* 11, 3.

frontiers | Frontiers in Marine Science

TYPE Original Research
PUBLISHED 29 November 2023
DOI 10.3389/fmars.2023.1233492



OPEN ACCESS

EDITED BY
Letterio Guglielmo,
Anton Dohrn Zoological Station Naples, Italy

REVIEWED BY
Vladimir G Dvoretsky,
Murmansk Marine Biological Institute, Russia
Emilia Trudnowska,
Polish Academy of Sciences, Poland
Gvm Gupta,
Centre for Marine Living Resources and Ecology (CMLRE), India

*CORRESPONDENCE
Shino Kumagai
shino2189@eis.hokudai.ac.jp

RECEIVED 02 June 2023
ACCEPTED 13 November 2023
PUBLISHED 29 November 2023

CITATION
Kumagai S, Matsuno K and Yamaguchi A (2023) Zooplankton size composition and production just after drastic ice coverage changes in the northern Bering Sea assessed via ZooScan.
*Front. Mar. Sci.* 10:1233492.
doi: 10.3389/fmars.2023.1233492



# Zooplankton size composition and production just after drastic ice coverage changes in the northern Bering Sea assessed via ZooScan

Shino Kumagai[1]*, Kohei Matsuno[1,2] and Atsushi Yamaguchi[1,2]

[1]Faculty/Graduate School of Fisheries Sciences, Hokkaido University, Hakodate, Hokkaido, Japan, [2]Arctic Research Center, Hokkaido University, Sapporo, Hokkaido, Japan

Drastic environmental changes were noted in the northern Bering Sea in 2018. A reduction in sea ice affected several trophic levels within the ecosystem; this resulted in delayed phytoplankton blooms, the northward shifting of fish stocks, and a decrease in the number of seabirds. Changes in the community composition of zooplankton were reported in 2022, but changes in zooplankton interactions and production have not been reported to date. Therefore, this study examined predator-prey interaction, secondary production, and prey availability for fish to understand the effect of early sea ice melt. Zooplankton size data were estimated from the size spectra obtained using ZooScan based on samples collected in 2017 and 2018. A cluster analysis based on biovolume showed that the zooplankton community could be divided into three groups (Y2017N, Y2017S, Y2018). Y2017N, characterized by low abundance, biomass, and production, Y2017S, characterized by high biovolume and production, which contributed with *Calanus* spp., and Y2018, characterized by low biovolume but high production, contributed with small copepods, and Bivalvia. In 2017, the highest biovolume group was observed south of St. Lawrence Island, and it was dominated by *Calanus* spp. and Chaetognatha. Normalized size spectra of this group showed the highest secondary production with present predator-prey interactions, suggesting that the area provides high prey availability for fish larvae and juveniles. In contrast, small copepods and bivalve larvae were dominant in this area in 2018, which contain less carbons and energy, suggesting the prevalence of low-nutrient foods in this year in relation to early sea ice melt.

KEYWORDS

**sea-ice reduction, zooplankton biomass, normalized biomass size spectra, predator-prey interactions, secondary production**

# 1 Introduction

The northern Bering Sea lies on a shallow shelf and has a maximum depth of 50 m. This region is influenced by the inflow of three different water masses: warm Alaskan Coastal Water (ACW) with low salinity and nutrient levels; cold Anadyr Water (AnW) with high salinity and nutrient levels; and Bering Shelf Water (BSW), the characteristics of which are between those of the ACW and AnW (Coachman et al., 1975). The continuous inflow of AnW supports high primary productivity, resulting in high biomass and trophic levels in this area (Springer et al., 1993).

Decreases in both the period and area of seasonal ice coverage in northern Being Sea have been recently reported (Grebmaier et al., 2015). In the winter of 2018, the area of sea ice coverage reached an historical minimum based on satellite observations recorded over 40 years (Cornwall, 2019), and the reduced sea ice extent resulted in early sea ice melting (Stabeno and Bell, 2019). The early sea-ice retreat has been largely attributed to relatively warm winds from the south accompanied by a westward shift of the Aleutian Low from its typical position (Stabeno and Bell, 2019; Basyuk and Zuenko, 2020). Irregular phenomena associated with early sea melt have been observed at several trophic levels: phytoplankton bloom delay (Kikuchi et al., 2020), the northward migration of subarctic fish such as pollack and Pacific cod (Stevenson and Lauth, 2019), and a decrease in the number of sea birds (Cornwall, 2019).

Zooplankton connect primary production and higher trophic levels. The abundance of small copepods increased during the summer of 2018 (Duffy-Anderson et al., 2019) because the delayed phytoplankton bloom resulted in delayed reproduction and large copepods did not reach their late developmental stage (Kimura et al., 2022). However, although the community structure of zooplankton and the population structure of copepods have been reported, changes in the size composition of zooplankton have not been reported. As another problem, copepod production is only estimated in the paper, but production of whole zooplankton taxa is not assumed due to lack of size data.

The size of zooplankton is reflective of the trophic level, and once the biomass of one size range is known, the abundance of other size ranges can be estimated (Sheldon et al., 1977). Obtaining such information is therefore important for understanding the ecosystem structure. In addition, fish select prey based on zooplankton size, and differences in prey species affect the growth rates of juveniles and the overwintering rates (Sheldon et al., 1977; O'Brien, 1979; Meeren and Næss, 1993). Therefore, determining the zooplankton size composition is not only important for assessing the ecosystem structure but also for determining its potential as a food resource for higher trophic levels.

Normalized Biomass Size Spectra (NBSS) were developed to analyze the size composition of marine organisms (Sheldon et al., 1977). They have been used in various oceans to analyze marine ecosystem structures and food chains (i.e. Garcia-Comas et al., 2011; Forest et al., 2012; Cornils et al., 2022). Characteristics of NBSS analysis can be explained by its slope and intercepts. Slope reflects abundance of zooplankton, and production and energy transportation can be explained by the slopes (Zhou, 2006). This is because NBSS slope explains ratio of large particles and small particles. When NBSS slope is steep, is means small particles are lots more than large particles. Therefore, NBSS slope can reflects energy transfer from zooplankton to fish (Sprules et al., 1988). The optical plankton counter (OPC) and laser optical plankton counter (LOPC) are the most common instruments used in NBSS analysis (e.g., Herman and Harvey, 2006; Barid et al., 2008); however, these instruments are only used to measure the size of zooplankton, and conducting an analysis of size alone may not correlate with the actual trophic level in the food web structure (e.g., large jellyfish feeding on phytoplankton). In addition, if NBSS analysis based only on size is used to interpret energy transfer within the food chain, the function of the food chain may be misinterpreted due to the opacity of the prey-predator relationship (Yurista et al., 2014). In contrast, ZooScan can be used to acquire and classify digital images of zooplankton (Gorsky et al., 2010), and the combination of size data and taxon information obtained from image analysis makes it suitable for use in conducting food chain analyses, such as those described above (Grosjean et al., 2004; Gorsky et al., 2010; Garcia-Comas et al., 2011).

Therefore, in this study, the zooplankton community structure and size composition in 2017 (normal sea ice melt year) and 2018 (early sea ice melt year) were investigated using ZooScan, and the results obtained from ZooScan for both years were compared to assess the effect of sea ice reduction on zooplankton size composition. Production of whole taxa was then estimated using size, taxon information, and *in situ* temperature, with the aim of clarifying whether production was passed on to higher trophic levels.

# 2 Materials and methods

## 2.1 Satellite data

Sea ice concentration (10-km resolution) was downloaded from the Advanced Microwave Scanning Radiometer 2 (ASMR2) supplied by the Japan Aerospace Exploration Agency via the Arctic Data Archive System (ADS), with the cooperation of the National Institute of Polar Research and Japan Aerospace Exploration Agency (JAXA). The data were then used to evaluate the sea ice coverage extent. Based on these data, the melt day (MD) was defined as the last date on which the sea ice concentration fell below 20% prior to the observed annual sea-ice minimum across the study region. Time since sea-ice melt (TSM) was also defined as the number of open-water days from the MD to the sampling date at each station.

## 2.2 Field samplings

Sampling was conducted by the 40$^{th}$ and 56$^{th}$ cruises of the T/S *Oshoro-maru* in the northern Bering Sea (62˚10'–66˚44'N, 166˚30'–174˚05'W) during July 11–22, 2017, and July 2–12, 2018 (Figure 1). Zooplankton samples were collected by towing a NORPAC net (0.45 m mouth diameter, 150 µm mesh) vertically from 5 m (22–71 m) just above the seafloor to the surface. The volume of water filtered

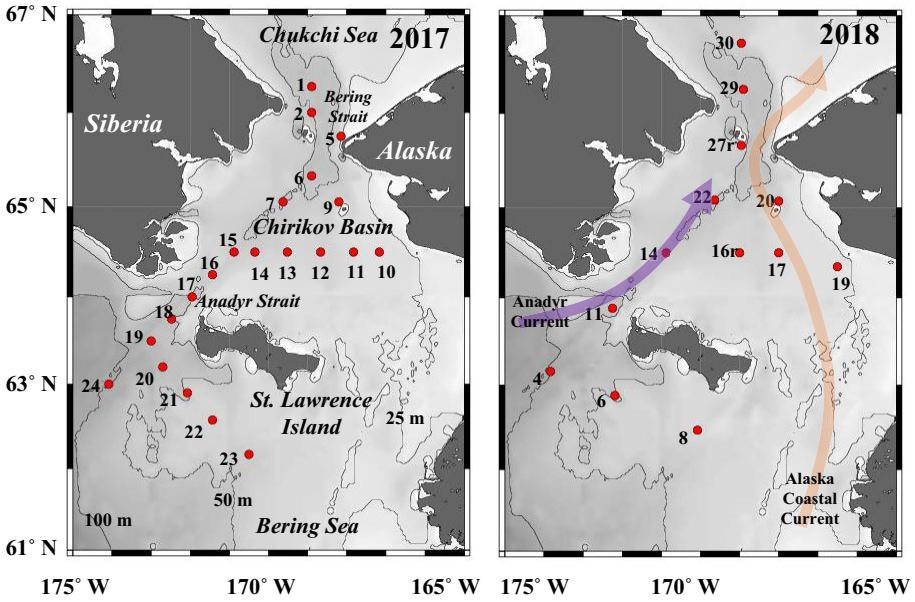


FIGURE 1
Location of stations in the northern Bering Sea during 11–22 July 2017and 2–12 July 2018. The numbers indicate station ID. Color arrows indicate main currents in this region.

through the net was estimated using a one-way flow meter (Rigosha Co., Ltd., Bunkyo-ku, Tokyo, Japan) attached to the center of the mouth. The collected zooplankton samples were immediately filled with 5% buffered formalin and transported to the laboratory. At the same station, the water temperature, salinity, and chlorophyll-a fluorescence values were measured using CTD (Conductivity Temperature Depth Profiler; Sea-Bird Electronics Inc., SBE911 plus).

## 2.3 Sample analysis

A total of 34 zooplankton samples were divided into 1/16–64 sections using a Motoda splitter (Motoda, 1959) and image data were obtained using ZooScan (Hydrooptic Inc.). First, the ZooScan scanning cell was filled with deionized water to scan the background image using VueScan (Version 9.5.24), and the divided zooplankton samples were then poured into the cell and scanned using VueScan. The scans of the samples were digitized using a minute function at 2400 dpi, where one pixel corresponded to 10.6 µm. Image data were semi-automatically separated per object using ZooProcess (Version 7.23) in Image J software (Version 1.410). All images scanned through ZooScan were uploaded onto the website Ecotaxa, where the gene level was semi-automatically identified based on datasets made from five manually identified samples per sampling year. All the images were manually checked to ensure that they had been correctly identified. Copepods were identified up to the genus level, and all other species were identified at the taxonomic level (from Order to Phylum). Images that could not be identified were classified as "unidentified organisms," and those containing more than one object were classified as "multiple." Images identified as "multiple" and "detritus" were excluded from further analysis. Copepods were divided into three groups: *Calanus* spp., Other large copepods (*Eucalanus* spp., *Metridia* spp., and *Neocalanus* spp.), and small copepods (*Acartia* spp., *Centropages* spp., *Microcalanus* spp., *Microsetella* spp., *Oithona* spp., *Oncaea* spp., *Pseudocalanus* spp., and Copepoda nauplii).

The size of each zooplankton was measured based on the study of Vandromme et al. (2012), using the ellipse major axis (*L major*, µm) and minor axis length *(L minor*, µm), which best fit the zooplankton image shape, and the volume of the ellipse (*volume*, $mm^3$) and an equivalent spherical diameter (ESD, µm) with the same volume as the ellipse were identified using the following respective equations,

$$Volume = \frac{4}{3}\pi\left(\frac{L\ major}{2}\right)\left(\frac{L\ minor}{2}\right)^2,$$

$$ESD = \sqrt[3]{\frac{Volume \times 3}{4\pi}}.$$

The biovolume (B: $mm^3\ m^{-2}$) was calculated using the filtered water volume (F: $m^{-3}$) calculated by using data of flowmeter, the tow distance (L), split ratio (s) and the elliptical volume (*Volume*, $mm^3$) via the following equation.

$$B = \frac{Volume \times L}{F \times s}$$

## 2.4 Data analysis

Based on vertical profiles in temperature and salinity, thickness of water mass (according to Danielson et al., 2020) was calculated at each station.

Zooplankton biovolumes ($mm^3$ $m^{-2}$) of 34 stations were used to conduct a cluster analysis, and they were transformed into fourth roots ($\sqrt[4]{X}$) to reduce the bias of abundant species. The similarities between the samples were examined using the Bray-Curtis similarity index. Dendrograms were created using the mean linkage method (unweighted pair group method using arithmetic means) and were classified into multiple groups by separating them at specific similarity levels (Field et al., 1982). Accompanying this analysis, similarity profile analysis (SIMPROF) was added to determine if groupings of the stations were statistically significant (at 5% significance level).The relationship between each sample and normalized hydrographic data (water temperature, salinity, chlorophyll-*a* fluorescence, MD, TSM and thickness in water masses) was evaluated using DistLM (distance based linear modeling) and a redundancy analysis (RDA). The parameters were selected by procedures consisting of Step-wise, $r^2$ and 999 permutations were used. The cluster analysis, DistLM, and RDA were conducted using the Primer 7 software (PRIMER-E Ltd., Albany, Auckland, New Zealand).

Differences in hydrographic (water temperature, salinity, chlorophyll-*a* fluorescence, and MD) and zooplankton size spectra parameters among the groups (identified by the cluster analysis based on zooplankton biovolume) were tested using the max-t method with a heteroscedastic consistent covariance estimation (HC3) (Herberich et al., 2010). The tests were conducted using R software with the packages "multcomp" and "sandwich" (version 4.1.2, R Core Team, 2021).

The NBSS analysis was conducted based on the size composition data obtained from ZooScan. Size data were used later analysis in the 300–3400 µm ESD range. Zooplankton larger than 3400 µm ESD (i.e., Cnidaria) were excluded from the analysis because they were not quantitatively sampled by net and were easily underestimated in ZooScan (Naito et al., 2019). Three ranges were set to categorize the sizes of zooplankton: small size (ESD 267–1024 µm), medium size (ESD 1024–2673 µm), and large size (ESD 2673–5759 µm). The NBSS X-axis is a log10 transformation of the biovolume for every log10 (0.25) ESD, (X: log10 zooplankton biovolume, [$mm^3$ $ind.^{-1}$]) and the Y-axis is the log10 transformation of the integrated biovolume of the size classes classified by 100 µm ESD divided by the biovolume difference between adjacent size classes (Δbiovolume [$mm^3$]) (Y: log10 zooplankton biovolume [$mm^3$ $m^{-3}$]/Δbiovolume [$mm^3$]). From X and Y, the linear equation of the NBSS is defined as $Y = aX + b$. Comparing the NBSS between the clustered groups, ANCOVA was performed using StatView, with the NBSS slope (a) applied as a response variable and intercept and (b) cluster groups applied as explanatory variables.

Zooplankton biomass and production were determined using ZooScan image data. First, the individual dry weight (*DWind*: mg DW $ind^{-1}$) was calculated from the biovolume per individual ($mm^3$ $ind.^{-1}$), assuming that the density was equivalent to water ($mm^3$ = mg), and the result was multiplied by the water content for each taxon (cf. Omori, 1969; Kiørboe, 2013; Nakamura et al., 2017; Matsuno unpublished data). The biomass per taxon was calculated using the following equation,

$$Biomass = \frac{\sum DWind}{s \times F} \times L ,$$

where $s$ is the split ratio, $F$ is the volume of filtered water ($m^3$), and $L$ is the towing distance (m). To estimate production (mg C $m^{-2}$ $day^{-1}$), the respiration rate (R: µL $O_2$ $ind.^{-1}$ $h^{-1}$) was calculated using the following equation (cf. Ikeda, 1985),

$$Ln(R) = -0.399 + 0.801 \times Ln\ (DWind) + 0.069 \times T,$$

where *DWind* is the dry weight per individual, and $T$ is the integrated mean water temperature at the sampling station. From the respiration rate, the production per individual, *Pind* (µg C $ind^{-1}$ $day^{-2}$) was estimated using the following equation (cf. Ikeda and Motoda, 1978),

$$Pind = \frac{R \times 12}{22.4} \times 0.75 \times 0.97 \times \frac{24}{1000}.$$

To calculate production (mg C $m^{-2}$ $day^{-1}$), Pind was summed for each taxon, divided by the volume of filtered water ($m^3$), and then multiplied by the towing depth.

# 3 Results

## 3.1 Hydrography

In both years, there were similar variations in water temperature and salinity from east to west and with cold saline waters distributed on the western side (cf. Figure 2 and 3 in Kimura et al., 2022). On the other hand, water mass distributions were slightly different between the years (Figure 2). Warm Shelf Water (wSW) covered at surface layer in both years, and cold Shelf Water (cSW) and Anadyr Water (AnW) occupied below the water mass. However, Modified Winter Water (MWW) and Winter Water (WW) were only observed in the south of the St. Lawrence Island during 2017. Chlorophyll *a* fluorescence was higher in the Bering Strait during both years (cf. Figure 2 and 3 in Kimura et al., 2022). The MD occurred from March 23 to April 29 in 2018, which was earlier than in 2017 (April 4 to May 11) (cf. Figure 2 and 3 in Kimura et al., 2022).

## 3.2 Zooplankton community

Cluster analysis based on the biovolumes of all zooplankton taxa revealed three groups (Y2017N, Y2017S, Y2018) with similarities of 62% and 65% (Figure 3A). By plotting the groups on a geological map, their spatial and interannual distributions were separated (Figure 3B). Y2017N was found from the Bering Strait to the Chirikov Basin in 2017 (Figure 3B); Y2017S was distributed along the Alaskan coast and southwest of St. Lawrence Island during both years; and Y2018 was spread widely from the Bering Strait to the southwest of St. Lawrence Island in 2018. Y2017N was dominated by *Calanus* spp. and other large copepods in similar proportions (Figure 3C); Y2017S (with the highest observed biovolume) was dominated by *Calanus* spp. and characterized by

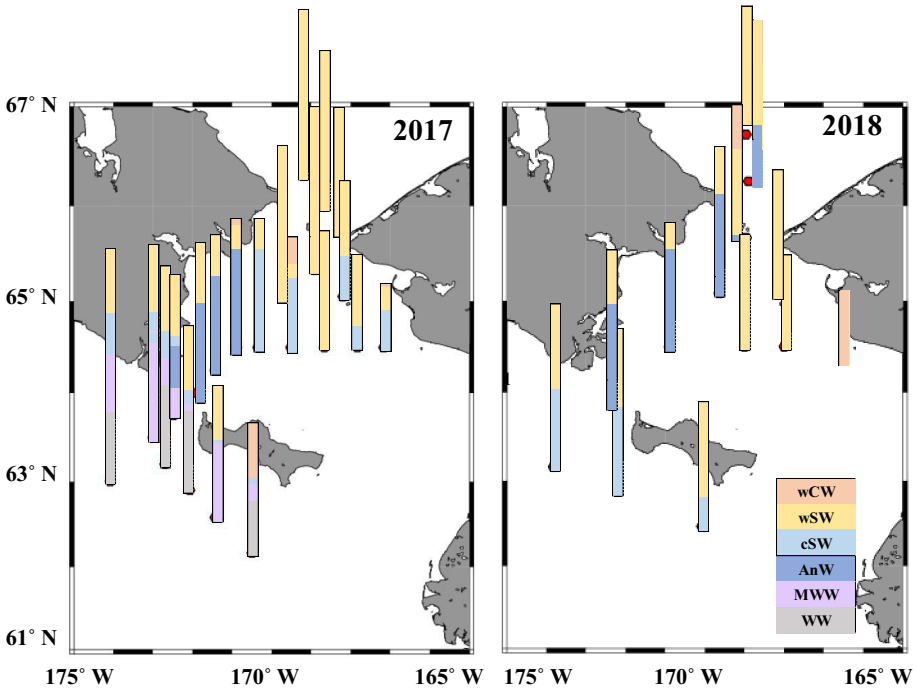


FIGURE 2
Spatial distribution of water masses in the northern Bering Sea during 11–22 July 2017 and 2–12 July 2018. Definition of water mass is according to Danielson et al. (2020). wCW, warm Coastal Water; wSW, warm Shelf Water; cSW, cool Shelf Water; AnW, Anadyr Water; MWW, Modified Winter Water; WW, Winter Water.

the contribution of Euphausiacea, small copepods, and Chaetognatha; and Y2018 contained the lowest biovolume but was dominated by small copepods and other large copepods. Each group was separately distributed in the RDA (Figure 4). Comparing hydrographic data among the groups, only salinity exhibited significant difference; higher value was seen in the Y2017N (32.3) than in the Y2018 (31.9) (Table 1).

An NBSS analysis based on size composition was performed for the three groups classified by the cluster analysis. The results showed that the slope of Y2018 was significantly steeper (-0.8241) than that of Y2017N (-0.6843) (Figure 5, Table 1). Intercepts in NBSS were not different among the group significantly (Table 1). Biovolumes were summarized by 0.25 on the log10 axis and compared to NBSS plots, which clearly showed the contribution of each taxon to size classes (Figure 6). For all taxa, ESD 311–771 µm (-1.75–0 in log10 ($mm^3$ $ind.^{-1}$)) with small copepods dominated, but *Calanus* spp. showed a high contribution at an ESD range of 1132–2439 µm (0–1 in log10 ($mm^3$ $ind.^{-1}$)). In Y2018, with the significantly steeper NBSS slope), Bivalvia highly contributed to the size class of ESD 300–311 µm (-2 to -1.75, log10 ($mm^3$ $ind.^{-1}$)) (Figure 6). other large copepods were dominant in the larger size classes of groups A and C, whereas Chaetognatha was dominant in the same size class of Y2017S. Euphausiacea was particularly abundant in the middle size class of groups Y2017N and Y2018.

A comparison between the size range and the available prey for fish (Pacific cod) (cf. Jacobsen et al., 2020) revealed no yolk-sac larvae specimens in the predator size classes (Figure 6). In Y2017N, other large copepods and Euphausiacea dominated the late larval and early juvenile stage predator size class; in Y2017S, large *Calanus* spp. dominated the late larvae to early juveniles predator size class but Chaetognatha was dominant in the late juvenile stage; and in Y2018, small copepods were dominant in the late larval stage predator size class.

Biomass ranged from 4.60–11.49 g DW $m^{-2}$ and was the highest and lowest in Y2017S and Y2017N, respectively (Figure 7A, Supplementary Table 1). Y2017N was characterized by a high proportion of *Calanus* spp., other large copepods, and Euphausiacea (Figure 7A). Y2017S, which had the highest biomass among the three groups, was dominated by *Calanus* spp. In Y2018, small copepods dominated, followed by *Calanus* spp. and other large copepods (Figure 7A), and the proportion of Bivalvia was higher (9.14%) than that of the other groups (0.05–0.2%). Production ranged from 52.6–119 mg C $m^{-2}$ $day^{-1}$ in the three groups, with the highest in Y2017S and the lowest in Y2017N (Figure 7B; Supplementary Table 2). Y2017N, which showed the lowest production rates, showed a high contribution from *Calanus* spp., other large copepods, and Euphausiacea. Production was dominated by copepods in Y2017S (66%), whereas small copepods supported the production of Y2018, which was also characterized by the production of Bivalvia. Euphausiacea showed the second highest production following copepods in all three groups, ranging from 6.68–13.93 mg C $m^{-2}$.

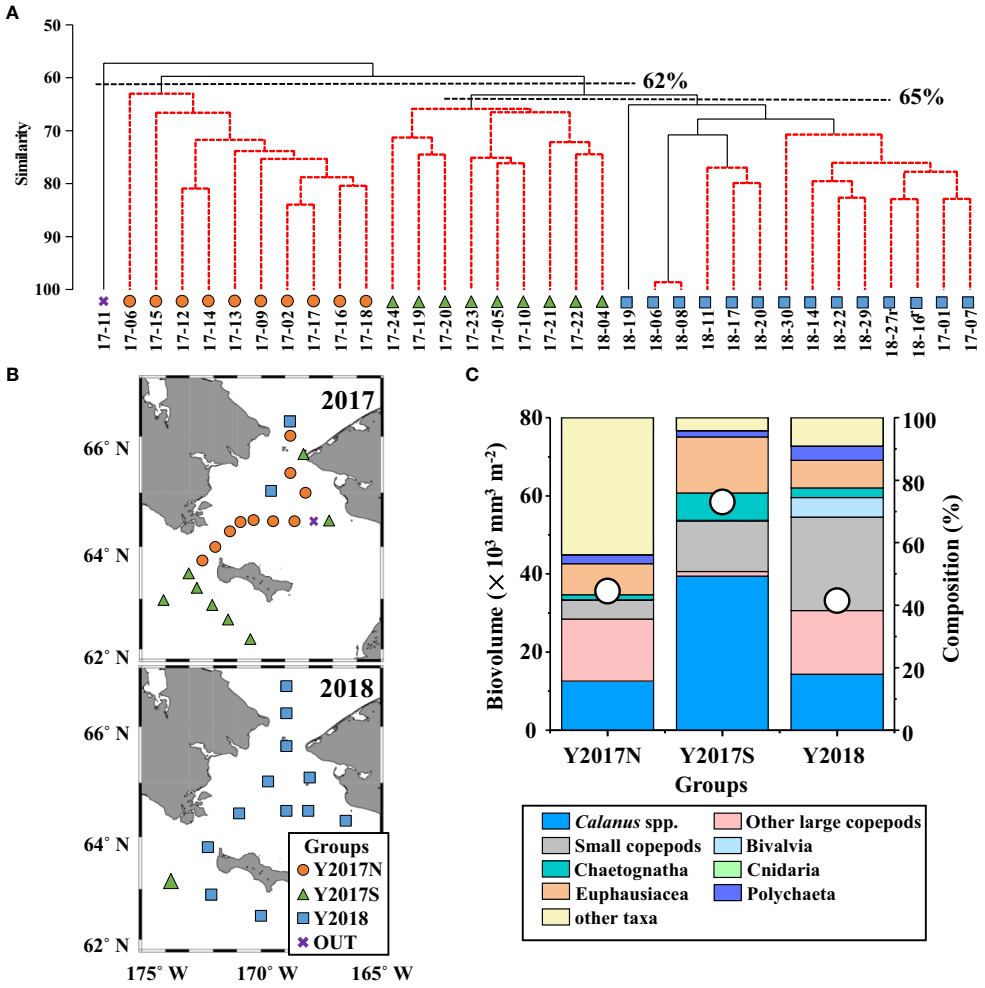


FIGURE 3
**(A)** Results of cluster analysis based on mesozooplankton biovolume using Bray–Curtis similarity connected with UPGMA in the northern Bering Sea during July 2017 and 2018. Three groups (Y2017N, Y2017S, Y2018) were identified with a similarity of 62% and 65% (dashed lines). The samples were named using the year and station ID. **(B)** Horizontal distribution of the three groups in the northern Bering Sea during July 2017 and 2018 identified by cluster analysis (cf. **A**). **(C)** Total biovolume and composition of each group.

# 4 Discussion

## 4.1 Limitation of ZooScan

It is not always possible to classify small objects (especially below 200 μm ESD) via image analysis with ZooScan, as it has a pixel resolution of 10.6 μm (Gorsky et al., 2010). Many studies using ZooScan have focused on > 300 μm ESD zooplankton (i.e., Colas et al., 2017), and we therefore also only analyzed this size range. The parameters of abundance and biovolume accuracy obtained using ZooScan are largely consistent with the microscopic counts and size measurements of copepods (Gorsky et al., 2010; Garcia-Comas et al., 2011; Cornils et al., 2022), and significant regression is present for ESD 1–6 mm-sized copepods, in particular (Forest et al., 2012). However, abundance and biomass based on ZooScans of Chaetognatha, Appendicularia, and Cnidaria are likely to be underestimated because it is difficult to analyze transparent objects using ZooScan and there is large variability in the organic matter content of gelatinous zooplankton (Lehette and Hernandez-Leon, 2009; Naito et al., 2019; Cornils et al., 2022). Also, they are not efficiently caught by nets. Therefore, a considerable amount of attention to detail is required when analyzing such taxa with ZooScan.

## 4.2 NBSS analysis

The slope and intercept of the NBSS explain the zooplankton size composition characteristics: the NBSS intercept is reflected by zooplankton standing stock and primary production, whereas the slope is reflected by productivity and trophic levels (Zhou, 2006). In a typical marine ecosystem, the NBSS slope approaches -1 (Platt and Denman, 1977; Kerr and Dickie, 2001). In this study, all slopes were less than -1: this indicated that larger objects were dominant, which is commonly observed after phytoplankton blooms (Vandromme et al., 2014). NBSS slopes can be easily altered by

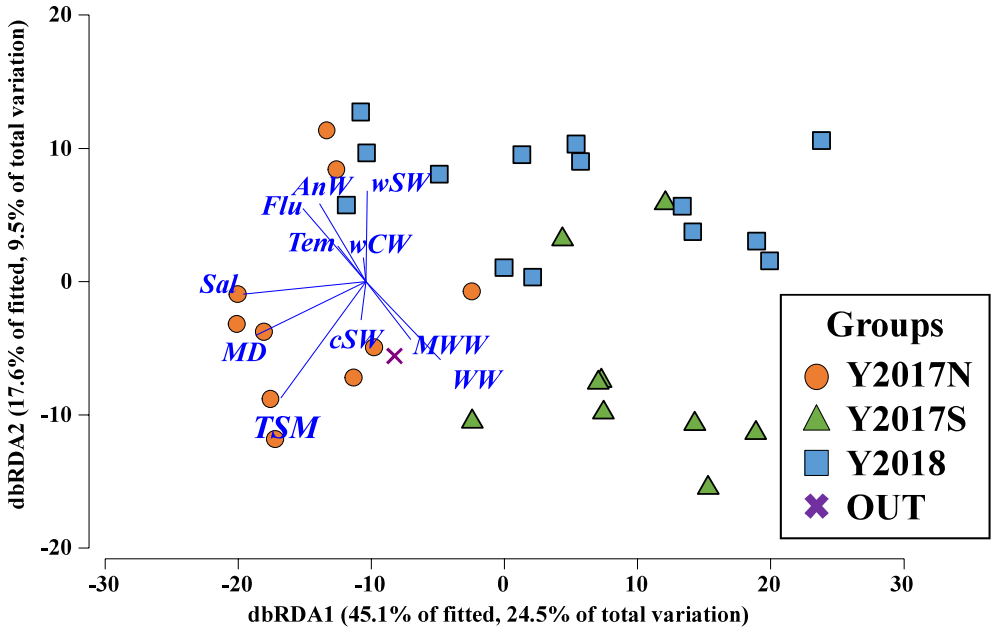


FIGURE 4
dbRDA plot of the three groups with environmental parameters. The direction of the lines indicate the relationship between environmental parameters and groups identified by cluster analysis (cf. Figure 3A) in the northern Bering Sea during July in 2017 and in 2018. Tem, water-column integrated mean temperature; Sal, water-column integrated mean salinity; Flu, water-column integrated fluorescence; MD, melt day; TSM, time since melt day to field sampling; wCW, warm Coastal Water; wSW, warm Shelf Water; cSW, cool Shelf Water; AnW, Anadyr Water; MWW, Modified Winter Water; WW, Winter Water.

top-down and bottom-up effects within an ecosystem (Suthers et al., 2006). In the top-down case, the slope of the NBSS becomes steeper as middle-to large-sized plankton decrease with predation by mammals and fishes. Therefore, a negative relationship is assumed between predator abundance and slope (Suthers et al., 2006). In a bottom-up effect, the slope becomes steeper as primary production increases, consequently increasing the size of small zooplankton (Moore and Suthers, 2006). When discussing top-down and bottom-up effects, it is important to clarify the actual prey-predator relationship (Yurista et al., 2014). As a result, an increasing number of reports have combined NBSS analysis with ZooScan to reveal taxonomic information (i.e., Cornils et al., 2022).

## 4.3 Characteristics of clustering groups

A cluster analysis based on the biovolume was used to reveal regional and interannual changes in zooplankton communities (Matsuno et al., 2012). The distribution and composition showed similar tendencies to those of microscopic analyses (cf. Figure 4 and 5 in Kimura et al., 2022), which suggests that identification at the taxon level (genus level for copepods) using the ZooScan approach can be used to detect trends at a level similar to that detected via microscopic analysis.

In northern Bering Sea, zooplankton community changes under the influence of water masses (Kimura et al., 2020). The water

TABLE 1 Inter-group comparison of hydrographic and zooplankton size spectra parameters in the northern Bering Sea during July in 2017 and in 2018.

| Parameters | Groups | | | Max-t test | | |
|---|---|---|---|---|---|---|
| | Y2017N (10) | Y2017S (9) | Y2018 (14) | | | |
| Temperature | 3.92 ± 0.87 | 3.44 ± 1.17 | 4.50 ± 1.52 | Not detected | | |
| Salinity | 32.3 ± 0.30 | 31.9 ± 0.17 | 32.0 ± 0.93 | Y2017S$^{2}$ | Y2018$^{1,2}$ | Y2017N$^{1}$ |
| Fluorescence | 21.8 ± 13.2 | 15.2 ± 7.57 | 19.9 ± 10.3 | Not detected | | |
| Melt Day | 108 ± 13.2 | 108 ± 14.4 | 107 ± 14.8 | Not detected | | |
| TSM | 88 ± 16.4 | 88 ± 13.7 | 81 ± 12.9 | Not detected | | |
| Slope in NBSS | -0.683 ± 0.089 | -0.705 ± 0.215 | -0.901 ± 0.260 | Y2018$^{2}$ | Y2017S$^{1,2}$ | Y2017N$^{1}$ |
| Intercept in NBSS | 0.828 ± 0.155 | 1.005 ± 0.261 | 0.845 ± 0.338 | Not detected | | |

Different superscript numbers in the Max-t test + HC3 column indicate significant differences between regions. NS, not significant.

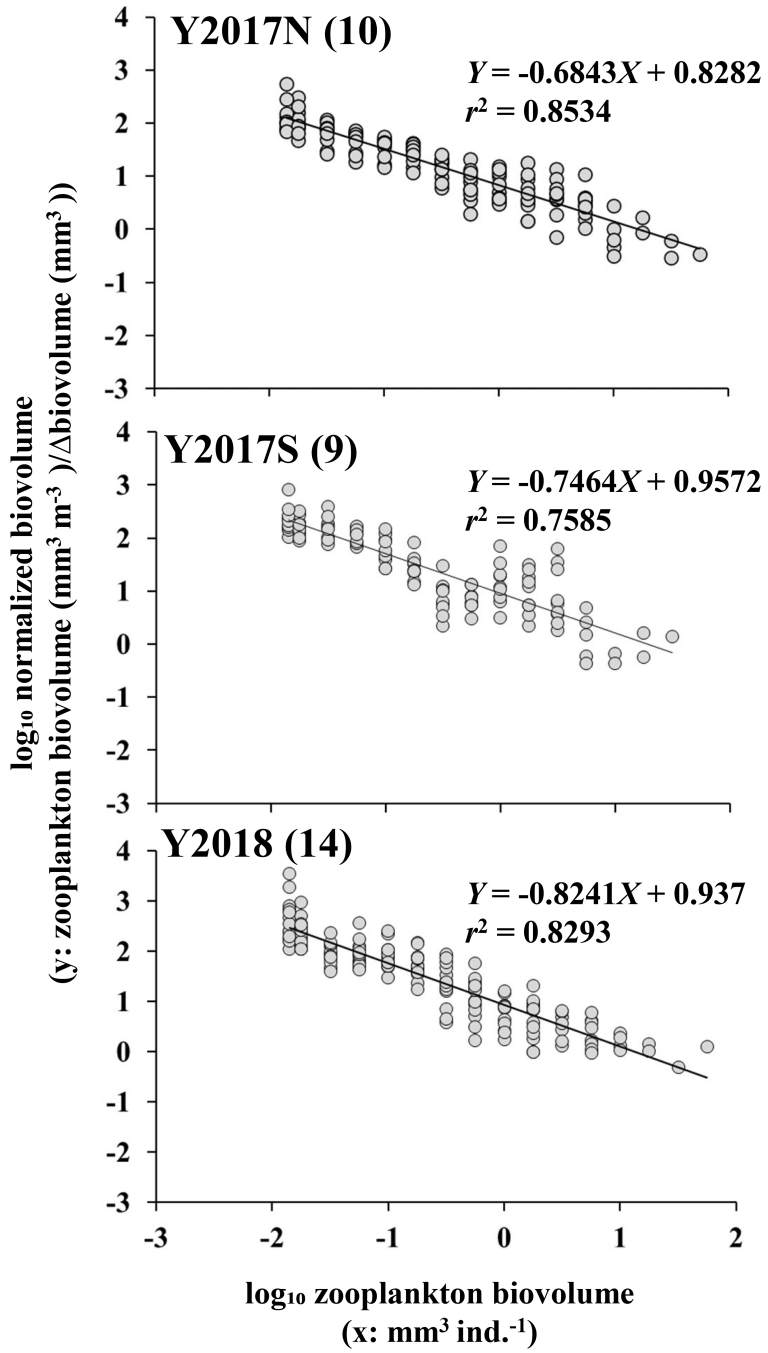


FIGURE 5
NBSS of three groups identified from cluster analysis of mesozooplankton biovolume (cf. Figure 3A) in the northern Bering Sea during July 2017 and 2018. Numbers in parenthesis indicate the number of stations belonging to each group.

masses changes seasonally (Danielson et al., 2020), so it is well reported that zooplankton communities are different between months. However, since there is no report about difference between shorter time scale, such as week. Thus, in this study, sampling time between two years differ only 11 days, which potentially influences zooplankton community, but quantitative evaluation (or back calculation) is not possible due to the lack of information.

Y2017N was observed in 2017 from the Bering Strait to the Chirikov Basin, and it corresponds to the Y2017N presented in our previous study (Kimura et al., 2022). This group was characterized by low abundance (Table 2 in Kimura et al., 2022) and biomass, and small copepods dominated the small size classes. The group showed higher salinity than the other group, which means AnW mainly occupied with water column at the station observed Y2017N. The middle class of this group was dominated by other large copepods

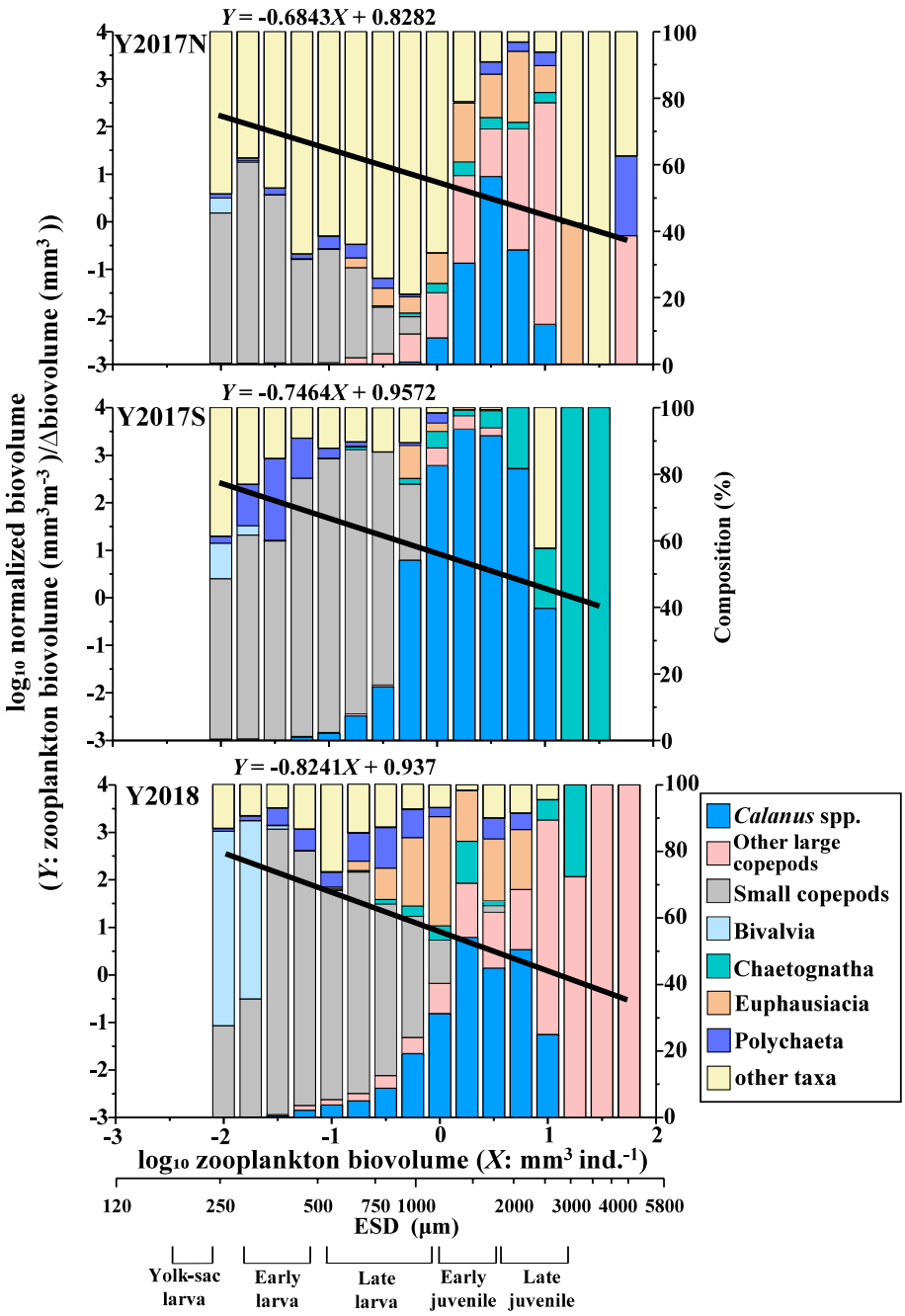


FIGURE 6
Species composition and biovolume within the interval of 0.25 in log10, and the NBSS line of the three groups identified from conducting a cluster analysis of mesozooplankton biovolume (cf. Figure 3C) in the northern Bering Sea during July 2017 and 2018. The species composition was calculated by summarizing the biovolume for all specimens in each size class. Prey size range for each stage of fish are shown at the bottom horizontal axis (cf. Jacobsen et al., 2020).

and Euphausiacea transported from Anadyr Bay (Springer et al., 1989; Ashjian et al., 2010; Moore et al., 2010). Euphausiacea dominated 60%–90% of the stomach contents of cetaceans in the study area; they are considered to play an important role in the food web but are not likely to establish expatriates in the present state (Moore et al., 2010). In Euphausiacea, *Thysanoessa inermis*, *T. raschii*, *Meganyctiphanes norvegica* are carnivorous, which can limit the abundance of *Calanus* spp. (Bamstedt and Karlson, 1998). The occurrence of other large copepods (composed of *Eucalanus* spp., *Metridia* spp., and *Neocalanus* spp.) was consistent with the characteristics of a community found during the summer in a previous study (Eisner et al., 2013). In the Chirikov Basin, the zooplankton community structure showed monthly changes accompanying surface water mass changes from June to September (Kimura et al., 2020). During June and July, other large copepods and Euphausiacea were abundant due to the inflow of AnW, *Calanus* spp., and Euphausiacea. In contrast, in August, the number of Bivalvia larvae, barnacle larvae, and Appendicularia

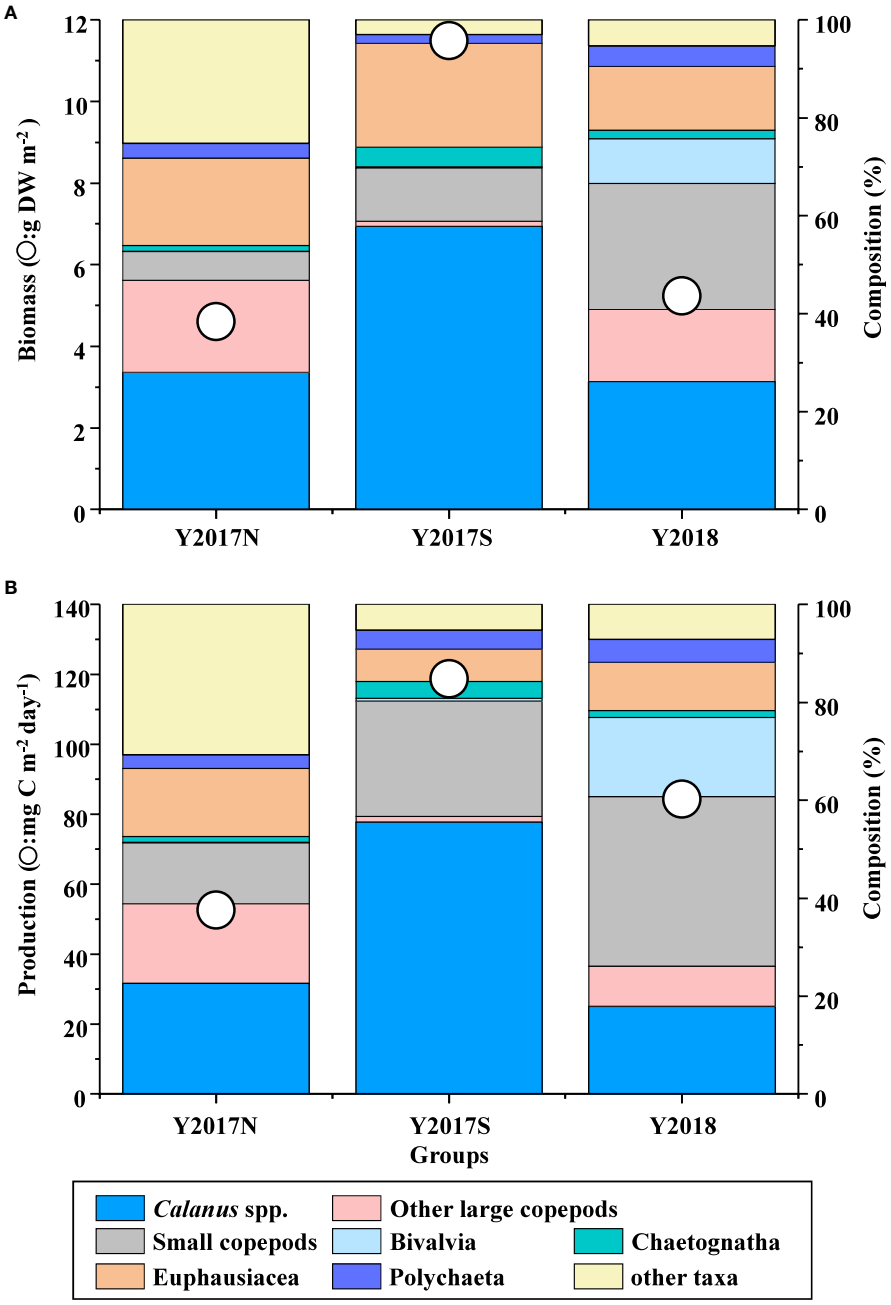


FIGURE 7
**(A)** Species composition and mean biomass and **(B)** production in each group as identified from conducting a cluster analysis of mesozooplankton biovolume (cf. Figure 3A) in the northern Bering Sea during July 2017 and 2018.

increased significantly. The community was then dominated by *Calanus* nauplii and other small copepods (*Centropages* spp. and Cyclopoida) (Kimura et al., 2020). The NBSS slope of Y2017N is gentle due to the dominance of *Calanus* spp., other large copepods, and Euphausiacea in the middle- and large-size classes, and it has been suggested that the slope of the NBSS will become steeper with an increase in benthic larvae (Matsuno et al., 2012; Kimura et al., 2020).

The NBSS slopes of Y2017N and Y2017S (seen south of St. Lawrence Island) were similar, but their compositions differed: *Calanus* spp. were dominant in the middle-sized class in Y2017S, but not in Y2017N. South of St. Lawrence Island, winter water is distributed in the lower layers where *Calanus glacialis* is abundant (Pinchuk and Eisner, 2017). It is also known that in cold years (late sea-ice retreat), the abundance of large copepods (*C. glacialis*) increases while that of small copepods and Cnidaria decreases (Ershova et al., 2015). In 2017, late sea ice melt (compared to 2018) induced ice-edge blooms in late April (Kikuchi et al., 2020); therefore, large copepods had grown to the C5 stage by July when our survey was conducted (Kimura et al., 2022). In other words,

Y2017S, as seen in this study, is the community generally found south of St. Lawrence Island during the summer of cold years. According to the results of the size analysis, the zooplankton abundance in the middle-sized class was low, and the large-sized class was dominated by Chaetognatha. Chaetognatha is a typical copepod predator (Feigenbaum, 1982; Kimmel et al., 2006); it is therefore likely that it fed on middle-sized copepods in Y2017S, which resulted in their decreased abundance. This suggests that the food chain was functional in Y2017S.

The small size glass of Y2018 (which produced the steepest NBSS slope) was dominated by Bivalvia larvae, and this is consistent with the large seasonal occurrence of Bivalvia larvae observed in the study area (Moore et al., 2003; Moore et al., 2006). Changes in the slope of the NBSS due to the dominance of small copepods have also been reported in the Chukchi Sea (Matsuno et al., 2012) and Atlantic sector of the Arctic Ocean (Basedow et al., 2010). As Bivalvia larvae typically settle 2–6 weeks after emergence (Steidinger and Walker, 1984), the steep slope of the NBSS in Y2018 does not indicate high productivity, but it rather indicates the seasonal recruitment of meroplankton.

## 4.4 Impact of early sea-ice melt on higher trophic levels

Sea ice melted from April to May in 2017, resulting in an ice-edge bloom and early copepod reproduction that induced a high abundance of large (late stage) copepods during summer (Kimura et al., 2022). However, sea ice melted earlier (from March to April) in 2018; therefore, an ice-edge bloom did not occur, and an open-water bloom occurred instead (Kikuchi et al., 2020). The reproduction of copepods was delayed in relation to the late open-water bloom, which resulted in a decreased abundance of large copepods during summer (Duffy-Anderson et al., 2019; Kimura et al., 2022). In this study, the results of the ZooScan analysis showed clear annual variations, with groups Y2017N and Y2017S dominating in 2017 and Y2018 dominating in 2018.

Y2017S, observed in 2017, exhibited the highest biomass. *Calanus* spp. largely contributed to this group, and this was attributed to late sea ice melting in cold years, as mentioned above (Ershova et al., 2015; Kimura et al., 2022). A high abundance of benthic larvae (Grebmeier et al., 2006) and a high biomass of copepods have been observed South of St. Lawrence Island (Kimura et al., 2022). According to the NBSS results, Y2017S was the most productive community with a functioning food chain among the three groups. This result means that the south of St. Lawrence Island is not only an important area for maintaining the zooplankton population, but also for efficiently transferring production to higher trophic levels.

Y2018 had the lowest biovolume, and this group corresponded to group D reported by Kimura et al. (2022). The biomass of Y2018 in this study was similar to that of Y2017N. However, production was higher than that of Y2017N because of the high production of small copepods. Large copepods in the study area are efficient prey for higher trophic levels, as they store rich lipids in their body (Lee, 1974), whereas small copepods rarely store lipids because of their low nutrient content (Norrbin et al., 1990). The small copepods in this study contained minimal amounts of lipids (Kimura et al., 2022). This group was also characterized by the dominance of Bivalvia larvae in the small class due to the seasonal reproduction of meroplankton. The carbon content of Bivalvia larva was 1.4–1.5%, which was much lower than that of copepods (Viverberg and Frank, 1976; Steidinger and Walker, 1984) and indicated that the food quality was too low for higher trophic levels. Lowering the nutrients and fats of prey decreases the winter survival rate of fish such as salmon or Arctic cod (Heintz et al., 2013). Therefore, it is suggested that in Y2018, the production of low fat meroplankton and small zooplankton was not transferred sufficiently to higher trophic levels, which might have affected their abundance (Springer et al., 1989; Huntington et al., 2020).

Fish generally exhibit grazing selectivity (for example, O'Brien, 1979). It is difficult for fish to detect small prey (and they contain low levels of nutrients); therefore, they tend to prey on larger foods (O'Brien, 1979). Walleye pollack (*Theragra chalcogramma*) is an abundant species in the study area and it preys on small copepods when they dominate in warm years, whereas it prays on large copepods and Euphausiacea when they dominate in cold years. This is likely because they graze on larger species during summer to efficiently store lipids for overwintering (Coyle et al., 2011; Heintz et al., 2013). Therefore, the prey-size composition provides important information about the survival rate of fish. To compare the growth stage of the fish larvae with the prey size, we determined the available prey size range for each growth stage. In this study, the available prey size for yolk-sac larvae was not detected, possibly because ZooScan could not analyze copepod eggs, which are the main food source for yolk-sac larvae. From late larvae to early juveniles, the most important period for survival (Jacobsen et al., 2020), the available food differed across the groups. Fat-rich other large copepods and Euphausiaceae with rich fats were relatively abundant in Y2017N and Y2018; however, their biovolumes were low. Therefore, because the rate at which fish encountered these foods was low and they experienced low food availability. When fish do not receive sufficient energy, their populations and survival rates are affected (Springer et al., 1989; Heintz et al., 2013; Huntington et al., 2020). In contrast, large and fat-rich *Calanus* spp. was found to be abundant in Y2017S, which suggested that it was readily available to fish. In addition, sufficient Chaetognatha populations for fish were seen in Y2017S; therefore, production by small and large copepods was efficiently transferred to fish in Y2017S.

In conclusion, the zooplankton community and size compositions in the northern Bering Sea differed between 2018 (an early sea ice melt year) and 2017 (a normal sea ice melt year). In 2017, Y2017N (dominated by other large copepods and Euphausiacea) was observed in the Chirikov Basin and was influenced by ACW, whereas Y2017S (dominated by *Calanus* spp. and Chaetognatha) was distributed to the south of St. Lawrence Island. In 2018, however, Y2017S was observed in the same area as that in 2017, and Y2018 (dominated by small copepods and Bivalvia) was distributed widely in the northern Bering Sea. The NBSS analysis showed that the slopes of groups Y2017N and Y2017S were similar; however, the species composition differed between the groups. Y2017N was dominated by medium- or large-

sized plankton (other large copepods and Euphausiacea) transported from Anadyr Bay. In contrast, the middle-sized class of Y2017S was dominated by *Calanus* spp., which is consistent with the community observed during summer in cold years. The abundance of the middle-sized class in this group was low, and this may have been due to Chaetognatha grazing on middle-sized copepod classes. The NBSS slope of Y2018 was the steepest in relation to the seasonal occurrence of Bivalvia larvae. In 2018, secondary production in the study area increased due to the increased abundance of small copepods, and production was contributed to by small copepods and Bivalvia larvae. As these small zooplankton are considered low-nutritional prey, the number of higher trophic levels may have decreased.

## Data availability statement

The original contributions presented in the study are included in the article/Supplementary Material. Further inquiries can be directed to the corresponding author.

## Ethics statement

The manuscript presents research on animals that do not require ethical approval for their study.

## Author contributions

KM and AY designed the study; AY performed field sampling; SK analyzed the samples; SK and KM analyzed the data; and SK and KM wrote the paper with contributions from all authors. All authors contributed to the article and approved the submitted version.

## Funding

The author(s) declare financial support was received for the research, authorship, and/or publication of this article. This study was funded by the Arctic Challenge for Sustainability (ArCS) (Program Grant Number JPMXD1300000000) and the Arctic Challenge for Sustainability II (ArCS II) (Program Grant Number JPMXD1420318865) projects. This work was also supported by the Environment Research and Technology Development Fund (JPMEERF20214002) of the Environmental Restoration and Conservation Agency of Japan. Furthermore, this work was partially supported by the Japan Society for the Promotion of Science (JSPS) KAKENHI, Grant Numbers JP21H02263 (B), JP20K20573 (Pioneering), JP20H03054 (B), JP20J20410 (B), JP19H03037 (B), JP18K14506 (Early Career Scientists), and JP17H01483 (A).

## Acknowledgments

We thank the captain, officers, crew, and researchers onboard the T/S Oshoro-Maru (Hokkaido University) for their crucial contributions to field sampling. The archived ADS dataset was provided by the Arctic Data archive System (ADS) developed by the National Institute of Polar Research.

## Conflict of interest

The authors declare that the research was conducted in the absence of any commercial or financial relationships that could be construed as a potential conflict of interest.

## Publisher's note



## Supplementary material

The Supplementary Material for this article can be found online at: https://www.frontiersin.org/articles/10.3389/fmars.2023.1233492/full#supplementary-material

## References

Ashjian, C. J., Braund, S. R., Campbell, R. G., George, J. C. C., Kruse, J., Maslowski, W., et al. (2010). Climate variability, oceanography, bowhead whale distribution, and iñupiat subsistence whaling near barrow, Alaska. *arctic institute North America* 63, 179–194. doi: 10.14430/arctic973

Bamstedt, U., and Karlson, K. (1998). Euphausiid predation on copepods in coastal waters of the Northeast Atlantic. *Mar. Ecol. Prog. Ser.* 172, 149–168. doi: 10.3354/meps172149

Barid, M. E., Timko, P. G., Middleton, T. J., Cox, D. R., and Suthers, I. M. (2008). Biological properties across the Tasman Front off southeast Australia. *Deep Sea Res.* 55, 1438–2455.

Basedow, S. L., Tande, K. S., and Zhou, M. (2010). Biovolume spectrum theories applied: spatial patterns of trophic levels within a mesozooplankton community at the polar front. *J. Plankton Res.* 32, 1105–1119. doi: 10.1093/plankt/fbp110

Basyuk, E., and Zuenko, Y. (2020). Extreme oceanographic conditions in the northwestern Bering Sea in 2017–2018. *Deep-Sea Res. II* 181–182, 104909. doi: 10.1016/j.dsr2.2020.104909

Coachman, L. K., Aagaard, K., and Tripp, E. B. (1975). *Bering Strait the Regional Physical Oceanography* Vol. 172 (Seattle, Washington: University of Washington Press).

Colas, F., Tardivela, M., Perchocb, J., Lunvenb, M., Foresta, B., Guyaderc, G., et al. (2017). The ZooCAM, a new in-flow imaging system for fast onboard counting, sizing and classification of fish eggs and metazooplankton. *Prog. Oceanogr.* 166, 54–65. doi: 10.1016/j.pocean.2017.10.014

Cornils, A., Thomisch, K., Hase, J., Hildebrandt, N., Auel, H., and Niehoff, B. (2022). Testing the usefulness of optical data for long-term monitoring of zooplankton: taxonomic composition, abundance, biomass, and size spectra from ZooScan image analysis. *Limnol. Oceanogr-Meth.* 20, 428–450. doi: 10.1002/lom3.10495

Cornwall, W. (2019). Vanishing Bering Sea ice poses a climate puzzle. *Science* 364, 616–617. doi: 10.1126/science.364.6441.616

Coyle, K. O., Eisner, L. B., Mueter, F. J., Pinchuk, A. I., Janout, M. A., Cieciel, K. D., et al. (2011). Climate change in the southeastern Bering Sea: impacts on pollock stocks and implications for the oscillating control hypothesis. *Fish. Oceanogr.* 20, 139–156. doi: 10.1111/j.1365-2419.2011.00574.x

Danielson, S. L., Ahkinga, O., Ashjian, C., Basyuk, E., Cooper, L. W., Eisner, L., et al. (2020). Manifestation and consequences of warming and altered heat fluxes over the Bering and Chukchi Sea continental shelves. *Deep. Sea. Res. II.* 177, 104781. doi: 10.1016/j.dsr2.2020.104781

Duffy-Anderson, J. T., Stabeno, P., Andrews, A. G.III, Cieciel, K., Deary, A., Farley, E., et al. (2019). Responses of the northern Bering Sea and southeastern Bering Sea pelagic ecosystems following record-breaking low winter sea ice. *Geophys. Res. Lett.* 46, 9833–9842. doi: 10.1029/2019GL083396

Eisner, L., Hillgruber, N., Martinson, E., and Maselko, J. (2013). Pelagic fish and zooplankton species assemblages in relation to water mass characteristics in the northern Bering and southeast Chukchi Seas. *Polar Biol.* 36, 87–113. doi: 10.1007/s00300-012-1241-0

Ershova, E. A., Hopcroft, R. R., and Kosobokova, K. N. (2015). Inter-annual variability of summer mesozooplankton communities of the western Chukchi Sea: 2004–2012. *Polar Biol.* 38, 1461–1481. doi: 10.1007/s00300-015-1709-9

Feigenbaum, D. (1982). Feeding by the chaetognath, *Sagitta elegans*, at low temperatures in Vineyard Sound, Massachusetts. *Am. Soc. Limnology Oceanography* 27, 699–6706. doi: 10.4319/lo.1982.27.4.0699

Field, J. G., Clarke, K. R., and Warwick, R. M. (1982). A practical strategy for analyzing multispecies distribution patterns. *Mar. Ecol.* 8, 37–52. doi: 10.3354/meps008037

Forest, A., Stemmann, L., Picheral, M., Burdorf, L., Robert, D., Fortier, L., et al. (2012). Size distribution of particles and zooplankton across the shelf basin system in southeast Beaufort Sea: combined results from an Underwater Vision Profiler and vertical net tows. *Biogeoscience* 9, 1301–1320. doi: 10.5194/bg-9-1301-2012

Garcia-Comas, C., Stemmann, L., Icanez, F., Berline, L., Mazzocchi, M. G., Gasparini, S., et al. (2011). Zooplankton long-term changes in the NW Mediterranean Sea: Decadal periodicity forced by winter hydrographic conditions related to large-scale atmospheric changes? *J. Mar. Syst.* 87, 216–226. doi: 10.1016/j.jmarsys.2011.04.003

Gorsky, G., Ohman, M. D., Picheral, M., Gasparini, S., Stemmann, L., Romagnan, J., et al. (2010). Digital zooplankton image analysis using the ZooScan integrated system. *J. Plankton Res.* 32, 285–303. doi: 10.1093/plankt/fbp124

Grebmaier, J. M., Bluhm, B. A., Cooper, L. W., Danielson, S. L., Arrigo, K. R., Blanchard, A. L., et al. (2015). Ecosystem characteristics and processes facilitating persistent macrobenthic biomass hotspots and associated benthivory in the Pacific Arctic. *Prog. Oceanogr* 136, 92–114. doi: 10.1016/j.pocean.2015.05.006

Grebmeier, J. M., Cooper, L. W., Feder, H. M., and Sirenko, B. I. (2006). Ecosystem dynamics of the pacific-influenced northern Bering and Chukchi seas in the Amerasian Arctic. *Prog. Oceanogr.* 71, 331–361. doi: 10.1016/j.pocean.2006.10.001

Grosjean, P., Picheral, M., Warembourg, C., and Gorsky, G. (2004). Enumeration, measurement, and identification of net zooplankton samples using the ZOOSCAN digital imaging system. *ICES. J. Mar. Sci.* 61, 518–525. doi: 10.1016/j.icesjms.2004.03.012

Heintz, R. A., Siddon, E. C., Farley, J. E.V., and Napp., J. (2013). Correlation between recruitment and fall condition of age-0 pollock (Theragra chalcogramma) from the eastern Bering Sea under varying climate conditions. *Deep-Sea Res. II* 94, 150–156. doi: 10.1016/j.dsr2.2013.04.006

Herberich, E., Sikorski, J., and Hothorn, T. (2010). A Robust procedure for comparing multiple means under heteroscedasticity in unbalanced designs. *PLoS One* 5, e9788. doi: 10.1371/journal.pone.0009788

Herman, A. W., and Harvey, M. (2006). Application of normalized biomass size spectra to laser optical plankton counter net intercomparisons of zooplankton distributions. *J. Geophy. Res.* 111, C05S05.

Huntington, H. P., Danielson, S. L., Wiese, F. K., Baker, M., Boveng, P., Citta, J. J., et al. (2020). Evidence suggests potential transformation of the Pacific Arctic ecosystem is underway. *Nat. Clim. Change* 10, 342–348. doi: 10.1038/s41558-020-0695-2

Ikeda, T. (1985). Metabolic rates of epipelagic marine zooplankton as a function of body mass and temperature. *Mar. Biol.* 85, 1–11. doi: 10.1007/BF00396409

Ikeda, T., and Motoda, S. (1978). Zooplankton production in the Bering Sea calculated from 1957-1970 Oshoro-Maru data. *Mar. Sci. Comms.* 4, 329–346.

Jacobsen, S., Nielsel, K. K., Kristiansen, R., Grønkjær, P., Gaard, E., and Steingrund, P. (2020). Diet and prey pregerences of larval and pelagic juvenile Faroe Plateau cod (*Gadus morhua*). *Mar. Biol.* 167, 122. doi: 10.1007/s00227-020-03727-5

Kerr, S. R., and Dickie, L. M. (2001). *The Biomass Spectrum* (New York: Columbia University Press).

Kikuchi, G., Abe, H., Hirawake, T., and Samhythm, M. (2020). Distinctive spring phytoplankton bloom in the Bering Strait in 2018: A year of historically minimum sea ice extent. *Deep-Sea Res. II* 181–182, 104905. doi: 10.1016/j.dsr2.2020.104905

Kimmel, D. G., Roman, M. R., and Zhang, X. (2006). *Limnol. Oceangr.* 51, 131–141. doi: 10.4319/lo.2006.51.1.0131

Kimura, F., Abe, Y., Matsuno, K., Hopcroft, R. R., and Yamaguchi, A. (2020). Seasonal changes in the zooplankton community and population structure in the northern Bering Sea from June to September 2017. *Deep-Sea Res. II* 181–182, 104901. doi: 10.1016/j.dsr2.2020.104901

Kimura, F., Matsuno, K., Abe, Y., and Yamaguchi, A. (2022). Effects of early sea-ice reduction on zooplankton and copper pod population structure in the northern Bering Sea during the summers of 2017 and 2018. *Front. Mar. Sci.* 9, 808910. doi: 10.3389/fmars.2022.808910

Kiørboe, T. (2013). Zooplankton body composition. *Limnol. Oceanogr.* 58 (5), 1843–1850. doi: 10.4319/lo.2013.58.5.1843

Lee, R. F. (1974). Lipids of arctic zooplankton. *Comp. Biochem. Physiol.* B51, 263–266.

Lehette, P., and Hernandez-Leon, S. (2009). Zooplankton biomass estimation from digitized images: a comparison between subtropical and Antarctic organisms. *Limnol. Oceanogr.: Methods* 7, 304–308. doi: 10.4319/lom.2009.7.304

Matsuno, K., Yamaguchi, A., and Imai, I. (2012). Biomass size spectra of mesozooplankton in the Chukchi Sea during the summers of 1991/1992 and 2007/2008: and analysis using optical plankton counter data. *ICES J. Mar. Sci.* 69, 1205–1217.

Meeren, T. D., and Næss, T. (1993). How does cod (*Gadus morhua*) cope with variability in feeding conditions during early larval stages? *Mar. Biol.* 116, 637–647. doi: 10.1007/bf00355482

Moore, S. E., George, J. C. C., Sheffield, G., Bacon, J., and Ashjian, C. J. (2010). Bowhead whale distribution and feeding near barrow, Alaska, in late summer 2005–06. *Arctic Institute North America.* 63, 195–205. doi: 10.14430/arctic974

Moore, S. E., Grebmeier, J. M., and Davis, J. R. (2003). Gray whale distribution relative to forage habitat in the northern Bering Sea: current conditions and retrospective summary. *Can. J. Zool.* 81, 734–742. doi: 10.1139/z03-043

Moore, S. E., Stafford, K. M., Mellinger, D. K., and Hildebrand, J. A. (2006). Listen to large whales in the offshore waters of Alaska. *Bioscience* 56, 49–55. doi: 10.1139/z03-043

Moore, S. K., and Suthers, I. M. (2006). Evaluation and correction of subresolved particles by the optical plankton counter in three Australian estuaries with pristine to highly modified catchments. *J. Geophys. Res.* 111, 148–227. doi: 10.1029/2005JC002920

Motoda, S. (1959). Device for a simple plankton apparatus. *Mem. Fac. Fish. Hokkaido Univ.* 7, 73–94.

Naito, A., Abe, Y., Matsuno, K., Nishizawa, B., Kanna, N., Sugiyama, S., et al. (2019). Surface zooplankton size and taxonomic composition in Bowdoin Fjord, north-western Greenland: a comparison of ZooScan, OPC, and microscopic analyses. *Polar Sci.* 19, 120–129. doi: 10.1016/j.polar.2019.01.001

Nakamura, Y., Somiya, R., Suzuki, N., Hidaka-Umetsu, M., Yamaguchi, A., and Lindsay, D. J. (2017). Optics-based surveys of large unicellular zooplankton: a case study on radiolarians and paederines. *Plankton Benthos Res.* 12, 95–103. doi: 10.3800/pbr.12.95

Norrbin, M. F., Olsen, R. E., and Tande, K. S. (1990). Seasonal variation in lipid class and fatty acid composition of two small copepods in Balsqorden, northern Norway. *Mar. Biol.* 105, 205–211. doi: 10.1007/BF01344288

O'Brien, W. J. (1979). The predator–prey interaction of planktivorous fish and zooplankton: Recent research with planktivorous fish and their zooplankton prey shows the evolutionary thrust and parry of the predator-prey relationship. *Am. Sci.* 67, 572–581.

Omori, M. (1969). Weight and chemical composition of important oceanic zooplankton in the north Pacific Ocean. *Mar. Biol.* 3, 2–10. doi: 10.1007/BF00355587

Pinchuk, A. I., and Eisner, L. B. (2017). Spatial heterogeneity in zooplankton summer distribution in the eastern Chukchi Sea in 2012–2013 as a result of large-scale interactions of water masses. *Deep-Sea Res. II* 1135, 27–39. doi: 10.1016/j.dsr2.2016.11.003

Platt, T., and Denman, K. (1977). Organisation in the pelagic ecosystem. *Helgoländer Wiss. Meeresunters* 30, 575–581. doi: 10.1007/BF02207862

R Core Team. (2021). *R: a language and environment for statistical computing* (Vienna, Australia: R Foundation for Statistical Computing). Available at: https://www.R-project.org/.

Sheldon, R. W., Sutcliffe, J. W.H., and Parajape, M. A. (1977). Structure of pelagic food chain and relationship between plankton and fish production. *J. Fish. Res* 34, 2344–2353. doi: 10.1139/f77-314

Springer, A. M., McRoy, C. P., and Turco, K. R. (1989). The paradox of pelagic food webs in the northern Bering Sea – II Zooplankton communities. *Cont. Shelf Res.* 9, 359–386. doi: 10.1016/0278-4343(89)90039-3

Springer, A. M., McRoy, C. P., and Turco, K. R. (1993). The paradox of pelagic food webs in the northern Bering Sea-II. Zooplankton communities. *Cont. Shelg Res.* 9, 359–386. doi: 10.1016/0278-4343(89)90039-3

Sprules, W. G., Munawar, M., and Jin, E. H. (1988). Plankton community stducture and size spectra in the Georgian Bay and North Channel ecosystems. *Hydrobiologia* 163, 135–140. doi: 10.1007/BF00026925

Stabeno, P. J., and Bell, S. W. (2019). Extreme conditions in the Bering Sea, (2017–2018): record-breaking low sea-ice extent. *Geophys. Res. Lett.* 46, 8952–8959. doi: 10.1029/2019GL083816

Steidinger, K. A., and Walker, M. L. (1984). *Marine plankton life cyclestrategies* (Boca Raton, Florida: CRC Press).

Stevenson, D. E., and Lauth, R. R. (2019). Bottom trawl surveys in the northern Bering Sea indicate recent shifts in the distribution of marine species. *Polar Biol.* 42, 407–421. doi: 10.1007/s00300-018-2431-1

Suthers, I. M., Taggart, C. T., Rissik, D., and Baird, M. E. (2006). Day and night ichthyoplankton assemblages and zooplankton biomass size spectrum in a deep ocean island wake. *Mar. Ecol. Prog. Ser.* 322, 225–238. doi: 10.3354/meps322225

Vandromme, P., Nogueira, E., Huret, M., Lopez-Urrutia, A., Gonzalez, G. G., Sourisseau, M., et al. (2014). Springtime zooplankton size structure over the continental shelf of the Bay of Biscay. *Ocean Sci.* 10, 821–835. doi: 10.5194/os-10-821-2014

Vandromme, P., Stemmann, L., Garcia-Comas, C., Berline, L., Sun, X., and Gorsky, G. (2012). Assessing biases in computing size spectra of automatically classified zooplankton from imaging systems: A case study with the ZooScan integrated system. *Methods Oceanogr.* 1–2, 3–21. doi: 10.1016/j.mio.2012.06.001

Viverberg, J., and Frank, T. H. H. (1976). The chemical composition and energy contents of copepods and cladocerans in relation to their size. *Freshw. Biol.* 6, 333–345. doi: 10.1111/j.1365-2427.1976.tb01618.x

Yurista, P. M., Yule, D. L., Balge, M., VanAlstine, J. D., Thompson, J. A., Gamble, A. E., et al. (2014). A new look at the Lake Superior biomass size spectrum. *Can. J. Fish. Aquat. Sci.* (NRC Research Press), Vol. 71, 1324–1333.

Zhou, M. (2006). What determines the slope of a plankton biomass spectrum? *J. Plankton Res.* 28, 437–448. doi: 10.1093/plankt/fbi119

frontiers | Frontiers in Marine Science

TYPE Original Research
PUBLISHED 22 December 2023
DOI 10.3389/fmars.2023.1304493



OPEN ACCESS

EDITED BY
Satya Panigrahi,
Indira Gandhi Centre for Atomic Research (IGCAR), India

REVIEWED BY
Ajit Kumar Mohanty,
Indira Gandhi Centre for Atomic Research (IGCAR), India
Ginevra Boldrocchi,
University of Insubria, Italy

*CORRESPONDENCE
Angelo Bonanno
angelo.bonanno@cnr.it

†These authors have contributed equally to this work

RECEIVED 29 September 2023
ACCEPTED 08 December 2023
PUBLISHED 22 December 2023

CITATION
Barra M, Guglielmo L, Bonanno A, Mangoni O, Rivaro P, Rumolo P, Falco P, Basilone G, Fontana I, Ferreri R, Giacalone G, Aronica S, Minutoli R, Memmola F, Granata A and Genovese S (2023) Vertical structure characterization of acoustically detected zooplankton aggregation: a case study from the Ross Sea. *Front. Mar. Sci.* 10:1304493. doi: 10.3389/fmars.2023.1304493



# Vertical structure characterization of acoustically detected zooplankton aggregation: a case study from the Ross Sea

Marco Barra[1], Letterio Guglielmo[2], Angelo Bonanno[3]*, Olga Mangoni[4], Paola Rivaro[5], Paola Rumolo[1], Pierpaolo Falco[6], Gualtiero Basilone[3], Ignazio Fontana[3], Rosalia Ferreri[3], Giovanni Giacalone[3], Salvatore Aronica[3], Roberta Minutoli[7], Francesco Memmola[6], Antonia Granata[7†] and Simona Genovese[3†]

[1]National Research Council (CNR), Institute of Marine Sciences, Naples, Italy, [2]Integrative Marine Ecology Department, Stazione Zoologica Anton Dohrn, Naples, Italy, [3]National Research Council (CNR), Institute for the Study of the Anthropic Impacts and Sustainability in the Marine Environment, SS Capo Granitola, Campobello Di Mazara, Trapani, Italy, [4]Department of Biology, University of Naples Federico II, Napoli, Italy, [5]Department of Chemistry and Industrial Chemistry, University of Genova, Genoa, Italy, [6]Department of Life and Environmental Sciences, Marche Polytechnic University, Ancona, Italy, [7]Department of Chemical, Biological, Pharmaceutical and Environmental Sciences, University of Messina, Messina, Italy

Acoustic data were collected by means of Simrad EK60 scientific echosounder on board the research vessel "Italica" in the Ross Sea during the 2016/2017 austral summer as part of the P-Rose and CELEBeR projects, within the framework of the Italian National Research Program in Antarctica (PNRA). Sampling activities also involved the collection of vertical hydrological profiles using the SBE 9/11plus oceanographic probe. Acoustic data were processed to extract three specific scattering structures linked to *Euphausia superba*, *Euphausia crystallorophias* and the so called Sound-Scattering Layers (SSLs; continuous and low-density acoustic structures constituted by different taxa). Four different sectors of the study area were considered: two southern coastal sectors (between the Drygalski Ice Tongue and Coulman Island), a northern sector (~30 nmi East of Cape Hallett) and an offshore one spanning about 2 degrees of latitude from Coulman Island south to the Drygalski Ice Tongue. The vertical structure of each group in each area was then analyzed in relation to the observed environmental conditions. Obtained results highlighted the presence of different vertical structures (both environmental and acoustic) among areas, except for the two southern coastal sectors that were found similar. GAM modelling permitted to evidence specific relationships between the environmental factors and the vertical distribution of the considered acoustic groups,

letting to hypothesize the presence of trophic relationships and differences in SSL species composition among areas. The advantages of acoustic techniques to implement opportunistic monitoring strategies in endangered ecosystems are also discussed.

KEYWORDS

*Euphausia superba*, *Euphausia crystallorophias*, vertical distribution, Ross Sea, sound scattering layers

## 1 Introduction

The use of active acoustic techniques to study life in the ocean began about a century ago (Kimura, 1929; Sund, 1935). From the earliest applications, the importance of such techniques and the impact they would have on our ability to study marine species in the water column became clear (Benoit-Bird and Lawson, 2016). Over the years, there has been considerable progress in both the development of increasingly reliable electroacoustic instrumentation and the development of faster and more sophisticated data analysis algorithms. Furthermore, for several years now, acoustic instruments specifically designed to study marine organisms in the water column have played a very important role in the assessment of commercial fish stocks and their management (Fernandes et al., 2002; Muradian et al., 2017; Bonanno et al., 2021; Leonori et al., 2021). The availability of acoustic data, acquired for the assessment of commercially exploited species, often with time series spanning decades, has made it possible to carry out multiple studies on the habitat suitability, spatial distribution and fluctuations in abundance of these species in relation to indices of natural climate variability in various regions (Lluchbelda et al., 1992; Gutierrez et al., 2007; Barange et al., 2009; Barra et al., 2015; Bonanno et al., 2015; Schismenou et al., 2017; Ben Abdallah et al., 2018; Bonanno et al., 2018; Zgozi et al., 2018; De Felice et al., 2021). In addition, acoustic techniques allow the acquisition of scattering volume profiles of the water column with high vertical resolution over large spatial scales in a quasi-synoptic way. Taking advantage of such features, an important area of marine ecology, focusing on spatial distribution of organisms in the water column in relation to environmental forcings, has strongly developed over the years. In this context, since many organisms aggregate in areas with particular environmental characteristics, acoustic observations, together with hydrographic and current measurements (often estimated from satellite data or through ocean circulation models) are used to understand the interaction of biological and physical processes underlying animal aggregations (Murase et al., 2009; Davis et al., 2017; Leonori et al., 2017).

Acoustics have also become an important part of plankton research (Greenlaw and Johnson, 1982) allowing scientists to monitor zooplankton movements in the water column in response to physical and chemical characteristics of the ocean. Just to give some examples, Cheriton et al. (2007) studied zooplankton aggregations occupying vertical scales of the order of 1 m and horizontal scales of kilometers. The authors showed how such layers are associated with the pycnocline in calm conditions while being strongly modified by wind and the movement of water masses with different characteristics from those in which these layers were formed. Ianson et al. (2011), analyzing acoustic data from multifrequency scientific echosounders, highlighted the influence of turbulent flow in the aggregation of *Euphausia pacifica*. The acquisition of acoustic data using an autonomous underwater vehicle made it possible to sample previously inaccessible areas under the ice in Antarctica, revealing the importance of the ice edge for krill (Brierley et al., 2002). Acoustics also allowed researchers to examine an important strategy used by copepods to hide from predators: overwintering at depth (Bagoien et al., 2001).

The ability of acoustics to examine multiple types of organisms at once has played an important role in identifying how the avoidance and foraging strategies of predators change depending on the time of day. For example, in the waters of Oahu (Hawaii), zooplankton, fish and dolphins all concentrate on one depth and are very active at dusk, but each group uses very different tactics during the rest of the night (Benoit-Bird & McManus, 2014).

The present study reports some of the results of an oceanographic survey, carried out in the austral summer of 2016/2017 in the waters of the Ross Sea as part of the P-ROSE project ("Plankton biodiversity and functioning of the Ross Sea ecosystems in a changing Southern Ocean" - PNRA16 00239), within the framework of the Italian National Research Program in Antarctica (PNRA). Part of the data analyzed were also collected during the activities of the CELEBeR project ("CDW Effects on glacial melting and on Bulk of Fe in the Western Ross sea" - PNRA16 00207).

The Ross Sea is a highly productive ecosystem whose food web is very complex and characterized by multiple trophic pathways (Hopkins, 1987; Smith et al., 2007; Pinkerton and Bradford-Grieve, 2014; Smith et al., 2014). Regarding the application of acoustic techniques for the study of marine organisms in this specific area of Antarctica, over the past decades, most efforts focused on studying the spatial distribution of a few key species such as *Euphausia superba*, *Euphausia crystallorophias* and *Pleuragramma antarctica*,

using both net sampling and acoustic techniques (Guglielmo et al., 1997; Azzali and Kalinowski, 2000; Granata et al., 2002; Sala et al., 2002; Azzali et al., 2006; Granata et al., 2009; Guglielmo et al., 2009; La Mesa et al., 2010; Naganobu et al., 2010; Davis et al., 2017; Leonori et al., 2017). In contrast, only little information is available on the characteristics and extent of sound-scattering layers that are ubiquitous acoustic structures commonly found in all oceans and representing a large percentage of the pelagic biomass (Blanluet et al., 2019; Geoffroy et al., 2019).

In the present study, according to well-known procedures available in literature (Fontana et al., 2022 and references therein), three distinct acoustic groups were identified (*E. crystallorophias*, *E. superba* and Sound-Scattering Layers) aiming at characterizing their vertical structure in relation to the environmental conditions (as inferred by CTD data) in four different sectors of the Ross Sea during the 2016/2017 summer.

# 2 Materials and methods

In the framework of the Italian National Research Program in Antarctica (PNRA), a multidisciplinary oceanographic survey is routinely carried out in the Ross Sea during the austral summer, partitioning the available vessel time among different research projects. During the 2016/2017 Austral summer, the P-ROSE project focused on the plankton biodiversity and functioning in some sectors of the Ross Sea. The planned sampling activities considered the collection of acoustic data and zooplankton samples along specific transects. Additional acoustic data were opportunistically collected in the sectors pertaining the CELEBeR project study area. Due to bad weather conditions, that led to a reduction in the time available for zooplankton and micronekton samplings, few (and unrepresentative) samples were collected in the area pertaining the P-ROSE project, while the zooplankton sampling was not foreseen in the other sectors considered in this study (CELEBeR project study area). Thus, for the purposes of this work, biological samples were not considered.

## 2.1 Acoustic data collection and processing

Acoustic data were collected from 08 January to 04 February 2017, on the board research vessel "Italica", in four sectors of the Ross Sea: area A1 located in the coastal waters between the Drygalski tongue and Cape Washington; area A2 located in coastal waters between Cape Washington and Coulman island; area A3 corresponding to the off-shore sector between Coulman island and the Drygalski tongue; area A4 is the one in front of Cape Hallett (Figure 1). Acoustic data were collected with a Simrad EK60 scientific echo-sounder working at three different frequencies (38 kHz, 120 kHz and 200 kHz) and calibrated following standard techniques (Foote et al., 1987).

The echo-sounder was configured to ping simultaneously at each frequency with a pulse duration of 1024 ms. Raw data were processed using the Echoview@ software package (Higginbottom et al., 2000) in order to extract all echoes related to the three considered groups, namely *Euphausia superba* (S), *Euphausia crystallorophias* (C) and Sound-Scattering Layers (SSL).

In each echogram, the analysis area was defined between 15 m and 200 m. The upper threshold (15 m) was chosen to avoid the effects of air bubbles due to bad weather conditions. The lower threshold (200 m) was chosen considering that most mesozooplankton occurs in the upper 200 m layer (Kasyan, 2023) and that the acoustic signal acquired by the transducer at 200 kHz was strongly attenuated. In order to remove background noise from the echograms collected at 38, 120 and 200 kHz, the method proposed by De Robertis & Higginbottom (2007) was adopted. In terms of krill species identification, *E. superba* and *E. crystallorophias* could be identified based on the equation proposed by Brierley et al. (1998) and La et al. (2015), respectively. Fontana et al. (2022), who worked on energetic and geometric parameters extracted from each aggregation and tested different clustering methods, highlighted that k-means performed better than other clustering methods, allowing the consistent classification of the two krill species. Consequently, acoustic data associated with the krill species were identified using the k-means method according to Fontana et al. (2022). All aggregations not linked to *E. superba* and *E. crystallorophias* were classified as "unknown" and removed from the analysis. SSLs were thus obtained by removing the identified krill aggregations (as well as background noise) from the acoustic data and ensuring the absence of other aggregations ("unknown" based on k-means approach; Fontana et al., 2022). NASC (Nautical Area Scattering Coefficient; MacLennan et al., 2002) values for the three above mentioned groups were extracted according to a grid characterized by a vertical resolution of 10 m and an elementary distance sampling unit (EDSU) of 0.5 nmi. The threshold level for the acoustic data analysis was set at -90 dB for the three frequencies. In relation to the aim of this study, density values (i.e. NASC) here analyzed were based on acoustic data acquired at 120 kHz, the most suitable frequency for detecting zooplankton aggregations (see Supplementary Figures S1–S4).

## 2.2 Hydrographic data

Temperature (°C), salinity (PSU), fluorescence (mg/m$^3$), depth (m) and oxygen (mg/l) data were acquired along the water column by means of the SBE 9/11plus multiparametric probe at the maximum frequency (24 Hz) with a descent speed of 1 m/s. 13 CTD stations were acquired in the A1 area, 12 in the A2 area, 12 in the A3 area and 13 in the A4 area (Figure 1). The data were processed and quality checked according to international procedures (SCOR Working Group, 1988), by using the CTD Sea Bird Electronics data processing software. Finally, the profiles were vertically averaged over 1-m-depth bins. The fluorescence sensor was calibrated (Chl-*a* = 1.5764 * Fluorescence + 0.2533; $R^{2 =}$ 0.8514) with chlorophyll-*a* samples collected *in situ* and analyzed following Holm-Hansen et al. (1965), using a spectrofluorometer (Shimadzu, Mod. RF - 6000; Shimadzu Corporation-Japan) checked daily with a Chl-*a* standard solution (Sigma-Aldrich).

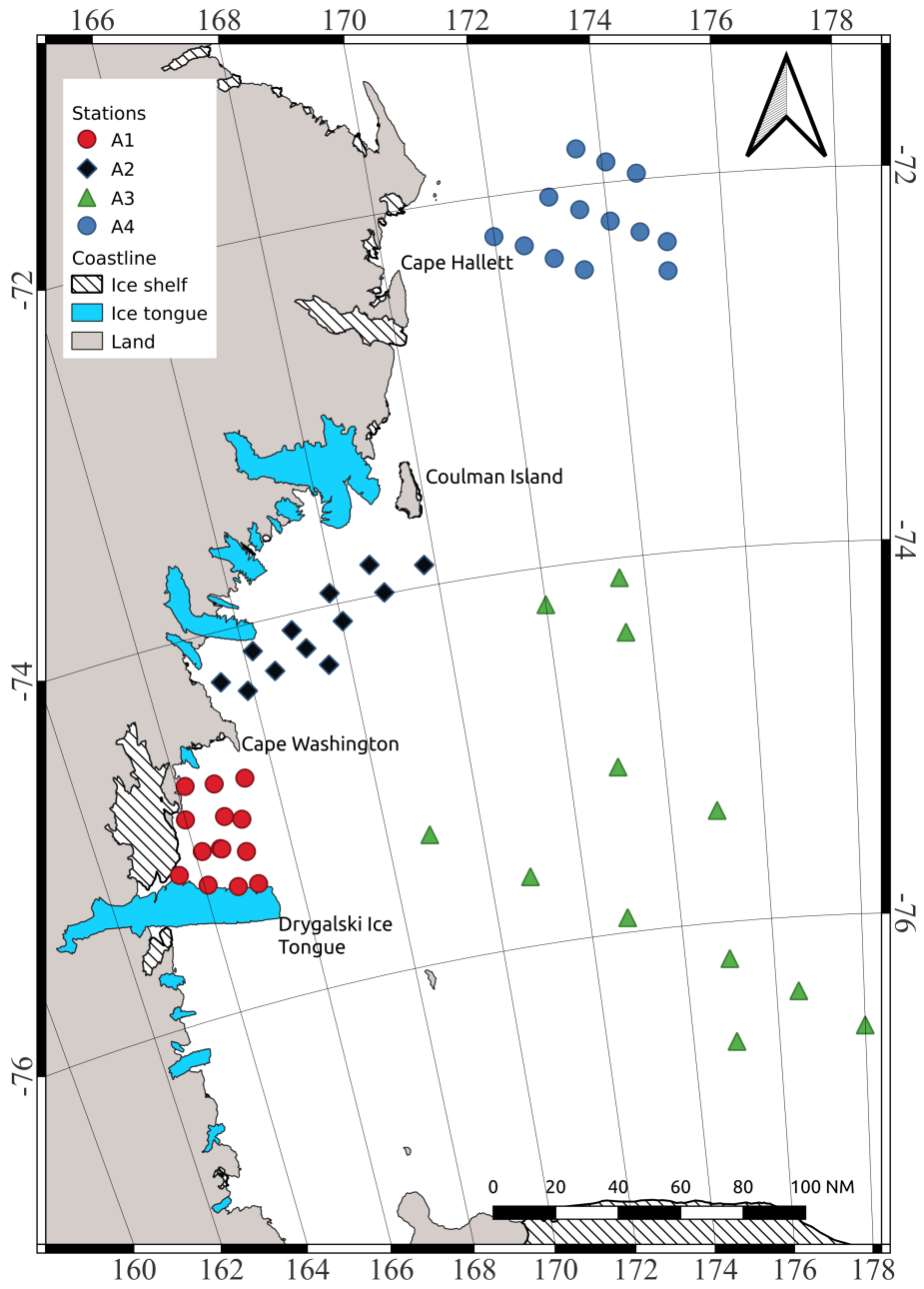


FIGURE 1
Study area and sampling stations.

## 2.3 Matching hydrographic and acoustic data

For each CTD station position, mean vertical NASC profiles at 120 kHz for the three considered groups (*E. crystallorophias*, *E. superba* and SSL) were obtained by averaging the NASC profiles of the EDSUs falling within 5 nmi from the CTD station. Furthermore, CTD related environmental parameters were vertically averaged each 10 m depth in order to obtain the same vertical resolution of acoustic data. The obtained dataset was thus fully balanced as for each station almost the same number of observations was available, allowing for consistent comparisons among sub-areas.

## 2.4 Statistical methods

In a first step, an exploratory data analysis on the environmental dataset was carried out. Boxplots and Kruskal-Wallis ANOVA (followed by Dunn's *post-hoc* test) were used to graphically evidence and evaluate the presence of significant differences in temperature, salinity, chlorophyll-a, and oxygen values among the four areas. The possible presence of structural patterns among environmental variables was also assessed by means of Principal Component Analysis (PCA). In particular, PCA was carried out on log-transformed values as, working on raw values, the distribution of PCA scores was highly skewed. *E. crystallorophias*, *E. superba* and

SSL NASC values were considered in the PCA as quantitative supplementary variables to evaluate possible relationships between NASC values and Principal Components (PCs). In a similar way, the area factor was included in the PCA as a qualitative supplementary variable thus allowing to evaluate possible significant effects in terms of area. In this context, the supplementary variables (qualitative and quantitative) do not influence the PCA that is thus based on environmental dataset only.

For each station, the average S, C and SSL NASC values were computed along with the vertical mass center (i.e. the NASC-weighted average depth, highlighting the depth where most of the biomass was concentrated) for the three groups. Similarly to what was done on the environmental dataset, boxplot and Kruskal-Wallis ANOVA followed by Dunn's *post-hoc* test were used to visualize and to test the differences in terms of NASC and mass center among areas for the three groups (SSL, C and S). The analysis of the relationship between environmental variables and C, S and SSL was carried out by means of Generalized Additive Models (GAM). The variables selection was carried out according to Wood's guidelines (Wood, 2001) and evaluating at each step the presence of deviation from the main assumptions (influential points, residuals distribution and multicollinearity). In particular, SSL NASC values, due to the highly right-skewed distribution, were modeled using Gamma error distribution with a log-link function. In the case of C and S, due to the large proportion of zero values and to the highly skewed strictly positive values, a presence/absence approach was used; NASC values for such groups were coded as binary variables and a binomial error family with logit-link function was used for modelling. To test the possible relationship between the vertical distribution of krill species (i.e. C and S) and SSL, the effect of C and S NASC was tested in the SSL model and the effect of SSL NASC was evaluated in the C and S models. All statistical analyses were carried out by means of R statistical software (R Core Team, 2023) by using "FactoMineR" (Le et al., 2008) and "mgcv" (Wood, 2011) packages.

# 3 Results

## 3.1 Environmental analysis

In a first step, CTD vertical profiles were inspected and averaged to highlight differences between areas in terms of temperature, salinity, Chl-*a* and oxygen (Supplementary Figure S5). Considering the average profiles by area, the A1 and A2 areas showed very similar shapes in terms of temperature (Figure 2), characterized by an almost linear decreasing trend from surface to 50 m depth, followed by a smooth decrease in temperature up to 100 m depth where temperature values almost stabilize. In such areas, and particularly in the A2 area, a small inversion was observed at the surface in terms of trends (i.e. the temperature increases with depth in the first part of the vertical profile and then starts to decrease). In addition, the two areas showed different temperature values at surface (~0.75°C in A1 and ~0°C in A2). The A3 area showed almost the same temperature profile of A1 and A2 areas, but here a step was observed around 30 m depth and temperature values were more variable below 100 m depth. Finally, in the A4 area the average temperature profile was quite different from the other ones with temperature almost stable from the surface till 40 m, while increasing from 50 m depth up to about 160 m depth where it stabilizes. In terms of salinity, average vertical profiles showed pairwise similarity, with A1 and A2 areas which showed an increasing trend from the surface up to 100 m depth followed by almost stable salinity values, while A3 and A4 areas were characterized by a very low variability from the surface up to 50 m depth followed by an increasing trend up to 200 m depth. Concerning the average Chl-*a* profiles, in the A1, A2 and A3 areas a clear maximum was observed at different depths and with different values depending on the area (Figure 2). On the contrary, in the A4 area, Chl-*a* values increased along the first few meters and then remained almost constant up to 50 m depth, where they started to decrease. Oxygen values showed an almost sigmoidal shape in all areas, but with a different degree of variation depending on the area.

Non-parametric ANOVA (Kruskal-Wallis rank sum test) showed significant differences between areas ($H_{(3)} = 36.902$, p-value = $4.8\times10^{-08}$ for temperature; $H_{(3)} = 38.484$, p-value = $2.2\times10^{-08}$ for salinity; $H_{(3)} = 29.913$, p-value = $1.4\times10^{-06}$ for Chl-*a*; $H_{(3)} = 24.99$, p-value = $1.6\times10^{-05}$ for oxygen). *Post-hoc* tests showed: A1 and A2 to be similar in terms of temperature; pairwise similar in salinity (A1 - A2 and A3 - A4); pairwise similar in Chl-*a* (A1 - A3 and A2 - A4); A1, A2 and A3 similar for oxygen but all different from the A4 area (Figure 3).

Principal component analysis was also carried out to highlight structural patterns among variables, species density (i.e. species NASC included in the analysis as quantitative supplementary variables) and identified areas (included in the analysis as a qualitative supplementary variable). Results from the PCA showed that the first and second PCA axes explained a large amount of variance (~82%), highlighting the presence of strong variables patterns (Figure 4A). In particular, obtained results (Figure 4A) evidenced a strong association on the first axis of depth, salinity and Chl-*a* (correlation values -0.88, 0.86 and 0.81, respectively) and relatively lower correlations with oxygen, temperature and SSL NASC (0.6, 0.57 and 0.51, respectively). On the second axis, the only significantly associated variables were temperature and oxygen (0.76 and -0.73 respectively) that were inversely related each other (Figure 4A). The area factor resulted also significantly associated to both the 1$^{th}$ and 2$^{nd}$ axes (Figure 4B), thus confirming the similarities between A1 and A2 areas that were in turn quite different from A3 and A4 areas.

## 3.2 SSL, krill aggregations and distribution patterns

Some echograms of the three acoustically-detected zooplankton groups at different frequencies in the four considered areas are shown in Supplementary Figures S1–S4.

For each CTD station, the presence of the three groups was assessed, evaluating also the co-occurrence of C and S (Figure 5). The group showing the lower presence among stations was S (with only 18 positive stations), followed by C (with 42 positive stations), while SSL was ubiquitous. C and S were found co-occurring in 11 stations (Figure 5, bottom-right panel).

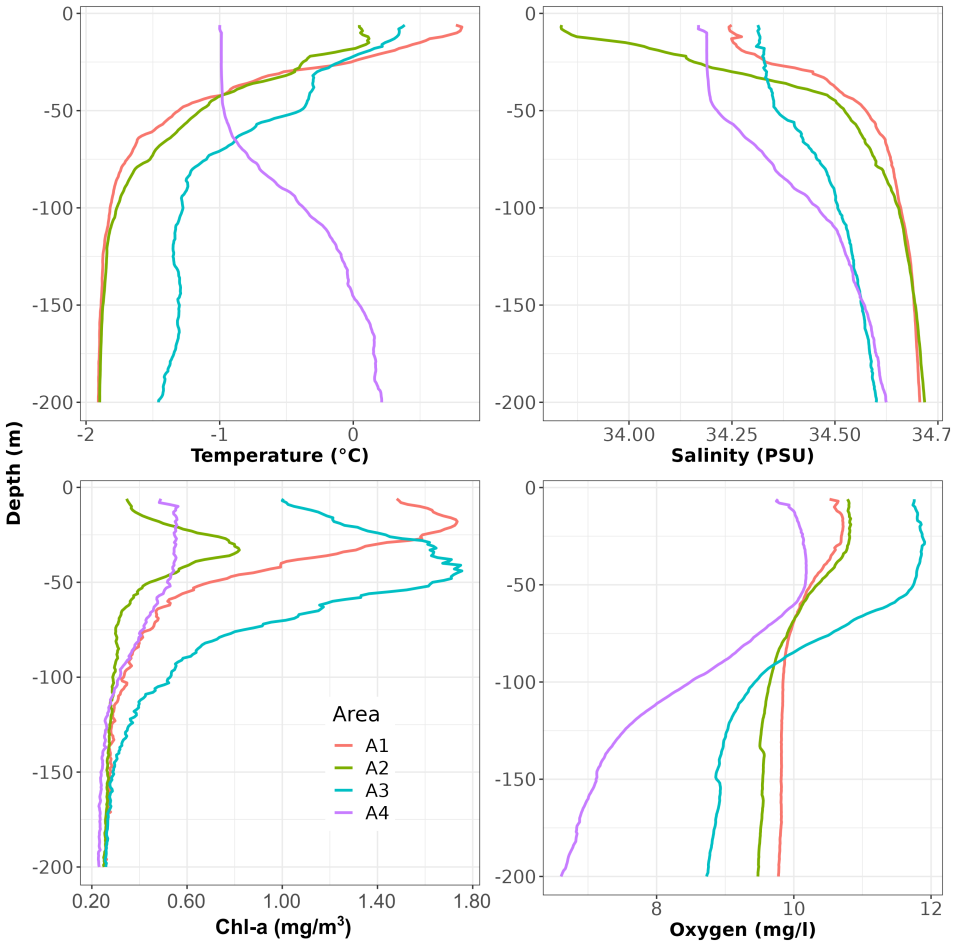


FIGURE 2
Depth-averaged vertical profiles by area of temperature, salinity, Chl-*a* and oxygen.

No significant difference was found among the four considered areas in terms of average NASC values for C and S, while significant differences ($H_{(3)}$ = 27.644, p-value < 0.05) were evidenced for SSL (Figure 6). In particular, according to the *post-hoc* test results, SSL NASC values were similar among the A1, A2 and A3 areas which resulted significantly different from the A4 one.

For each station, the vertical mass center (GC) of the three groups showed significant differences for S ($H_{(3)}$ = 7.4967, df = 2, p-value < 0.05) with deeper GC in the A1 than in A3 and A4 areas (the A2 area was excluded for this species as only one positive station was present).

In the C case, significant differences ($H_{(3)}$ = 11.819, df = 3, p-value <0.05) were found with a pairwise similarity between A1-A2 and A3-A4 areas (Figure 6). Finally, SSL GCs were also found significantly different among all areas ($H_{(3)}$ = 21.406, df = 3, p-value < 0.05), except for the comparison A1-A4.

## 3.3 Modelling the vertical distribution of SSL, *E. crystallorophias* (C) and *E. superba* (S)

The vertical distribution of SSL was found to be significantly related to the area factor, to the logarithm of C NASC, to the interaction between area factor and depth as well as to the interaction among area, Chl-*a* and temperature (Table 1). The obtained model explained about 63% of the total deviance (Table 1) and evidenced a different effect of depth among the considered areas (Figure 7). In A1 area, SSL NASC values decreased with depth from the surface till 50 m where they started to increase again up to ~110 m; below such depth, SSL NASC decreased again till 200 m. In A2 area, the SSL NASC values rapidly decreased to 0 from the surface till about 70 m, to increase again from about 120 m up to 200 m. In A3 area, the depth effect was bell shaped and centered around 100 m while in A4 area the depth effect monotonically decreased from the surface up to 75 m. In addition, for all areas SSL NASC almost linearly increased according to the (shifted) logarithm of C NASC values (Figure 7). Finally, the temperature - Chl-*a* interaction showed different behavior according to the area factor. In A1 and A2 areas, higher SSL NASC were linked mainly to higher temperature even if slightly lower values were estimated for lower Chl-*a* values. In A3 and A4 areas, the relationship among temperature, Chl-*a* and SSL NASC values was much more complex, evidencing different effects in relation to specific combination of Chl-*a* and temperature values (e.g. in A3 area higher SSL values were found related to higher Chl-*a* but the effect direction and magnitude was modulated by temperature values).

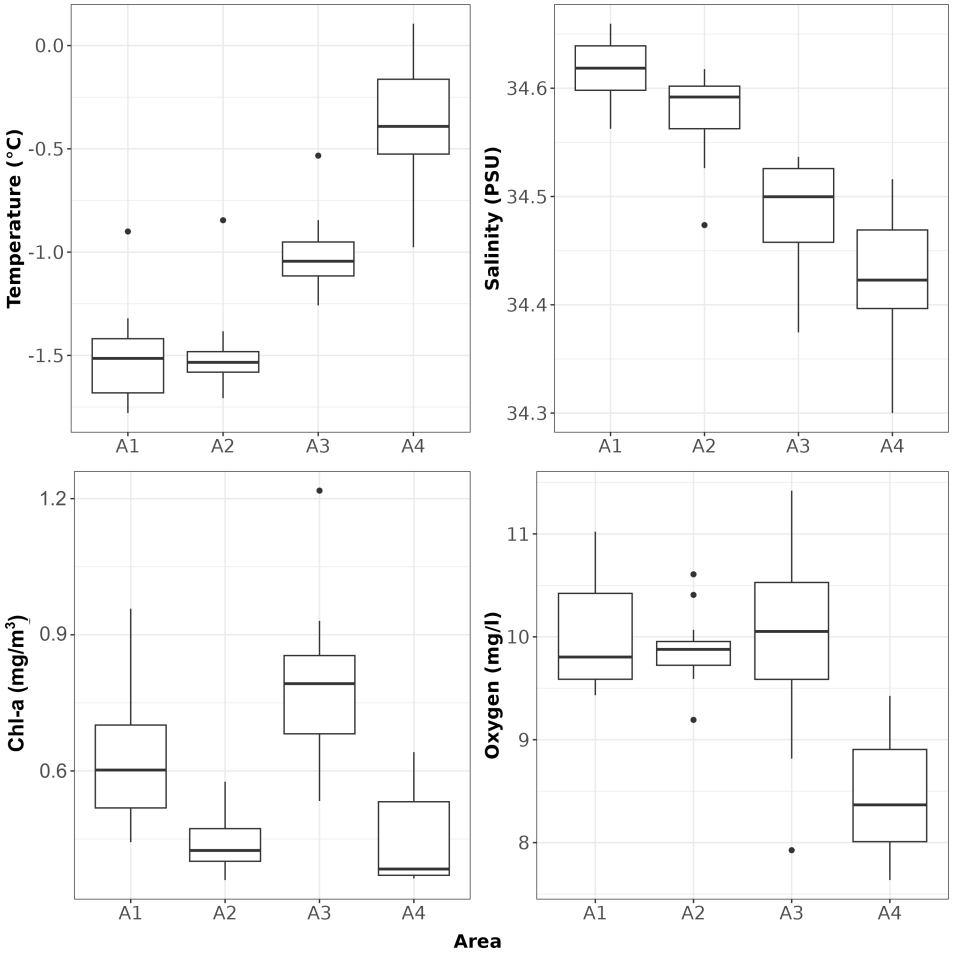


FIGURE 3
Boxplot of CTD derived temperature, salinity, Chl-*a* and oxygen.

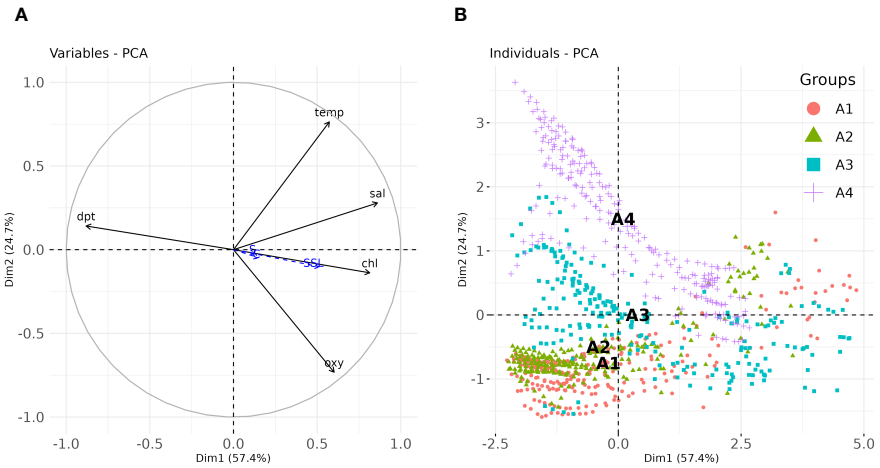


FIGURE 4
**(A)** Factor-Variables correlation plot and **(B)** Scatterplot of observations in the PC space. Area labels in panel **(B)** represent the centroid of each group. temp, Temperature (°C); sal, salinity (PSU); chl, Chl-*a* (mg/m$^3$); dpt, depth (m); oxy, oxygen (mg/l).

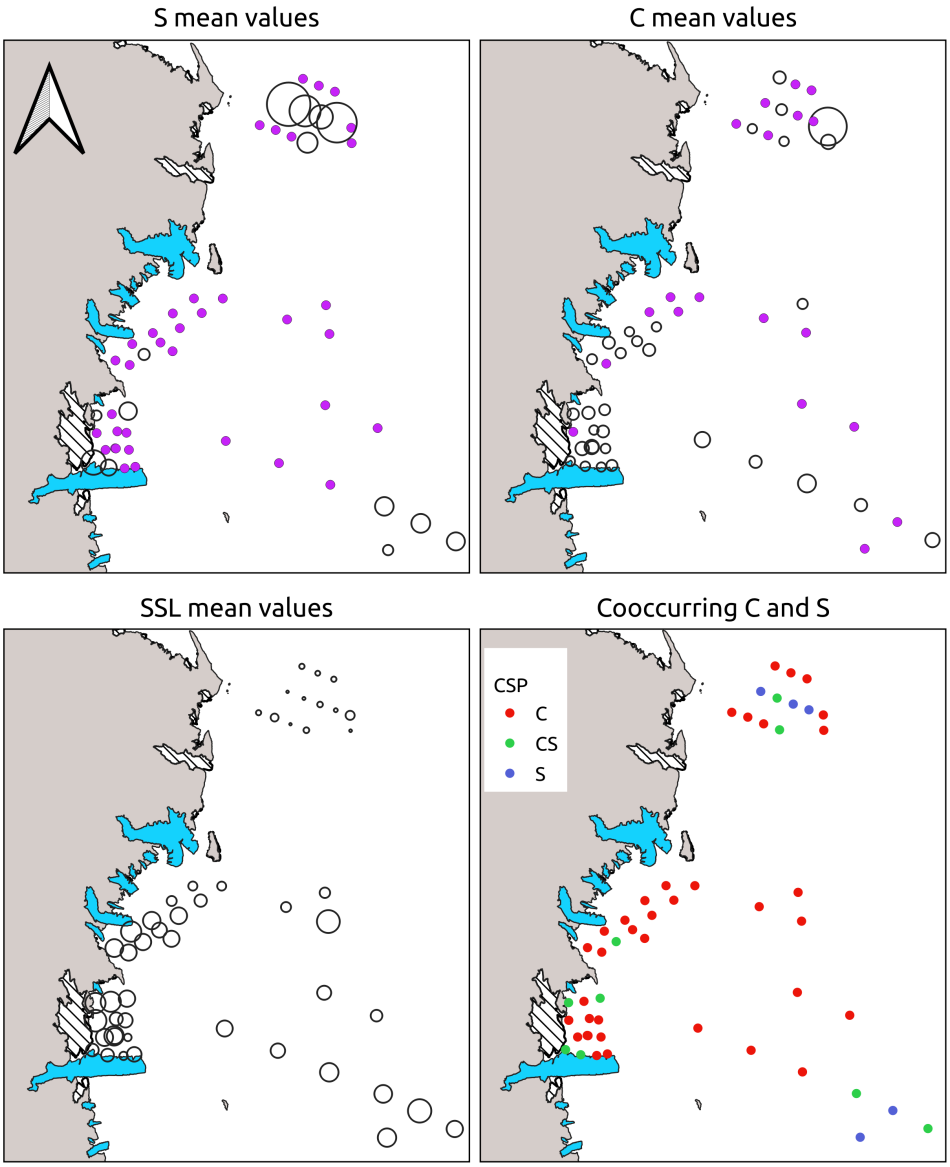


FIGURE 5
Proportional representation of station-averaged C, S and SSL NASC values. Points in purple represent group absence. The bottom right panel represent the station positive for S (blue points), for C (red points) or for both (green points - CS).

In the case of C NASC, the binomial GAM approach explained about 50% of the total deviance and showed that the probability of C presence was significantly related to the area-depth interaction, the oxygen-salinity interaction and the SSL NASC (Table 2). In terms of depth, in A1 and A3 areas the effect was almost bell-shaped but with peaks occurring at different depths (Figure 8). In A2 and A4 areas the depth effect was characterized by a more complex shape with 2 peaks occurring at different depth. Furthermore, for all areas considered, the C probability of presence was positively influenced by the square root of SSL NASC. Specifically, the C probability of presence increased from 0 to 0.5 when transformed SSL NASC values were between 0 and 0.8, decreased from 0.5 to 0.2 for transformed SSL NASC values between 1 and 1.8, and increased again to 0.8 for transformed SSL NASC values greater than 1.8. Finally, the interaction between oxygen and salinity led to an increase in C probability of presence for higher salinity and increasing oxygen from low to mid-low values, followed by a decrease for oxygen values from mid-low to medium levels. Then, for medium to high oxygen levels, the C probability of presence showed an increase with increasing oxygen for high salinity values.

The GAM model for S presence/absence explained ~44% of the total deviance, highlighting again different depth patterns in relation to the area factor (Table 3). In A3 and A4 areas, the probability of S presence decreased almost similarly from the surface to 200 m, with a change in slope at 120 m and a different behavior between the two areas at the surface. On the contrary, the depth effect in A1 area was bell-shaped, with the peak occurring at around 100 m depth (Figure 9). The interaction between Chl-*a* and

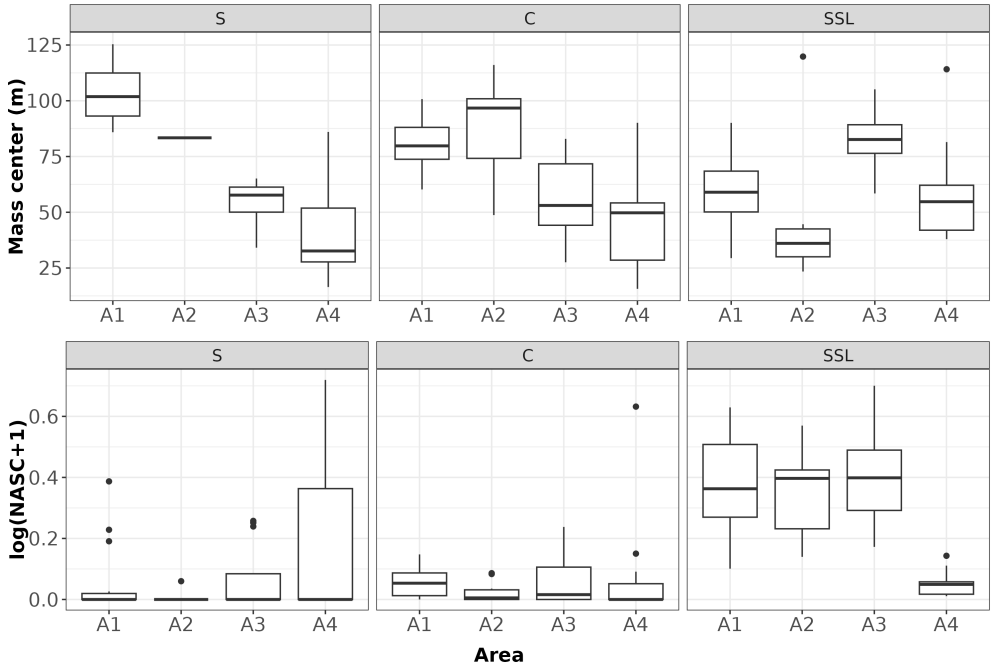


FIGURE 6
Boxplot of NASC and Mass center by acoustic groups (S: *Euphausia superba*; C: *Euphausia crystallorophias*; SSL: Sound Scattering Layers) and areas. Note that in the statistical test, the case "S" in the A2 area was not considered as only one positive station was present.

TABLE 1 SSL (Sound Scattering Layer) NASC model summary.

| Parametric coefficients | | | | |
|---|---|---|---|---|
| | Estimate | Std.Error | t-value | Pr(>\|t\|) |
| (Intercept) | -0.8791 | 0.2032 | -4.326 | 1.69E-05 |
| groupA2 | -0.8272 | 0.2385 | -3.469 | 0.000547 |
| groupA3 | -0.1365 | 0.2461 | -0.555 | 0.579171 |
| groupA4 | -3.07 | 0.9583 | -3.204 | 0.001404 |
| **Approximate significance of smooth terms** | | | | |
| | edf | Ref.df | F | p-value |
| s(depth):areaA1 | 4.74 | 5.834 | 13.045 | < 2.00E-16 |
| s(depth):areaA2 | 4.741 | 5.809 | 13.762 | < 2.00E-16 |
| s(depth):areaA3 | 3.362 | 4.209 | 9.38 | < 2.00E-16 |
| s(depth):areaA4 | 2.818 | 3.539 | 3.266 | 1.64E-02 |
| s(Chl-*a*,temperature):areaA1 | 5.842 | 7.69 | 3.282 | 1.41E-03 |
| s(Chl-*a*,temperature):areaA2 | 2.106 | 2.206 | 8.434 | 1.99E-04 |
| s(Chl-*a*,temperature):areaA3 | 7.842 | 10.559 | 3.165 | 5.05E-04 |
| s(Chl-*a*,temperature):areaA4 | 11.632 | 13.455 | 5.123 | 2.00E-16 |
| s(NASC_C) | 2.176 | 2.71 | 21.185 | 2.00E-16 |

R-sq.(adj) = 0.505 Deviance explained = 63.2%.
REML = -877.55 Scale est. = 1.0888 n = 969.

10.3389/fmars.2023.1304493

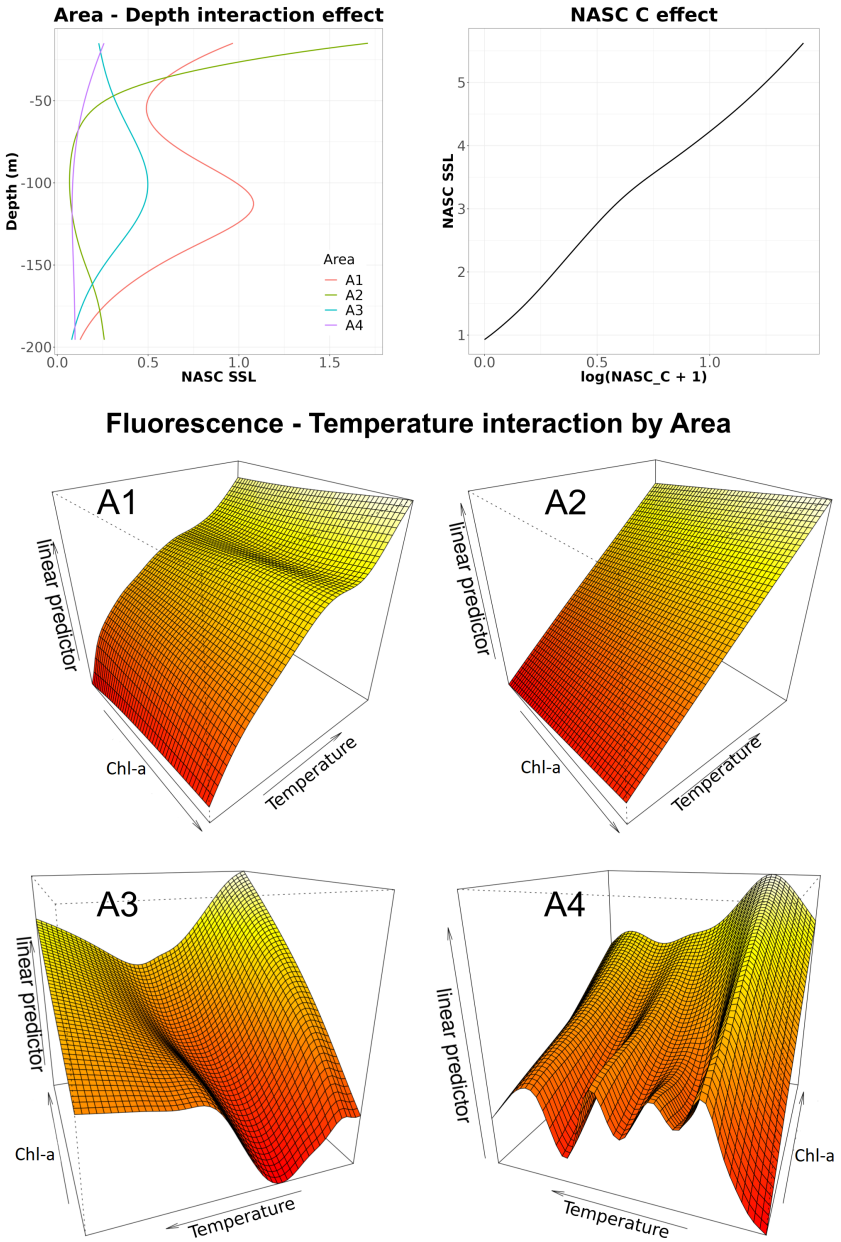


FIGURE 7
Effects of the significant terms in the SSL (Sound Scattering Layer) NASC model. The interaction between Chl-*a* and temperature as well as depth were evaluated by area factor.

oxygen was quite complex, showing a low probability of presence at low oxygen and Chl-*a* levels and the highest probability at higher Chl-*a* and lower oxygen levels.

## 4 Discussion

In the present study, active acoustic techniques were used to characterize the vertical structure of *E. crystallorophias*, *E. superba* and SSL in four different areas of the Ross Sea. SSLs were found mostly ubiquitous while *E. crystallorophias* and *E. superba* showed a patchy distribution with the latter patchier than the former. Some differences and similarities among areas were also observed in terms of both environmental parameters and vertical distributions of the three acoustic groups. The A1 and A2 areas showed high degree of similarity for temperature, salinity and oxygen but not for Chl-*a* (Figure 2). For the two areas, the average vertical profiles of the three acoustic groups were also found similar (Supplementary Figures S6, S7), even if S was found in only one station in area A2, thus making it difficult a direct comparison for this species. The A3 and A4 areas were found different from each other and from the A1 and A2 areas both in terms of hydrological vertical profiles and acoustic vertical profiles of S, C and SSL (Supplementary Figures S6, S7). Such results, likely due to difference among areas in terms of phytoplankton and zooplankton communities, confirm the complexity of the marine ecosystem structure in the Ross Sea

TABLE 2 Model summary for the probability of presence of C.

| Parametric coefficients | | | | |
|---|---|---|---|---|
| | Estimate | Std. Error | z value | Pr(>\|z\|) |
| (Intercept) | -5.2719 | 0.7408 | -7.117 | 1.11E-12 |
| **Approximate significance of smooth terms** | | | | |
| | edf | Ref.df | Chi.sq | p-value |
| s(depth):areaA1 | 3.368 | 4.206 | 42.26 | < 2e-16 |
| s(depth):areaA2 | 4.396 | 5.318 | 34.86 | 3.21E-06 |
| s(depth):areaA3 | 4.132 | 4.997 | 21.85 | 0.00055 |
| s(depth):areaA4 | 8.692 | 8.936 | 23.22 | 0.00556 |
| s(oxygen,salinity) | 24.632 | 26.816 | 56.15 | 0.00104 |
| s(SSL NASC) | 6.908 | 7.979 | 51.14 | < 2e-16 |

R-sq.(adj) = 0.459 Deviance explained = 50.6%.
UBRE = -0.44594 Scale est. = 1 n = 969.

(Faranda et al., 2000). The western Ross Sea is known to represent a mosaic of functionally different marine subsystems, characterized by different levels of primary production (Saggiomo et al., 2002; Ducklow et al., 2006; Arrigo et al., 2008; Mangoni et al., 2018), with the most productive area to the west of the 175$^{th}$ meridian. Furthermore, the west coast of the Ross Sea is characterized by two blooms based on different spatial and temporal scales (Di Tullio and Smith, 1996; Arrigo et al., 1999; Innamorati et al., 2000; Smith and Asper, 2001; Arrigo et al., 2008). In this area, the phytoplankton community shows a well-defined biogeographic distribution

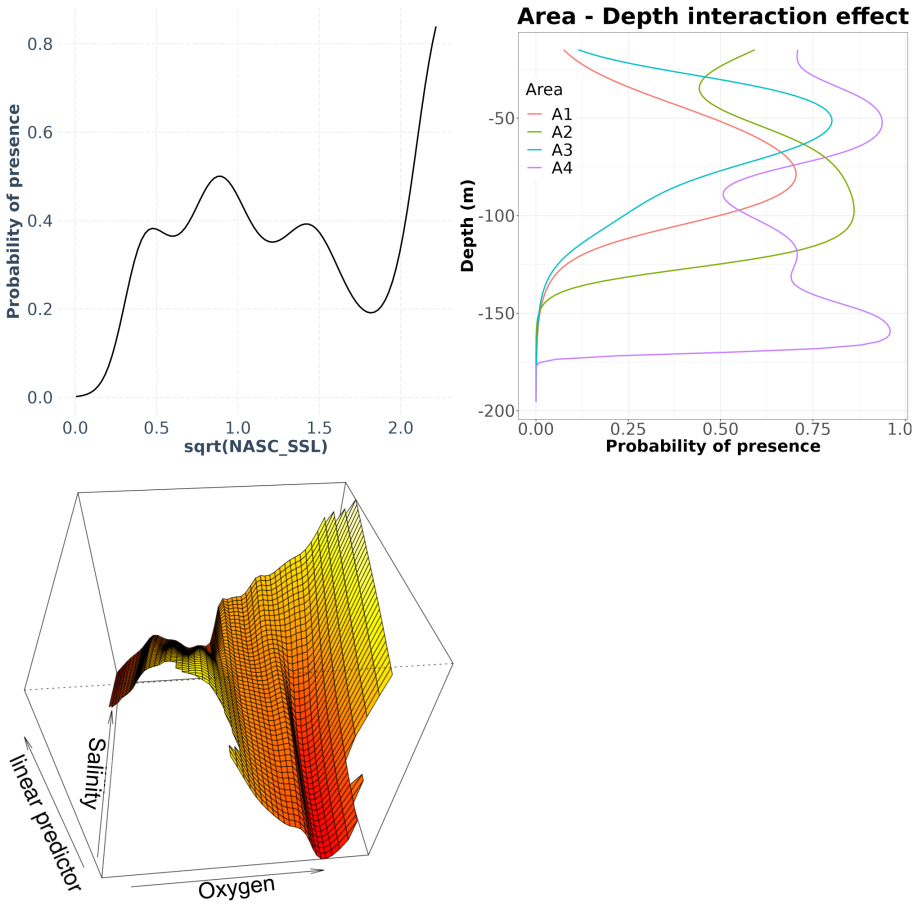


FIGURE 8
Effects of the significant terms in the *Euphausia crystallorophias* (C) presence/absence model. The depth was also evaluated by area factor.

TABLE 3 Model summary for the probability of presence of S.

| Parametric coefficients | | | | |
|---|---|---|---|---|
| | Estimate | Std. Error | z value | Pr(>\|z\|) |
| (Intercept) | -18.6 | 12.65 | -1.427 | 0.153 |
| **Approximate significance of smooth terms** | | | | |
| | edf | Ref.df | Chi.sq | p-value |
| s(depth):areaA1 | 3.026 | 3.821 | 11.638 | 0.01719 |
| s(depth):areaA3 | 1.812 | 2.239 | 2.788 | 0.27668 |
| s(depth):areaA4 | 1.515 | 1.822 | 9.328 | 0.00658 |
| te(Chl-*a*,oxy) | 12.998 | 14.194 | 35.035 | 0.00157 |

R-sq.(adj) = 0.352 Deviance explained = 44.8%.
UBRE = -0.6682 Scale est. = 1n = 741.
Note that area 2 was excluded from the analysis as in such area only one station was positive for S.

(Nuccio et al., 2000; Saggiomo et al., 2000) with blooms of haptophytes (*Phaeocystis antarctica*) dominating the larger Ross Sea polynya during spring and early summer, and diatoms (most frequently *Fragirariopsis curta*, *F. cylindricus*, *Nitzschia* and *Chaetoceros* spp.) in the open waters and the marginal ice zones of the western Ross Sea during summer (Di Tullio and Smith, 1996; Arrigo et al., 1999; Sweeney et al., 2000; Mangoni et al., 2004; Sedwick et al., 2011; Smith et al., 2014; Misic et al., 2017). Less rich zones are mainly dominated by dinoflagellates and other flagellates (Smith et al., 2014; Mangoni et al., 2017; Phan-Tan et al., 2018). Bolinesi et al. (2020), working on data collected in the same expedition of the P-Rose Project (austral summer 2016/2017), reported higher phytoplankton biomass values (in terms of chlorophyll-a concentrations) in Terra Nova Bay (Area A1), compared to the values in A2 area. Moreover, in the south-central Ross Sea (Area A3) the phytoplankton community exhibited high variability both in terms of biomass and structure, associated to a latitudinal effect. The A4 area sub-system was different from the other areas showing a completely different arrangement of chemicals and biological variables (Bolinesi et al., 2020).

Zooplankton is the most important factor in regulating food web dynamics and ecological interactions in the Ross Sea (Hopkins, 1987; Saino and Guglielmo, 2000; Ainley et al., 2010; Ainley et al., 2015; Minutoli et al., 2017; Smith et al., 2017; Kiko et al., 2020) with gelatinous zooplankton, comprising jellyfish, ctenophores and chordate tunicates (Pagès, 1997), showing a ubiquitous behavior (Richardson et al., 2009; Schaub et al., 2018; Verhaegen et al., 2021). Nonetheless, zooplankton abundance varies greatly over the continental shelf and its assemblages, beyond copepods, are mainly composed by fish larvae, euphausiids, hyperiid and gammarid amphipods, pteropods, chaetognaths, and ostracods (Guglielmo et al., 1990; Guglielmo et al., 1992; Hecq et al., 1992; Hunt et al., 2008; Stevens et al., 2015; Smith et al., 2017; Granata et al., 2022; Kim et al., 2022). In the coastal area (corresponding to A1 and A2 areas) copepods are the dominant group (Carli et al., 1990; Zunini Sertorio et al., 1990; Carli et al., 1992; Hecq et al., 1992; Zunini Sertorio et al., 1992; Carli et al., 2000; Zunini Sertorio et al.,

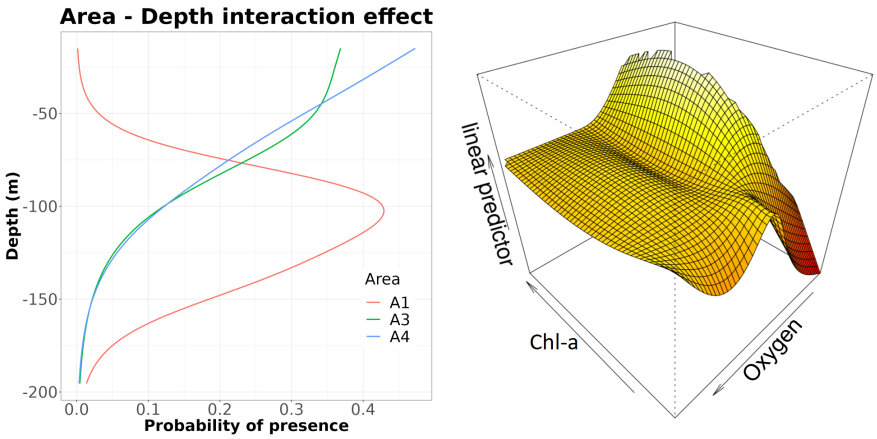


FIGURE 9
Effects of the significant terms in the *Euphausia Superba* (S) presence/absence model. Note that, as in A2 area only one station was positive for S, such area was excluded from the analysis.

2000; Pane et al., 2004; Guglielmo et al., 2015; Smith et al., 2017; Bonello et al., 2020; Grillo et al., 2022; Kim et al., 2022), representing in austral summer more than 70% of the total community, while the remaining species are pelagic amphipods (Minutoli et al., 2023), *Limacina helicina antarctica* (Accornero et al., 2003; Manno et al., 2010), postlarval and juvenile stages of *Pleuragramma antarcticum* (Guglielmo et al., 1997; Granata et al., 2000; Granata et al., 2002; Granata et al., 2009), and calyptopis and furcilia stages of *Euphausia crystallorophias* (Guglielmo et al., 2009).

In the offshore waters between 170° and 175°E (corresponding to A3 area) and in the southern part of Terra Nova Bay, juvenile *Pleuragramma antarcticum* show higher abundance with respect to postlarvae (Guglielmo et al., 1998; Granata et al., 2000; Granata et al., 2002; Granata et al., 2009) which showed higher abundances in Terra Nova Bay (Area A1).

In the norther part of the Ross Sea (area A4 in this study), high abundance of copepods was found during the 1989-90 summer season, particularly in the upper 100 m with dominant species represented by adults of *Calanoides acutus*, *Calanus propinquus*, *Metridia gerlachei* and *Rhincalanus nasutus* (Zunini Sertorio et al., 2000). On the contrary, *L. helicina antarctica* and *P. antarcticum* larvae showed relatively low abundance (Kim et al., 2022), compared to coastal areas such as Terra Nova Bay (Area A1).

In all considered areas, SSLs showed similar average NASC values except in A4 area characterized by lower values (Figure 6). SSLs are commonly observed in all oceans, spanning different spatial and temporal scales likely due to the species composition that, although almost unknown, appears mainly composed of mesozooplankton, macrozooplankton, micronekton organisms, fish larvae and juveniles (Blanluet et al., 2019; Geoffroy et al., 2019). SSL backscatter values also show temporal and spatial variation as well as seasonal changes in species composition. For instance, in the Barents Sea, Geoffroy et al. (2019) observed a latitudinal decrease (south to north) in SSL Sv (Volume backscattering strength) that was consistent with previous studies (Siegelman-Charbit and Planque, 2016; Knutsen et al., 2017). However, the latitudinal trend found by the authors evidenced changes with seasons (being present in January but not in August), thus highlighting a complex interaction between spatial and temporal variations. Also in our case, while the southern areas were characterized by similar SSL NASC values, the northern one showed lower NASC values, letting us to hypothesize that SSL latitudinal gradients also exists in the Ross Sea. Despite the similar densities among A1, A2 and A3 areas, the vertical SSL structure showed different relationships with environmental conditions. In A1 and A2 areas, the vertical profiles of SSL were quite similar, but in A1 area a small increase in SSL NASC was observed between 75 and 100 m depth. The modelling approach highlighted the importance of depth in both areas as well as the influence of the interaction between temperature and Chl-*a* (Figure 7). As far as this latter aspect is concerned, most of the SSL NASC variation is linked to increasing temperature and modulated by Chl-*a*. Indeed, in A1 and A2 areas, even if the vertical SSL NASC profiles followed a decreasing trend in the upper layer, in A1 area SSL NASC values below 50 m depth were higher than in the A2 area (Figure 2), likely associated to higher Chl-*a* below such depth in A1 area. In A3 and A4 areas, the shape of interaction between Chl-*a* and temperature was much more complex, highlighting a different response of SSL assemblages to vertical environmental gradients and letting us to hypothesize a different species composition in SSL.

The presence/absence average vertical profiles for C (Supplementary Figure S7) also highlighted some similarities between the A1 and A2 areas, showing deeper maxima than in the A3 and A4 areas. In this case, the binomial GAM approach highlighted the importance of the interaction between salinity and oxygen as well as the effect of SSL NASC, included in the model as predictor (Figure 9). Overall, higher probability of presence of C was found for higher oxygen values but modulated by salinity. Such complex interaction, likely reflects the different oxygen and salinity levels found in the four areas. In addition, higher SSL NASC values were associated to higher probability of presence of C, likely indicating a trophic relationship between the two acoustic groups. In this context, gut content analyses of *E. crystallorophias* revealed phytoplankton, protozoans and metazoans as food items (Kattnerll and Hagen, 1998), even if more investigations indicate that such species may switch from algae to other food sources (Pakhomov et al., 1998; Ko et al., 2016). In addition, fatty acid and stable isotopic analyses suggested that *E. crystallorophias* apparently occupies a trophic niche different from *E. superba* (Ko et al., 2016; Yang et al., 2016; De Felice et al., 2022). This wide diversification in food sources could support the hypothesized trophic link between SSL and the presence of *E. crystallorophias*.

In the case of S, the modelling approach highlighted the importance of depth (similarly to SSL and C) and the effect of the interaction between Chl-*a* and oxygen; the latter evidencing highest probability of presence for relatively lower oxygen and higher Chl-*a* values. Also in this case the complex shape of the oxygen-Chl-*a* interaction surface likely reflects trophic effects as well as the different oxygen-Chl-*a* combination in the different areas. *Euphausia superba* is a key species in the Southern Ocean that serves as a link between primary production and higher trophic levels. Here, *E. superba* is essentially herbivorous, with a great contribution of nanoplankton (2–20 μm) particles in its diet, especially during the austral spring and autumn when phytoplankton blooms occur (Mangoni et al., 2019; Saggiomo et al., 2021). Differently from the *E. crystallorophias*, the lack of significant relationship between *E. superba* and SSL could be justified by the prevalence of phytoplankton in *E. superba* diet.

Despite the unavailability of biological samples, it is important to highlight the monitoring-related perspective of the methodology. Acoustic methods are relatively non-invasive and allow to cover large sectors in a quasi-synoptic way without impacting other survey-related activities (except for the needs to sample specific acoustic structure identified on ecograms along the route). Such methods permit to optimize biological sampling by sampling only specific acoustic targets (such features is particularly important for endangered species or ecosystems). In this context, the wide-band technology in conjunction with a multifrequency approach and pattern recognition algorithms (e.g. Aronica et al., 2019; Fontana et al., 2022; Giacalone et al., 2022) could also improve the reliability of acoustic estimates and reduce the sampling effort. Finally, from an operational point of view only 3 or 4 researchers/technicians are

necessary to continuously acquire acoustic dataset during the survey, thus permitting the development of "opportunistic" monitoring programs with highly positive benefit–cost ratio. Considering the importance of mid-trophic levels organisms from the ecological point of view, as well as that the Southern Ocean plays an important role in carbon sequestration (DeVries, 2014) through still poorly understood mechanisms involving mid-tropic levels organisms (Tournier et al., 2021), it is important to increase the monitoring effort on yearly basis during multidisciplinary surveys, thus developing a time series of detailed information about the vertical structure and the daily vertical migration of the zooplankton community.

## Data availability statement

The raw data supporting the conclusions of this article will be made available by the authors, without undue reservation.

## Author contributions

MB: Conceptualization, Data curation, Formal analysis, Investigation, Methodology, Software, Supervision, Writing – original draft, Writing – review & editing. LG: Conceptualization, Methodology, Supervision, Writing – original draft, Writing – review & editing. AB: Conceptualization, Data curation, Investigation, Supervision, Writing – original draft, Writing – review & editing. OM: Conceptualization, Data curation, Methodology, Supervision, Validation, Writing – original draft. PRi: Conceptualization, Data curation, Investigation, Methodology, Supervision, Writing – original draft. PRu: Conceptualization, Methodology, Supervision, Writing – original draft, Writing – review & editing. PF: Data curation, Investigation, Supervision, Writing – original draft, Writing – review & editing. GB: Conceptualization, Data curation, Methodology, Writing – original draft. IF: Data curation, Investigation, Methodology, Writing – original draft, Writing – review & editing. RF: Data curation, Methodology, Supervision, Writing – original draft, Writing – review & editing. GG: Conceptualization, Data curation, Methodology, Software, Writing – original draft. SA: Conceptualization, Data curation, Investigation, Software, Writing – original draft. RM: Conceptualization, Data curation, Methodology, Writing – original draft. FM: Data curation, Investigation, Writing – original draft. AG: Conceptualization, Data curation, Investigation, Methodology, Supervision, Writing – original draft, Writing – review & editing. SG: Conceptualization, Data curation, Methodology, Software, Supervision, Writing – original draft, Writing – review & editing.

## Funding

The author(s) declare financial support was received for the research, authorship, and/or publication of this article. This study was funded by the Italian National Program for Antarctic Research, in the framework of the Projects P-ROSE (PNRA16_00239) and CELEBeR (PNRA16_00207).

## Acknowledgments

The authors express their gratitude to Italian Antarctic National Program (PNRA) and the scientific personnel and crew of the research vessel Italica for logistical support.

## Conflict of interest

The authors declare that the research was conducted in the absence of any commercial or financial relationships that could be construed as a potential conflict of interest.

The author(s) declared that they were an editorial board member of Frontiers, at the time of submission. This had no impact on the peer review process and the final decision.

## Publisher's note



## Supplementary material

The Supplementary Material for this article can be found online at: https://www.frontiersin.org/articles/10.3389/fmars.2023.1304493/full#supplementary-material

SUPPLEMENTARY FIGURE 1
Example of echograms acquired at 38 kHz (upper panel) and at 120 kHz (lower panel) in the A1 area.

SUPPLEMENTARY FIGURE 2
Example of echograms acquired at 38 kHz (upper panel) and at 120 kHz (lower panel) in the A2 area.

SUPPLEMENTARY FIGURE 3
Example of echograms acquired at 38 kHz (upper panel) and at 120 kHz (lower panel) in the A3 area.

SUPPLEMENTARY FIGURE 4
Example of echograms acquired at 38 kHz (upper panel) and at 120 kHz (lower panel) in the A4 area.

SUPPLEMENTARY FIGURE 5
Average vertical profiles by area and depth (thick red lines) and vertical profiles by station and area (thin lines) of temperature (°C), salinity (PSU), chlorophyll-a ($mg/m^3$) and oxygen ($mg/m^3$).

SUPPLEMENTARY FIGURE 6
Comparison between the vertical profiles of temperature (°C), salinity (PSU), chlorophyll-a ($mg/m^3$) and oxygen ($mg/m^3$) and NASC C, S and SSL ones. All variables were scaled in order to allow a clear representation on a common x scale.

SUPPLEMENTARY FIGURE 7
Model-predicted vs. observed average SSL NASC profiles and probability of presence of C and S by area. Note that in the case of S, area A2 was excluded from the analysis as only one station was found positive for such group.

# References


Accornero, A., Manno, C., Esposito, F., and Gambi, M. C. (2003). The vertical flux of particulate matter in the polynya of Terra Nova Bay: Part II. Biological components. *Antarct. Sci.* 15, 175–188. doi: 10.1017/S0954102003001214

Ainley, D. G., Ballard, G., Blight, L. K., Ackley, S., Emslie, S. T., Lescroel, A., et al. (2010). Impacts of cetaceans on the structure of Southern Ocean food webs. *Mar. Mamm. Sci.* 26 (2), 482–489. doi: 10.1111/j.1748-7692.2009.00337.x

Ainley, D. G., Ballard, G., Jones, R. M., Jongsomjit, D., Pierce, S. D., Smith, W. O. Jr, et al. (2015). Trophic cascades in the western Ross Sea, Antarctica: revisited. *Mar. Ecol. -Prog. Ser.* 534, 1–16. doi: 10.3354/meps11394

Aronica, S., Fontana, I., Giacalone, G., Lo Bosco, G., Rizzo, R., Mazzola, S., et al. (2019). Identifying small pelagic Mediterranean fish schools from acoustic and environmental data using optimized artificial neural networks. *Ecol. Inform.* 50, 149–161. doi: 10.1016/j.ecoinf.2018.12.007

Arrigo, K. L., Robinson, D. H., Worthen, D. L., Dunbar, R. B., Di Tullio, G. R., VanWoert, M., et al. (1999). Phytoplankton community structure and the drawdown of nutrients and CO2 in the southern ocean. *Science* 283 (5400), 365–367. doi: 10.1126/science.283.5400.365

Arrigo, K. R., Van Dijken, G. L., and Bushinsky, S. (2008). Primary production in the southern ocean 1997-2006. *J. Geophys. Res.* 113, C08004. doi: 10.1029/2007JC004551

Azzali, M., and Kalinowski, J. (2000). "Spatial and temporal distribution of krill *Euphausia superba* biomass in the Ross Sea, (1989-1990 and 1994)," in *Ross Sea ecology*. Eds. F. M. Faranda, L. Guglielmo and A. Ianora (Berlin, Heidelberg: Springer-Verlag), 433–455. doi: 10.1007/978-3-642-59607-0_31

Azzali, M., Leonori, I., De Felice, A., and Russo, A. (2006). Spatial-temporal relationships between two euphausiid species in the Ross Sea. *Chem. Ecol.* 22, S219–S233. doi: 10.1080/02757540600670836

Bagoien, E., Kaartvedt, S., Aksnes, D. L., and Eiane, K. (2001). Vertical distribution and mortality of overwintering Calanus. *Limnol. Oceanogr.* 46, 1494–1510. doi: 10.4319/lo.2001.46.6.1494

Barange, M., Coetzee, J., Takasuka, A., Hill, K., Gutierrez, M., Oozeki, Y., et al. (2009). Habitat expansion and contraction in anchovy and sardine populations. *Prog. Oceanogr.* 83 (1-4), 251–260. doi: 10.1016/j.pocean.2009.07.027

Barra, M., Petitgas, P., Bonanno, A., Somarakis, S., Woillez, M., Machias, A., et al. (2015). Interannual changes in biomass affect the spatial aggregations of anchovy and sardine as evidenced by geostatistical and spatial indicators. *PloS One* 10 (8), e0135808. doi: 10.1371/journal.pone.0135808

Ben Abdallah, L., Barra, M., Gaamour, A., Khemiri, S., Genovese, S., Mifsud, R., et al. (2018). Small pelagic fish assemblages in relation to environmental regimes in the Central Mediterranean. *Hydrobiologia* 821, 113–134. doi: 10.1007/s10750-018-3540-0

Benoit-Bird, K. J., and Lawson, G. L. (2016). Ecological insights from pelagic habitats acquired using active acoustic techniques. *Annu. Rev. Mar. Sci.* 8, 463–490. doi: 10.1146/annurev-marine-122414-034001

Benoit-Bird, K. J., and McManus, M. A. (2014). A critical time window for organismal interactions in a pelagic ecosystem. *PloS One* 9, e97763. doi: 10.1371/journal.pone.0097763

Blanluet, A., Doray, M., Berger, L., Romagnan, J. B., Le Bouffant, N., Lehuta, S., et al. (2019). Characterization of sound scattering layers in the Bay of Biscay using broadband acoustics, nets and video. *PloS One* 14 (10), e0223618. doi: 10.1371/journal.pone.0223618

Bolinesi, F., Saggiomo, M., Ardini, F., Castagno, P., Cordone, A., Fusco, G., et al. (2020). Spatial-related community structure and dynamics in phytoplankton of the Ross Sea, Antarctica. *Front. Mar. Sci.* 7. doi: 10.3389/fmars.2020.574963

Bonanno, A., Barra, M., De Felice, A., Giannoulaki, M., Iglesias, M., Leonori, I., et al. (2021). Acoustic correction factor estimate for compensating vertical diel migration of small pelagics. *Mediterr. Mar. Sci.* 22 (4), 784–799. doi: 10.12681/mms.25120

Bonanno, A., Barra, M., Mifsud, R., Basilone, G., Genovese, S., Di Bitetto, M., et al. (2018). Space utilization by key species of the pelagic fish community in an upwelling ecosystem of the Mediterranean Sea. *Hydrobiologia* 821, 173–190. doi: 10.1007/s10750-017-3350-9

Bonanno, A., Zgozi, S., Basilone, G., Hamza, M., Barra, M., Genovese, S., et al. (2015). Acoustically detected pelagic fish community in relation to environmental conditions observed in the Central Mediterranean Sea: a comparison of Libyan and Sicilian-Maltese coastal areas. *Hydrobiologia* 755, 209–224. doi: 10.1007/s10750-015-2234-0

Bonello, G., Grillo, M., Cecchetto, M., Giallain, M., Granata, A., Guglielmo, L., et al. (2020). Distributional records of ross sea (Antarctica) planktic copepoda from bibliographic data and samples curated at the Italian national antarctic museum (MNA): checklist of species collected in the ross sea sector from 1987 to 1995. *ZooKeys* 969, 1–22. doi: 10.3897/zookeys.969.52334

Brierley, A. S., Fernandes, P. G., Brandon, M. A., Armstrong, F., Millard, N. W., McPhail, S. D., et al. (2002). Antarctic krill under sea ice: elevated abundance in a narrow band just south of ice edge. *Science* 295 (5561), 1890–1892. doi: 10.1126/science.1068574

Brierley, A. S., Ward, P., Watkins, J. L., and Goss, C. (1998). Acoustic discrimination of Southern Ocean zooplankton. Deep-Sea Res. *Part II: Topical Studies in Oceanography* 45 (7), 1155–1173. doi: 10.1016/S0967-0645(98)00025-3

Carli, A., Feletti, M., Mariottini, G. L., and Pane, L. (1992). Contribution to the study of Copepods collected during the Italian oceanographic campaign in Antarctica 1989-90. *Nat. Sc. Com. Ant. Ocean. Camp.*, 1987–1988.

Carli, A., Mariottini, G. L., and Pane, L. (1990). Contribution to the study of Copepods collected in Terra Nova Bay (Ross Sea). *Nat. Sc. Com. Ant. Ocean. Camp.*, 1987–1988.

Carli, A., Pane, L., and Stocchino, C. (2000). "Planktonic Copepods in Terra Nova Bay (Ross Sea): Distribution and relationship with environmental factors," in *Ross Sea Ecology Italian Antarctic expeditions, (1987-1995)*. Eds. F. M. Faranda, L. Guglielmo and A. Ianora (Berlin: Springer), 309–321.

Cheriton, O. M., McManus, M. M., Holliday, D. V., Greenlaw, C. F., Donaghay, P. L., and Cowles, T. J. (2007). Effects of mesoscale physical processes on thin zooplankton layers at four sites along the west coast of the U.S. *Estuaries Coasts: J. ERF* 30, 575–590. doi: 10.1007/BF02841955

Davis, L. B., Hofmann, E. E., Klinck, J. M., Pinones, A., and Dinniman, M. S. (2017). Distributions of krill and Antarctic silverfish and correlations with environmental variables in the western Ross Sea, Antarctica. *Mar. Ecol. -Prog. Ser.* 584, 45–65. doi: 10.3354/meps12347

De Felice, A., Biagiotti, I., Canduci, G., Costantini, I., Malavolti, S., Giuliani, G., et al. (2022). Is it the same every summer for the euphausiids of the ross sea? *Diversity-Basel* 14, 433. doi: 10.3390/d14060433

De Felice, A., Iglesias, M., Saraux, C., Bonanno, A., Tičina, V., Leonori, I., et al. (2021). Environmental drivers influencing the abundance of round sardinella (*Sardinella aurita*) and European sprat (*Sprattus sprattus*) in different areas of the Mediterranean Sea. *Mediterr. Mar. Sci.* 22(4), 812–826. doi: 10.12681/mms.25933

De Robertis, A., and Higginbottom, I. (2007). A post-processing technique to estimate the signal-to-noise ratio and remove echosounder background noise. *ICES J. Mar. Sci.* 64, 1282–1291. doi: 10.1093/icesjms/fsm112

DeVries, T. (2014). The oceanic anthropogenic $CO_2$ sink: storage, air-sea fluxes, and transports over the industrial era. *Glob. Biogeochem. Cycle* 28 (7), 631–647. doi: 10.1002/2013GB004739

Di Tullio, G. R., and Smith, W. O. Jr (1996). Spatial patterns in phytoplankton biomass and pigment distributions in the Ross Sea. *J. Geophys. Res.* 101, 18467–18477. doi: 10.1029/96JC00034

Ducklow, H. W., Fraser, W., Karl, D. M., Quetin, L. B., Ross, R. M., Smith, R. C., et al. (2006). Water-column processes in the West Antarctic Peninsula and the Ross Sea: Interannual variations and foodweb structure. *Deep-Sea Res. Part II-Top. Stud. Oceanogr.* 53, 834–852. doi: 10.1016/j.dsr2.2006.02.009

Faranda, F. M., Guglielmo, L., and Ianora, A. (2000). "The italian oceanographic cruises in the ross sea, (1987-95): Strategy, general considerations and description of the sampling sites," in *Ross Sea Ecology Italian antarctic expeditions, (1987-1995)*. Eds. F. M. Faranda, L. Guglielmo and A. Ianora (Berlin: Springer), 1–13.

Fernandes, P. G., Gerlotto, F., Holliday, D. V., Nakken, O., and Simmonds, E. J. (2002). Acoustic applications in fisheries science: the ICES contribution. *ICES Mar. Sci. Symp.* 215, 483–492. doi: 10.17895/ices.pub.8889

Fontana, I., Barra, M., Bonanno, A., Giacalone, G., Rizzo, R., Mangoni, O., et al. (2022). Automatic classification of acoustically detected krill aggregations: a case study from Southern Ocean. *Environ. Modell. Software* 151, 105357. doi: 10.1016/j.envsoft.2022.105357

Foote, K. G., Knudsen, H. P., Vestnes, G., MacLennan, D. N., and Simmonds, E. J. (1987). Calibration of acoustic instruments for fish density estimation: a practical guide. *ICES Cooperative Res. Rep.* 144, 82. doi: 10.1121/1.396131

Geoffroy, M., Daase, M., Cusa, M., Darnis, G., Graeve, M., Santana Hernández, N., et al. (2019). Mesopelagic sound scattering layers of the High Arctic: Seasonal variations in biomass, species assemblage, and trophic relationships. *Front. Mar. Sci.* 6. doi: 10.3389/fmars.2019.00364

Giacalone, G., Barra, M., Bonanno, A., Basilone, G., Fontana, I., Calabrò, M., et al. (2022). A pattern recognition approach to identify biological clusters acquired by acoustic multi-beam in Kongsfjorden. *Environ. Modell. Software* 152, 105401. doi: 10.1016/j.envsoft.2022.105401

Granata, A., Cubeta, A., Guglielmo, L., Sidoti, O., Greco, S., Vacchi, M., et al. (2002). Ichthyoplankton abundance and distribution in the Ross Sea during 1987–1996. *Polar Biol.* 25, 187–202. doi: 10.1007/s00300-001-0326-y

Granata, A., Guglielmo, L., Greco, S., Vacchi, M., Sidoti, O., Zagami, G., et al. (2000). "Spatial distribution and feeding habits of larval and juvenile *Pleuragramma antarcticum* in the Western Ross Sea (Antarctica)," in *Ross Sea ecology*. Eds. F. Faranda, L. Guglielmo and A. Ianora (Berlin Heidelberg New York: Springer), 369–393.

Granata, A., Weldrick, C. K., Bergamasco, A., Saggiomo, M., Grillo, M., Bergamasco, A., et al. (2022). Diversity in zooplankton and sympagic biota during a period of rapid sea ice change in Terra Nova Bay, Ross Sea, Antarctica. *Diversity-Basel* 14 (6), 425. doi: 10.3390/d14060425

Granata, A., Zagami, G., Vacchi, M., and Guglielmo, L. (2009). Summer and spring trophic niche of larval and juvenile *Pleuragramma antarcticum* in the Western Ross Sea, Antarctica. *Polar Biol.* 32, 369–382. doi: 10.1007/s00300-008-0551-8

Greenlaw, C. F., and Johnson, R. K. (1982). Physical and acoustical properties of zooplankton. *J. Acoust. Soc Am.* 72, 1706–1710. doi: 10.1121/1.388663

Grillo, M., Huettmann, F., Guglielmo, L., and Schiaparelli, S. (2022). Three-dimensional quantification of copepods predictive distributions in the Ross Sea: first data based on a machine learning model approach and open access (FAIR) data. *Diversity-Basel* 14, 355. doi: 10.3390/d14050355

Guglielmo, L., Arena, G., Brugnano, C., Guglielmo, R., Granata, A., Minutoli, R., et al. (2015). MicroNESS: an innovative opening–closing multinet for under pack-ice zooplankton sampling. *Polar Biol.* 38 (12), 2035–2046. doi: 10.1007/s00300-015-1763-3

Guglielmo, L., Costanzo, G., Manganaro, A., and Zagami, G. (1990). Spatial and vertical distribution of zooplanktonic communities in Terra Nova Bay (Ross Sea). *Nat. Sc. Com. Ant. Ocean. Camp* 1987-88, Data Rep I, 257–398.

Guglielmo, L., Costanzo, G., Zagami, G., Manganaro, A., and Arena, G.(1992).Zooplankton ecology in the southern ocean. *Nat. Sc. Com. Ant. Ocean. Camp* 1989-90, Data Report Part II, 301–468.

Guglielmo, L., Donato, P., Zagami, G., and Granata, A. (2009). Spatiotemporal distribution and abundance of *Euphausia crystallorophias* in Terra Nova Bay (Ross Sea, Antarctica) during austral summer. *Polar Biol.* 32, 347–367. doi: 10.1007/s00300-008-0546-5

Guglielmo, L., Granata, A., and Greco, S. (1997). Distribution and abundance of postlarval and juvenile *Pleuragramma antarcticum* (Pisces, Nototheniidae) off Terra Nova Bay (Ross Sea, Antarctica). *Polar Biol.* 19, 37–51. doi: 10.1007/s003000050214

Gutierrez, M., Swartzman, G., Bertrand, A., and Bertrand, S. (2007). Anchovy (*Engraulis ringens*) and sardine (*Sardinops sagax*) spatial dynamics and aggregation patterns in the Humboldt Current ecosystem, Peru, from 1983-2003. *Fish Oceanogr.* 16, 155–168. doi: 10.1111/j.1365-2419.2006.00422.x

Hecq, J. H., Magazzù, G., Goffart, A., Catalano, G., Vanucci, S., and Guglielmo, L. (1992). "Distribution of Planktonic Components related to structure of water masses in the Ross Sea during the V$^{th}$ Italiantartide Expedition," in *Atti 9° Congresso A.I.O.L. S. Margherita Ligure*, , 20-23 November 1990. 665–678.

Higginbottom, I. R., Pauly, T. J., and Heatley, D. C. (2000). "Virtual echograms for visualization and post-processing of multiple-frequency echosounder data," in *Proceedings of the Fifth European Conference on Underwater Acoustics, ECUA 2000*, Lyon, France, P. Chevret and M.E. Zakharia.

Hopkins, T. L. (1987). Midwater food web in McMurdo Sound, Ross Sea, Antarctica. *Marine Biology.* 96, 93–106.

Holm-Hansen, O., Lorenzen, C. J., Holmes, R. W., and Strickland, J. D. H. (1965). Fluorometric determination of chlorophyll. *ICES J. Mar. Sci.* 30 (1), 3–15. doi: 10.1093/icesjms/30.1.3

Hunt, B. P. V., Pakhomov, E. A., Hosie, G. W., Siegel, V., Ward, P., and Bernard, K. (2008). Pteropods in southern ocean ecosystems. *Prog. Oceanogr.* 78, 193–221. doi: 10.1016/j.pocean.2008.06.001

Ianson, D., Allen, S. E., Mackas, D. L., Trevorrow, M. V., and Benfield, M. C. (2011). Response of *Euphausia pacifica* to small-scale shear in turbulent flow over a sill in a fjord. *J. Plankton Res.* 33, 1679–1695. doi: 10.1093/plankt/fbr074

Innamorati, M., Mori, G., Massi, L., Lazzara, L., and Nuccio, C. (2000). "Phytoplankton biomass related to environmental factors in the Ross Sea," in *Ross Sea Ecology Italian antarctic expeditions, (1987–1995)*. Eds. F. M. Faranda, L. Guglielmo and A. Ianora (Berlin: Springer), 259–273.

Kasyan, V. V. (2023). Recent changes in composition and distribution patterns of summer mesozooplankton off the western Antarctic Peninsula. *Water* 15 (10), 1948. doi: 10.3390/w15101948

Kattnerll, G., and Hagen, W. (1998). Lipid metabolism of the Antarctic euphausiid *Euphausia crystallorophias* and its ecological implications. *Mar. Ecol. -Prog. Ser.* 170, 203–213. doi: 10.3354/meps170203

Kiko, R., Bianchi, D., Grenz, C., Hauss, H., Iversen, M., Kuma, S., et al. (2020). Editorial: zooplankton and nekton: gatekeepers of the biological pump. *Front. Mar. Sci.* 7. doi: 10.3389/fmars.2020.00545

Kim, S. H., Kim, B. K., Lee, B., Son, W., Jo, N., Lee, J., et al. (2022). Distribution of the mesozooplankton community in the Western Ross Sea region marine protected area during late summer bloom. *Front. Mar. Sci.* 9. doi: 10.3389/fmars.2022.860025

Kimura, K. (1929). On the detection of fish groups by an acoustic method. *J. Imp. Fish. Inst. Tokyo* 24, 451–458.

Knutsen, T., Wiebe, P. H., Gjøsæter, H., Ingvaldsen, R. B., and Lien, G. (2017). High latitude epipelagic and mesopelagic scattering layers - a reference for future Arctic ecosystem change. *Front. Mar. Sci.* 4. doi: 10.3389/fmars.2017.00334

Ko, A.-R., Yang, E. J., Kim, M.-S., and Ju, S.-J. (2016). Trophodynamics of euphausiids in the Amundsen Sea during the austral summer by fatty acid and stable isotopic signatures. *Deep-Sea Res. Part II-Top. Stud. Oceanogr.* 123, 78–85. doi: 10.1016/j.dsr2.2015.04.023

La, H. S., Lee, H., Fielding, S., Kang, D., Ha, H. K., Atkinson, A., et al. (2015). High density of ice krill (*Euphausia crystallorophias*) in the Amundsen sea coastal polynya, Antarctica. Deep-Sea Res. *Part I: Oceanographic Res. Papers* 95, 75–84. doi: 10.1016/j.dsr.2014.09.002

La Mesa, M., Catalano, B., Russo, A., Greco, S., Vacchi, M., and Azzali, M. (2010). Influence of environmental conditions of spatial distribution and abundance of early life stages of Antarctic silverfish, *Pleuragramma antarcticum* (Nototheniidae), in the Ross Sea. *Antarct. Sci.* 22, 243–254. doi: 10.1017/S0954102009990721

Le, S., Josse, J., and Husson, F. (2008). FactoMineR: an R package for multivariate analysis. *J. Stat. Software* 25 (1), 1–18. doi: 10.18637/jss.v025.i01

Leonori, I., De Felice, A., Canduci, G., Costantini, I., Biagiotti, I., Giuliani, G., et al. (2017). Krill distribution in relation to environmental parameters in mesoscale structures in the Ross Sea. *J. Mar. Syst.* 166, 159–171. doi: 10.1016/j.jmarsys.2016.11.003

Leonori, I., Tičina, V., Giannoulaki, M., Hattab, T., Iglesias, M., Bonanno, A., et al. (2021). History of hydroacoustic surveys of small pelagic fish species in the European Mediterranean Sea. *Mediterr. Mar. Sci.* 22 (4), 751–768. doi: 10.12681/mms.26001

Lluch-belda, D., Schwartzlose, R. A., Serra, R., Parrish, R., Kawasaki, T., Hedgecock, D., et al. (1992). Sardine and anchovy regime fluctuations of abundance in four regions of the world oceans: a workshop report. *Fish Oceanogr.* 114, 339–347. doi: 10.1111/j.1365-2419.1992.tb00006.x

MacLennan, D., Fernandes, P., and Dalen, J. (2002). A consistent approach to definitions and symbols in fisheries acoustics. *ICES J. Mar. Sci.* 59, 365–369. doi: 10.1006/jmsc.2001.1158

Mangoni, O., Modigh, M., Conversano, F., Carrada, G. C., and Saggiomo, V. (2004). Effects of summer ice coverage on phytoplankton assemblages in the Ross Sea, Antarctica. *Deep-Sea Res. Part I-Oceanogr. Res. Pap.* 51, 1601–1617. doi: 10.1016/j.dsr.2004.07.006

Mangoni, O., Saggiomo, M., Bolinesi, F., Castellano, M., Povero, P., Saggiomo, V., et al. (2019). Phaeocystis Antarctica unusual summer bloom in stratified Antarctic coastal waters (Terra Nova Bay, Ross Sea). *Mar. Environ. Res.* 151, 104733. doi: 10.1016/j.marenvres.2019.05.012

Mangoni, O., Saggiomo, V., Bolinesi, F., Escalera, L., and Saggiomo, M. (2018). A review of past and present summer primary production processes in the Ross Sea in relation to changing ecosystems. *Ecol. Quest.* 29, 75–85. doi: 10.12775/EQ.2018.024

Mangoni, O., Saggiomo, V., Bolinesi, F., Margiotta, F., Budillon, G., Cotroneo, Y., et al. (2017). Phytoplankton blooms during austral summer in the Ross Sea, Antarctica: Driving factors and trophic implications. *PloS One* 12 (4), e0176033. doi: 10.1371/journal.pone.0176033

Manno, C., Tirelli, V., Accornero, A., and Fonda Umani, S. (2010). Importance of the contribution of *Limacina helicina* faecal pellets to the carbon pump in Terra Nova Bay (Antarctica). *J. Plankton Res.* 32 (2), 145–152. doi: 10.1093/plankt/fbp108

Minutoli, R., Bergamasco, A., Guglielmo, L., Swadling, K. M., Bergamasco, A., Veneziano, F., et al. (2023). Species diversity and spatial distribution of pelagic amphipods in Terra Nova Bay (Ross Sea, Southern Ocean). *Polar Biol.* 46, 821–835. doi: 10.1007/s00300-023-03166-0

Minutoli, R., Brugnano, C., Granata, A., Zagami, G., and Guglielmo, L. (2017). Zooplankton electron transport system activity and biomass in the western Ross Sea (Antarctica) during austral summer 2014. *Polar Biol.* 40, 1197–1209. doi: 10.1007/s00300-016-2043-6

Misic, C., Covazzi Harriague, A., Mangoni, O., Cotroneo, Y., Aulicino, G., and Castagno, P. (2017). Different responses of the trophic features of particulate organic matter to summer constraints in the Ross Sea. *J. Mar. Syst.* 166, 132–143. doi: 10.1016/j.jmarsys.2016.06.012

Muradian, M. L., Branch, T. A., Moffitt, S. D., and Hulson, P. J. F. (2017). Bayesian stock assessment of Pacific herring in Prince William sound Alaska. *PloS One* 12 (2), e0172153. doi: 10.1371/journal.pone.0172153

Murase, H., Nagashima, H., Yonezaki, S., Matsukura, R., and Kitakado, T. (2009). Application of a generalized additive model (GAM) to reveal relationships between environmental factors and distributions of pelagic fish and krill: a case study in Sendai Bay, Japan. *ICES J. Mar. Sci.* 66, 1417–1424. doi: 10.1093/icesjms/fsp105

Naganobu, M., Murase, H., Nishiwaki, S., Yasuma, H., Matsukura, R., Takao, Y., et al. (2010). Structure of the marine ecosystem of the Ross Sea, Antarctica-overview and synthesis of the results of a Japanese multidisciplinary study by Kaiyo-Maru and JARPA. *Bull. Jpn. Soc Fish. Oceanogr.* 74, 1–12.

Nuccio, C., Innamorati, M., Lazzara, L., Mori, G., and Massi, L. (2000). "Spatial and temporal distribution of phytoplankton assemblage in the Ross Sea," in *Ross Sea Ecology Italian antarctic expeditions, (1987–1995)*. Eds. F. M. Faranda, L. Guglielmo and A. Ianora (Berlin: Springer), 231–246.

Pagès, F. (1997). The gelatinous zooplankton in the pelagic system of the Southern Ocean: a review. *Annales l'Institute Oceanographique* 73, 139–158.

Pakhomov, E. A., Perissinotto, R., and Froneman, P. W. (1998). Abundance and trophodynamics of *Euphausia crystallorophias* in the shelf region of the Lazarev Sea during austral spring and summer. *J. Mar. Syst.* 17, 313–324. doi: 10.1016/S0924-7963(98)00046-3

Pane, L., Feletti, M., Francomacaro, B., and Mariottini, G. L. (2004). Summer coastal zooplankton biomass and copepod community structure near the Italian Terra Nova base (Terra Nova Bay, Ross Sea, Antarctica). *J. Plankton Res.* 26, 1479–1488. doi: 10.1093/plankt/fbh135

Phan-Tan, L., Nguyen-Ngoc, L., Smith, W. O., and Doan-Nhu, H. (2018). A new dinoflagellate species, *Protoperidinium smithii* H. Doan-Nhu, L. Phan-Tan et L. Nguyen-Ngoc sp. nov., and an emended description of *Protoperidinium defectum* (Balech 1965) Balech 1974 from the Ross Sea, Antarctica. *Polar Biol.* 41, 983–992. doi: 10.1007/s00300-018-2262-0

Pinkerton, M. H., and Bradford-Grieve, J. M. (2014). Characterizing foodweb structure to identify potential ecosystem effects of fishing in the Ross Sea, Antarctica. *ICES J. Mar. Sci.* 71, 1542–1553. doi: 10.1093/icesjms/fst230

R Core Team. (2023). *R: A Language and Environment for Statistical Computing*_ (Vienna, Austria: R Foundation for Statistical Computing). Available at: https://www.R-project.org/.

Richardson, A., Bakun, A., Hays, G., and Gibbons, M. (2009). The jellyfish joyride: causes, consequences and management responses to a more gelatinous future. *Trends Ecol. Evol.* 24, 312–322. doi: 10.1016/j.tree.2009.01.010

Saggiomo, M., Escalera, L., Bolinesi, F., Rivaro, P., Saggiomo, V., and Mangoni, O. (2021). Diatom diversity during two austral summers in the Ross Sea (Antarctica). *Mar. Micropaleontol.* 165, 101993. doi: 10.1016/j.marmicro.2021.101993

Saggiomo, V., Carrada, G. C., Mangoni, O., Marino, D., and Ribera d'Alcalà, M. (2000). "Physiological and ecological aspects of primary production in the Ross Sea," in *Ross Sea Ecology - Italian Antarctic Expeditions, (1987–1995)*. Eds. F. M. Faranda, L. Guglielmo and A. Ianora (Berlin: Springer-Verlag), 247–258.

Saggiomo, V., Catalano, G., Mangoni, O., Budillon, G., and Carrada, G. C. (2002). Primary production processes in ice-free waters of the Ross Sea (Antarctica) during the austral summer 1996. *Deep-Sea Res. Part II-Top. Stud. Oceanogr.* 49, 1787–1801. doi: 10.1016/S0967-0645(02)00012-7

Saino, N., and Guglielmo, L. (2000). "ROSSMIZE expedition: distribution and biomass of birds and mammals in the western ross sea," in *Ross Sea Ecology Italian Antarctic Expeditions, (1987–1995)*. Eds. F. M. Faranda, L. Guglielmo and A. Ianora (Berlin: Springer- Verlag), 469–478.

Sala, A., Azzali, M., and Russo, A. (2002). Krill of the Ross Sea: distribution, abundance and demography of *Euphausia superba* and *Euphausia crystallorophias* during the Italian Antarctic Expedition (January–February 2000). *Sci. Mar.* 66, 123–133. doi: 10.3989/scimar.2002.66n2123

Schaub, J., Hunt, B. V., Pakhomov, E., Holmes, K., Lu, Y., and Quayle, L. (2018). Using unmanned aerial vehicles (UAVs) to measure jellyfish aggregations. *Mar. Ecol.-Prog. Ser.* 591, 29–36. doi: 10.3354/meps12414

Schismenou, E., Tsoukali, S., Giannoulaki, M., and Somarakis, S. (2017). Modelling small pelagic fish potential spawning habitats: eggs vs spawners and in *situ* vs satellite data. *Hydrobiologia* 788, 17–32. doi: 10.1007/s10750-016-2983-4

SCOR Working Group (1988). *The acquisition, calibration and analysis of CTD data. UNESCO Technical Papers in Marine Science*. 54. Available at: https://www.jodc.go.jp/info/ioc_doc/UNESCO_tech/096989eb.pdf.

Sedwick, P. N., Marsay, C. M., Sohst, B. M., Aguilar-Islas, A. M., Lohan, M. C., Long, M. C., et al. (2011). Early season depletion of dissolved iron in the Ross Sea polynya: implications for iron dynamics on the Antarctic continental shelf. *J. Geophys. Res.* 116, C12019. doi: 10.1029/2010JC006553

Siegelman-Charbit, L., and Planque, B. (2016). Abundant mesopelagic fauna at oceanic high latitudes. *Mar. Ecol. .-Prog. Ser.* 546, 277–282. doi: 10.3354/meps11661

Smith, W. O. Jr., Ainley, D. G., Arrigo, K. R., and Dinniman, M. S. (2014). The oceanography and ecology of the Ross Sea. *Annu. Rev. Mar. Sci.* 6, 469–487. doi: 10.1146/annurev-marine-010213-135114

Smith, W. O. Jr., Ainley, D. G., and Cattaneo-Vietti, R. (2007). Trophic interactions within the Ross Sea continental shelf ecosystem. *Philos. Trans. R. Soc Lond. Ser. B-Biol. Sci.* 362, 95–111. doi: 10.1098/rstb.2006.1956

Smith, W. O. Jr., and Asper, V. (2001). The influence of phytoplankton assemblage composition on biogeochemical characteristics and cycles in the southern Ross Sea, Antarctica. *Deep Sea Res. Part I-Oceanogr. Res. Pap.* 48, 137–161. doi: 10.1016/S0967-0637(00)00045-5

Smith, W. O. Jr., Delizo, L. M., Herbolsheimer, C., and Spencer, E. (2017). Distribution and abundance of mesozooplankton in the Ross Sea, Antarctica. *Polar Biol.* 40, 2351–2361. doi: 10.1007/s00300-017-2149-5

Stevens, C. J., Pakhamov, E. A., Robinson, K. V., and Hall, J. A. (2015). Mesozooplankton biomass, abundance and community composition in the Ross Sea and the Pacific sector of the Southern Ocean. *Polar Biol.* 38, 275–286. doi: 10.1007/s00300-014-1583-x

Sund, O. (1935). Echo sounding in fisheries research. *Nature* 135, 953. doi: 10.1038/135953a0

Sweeney, C., Smith, W. O. Jr., Hales, B., Bidigare, R. R., Carlson, C. A., Codispoti, L. A., et al. (2000). Nutrient and carbon removal ratios and fluxes in the Ross Sea, Antarctica. *Deep-Sea Res. Part II-Top. Stud. Oceanogr.* 47, 3395–3421. doi: 10.1016/S0967-0645(00)00073-4

Tournier, M., Goulet, P., Johnson, M., Nerini, D., Fonvieille, N., and Guinet, C. (2021). A novel animal-borne miniature echosounder to observe the distribution and migration patterns of intermediate trophic levels in the Southern Ocean. *J. Mar. Syst.* 223, 103608. doi: 10.1016/j.jmarsys.2021.103608

Verhaegen, G., Cimoli, E., and Lindsay, D. (2021). Life beneath the ice: jellyfish and ctenophores from the Ross Sea, Antarctica, with an image-based training set for machine learning. *Biodiver. Data J.* 9, e69374. doi: 10.3897/BDJ.9.e69374

Wood, S. N. (2001). mgcv: GAMs and generalized ridge regression for R. *R News* 1 (2), 20–25.

Wood, S. N. (2011). Fast stable restricted maximum likelihood and marginal likelihood estimation of semiparametric generalized linear models. *J. R. Stat. Soc Ser. B-Stat. Methodol.* 73 (1), 3–36. doi: 10.1111/j.1467-9868.2010.00749.x

Yang, G., Li, C., and Wang, Y. (2016). Fatty acid composition of *Euphausia superba*, *Thysanoessa macrura* and *Euphausia crystallorophias* collected from Prydz Bay, Antarctica. *J. Ocean Univ. China* 15, 297–302. doi: 10.1007/s11802-016-2791-5

Zgozi, S., Barra, M., Basilone, G., Hamza, M., Assughayer, M., Nfate, A., et al. (2018). Habitat suitability modelling for a key small pelagic fish species (*Sardinella aurita*) in the central Mediterranean sea. *Hydrobiologia* 821, 83–98. doi: 10.1007/s10750-017-3265-5

Zunini Sertorio, T., Licandro, P., Ossola, C., and Artegiani, A. (2000). "Copepod communities in the pacific sector of the southern ocean in early summer," in *Ross Sea Ecology* (Berlin/Heidelberg, Germany: Springer), 291–307.

Zunini Sertorio, T., Licandro, P., Ricci, F., and Giallain, M. (1992). Antarctica, N.S.C. for A study on ross sea copepods. *Nat. Sc. Com. Ant. Ocean. Camp.* 90, 217–246. doi: 10.1007/978-3-642-59607-0_23

Zunini Sertorio, T., Salemi Picone, P., Bernat, P., Cattini, E., and Ossola, C. (1990). Copepods collected in sixteen stations during the Italian Antarctic Expedition 1987-1988. *Nat. Sc. Com. Ant. Ocean. Camp.* 1988, 67–125.

frontiers | Frontiers in Marine Science

TYPE Original Research
PUBLISHED 22 February 2024
DOI 10.3389/fmars.2024.1339413



OPEN ACCESS

EDITED BY
Letterio Guglielmo,
Anton Dohrn Zoological Station Naples, Italy

REVIEWED BY
Ajit Kumar Mohanty,
Indira Gandhi Centre for Atomic Research (IGCAR), India
Ruifeng Zhang,
Shanghai Jiao Tong University, China

*CORRESPONDENCE
Zhibo Lu
luzhibo@tongji.edu.cn
Jianfeng He
hejianfeng@pric.org.cn

RECEIVED 11 December 2023
ACCEPTED 07 February 2024
PUBLISHED 22 February 2024

CITATION
Chen Z, Zheng H, Gao Y, Lan M, Luo G, Lu Z and He J (2024) Spatial distribution and diversity of the heterotrophic flagellates in the Cosmonaut Sea, Antarctic.
*Front. Mar. Sci.* 11:1339413.
doi: 10.3389/fmars.2024.1339413



# Spatial distribution and diversity of the heterotrophic flagellates in the Cosmonaut Sea, Antarctic

Zhiyi Chen[1,2], Hongyuan Zheng[2,3], Yuan Gao[2], Musheng Lan[2], Guangfu Luo[2], Zhibo Lu[4*] and Jianfeng He[2*]

[1]College of Civil Engineering and Architecture, Zhejiang University of Water Resources and Electric Power, Zhejiang, Hangzhou, China, [2]Ministry of Natural Resources Key Laboratory for Polar Science, Polar Research Institute of China, Shanghai, China, [3]Ocean Institute, Northwestern Polytechnical University, Jiangsu, Taicang, China, [4]College of Environmental Science and Engineering, Tongji University, Shanghai, China

As predators of bacteria and viruses and as food sources for microzooplankton, heterotrophic flagellates (HFs) play an important role in the marine micro-food web. Based on the global climate change's impact on marine ecosystems, particularly sea ice melting, we analyzed the community composition and diversity of heterotrophic flagellates, focusing on the Antarctic Cosmonaut Sea. During the 36th China Antarctic research expedition (2019-2020), we collected seawater samples, subsequently analyzing HFs through IlluminaMiSeq2000 sequencing to assess community composition and diversity. Notable variations in HFs abundance were observed between the western and eastern sectors of the Cosmonaut Sea, with a distinct concentration at a 100-meter water depth. Different zones exhibited diverse indicators and dominants taxa influenced by local ocean currents. Both the northern Antarctic Peninsula and the western Cosmonaut Sea, where the Weddell Eddy and Antarctic Land Slope Current intersect, showcased marine stramenopiles as dominant HFs species. Our findings offer insights into dominant taxa, spatial distribution patterns among heterotrophic flagellates, correlations between taxa distribution and environmental factors, and the exploration of potential indicator taxa.

KEYWORDS

**heterotrophic flagellates, biodiversity, Cosmonaut Sea, Antarctic, climate change community ecology**

## 1 Introduction

Global warming and sea ice melt alter polar habitats and marine protozoan communities. It is predicted that 79% of endemic species in Antarctic waters will face a reduction in suitable temperature habitat in this century because of global climate change (Griffiths et al., 2017), including Heterotrophic flagellates (HFs). HFs are widely distributed in the global oceans, occurring in all the world's major seas, including the Arctic Ocean and

the Southern Ocean. They have different taxonomic compositions and characteristics in different geographic regions (Sohrin et al., 2010). They are central in marine food webs, controlling phytoplankton biomass and consuming most bacterial biomass (del Campo and Ruiz-Trillo, 2013). Moreover, their feeding rate directly impacts the ecosystem's material cycling and nutrient regeneration, which can significantly affect the plankton community structure (Seenivasan et al., 2013).

Although all levels of the marine microbial food web may be affected by climate change (Fortier et al., 2006; Falk-Petersen et al., 2007; Laidre et al., 2008), microphytoplankton are particularly sensitive to environmental change (Li et al., 2009). The biomass of HFs is concentrated in this particle size range (Rodriguez-Martinez et al., 2013). Heterotrophic flagellates can control the phytoplankton biomass (Verity et al., 2002) and target bacteria (Christaki et al., 2021), viruses, and colloids for feeding (Arndt et al., 2000; Sherr and Sherr, 2002). However, the complexity and importance of HFs taxa have not received sufficient attention in the literature (Monier et al., 2013; Lovejoy, 2014). Phytoplankton are important food sources for some HF taxa. The miniaturization of phytoplankton has, in some cases, been found to have a more significant impact on microscopic unicellular predators (like flagellates) than other large predators in the micro food web (Li et al., 2009; Worden et al., 2015). This implies that the miniaturization shift of phytoplankton taxa could directly affect the community structure and biodiversity of HFs in the context of climate change. Numerous studies have reported that the global distribution of HFs is environmentally driven and is not subject to any dispersal constraints (neither distance nor isolation) (Azovsky et al., 2020), with different community structures in different geographic regions (Sohrin et al., 2010). Although there is high regional diversity, the low global diversity and regional endemism need further investigation.

There has been limited research on the spatial distribution and diversity of HFs in polar seas and ice zones. Nevertheless, in recent years, the Cosmonaut Sea has received much attention. It is in the western part of the Antarctic Entebbe Land (Hunt et al., 2007), with a longitude range of 30°E to 60°E. It represents an area of significant variability in the annual sea ice extent (Comiso and Gordon, 1987). There are relatively substantial regional differences in the Antarctic Sea variability between sectors under the influence of climate change (Convey and Peck, 2019), with regional ablation and sea ice in the different seas. Large fluctuations in the sea ice distribution in the Cosmonaut Sea are also present in winter and summer. As a region in the Southern Ocean with less research information, the current state and future ecosystem trends in the Cosmonaut Sea also deserve further investigation. Previous studies have not focused on HFs or microscopic protists that exist as predators in micro food webs, so we attempted to explore this.

In this study, we surveyed the abundance and biodiversity of HFs taxa in the Antarctic Cosmonaut Sea using samples from China's 36$^{th}$ Antarctic Scientific Expedition. After sequencing the community diversity of the microplankton using Illumina, ten taxa were selected for analysis. This study will address the dominant taxa and differences in the spatial distribution of heterotrophic flagellates in the Antarctic Cosmonaut Sea seawater. In contrast, the correlation between taxa distribution and environmental factors will be explored, and the possibility of some taxa as indicators will be further explored. The differences in the distribution of the dominant HFs taxa in the sea were also investigated to provide a basis for further exploration of the possible trends in the community structure of the HFs under the influence of climate change.

# 2 Materials and methods

## 2.1 Sample collection

During China's 36$^{th}$ Antarctic Scientific Expedition (CHINARE), from December 6, 2019, to January 6, 2020, there were a total of 56 stations in nine sections of the Cosmonaut Sea (62–70°S, 35–78°E; Figure 1), and 24 Niskin bottles Sea-Bird Electronics 911 plus CTD (Bellevue, USA) was used to collect the seawater samples. Each station collected the samples at different water depths, from the surface to the seabed, and simultaneously observed various physical and chemical parameters, such as the seawater temperature, salinity, and nutrient salts. Samples of the biological community composition and biodiversity were also obtained.

The biodiversity samples were taken back to the laboratory to filter out the microbial film samples using 0.2 μm polycarbonate membranes (all membranes are from Whatman, UK, 47 mm in diameter), stored at -80 °C, and transported to the laboratory to determine the microbial diversity. For the property analysis, after the second filtration, the water sample was retained for nutrient analysis. During the sampling process, a total of 11 variables were measured to explain the variation in the abundance of the HFs, including the water depth, temperature, salinity, total Chlorophyll a (Chl *a*), dissolved oxygen (DO), ammonium, phosphate, silicate, nitrate, nitrite, and total nitrogen. The DO, ammonium, phosphate, silicate, nitrate, nitrite, and total nitrogen were analyzed using a four-channel continuous flow Technicon AA3 Auto-Analyzer (Luebbe, 1997). The Chl *a* was measured with a 10AU field fluorometer (Turner Designs, Sunnyvale, CA, USA) after filtering part of the water samples with a GF/F glass fiber filter membrane. The abundance of the bacteria and eukaryotic plankton was determined by flow cytometry using a BD FACSCalibur™ flow cytometer for detection.

## 2.2 PCR and Illumina MiSeq sequencing

The seawater samples from the Cosmonaut Sea were sequenced based on the eukaryotic plankton diversity lineage using the Illumina MiSeq ultra-high-throughput sequencing platform. The total genomic DNA samples were extracted using the OMEGA Soil DNA Kit (M5635-02; Omega Bio-Tek, Norcross, GA, USA). The quantity and quality of the extracted DNA were measured using a NanoDrop NC2000 spectrophotometer (Thermo Fisher Scientific, Waltham, MA, USA) and agarose gel electrophoresis, respectively. Then, polymerase chain reaction amplification of the eukaryotic *18S*

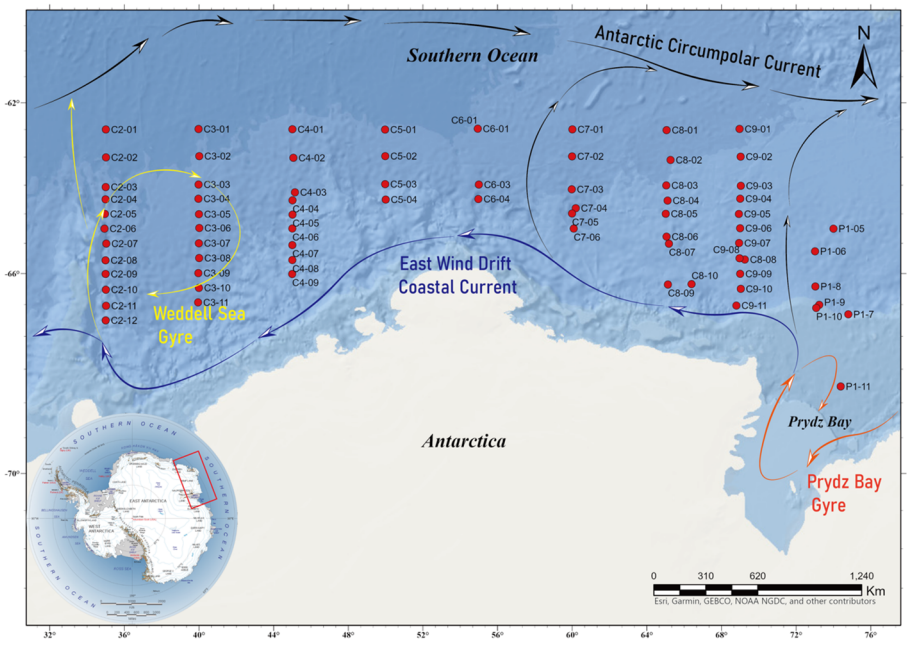


FIGURE 1
Location of the sampling stations and currents.

ribosomal RNA (rRNA) gene V3–V4 region was performed using the forward primer 547F (5′-CCAGCASCYGCGGTAATTCC-3′) and the reverse primer V4R (5′-ACTTTCGTTCTTGATYRA-3′). After the quantification step, the amplicons were pooled in equal amounts, and pair-end 2 × 250 bp sequencing was performed using the Illumina MiSeq platform with the MiSeq Reagent Kit v3 at Shanghai Personal Biotechnology Co. Ltd (Shanghai, China). The detailed conditions and laboratory analysis are specified in a previous study (Chen et al., 2021). The classify-sklearn naïve Bayes taxonomy classification probe (Bokulich et al., 2018) was used to classify and assign the non-single amplicon sequence variants (ASVs) and label the original data according to the UNITE Release 8.0 (fungal) database (Koljalg et al., 2013). Specific taxonomic groups were screened out, with 10 main target analysis taxa.

## 2.3 Diversity and community structure analysis

The samples were subjected to ultra-high throughput sequencing and database matching for classification and name annotation, the HFs taxa were screened based on existing studies, and the screened data were used for biodiversity calculations. The samples from nine sections of the Cosmonaut Sea with a total of 56 stations were divided into zones according to the reported current distribution. Sections C2 and C3 were divided into zone A, section C4 into zone B, sections C5, C6, and C7 into zone C, section C8 into zone D, and sections C9 and P1 and station C8–08 into zone E. The analysis of the samples was conducted according to these five zones (Figure 1).

An alpha biodiversity analysis was performed using R (v4.1.3) (http://www.R-project.org/), and alpha diversity indices based on the ASV levels were calculated, including the Chao1 richness estimates, observed species, Shannon diversity index, Simpson index, and goods coverage (Table 1). The results of a Principal Coordinate Analysis (PCoA) of the HFs communities were generated using the vegan package and ggplot2 package. Then, ArcGIS pro 3.0 (Zheng et al., 2023) was used to generate the sampling station maps and bubble sector maps of the HFs community distribution at different water depths. The Ocean Data View software (Schlitzer, 2021) was used to generate the overall abundance and α-diversity index of the HFs for different water depths, the difference maps of each environmental factor in the different sections, and the bubble maps of the difference in abundance for each clade of MASTs at different water depths.

To explore the correlation between the environmental factors and HFs taxa, a redundancy analysis (RDA) was performed using CANOCO 5.2 software (Microcomputer Power, Ithaca, USA) to investigate the relationship between the differences in the HFs community structure and environmental variables across the samples and assess community variation (based on the relative abundance of all the operational taxonomic units/ASVs) and the environmental variables (temperature, salinity, nutrients, Chl *a*, eukaryotic plankton, and bacteria) at the sampling sites. A linear regression analysis was used to determine the relationship between the two variables. Pearson and Spearman correlations between the HFs taxa and environmental factors were visualized using the psych package in R (v4.1.3) and vegan. An indicator species analysis (Ind Val) was performed using the indicspecies package in the R (v4.1.3) software to identify indicator species in each study area (Dufrene and Legendre, 1997).

TABLE 1 Comparison of the main dominant and indicator taxa differences in the heterotrophic flagellates in the Cosmonaut Sea, Antarctic.

| Zone | Indicator taxa | Dominant taxa |
|---|---|---|
| A | Cryomonadida | Cryomonadida |
| | MAST-9 | MAST-1C |
| | | MAST-9 |
| B | Cryomonadida | Cryomonadida |
| | | MAST-1C |
| | | MAST-9 |
| C | Cryomonadida | Cryomonadida |
| | MASTs | MASTs |
| | MAST-3 | MAST-9 |
| D | MASTs | MASTs |
| | MAST-1C | Opalozoa |
| | MAST-9 | MAST-1C |
| E | MASTs | MASTs |
| | MAST-1C | MAST-3 |
| | MAST-7 | MAST-1C |

# 3 Results

## 3.1 Geographical distribution characteristics

Data on the temperature, salinity, Chl *a*, and various nutrients were obtained during the sampling process for the samples at different water depths. A total of 11 variables were examined to explain the differences in the HFs community structure and abundance. The longitudinal differences in the environmental factors were plotted for each section (Supplementary Figure S1).

The seawater temperature in the Cosmonaut Sea decreased and then increased with depth in the range of 0 to 200 m. At the same time, the water temperature below 200 m was relatively constant. The seawater salinity appeared to rise significantly with increasing depth, and the surface ocean salinity was lower when compared with the deeper water layer. The horizontal distribution trends of the DO and Chl *a* were similar, with relatively higher concentrations of DO and Chl *a* at the stations with higher latitudes. The concentration of DO was relatively high at the surface ocean, and at some stations, the DO peaked at a water depth of 25 m and gradually decreased with increasing water depth. However, there was a slight increase in DO concentration in the deep seawater samples at more than 300 m depth. The Chl *a* was basically concentrated within the upper 100 m, and the peak was concentrated at a depth of 25 m to 75 m. Comparatively, the Chl *a* concentration was higher in the mid-sea of the Cosmonaut Sea than in the other regions.

Most of the stations showed a trend of an increasing phosphate concentration with increasing water depth, and some of the stations reached a peak at around 200 m in depth. The silicate and phosphate concentrations were similar, with a clear trend of increasing concentration with increasing water depth, and the peak occurred in the deep layer below 1500 m. Nitrate concentrations were notably higher than those of nitrite and ammonium salts. At the majority of stations, nitrate levels exhibited a slight increase within the 100–200 m depth range, followed by a decrease as water depth increased. The highest concentrations of nitrite and ammonium were primarily found in the 0–100 m range. Specifically, the nitrite peak occurred at depths between 0–50 m, while the ammonium peak was more concentrated in the 50–100 m range. Both nitrite and ammonium demonstrated a gradual decline and eventually leveled off.

## 3.2 Alpha-biodiversity analysis of heterotrophic flagellates

A total of 642 species were screened from all the samples, with 95.6% of the samples with a good coverage of above 90% and 87.7% of the samples with a coverage above 97%. In terms of the overall abundance at each station (Figure 2), the abundance in areas A and B was significantly higher than that in the other seas, while the abundance of the HFs showed a trend of increasing and then decreasing from the surface ocean with the increase in the water depth. The HFs were mainly distributed within the top 100 m, and the peak abundance at most stations appeared at 25-75 m in depth. With the increase in the water depth, the abundance of the HFs in the near-bottom samples in zone E showed a significant increase. The high values of Shannon's index and Simpson's diversity index were concentrated in zone E. Most occurred in the water depth range of 200–2000 m, and the number of species observed in this area was also more than that in the other areas. Furthermore, the biodiversity indices in zones A and B were relatively low. However, the diversity of the HFs in the near-land stations in zone A was similar to that in zone E. Meanwhile, most of the high values of the ACE index and Chao1 index were found at stations in the P1 section, which is relatively close to the Antarctic continental region. This indicates that the HFs diversity and species distribution uniformity were higher in the eastern Cosmonaut Sea than in the western sea. The diversity of the HFs was higher in the near-land waters than in the distant waters. Overall, the overall abundance of the HFs was higher in the western Cosmonaut Sea, in the shallow layer starting from the surface ocean to 100 m in depth, than in the eastern sea, and they were rarer in the mid-sea.

The overall abundance, community structure composition, and dominant taxa of the HFs differed with depth. A principal coordinate analysis of all the samples (Figure 3) showed that the HFs community confidence ellipses at water depths of 0 to 50 m deviated significantly ($p < 0.05$) from the depths of 75 m and 100 m. The community confidence ellipses of the samples at water depths greater than 100 m had a large overlap. This indicates a significant similarity between the HFs communities in the water column at depths of 0–50 m, with depths of 75–100 m being the overlap region, and a large difference in the samples at depths greater than 100 m. There was also a significant similarity between the HFs communities at depths greater than 100 m.

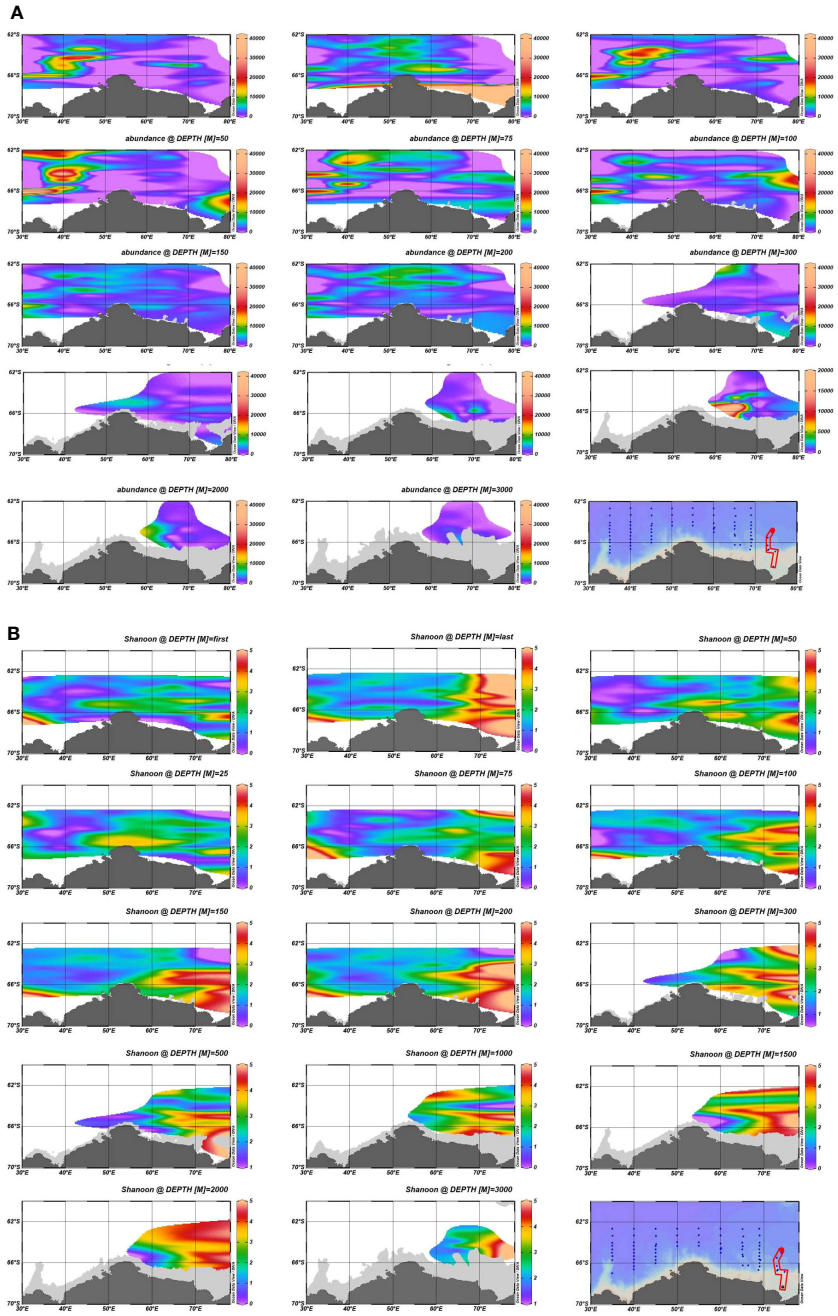


FIGURE 2
Comparison of the abundance and diversity indices of the ASVs based on the *18S* ribosomal RNA (rRNA) gene library at different water depths: **(A)** difference plots of the overall abundance at different water depths; **(B)** difference plots of the α diversity-Shannon index at the different water depths.

## 3.3 Taxonomy composition of heterotrophic flagellates

A total of 10 HFs taxa were screened in this study. The more common taxa, such as Cryomonadida, MASTs, and Picozoa, were distributed in all the sections and depths (Figure 4). Cryomonadida, Marine stramenopiles (MASTs), and Opalozoa were relatively more abundant overall, and Cryomonadida was detected in all the samples. The abundance of Cryonmonadida and the MASTs tended to decrease with increasing depth, while a slight increase was observed in the near-shelf samples. However, the abundance of Opalozoa was relatively low in the shallow layer (25–100 m). It was not even detected at some of the stations. At the same time, it was abundantly distributed in the deep layer and near the seafloor, with an overall trend of increasing with depth.

The other relatively common HFs taxa were Picozoa, choanoflagellates, *Apusomonadidae*, and Telonemia, which were relatively less abundant. Except for *Apusomonadidae*, which was detected only at some stations and depths, the other three HFs were distributed in all the sections and depths. Picozoa was observed in

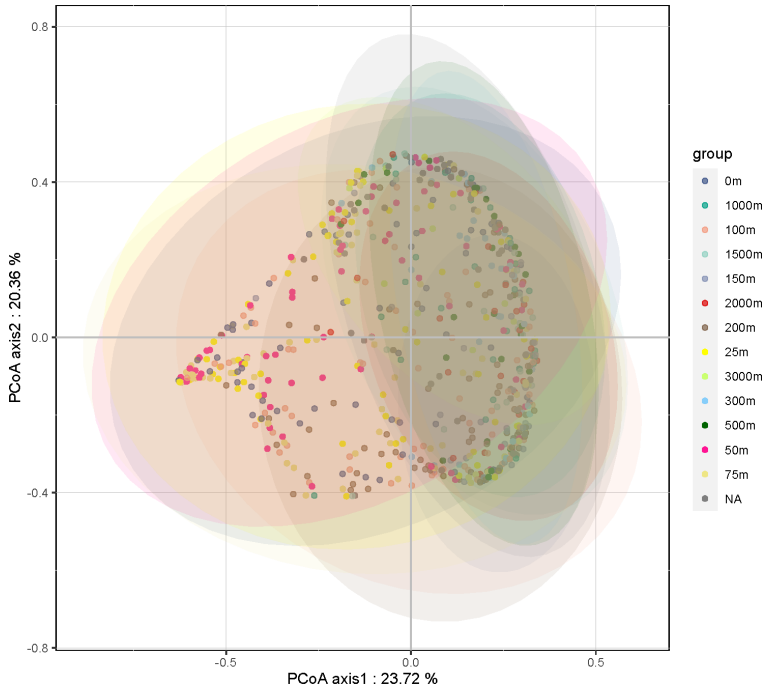


FIGURE 3
Results of the Principal Coordinate Analysis (PCoA) analysis of the heterotrophic flagellate communities in the samples at different water depths.

78.5% of the samples, mainly in the east-west area, and concentrated in the water layer between 75 m and 300 m. The choanoflagellates were observed in 71.6% of the samples, mainly in the east-west area of the Cosmonaut Sea, with peaks at 100 m and 150 m. Then, Telonemia was mainly found on the east side of the Cosmonaut Sea, with a relatively high abundance in the shallow layer. Telonemia was observed in 57.0% of the samples.

*Apusomonadidae* was concentrated in the western part of the Cosmonaut Sea, mainly at 150 to 200 m in depth and near the seafloor. The overall abundance was relatively low for *Palpitomonas*, Ancryomonadida, and Jakobida. Additionally, *Palpitomonas* was mainly distributed in the eastern Cosmonaut Sea, mostly in the surface ocean samples. Ancryomonadida was concentrated at the stations on the western side of the Cosmonaut Sea near the Antarctic continental region. The occurrence in the samples from 0 to 200 m in depth was rare, except for a small number of detections in the individual seafloor samples, and they were not found in all the samples over 300 m. Jakobida was found in the samples at all water depths, mainly in the near Antarctic continental waters.

The dominant taxon on the west and mid-sea was Cryomonadida, with some stations being dominated by MASTs. On the east side, the dominant taxon was MASTs. At depths greater than 100 m, Cryomonadida decreased substantially, and from 200 m in depth, the dominant position of Cryomonadida was occupied by MASTs and Opalozoa. Beyond 200 m, deep-sea samples were only collected in sections C8, C9, and P1 and station C7-06 on the eastern side, and the results showed that MASTs still dominated in the deep-sea layer. While Opalozoa also occurred in a high proportion at several stations, and the proportion of Picozoa and choanoflagellates also increased.

To compare the differences in the distribution of the HFs in the study area and whether each taxon could serve as an indicator species for the area, the indicator value (Ind Val) was used to determine the indicator taxa for each sea area. Based on the indicator value (Table 1), the indicator taxon/taxa in zone A were Cryomonadida and MAST-9, in zone B was Cryomonadida, in zone C were Cryomonadida, MASTs, and MAST-3, in zone D were MASTs, MAST-1C, and MAST-9, and in zone E were MASTs, MAST-1C, MAST-7, MAST-8, MAST-3, MAST-2, *Palpitomonas*, Telonema, and Cryomonadida.

## 3.4 Taxonomy composition of marine stramenopiles

Marine stramenopiles, as an important taxon of HFs, were targeted using 13 clades in this study. MAST-1, a common clade of MASTs, was detected in most samples and accounted for more than 50% of the total MASTs in nearly half of the samples. The distribution of MAST-1 in the global waters also varied greatly, with a significantly higher density in the Antarctic Peninsula than that in the other global oceans (Massana et al., 2006; Massana, 2011). MAST-1C had a relatively high overall abundance, accounting for more than 50% of that of MAST-1 in 72% of the samples. The abundance of MAST-1C was higher in the east and west areas of the Cosmonaut Sea than that in the mid-sea, and its distribution directly affected the overall distribution of the MASTs

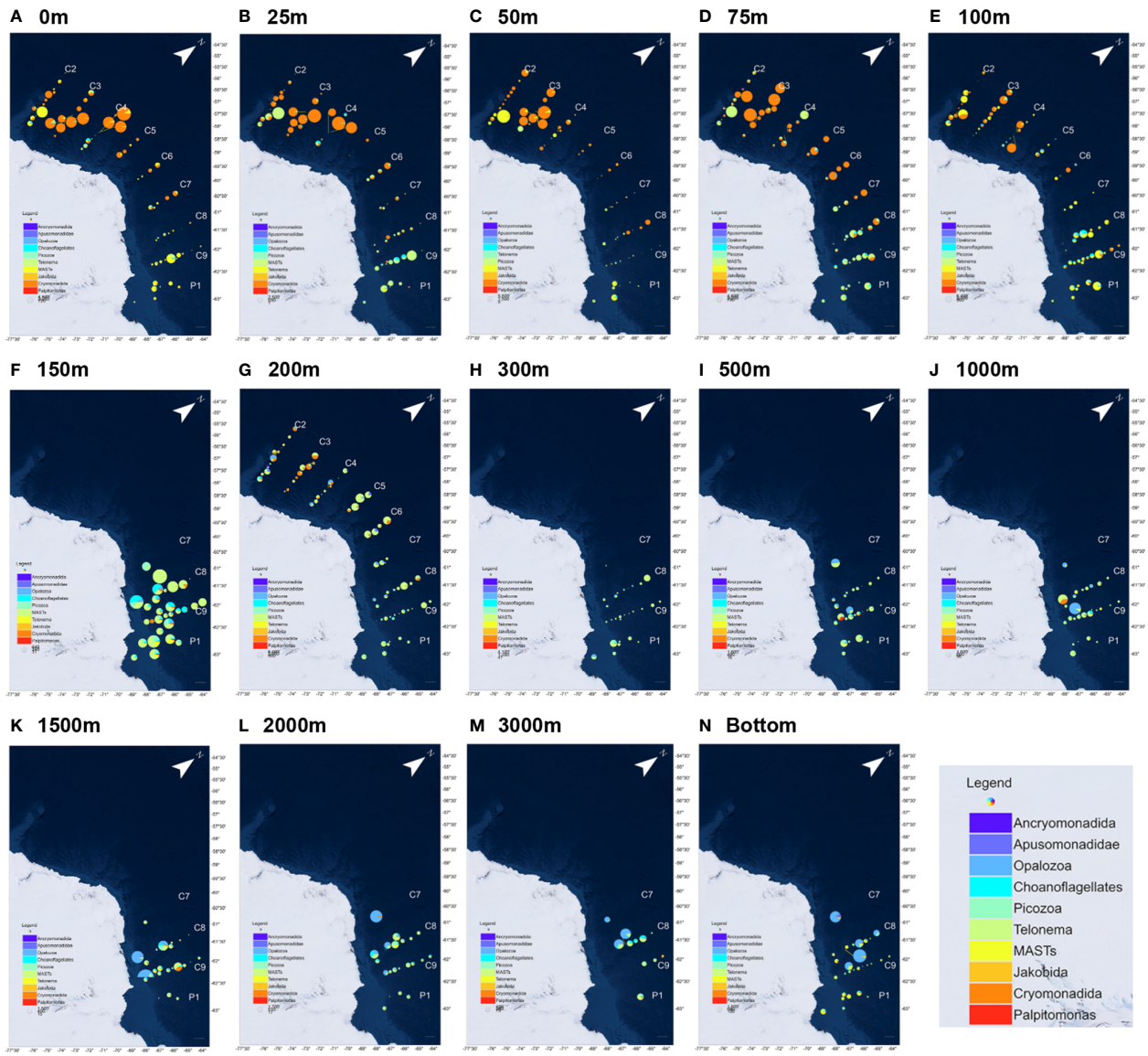


FIGURE 4
Community structure of the heterotrophic flagellates at different water depths in the nine sections of the Antarctic Astronaut Sea. The bubble size represents the relative abundance of the heterotrophic flagellates at the station, and the sector area represents the proportion of the taxon in the heterotrophic flagellate community at the station. as represents the maximum water depth (bottom) of the sample that was collected at the station. **(A–N)** corresponds to the HFs distribution at different seawater depths.

(Figure 5). Moreover, the distribution of MAST-1A was concentrated in the east side of the Cosmonaut Sea, and high values were also observed at individual stations in the west side of the near-continental sea, being concentrated in the samples from 0 to 100 m in depth. The abundance of MAST-1A decreased in the samples at a water depth of over 100 m, but it was also distributed in large numbers in the near-shelf samples. MAST-1B was concentrated in the water layer from 100 m to 300 m, with only a few or no detections in the samples from the other depths. Then, MAST-1D was the least abundant clade of MAST-1 and was mainly distributed in deeper waters below 1000 m.

MAST-3 and MAST-9 were the second most abundant clades after MAST-1. MAST-3 was concentrated in the 50 m to 100 m deep water layer, with a high relative abundance in the near-shelf samples. MAST-9 was concentrated in the 75 m to 200 m deep water layer and near-shelf samples, with a relatively higher abundance in the mid-sea. MAST-7 was more abundant in the samples from 50 m to 150 m. Additionally, MAST-8 was more evenly distributed, with high values occurring at the stations in both the shallow and deep ocean layers. MAST-2 was relatively rare and was mainly distributed in the surface and near-shelf samples. In previous studies, MAST-4 was hardly found in the polar ocean, most of which was distributed in tropical, subtropical, and temperate waters (Massana et al., 2006; Massana, 2011; Massana et al., 2015). In this study, MAST-4 was detected in the deep-sea samples from the eastern side of the Cosmonaut Sea at about

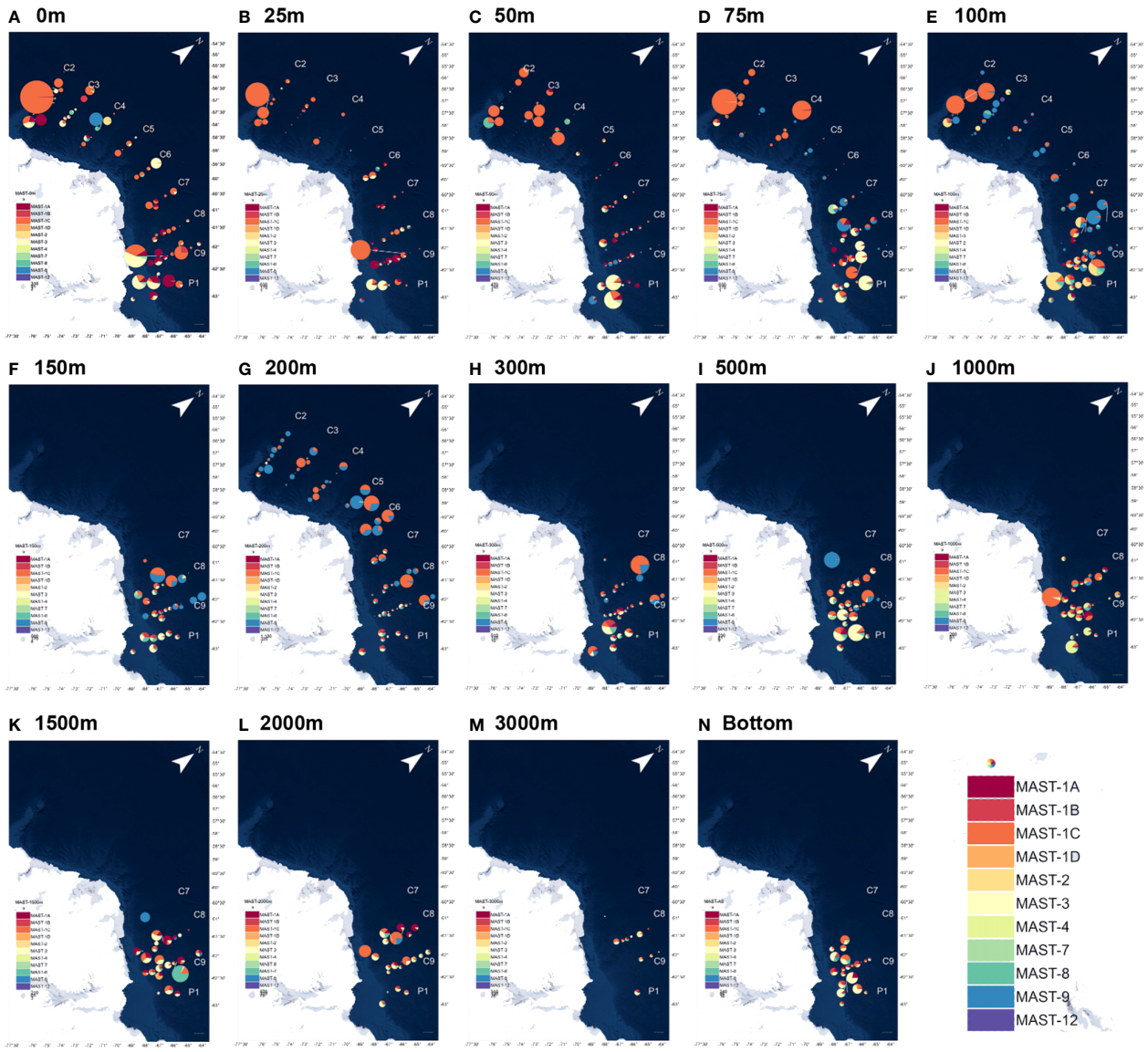


FIGURE 5
Community structure differences in the heterotrophic flagellate marine stramenopile (MAS) taxa at the different water depths in the nine sections of the Antarctic Astronaut Sea. The bubble size represents the relative abundance of the MASTs at the station site, and the sector area represents the proportion of the taxa among the various clades of MASTs at the site. as represents the maximum water depth (bottom) of the samples that were collected at the station site. **(A–N)** corresponds to the HFs distribution at different seawater depths.

2000 m and occurred sporadically in the surface ocean samples. MAST-12 was mostly found in samples from 25 to 100 m in depth, and MAST-11 and MAST-23 were only detected in a few samples.

## 3.5 Effects of environmental factors and biological interactions on community structure

A Spearman correlation matrix analysis (Figure 6) revealed significant correlations between most HFs taxa in the Cosmonaut Sea and 11 environmental factors at the $p < 0.01$ level. However, some correlations were weak, indicating that environmental factors influenced different taxa to varying extents. Notably, salinity exhibited a significant negative correlation with Cryomonadida and a significant positive correlation with MAST-9. Conversely, DO had a significant positive correlation with Cryomonadida and a significant negative correlation with MAST-9. MAST-9 was the taxon most responsive to temperature variations, displaying an opposing trend to the generally negative correlation observed with other HFs taxa. Water depth correlated significantly and negatively with Cryomonadida, while Chl *a* and silicates across all grain sizes were significantly and positively correlated with this taxon. Among the 11 environmental factors, nitrite showed significant correlations with several HFs taxa. It was negatively correlated with MAST-1A, MAST-1B, MAST-2, MAST-7, and MAST-8, but positively

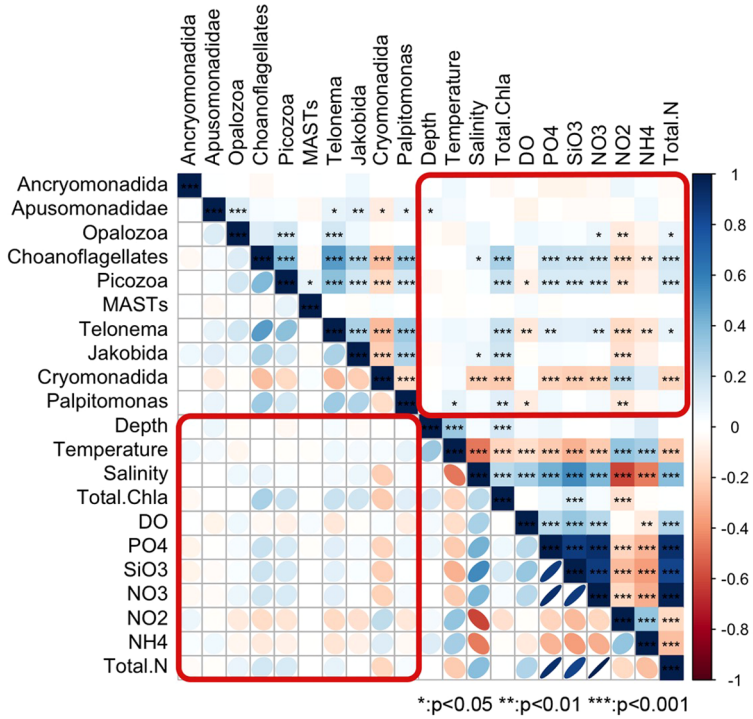


FIGURE 6
Clustering matrix of the correlations between the environmental factors and various groups of heterotrophic flagellates; the color, size, and gradient of the symbols indicate the Spearman's correlation coefficients.

correlated with Cryomonadida. Overall, Cryomonadida emerged as a distinct taxon, exhibiting correlations with environmental factors that were generally opposite to those of other taxa.

Six of the HFs taxa were moderately significantly correlated with at least two of the other taxa. Cryomonadida was more specific when compared to the other taxa, as it was negatively correlated with the taxa with which it was correlated. Specifically, it was weakly negatively correlated with nine taxa (including five clades of MAST), with the strongest correlations with MAST-1A and Telonema. Compared with the other taxa, stronger correlations were observed between choanoflagellates, Picozoa, and Telonemia, which were also moderately positively correlated with *Palpitomonas* and MAST-1A and weakly negatively correlated with Cryomonadida.

# 4 Discussion

## 4.1 Dominant group differences and potential indications

Taxa with a higher relative abundance are not necessarily indicative taxa, but rather indicator taxa that can show the specificity of some of the HFs taxa in the region. In the study area, the main dominant and indicator taxa overlapped well, but there were some differences (Supplementary Table S1). For example, in zones A and B of the Cosmonaut Sea, where MAST-1C was the clade of MASTs with the highest relative abundance, the distribution of the MASTs in the zone was more balanced when compared with that of the other taxa. The dominant and indicator taxa overlapped in most areas, and the east and west sides of the Cosmonaut Sea had obvious differences in the dominant and indicator taxa, with Cryomonadida as the dominant and indicator taxa in Zones A and B, and MASTs and their clades in Zones D and E. Zone C, which is in the middle of the sea, served as an intermediate zone for the shift in dominance between Cryomonadida and MASTs. Some taxa were present in most regions as indicator taxa, such as Cryomonadida, Telonemia, and some clades of the MASTs.

In the tropical and subtropical oceans, most of the dominant HFs taxa in the surface layer belonged to MASTs, Picozoa, and Opalozoa, and in the deep sea, Opalozoa and Diplonemea comprised most of the HFs signal (Obiol et al., 2021). This agrees with the results of this study on the differences in the distribution of the HFs dominant taxa at the different water depths, except that Diplonemea was detected in only a few samples from the Cosmonaut Sea so that they may be more adapted to a higher temperature environment. This is also similar to the global distribution of the MAST subgroup MAST-4, which is rarely found in polar oceans (Massana et al., 2006; Lovejoy and Potvin, 2011; Lovejoy, 2014; Thaler and Lovejoy, 2015). Comparatively, MAST-1 has shown greater adaptability in polar oceans. Although it is the main dominant subgroup of MASTs in temperate and subtropical waters, it also co-occurs with other subgroups to a certain extent (Massana et al., 2006). The choanoflagellates also revealed a clear separation into warm and cold-water clusters,

which was attributed to temperature and ocean currents (Rodriguez-Martinez et al., 2013; Nitsche and Arndt, 2015; Thomsen and Østergaard, 2017). Large taxa with global distributions may obscure most HFs-specific taxa with climatic preferences due to their low numbers (Azovsky et al., 2020). Subsequent studies on the regional specificity of HFs may therefore need to focus more on the less abundant taxa.

## 4.2 Influence of ocean currents on heterotrophic flagellates' regional distribution

Geographically, the Antarctic Cosmonaut Sea is bordered by the Weddell Sea Gyre Eastern Branch (WSG) to the west, it intersects with the Weddell Sea Deep Water (Aoki et al., 2020), the Antarctic Slope Current (ASC) is to the south, the Prydz Bay Gyre (PBG) is to the east, and the southern boundary of the Antarctic Circumpolar Current (ACC) is to the north (Orsi et al., 1995; Williams et al., 2010; Anderson and Hansen, 2020; Yang et al., 2024). Among them, sections C2 and C3 are in the inner rotation of WSG; C4 is on the outer side of WSG; the C5, C6, and C7 northern stations are in the ACC, and C9, P1, and C8-08 are in the inner rotation of the PBG (Figure 1). Based on the differences in the abundance and community structure of the HFs in each section, the areas that were delineated with the currents were more consistent, and sections C2, C3, and C4 are all distributed in the WSG. This may be because the area is at the intersection between the ASC and the PBG, and the direction of the ASC runs from east to west along the Antarctic continental margin. This may bring microorganisms from the eastern waters of the Cosmonaut Sea to the west. They may mix with the shelf water near the shelf front (Bibik et al., 1988; Klyausov and Lanin, 1988; Comiso et al., 2017; Li et al., 2022), which could be why the distribution and abundance of the dominant species of the HFs communities in this part of the region and at depth differed significantly from other stations in the region.

By comparing the structure and dominant species of the HFs communities in the northern Antarctic Peninsula (Chen et al., 2021) and the Cosmonaut Sea, it was found that the distribution of the HFs in these two regions is likely closely related to ocean currents, and both the northern Antarctic Peninsula and the southwestern Cosmonaut Sea are areas where the WSG and the ASC act together, and their dominant species was MASTs. Some stations in sections C5, C6, and C7 are within the ACC, the most extensive ocean current in the world, circumnavigating the Southern Ocean and being composed of an eastward flowing mean current and a small transient eddy. If the average position of the ACC shifts southward, it will alter the habitat range of the different species with profound effects on marine ecosystems (Cristofari et al., 2018; Meijers et al., 2019).

There are some differences in the drivers of microbial distribution in the surface and deep seas. In the surface ocean, spatial environmental differences significantly influence microbial distribution (Villarino et al., 2022). In the deep sea, the influence of the ocean distance (the shortest path between two sites while avoiding land) (Villarino et al., 2022), ocean circulation, and water mass interactions (Ghiglione et al., 2012; Wilkins et al., 2013) is more significant. It has also been proposed that bacterioplankton are water-mass specific, and interactive mixing of the water masses creates either convergence or divergence in the regional distributions of the marine microbial communities (Hernando-Morales et al., 2017). As predators, HFs in the marine micro-food web are selective for bacterial predation, potentially selectively targeting actively growing bacteria (Anderson and Hansen, 2020). The differences in the bacterial biomes may further affect the community structure of the HFs. In addition, there was a certain gradient change in the environmental factors at different ocean depths in the region [(Han et al., 2022), Supplementary Figure S1]. Therefore, the existence of a bathymetric gradient in the distribution of HFs communities supports, to some extent, the differences in the microbial community impact mechanisms between the surface ocean and deep ocean.

## 4.3 Prospects with climate change

The eastern waters of the Cosmonaut Sea are influenced by the PBG, which intersects the ASC and converges northward in a clockwise direction northward toward the southern boundary of the ACC. The shelf water along the Antarctic continent sinks to form the low-temperature and high-density Antarctic bottom water mass (AABW), which forms the Southern Ocean through overturning circulation with the upper relatively warm water mass (Armour et al., 2016; Stuecker et al., 2018). The bottom water mass also flows into the deep ocean layers of most oceans (Patara and Boning, 2014; Patara et al., 2016), and Weddell Sea- and Prydz Bay-sourced AABW are blended and exported mainly to the Atlantic and Indian oceans (Solodoch et al., 2022). The upwelling of the Southern Ocean's overturning circulation carries deep-sea plankton and nutrients, to shallower depths (Thomson et al., 2010; Han et al., 2022), and the surface plankton communities and nutrients can also be transported to the deep sea (Jiao et al., 2018). Therefore, the community ecology of the HFs in the deeper layers of the Cosmonaut Sea is also affected by overturning circulation. Some of the pelagic HFs will be transported to the bottom layer. There will be HFs carried with the Southern Ocean's bottom water mass to other Antarctic waters and even the deeper layers of the Atlantic Ocean and Indian Ocean.

At the circumpolar scale, the overall variability in the plankton biomass per unit area in the Southern Ocean waters is small (Behrenfeld et al., 2017), with local factors, such as sea ice, glaciers, and changes in the seawater stratification under the influence of circulation affecting the plankton community in the Southern Ocean waters to a greater extent (Schofield et al., 2018; Kim et al., 2020). Freshwater fluxes in the circumpolar zone of the ACC will gradually increase under the influence of sea ice melt, increased net precipitation, and glacier breakup (Downes and Hogg, 2013). Moreover, Antarctic Circumpolar Deep-Water formation and export will continue to decrease due to warming and the renewal of the surface ocean waters near the Antarctic continent (Azaneu et al., 2013; Desbruyeres et al., 2017). The overall transport of the Southern Ocean overturning currents will increase, with

implications for the stability of the ice shelves, glaciers, and the Antarctic ice cap. The effect on the nature and circulation of the Southern Ocean water masses (Abernathey et al., 2016; Pellichero et al., 2018; Swart et al., 2018) could directly affect pelagic plankton in the middle and upper ocean (Doney et al., 2012).

Furthermore, it could directly affect the transportation of DO and nutrients in the deep Antarctic seawater. It has been found that the Surface waters that are south of the ACC have stronger freshening rates than those of the intermediate or bottom waters (Menezes et al., 2017; Morley et al., 2020). This means that impacts on the micro-plankton in the surface ocean will occur more quickly (Doney et al., 2012). Therefore, species that are more resilient to disturbances, such as freshening due to climate warming in Antarctica, will be more likely to be less affected (Alcaman-Arias et al., 2021). This implies that as the climate gradually warms, the overall community structure and distribution of the HFs is likely to shift from the original seawater habitat structure to a freshwater habitat structure. The dominance of the taxa that are more adapted to higher temperature and lower salinity water bodies may gradually increase.

This study only discusses heterotrophic flagellate data from a single summer year, with temporal and spatial limitations, which require the subsequent establishment of a long-term dynamic monitoring database to materialize the evaluation of the response and feedback of marine ecosystems to global climate change. Moreover, regionally representative and environmentally indicative taxa could be selected. In addition to focusing on the dominant taxa, further attention should be paid to some taxa (e.g., MAST-4) that are less abundant but have obvious regional distribution characteristics.

## 5 Conclusion

Investigating the spatial distribution and diversity of heterotrophic flagellates (HFs) in polar seas and ice zones is essential. Our study revealed that the western Cosmonaut Sea had a significantly higher HFs abundance than its eastern counterpart, primarily within the top 100 m. Dominant HFs taxa, such as Cryomonadida in the western and MASTs and Opalozoa in the eastern regions, were influenced by local ocean currents. Specifically, the western Cosmonaut Sea's HFs diversity was shaped by a combination of the Antarctic Circumpolar Current (ACC) and the Weddell Eddy, similar to the northern Antarctic Peninsula. Long-term monitoring of HF and the construction of an ecological database are recommended for assessing climate change impacts on HFs and the marine food web.

## Data availability statement

The datasets presented in this study can be found in online repositories. The names of the repository/repositories and accession number(s) can be found below: https://zenodo.org/records/10156730.

## Author contributions

ZC: Conceptualization, Data curation, Methodology, Supervision, Visualization, Writing – original draft, Writing – review & editing, Formal analysis, Software, Validation. HZ: Visualization, Writing – review & editing, Funding acquisition, Validation. YG: Investigation, Methodology, Writing – review & editing. ML: Investigation, Writing – review & editing. GL: Writing – review & editing, Investigation. ZL: Writing – review & editing, Project administration, Validation, Supervision. JH: Funding acquisition, Writing – review & editing, Project administration, Supervision, Resources, Validation.

## Funding

The author(s) declare financial support was received for the research, authorship, and/or publication of this article. This study was generously supported by the China Central University Foundation (Grant No. 23GH02026, achieved by HZ), the Taicang Basic Research Program (Grant No. TC2023JC34, achieved by HZ), and the National Natural Science Foundation of China (Grant No. 41976230).

## Acknowledgments

We express our deepest gratitude to the crew of R/V Xuelong for their exceptional support during on-site sampling.

## Conflict of interest

The authors declare that the research was conducted in the absence of any commercial or financial relationships that could be construed as a potential conflict of interest.

## Publisher's note



## Supplementary material

The Supplementary Material for this article can be found online at: https://www.frontiersin.org/articles/10.3389/fmars.2024.1339413/full#supplementary-material

# References


Abernathey, R. P., Cerovecki, I., Holland, P. R., Newsom, E., Mazlo, M., and Talley, L. D. (2016). Water-mass transformation by sea ice in the upper branch of the Southern Ocean overturning. *Nat. Geosci.* 9, 596. doi: 10.1038/ngeo2749

Alcaman-Arias, M. E., Fuentes-Alburquenque, S., Vergara-Barros, P., Cifuentes-Anticevic, J., Verdugo, J., Polz, M., et al. (2021). Coastal bacterial community response to glacier melting in the western antarctic peninsula. *Microorganisms* 9. doi: 10.3390/microorganisms9010088

Anderson, R., and Hansen, P. J. (2020). Meteorological conditions induce strong shifts in mixotrophic and heterotrophic flagellate bacterivory over small spatio-temporal scales. *Limnol. Oceanogr.* 65, 1189–1199. doi: 10.1002/lno.11381

Aoki, S., Katsumata, K., Hamaguchi, M., Noda, A., Kitade, Y., Shimada, K., et al. (2020). Freshening of antarctic bottom water off cape darnley, east Antarctica. *J. Geophysical Research-Oceans* 125. doi: 10.1029/2020JC016374

Armour, K. C., Marshall, J., Scott, J. R., Donohoe, A., and Newsom, E. R. (2016). Southern Ocean warming delayed by circumpolar upwelling and equatorward transport. *Nat. Geosci.* 9, 549. doi: 10.1038/ngeo2731

Arndt, H., Dietrich, D., Auer, B., Cleven, E.-J., Grafenhan, T., Weitere, M., et al. (2000). Functional diversity of heterotrophic flagellates in aquatic ecosystems. *Systematics Assoc. Special volume* 59, 240–268.

Azaneu, M., Kerr, R., Mata, M. M., and Garcia, C. (2013). Trends in the deep Southern Ocean, (1958-2010): Implications for Antarctic Bottom Water properties and volume export. *J. Geophysical Research-Oceans* 118, 4213–4227. doi: 10.1002/jgrc.20303

Azovsky, A. I., Chertoprud, E. S., Garlitska, L. A., Mazei, Y. A., and Tikhonenkov, D. V. (2020). Does size really matter in biogeography? Patterns and drivers of global distribution of marine micro- and meiofauna. *J. Biogeogr.* 47, 1180–1192. doi: 10.1111/jbi.13771

Behrenfeld, M. J., Hu, Y. X., O'malley, R. T., Boss, E. S., Hostetler, C. A., Siegel, D. A., et al. (2017). Annual boom-bust cycles of polar phytoplankton biomass revealed by space-based lidar. *Nat. Geosci.* 10, 118–11+. doi: 10.1038/ngeo2861

Bibik, V., Maslennikov, V., Pelevin, A., Polonsky, V., and Solyankin, E. (1988). "The current system and the distribution of waters of different modifications in the Cooperation and Cosmonaut Seas," in *Interdisciplinary investigations of pelagic ecosystem in the Cooperation and Cosmonaut Seas* (VNIRO Publishers, Moscow), 16–43.

Bokulich, N. A., Kaehler, B. D., Rideout, J. R., Dillon, M., Bolyen, E., Knight, R., et al. (2018). Optimizing taxonomic classification of marker-gene amplicon sequences with QIIME 2's q2-feature-classifier plugin. *Microbiome* 6, 1–17. doi: 10.1186/s40168-018-0470-z

Chen, Z. Y., He, J. F., Cao, S. N., Lu, Z. B., Lan, M. S., Zheng, H. Y., et al. (2021). Diversity and distribution of heterotrophic flagellates in seawater of the Powell Basin, Antarctic Peninsula. *Polar Res.* 40. doi: 10.33265/polar.v40.5389

Christaki, U., Gueneugues, A., Liu, Y., Blain, S., Catala, P., Colombet, J., et al. (2021). Seasonal microbial food web dynamics in contrasting Southern Ocean productivity regimes. *Limnol. Oceanogr.* 66, 108–122. doi: 10.1002/lno.11591

Comiso, J. C., Gersten, R. A., Stock, L. V., Turner, J., Perez, G. J., and Cho, K. (2017). Positive trend in the antarctic sea ice cover and associated changes in surface temperature. *J. Climate* 30, 2251–2267. doi: 10.1175/JCLI-D-16-0408.1

Comiso, J. C., and Gordon, A. L. (1987). Recurring polynyas over the cosmonaut sea and the maud rise. *J. Geophysical Research-Oceans* 92, 2819–2833. doi: 10.1029/JC092iC03p02819

Convey, P., and Peck, L. S. (2019). Antarctic environmental change and biological responses. *Sci. Adv.* 5. doi: 10.1126/sciadv.aaz0888

Cristofari, R., Liu, X., Bonadonna, F., Cherel, Y., Pistorius, P., Le Maho, Y., et al. (2018). Climate-driven range shifts of the king penguin in a fragmented ecosystem. *Nat. Climate Change* 8, 245–24+. doi: 10.1038/s41558-018-0084-2

del Campo, J., and Ruiz-Trillo, I. (2013). Environmental survey meta-analysis reveals hidden diversity among unicellular opisthokonts. *Mol. Biol. Evol.* 30, 802–805. doi: 10.1093/molbev/mst006

Desbruyeres, D., Mcdonagh, E. L., King, B. A., and Thierry, V. (2017). Global and full-depth ocean temperature trends during the early twenty-first century from Argo and repeat hydrography (vol 30, pg 1985, 2017). *J. Climate* 30, 7577–7577. doi: 10.1175/JCLI-D-16-0396.1

Doney, S. C., Ruckelshaus, M., Duffy, J. E., Barry, J. P., Chan, F., English, C. A., et al. (2012). *Climate Change Impacts on Marine Ecosystems, Annual Review of Marine Science*, Vol. 4, 11–37. doi: 10.1146/annurev-marine-041911-111611

Downes, S. M., and Hogg, A. M. (2013). Southern ocean circulation and eddy compensation in CMIP5 models. *J. Climate* 26, 7198–7220. doi: 10.1175/JCLI-D-12-00504.1

Dufrene, M., and Legendre, P. (1997). Species assemblages and indicator species: The need for a flexible asymmetrical approach. *Ecol. Monogr.* 67, 345–366. doi: 10.2307/2963459

Falk-Petersen, S., Pavlov, V., Timofeev, S., and Sargent, J. R. (2007). Climate variability and possible effects on arctic food chains: The role of Calanu. *Arctic Alpine Ecosystems and People in a Changing Environmentt* (Springer, Berlin, Heidelberg). doi: 10.1007/978-3-540-48514-8_9

Fortier, L., Sirois, P., Michaud, J., and Barber, D. (2006). Survival of Arctic cod larvae (Boreogadus saida) in relation to sea ice and temperature in the Northeast Water Polynya (Greenland Sea). *Can. J. Fisheries Aquat. Sci.* 63, 1608–1616. doi: 10.1139/f06-064

Ghiglione, J. F., Galand, P. E., Pommier, T., Pedros-Alio, C., Maas, E. W., Bakker, K., et al. (2012). Pole-to-pole biogeography of surface and deep marine bacterial communities. *Proc. Natl. Acad. Sci. United States America* 109, 17633–17638. doi: 10.1073/pnas.1208160109

Griffiths, H. J., Meijers, A. J. S., and Bracegirdle, T. J. (2017). More losers than winners in a century of future Southern Ocean seafloor warming. *Nat. Climate Change* 7, 749–74+. doi: 10.1038/nclimate3377

Han, M., Cao, S. N., Luo, G. F., He, J. F., Liang, Y. T., Chen, X. C., et al. (2022). Distributions of virio- and picoplankton and their relationships with ice-melting and upwelling in the Indian Ocean sector of East Antarctica. *Deep-Sea Res. Part Ii-Topical Stud. Oceanogr.* 197. doi: 10.1016/j.dsr2.2022.105044

Hernando-Morales, V., Ameneiro, J., and Teira, E. (2017). Water mass mixing shapes bacterial biogeography in a highly hydrodynamic region of the Southern Ocean. *Environ. Microbiol.* 19, 1017–1029. doi: 10.1111/1462-2920.13538

Hunt, B., Pakhomov, E., and Trotsenko, B. (2007). The macrozooplankton of the Cosmonaut Sea, east Antarctica (30 E–60 E), 1987–1990. *Deep Sea Res. Part I: Oceanographic Res. Papers* 54, 1042–1069. doi: 10.1016/j.dsr.2007.04.002

Jiao, N., Wang, H., Xu, G., and Aricò, S. (2018). Blue carbon on the rise: challenges and opportunities. *Natl. Sci. Rev.* 5, 464–468. doi: 10.1093/nsr/nwy030

Kim, S., Kim, J. H., Lim, J. H., Jeong, J. H., Heo, J. M., and Kim, I. N. (2020). Distribution and control of bacterial community composition in marian cove surface waters, King George Island, Antarctica during the summer of 2018. *Microorganisms* 8. doi: 10.3390/microorganisms8081115

Klyausov, A., and Lanin, V. (1988). On the near-shelf frontal zone in the Commonwealth and Cosmonaut Sea. *Interdisciplinary investigations of pelagic ecosystem in the commonwealth and cosmonaut seas* (Moscow: VNIRO Publishers), 56–62.

Koljalg, U., Nilsson, R. H., Abarenkov, K., Tedersoo, L., Taylor, A. F. S., Bahram, M., et al. (2013). Towards a unified paradigm for sequence-based identification of fungi. *Mol. Ecol.* 22, 5271–5277. doi: 10.1111/mec.12481

Laidre, K. L., Stirling, I., Lowry, L. F., Wiig, O., Heide-Jorgensen, M. P., and Ferguson, S. H. (2008). Quantifying the sensitivity of Arctic marine mammals to climate-induced habitat change. *Ecol. Appl.* 18, S97–125. doi: 10.1890/06-0546.1

Li, W. K. W., Mclaughlin, F. A., Lovejoy, C., and Carmack, E. C. (2009). Smallest algae thrive as the arctic ocean freshens. *Science* 326, 539–539. doi: 10.1126/science.1179798

Li, H. B., Xu, Z. Q., Mou, W. X., Gao, L. B., Zu, Y. C., Wang, C. F., et al. (2022). Planktonic ciliates in different water masses of Cosmonaut and Cooperation Seas (Indian sector of the Southern Ocean) during austral summer. *Polar Biol.* 45, 1059–1076. doi: 10.1007/s00300-022-03057-w

Lovejoy, C. (2014). Changing views of arctic protists (Marine microbial eukaryotes) in a changing arctic. *Acta Protozoologica* 53, 91–100. doi: 10.4467/16890027AP.14.009.1446

Lovejoy, C., and Potvin, M. (2011). Microbial eukaryotic distribution in a dynamic Beaufort Sea and the Arctic Ocean. *J. Plankton Res.* 33, 431–444. doi: 10.1093/plankt/fbq124

Luebbe, B. (1997). Inc. Bran luebbe autoAnalyzer applications: autoAnalyzer method no: G-172-96 nitrate and nitrite in water and seawater.

Massana, R. (2011). Eukaryotic picoplankton in surface oceans. *Annu. Rev. Microbiol.* 65, 91–110. doi: 10.1146/annurev-micro-090110-102903

Massana, R., Gobet, A., Audic, S., Bass, D., Bittner, L., Boutte, C., et al. (2015). Marine protist diversity in European coastal waters and sediments as revealed by high-throughput sequencing. *Environ. Microbiol.* 17, 4035–4049. doi: 10.1111/1462-2920.12955

Massana, R., Terrado, R., Forn, I., Lovejoy, C., and Pedros-Alio, C. (2006). Distribution and abundance of uncultured heterotrophic flagellates in the world oceans. *Environ. Microbiol.* 8, 1515–1522. doi: 10.1111/j.1462-2920.2006.01042.x

Meijers, A. J. S., Meredith, M. P., Murphy, E. J., Chambers, D. P., Belchier, M., and Young, E. F. (2019). The role of ocean dynamics in king penguin range estimation. *Nat. Climate Change* 9, 120–121. doi: 10.1038/s41558-018-0388-2

Menezes, V. V., Macdonald, A. M., and Schatzman, C. (2017). Accelerated freshening of Antarctic Bottom Water over the last decade in the Southern Indian Ocean. *Sci. Adv.* 3. doi: 10.1126/sciadv.1601426

Monier, A., Terrado, R., Thaler, M., Comeau, A., Medrinal, E., and Lovejoy, C. (2013). Upper Arctic Ocean water masses harbor distinct communities of heterotrophic flagellates. *Biogeosciences* 10, 4273–4286. doi: 10.5194/bg-10-4273-2013

Morley, S. A., Abele, D., Barnes, D. K. A., Cardenas, C. A., Cotte, C., Gutt, J., et al. (2020). Global drivers on southern ocean ecosystems: changing physical environments and anthropogenic pressures in an earth system. *Front. Mar. Sci.* 7. doi: 10.3389/fmars.2020.547188

Nitsche, F., and Arndt, H. (2015). Comparison of similar arctic and antarctic morphotypes of heterotrophic protists regarding their genotypes and ecotypes. *Protist* 166, 42–57. doi: 10.1016/j.protis.2014.11.002

Obiol, A., Muhovic, I., and Massana, R. (2021). Oceanic heterotrophic flagellates are dominated by a few widespread taxa. *Limnol. Oceanogr.* 66, 4240–4253. doi: 10.1002/lno.11956

Orsi, A. H., Whitworth, T., and Nowlin, W. D. (1995). On the meridional extent and fronts of the antarctic circumpolar current. *Deep-Sea Res. Part I-Oceanographic Res. Papers* 42, 641–673. doi: 10.1016/0967-0637(95)00021-W

Patara, L., and Boning, C. W. (2014). Abyssal ocean warming around Antarctica strengthens the Atlantic overturning circulation. *Geophysical Res. Lett.* 41, 3972–3978. doi: 10.1002/2014GL059923

Patara, L., Boning, C. W., and Biastoch, A. (2016). Variability and trends in Southern Ocean eddy activity in 1/12 degrees ocean model simulations. *Geophysical Res. Lett.* 43, 4517–4523. doi: 10.1002/2016GL069026

Pellichero, V., Sallee, J. B., Chapman, C. C., and Downes, S. M. (2018). The southern ocean meridional overturning in the sea-ice sector is driven by freshwater fluxes. *Nat. Commun.* 9. doi: 10.1038/s41467-018-04101-2

Rodriguez-Martinez, R., Rocap, G., Salazar, G., and Massana, R. (2013). Biogeography of the uncultured marine picoeukaryote MAST-4: temperature-driven distribution patterns. *ISME J.* 7, 1531–1543. doi: 10.1038/ismej.2013.53

Schlitzer, R. (2021) Ocean Data View. Available online at: https://odv.awi.de.

Schofield, O., Brown, M., Kohut, J., Nardelli, S., Saba, G., Waite, N., et al. (2018). Changes in the upper ocean mixed layer and phytoplankton productivity along the West Antarctic Peninsula. *Philos. Trans. R. Soc. a-Mathematical Phys. Eng. Sci.* 376. doi: 10.1098/rsta.2017.0173

Seenivasan, R., Sausen, N., Medlin, L. K., and Melkonian, M. (2013). Picomonas judraskeda gen. Et sp nov.: the first identified member of the picozoa phylum nov., a widespread group of picoeukaryotes, formerly known as 'Picobiliphytes'. *PloS One* 8. doi: 10.1371/journal.pone.0059565

Sherr, E. B., and Sherr, B. F. (2002). Significance of predation by protists in aquatic microbial food webs. *Antonie Van Leeuwenhoek* 81, 293–308. doi: 10.1023/A:1020591307260

Sohrin, R., Imazawa, M., Fukuda, H., and Suzuki, Y. (2010). Full-depth profiles of prokaryotes, heterotrophic nanoflagellates, and ciliates along a transect from the equatorial to the subarctic central Pacific Ocean. *Deep-Sea Res. Part Ii-Topical Stud. Oceanogr.* 57, 1537–1550. doi: 10.1016/j.dsr2.2010.02.020

Solodoch, A., Stewart, A. L., Hogg, A. M., Morrison, A. K., Kiss, A. E., Thompson, A. F., et al. (2022). How does antarctic bottom water cross the Southern Ocean? *Geophysical Res. Lett.* 49. doi: 10.1029/2021GL097211

Stuecker, M. F., Bitz, C. M., Armour, K. C., Proistosescu, C., Kang, S. M., Xie, S. P., et al. (2018). Polar amplification dominated by local forcing and feedbacks. *Nat. Climate Change* 8, 1076–107+. doi: 10.1038/s41558-018-0339-y

Swart, N. C., Gille, S. T., Fyfe, J. C., and Gillett, N. P. (2018). Recent Southern Ocean warming and freshening driven by greenhouse gas emissions and ozone depletion. *Nat. Geosci.* 11, 836–83+. doi: 10.1038/s41561-018-0226-1

Thaler, M., and Lovejoy, C. (2015). Biogeography of heterotrophic flagellate populations indicates the presence of generalist and specialist taxa in the Arctic Ocean. *Appl. Environ. Microbiol.* 81, 2137–2148. doi: 10.1128/AEM.02737-14

Thomsen, H. A., and Østergaard, J. B. (2017). Acanthoecid choanoflagellates from the Atlantic Arctic Region – a baseline study. *Heliyon* 3, e00345. doi: 10.1016/j.heliyon.2017.e00345

Thomson, P. G., Davidson, A. T., Van Den Enden, R., Pearce, I., Seuront, L., Paterson, J. S., et al. (2010). Distribution and abundance of marine microbes in the Southern Ocean between 30 and 80°E. *Deep Sea Res. Part II: Topical Stud. Oceanogr.* 57, 815–827. doi: 10.1016/j.dsr2.2008.10.040

Verity, P. G., Wassmann, P., Frischer, M. E., Howard-Jones, M. H., and Allen, A. E. (2002). Grazing of phytoplankton by microzooplankton in the Barents Sea during early summer. *J. Mar. Syst.* 38, 109–123. doi: 10.1016/S0924-7963(02)00172-0

Villarino, E., Watson, J. R., Chust, G., Woodill, A. J., Klempay, B., Jonsson, B., et al. (2022). Global beta diversity patterns of microbial communities in the surface and deep ocean. *Global Ecol. Biogeogr.* 31, 2323–2336. doi: 10.1111/geb.13572

Wilkins, D., Van Sebille, E., Rintoul, S. R., Lauro, F. M., and Cavicchioli, R. (2013). Advection shapes Southern Ocean microbial assemblages independent of distance and environment effects. *Nat. Commun.* 4. doi: 10.1038/ncomms3457

Williams, G. D., Nicol, S., Aoki, S., Meijers, A. J. S., Bindoff, N. L., Iijima, Y., et al. (2010). Surface oceanography of BROKE-West, along the Antarctic margin of the south-west Indian Ocean (30-80 degrees E). *Deep-Sea Res. Part Ii-Topical Stud. Oceanogr.* 57, 738–757. doi: 10.1016/j.dsr2.2009.04.020

Worden, A. Z., Follows, M. J., Giovannoni, S. J., Wilken, S., Zimmerman, A. E., and Keeling, P. J. (2015). Rethinking the marine carbon cycle: factoring in the multifarious lifestyles of microbes. *Science* 347, 1257594. doi: 10.1126/science.1257594

Yang, S., Zhou, M., and Cheng, X. (2024). Seasonal and interannual variability between upper ocean processes and the slope current in the region around the Cosmonauts Sea off East Antarctic. *Journal of Geophysical Research: Oceans* 129, e2023JC019636. doi: 1029/2023JC019636

Zheng, H., Chen, Z., Yang, K., Xiao, K., Zhu, J., Gao, Z., et al. (2023). Spatiotemporal variations, surface inventory, and cross regional impact of current-use organoamine pesticides in Chinese Marginal Seas. *J. Hazardous Materials* 451, 131213. doi: 10.1016/j.jhazmat.2023.131213

frontiers | Frontiers in Marine Science

TYPE Original Research
PUBLISHED 07 March 2024
DOI 10.3389/fmars.2024.1302498



OPEN ACCESS

EDITED BY
Antonia Granata,
University of Messina, Italy

REVIEWED BY
Won Young Lee,
Korea Polar Research Institute,
Republic of Korea
Richard O'Driscoll,
National Institute of Water and Atmospheric Research (NIWA), New Zealand

*CORRESPONDENCE
Iole Leonori
iole.leonori@cnr.it

RECEIVED 26 September 2023
ACCEPTED 21 February 2024
PUBLISHED 07 March 2024

CITATION
De Felice A, Biagiotti I, Costantini I, Canduci G and Leonori I (2024) Interactions between krill and its predators in the western Ross Sea. *Front. Mar. Sci.* 11:1302498. doi: 10.3389/fmars.2024.1302498



# Interactions between krill and its predators in the western Ross Sea

Andrea De Felice, Ilaria Biagiotti, Ilaria Costantini, Giovanni Canduci and Iole Leonori*

National Research Council – Institute for Marine Biological Resources and Biotechnology (CNR-IRBIM), Largo Fiera della Pesca, Ancona, Italy

Krill is a fundamental resource in the pelagic food web of the Ross Sea, constituting an important link between primary production and top predators. A series of Italian research voyages to the Ross Sea from 1994 to 2016 have contributed to our understanding of the dynamics of krill populations inhabiting the Ross Sea. Only the surveys in 1994 and 2004 reported information on krill's predators through visual census data, and 2004 data were not object of publication until now. Analyzing *Euphausia superba* and *Euphausia crystallorophias* abundance spatial distribution in the study area in relation to the distribution of its key natural predators have shown a significant relationship between the spatial distribution of minke whales' abundance and the density of *E. superba* biomass, indicating a classical predator-prey interaction. Moreover, krill biomass density data in the water column were analyzed together with the main environmental data from CTD samplings. The analysis of krill density data in relation to environmental factors throughout the water column revealed a significant relation between *E. superba* abundance and salinity, a result that may be linked to the presence of ice melting effects improving environment productivity conditions.

KEYWORDS

**krill, pelagic ecosystem, krill predators, Ross Sea, environment**

## 1 Introduction

The knowledge of krill role in the pelagic food webs in Antarctic and sub-Antarctic waters has been greatly enhanced through extensive research efforts focused on these crustaceans in such environments (Cavan et al., 2019; Testa et al., 2022). The dynamics of these animals could be influenced by many biotic and abiotic factors. Among the main biotic factors, we could mention prey availability, predators' presence, and competitors for food (Meyer et al., 2020), whereas, among the main abiotic factors, we could consider ice cover, water temperature, salinity, dissolved oxygen and water circulation (Leonori et al., 2017; Veytia et al., 2020; De Felice et al., 2022).

Many species rely on krill as a main food source in Antarctic waters. Focusing on the top predators of the pelagic food chain, penguins (Watters et al., 2020), seals (Melbourne-Thomas, 2020) and whales (Konishi et al., 2014; Smetacek, 2021), in particular, show a huge percentage of their diet as consisting in these small crustaceans (Trathan and Hill, 2016). One study, based on isotope analysis, dealing with penguins' diet in the Ross Sea (Jafari et al., 2021) has shown that the relative krill and fish consumption by Adélie penguins (*Pygoscelis adeliae*) and emperor penguins (*Aptenodites forsteri*) changed in relation to the prey availability, in function of seasonal sea ice dynamics and penguin life cycle phases. Dietary variability of Adélie penguin was already known, but not in emperor penguin. In contrast, other authors (Hong et al., 2021), from isotope analysis, found that emperor penguins in the Ross Sea maintain preference for the typology of prey (Antarctic silverfish), while Adélie penguin chicks at Cape Hallett mostly fed on Antarctic krill (*Euphausia superba*), since this krill species is particularly abundant there, but Adélie penguin chicks at Inexpressible Island, located near Terra Nova Bay, mainly fed on both Antarctic silverfish and ice krill (*Euphausia crystallorophias*), demonstrating a regional characterization of the diet and an adaptation to prey availability. In any case krill reveals to be one of the preferred preys, at least for Adélie penguin.

Seals are very important krill consumers. Crabeater seals prefer to breed close to krill and are sensible to the conditions of seasonal sea for breeding success. Weddell seals are less dependent on krill as a food source and remain connected to the stable ice and to the preys that can be found there (Wege et al., 2021). Trathan et al. (2022) found a positive response relationship between predator offspring mass (Antarctic fur seals, gentoo penguins and macaroni penguins) and the spatial distribution of krill, measuring the patchiness in krill distribution, while they found little relation between predator performance and krill density levels at South Georgia. This result evidence the importance of the information derived from krill spatial distribution when studying krill predators' diet and breeding success.

Marine mammals often play a fundamental role concerning krill predation. Miller et al. (2019) have shown that blue whales prefer to concentrate where Antarctic krill swarms are bigger and shallower in order to maximize the energy intake respect to the predation effort. The spatial distribution of minke whales (*Balaenoptera bonaerensis)* in the Ross Sea was studied together with the distribution of Antarctic and ice krill using Generalized Additive Models (GAMs); the results showed that the distribution of these whales was influenced by many factors, such as longitude, distance from shelf break, oceanographic conditions, and densities of both krill species.

Following the examples given above, it could be expected that the spatial distributions of these top predators would overlap, at least partially, with those of the krill species, especially *Euphausia superba*, in the Ross Sea.

For similar reasons, krill preys, mainly represented by phytoplankton species and at a minor level by mesozooplankton species (Hellessey et al., 2020; De Felice et al., 2023), could influence abundance level and spatial distribution of Euphausiids in Antarctica. Different krill species are competitors for food, a fact evidenced by their similar feeding appendages and their diet (Haberman et al., 2003). It is also important to note, at least in the Ross Sea, that the cores of the two most relevant krill populations, *E. superba* and *E. crystallorophias*, tend to separate spatially, passing from austral spring to austral summer (Azzali et al., 2006; Leonori et al., 2017). The abovementioned behavior represents a potential strategy for reducing the risk of starvation resulting from competition for food resources.

The main aim of this work was to investigate potential correlations between the spatial distribution of krill biomass density and the distribution of krill predators in January 2004, having the opportunity of available data on krill predators. The prevalent localization of krill in the water column and the possible influence on the krill density of environmental variables along the water column were also studied, benefitting from *in situ* CTD data acquired during the acoustic survey.

# 2 Materials and methods

## 2.1 Study area, target species and sampling procedures

Acoustic and biological data concerning *E. superba and E. crystallorophias* came from an acoustic survey conducted in the western sector of the Ross Sea (Antarctica) and the adjacent Southern Ocean in January 2004. The study was conducted within the framework of the 19$^{th}$ Italian National Program for Research in Antarctica (PNRA) Expedition aboard the research vessel "Italica". The area boundary coordinates were 69° and 76° S latitude and 165° E and 175° W longitude. The acoustic survey targeting krill was carried out from 28/12/2003 to 23/01/2004, synoptically with the census on krill predators. Both the acoustic and the visual surveys were taken 24 hours a day. The acoustic monitoring followed CCAMLR guidelines and focused on the top 200 m of the water column, the stratum with the core of krill abundance in the study area, as confirmed by the scarce krill abundance level found in the stratum between 200 and 300 meters during the following 2014 survey (Leonori et al., 2017). Krill swarms were monitored acoustically at three frequencies (38, 120, and 200 kHz), in order to separate krill echoes from non-target signals and separate the two krill species between them. Krill aggregations were identified in echograms on the base of the experience from the previous surveys and relying on frequency comparison methodology as described in Azzali et al. (2004a) to discriminate in the categories "*E. superba*", "*E. crystallorophias*" and "other". Periodical trawl hauls were carried out to obtain ground truth information. Bottom depth ranged from about 300 to 3500 m; the highest depths were in the northern area at the border between the Ross Sea and the Southern Ocean. Specimens were collected by means of the HPRI-1000 plankton net (mesh size 1 mm), which was designed by CNR-IRBIM (Ancona, Italy); haul position was decided on the basis of the observation of krill swarms during the acoustic survey (Azzali et al., 2004b; De Felice et al., 2023). The sampling net was equipped with SIMRAD ITI system that allowed, by acoustic wireless connection, to know information about the catch stratum,

such as temperature, net depth and vertical opening. Oceanographic sampling was carried out by means of CTD probe Sea Bird Electronics SBE 911 plus.

For what concerns biomass estimation procedure, the density contrast (g) and sound speed contrast (h) coefficients applied for the two species were derived from Foote et al. (1990); the average tilt angle was hypothesized to be 15°. The fluid sphere model was applied for biomass calculation (Simmonds and MacLennan, 2005) in all the acoustic surveys carried out in the Ross Sea since 1989 by the CNR Institute of Ancona. The fluid sphere model has been improved in time (Anderson, 1950; Johnson, 1977; Stanton et al., 1993; Macaulay, 1994) and represents a valid tool for krill biomass evaluation. Hewitt et al. (2004) length-weight relationship was used for conversion from numbers to biomass. Biomass estimates were expressed as mean krill density per elementary statistical sampling rectangle (Simmonds and MacLennan, 2005). The ESSR method has been employed in all previous surveys, because it is suitable for acoustic monitoring of large areas. Western Ross Sea was subdivided into rectangular grid cells, spaced at intervals of 1° in longitude, but variable in latitude, according to the Earth's curvature variation at the poles. All rectangles had an area of 600 $nm^2$; the origin of the grid (rectangle A0) was set at coordinates 64° 25.1′ S 164°30.0′ E. Numbers and letters (in alphabetical order) proceed from the coast to offshore and southwards. Species abundance and biomass in each rectangle were estimated from the average NASC value of the Elementary Sampling Distance Units (ESDUs) laying within the rectangle.

## 2.2 Study of the relationships between krill, its predators and environmental parameters

Up to now, several acoustic surveys were conducted in the western Ross Sea during Italian expeditions to Antarctica (De Felice et al., 2022), but synoptic information on krill predators was often lacking. Apart from the survey held in January 2004 (Azzali et al., 2004b), only the two surveys carried out in 1994 had this information that was reported in Saino and Guglielmo (2000); however, krill dataset was not studied in relation with its predator dataset at that time, but data were analyzed and reported separately.

In the present paper krill distribution was studied both as spatial distribution over the whole study area in relation with the main krill predators and also along the water column at selected haul positions in relation with environmental parameters.

Consequently, as a first approach, the spatial distribution of krill biomass density within the study area was analyzed using multiple regression analysis (DISTLM), together with estimates of abundance of the main krill natural predators derived from visual census (strip transect methodology) conducted during the survey.

Visual census on krill predators took place from a dedicated platform located at 14 meters (level of the ship's bridge) on the right side of the ship. Individuals spotted on that side within a strip of varying width, dependent on visibility and weather conditions, were considered. The census of krill predators was achieved with both traditional and digital binoculars; the latter allowed to take photos of the observed animals and store them, with relative time and geographical position, in the acoustic database. This allowed a more accurate recognition of the animals and facilitated the studying of the interaction between krill and its predators. Density values were calculated taking into account the number of individuals sighted for each species within each statistical rectangle (as defined for the estimation of krill biomass) and the total observed area (number of miles with sighting activity multiplied by the strip's width). Four predator species were selected based on their dietary dependence on krill and their average krill consumption (minke whale) or the high density of these predators, as determined from visual census (crabeater seal, emperor penguin and Adélie penguin). Marine birds, as skuas and petrels, were not considered in this analysis, even if petrel species in particular presented very high densities, since they can predate krill only at surface and the relative data collected by means of visual census could contain more bias, since these animals usually follow the vessel, with the risk of multiple counts for the same specimen. In general, krill predators' species identified in the study area were the same as reported in Saino and Guglielmo (2000) and are comparable to what found by Double et al. (2015) and Naganobu et al. (2006) for the portion of the area that is common with the data presented in this work. Limiting to penguins, seals and marine mammals, the species that were observed in decent numbers were respectively: Adélie penguin, emperor penguin, crabeater seal, Weddell seal, minke whale and killer whale. No humpback whales were observed and there was only one sighting of blue whale, but not during official visual census monitoring. The aforementioned data was averaged within the same statistical rectangles to prepare them for subsequent analysis with DISTLM, using the best "AIC (Akaike Information Criterion)" as selection criterion. Data were log (x+1) normalized and were formatted for processing using GIS software.

In second instance, acoustic data was matched with CTD data corresponding to the fishing stations in the core abundance areas for the two krill populations, that corresponded respectively with their highest catches with the trawl (Figure 1). Hauls nos. 1, 27, 28 and 30 were selected for *E. superba*, while hauls nos. 7, 8, 10, 13, 17 were selected for *E. crystallorophias*. The density of krill (Nautical Area Scattering Coefficient in $m^2/nm^2$) measured at the frequency of 120 kHz, which is the reference for biomass calculation, was obtained by layers of 20 meters stretching from 15 up to 195 meters (Azzali et al., 2004a; Leonori et al., 2017). The above data was then analyzed by means of DISTLM, using the best "AIC" as selection criterion. Temperature data were log (x+2) normalized, because values could be below -1°C in some cases, while the other variables were log (x+1) normalized.

Figure 2 shows vertical profiles of fluorescence (as proxy for phytoplankton) and krill density, after normalizing the data for hauls where the fluorescence parameter was available. This was done to visually check any potential correspondence in abundance peaks, which could indicate predator-prey interaction.

10.3389/fmars.2024.1302498

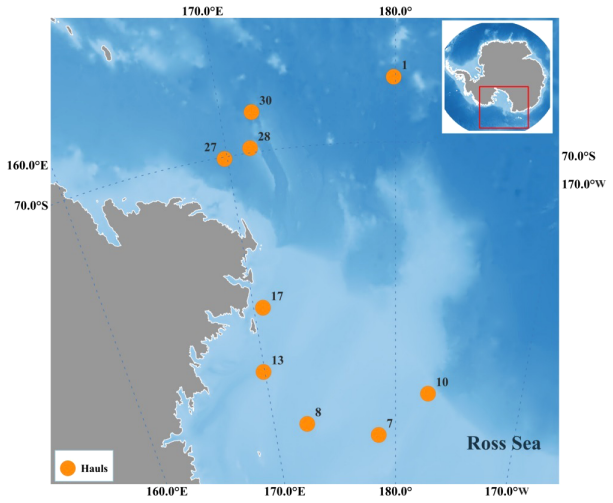


FIGURE 1
Geographic positions of the pelagic hauls with the highest catch levels of *E. superba* and *E. crystallorophias*.

# 3 Results

## 3.1 Spatial distribution of krill in relation to the density of their main natural predators

Krill biomass density data from the two species was studied by DISTLM analysis against abundance of the main natural predators. Maps depicting the spatial distribution of *E. superba*, *E. crystallorophias* and of natural krill predators are reported in Figure 3. The results of this analysis are shown in Tables 1 and 2; the only statistically significant relationship observed was between the density of minke whales and the biomass density of *E. superba* with a best estimate for AIC criterion being 235.49 for the model considering only minke whale density as explanatory variable.

## 3.2 Krill density in relation to environmental parameters

Table 3 shows the results of the multivariate multiple regression applied to krill density data and CTD data recorded throughout the water column. The main environmental parameters measured by CTD probe were averaged within the corresponding depth ranges as it was done for krill density. The analysis was carried out considering one krill species at a time versus all the environmental parameters (temperature, salinity and water density) except for fluorescence, as the fluorimeter broke after the first 10 stations.

Due to autocorrelation issues between water density and salinity, water density was discarded from the analysis.

Salinity exhibited a highly significant correlation with *E. superba* density, with AIC being -1.8898 in the best model considering only this correlation.

Examining in detail Table 4, which provides insights into the vertical distribution of krill in the water column in relation with fluorescence peaks, as proxy of phytoplankton, it becomes evident that *E. superba* in proximity of the considered stations tended to be located within the first 40 meters, apart from station 30 where it was abundant up to about 60 meters. On the contrary, *E. crystallorophias* was generally located in deeper strata, specifically within depth intervals of 80-120 meters at station 7, 40-80 meters and 140-200 meters at station 8, 60-120 meters at station 13, and finally within 100 meters at station 17. The overall vertical distribution bands for the two species were not significantly different, as the trend showed that *E. superba* predominantly occupied the upper meters of the water column while *E. crystallorophias* presented peaks of abundance below 40-60 meters. This suggests circadian movements along the water column, potentially associated with the time of day.

# 4 Discussion

Multiple regression analysis applied to krill biomass data and krill predators' abundance data showed a significant relationship for Antarctic krill only in the case of *Balaenoptera bonaerensis*. This result is in agreement with the literature that identifies in particular Antarctic krill as preferred prey for the numerous specimens of *B. bonaerensis* present in the Ross Sea and surrounding areas (Tamura and Konishi, 2009; Murase et al., 2013; Ishikawa et al., 2022). It suggests that minke whales tend to reside in areas with a high abundance of *E. superba* for feeding purposes. Several other species of marine mammals have krill as their main prey, for example humpback whale (Pallin et al., 2023), blue whale (Miller et al., 2019) and other baleen whales (Savoca et al., 2021) and in certain cases it was demonstrated that their migration seems to be well coordinated with environmental conditions and krill availability (Szesciorka et al., 2020). Our study area involves the western Ross Sea and the portion of the Southern Ocean bordering with it, extending from 69° to 76° S in latitude and from 165° E to 175° W in longitude. Considering the results by Double et al. (2015), going from 65° to 70° S of latitude we have sightings of humpback whales, blue whales, fin whales and minke whales, but south of 70° S the only marine mammals that were identified were minke whales and killer whales. These results are quite consistent with our study, confirming the predominant presence of *B. bonaerensis* and *Orcinus orca* in the Ross Sea among marine mammals, and, for the first species, its strong dependence on krill as a food source. It is highly probable that minke whales concentrate in the area north of Cape Adare, because they can find big *E. superba* swarms that can give a high energy level with limited efforts, a mechanism similar to what described by Miller et al. (2019) for *Balaenoptera musculus*. Minke whale exhibits also a marked preference for *E. superba* respect to *E. crystallorophias*; this fact is reflected by the difference in abundance of B. bonaerensis comparing the core of its distribution (and core for Antarctic krill) in the northern part of the study area, respect to the core of the distribution of ice krill in the central coastal part of the Ross Sea, where minke whales are present, but in much lower density. The spatial distribution of *E. superba* and *E. crystallorophias* in January 2004 reflects quite well what has been observed for all the years in which the acoustic survey

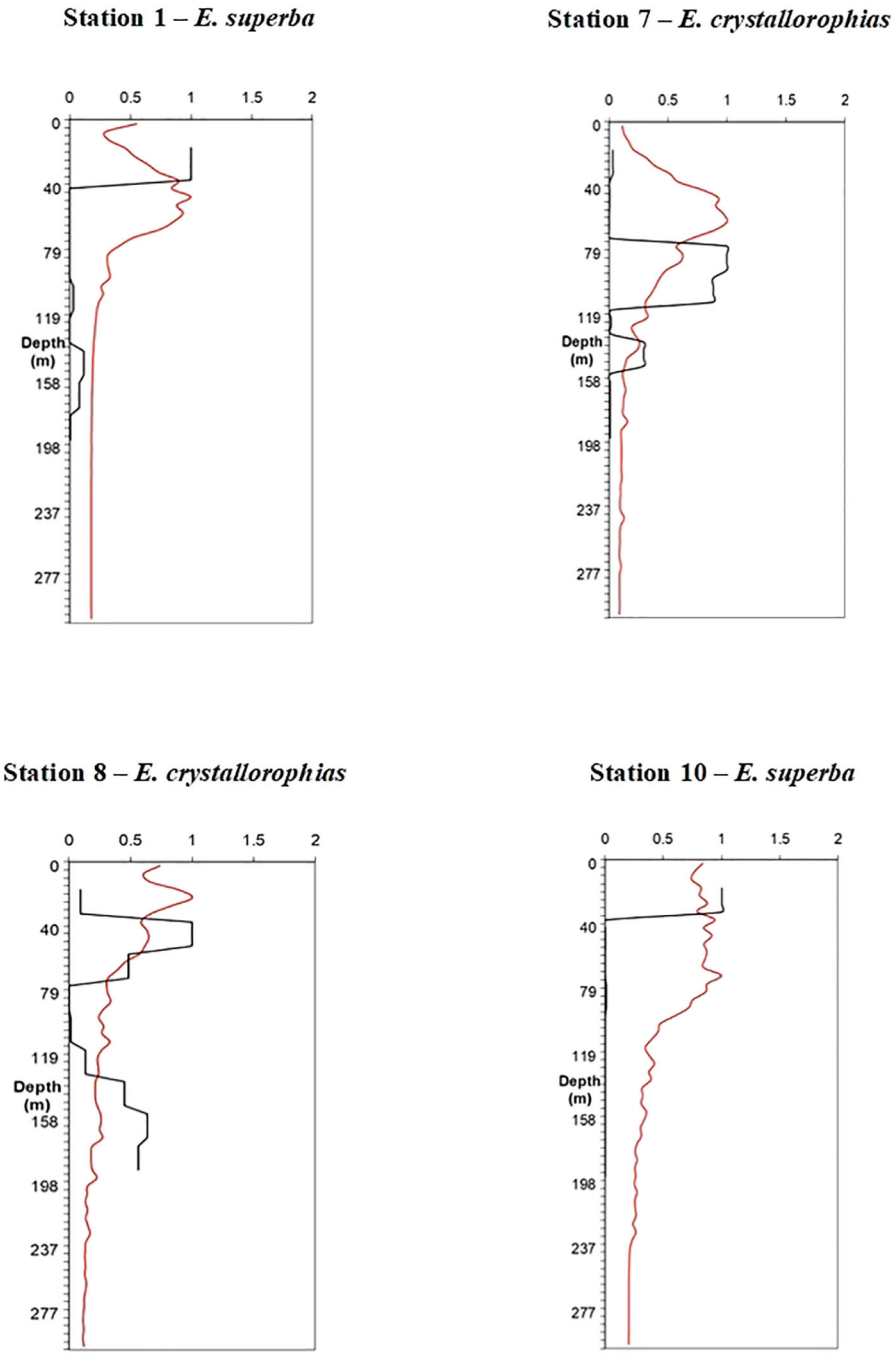


FIGURE 2
Vertical profiles of krill density compared with fluorescence for hauls 1, 7, 8 and 10 where the fluorimeter was operative. In black krill density profile, in red fluorescence.

was conducted in December-January (Davis et al., 2017; Leonori et al., 2017; De Felice et al., 2022) with Antarctic krill concentrated along the northwestern shelf break and ice krill mainly found in the central part. This could be a good condition for krill to avoid competition for food, and predators highly specialized with a diet based prevalently on krill, adapt to this distribution.

An exception in our dataset was constituted by crabeater seal (*Lobodon carcinophagus*) that has a relatively high dependence on krill as a food source (Nachtsheim et al., 2017; Bengtson and Stewart, 2018), but did not show a significant relation with krill biomass spatial distribution. A possible explanation could be that crabeater seals are observed and registered easily while they are resting on ice sheets but are less visible when in the water actively feeding on krill. Almost all the sightings of this species were relative to individuals resting on ice and their spatial distribution (Figure 3), resulting from our study, confirms that they are found prevalently on floating sea ice during austral summer, quite far from the coast, in contrast to Weddell seals that are mainly found on stable ice

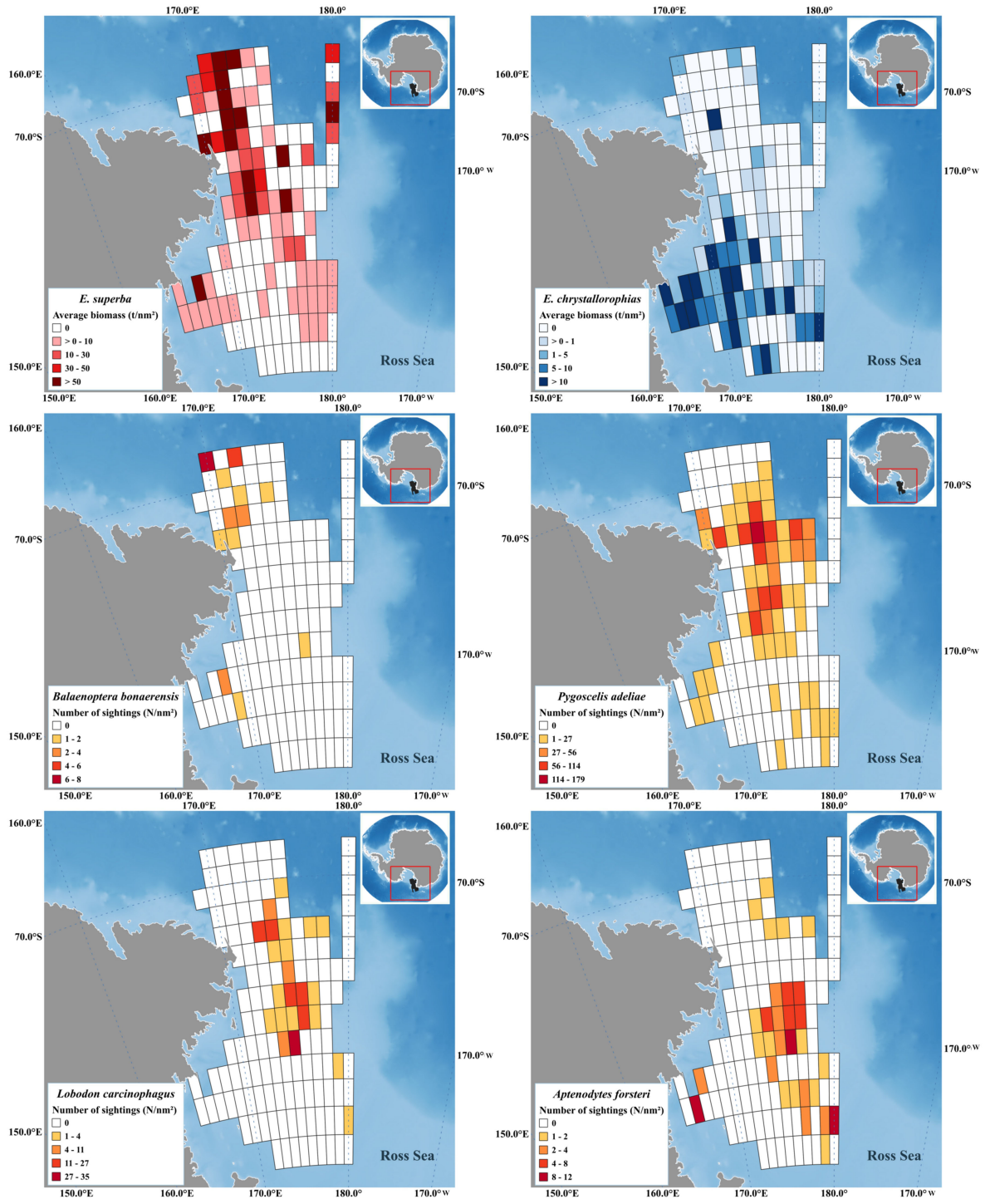


FIGURE 3
Spatial distribution of *E. superba* and *E. crystallorophias* density (above) in comparison with the spatial distribution of krill's natural predators in January 2004 (below) along the grid of statistical rectangles in use for the estimation of krill biomass.

along the coast (Wege et al., 2021). Another possible reason for the absence of a correlation between the spatial distribution of krill and crabeater seals in western Ross Sea could be a switch in the diet composition by these animals in years when krill biomass is not particularly abundant, such as the year considered in this work (Leonori et al., 2017). It is not known how adaptable these seals could be for the diet, being considered highly specialists in feeding krill, but they have shown a shift in the diet towards other prey in the Antarctic Peninsula when krill biomass was at low levels (Hückstädt et al., 2012).

10.3389/fmars.2024.1302498

TABLE 1 Results of DISTLM models run on *E. superba* density values vs. the abundance of its main predators.

| SEQUENTIAL TESTS | | | | | | | |
|---|---|---|---|---|---|---|---|
| Variable | $R^2$ | SS(trace) | Pseudo-F | P | Prop. | Cumul. | res.df |
| *B. bonaerensis* density (N/nm$^2$) | 5.73E-02 | 54.266 | 6.6206 | **0.0068** | **5.73E-02** | 5.73E-02 | 109 |
| *L. carcinophagus* (N/nm$^2$) | 5.80E-02 | 0.69622 | 8.42E-02 | 0.773 | 7.35E-04 | 5.80E-02 | 108 |
| *P. adeliae* (N/nm$^2$) | 6.10E-02 | 2.822 | 0.33931 | 0.558 | 2.98E-03 | 6.10E-02 | 107 |
| *A. forsteri* (N/nm$^2$) | 6.11E-02 | 0.10233 | 1.22E-02 | 0.9099 | 1.08E-04 | 6.11E-02 | 106 |

| BEST SOLUTION | | | | |
|---|---|---|---|---|
| AIC | $R^2$ | RSS | No. Variables | Selections |
| 235.49 | 5.73E-02 | 893.42 | 1 | *B. bonaerensis* density |

Statistically significant values were evidenced in bold.

The situation for what concerns dietary preferences in penguins living in Antarctica is varied, in the sense that different results were obtained in different researches. Emperor penguin (*A. forsteri*) seems to be less dependent on krill as a food source (Putz, 1995; Gales et al., 1990; Zimmer et al., 2007), showing a wider range of possible preys also depending on the study area. When comparing emperor penguin and Adélie penguin, basing on stable isotope analysis (Hong et al., 2021), it was found that emperor penguins in the Ross Sea maintain preference for the typology of prey (Antarctic silverfish), while Adélie penguin chicks at Cape Hallett versus Terra Nova Bay presented a regional characterization of the diet and an adaptation to prey availability. By contrast, another study, based on isotope analysis, dealing with penguins' diet in the Ross Sea (Jafari et al., 2021) has shown that the relative krill and fish consumption by Adélie penguins (*Pygoscelis adeliae*) and emperor penguins (*Aptenodites forsteri*) changed in relation to the prey availability, in function of seasonal sea ice dynamics and penguin life cycle phases. Dietary variability of Adélie penguin is generally confirmed by the various studies, but it is not always the case for emperor penguin. However, krill reveals to be one of the preferred prey, at least for Adélie penguin. In conclusion, it is not surprising that we have not found any relation between krill and emperor penguin, but it could be expected to find it with Adélie penguin; a possible reason for not finding any relation could be that we monitored these penguins during phases of active movement to or from feeding areas. Jafari et al. (2021) identified in spring and summer an active feeding period for *P. adeliae*, but we should take into account that duration of foraging trips by these animals could be very different within Antarctic areas (Juáres et al., 2016; Olmastroni et al., 2020).

As regards krill vertical distribution along the water column, the results have evidenced that the highest densities of the two krill species under investigation were mainly located within the first 100 meters, with occasional exceptions for *E. crystallorophias*, which in some cases was found even deeper. These results seem to be in line with those of other authors for the summer season, particularly in the case of *E. superba* (Pauly et al., 2000; Amakasu et al., 2011). However, it has been suggested that *E. superba* swarms make more than one vertical migration per day (Swadling, 2006). Probably, we could not detect migrations from the surface to deeper waters and back for *E. superba* due to the limited number of hauls considered, covering the daily time span only partially. However, it was possible to identify these movements for *E. crystallorophias*. In the initial stations, where the fluorescence data were available, a certain correspondence could be observed between the fluorescence peak and the peak of krill density when *E. superba* predominated (stations 1 and 10). By contrast, when *E. crystallorophias* prevailed (stations 7 and 8), the krill peak density was slightly deeper than that of fluorescence.

For what concerns the possible relations between krill and environmental parameters along the water column, the only significant one was found between Antarctic krill and salinity. This relation seems to be a similar result to the inverse correlation found by Leonori et al. (2017) between *E. superba* biomass and salinity in the water column. A possible interpretation for this relation is that a decrease in salinity could be associated with ice melting conditions that often mean higher availability of food freed from entrapping ice (Nicol, 2006; Murase et al., 2013) and consequently an increase in prey availability for

TABLE 2 Results of DISTLM models run on *E. crystallorophias* density values vs. the abundance of its main predators.

| SEQUENTIAL TESTS | | | | | | | |
|---|---|---|---|---|---|---|---|
| Variable | $R^2$ | SS(trace) | Pseudo-F | P | Prop. | Cumul. | res.df |
| *B. bonaerensis* density (N/nm$^2$) | 1.808E-3 | 1.0524 | 0.19742 | 0.6738 | 1.808E-3 | 1.808E-3 | 109 |
| *L. carcinophagus* (N/nm$^2$) | 1.2018E-2 | 5.9434 | 1.1161 | 0.2966 | 1.021E-2 | 1.2018E-2 | 108 |
| *P. adeliae* (N/nm$^2$) | 2.6969E-2 | 8.7025 | 1.644 | 0.198 | 1.495E-2 | 2.6969E-2 | 107 |
| *A. forsteri* (N/nm$^2$) | 6.0497E-2 | 19.516 | 3.7828 | 0.0541 | 3.3528E-2 | 6.0497E-2 | 106 |

TABLE 3 Results of multivariate multiple regression on Antarctic krill density data and environmental parameters measured by CTD probe for layers of 20 meters between 15 and 195 meters.

| SEQUENTIAL TESTS | | | | | | | |
|---|---|---|---|---|---|---|---|
| Variable | $R^2$ | SS(trace) | Pseudo-F | P | Prop. | Cumul. | res.df |
| Temp | 4.09E-02 | 1.3912 | 1.3658 | 0.2483 | 4.09E-02 | 4.09E-02 | 32 |
| **Sal** | 0.20678 | 5.6367 | 6.4817 | **0.0131** | 0.16585 | **0.20678** | 31 |
| **BEST SOLUTION** | | | | | | | |
| AIC | $R^2$ | RSS | | No. Variables | | Selections | |
| 0.21346 | 0.10504 | 30.417 | | 1 | | Salinity | |

Statistically significant values were evidenced in bold.

TABLE 4 Depth intervals in which *E. superba* and *E. crystallorophias* swarms occurred in concomitance with the fishing hauls selected for the analyses and local starting time of trawling operations.

| Species | Haul No. | Haul starting hour (hh.mm) | Depth interval with krill highest density (m) |
|---|---|---|---|
| *E. superba* | 1 | 15.01 | 20-40 |
| | 10 | 23.04 | 20-40 |
| | 27 | 01.09 | 20-40 |
| | 28 | 09.27 | 20-40 |
| | 30 | 06.22 | 20-60 |
| *E. crystallorophias* | 7 | 10.17 | 80-120 |
| | 8 | 23.22 | 40-80; 140-200 |
| | 13 | 18.03 | 60-120 |
| | 17 | 01.35 | 20-100 |

krill, once again confirming the importance of the trophic factor for these animals. This result could also be connected to the buoyancy of krill. Krill is capable to swim changing stratum in water column quite well, as also evidenced by the data from this paper, but in certain condition, such as when their stomach is full and they rest, they are transported passively downwards (Tarling and Thorpe, 2017) and the extent of this transport could depend on salinity.

## 5 Conclusion

The analyses presented in this paper focused on the interactions between krill and its predators. The spatial distribution of *E. superba* and *E. crystallorophias* was studied together with four predator species; the results evidenced a relation between the abundance of *B. bonaerensis* and the biomass density of *E. superba*, confirming the high dependence of minke whales on krill as a prey. Krill density, particularly that of *E. superba*, showed a significant correlation only with salinity throughout the water column, a result that could be linked to local increases in productivity due to ice melting, but also to the regulation of water density of krill sinking, when resting, in relation to the buoyancy of these animals.

## Data availability statement

The raw data supporting the conclusions of this article will be made available by the authors, upon pertinent request.

## Ethics statement

The manuscript presents research on animals that do not require ethical approval for their study.

## Author contributions

AD: Conceptualization, Writing – review & editing, Data curation, Formal Analysis, Methodology, Writing – original draft, Validation. IB: Data curation, Writing – review & editing, Validation. IC: Data curation, Writing – review & editing, Validation, Visualization. GC: Data curation, Writing – review & editing, Validation. IL: Conceptualization, Formal Analysis, Methodology, Supervision, Writing – review & editing, Data curation.

## Funding

The author(s) declare financial support was received for the research, authorship, and/or publication of this article. Authors are grateful to the Italian National Antarctic Scientific Commission (CSNA) and the Italian National Research Program in Antarctica (PNRA) for financial support: research project 2002/8.4 (KEP).

## Acknowledgments

The authors would like to thank the Italian National Research Program in Antarctica (PNRA). Special thanks go to Dr. Massimo

Azzali for inspiring this work. We also wish to express our gratitude to the crew of R/V Italica and all the researchers involved for their assistance in conducting the scientific surveys.

## Conflict of interest

The authors declare that the research was conducted in the absence of any commercial or financial relationships that could be construed as a potential conflict of interest.

## Publisher's note



## References

Amakasu, K., Ono, A., Hirano, D., Moteki, M., and Ishimaru, T. (2011). Distribution and density of Antarctic krill (*Euphausia superba*) and ice krill (E. crystallorophias) off Adelie Land in austral summer 2008 estimated by acoustical methods. *Pol. Sci.* 5, 187–194. doi: 10.1016/j.polar.2011.04.002

Anderson, V. C. (1950). Sound scattering from a fluid sphere. *J. Acoust. Soc Am.* 22, 426–431.

Azzali, M., Leonori, I., De Felice, A., and Russo, A. (2006). Spatial–temporal relationships between two euphausiid species in the Ross Sea. *Chem. Ecol.* 22, S219–S233. doi: 10.1080/02757540600670836

Azzali, M., Leonori, I., and Lanciani, G. (2004a). A hybrid approach to acoustic classification and length estimation of krill. *CCAMLR Sci.* 11, 33–58.

Azzali, M., Russo, A., Sala, A., De Felice, A., and Catalano, B. (2004b). *Preliminary results of a survey on krill, environment and predators in CCAMLR Division 88.1 carried out in December 2003 and in January 2004 (Project 8.4). CCAMLR WG-EMM-04/71* (Hobart, Australia: CCAMLR), 23 p.

Bengtson, J. L., and Stewart, B. S. (2018). "Crabeater seal: *lobodon carcinophaga*," in *Encyclopedia of marine mammals, 3rd ed.* Eds. B. Würsig, J. G. M. Thewissen and K. M. Kovacs (Academic Press), 230–232, ISBN: . doi: 10.1016/B978-0-12-804327-1.00098-4

Cavan, E. L., Belcher, A., Atkinson, A., Hill, S. L., Kawaguchi, S., McCormack, S., et al. (2019). The importance of Antarctic krill in biogeochemical cycles. *Nat. Commun.* 10, 4742. doi: 10.1038/s41467-019-12668-7

Davis, L. B., Hofmann, E. E., Klinck, J. M., Piñones, A., and Dinniman, M. S. (2017). Distributions of krill and Antarctic silverfish and correlations with environmental variables in the western Ross Sea, Antarctica. *Mar. Ecol. Prog. Ser.* 584, 45–65. doi: 10.3354/meps12347

De Felice, A., Biagiotti, I., Canduci, G., Costantini, I., Malavolti, S., Giuliani, G., et al. (2022). Is it the same every summer for the euphausiids of the ross sea? *Divers.* 14, 433. doi: 10.3390/d14060433

De Felice, A., Manini, E., Biagiotti, I., and Leonori, I. (2023). Bioenergetics of *Euphausia superba* and *Euphausia crystallorophias* in the Ross Sea. *Divers.* 15, 480. doi: 10.3390/d15040480

Double, M. C., Miller, B. S., Leaper, R., Olson, P., Cox, M. J., Miller, E., et al. (2015). *Cruise report on blue whale research from the NZ/Aus Antarctic Ecosystems Voyage 2015 of the Southern Ocean Research Partnership* (International Whaling Commission).

Foote, K. G., Everson, I., Watkins, J. L., and Bone, D. G. (1990). Target strengths of antarctic krill (Euphausia superba) at 38 and 120 kHz. *J. Acoust. Soc Am.* 87, 16–24.

Gales, N. J., Klages, N. T. W., Williams, R., and Woehler, E. J. (1990). The diet of the emperor penguin, *Aptenodytes forsteri*, in Amanda Bay, Princess Elizabeth Land, Antarctica. *Ant. Sci.* 2, 23–28. doi: 10.1017/S0954102090000037

Haberman, K. L., Ross, R. M., and Quetin, L. B. (2003). Diet of the Antarctic krill (*Euphausia superba* Dana): II. Selective grazing in mixed phytoplankton assemblages. *J. Exp. Mar. Biol. Ecol.* 283, 97–113.

Hellessey, N., Johnson, R., Ericson, J. A., Nichols, P. D., Kawaguchi, S., Nicol, S., et al. (2020). Antarctic krill lipid and fatty acid content variability is associated to satellite derived chlorophyll a and sea surface temperatures. *Sci. Rep.* 10, 6060.

Hewitt, R. P., Watkins, J., Naganobu, N., Sushin, V., Brierley, A. S., Demer, D., et al. (2004). Biomass of antarctic krill in the scotia sea in January/February 2000 and its use in revising an estimate of precautionary yield. *Deep-Sea Res. II* 51, 1215–1236. doi: 10.1016/j.dsr2.2004.06.011

Hong, S.-Y., Gal, J.-K., Lee, B.-Y., Son, W.-J., Jung, J.-W., La, H.-S., et al. (2021). Regional differences in the diets of adélie and emperor penguins in the ross sea, Antarctica. *Anim.* 11, 2681. doi: 10.3390/ani11092681

Hückstädt, L. A., Burns, J. M., Koch, P. L., McDonald, B. I., Crocker, D. E., and Costa, D. P. (2012). Diet of a specialist in a changing environment: the crabeater seal along the western Antarctic Peninsula. *Mar. Ecol. Prog. Ser.* 455, 287–301. doi: 10.3354/meps09601

Ishikawa, H., Otsuki, M., Tamura, T., Konishi, K., Bando, T., Ishizuka, M., et al. (2022). Foraging ecology of mature male Antarctic minke whales (*Balaenoptera bonaerensis*) revealed by stable isotope analysis of baleen plates. *Pol. Sci.* 31, 100785. doi: 10.1016/j.polar.2021.100785

Jafari, V., Maccapan, D., Careddu, G., Sporta Caputi, S., Calizza, E., Rossi, L., et al. (2021). Spatial and temporal diet variability of Adélie (*Pygoscelis adeliae*) and Emperor (*Aptenodytes forsteri*) Penguin: a multi tissue stable isotope analysis. *Pol. Biol.* 44, 1869–1881. doi: 10.1007/s00300-021-02925-1

Johnson, R. K. (1977). Sound scattering from a fluid sphere revisited. *J. Acoust. Soc Am.* 61, 375–377.

Juáres, M. A., Santos, M., Mennucci, J. A., Coria, N. R., and Mariano–Jelicich, R. (2016). Diet composition and foraging habitats of Adélie and gentoo penguins in three different stages of their annual cycle. *Mar. Biol.* 163, 105. doi: 10.1007/s00227-016-2886-y

Konishi, K., Hakamada, T., Kiwada, H., Kitakado, T., and Walløe, L. (2014). Decrease in stomach contents in the Antarctic minke whale (*Balaenoptera bonaerensis*) in the Southern Ocean. *Pol. Biol.* 37, 205–215. doi: 10.1007/s00300-013-1424-3

Leonori, I., De Felice, A., Canduci, G., Costantini, I., Biagiotti, I., Giuliani, G., et al. (2017). Krill distribution in relation to environmental parameters in mesoscale structures in the Ross Sea. *J. Mar. Syst.* 166, 159–171. doi: 10.1016/j.jmarsys.2016.11.003

Macaulay, M. C. (1994). A generalized target strength model for euphausiids, with application to other zooplankton. *J. Acoust. Soc Am.* 95, 2452–2466.

Melbourne-Thomas, J. (2020). Climate shifts for krill predators. *Nat. Clim. Change* 10, 390–391. doi: 10.1038/s41558-020-0756-6

Meyer, B., Atkinson, A., Bernard, K. S., Brierley, A. S., Driscoll, R., Hill, S. L., et al. (2020). Successful ecosystem-based management of Antarctic krill should address uncertainties in krill recruitment, behaviour and ecological adaptation. *Commun. Earth Env.* 1, 28. doi: 10.1038/s43247-020-00026-1

Miller, E. J., Potts, J. M., Cox, M. J., Miller, B. S., Calderan, S., Leaper, R., et al. (2019). The characteristics of krill swarms in relation to aggregating Antarctic blue whales. *Sci. Rep.* 9, 16487. doi: 10.1038/s41598-019-52792-4

Murase, H., Kitakado, T., Hakamada, T., Matsuoka, K., Nishiwaki, S., and Naganobu, M. (2013). Spatial distribution of Antarctic minke whales (*Balaenoptera bonaerensis*) in relation to spatial distributions of krill in the Ross Sea, Antarctica. *Fish. Ocean.* 22, 154–173. doi: 10.1111/fog.12011

Nachtsheim, D. A., Jerosch, K., Hagen, W., Plotz, J., and Bornemann, H. (2017). Habitat modelling of crabeater seals (*Lobodon carcinophaga*) in the Weddell Sea using the multivariate approach Maxent. *Pol. Biol.* 40, 961–976. doi: 10.1007/s00300-016-2020-0

Naganobu, M., Nishiwaki, S., Yasuma, H., Matsukura, R., Takao, Y., Taki, K., et al. (2006). *Interactions between oceanography, krill and baleen whales in the Ross Sea and Adjacent Waters: An overview of Kaiyo Maru-JARPA joint survey in 2004/05*. Paper SC/D06/J23 presented to the JARPA Review Meeting, December 2006 (unpublished). 33pp.

Nicol, S. (2006). Krill, currents, and sea ice: *Euphausia superba* and its changing environment. *Biosci.* 56, 111–120. doi: 10.1641/0006-3568(2006)056[0111:KCASIE]2.0.CO;2

Olmastroni, S., Fattorini, N., Pezzo, F., and Focardi, S. (2020). Gone fishing: Adélie penguin site-specific foraging tactics and breeding performance. *Ant. Sci.* 32, 199–209. doi: 10.1017/S0954102020000085

Pallin, L. J., Kellar, N. M., Steel, D., Botero-Acosta, N., Scott Baker, C., Conroy, J. A., et al. (2023). A surplus no more? variation in krill availability impacts reproductive rates of antarctic baleen whales. *Glob. Ch. Biol.* 29, 2108–2121. doi: 10.1111/gcb.16559

Pauly, T., Nicol, S., Higginbottom, I., Hosie, G., and Kitchener, J. (2000). Distribution and abundance of antarctic krill (*Euphausia superba*) off east antarctica (80-150°E) during the austral summer of 1995/1996. *Deep-Sea Res. II* 47, 2465–2488.

Putz, K. (1995). The post-moult diet of Emperor Penguins (*Aptenodytes forsteri*) in the eastern Weddell Sea, Antarctica. *Pol. Biol.* 15, 457 463.

Saino, N., and Guglielmo, L. (2000). "ROSSMIZE expedition: Distribution and biomass of birds and mammals in the western ross sea," in *Ross sea ecology*. Ed. F. M. Faranda, et al (Heidelberg: Springer-Verlag Berlin).

Savoca, M. S., Czapanskiy, M. F., Kahane-Rapport, S. R., Gough, W. T., Fahlbusch, J. A., Bierlich, K. C., et al. (2021). Baleen whale prey consumption based on high-resolution foraging measurements. *Nat.* 599, 85–90. doi: 10.1038/s41586-021-03991-5

Simmonds, E. J., and MacLennan, D. N. (2005). *Fisheries acoustics* (Oxford: Blackwell Science), 456.

Smetacek, V. (2021). A whale of an appetite. *Nat.* 599, 33–34.

Stanton, T. K., Clay, C. S., and Chu, D. (1993). Ray representation of sound scattering by weakly scattering deformed fluid cylinders: Simple physics and application to zooplankton. *J. Acoust. Soc Am.* 94, 3452–3454.

Swadling, K. M. (2006). Krill migration: up and down all night. *Curr. Biol.* 16, R173–R175. doi: 10.1016/j.cub.2006.02.044

Szesciorka, A. R., Ballance, L. T., Širović, A., Rice, A., Ohman, M. D., Hildebrand, J. A., et al. (2020). Timing is everything: Drivers of interannual variability in blue whale migration. *Sci. Rep.* 10, 7710. doi: 10.1038/s41598-020-64855-y

Tamura, T., and Konishi, K. (2009). Feeding habits and prey consumption of Antarctic minke whale (*Balaenoptera bonaerensis*) in the Southern Ocean. *J. Northw. Atl. Fish Sci.* 42, 13–25. doi: 10.2960/J.v42.m652

Tarling, G. A., and Thorpe, S. E. (2017). Oceanic swarms of Antarctic krill perform satiation sinking. *Proc. R. Soc B* 284, 20172015. doi: 10.1098/rspb.2017.2015

Testa, G., Neira, S., Giesecke, R., and Pinones, A. (2022). Projecting environmental and krill fishery impacts on the Antarctic Peninsula food web in 2100. *Prog. Ocean.* 206, 102862. doi: 10.1016/j.pocean.2022.102862

Trathan, P. N., Fielding, S., Warwick-Evans, V., Freer, J., and Perry, F. (2022). Seabird and seal responses to the physical environment and to spatio-temporal variation in the distribution and abundance of Antarctic krill at South Georgia, with implications for local fisheries management. *ICES J. Mar. Sci.* 79, 2373–2388. doi: 10.1093/icesjms/fsac168

Trathan, P. N., and Hill, S. L. (2016). "The importance of krill predation in the southern ocean," in *Biology and ecology of Antarctic krill. Advances in polar ecology*. Ed. V. Siegel (Springer, Cham). doi: 10.1007/978-3-319-29279-3_9

Veytia, D., Corney, S., Meiners, K. M., Kawaguchi, S., Murphy, E. J., and Bestley, S. (2020). Circumpolar projections of Antarctic krill growth potential. *Nat. Clim. Change* 10, 568–575. doi: 10.1038/s41558-020-0758-4

Watters, G. M., Hinke, J. T., and Reiss, C. S. (2020). Long-term observations from Antarctica demonstrate that mismatched scales of fsheries management and predator-prey interaction lead to erroneous conclusions about precaution. *Sci. Rep.* 10, 2314. doi: 10.1038/s41598-020-59223-9

Wege, M., Salas, L., and LaRue, M. (2021). Ice matters: Life-history strategies of two Antarctic seals dictate climate change eventualities in the Weddell Sea. *Glob. Change Biol.* 27, 6252–6262. doi: 10.1111/gcb.15828

Zimmer, I., Piatkowski, U., and Brey, T. (2007). The trophic link between squid and the emperor penguin *Aptenodytes forsteri* at Pointe Geologie, Antarctica. *Mar. Biol.* 152, 1187–1195. doi: 10.1007/s00227-007-0766-1

frontiers | Frontiers in Marine Science

TYPE Original Research
PUBLISHED 27 March 2024
DOI 10.3389/fmars.2024.1308542



OPEN ACCESS

EDITED BY
Antonia Granata,
University of Messina, Italy

REVIEWED BY
Hauke Flores,
Alfred Wegener Institute Helmholtz Centre for Polar and Marine Research (AWI), Germany
David Kimmel,
National Oceanic and Atmospheric Administration, United States

*CORRESPONDENCE
Christine Gawinski
Christine.gawinski@uit.no

RECEIVED 06 October 2023
ACCEPTED 28 February 2024
PUBLISHED 27 March 2024

CITATION
Gawinski C, Daase M, Primicerio R, Amargant-Arumí M, Müller O, Wold A, Ormańczyk MR, Kwasniewski S and Svensen C (2024) Response of the copepod community to interannual differences in sea-ice cover and water masses in the northern Barents Sea. *Front. Mar. Sci.* 11:1308542. doi: 10.3389/fmars.2024.1308542



# Response of the copepod community to interannual differences in sea-ice cover and water masses in the northern Barents Sea

Christine Gawinski[1]*, Malin Daase[1,2], Raul Primicerio[1], Martí Amargant-Arumí[1], Oliver Müller[3], Anette Wold[4], Mateusz Roman Ormańczyk[5], Slawomir Kwasniewski[5] and Camilla Svensen[1]

[1]Department of Arctic and Marine Biology, UiT The Arctic University of Norway, Tromsø, Norway, [2]Department of Arctic Biology Research, The University Centre in Svalbard, Longyearbyen, Svalbard, Norway, [3]Department of Biological Sciences (BIO), University of Bergen, Bergen, Norway, [4]Norwegian Polar Institute, Tromsø, Norway, [5]Department of Marine Ecology, Institute of Oceanology, Polish Academy of Sciences, Sopot, Poland

The reduction of Arctic summer sea ice due to climate change can lead to increased primary production in parts of the Barents Sea if sufficient nutrients are available. Changes in the timing and magnitude of primary production may have cascading consequences for the zooplankton community and ultimately for higher trophic levels. In Arctic food webs, both small and large copepods are commonly present, but may have different life history strategies and hence different responses to environmental change. We investigated how contrasting summer sea-ice cover and water masses in the northern Barents Sea influenced the copepod community composition and secondary production of small and large copepods along a transect from 76°N to 83°N in August 2018 and August 2019. Bulk abundance, biomass, and secondary production of the total copepod community did not differ significantly between the two years. There were however significant spatial differences in the copepod community composition and production, with declining copepod abundance from Atlantic to Arctic waters and the highest copepod biomass and production on the Barents Sea shelf. The boreal *Calanus finmarchicus* showed higher abundance, biomass, and secondary production in the year with less sea-ice cover and at locations with a clear Atlantic water signal. Significant differences in the copepod community between areas in the two years could be attributed to interannual differences in sea-ice cover and Atlantic water inflow. Small copepods contributed more to secondary production in areas with no or little sea ice and their production was positively correlated to water temperature and ciliate abundance. Large copepods contributed more to secondary production in areas with extensive sea ice and their production was positively correlated with chlorophyll *a* concentration. Our results show how pelagic communities might function in a

future ice-free Barents Sea, in which the main component of the communities are smaller-sized copepod species (including smaller-sized *Calanus* and small copepods), and the secondary production they generate is available in energetically less resource-rich portions.

KEYWORDS

**sea-ice cover, copepod community composition, secondary production, northern Barents Sea, interannual variability, sea-ice melt**

## 1 Introduction

One of the most noticeable consequences of ongoing climate change is the decline of Arctic summer sea ice (Pörtner et al., 2019). Sea ice is melting earlier and forming later in the season, resulting in a prolonged open water period with increased light transmission to the upper ocean (Wassmann and Reigstad, 2011). The seasonally ice-covered Barents Sea is experiencing the highest rates of warming amongst all regions of the Arctic (Isaksen et al., 2022) and it is projected to be ice-free during winter beyond the year 2061 (Onarheim and Årthun, 2017). These physical alterations have major impacts on biological processes in the Barents Sea, as sea ice constitutes a unique habitat for sea ice algae and further controls light availability and mixing in the upper ocean, which regulates the onset of phytoplankton blooms (Sakshaug et al., 1991). The blooms typically follow the northwards retreat of sea ice in spring and summer, as the melting ice creates the stratified surface layer and increased light transmittance that are necessary for bloom formation. Once surface nitrate and silicate are depleted, the phytoplankton community changes from a diatom-dominated system to one dominated by flagellates and ciliates (Rat'kova and Wassmann, 2002). Timing and quality of the bloom are critical for the biomass and reproductive success of secondary producers.

Associated with the diatom-dominated system are large, lipid-rich copepods of the genus *Calanus* that have developed a reproductive cycle that is tightly linked to the ice algae and spring phytoplankton blooms (Falk-Petersen et al., 2009). The Arctic species *Calanus hyperboreus* reproduces during winter, entirely based on internal lipid reserves that were build up during the previous growth season (Falk-Petersen et al., 2009). *C. glacialis* on the other hand usually spawns just before or during the ice algae bloom (Søreide et al., 2010), while the boreal species *C. finmarchicus* reproduces during the open water spring bloom (Hirche, 1996). Offspring of *C. hyperboreus* and *C. glacialis* are dependent on the phytoplankton spring bloom for growth and accumulation of energy reserves that are needed for diapause (Falk-Petersen et al., 2009; Søreide et al., 2010). Nauplii and young copepodids (CI-III) of *C. finmarchicus* feed during the spring bloom, while the development of older copepodids (CIV-V) is fueled by grazing on microzooplankton during the summer (Svensen et al., 2019). In late summer, *Calanus* spp. that have acquired enough lipids for diapause descend into deeper water layers to hibernate at depth until the next spring bloom (Falk-Petersen et al., 2009). While *Calanus* spp. often dominate the mesozooplankton community in terms of biomass, smaller copepods (adult body size <2 mm; Svensen et al., 2019), such as *Oithona similis*, usually dominate in terms of numbers (Gallienne and Robins, 2001; Madsen et al., 2008). These copepods are closely associated with the microbial food web occurring in late summer and autumn, as they are omnivores (Lischka and Hagen, 2007). In contrast to *Calanus* spp., they reproduce year-round, with greatest abundance of eggs and nauplii occurring during spring and summer (Ashjian et al., 2003; Madsen et al., 2008).

The reduction of summer sea-ice cover due to climate change can lead to increased primary production in parts of the Barents Sea, depending on the prevalent nutrient and stratification regimes (Randelhoff et al., 2020). With a retreat of the seasonal ice zone northwards, regions previously covered by ice will likely experience a prolonged phytoplankton growing season and higher primary production, if sufficient nutrients are available. The southern edge of the seasonal ice zone is expected to become less productive due to increased thermal stratification and the resulting decrease in nutrients supplied to the surface layers (Wassmann and Reigstad, 2011). These changes will likely affect the zooplankton community by altering the composition of the grazers. In the Bering Sea, large-sized *Calanus* spp. were found to be more abundant during cold periods with extensive sea-ice cover (Coyle and Pinchuk, 2002; Hunt et al., 2011; Stabeno et al., 2012; Eisner et al., 2014; Kimmel et al., 2018, Kimmel et al., 2023), while small copepods (e.g. *Oithona* spp. and *Pseudocalanus* spp.) were more abundant during warm periods with less sea-ice cover (Stabeno et al., 2012; Kimmel et al., 2018, Kimmel et al., 2023). Similar observations have been made in Svalbard fjords and the northern Barents Sea, where higher abundance of small copepods has been linked to warmer periods (Balazy et al., 2018) and the abundance of *Calanus* spp. was influenced by Atlantic water inflow and sea-ice cover (Dalpadado et al., 2003; Daase and Eiane, 2007; Blachowiak-Samolyk et al., 2008; Dalpadado et al., 2012; Stige et al., 2019).

Secondary production is key in understanding how climate related changes, such as a reduction of sea ice, may impact the transfer of energy in Arctic marine food webs. Secondary production refers to the biomass produced by consumers, such as

copepods, in a given unit of time (e.g., mg C $m^{-2}$ $d^{-1}$). The Barents Sea is a highly productive fishing ground and *Calanus* spp. are a crucial food source for many small and juvenile planktivorous fish such as the Barents Sea capelin (*Mallotus villosus*), Atlantic herring (*Clupea harengus*) and polar cod (*Boreogadus saida*) (Hassel et al., 1991; Huse and Toresen, 1996; Bouchard et al., 2017). Small copepods, such as *O. similis* and *Pseudocalanus* spp. are food for fish larvae and other larger zooplankton, such as krill, amphipods, chaetognaths, ctenophores, and hydrozoans (Turner, 2004). Eggs and nauplii of both small and large copepods form a substantial part of the diet of the early larval stages of polar cod. Here, small copepods are especially important to polar cod larvae hatching during the winter months, when other food sources are scarce (Geoffroy and Priou, 2020). In the Bering Sea, sea-ice concentration was found to impact secondary production of *Calanus* spp., which was low during warm periods with less sea-ice cover (Kimmel et al., 2018, Kimmel et al., 2023). In the Barents Sea previous research on secondary production has mainly focused on the southern regions close to the polar front (Basedow et al., 2014; Dvoretsky and Dvoretsky, 2024a) and the eastern Barents Sea (Dvoretsky and Dvoretsky, 2009; Dvoretsky and Dvoretsky, 2024b) and primarily on large *Calanus* spp. (Slagstad et al., 2011). Gaining insights into the effects of sea-ice reduction on copepod secondary production in the Barents Sea is of great social and economic significance, especially since interannual sea-ice concentrations in the northern Barents Sea are highly variable due to climate change (Efstathiou et al., 2022).

In the present study, we evaluate how a reduction in sea-ice cover influenced the copepod community composition and their secondary production in the upper 100 m of the northern Barents Sea. We further examined the relationship between copepod secondary production and environmental and biological drivers, such as hydrography, protist community composition and bacterial and primary production. Zooplankton samples were collected in August 2018, a year with reduced sea-ice cover, and in August 2019, a year with extensive sea-ice cover along a transect spanning 76-83° N. We address the following research questions through direct hypothesis testing: Did differences in sea-ice cover between the two years (I) affect the total copepod secondary production and (II) change the contribution of different species to the total copepod secondary production? Additionally, we explore whether patterns in community composition or secondary production correlated with other environmental or biological factors through multivariate descriptive analyses.

We expect the total copepod secondary production to be higher in the summer with reduced sea-ice cover (2018) due to an extended period of primary production. However, this would likely be accompanied by a change in the copepod community composition, because diatom blooms terminate earlier in a year with reduced sea-ice cover and the community of primary producers becomes dominated by flagellates and ciliates earlier in the season, which favors the growth of small copepods (e.g. *O. similis*) (Gallienne and Robins, 2001). We therefore hypothesize that small copepods will contribute more to the total copepod secondary production during the summer with reduced sea-ice cover (2018), whereas large copepods (e.g. *Calanus* spp.) will contribute more when the summer sea-ice cover is more extensive (2019). Furthermore, we expect the quantity and relative contribution of small copepod production to total copepod production to be higher in habitats with higher water temperatures and a higher abundance of ciliates and dinoflagellates. Conversely, in habitats characterized by colder water temperatures and higher concentrations of chlorophyll *a*, which are typically associated with increased phytoplankton biomass and greater diatom abundance, we expect the production of large *Calanus* spp. and their contribution to total copepod production to be higher.

# 2 Material and methods

## 2.1 Study area

Samples and measurements were collected in the northern Barents Sea as part of The Nansen Legacy project, during cruises of RV *Kronprins Haakon* in August 2018 (06.-23.08.2018) and August 2019 (05.-27.08.2019). The study sections, where stations were located, covered an environmental gradient from Atlantic to Arctic waters (76°-83° N, Table 1; Figures 1A, C). Samples were collected at 8 stations in 2018 and 6 stations in 2019 and were categorized according to their locations. Station P1 was in Atlantic waters south of the polar front and is seen as a representative of 'Atlantic' environmental conditions. Stations P2-P5 were located north of the polar front on the Barents Sea shelf and are seen as representing 'Barents Sea shelf' conditions and stations P7, PICE1 and SICE2-3 were located in the deeper Arctic Ocean basin, representing 'Arctic Ocean basin' conditions. Stations P1-P5 were visited in both years, and among these stations P4 and P5 were in ice-free waters at the time of sampling in 2018 and in ice-covered waters during sampling in 2019 (Table 1). PICE1 and SICE2-3, only visited in 2018, were also ice covered, as well as P7, which was only visited in 2019.

## 2.2 Zooplankton sampling

Zooplankton was collected with stratified net hauls using two separate MultiNet® Type Midi (HYDRO-BIOS Apparatebau GmbH, net opening 0.25 $m^2$), one with 64 µm and one with 180 µm mesh size net bags. The depth intervals for the shallow shelf stations were: bottom-200, 200-100, 100-50, 50-20 and 20-0 m. Where bottom depth exceeded 600 m, zooplankton was collected from the following depth strata: bottom-600, 600-200, 200-50, 50-20, 20-0 m. The 180 µm net was hauled with a speed of 0.5 m $s^{-1}$ and the 64 µm with a speed of 0.3 m $s^{-1}$ to warrant optimal water filtering. All samples were processed immediately upon retrieval of the nets. The samples were concentrated on 64 µm and 180 µm sieves respectively, gently flushed with filtered sea water, and stored in 125 mL bottles with 4% formaldehyde-seawater solution free from acid. Due to unpredictable failures of water flow meters installed in the plankton nets used, the volume of filtered water was calculated based on a regression equation describing the

TABLE 1 Location and bottom depth at the stations where zooplankton samples were collected in August 2018 and August 2019.

| 2018 station # | Date of sampling | Latitude | Longitude | Bottom depth (m) | Ice covered on day of sampling | Days since ice retreat (< 15% sea ice concentration) | comments | 2019 station # | Date of sampling | Latitude | Longitude | Bottom depth (m) | Ice covered on day of sampling | Days since ice retreat (< 15% sea ice concentration) | comments |
|---|---|---|---|---|---|---|---|---|---|---|---|---|---|---|---|
| P1 | Aug 09 | 76.00 | 31.23 | 325 | no | 219 | always ice free | P1 | Aug 08 | 76.00 | 31.22 | 325 | no | 92 | 11 days of loose drift ice in May |
| P2 | Aug 10 | 77.50 | 34.00 | 192 | no | 88 | | P2 | Aug 12 | 77.50 | 33.99 | 186 | no | 43 | |
| P3 | Aug 12 | 78.75 | 34.00 | 305 | no | 83 | | P3 | Aug 13 | 78.75 | 34.00 | 307 | no | 45 | |
| P4 | Aug 14 | 79.75 | 34.00 | 335 | no | 73 | | P4 | Aug 14 | 79.69 | 34.23 | 353 | yes | 32 | loose drift ice 6 days before and 2 days after sampling |
| P5 | Aug 15 | 80.50 | 34.00 | 163 | no | 79 | | P5 | Aug 15 | 80.50 | 33.99 | 163 | yes | 0 | ice covered for another 16 days |
| PICE1 | Aug 17 | 83.35 | 31.58 | 3930 | yes | 0 | always ice covered | | | | | | | | |
| SICE2 | Aug 19 | 83.34 | 29.30 | 3920 | yes | 0 | always ice covered | | | | | | | | |
| SICE3 | Aug 20 | 83.23 | 25.87 | 3911 | yes | 0 | always ice covered | | | | | | | | |
| | | | | | | | | P7 | Aug 21 | 81.93 | 29.14 | 3300 | yes | 0 | always ice covered |

The presence of ice cover (yes/no) and the number of days that have passed since the ice retreated from each station are indicated.





10.3389/fmars.2024.1308542

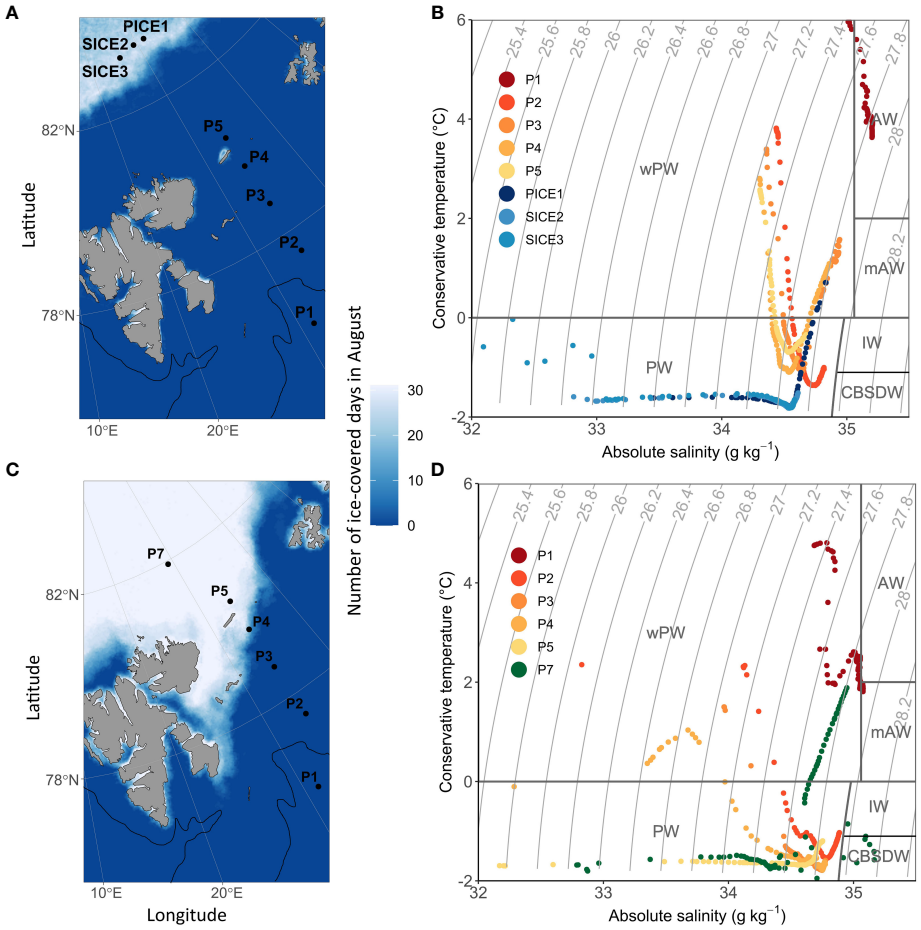


FIGURE 1
Location of the sampling stations and sea-ice cover during the sampling period (indicated as number of ice-covered days during August) in 2018 **(A)** and 2019 **(C)**. The approximate location of the polar front based on the 200 m isobath is indicated with a black line. During the sampling campaign in 2018, sea ice was only present at stations PICE1 and SICE2-3 in the Arctic Ocean basin. During the 2019 sampling campaign, sea ice was present at P4, P5 and P7. **(B)** shows a t-s-plot of water masses in 2018 and **(D)** in 2019 (PW, Polar Water; IW, Intermediate Water; CBSDW, Cold Barents Sea Dense Water; wPW, warm Polar Water; AW, Atlantic Water; mAW, modified Atlantic Water, following definitions by Sundfjord et al., 2020).

relationship between the volume of water filtered through the net and depth strata:

$$\text{Volume filtered } (m^3) = -1.2682 + 0,3298 * (\text{lower layer depth } [m] - \text{upper layer depth } [m])\ (N = 537,\ R2 = 0.789,\ p = 0.000)\,.$$

The equation is based on a data set consisting of numerous zooplankton collections using MultiNet plankton nets conducted in the Barents Sea area, e.g. from projects 'On Thin Ice', 'Cabanera', 'MariClim'. This model equation is valid for depth strata ranging from 20 m to 400 m. For water layers <20 m, the volume of filtered water was calculated based on the relationship: Volume filtered ($m^3$) = net opening area * (lower layer depth [m] - upper layer depth [m]), assuming the filtration efficiency declared by the manufacturer (in the range of 90%).

Zooplankton samples were analyzed under an Olympus SZX7 dissecting microscope (OM Digital Solutions GmbH) equipped with an ocular micrometer following methods described in Postel et al. (2000) and Kwasniewski et al. (2010). In the first step, the zooplankton sample was filtered from the preservative solution of formaldehyde, suspended in a beaker with fresh water and then all large zooplankton (total length >5 mm) were removed, identified, and counted in their entirety. Smaller zooplankton (total size <5 mm) were identified and counted from sub-samples taken from a fixed sample volume using a macro pipette. In this case, at least five subsamples were analyzed in detail, assuming that the number of organisms identified and counted was not less than 500 individuals. If the number of individuals in 5 subsamples was smaller, further subsamples were taken until at least 500 zooplankton individuals from the smaller than 5 mm fraction were identified and counted. All zooplankton individuals were identified to the lowest possible taxonomic level, also specifying developmental stage (copepodid stage for copepods). The remaining sample was scanned to detect rare species and developmental stages. The species distinction between *Calanus finmarchicus*, *C. glacialis* and younger developmental stages of *C. hyperboreus* was made based on the length of the prosome, using the size classes established in the study by Kwasniewski et al. (2003). This approach likely introduces some bias in our data, as studies

using molecular tools have shown a high but regionally variable overlap in prosome lengths of *C. finmarchicus* and *C. glacialis*, which often leads to an underestimation of *C. glacialis* (e.g., Gabrielsen et al., 2012; Choquet et al., 2018). However, as the results of molecular species analysis for our study region are currently not available to us and the vast majority of ecological studies of zooplankton to date, including studies on species distribution patterns, are based on using size classes to distinguish between *Calanus* species (e.g. Unstad and Tande, 1991; Hirche et al., 1994; Basedow et al., 2004; Kosobokova and Hirche, 2009; Kosobokova et al., 2011; Wold et al., 2023), our data should nevertheless provide insights into *Calanus* species distribution in comparison with previous observations. We followed Roura et al. (2018), who defines small copepods as those having adult body size of <2 mm. Consequently, abundance of 'small copepods' was represented by *Acartia longiremis*, *Centropages hamatus*, Harpacticoida spp. indet., *Oithona atlantica*, *O. similis*, *Microcalanus* spp., *Microsetella norvegica*, *Neomormonilla* spp., *Oncaea* spp., *Pseudocalanus* spp., *Scolecithricella minor* and *Triconia borealis*. Abundance of 'large copepods' was represented by Aetideidae, *C. finmarchicus*, *C. glacialis*, *C. hyperboreus*, *Gaetanus tenuispinus*, *Heterorhabdus norvegicus*, *Metridia longa*, *Scaphocalanus brevicornis* and *Paraeuchaeta* spp. The samples from the 64 µm and 180 µm gauze nets were analyzed separately, and the analytical results were then combined. Abundance data of copepod nauplii, all stages of 'small copepods', as well as all early developmental stages (CI-CIII) of 'large copepods', were obtained from the 64 µm net results. Abundance data of older developmental stages (CIV-adult) of 'large copepods' were based on 180 µm net results. Copepod abundance was converted into biomass, based on species and stage-specific carbon mass relationships (Supplementary Table 1). Copepod stage specific carbon mass was obtained from literature if available. For copepod species and life stages for which no published carbon mass was available, a conversion factor of 0.4 (individual dry weight to carbon weight) was used (Peters and Downing, 1984). For further analyses, we only used data on copepod abundance (ind. $m^{-2}$) and biomass (mg C $m^{-2}$) integrated for the upper 100 m at individual stations (including three net sampling depth strata: 0-20, 20-50 and 50-100/50-200 m). In the case where samples were taken over a depth range of 50-200 m (P7, PICE1, SICE2, SICE3), the abundance in the 50-100 m depth strata was calculated as one third of the abundance of the 50-200 m depth strata, assuming an even distribution of zooplankton in this layer of water. While this approach might potentially lead to an underestimation of copepod production in these depth strata, a comparison using one third or the total abundance or biomass in the 50-200 m depth layer indicated that it had minimal impact in our study and did not change the main results or conclusions. This is due to the comparatively low abundance and biomass in the deep layers of the Arctic Ocean basin (P7, PICE1, SICE2, SICE3).

## 2.3 Secondary production calculation

Daily copepod secondary production $p$ (mg C $m^{-2}$ $d^{-1}$) in the upper 100 m was calculated using the following Equation 1, (Runge and Roff, 2000):

$$p = \sum Bi \times gi \quad (1)$$

Where $Bi$ is copepod stage specific biomass for the upper 100 m (mg C $m^{-2}$) and $gi$ stage specific growth rate ($d^{-1}$).

Here, $gi$ was determined for nauplii, copepodids and adults of individual broadcast-spawning and sac-spawning copepod species using the multiple linear regression model of Hirst and Lampitt (1998), taking temperature and body weight into consideration (Table 2; Supplementary Table 1: distinction of broadcast- and sac-spawning copepod species). We chose the Hirst and Lampitt (1998) growth model, as it reflects the physiological performances of copepods at low water temperatures relatively realistically and has been used in previous studies on copepod secondary production in Arctic regions (e.g. Liu and Hopcroft, 2006; Madsen et al., 2008). This global model can be used to calculate growth rates of actively growing copepod populations in the epipelagic layer of polar to tropical regions (Hirst and Lampitt, 1998). The present study focuses solely on the upper 100 m water column, as copepods found in this depth range are assumed to be active. We are aware that some copepods below 100 m will be active and hence contribute to the total copepod production in the ecosystem. Therefore, our production estimates may be considered conservative. An alternative approach would be to estimate production for the entire water column – hence also to include the deeper communities. However, we believe this would significantly overestimate the production estimates. Diapause plays a crucial role in the life cycle of *Calanus* spp., where individuals that have acquired enough lipids descend into deeper water layers in late summer, to hibernate at depth until the next spring bloom (Falk-Petersen et al., 2009). Therefore, including hibernating individuals below 100 m (Ashjian et al., 2003) would overestimate secondary production. The majority of small copepod species, such as *Oithona* spp. and *Pseudocalanus* spp., can be found above a depth of 150 m in summer months in Arctic waters, with highest abundance recorded in the upper 50 m water column (Lischka and Hagen, 2005; Madsen et al., 2008; Darnis and Fortier, 2014). Mesopelagic, omnivorous copepods, such as *Metridia longa* and *Microcalanus* spp., and carnivorous copepods, such as *Paraeuchaeta* spp., are only sporadically found in the upper

TABLE 2 Equations used to calculate stage specific growth rates of sac spawning and broadcast spawning copepods, after Hirst and Lampitt (1998).

| | | |
|---|---|---|
| sac spawners | nauplii + copepodids | $log_{10}g = -1.4647 + 0.0358[T]$ |
| | adults | $log_{10}g = -1.7726 + 0.0385[T]$ |
| broadcast spawners | nauplii + copepodids | $log_{10}g = 0.0111[T] - 0.2917[log_{10}BW] - 0.6447$ |
| | adults | $log_{10}g = 0.6516 - 0.5244[log_{10}BW]$ |

100 m (Darnis and Fortier, 2014) and are therefore not the focus of the present study. Furthermore, currently there is a shortage of models that can accurately estimate the growth rates of these kind of copepods (Kobari et al., 2019). We therefore decided to use the first approach of estimating secondary production for the upper 100 m only, with a potential underestimation of production – rather than to include all depth layers and risk an overestimation of the production.

## 2.4 Supplementary physical and biological data

In addition to sea-ice cover, multiple other biological and environmental factors can influence the copepod community composition and their production, such as water temperature and salinity (e.g. Daase and Eiane, 2007; Trudnowska et al., 2016; Balazy et al., 2018), the protist community composition (e.g. Levinsen et al., 2000; Leu et al., 2011) and primary production (e.g. Svensen et al., 2019). We therefore included data on water column temperature and salinity, chlorophyll *a* concentration, protist abundance, primary production, and bacterial production rates, collected during the same cruises as part of The Nansen Legacy project, in our statistical analyses. Detailed sampling procedures for the environmental and biological properties measured can be found in The Nansen Legacy sampling protocol (The Nansen Legacy, 2020).

### 2.4.1 Sea-ice concentration

A dataset containing daily sea-ice concentrations for each of the sampling stations in 2018 and 2019 was obtained from the data portal of the Norwegian Polar Institute (Steer and Divine, 2023). Daily sea-ice concentrations were derived from a 6.25 km resolution gridded sea-ice concentration product based on AMSR-E and AMSR2 passive microwave sensors. The satellite derived sea-ice concentration dataset was complemented with local sea-ice concentration from visual bridge-based sea ice observations, conducted following ASSIST Ice Watch protocol during some of the Nansen Legacy cruises to the study area. To visualize the sea-ice cover during the study period, AMSR2 sea-ice concentration data were obtained from the data archive of the University Bremen (Spreen et al., 2008) for the Svalbard region for each day in August 2018 and August 2019. The data was then processed by classifying each grid cell (3.125 km grid spacing) in the Barents Sea as either ice-free (0) or ice-covered (1) based on a threshold of less than 15 % sea-ice coverage representing ice-free conditions. Finally, the number of ice-covered days for each grid cell was determined by summing up the number of days classified as ice-covered, giving a range between 0-31 days of ice cover in August.

### 2.4.2 Hydrography

Data on hydrography of the sampling area was obtained from the Svalbard Integrated Arctic Earth Observing System (SIOS) data portal (Ingvaldsen, 2022; Reigstad, 2022). The data, consisting of depth profiles of water column salinity and temperature, were obtained using a rosette-mounted conductivity-temperature-depth (CTD) sensors mounted on the SBE911+ probe from Sea-Bird Electronics. Data were processed following standard procedures as recommended by the manufacturer and were averaged to 1 m vertical bins before plotting. We applied the suggested water mass definitions for the central and northern Barents Sea (Sundfjord et al., 2020), based on conservative temperature CT, absolute salinity SA and potential density values, following TEOS-10 convention.

### 2.4.3 Chlorophyll *a*

Values of acid-corrected chlorophyll *a* concentration at the stations along the transect were obtained from the SIOS data portal (Vader, 2022a, Vader, 2022b). Water for the measurements was collected with 10 L Niskin bottles mounted on a CTD rosette at nine depths: 5, 10, 20, 30, 40, 50, 60, 90 m and at the fluorescence maximum. Chlorophyll *a* was extracted with methanol using GF/F filters following the Holm-Hansen and Riemann (1978) procedure and its concentration was measured on board, using a Turner Design AU10 fluorometer.

### 2.4.4 Protist abundance

Abundance data of pelagic marine protists (cells $L^{-1}$) at the study stations were obtained from the SIOS data portal (Assmy et al., 2022a, Assmy et al., 2022b). Samples were collected with Niskin bottles mounted on a CTD rosette at depths: 5, 10, 30, 60, 90 m and at deep chlorophyll maximum. The samples were preserved using a mixture of glutaraldehyde and hexamethylenetetramine-buffered formalin at final concentrations of 0.1% and 1%, respectively. The organisms were identified and counted under an inverted microscope according to the Utermöhl method (Utermöhl, 1958).

### 2.4.5 Primary production

Primary production rates at selected stations (2018: P1, P2, P4, PICE; 2019: P1, P4, P5, P7) were estimated by measuring $^{14}C$ uptake during *in situ* incubations. Water was collected from a CTD rosette at 10, 20, 40, 60, 90 m and at the fluorescence maximum. The samples were stored in a dark and cold environment until processing, no longer than one hour. Two 250 mL polystyrene incubation bottles, one clear and one dark, were filled with water from each depth. $NaH_{14}CO_3$ was added to each incubation bottle to a final activity of 0.1 mCi/mL. Two 250 µL subsamples of each incubation bottle were fixed with 250 µL pure ethanolamine to quantify total added carbon. Both bottles were then incubated at their corresponding sampling depths, attached to a freely drifting mooring rig. After 18 to 24 hours, the bottles were recovered, and their contents filtered onto 25 mm Whatman GF/F filters at low vacuum pressure. The filters were transferred to 20 mL scintillation vials, and 750 µL concentrated HCl was added to remove the unincorporated inorganic carbon. The samples were stored in the dark until analysis, at which point 10 mL of scintillation cocktail (Ecolume) was added before analysis in a scintillation counter (Tricarb). Samples were counted for 10 minutes.

### 2.4.6 Bacterial production

Bacterial production rates at selected stations (2018: P1-P5, PICE; 2019: P1-P5, P7) were measured using the method of 3H-leucine incorporation according to Smith and Azam (1992). In short, four replicates of 1.5 mL of seawater, collected at depths of 5, 10, 20, 40, 60, 90, 120 m and at maximum fluorescence using Niskin bottles mounted on a CTD rosette, were distributed in 2 mL Eppendorf vials. To one replicate, 80 µL of 100% trichloroacetic acid (TCA) were immediately added to serve as control. All replicates were incubated with 3H-leucine (25-nM final concentrations) for 2h at *in situ* temperature (temperature measured at the sampling depth) and stopped through addition of 80 µL of 100% TCA. For the analysis, samples were first centrifuged for 10 min at 14,800 rpm and subsequently washed with 5% TCA (repeated three times). 5 mL of scintillation liquid (Ultima Gold) was added after the final step and the radioactivity in the samples was counted on a Perkin Elmer Liquid Scintillation Analyzer Tri-Carb, 2800TR. The measured leucine incorporation was converted to µg carbon incorporated per L per hour according to Simon et al. (1992). Datasets for bacterial production measurements in August 2018 and August 2019 can be found at NMDC (Müller, 2023a, Müller, 2023b).

## 2.5 Statistical analyses

Data on copepod abundance (ind. $m^{-2}$), biomass (µg C $m^{-2}$) and secondary production (µg C $m^{-2}$ $d^{-1}$) were aggregated at different taxonomic resolutions, combining across all developmental stages, using the following groupings: Calanoida nauplii, *Calanus finmarchicus*, *C. glacialis*, *C. hyperboreus*, *Microcalanus* spp., *Pseudocalanus* spp., Cyclopoida nauplii, *Oithona* spp., other Cyclopoida (including predominantly *Triconia borealis*), *Microsetella norvegica* and 'other copepods' (Table 3, representative species and life stages used in the grouping). Data was tested for normal distribution using the Shapiro-Wilk test. Prior to the analysis, data on abundance were fourth root transformed and data on biomass and secondary production were $\log_{10}(x+1)$ transformed to approximate the normal distribution and stabilize variances. All statistical analyses of the copepod community were performed on abundance, biomass, and secondary production data from three depth strata (0-20, 20-50, 50-100 m) at stations along the study transect in 2018 and 2019. Because of non-replicated zooplankton tows, we used the different depth strata as replicates within each station, to be able to perform statistical tests on the dataset.

To test whether bulk abundance, biomass, and secondary production of the total copepod community and of individual copepod species differed significantly between the two years (2018 and 2019) and locations (stations P1, P2, P3, P4, P5, which were sampled in both years), two-ways Analyses of Variance (ANOVA) were performed for the dominant copepod species mentioned above.

To test whether there was a significant difference in copepod community composition between the two years (2018 and 2019) and locations (stations P1, P2, P3, P4, P5), a permutation test was performed for a Constrained Correspondence Analysis (CCA) on abundance data and for a Redundancy Analysis (RDA) on biomass and secondary production data. Due to the nature of the data, a CCA was chosen for the abundance data (count data appropriate for Chi-square distances) and an RDA for biomass and secondary production data (both continuous variables appropriate for Euclidean distances). The explanatory variables in the CCA and RDAs included year and location. The interaction term (year x location) was included in the model to capture interannual differences of the copepod community along the transect. The significance of the overall model and individual terms were obtained by permutation testing (1000 permutations) at a significance level of $\alpha = 0.05$.

To test the effect of environmental variables on the copepod community composition at stations in the two years, a CCA was performed on abundance data, whereas an RDA was performed on biomass and secondary production data. Included stations were P1-P5, P7, PICE1, SICE2, SICE3. The explanatory variables in the CCA and RDAs were selected based on ecological relevance and included water temperature (conservative temperature, °C) and salinity (absolute salinity, g $kg^{-1}$), number of ice-free days, and integrated chlorophyll *a* concentration (mg Chl a $m^{-2}$ for the upper 100 m water column). Because temperature and number of ice-free days were highly correlated, the temperature residuals were extracted

TABLE 3 Copepod groupings used for the statistical analyses, with representative species and life stages.

| Groupings used in the statistical analyses | Main copepod species and life stages |
|---|---|
| Calanoida nauplii | *Calanus* spp., *Pseudocalanus* spp. and other Calanoida nauplii |
| *Calanus finmarchicus* | *Calanus finmarchicus* CI-CVI |
| *C. glacialis* | *C. glacialis* CI-CVI |
| *C. hyperboreus* | *C. hyperboreus* CI-CVI |
| *Microcalanus* spp. | *Microcalanus* spp. CI-CVI |
| *Pseudocalanus* spp. | *Pseudocalanus* spp. CI-CVI |
| Cyclopoida nauplii | *Oithona* spp. and other Cyclopoida nauplii |
| *Oithona* spp. | *Oithona similis* CI-CVI, *Oithona atlantica* CI-CVI |
| other Cyclopoida | *Triconia borealis*, *Oncaea* spp. CI-CVI |
| *Microsetella norvegica* | *Microsetella norvegica* CI-CVI |
| other copepods | Aetideidae, *Acartia longiremis*, *Centropages hamatus*, *Gaetanus tenuispinus*, *Heterorhabdus norvegicus*, Harpacticoida spp. indet., *Neomormonilla* spp., *Metridia longa*, *Scaphocalanus brevicornis*, *Scolecithricella minor*, *Paraeuchaeta* spp. |

using a linear model relating temperature to ice-free days. These temperature residuals were further used in the analyses and were representative of temperature variations within the water column decoupled from the spatial trend in sea-ice cover. Using temperature residuals also ensured that secondary production was not correlated with the same temperature data set that was used in the secondary production calculations. Model assumptions (linearity, variance heterogeneity and normality) were checked via exploratory data analyses and regression diagnostics. Salinity was square root transformed and number of ice-free days was $\log_{10}(x+1)$ transformed, due to their skewed distributions. The significance of the overall model and individual terms were obtained by permutation testing (1000 permutations) at a significance level of $\alpha = 0.05$.

In the constrained multivariate analysis, we could only include salinity, temperature, integrated chlorophyll *a*, and number of ice-free days as explanatory variables, due to missing values of other biological and environmental drivers at some of the sampling stations. However, primary production rate, bacterial production rate, ciliate abundance, dinoflagellate abundance and diatom abundance can be of high ecological relevance to secondary production. To explore the relationship between copepod secondary production and these additional environmental and biological drivers, a Principal Component Analysis (PCA) was performed on the copepod secondary production variables, and the explanatory variables were then superimposed on the biplot by relating these to the principal components (PC1, PC2).

All data processing, statistical analyses and visualizations were performed using R version 4.2.2. The multivariate ordination analyses and permutation tests were performed with R package Vegan (Oksanen et al., 2023). Station maps were plotted in R using the GGOceanmaps package (Vihtakari, 2022) and Bathymetry data from the National Geophysical Data Center (NOAA National Geophysical Data Center 2009).

# 3 Results

## 3.1 Physical properties: sea ice and hydrography

Sea-ice cover and water mass distribution in the study area varied between the two years. In August 2018, the ice edge was at 83°N, while it extended as far south as 80°N in 2019 (Figures 1A, C). Analysis of the sea-ice concentration in the Barents Sea in the weeks prior to the sampling campaigns revealed that in 2018 the Atlantic station P1 had been ice-free (defined as consecutive days with < 15% sea ice concentration) for 219 days, while it had only been ice-free for 92 days in 2019 (Table 1). The Barents Sea shelf stations P2, P3, P4 and P5 north of the polar front had been ice-free respectively for 88, 83, 73 and 79 days in 2018 and 43, 45, 32 and 0 days in 2019 (Table 1). All stations in the Arctic Ocean basin in 2018 (PICE1, SICE2, SICE3) and 2019 (P7) were ice covered in August (Table 1). In 2018, the sea ice in the study area started to melt around mid-May and did not form again until approximately mid-December. In 2019, on the other hand, the sea ice started to melt roughly by the end of June and formed again by the beginning of October (Amargant-Arumí et al., 2024).

The upper 100 m water column was warmer and more saline in 2018 than in 2019. In 2018, Atlantic Water was only observed at station P1, while this water mass was not present there in 2019 and was substituted with warm Polar Water (Figures 1B, D). Stations P2, P3, P4 and P5 north of the polar front were characterized by warm Polar Water in the surface layers and Polar Water in deeper layers in both years. In 2019, both temperature and salinity of the water masses decreased from south to north over the Barents Sea shelf. The Arctic Ocean basin stations in 2018 (PICE1, SICE2-3) and 2019 (P7) were characterized by Polar Water in the surface layers and warm Polar Water in deeper layers (Figures 1B, D).

## 3.2 Copepod community composition

### 3.2.1 Copepod depth distribution

In general, the majority of the copepods were found in the upper 100 m of the water column. At the Atlantic station P1, 85% of the entire copepod community was found in the upper 100 m in 2018, and 95% in 2019 (Figures 2A, B, diamonds representing the percentage of the copepod community that resided in the upper 100 m). On the Barents Sea shelf (stations P2-P5) approximately 66-91% of the entire copepod community was in the upper 100 m in 2018 and 84-94% in 2019 (Figures 2A, B). In the Arctic Ocean basin between 47-57% of the whole copepod community were found in the upper 100 m in 2018 (stations PICE1, SICE2-3) and 49% in 2019 (station P7, Figures 2A, B). It should be recalled that the stations in the Arctic Ocean basin were located in much deeper areas of the ocean. Of the *Calanus* population at the Atlantic station P1, 4% was found in the upper 100 m of water in 2018, while it was as much as 40% in 2019 (data not shown). On the Barents Sea shelf, 51-94% of the *Calanus* spp. community was found in the upper 100 m in 2018 and 68-94% in 2019 (data not shown). In the Arctic Ocean basin, between 72-100% of the *Calanus* spp. community was in the upper 100 m in 2018 (stations PICE1, SICE2-3) and 92% in 2019 (P7, data not shown). As the present study focuses solely on the secondary production occurring in the upper 100 m water column, e.g. does not considering *Calanus* spp. below 100 m in hibernation, the focus of the following chapters lays exclusively on the depth range of 0-100 m.

### 3.2.2 Copepod abundance

Copepod abundance in the upper 100 m was highest at the Atlantic station P1 in both years and amounted to 1052 and 1023 x $10^3$ ind. $m^{-2}$ in 2018 and 2019, respectively. The copepod community was numerically dominated by small copepods and cyclopoid nauplii (Figures 2A, B). The small copepod *Microsetella norvegica* and its nauplii were found almost exclusively at the Atlantic station P1. The total abundance of this species, including nauplii, was 225 x $10^3$ ind. $m^{-2}$ in 2018 and 40 x $10^3$ ind. $m^{-2}$ in 2019. The large copepods *Calanus* spp. reached abundance of 0.4 x $10^3$ ind. $m^{-2}$ in 2018 and 5 x $10^3$ ind. $m^{-2}$ in 2019, representing less than 0.5% of total copepod abundance in both years. Other large copepods, e.g. *Metridia longa*, were virtually absent at station P1

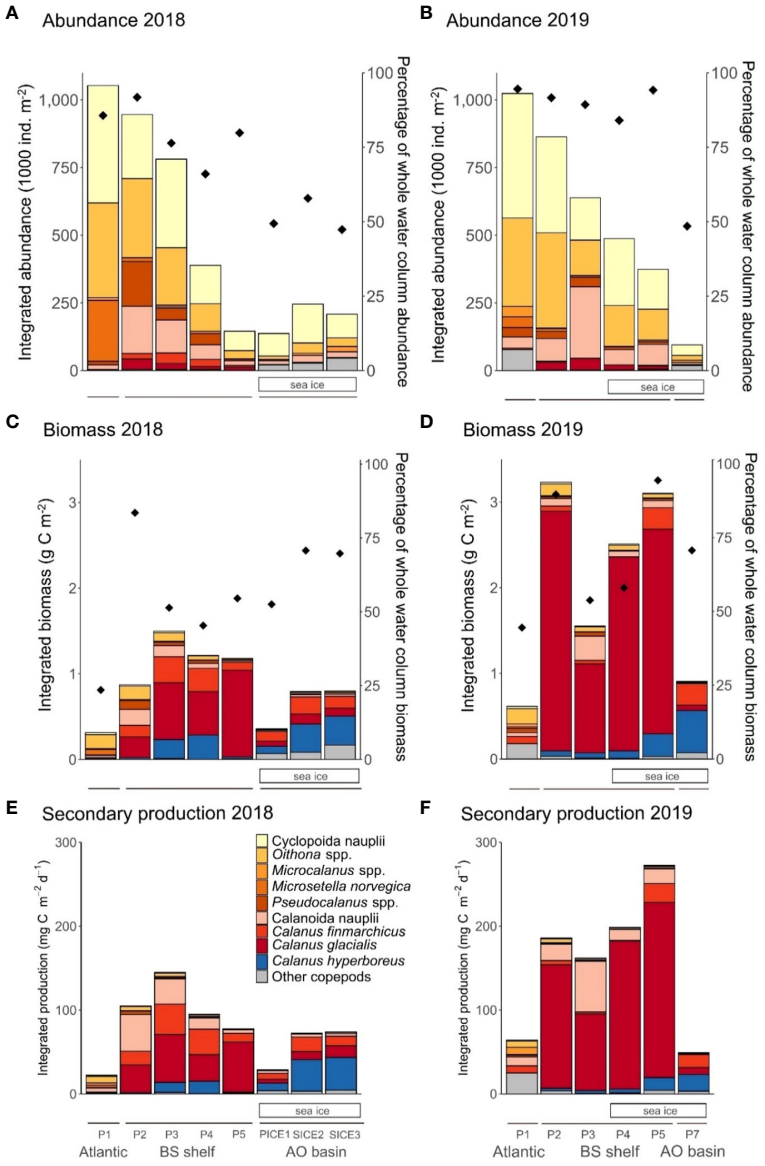


FIGURE 2
Abundance (upper panels), biomass (middle panels) and secondary production (lower panels) of dominating copepods within the upper 100 m layer at the southernmost station P1 (Atlantic), on the Barents Sea shelf (BS shelf) and in the Arctic Ocean basin (AO basin) in 2018 (left side graphs) and 2019 (right side graphs). Integrated abundance (1000 ind. $m^{-2}$) in 2018 (panel **(A)**) and 2019 (panel **(B)**), integrated biomass (g C $m^{-2}$) in 2018 (panel **(C)**) and 2019 (panel **(D)**) and integrated secondary production (mg C $m^{-2}$ $d^{-1}$) in 2018 (panel **(E)**) and 2019 (panel **(F)**) with proportions for individual copepod groups shown in the legend. Diamonds represent the percentage of the copepod community abundance (panels **(A, B)**) and biomass (panels **(C, D)**) that was located in the upper 100 m. Solid lines below the figure panels indicate the respective regions of the study section. Sea-ice cover is indicated with white rectangles under the graphs.

in 2018, whereas they represented up to 4% of the total copepod abundance at this station in 2019.

On the Barents Sea shelf (stations P2-P5) copepod abundance ranged between 145-946 x $10^3$ ind. $m^{-2}$ in 2018 and 374-863 x $10^3$ ind. $m^{-2}$ in 2019. The community was numerically dominated by small copepods and copepod nauplii in both years (Figures 2A, B). *Calanus* spp. and especially individuals in the size range of *C. glacialis*, contributed more to total abundance there. In terms of abundance, *Calanus* spp. made up 6-12% of the copepod community in 2018 (18-62 x $10^3$ ind. $m^{-2}$) and accounted for 4-7% (16-44 x $10^3$ ind. $m^{-2}$) in 2019. The species composition of the *Calanus* complex differed between the two years. *C. finmarchicus* made up 31-67% of the *Calanus* abundance on the Barents Sea shelf in 2018 and 1-17% in 2019. C. *glacialis* made up 29-68% in 2018 and 73-97% in 2019. C. *hyperboreus* made up 0.5-5% in 2018 and 1-10% in 2019. Copepod nauplii made up more than half of the total abundance of Copepoda on the shelf in both years, with cyclopoid nauplii being more abundant than calanoid nauplii. The only exception was station P3 in 2019, where the highest nauplii abundance was recorded (420 x $10^3$ ind. $m^{-2}$) and the nauplii

assemblage was dominated by calanoid nauplii, with 63% contribution to total nauplii abundance.

In the Arctic Ocean basin copepod abundance in the upper 100 m of the ocean was low in both years, ranging from 137-246 x $10^3$ ind. $m^{-2}$ in 2018 (stations PICE1 and SICE2, respectively) and 95 x $10^3$ ind. $m^{-2}$ in 2019 (station P7) (Figures 2A, B). This was only a fraction (9-23%) of the abundance found at the Atlantic station P1. The copepod community in both years consisted mainly of copepod nauplii (48-76% of total abundance) and small copepods (24-46% of total abundance), while large copepods played a minor role (0-6% of the total abundance). As for *Calanus* spp., *C. finmarchicus* accounted for approximately 60-70% in both years, while *C. hyperboreus* only accounted for 7-26% in 2018 and 34% in 2019.

### 3.2.3 Copepod biomass

In both years, the copepod biomass in the upper 100 m was highest on the Barents Sea shelf and lower at the Atlantic station and in the Arctic Ocean basin. The copepod biomass at the Atlantic station P1 amounted to 0.31 g C $m^{-2}$ in 2018 and 0.61 g C $m^{-2}$ in 2019. In 2018, *Oithona* spp., *Microsetella norvegica* (Figures 2C, D) and the nauplii of both small copepods contributed most to the copepod biomass. In 2019, the copepod biomass consisted mainly of *Oithona* spp., other small copepods (e.g. *Pseudocalanus* spp., *Triconia borealis*, *Microcalanus* spp., *Microsetella norvegica*) and *Metridia longa* (other copepods in Figures 2C, D).

Copepod biomass was the highest on the Barents Sea shelf, with a maximum of 1.50 g C $m^{-2}$ at station P3 in 2018 and a maximum of 3.21 g C $m^{-2}$ at station P2 in 2019. The main component of copepod biomass on the Barents Sea shelf was *Calanus* spp. in both years, except at the southernmost station P2 in 2018, where small copepods and copepod nauplii together accounted for 55% of the total copepod biomass, and station P3 in 2019, where calanoid nauplii constituted 18%. *Calanus* in the size range of *C. finmarchicus* made up 8-34% of *Calanus* spp. biomass on the Barents Sea shelf in 2018 and 24-44% in 2019. *C. glacialis* made up 48-90% in 2018 and 82-96% in 2019. *C. hyperboreus* made up 2-27% in 2018 and 2-9% in 2019 (Figures 2C, D).

Copepod biomass was considerably lower in the Arctic Ocean basin than in the south, with 0.06-0.80 g C $m^{-2}$ in 2018 and 0.90 g C $m^{-2}$ in 2019. Here the biomass was mainly composed of *Calanus* spp. and other large copepods and *C. hyperboreus* contributed up to 60% in *Calanus* spp. biomass in both years (Figures 2C, D).

### 3.2.4 Copepod secondary production

The secondary production of copepods in the upper 100 m was highest on the Barents Sea shelf and lower at the Atlantic station P1 and at stations in the Arctic Ocean basin. At the Atlantic station P1, total estimated secondary production was 22.3 and 64.3 mg C $m^{-2}$ $d^{-1}$ in 2018 and 2019, respectively. Small copepods (13.8 and 19.3 mg C $m^{-2}$ $d^{-1}$ 2018 and 2019, respectively) and their nauplii (1.8 and 1.4 mg C $m^{-2}$ $d^{-1}$ 2018 and 2019, respectively) contributed considerably to the total copepod secondary production (Figures 2E, F). The production of large copepods at the Atlantic station was only 1.9 mg C $m^{-2}$ $d^{-1}$ in 2018 while it was 32.7 mg C $m^{-2}$ $d^{-1}$ in 2019.

The total estimated secondary production on the Barents Sea shelf ranged between 77.6-144.8 mg C $m^{-2}$ $d^{-1}$ in 2018 and 162.1-272.2 mg C $m^{-2}$ $d^{-1}$ in 2019. There was a change between years in the relative contribution of different groups to total secondary production of copepods on the Barents Sea shelf. In 2018, copepod nauplii and small copepods accounted for a large part of the production in the southern-most part of the Barents Sea shelf (stations P2), while *Calanus* spp. accounted for the majority of production in the remaining northern part (stations P3, P4, P5). In 2019, *Calanus* spp. accounted for most of the copepod secondary production at all stations except station P3, where calanoid nauplii had a higher share in production, amounting to 37.2% (Figures 2E, F). *C. finmarchicus* made up 13-39% of *Calanus* spp. production on the Barents Sea shelf in 2018 and 0.2-9% in 2019. C. *glacialis* made up 41-83% in 2018 and 83-97% in 2019. C. *hyperboreus* made up 2-19% in 2018 and 2-6% in 2019 (Figures 2C, D).

The secondary production of copepods in the Arctic Ocean basin ranged from 28.9-74.0 mg C $m^{-2}$ $d^{-1}$ in 2018 to 49.2 mg C $m^{-2}$ $d^{-1}$ in 2019 and resulted mainly from the production of *Calanus* spp. (72-89% in 2018, 89% in 2019) (Figures 2E, F).

## 3.3 Distribution of copepod communities in relation to ecological drivers

### 3.3.1 Differences in bulk abundance, biomass, and secondary production

There were no significant differences in mean abundance, biomass, and secondary production of the bulk copepod community between the two years (2018, 2019). In contrast, the mean abundance of the bulk copepod community was significantly different between locations (upper 100 m, stations P1-P5, two-way ANOVA, $p < 0.001$, Supplementary Table 2). Post-hoc testing showed that the mean abundance decreased from south to north (Supplementary Figure 1A).

The only copepod species for which significant interannual differences were found was *C. finmarchicus*. The mean abundance, biomass, and secondary production of *C. finmarchicus* were significantly different between the two years (abundance, $p < 0.001$; biomass, $p = 0.007$; secondary production, $p = 0.001$, Supplementary Table 2) and the interaction between year and location had a significant effect (abundance, $p = 0.018$; biomass, $p = 0.003$; secondary production, $p = 0.002$, Supplementary Table 2). Post-hoc testing showed that the mean abundance, biomass, and secondary production of *C. finmarchicus* were higher in 2018 than in 2019 at station P2, P3 and P4 (Supplementary Figures 1, panels 7A–C).

Significant differences between locations were found for *Calanus* spp. and the small copepods *Oithona similis* and *Microsetella norvegica*. The mean biomass of the large copepods *Calanus* spp. was significantly different between the locations (biomass, $p = 0.03$, Supplementary Table 2). Post-hoc testing showed that the mean bulk biomass of *Calanus* spp. was lower at the Atlantic station P1 than at the Barents Sea shelf stations P2-P5 (Supplementary Figures 1, panel 5B). The mean bulk abundance,

biomass, and secondary production of *Oithona* spp., *Pseudocalanus* spp., *Microcalanus* spp., *Microsetella norvegica* and remaining small copepods combined were significantly different between locations (abundance, p = 0.006; biomass, p = 0.003, secondary production, p < 0.001, Supplementary Table 2). Post-hoc testing showed that the mean bulk abundance, biomass, and secondary production of small copepods decreased from south to north (Supplementary Figures 1, panels 10A–C). The mean abundance, biomass, and secondary production of the small copepods *O. similis* and *M. norvegica* varied significantly with location (*O. similis* abundance, p = 0.038; *O. similis* biomass, p = 0.020; *O. similis* secondary production, p = 0.018 and *M. norvegica* abundance, p = 0.013; *M. norvegica* biomass, p = 0.013; *M. norvegica* production, p = 0.002, Supplementary Table 2). Post-hoc testing showed that the mean abundance, biomass, and secondary production of both copepods decreased from south to north.

### 3.3.2 Copepod community composition

Multivariate analyses showed that there was no significant difference in terms of mean abundance, biomass, and secondary production of the copepod community between the two years (Table 4). The copepod community differed significantly in terms of mean abundance, biomass, and secondary production between locations (permutation test for stations P1-P5, using copepod groupings in Table 3, CCA abundance, p = 0.001; RDA biomass, p = 0.001; RDA production, p = 0.001, Table 4). Mean abundance, biomass, and secondary production of the copepod community differed significantly when testing for the interaction between year and location simultaneously (CCA abundance, p = 0.004; RDA biomass, p = 0.011; RDA production, p = 0.049, Table 4).

TABLE 4 Results of permutation testing of the copepod community in the upper 100 m (three depth strata 0-20, 20-50, 50-100 m) in relation to the two study years (2018 and 2019) and locations (stations P1-P5).

| | Factor | Variance explained (%) | p-value |
|---|---|---|---|
| Abundance | Model (Year, Location) | 59.86 | 0.001 (**) |
| | Year | 1.31 | 0.455 |
| | Location | 45.28 | 0.001 (***) |
| | Year x location | 13.27 | 0.004 (**) |
| Biomass | Model (Year, Location) | 61.96 | 0.001 (***) |
| | Year | 1.05 | 0.588 |
| | Location | 50.27 | 0.001 (***) |
| | Year x location | 10.64 | 0.011 (*) |
| Production | Model (Year, Location) | 58.49 | 0.001 (***) |
| | Year | 2.70 | 0.257 |
| | Location | 41.30 | 0.001 (***) |
| | Year x location | 14.49 | 0.049 (*) |

Permutation testing was performed for a Constrained Correspondence Analysis (CCA) on copepod abundance data and for a Redundancy Analysis (RDA) on copepod biomass and copepod secondary production data. Copepods were grouped into Calanoida nauplii, *Calanus finmarchicus, C. glacialis, C. hyperboreus, Microcalanus* spp., *Pseudocalanus* spp., Cyclopoida nauplii, *Oithona* spp., other Cyclopoida, *Microsetella norvegica*, other copepods. Significance codes are indicated as '***' 0.001, '**' 0.01, '*' 0.05.

The constrained ordination models that explained the differences in copepod community abundance (Figure 3A; CCA, p <0.01), biomass (Figure 3B; RDA, p <0.01) and secondary production (Figure 3C; RDA, p <0.01) between locations within and between the two years included salinity, temperature, chlorophyll *a* and number of ice-free days as explanatory variables. Of the explanatory variables, only number of ice-free days was significant (p = 0.001, for abundance, biomass, secondary production, Table 5). The CCA explained 27.16% of total variation in the abundance data (Table 5), with the first axis accounting for 18.05% and the second axis for 4.81%. The RDA explained 27.43% of total variation in the biomass data (Table 5), with the first axis accounting for 19.38% and the second axis for 5.15%. The RDA accounted for 28.77% of total variation in the secondary production data (Table 5), with the first axis accounting for 20.35% and the second axis for 5.72% of the explained variability. The first axis of the CCA and of the two RDAs was significant (p = 0.001, for abundance, biomass, secondary production) and was primarily related to ice-free days, which contributed most to the observed variation. The second axis of the CCA and of the two RDAs was related to higher temperature and salinity on one end (Atlantic Water) and higher chlorophyll *a* concentrations on the other end, but was not significant. Samples clustered by characteristic geographical area, with the Atlantic station P1, the Barents Sea shelf stations (P2-P5) and the Arctic Ocean basin stations (PICE1, SICE2-3, P7) separating within the ordination plane. There was no clear distinction between samples from 2018 and 2019 in the ordination (Figures 3A–C). Copepod abundance, biomass, and secondary production were positively correlated with chlorophyll *a* at the Barents Sea shelf stations and positively correlated with salinity and temperature at the Atlantic station. A negative correlation was found between copepod abundance, biomass and secondary production and number of ice-free days for the Arctic Ocean basin stations. The analyses showed that the abundance, biomass, and secondary production of *Microsetella norvegica*, *Pseudocalanus* spp. and *Oithona* spp. were positively correlated with number of ice-free days, water temperature and salinity. The abundance, biomass, and secondary production of *Calanus glacialis* was positively correlated with chlorophyll *a* concentration. The abundance, biomass, and secondary production of *C. hyperboreus, Microcalanus* spp. and other copepods (e.g. *Metridia longa*, *Paraeuchaeta* spp.) was negatively correlated with number of ice-free days (Figures 3A–C). This shows that distinct copepod communities were found in the southern and northern parts of the study transect (spread along the first axis), with *M. norvegica*, *Pseudocalanus* spp., *Oithona* spp. and *C. glacialis* being characteristic for the Atlantic and shelf community, and *C. hyperboreus, C. finmarchicus, Microcalanus* spp., *M. longa*, and *Paraeuchaeta* spp. characteristic for the Arctic Ocean basin community. The communities were either located in Atlantic

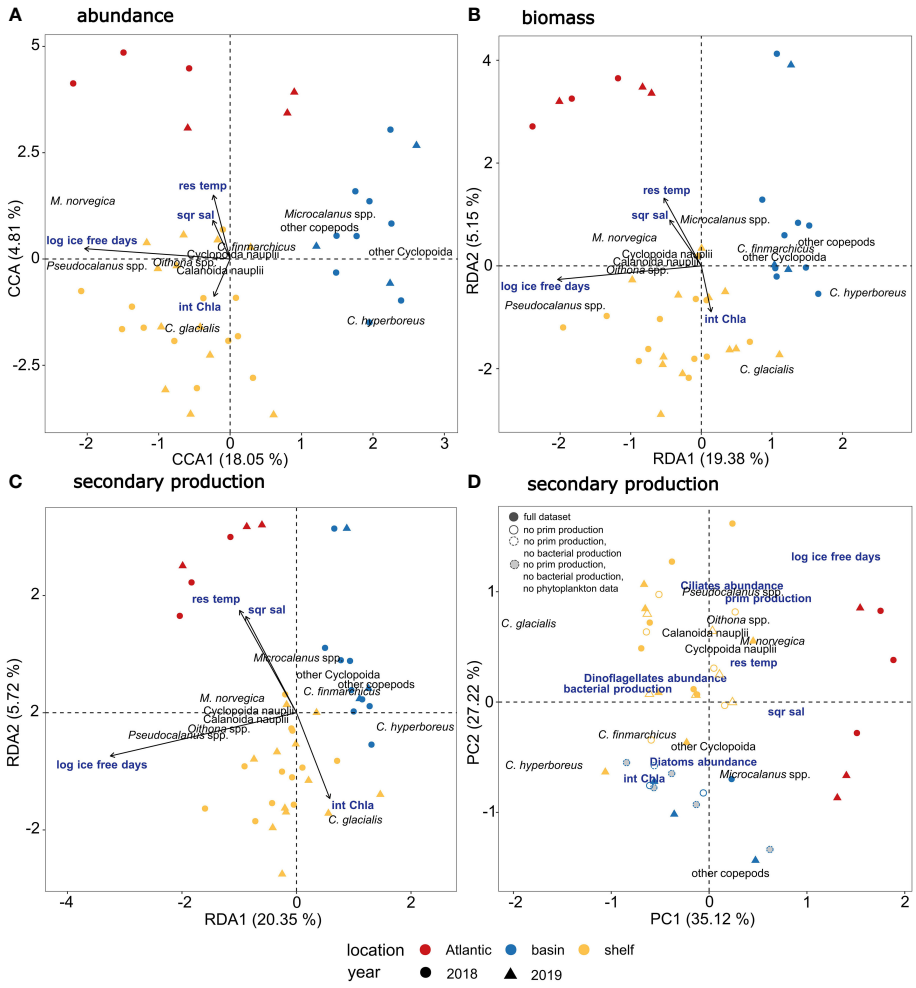


FIGURE 3
Multivariate analyses of copepod communities in relation to environmental and biological factors. **(A)** Triplot showing relationship between copepod abundance (based on fourth root transformed abundance data expressed as ind. $M^{-2}$ in three depth strata from 0-20, 20-50, 50-100 m) and environmental factors (int Chl *a* = integrated chlorophyll *a* concentration, sqr sal = square root transformed salinity, res temp = residuals of temperature and log ice free days = log transformed number of ice-free days) using Constrained Correspondence Analysis (CCA). **(B)** Triplot showing relationship between copepod biomass (based on $\log_{10}(x+1)$ transformed biomass data expressed as µg C $m^{-2}$) and environmental factors using Redundancy Analysis (RDA). **(C)** Triplot showing relationship between copepod secondary production (based on $\log_{10}(x+1)$ transformed secondary production data expressed as µg C $m^{-2}$ $d^{-1}$) and environmental factors using Redundancy Analysis (RDA). **(D)** Biplot showing Principal Component Analysis of copepod secondary production with overlaid potential drivers of secondary production, including log-transformed number of ice-free days, square root transformed salinity, residuals of temperature, integrated chlorophyll *a* concentration, bacterial production, primary production, abundance of ciliates, dinoflagellates, and diatoms. Solid filled symbols indicate samples with full dataset of environmental and biological variables, symbols with solid lines indicate that primary production was not measured, symbols with dashed lines indicate that primary production and bacterial production were not measured, grey-filled symbols with dashed lines indicate that primary production, bacterial production, and phytoplankton community composition were not measured.

waters with low phytoplankton biomass, i.e. low integrated chlorophyll *a*, or in other water masses with higher phytoplankton biomass (sample points spread along the second axis).

A Principal Component Analysis (PCA) revealed that the secondary production of small copepods (e.g. *Oithona* spp., *Pseudocalanus* spp., *M. norvegica*) on the Barents Sea shelf and in the Atlantic region was positively correlated with number of ice-free days and was furthermore associated with a higher primary production rate and ciliate abundance (Figure 3D). The secondary production of *C. finmarchicus* and *C. hyperboreus* and other copepods in the Arctic Ocean basin was positively correlated with integrated chlorophyll *a* values, and also associated with higher diatom abundance. The high secondary production of *C. glacialis* on the Barents Sea shelf was associated with a higher bacterial production rate and higher dinoflagellate abundance. Both the bacterial production rate and dinoflagellate abundance were negatively correlated with salinity and temperature (Figure 3D). Hence, different environmental drivers seemed to influence the copepod communities in the southern and northern parts of the study area.

TABLE 5 Results of permutation testing of the copepod community in the upper 100 m (three depth strata 0-20, 20-50, 50-100 m) at stations P1-5, P7, PICE1, SICE2 and SICE3 in relation to environmental and biological variables (int_Chla = integrated chlorophyll a concentration, res_temp = residuals of temperature, log_ice_free_days = log transformed number of ice-free days and sqr_sal = square root transformed salinity.

| | Factor | Variance explained (%) | p-value |
|---|---|---|---|
| Abundance | Model (int_Chla, res_temp, log_ice_free_days, sqr_sal) | 27.16 | 0.001*** |
| | int_Chla | 2.18 | 0.360 |
| | res_temp | 3.77 | 0.091. |
| | log_ice_free_days | 17.52 | 0.001*** |
| | sqr_sal | 3.69 | 0.106 |
| Biomass | Model (int_Chla, res_temp, log_ice_free_days, sqr_sal) | 27.43 | 0.001*** |
| | int_Chla | 1.87 | 0.447 |
| | res_temp | 3.96 | 0.053. |
| | log_ice_free_days | 18.31 | 0.001*** |
| | sqr_sal | 3.29 | 0.124 |
| Production | Model (int_Chla, res_temp, log_ice_free_days, sqr_sal) | 28.77 | 0.001*** |
| | int_Chla | 2.22 | 0.324 |
| | res_temp | 3.97 | 0.080. |
| | log_ice_free_days | 18.50 | 0.001*** |
| | sqr_sal | 4.11 | 0.058. |

Copepods were grouped into Calanoida nauplii, *Calanus finmarchicus, C. glacialis, C. hyperboreus, Microcalanus* spp., *Pseudocalanus* spp., Cyclopoida nauplii, *Oithona* spp., other Cyclopoida, Microsetella norvegica, other copepods. Significance codes are indicated as '***' 0.001, '.' 0.1.

# 4 Discussion

## 4.1 Effect of interannual variation of sea-ice cover on copepod secondary production

Since the cold climate period in the late 1970s, the Barents Sea has undergone a warming trend (Bagøien et al., 2020), marked by notable interannual and multidecadal variability, resulting in an overall sea surface temperature increase of about 1.5°C (Mohamed et al., 2022). In this perspective, the two investigated years were both relatively warm years, although on a generally slightly cooling trend since the record warm year 2016 (Bagøien et al., 2020). There were differences in environmental drivers in the Barents Sea between the two years of study, which influenced the pelagic community and its production. Most notably, in August 2018, there was no sea-ice cover across the Barents Sea shelf and the hydrography in the southernmost part of the section was shaped by Atlantic water masses. In 2019, parts of the Barents Sea shelf were still ice-covered and water temperature at the study stations was overall lower. In the ice-free summer of 2018, the microbial community in the study area was in a late post-bloom stage, while in 2019, remnants of a marginal ice-zone bloom were still observed (Kohlbach et al., 2023; Amargant-Arumí et al., 2024). Even though the microbial community in 2018 was in a later seasonal succession stage than in 2019, both communities sustained comparable primary production averaged across the transect (Amargant-Arumí et al., 2024). To understand how climate change affects the entire pelagic ecosystem, it is crucial to understand how this energy is transferred to higher trophic levels. The Barents Sea as a highly productive fishing ground and depends on copepods as key food sources for many fish species (Hassel et al., 1991; Huse and Toresen, 1996; Bouchard et al., 2017). It is therefore important to understand how the productivity patterns of copepods may be altered by changes in environmental conditions. Despite the contrasting sea-ice regimes in the two years, we did not find any statistically significant interannual differences in the mean copepod secondary production (Table 4), even though a comparison of the total integrated copepod biomass and secondary production between the two years (integrated for the upper 100 m) suggested that both were higher in 2019 than 2018 (Figures 2C–F). Instead, we found that spatial rather than interannual differences dominated the variation of copepod secondary production across the study region. Integrated bulk copepod secondary production for the upper 100 m ranged between 22.3-64.3 mg C $m^{-2}$ $d^{-1}$ in the Atlantic region, 77.6-272.2 mg C $m^{-2}$ $d^{-1}$ on the Barents Sea shelf and 28.9-74.0 mg C $m^{-2}$ $d^{-1}$ in the Arctic Ocean basin (Figures 2E, F). These values are comparable to data reported for the eastern Barents Sea (13.6-128 mg C $m^{-2}$ $d^{-1}$, assuming a dry mass to carbon mass relationship of 0.4 and integrating for the upper 100 m, Dvoretsky and Dvoretsky, 2024a) and the Barents Sea polar front (mean 70 ± 8.8 mg C $m^{-2}$ $d^{-1}$, for the whole water column, Dvoretsky and Dvoretsky, 2024b).

One possible explanation for the absence of interannual variability in the analyzed dataset is that potential interannual differences may have been masked by natural heterogeneity in the depth and spatial distribution of copepods, which is a natural feature of zooplankton and not an effect of climate change. Although the distribution of copepods within the three distinguished depth layers (0-20, 20-50, 50-100 m) did not differ much (Supplementary Figures 2-4 for copepod abundance, biomass and secondary production, respectively), similarly to the zooplankton distribution in the same region described by Wold et al. (2023), the within-group variability of copepod occurrence data across different depth layers at a station was nevertheless high. This reduced the power of the analyses and potentially masked interannual variability. Furthermore, using depth layers as replicates introduces pseudoreplication, which may lead to optimistic estimates affecting the statistical inference. But the large variance observed within stations implies that effect size must be large for significant effects to emerge. To address these challenges, a sampling plan which involves replicate sampling with vertical resolution across multiple stations within each region would be crucial, enabling the inclusion of depth as a predictor in the statistical model to correct for potential differences between depths. Unfortunately, this is a very challenging sampling plan both at sea and in the laboratory and could not be implemented, even for such a large-scale research program as The Nansen Legacy. Further

sampling efforts are needed to conclusively answer the important question of the effect of sea-ice reduction on the bulk copepod secondary production and should ideally focus on specific regions to investigate long-term trends. Despite its potential, this approach would require long-term monitoring and additional resources, posing practical challenges. At present we can discuss the question of the effects of interannual variation in sea-ice cover on copepod production based on results from short-term studies such as the present one, which, despite their limitations, provide new insights into how copepod communities respond to changes in water masses and sea ice cover.

It has previously been suggested that as the Arctic continues to warm and sea ice declines, large copepods may become less important for copepod secondary production, while the proportion of small copepods in the copepod community increases (Kimmel et al., 2018, Kimmel et al., 2023) and our observations support this notion. We found significant differences in the copepod community composition and production when comparing individual sampling sites between the two years. These changes could mainly be linked to differences in sea-ice cover at the stations between the two years. Small copepods showed the highest contribution to total copepod production at the warmer stations, but *Calanus* spp. was overall the largest contributor to secondary production in both years. The differences in community composition and secondary production of small and large copepods in 2018 and 2019 were consequences of the interplay of the sea-ice retreat, the phytoplankton bloom status and Atlantic water inflow. In the following we discuss each of these factors in the context of copepod community production.

## 4.2 Higher water temperature and the specific structuring of the microbial food web promoted secondary production of small copepods

Daily secondary production rates of 1.0-9.7 mg C $m^{-2}$ $d^{-1}$ for small copepods on the Barents Sea shelf are in good agreement with secondary production rates previously recorded in other Arctic regions. The maximum secondary production of small copepods in Disko Bay, western Greenland, in the upper 50 m water column was estimated as 15.5 mg C $m^{-2}$ $d^{-1}$ in October (Madsen et al., 2008). Secondary production values of 2.7-16.1 mg C $m^{-2}$ $d^{-1}$ were reported for small copepods in Ura Bay, when aggregating Dvoretsky and Dvoretsky (2012) mean daily secondary production rates of different copepod species and converting them to carbon mass, using a conversion factor of 0.4 (Peters and Downing, 1984). When comparing the integrated secondary production of small copepods reported in the present study to the integrated primary production in 2018, it becomes apparent that small copepods played a moderate role for carbon transport to higher trophic levels. At the Atlantic station P1, the integrated primary production in the upper 100 m was 632 mg C $m^{-2}$ $d^{-1}$ (Amargant-Arumí et al., 2024) and secondary production of small copepods was 13.8 mg C $m^{-2}$ $d^{-1}$, which equals an energy transfer of 2.2%. On the Barents Sea shelf, integrated primary production was between 652-710 mg C $m^{-2}$ $d^{-1}$ (stations P4 and P2, respectively, Amargant-Arumí et al., 2024) and secondary production of small copepods was 4.3-9.7 mg C $m^{-2}$ $d^{-1}$ (stations P4 and P2, respectively), equal to an energy transfer of 0.6-1.4%.

There were no significant interannual differences in secondary production of small copepods, but variations were observed between locations, with highest production occurring in warm waters in the southernmost part of the transect. In 2018, water temperatures in the study area were overall higher, less sea-ice was present and chlorophyll *a* concentrations were low (Kohlbach et al., 2023). In August 2018, the protist community was in a late-summer oligotrophic state, dominated by small-sized autotrophic and heterotrophic protists, predominantly flagellates and ciliates (Kohlbach et al., 2023). Highest primary production in 2018 was observed at the southernmost station of the transect (P1), where the growth of small pico- and nano-flagellated cells was sustained by nutrient input through Atlantic Water inflow (Amargant-Arumí et al., 2024). Along the rest of the transect, primary production was overall low and no latitudinal structuring of the microbial community was observed (Amargant-Arumí et al., 2024). In 2019, on the other hand, the microbial community was latitudinally structured (Kohlbach et al., 2023), with highest primary and bacterial production occurring close to the sea-ice edge (around station P4, Amargant-Arumí et al., 2024). With increasing distance to the ice-edge, higher nutrient and chlorophyll *a* concentrations were observed at deeper water layers at the southern stations. The southernmost station P1 was dominated by late-summer protist communities, including high numbers of ciliates in both years (Kohlbach et al., 2023). Our analyses showed that secondary production of small copepods (e.g. *Oithona* spp.) had a positive relationship with the number of ice-free days, which was strongly correlated with the overall water temperature in the study area (Figure 3). A positive relationship between secondary production of *O. similis* and temperature has previously been demonstrated by Balazy et al. (2021). This can be explained by the fact that egg hatching and developmental rates of copepods are positively correlated with temperature, resulting in higher secondary production at higher temperature (Nielsen et al., 2002; Dvoretsky and Dvoretsky, 2009). The development and growth of small copepods appears to depend more directly on water temperature than that of large copepods, whose production is more food dependent. Because of their size, small copepods live in conditions close to food saturation (Kiørboe and Sabatini, 1995). Furthermore, species of the genus *Oithona* prey upon a larger variety of prey items including dinoflagellates, phytoplankton, and faecal material (Gallienne and Robins, 2001), with a preference for swimming prey particles such as ciliates (Svensen and Kiørboe, 2000; Zamora-Terol et al., 2013). This makes them able to sustain higher productivity in low chlorophyll *a* conditions (Sabatini and Kiørboe, 1994), as has been observed in this study in 2018 and explains the positive correlation of secondary production with ciliate abundance that we observed. In the Bering Sea, both the abundance and secondary production of the small copepods *Oithona* spp. and *Pseudocalanus* spp. were higher during a warm period (2001–2005) compared to a cold period (2007–2011) (Hunt et al., 2011; Stabeno et al., 2012; Eisner et al., 2014; Kimmel et al., 2018). In the Barents Sea, higher abundance of small copepods has

previously been linked to higher water temperatures (Trudnowska et al., 2016; Balazy et al., 2018).

## 4.3 Water mass distribution shaped the spatial pattern of secondary production of *Calanus finmarchicus*

The daily secondary production rates of large copepods in the range of 50.8-250.7 mg C $m^{-2}$ $d^{-1}$ for the Barents Sea shelf reported in this study are in good agreement with secondary production previously recorded in other Arctic regions. The highest secondary production rates for *Calanus* spp. of 250 mg C $m^{-2}$ $d^{-1}$ have been estimated in Disko Bay, western Greenland, in the upper 50 m water column in May/June (Madsen et al., 2001). Dvoretsky and Dvoretsky (2012) reported secondary production values of 13.3-14.0 mg C $m^{-2}$ $d^{-1}$ for large copepods in Ura Bay (low copepod biomass in coastal Barents Sea area). When comparing the integrated secondary production of large copepods to the integrated primary production in 2019 it becomes apparent that large copepods were especially important for energy transfer to higher trophic levels in the marginal ice zone. On the Barents Sea shelf, integrated primary production in the upper 100 m was 261-551 mg C $m^{-2}$ $d^{-1}$ (stations P5 and P4, respectively) and secondary production of large copepods was 182.8-250.7mg C $m^{-2}$ $d^{-1}$ (stations P4 and P5, respectively), equivalent to an energy transfer of 33.2-96.1%. At the Atlantic station P1, energy transfer only equaled 10%, based on an integrated primary production of 340 mg C $m^{-2}$ $d^{-1}$ and secondary production of large copepods of 32.7 mg C $m^{-2}$ $d^{-1}$.

We observed overall higher abundance, biomass, and secondary production of *Calanus* in the size range of the boreal species *C. finmarchicus* in the year that was characterized by presence of Atlantic Water in the southern part of the study area (2018). The recent Arctic winter sea-ice retreat in the Barents Sea has been linked to a strengthening of the Atlantic water inflow into this region and warming of the water masses (Årthun et al., 2012) i.e. 'Atlantification'. As a result of this event, an increasing number of organisms from boreal regions can be advected into the Arctic (Freer et al., 2022). Currently, low water temperatures prevent the boreal species *C. finmarchicus* from establishing a population that can successfully reproduce in the Arctic Ocean (Ji et al., 2012). However, this may change with continued ocean warming and a prolonged retreat of the ice edge (Tarling et al., 2022). A modelling study by Slagstad et al. (2015) showed that with rising water temperature and increasing Atlantic water inflow, the production areas of *C. finmarchicus* will steadily expand into the Greenland Sea, northern Barents Sea, and western Kara Sea. Likewise, warming and an extended growth season due to earlier sea-ice retreat have been suggested to increase the suitability of pelagic habitats in the Fram Strait for *C. finmarchicus* (Freer et al., 2022; Tarling et al., 2022). The large fraction of smaller *Calanus* found on the Barents Sea shelf in our study indicates an advection of *C. finmarchicus* onto the shelf from the southern Barents Sea (Gluchowska et al., 2017), while those in the Arctic Ocean basin are transported into this region with the West Spitsbergen Current (Basedow et al., 2018).

## 4.4 Differences in sea-ice cover influenced *Calanus glacialis* reproduction

Significantly higher secondary production of the larger *Calanus* (i.e. *C. glacialis*) was observed in the year with extensive sea-ice cover (2019), when chlorophyll *a* concentrations were higher and the protist community was in a late-bloom stage and showed a dominance of autotrophs and large-celled phytoplankton, in particular diatoms (Kohlbach et al., 2023). Highest primary production in 2019 was found at station P5 closest to the ice edge on the Barents Sea shelf. The marginal ice zone bloom had a typical south-to-north progression, where primary production shifted into deeper water layers in the southern parts of the study area (Amargant-Arumí et al., 2024). The sea-ice breakup in 2019 was at the beginning of July, compared to mid-May in 2018, and likely resulted in a longer ice-algae season and an extended spring bloom in 2019 (Kohlbach et al., 2023). This was supported by high numbers of calanoid nauplii observed close to the ice edge at station P3 in 2019, and the presence of CI and CII at the stations south of P3, that may indicate that reproduction took place some weeks earlier. Overall, higher abundance of older *Calanus* copepodids in 2018 compared to 2019 indicated that reproduction in 2018 had started earlier than in 2019. In 2018 biomass and secondary production of *C. glacialis* (i.e. the larger size fraction of the *Calanus* population) on the Barents Sea shelf were however generally lower than in 2019, possibly due to a mismatch between the reproduction of the species and the bloom phenology, and consequently lower recruitment. The life history strategy of *C. glacialis* is tightly linked to the distribution and timing of sea-ice cover and the resulting timing of the ice-algae and phytoplankton blooms (Falk-Petersen et al., 2009; Daase et al., 2013; Feng et al., 2016, Feng et al., 2018). The nutritional quality of both ice algae and phytoplankton is highest at the beginning of the bloom (Søreide et al., 2010; Leu et al., 2011) and *C. glacialis* females can increase their reproductive output if an ice algae bloom is available to fuel egg maturation, while they must rely to a large extent on internal energy reserves from the previous feeding season in the absence of an ice algae bloom (Søreide et al., 2010). The reduction of sea-ice thickness and extent alters the current primary production regime, shortening the growth period of ice algae and advancing the onset of the open water phytoplankton growth season (Arrigo et al., 2008; Søreide et al., 2010). At sub-zero temperatures, the species' nauplii require about three weeks to develop to the first naupliar stage that feeds (Daase et al., 2011). If the phytoplankton bloom occurs shortly after the ice algae bloom, the new generation may miss the early, high-quality food phase of the bloom, thus reducing the reproductive success.

*C. glacialis* secondary production was higher in the ice-covered northern parts of the study area in 2019. However, this trend was not significant, likely due to high within-group variance compared to the number of replicates in this study. Our observations nevertheless agree with previous studies showing elevated secondary production of large *Calanus* spp. during a cold period (2007–2011) compared to a warm period with reduced sea-ice cover (2001–2005) in the Bering Sea (Hunt et al., 2011; Stabeno et al., 2012; Eisner et al., 2014; Kimmel et al., 2018, Kimmel et al., 2023).

While a mismatch scenario between *C. glacialis* reproduction and the phytoplankton bloom may explain the interannual variation in the local *Calanus* population in the Barents Sea, there is so far little evidence that sea-ice loss has been detrimental to *Calanus* populations in other parts of the European Arctic. Studies from Svalbard fjords suggest that warming and sea-ice loss benefit *C. glacialis* populations (Hatlebakk et al., 2022). Life history models by Feng et al. (2016); Feng et al. (2018) showed that early ice retreat, warming, increased phytoplankton food availability and prolonged growth season overall create favorable conditions for *C. glacialis* development, leading to a northward expansion of well prospering populations of the species as the sea ice retreats. This has been confirmed by observations from the polar basin, indicating a northwards expansion of *C. glacialis* (Kvile et al., 2019; Ershova et al., 2021).

It should be noted that due to the identification of *C. finmarchicus* and *C. glacialis* based on size alone, there is a possibility of an underestimation of *C. glacialis* abundance, as the prosome lengths of the early developmental stages of the two species may overlap for populations thriving in convergence areas. Additionally, because we only looked at communities within the upper 100 m of the water column for this study, we may also have missed parts of the *Calanus* population that have likely already descended to greater depths at this time of the year. However, including diapausing *Calanus* spp. in production estimates would likely result in an overestimation of secondary production in this area. Also, even if some *Calanus* spp. in the two years might have been misidentified, the conclusion that secondary production of large copepods in 2018 was mainly driven by *Calanus* within the size range of *C. finmarchicus* and in 2019 by *Calanus* within the size range of *C. glacialis*, would remain the same, as the differences in secondary production between the two years were pronounced.

While our data indicates that differences in bloom phenology and food availability between the two years may explain the observed changes in community composition from larger to smaller species, the presence of sea ice itself and its effect on visual predation risk may have played an important role. A recent study from the Barents Sea suggests that the prevalence of large copepods in deeper troughs and under sea ice is best explained by top-down control (Langbehn et al., 2023). Large copepods, such as *Calanus* spp., experience a reduced visual predation risk and subsequent increased survival rate where sea ice shades the water. The increased predation risk in open waters can therefore shift the community to a dominance of smaller species (Aarflot et al., 2019; Langbehn et al., 2023), which is also in accordance with our observations.

## 4.5 Changes in copepod secondary production and the marine food web

Even though our results suggest that the total secondary production in a year with less sea-ice cover is not different from a year with extended sea-ice cover, we speculate that the shift towards smaller organisms may affect the food quality and availability for planktivorous organisms, ultimately leading to food web changes. In terms of biomass, calanoid copepods are the major component of the mesozooplankton community in the Arctic (Falk-Petersen et al., 2009), due to their high lipid content that can account for 50-70% of their dry mass (Falk-Petersen et al., 2009). The lipid content of *Calanus* spp. is size rather than species specific and a shift in dominance from larger to smaller *Calanus* individuals would lead to a reduction in lipid production at the individual level, but not necessary on population level, if overall turn-over rates increase (Renaud et al., 2018). Early larval stages of many fish species, such as Atlantic herring (*Clupea harengus*), Atlantic cod (*Gadus morhua*), haddock (*Melanogrammus aeglefinus*), Alaska pollock (*Gadus chalcogrammus)* and polar cod (*Boreogadus saida*) have a specific prey preference for calanoid nauplii, due to their high lipid content in comparison to other copepod nauplii (Kane, 1984; Napp et al., 2000; Swalethorp et al., 2014; Bouchard and Fortier, 2020). Even though cyclopoid copepods, such as those of *Oithona* spp., are often found in much higher abundance than calanoid copepods, their contribution to the diet of these fish species is considerably less important (Kane, 1984; Napp et al., 2000; Swalethorp et al., 2014). In some Arctic regions, low abundance of preferred prey (e.g. *Calanus* spp., *Pseudocalanus* spp., and *Temora longicornis*) has been linked to lower recruitment of pollock (Kimmel et al., 2018) and mackerel (Lafontaine, 1999; Paradis et al., 2012). Similar to the observed trends in other regions of the Arctic, we hypothesize that the recruitment of commercially and ecologically important fish species in the Barents Sea, such as polar cod, capelin, and Atlantic herring, may be lower in years with increased water temperature and reduced summer sea-ice, due to a shift towards a more generalist diet based on smaller-sized, less lipid-rich copepods.

Zooplankton groups other than copepods can be important both in terms of abundance and biomass in the Barents Sea. Meroplankton, e.g. Bivalvia and Echinodermata larvae, emerged across the study transect in summer (Wold et al., 2023) and high abundance of arrow worms (*Parasagitta elegans*), pteropods (*Limacina helicina*) and gelatinous zooplankton were observed (Van Engeland et al., 2023; Wold et al., 2023). In the present study, we focus solely on copepod secondary production, given the pivotal role of copepods in transferring energy to higher trophic levels in Barents Sea food webs (Pedersen et al., 2021). Most of the secondary production research has focused on copepods, as the majority of available growth rate models are tailored specifically to this group. Due to the complicated life cycle of some non-copepod groups, especially gelatinous zooplankton, determination of their growth rates can be difficult (Postel et al., 2000). Therefore, total secondary production in the study area is likely higher, especially in the Atlantic region and the Arctic Ocean basin, where the contribution of non-zooplankton groups was found to be larger than in the Arctic parts of the study area (Van Engeland et al., 2023; Wold et al., 2023). Copepods can also impact the biological carbon pump through feeding on phytoplankton and aggregates, as well as through fecal pellet production (Jumars et al., 1989). Larger, current-feeding copepods, such as *Calanus* spp., can increase the flux of particulate organic carbon (POC) through efficient grazing and production of large, fast sinking fecal pellets (e.g. Riser et al., 2008). Many small copepod taxa are particle-feeders and can decrease POC export efficiency through feeding on organic particles (e.g. Koski et al.,

2020; Koski and Lombard, 2022; Mooney et al., 2023). A shift of the copepod community towards smaller-sized species will possibly be reflected in a compositional and quantitative change of the vertical flux in the Barents Sea. Indications supporting this hypothesis are the lower vertical flux in the study area in 2018 with no attenuation with depth, while the vertical flux in 2019 was higher and showed a strong attenuation profile (Amargant-Arumí et al., 2024).

## 5 Conclusions

The Barents Sea, known for its high productivity, sustains a substantial commercial fishery. Despite declining sea-ice, the impact on lower trophic levels' productivity is still under debate. In particular, the impact of environmental change on copepod secondary production is not well understood at present. We expected to find higher total bulk copepod secondary production in a summer with reduced sea-ice cover, due to a hypothesized extended period of primary production and consequently higher food availability. However, our observations did not support this hypothesis. Instead, we found that spatial rather than interannual differences dominated the observed variation of copepod secondary production in the Barents Sea. Here, Atlantic waters in summer were characterized by a high contribution of small copepods to total copepod secondary production, as they benefited from higher water temperatures and a more abundant microbial food web in this region. Copepod secondary production on the northern Barents Sea shelf, the study focus area, was overall highest and mainly driven by large *Calanus* spp. Our study shows that if environmental conditions (e.g. the presence of sea ice or water temperature) change to an appropriate extent in a habitat from year to year, this will affect the copepod community composition and its production. There were significant interannual differences of the *Calanus* spp. community composition between the two years, with the smaller *C. finmarchicus* being more important for total copepod secondary production during the summer with less sea-ice cover and in habitats characterized by higher water temperatures and a pronounced Atlantic water signal. The larger *C. glacialis*, on the other hand, was more important in the summer with extensive sea-ice cover and in habitats with lower water temperatures, sea-ice cover and with the presence and higher contribution of diatoms to pelagic primary production.

Due to high spatial heterogeneity in copepod distribution and consequently high variability in secondary production, we still cannot conclude with high confidence which effect the sea-ice decline will have on bulk copepod secondary production in the Barents Sea. Despite its limitations, our study provides important insight into the copepod community response to changes in water masses and sea-ice cover. The results of our study confirm the observations that, as a result of Arctic warming and reduced sea ice, large copepods may become less important and smaller-sized copepod species (including smaller-sized Calanus and small copepods) more important components of pelagic communities, which will have consequences for the secondary production of copepods, as well as for the role of copepods in food webs, biogeochemical cycles, including the biological carbon pump, and other functions performed by them in the ecosystem.

## Data availability statement

The original contributions presented in the study are included in the article/Supplementary Material. Further inquiries can be directed to the corresponding author.

## Ethics statement

The manuscript presents research on animals that do not require ethical approval for their study.

## Author contributions

CG: Writing – review & editing, Writing – original draft, Visualization, Methodology, Investigation, Formal analysis, Data curation, Conceptualization. MD: Writing – review & editing, Writing – original draft, Visualization, Supervision, Methodology, Conceptualization. RP: Writing – review & editing, Visualization, Supervision, Software, Methodology, Formal analysis, Data curation, Conceptualization. MA-A: Writing – review & editing, Formal analysis, Data curation, Conceptualization. OM: Writing – review & editing, Formal analysis, Data curation, Conceptualization. AW: Writing – review & editing, Investigation, Data curation, Conceptualization. MO: Writing – review & editing, Formal analysis, Data curation. SK: Writing – review & editing, Writing – original draft, Supervision, Methodology, Formal analysis, Data curation. CS: Writing – review & editing, Writing – original draft, Supervision, Methodology, Funding acquisition, Data curation, Conceptualization.

## Funding

The author(s) declare financial support was received for the research, authorship, and/or publication of this article. This work was funded by the Research Council of Norway through the project The Nansen Legacy (RCN # 276730).

## Acknowledgments

We would like to thank the captain and crew of R/V Kronprins Haakon for their excellent support at sea during the Nansen Legacy research cruises in 2018 (JC1-2) and 2019 (Q3). We would like to thank the Institute of Oceanology of the Polish Academy of Sciences (IO PAN) for cooperation in laboratory analysis of zooplankton samples.

## Conflict of interest

The authors declare that the research was conducted in the absence of any commercial or financial relationships that could be construed as a potential conflict of interest.

## Publisher's note

All claims expressed in this article are solely those of the authors and do not necessarily represent those of their affiliated organizations, or those of the publisher, the editors and the reviewers. Any product that may be evaluated in this article, or claim that may be made by its manufacturer, is not guaranteed or endorsed by the publisher.

## Supplementary material

The Supplementary Material for this article can be found online at: https://www.frontiersin.org/articles/10.3389/fmars.2024.1308542/full#supplementary-material

## References


Aarflot, J. M., Aksnes, D. L., Opdal, A. F., Skjoldal, H. R., and Fiksen, Ø. (2019). Caught in broad daylight: topographic constraints of zooplankton depth distributions. *Limnol. Oceanogr.* 64, 849–859. doi: 10.1002/lno.11079

Amargant-Arumí, M., Müller, O., Bodur, Y. V., Ntinou, I. V., Vonnahme, T., Assmy, P., et al. (2024). Interannual differences in sea ice regime in the north-western Barents Sea cause major changes in summer pelagic production and export mechanisms. *Prog. Oceanogr.* 220, 103178. doi: 10.1016/j.pocean.2023.103178

Arrigo, K. R., van Dijken, G., and Pabi, S. (2008). Impact of a shrinking Arctic ice cover on marine primary production. *Geophys. Res. Lett.* 35, L19603. doi: 10.1029/2008GL035028

Årthun, M., Eldevik, T., Smedsrud, L. H., Skagseth, Ø., and Ingvaldsen, R. B. (2012). Quantifying the influence of Atlantic heat on Barents Sea ice variability and retreat. *J. Clim.* 25, 4736–4743. doi: 10.1175/JCLI-D-11-00466.1

Ashjian, C. J., Campbell, R. G., Welch, H. E., Butler, M., and van Keuren, D. (2003). Annual cycle in abundance, distribution, and size in relation to hydrography of important copepod species in the western Arctic Ocean. *Deep Sea Res. Part I* 50, 1235–1261. doi: 10.1016/S0967-0637(03)00129-8

Assmy, P., Gradinger, R., Edvardsen, B., Wold, A., Goraguer, L., Wiktor, J., et al. (2022a). Phytoplankton biodiversity nansen legacy JC1. doi: 10.21334/npolar.2022.c86f931f

Assmy, P., Gradinger, R., Edvardsen, B., Wold, A., Goraguer, L., Wiktor, J., et al. (2022b). Phytoplankton biodiversity nansen legacy Q3. doi: 10.21334/npolar.2022.dadccf78

Bagøien, E., Bogstad, B., Dalpadado, P., Dolgov, A. V., Eriksen, E., Fauchald, J., et al. (2020). *Working Group on the Integrated Assessments of the Barents Sea (WGIBAR).* (ICES Scientific Reports). 1 (42), 157. doi: 10.17895/ices.pub.5536

Balazy, K., Boehnke, R., Trudnowska, E., Søreide, J. E., and Błachowiak-Samołyk, K. (2021). Phenology of *Oithona similis* demonstrates that ecological flexibility may be a winning trait in the warming Arctic. *Sci. Rep.* 11, 18599. doi: 10.1038/s41598-021-98068-8

Balazy, K., Trudnowska, E., Wichorowski, M., and Błachowiak-Samołyk, K. (2018). Large versus small zooplankton in relation to temperature in the Arctic shelf region. *Pol. Res.* 37, 1427409. doi: 10.1080/17518369.2018.1427409

Basedow, S. L., Eiane, K., Tverberg, V., and Spindler, M. (2004). Advection of zooplankton in an Arctic fjord (Kongsfjorden, Svalbard). *Estuar. Coast. Shelf Sci.* 60, 113–124. doi: 10.1016/j.ecss.2003.12.004

Basedow, S. L., Sundfjord, A., von Appen, W.-J., Halvorsen, E., Kwasniewski, S., and Reigstad, M. (2018). Seasonal variation in transport of zooplankton into the Arctic Basin through the Atlantic gateway, Fram Strait. *Front. Mar. Sci.* 5. doi: 10.3389/fmars.2018.00194

Basedow, S. L., Zhou, M., and Tande, K. S. (2014). Secondary production at the polar front, Barents Sea, August 2007. *J. Mar. Syst.* 130, 147–159. doi: 10.1016/j.jmarsys.2013.07.015

Blachowiak-Samolyk, K., Søreide, J. E., Kwasniewski, S., Sundfjord, A., Hop, H., Falk-Petersen, S., et al. (2008). Hydrodynamic control of mesozooplankton abundance and biomass in northern Svalbard waters (79-81 N). *Deep Sea Res. Part II* 55, 2210–2224. doi: 10.1016/j.dsr2.2008.05.018

Bouchard, C., and Fortier, L. (2020). The importance of *Calanus glacialis* for the feeding success of young polar cod: a circumpolar synthesis. *Polar Biol.* 43, 1095–1107. doi: 10.1007/s00300-020-02643-0

Bouchard, C., Geoffroy, M., LeBlanc, M., Majewski, A., Gauthier, S., Walkusz,, et al. (2017). Climate warming enhances polar cod recruitment, at least transiently. *Prog. Oceanogr.* 156, 121–129. doi: 10.1016/j.pocean.2017.06.008

Choquet, M., Kosobokova, K., Kwaśniewski, S., Hatlebakk, M., Dhanasiri, A. K., Melle, W., et al. (2018). Can morphology reliably distinguish between the copepods *Calanus finmarchicus* and *C. glacialis*, or is DNA the only way? *Limnol. Oceanogr. Methods* 16, 237–252. doi: 10.1002/lom3.10240

Coyle, K. O., and Pinchuk, A. I. (2002). Climate-related differences in zooplankton density and growth on the inner shelf of the southeastern Bering Sea. *Prog. Oceanogr.* 55, 177–194. doi: 10.1016/S0079-6611(02)00077-0

Daase, M., and Eiane, K. (2007). Mesozooplankton distribution in northern Svalbard waters in relation to hydrography. *Polar Biol. 30* pp, 969–981. doi: 10.1007/s00300-007-0255-5

Daase, M., Falk-Petersen, S., Varpe, Ø., Darnis, G., Søreide, J. E., Wold, A., et al. (2013). Timing of reproductive events in the marine copepod *Calanus glacialis*: a pan-Arctic perspective. *Can. J. Fish. Aquat. Sci.* 70, 871–884. doi: 10.1139/cjfas-2012-0401

Daase, M., Søreide, J. E., and Martynova, D. (2011). Effects of food quality on naupliar development in *Calanus glacialis* at subzero temperatures. *Mar. Ecol. Prog. Ser.* 429, 111–124. doi: 10.3354/meps09075

Dalpadado, P., Ingvaldsen, R. B., and Hassel, A. (2003). Zooplankton biomass variation in relation to climatic conditions in the Barents Sea. *Polar Biol.* 26, 233–241. doi: 10.1007/s00300-002-0470-z

Dalpadado, P., Ingvaldsen, R. B., Stige, L. C., Bogstad, B., Knutsen, T., Ottersen, G., et al. (2012). Climate effects on Barents Sea ecosystem dynamics. *ICES J. Mar. Sci.* 69, 1303–1316. doi: 10.1093/icesjms/fss063

Darnis, G., and Fortier, L. (2014). Temperature, food and the seasonal vertical migration of key arctic copepods in the thermally stratified Amundsen Gulf (Beaufort Sea, Arctic Ocean). *J. Plankton Res.* 36, 1092–1108. doi: 10.1093/plankt/fbu035

Dvoretsky, V. G., and Dvoretsky, A. G. (2009). Life cycle of *Oithona similis* (Copepoda: Cyclopoida) in Kola Bay (Barents Sea). *Mar. Biol.* 156, 1433–1446. doi: 10.1007/s00227-009-1183-4

Dvoretsky, V. G., and Dvoretsky, A. G. (2012). Estimated copepod production rate and structure of mesozooplankton communities in the coastal Barents Sea during summer-autumn 2007. *Polar Biol.* 35, 1321–1342. doi: 10.1007/s00300-012-1175-6

Dvoretsky, V. G., and Dvoretsky, A. G. (2024a). Marine copepod assemblages in the Arctic: The effect of frontal zones on biomass and productivity. *Mar. Environ. Res.* 193, 106250. doi: 10.1016/j.marenvres.2023.106250

Dvoretsky, V. G., and Dvoretsky, A. G. (2024b). Local variability of Arctic mesozooplankton biomass and production: A case summer study. *Environ. Res.* 241, 117416. doi: 10.1016/j.envres.2023.117416

Efstathiou, E., Eldevik, T., Årthun, M., and Lind, S. (2022). Spatial patterns, mechanisms, and predictability of Barents Sea ice change. *J. Clim.* 35, 2961–2973. doi: 10.1175/JCLI-D-21-0044.1

Eisner, L. B., Napp, J. M., Mier, K. L., Pinchuk, A. I., and Andrews, III, A.G. (2014). Climate-mediated changes in zooplankton community structure for the eastern Bering Sea. *Deep Sea Res. Part II* 109, 157–171. doi: 10.1016/j.dsr2.2014.03.004

Ershova, E. A., Kosobokova, K. N., Banas, N. S., Ellingsen, I., Niehoff, B., Hildebrandt, N., et al. (2021). Sea ice decline drives biogeographical shifts of key *Calanus* species in the central Arctic Ocean. *Global Change Biol.* 27, 2128–2143. doi: 10.1111/gcb.15562

Falk-Petersen, S., Mayzaud, P., Kattner, G., and Sargent, J. R. (2009). Lipids and life strategy of Arctic *Calanus*. *Mar. Biol. Res.* 5, 18–39. doi: 10.1080/17451000802512267

Feng, Z., Ji, R., Ashjian, C., Campbell, R., and Zhang, J. (2018). Biogeographic responses of the copepod *Calanus glacialis* to a changing Arctic marine environment. *Global Change Biol.* 24, e159–e170. doi: 10.1111/gcb.13890

Feng, Z., Ji, R., Campbell, R. G., Ashjian, C. J., and Zhang, J. (2016). Early ice retreat and ocean warming may induce copepod biogeographic boundary shifts in the Arctic Ocean. *J. Geophys. Res.: Oceans* 121, 6137–6158. doi: 10.1002/2016JC011784

Freer, J. J., Daase, M., and Tarling, G. A. (2022). Modelling the biogeographic boundary shift of *Calanus finmarchicus* reveals drivers of Arctic Atlantification by subarctic zooplankton. *Global Change Biol.* 28, 429–440. doi: 10.1111/gcb.15937

Gabrielsen, T. M., Merkel, B., Søreide, J. E., Johansson-Karlsson, E., Bailey, A., Vogedes, D., et al. (2012). Potential misidentifications of two climate indicator species of the marine arctic ecosystem: *Calanus glacialis* and *C. finmarchicus*. *Polar Biol.* 35, 1621–1628. doi: 10.1007/s00300-012-1202-7

Gallienne, C. P., and Robins, D. B. (2001). Is *Oithona* the most important copepod in the world's oceans? *J. Plankton Res.* 23, 1421–1432. doi: 10.1093/plankt/23.12.1421

Geoffroy, M., and Priou, P. (2020). "Fish ecology during the polar night," in *POLAR NIGHT Marine Ecology: Life and Light in the Dead of Night*, 181–216 (Springer Cham).

Gluchowska, M., Trudnowska, E., Goszczko, I., Kubiszyn, A. M., Blachowiak-Samolyk, K., Walczowski, W., et al. (2017). Variations in the structural and functional diversity of zooplankton over vertical and horizontal environmental gradients en route to the Arctic Ocean through the Fram Strait. *PloS One* 12, e0171715. doi: 10.1371/journal.pone.0171715

Hassel, A., Skjoldal, H. R., Gjøsæter, H., Loeng, H., and Omli, L. (1991). Impact of grazing from capelin (*Mallotus villosus*) on zooplankton: a case study in the northern Barents Sea in August 1985. *Polar Res.* 10, 371–388. doi: 10.1111/j.1751-8369.1991.tb00660.x

Hatlebakk, M. K. V., Kosobokova, K. N., Daase, M., and Søreide, J. (2022). Contrasting life traits of sympatric *Calanus glacialis* and *C. finmarchicus* in a warming Arctic revealed by a year-round study in Isfjorden, Svalbard. *Front. Mar. Sci* 9, 877910. doi: 10.3389/fmars.2022.877910

Hirche, H.-J. (1996). Diapause in the marine copepod, *Calanus finmarchicus*—a review. *Ophelia* 44, 129–143. doi: 10.1080/00785326.1995.10429843

Hirche, H. J., Hagen, W., Mumm, N., and Richter, C. (1994). The Northeast Water polynya, Greenland Sea: III. Meso-and macrozooplankton distribution and production of dominant herbivorous copepods during spring. *Polar Biol.* 14, 491–503. doi: 10.1007/BF00239054

Hirst, A. G., and Lampitt, R. S. (1998). Towards a global model of in *situ* weight-specific growth in marine planktonic copepods. *Mar. Biol.* 132, 247–257. doi: 10.1007/s002270050390

Holm-Hansen, O., and Riemann, B. (1978). *Chlorophyll a determination: improvements in methodology* (Oikos), 438–447. doi: 10.2307/3543338

Hunt, G. L. Jr., Coyle, K. O., Eisner, L. B., Farley, E. V., Heintz, R. A., Mueter, F., et al. (2011). Climate impacts on eastern Bering Sea foodwebs: a synthesis of new data and an assessment of the Oscillating Control Hypothesis. *ICES J. Mar. Sci.* 68, 1230–1243. doi: 10.1093/icesjms/fsr036

Huse, G., and Toresen, R. (1996). A comparative study of the feeding habits of herring (*Clupea harengus*, Clupeidae, 1.) and capelin (*Mallotus villosus*, Osmeridae, müller) in the Barents Sea. *Sarsia* 81, 143–153. doi: 10.1080/00364827.1996.10413618

Ingvaldsen, R. (2022). *CTD data from Nansen Legacy Cruise - Joint cruise*. 1–2. doi: 10.21335/NMDC-714672628

Isaksen, K., Nordli, Ø., Ivanov, B., Køltzow, M.A.Ø., Aaboe, S., Gjelten, H. M., et al. (2022). Exceptional warming over the Barents area. *Sci. Rep.* 12, 1–18. doi: 10.1038/s41598-022-13568-5

Ji, R., Ashjian, C. J., Campbell, R. G., Chen, C., Gao, G., Davis, C. S., et al. (2012). Life history and biogeography of *Calanus* copepods in the Arctic Ocean: an individual-based modeling study. *Prog. Oceanogr.* 96, 40–56. doi: 10.1016/j.pocean.2011.10.001

Jumars, P. A., Penry, D. L., Baross, J. A., Perry, M. J., Frost, B. W., and Part, A. (1989). Closing the microbial loop: dissolved carbon pathway to heterotrophic bacteria from incomplete ingestion, digestion and absorption in animals. *Deep Sea Res.* 36 (4), 483–495. doi: 10.1016/0198-0149(89)90001-0

Kane, J. (1984). The feeding habits of co-occurring cod and haddock larvae from Georges Bank. *Mar. Ecol. Prog. Ser.* 16, 9–20. doi: 10.3354/meps016009

Kimmel, D. G., Eisner, L. B., and Pinchuk, A. I. (2023). The northern Bering Sea zooplankton community response to variability in sea ice: evidence from a series of warm and cold periods. *Mar. Ecol. Prog. Ser.* 705, 21–42. doi: 10.3354/meps14237

Kimmel, D. G., Eisner, L. B., Wilson, M. T., and Duffy-Anderson, J. T. (2018). Copepod dynamics across warm and cold periods in the eastern Bering Sea: implications for walleye pollock (*Gadus chalcogrammus*) and the Oscillating Control Hypothesis. *Fish. Oceanogr.* 27, 143–158. doi: 10.1111/fog.12241

Kiørboe, T., and Sabatini, M. (1995). Scaling of fecundity, growth and development in marine planktonic copepods. *Mar. Ecol. Prog. Ser.* 120, 285–298. doi: 10.3354/meps120285

Kobari, T., Sastri, A. R., Yebra, L., Liu, H., and Hopcroft, R. R. (2019). Evaluation of trade-offs in traditional methodologies for measuring metazooplankton growth rates: assumptions, advantages and disadvantages for field applications. *Prog. Oceanogr* 178, 102137. doi: 10.1016/j.pocean.2019.102137

Kohlbach, D., Goraguer, L., Bodur, Y. V., Müller, O., Amargant-Arumí,, Blix, K., et al. (2023). Earlier sea-ice melt extends the oligotrophic summer period in the Barents Sea with low algal biomass and associated low vertical flux. *Prog. Oceanogr* 103018. doi: 10.1016/j.pocean.2023.103018

Koski, M., and Lombard, F. (2022). Functional responses of aggregate-colonizing copepods. *Limnol. Oceanogr* 67, 2059–2072. doi: 10.1002/lno.12187

Koski, M., Valencia, B., Newstead, R., and Thiele, C. (2020). The missing piece of the upper mesopelagic carbon budget? Biomass, vertical distribution and feeding of aggregate-associated copepods at the PAP site. *Progr. Oceanogr* 181, 102243. doi: 10.1016/j.pocean.2019.102243

Kosobokova, K., and Hirche, H. J. (2009). Biomass of zooplankton in the eastern Arctic Ocean–a base line study. *Prog. Oceanogr.* 82, 265–280. doi: 10.1016/j.pocean.2009.07.006

Kosobokova, K. N., Hopcroft, R. R., and Hirche, H. J. (2011). Patterns of zooplankton diversity through the depths of the Arctic's central basins. *Mar. Biodiv.* 41, 29–50. doi: 10.1007/s12526-010-0057-9

Kvile, K.Ø., Ashjian, C., and Ji, R. (2019). Pan-Arctic depth distribution of diapausing Calanus copepods. *Biolog. Bull.* 237, 76–89. doi: 10.1086/704694

Kwasniewski, S., Gluchowska, M., Jakubas, D., Wojczulanis-Jakubas, K., Walkusz, W., Karnovsky, N., et al. (2010). The impact of different hydrographic conditions and zooplankton communities on provisioning Little Auks along the West coast of Spitsbergen. *Prog. Oceanogr.* 87, 72–82. doi: 10.1016/j.pocean.2010.06.004

Kwasniewski, S., Hop, H., Falk-Petersen, S., and Pedersen, G. (2003). Distribution of *Calanus* species in Kongsfjorden, a glacial fjord in Svalbard. *J. Plankton Res.* 25, 1–20. doi: 10.1093/plankt/25.1.1

Lafontaine, Y. (1999). Covariation in climate, zooplankton biomass and mackerel recruitment in the southern Gulf of St Lawrence. *Fish. Oceanogr.* 8, 139–149. doi: 10.1046/j.1365-2419.1999.00095.x

Langbehn, T. J., Aarflot, J. M., Freer, J. J., and Varpe, Ø. (2023). Visual predation risk and spatial distributions of large Arctic copepods along gradients of sea ice and bottom depth. *Limn. Oceanogr* 68 (6), 1388-1405. doi: 10.1002/lno.12354

Leu, E., Søreide, J. E., Hessen, D. O., Falk-Petersen, S., and Berge, J. (2011). Consequences of changing sea-ice cover for primary and secondary producers in the European Arctic shelf seas: timing, quantity, and quality. *Prog. Oceanogr.* 90, 18–32. doi: 10.1016/j.pocean.2011.02.004

Levinsen, H., Turner, J. T., Nielsen, T. G., and Hansen, B. W. (2000). On the trophic coupling between protists and copepods in arctic marine ecosystems. *Mar. Ecol. Prog. Ser.* 204, 65–77. doi: 10.3354/meps204065

Lischka, S., and Hagen, W. (2005). Life histories of the copepods Pseudocalanus minutus, P. acuspes (Calanoida) and Oithona similis (Cyclopoida) in the Arctic Kongsfjorden (Svalbard). *Polar Biology* 28, 910–921.

Lischka, S., and Hagen, W. (2007). Seasonal lipid dynamics of the copepods *Pseudocalanus minutus* (Calanoida) and *Oithona similis* (Cyclopoida) in the Arctic Kongsfjorden (Svalbard). *Mar. Biol.* 150, 443–454. doi: 10.1007/s00227-006-0359-4

Liu, H., and Hopcroft, R. R. (2006). Growth and development of *Neocalanus flemingeri/plumchrus* in the northern Gulf of Alaska: validation of the artificial-cohort method in cold waters. *J. Plankton Res.* 28, 87–101. doi: 10.1093/plankt/fbi102

Madsen, S. D., Nielsen, T. G., and Hansen, B. W. (2001). Annual population development and production by *Calanus finmarchicus, C. glacialis* and *C. hyperboreus* in Disko Bay, western Greenland. *Mar. Biol.* 139, 75–83. doi: 10.1007/s002270100552

Madsen, S. D., Nielsen, T. G., and Hansen, B. W. (2008). Annual population development and production by small copepods in Disko Bay, western Greenland. *Mar. Biol.* 155, 63–77. doi: 10.1007/s00227-008-1007-y

Mohamed, B., Nilsen, F., and Skogseth, R. (2022). Interannual and decadal variability of sea surface temperature and sea ice concentration in the Barents Sea. *Remote Sens* 14, 4413. doi: 10.3390/rs14174413

Mooney, B. P., Iversen, M. H., and Norrbin, F. (2023). Impact of *Microsetella norvegica* on carbon flux attenuation and as a secondary producer during the polar night in the subarctic Porsangerfjord. *Front. Mar. Sci* 10. doi: 10.3389/fmars.2023.996275

Müller, O. (2023a). *Bacterial production measurements (rate of production of biomass expressed as carbon by prokaryotes [bacteria and archaea]) during Nansen Legacy cruise 2018707* (University of Bergen). doi: 10.21335/NMDC-1815353537-2018707

Müller, O. (2023b). *Bacterial production measurements (rate of production of biomass expressed as carbon by prokaryotes [bacteria and archaea]) during Nansen Legacy cruise 2019706* (University of Bergen). doi: 10.21335/NMDC-1815353537-2019706

Napp, J. M., Kendall, A. W., and Schumacher, J. D. (2000). A synthesis of biological and physical processes affecting the feeding environment of larval walleye pollock (*Theragra chalcogramma)* in the eastern Bering Sea. *Fish. Oceanogr.* 9, 147–162. doi: 10.1046/j.1365-2419.2000.00129.x

Nielsen, T. G., Møller, E. F., Satapoomin, S., Ringuette, M., and Hopcroft, R. R. (2002). Egg hatching rate of the cyclopoid copepod *Oithona similis* in arctic and temperate waters. *Mar. Ecol. Prog. Ser.* 236, 301–306. doi: 10.3354/meps236301

NOAA National Geophysical Data Center. (2009). *ETOPO1 1 Arc-Minute Global Relief Model* (NOAA National Centers for Environmental Information). Available at: https://www.ngdc.noaa.gov/mgg/global/relief/ETOPO1/data/ice_surface/grid_registered/netcdf/. 2009. ETOPO1 1 Arc-Minute Global Relief Model.

Oksanen, J., Simpson, G., Blanchet, F., Kindt, R., Legendre, P., Minchin, P., et al. (2023). *vegan: Community Ecology Package. R package version 2.6-5*. Available online at: https://github.com/vegandevs/vegan.

Onarheim, I. H., and Årthun, M. (2017). Toward an ice-free barents sea. *Geophys. Res. Lett.* 44, 8387–8395. doi: 10.1002/2017GL074304

Paradis, V., Sirois, P., Castonguay, M., and Plourde, S. (2012). Spatial variability in zooplankton and feeding of larval Atlantic mackerel (*Scomber scombrus*) in the

southern Gulf of St. Lawrence. *J. Plankton Res.* 34, 1064–1077. doi: 10.1093/plankt/fbs063

Pedersen, T., Mikkelsen, N., Lindstrøm, U., Renaud, P. E., Nascimento, M. C., Blanchet, M. A., et al. (2021). Overexploitation, recovery, and warming of the Barents Sea ecosystem during 1950–2013. *Front. Mar. Sci.* 8, 732637. doi: 10.3389/fmars.2021.732637

Peters, R. H., and Downing, J. A. (1984). Empirical analysis of zooplankton filtering and feeding rates 1. *Limn. Oceanogr.* 29, 763–784. doi: 10.4319/lo.1984.29.4.0763

Pörtner, H.-O., Roberts, D. C., Masson-Delmotte, V., Zhai, P., Tignor, M., Poloczanska, E., et al. (2019). "Summary for policymakers," in *IPCC special report on the ocean and cryosphere in a changing climate*, vol. 7. .

Postel, L., Fock, H., and Hagen, W. (2000). *Biomass and abundance. ICES zooplankton methodology manual* Vol. 83 (London: Academic Press), 192.

Randelhoff, A., Holding, J., Janout, M., Sejr, M. K., Babin, M., Tremblay, J.-É., et al. (2020). Pan-Arctic Ocean primary production constrained by turbulent nitrate fluxes. *Front. Mar. Sci.* 7. doi: 10.3389/fmars.2020.00150

Rat'kova, T. N., and Wassmann, P. (2002). Seasonal variation and spatial distribution of phyto-and protozooplankton in the central Barents Sea. *J. Mar. Syst.* 38, 47–75. doi: 10.1016/S0924-7963(02)00169-0

Reigstad, M. (2022). *CTD data from Nansen Legacy Cruise - Seasonal cruise Q3*. doi: 10.21335/NMDC-1107597377

Renaud, P. E., Daase, M., Banas, N. S., Gabrielsen, T. M., Søreide, J. E., Varpe, Ø., et al. (2018). Pelagic food-webs in a changing Arctic: a trait-based perspective suggests a mode of resilience. *ICES J. Mar. Sci.* 75, 1871–1881. doi: 10.1093/icesjms/fsy063

Riser, C. W., Wassmann, P., Reigstad, M., and Seuthe, L. (2008). Vertical flux regulation by zooplankton in the northern Barents Sea during Arctic spring. *Deep Sea Res. Part II* 55, 2320–2329. doi: 10.1016/j.dsr2.2008.05.006

Roura, Á., Strugnell, J. M., Guerra, Á., González, Á.F., and Richardson, A. J. (2018). Small copepods could channel missing carbon through metazoan predation. *Ecol. Evo.* 8, 10868–10878. doi: 10.1002/ece3.4546

Runge, J. A., and Roff, J. C. (2000). The measurement of growth and reproductive rates. In: *ICES zooplankton methodology manual* Elsevier, 401–454.

Sabatini, M., and Kiørboe, T. (1994). Egg production, growth and development of the cyclopoid copepod *Oithona similis*. *J. Plankton Res.* 16, 1329–1351. doi: 10.1093/plankt/16.10.1329

Sakshaug, E., Slagstad, D., and Holm-Hansen, O. (1991). Factors controlling the development of phytoplankton blooms in the Antarctic Ocean—a mathematical model. *Mar. Chem.* 35, 259–271. doi: 10.1016/S0304-4203(09)90021-4

Simon, M., Cho, B. C., and Azam, F. (1992). Significance of bacterial biomass in lakes and the ocean: comparison to phytoplankton biomass and biogeochemical implications. *Mar. Ecol. Prog. Ser.* 86 (2), 103–110. doi: 10.3354/meps086103

Slagstad, D., Ellingsen, I. H., and Wassmann, P. (2011). Evaluating primary and secondary production in an Arctic Ocean void of summer sea ice: an experimental simulation approach. *Prog. Oceanogr.* 90, 117–131. doi: 10.1016/j.pocean.2011.02.009

Slagstad, D., Wassmann, P. F. J., and Ellingsen, I. (2015). Physical constrains and productivity in the future Arctic Ocean. *Front. Mar. Sci.* 2. doi: 10.3389/fmars.2015.00085

Smith, D. C., and Azam, F. (1992). A simple, economical method for measuring bacterial protein synthesis rates in seawater using 3H-leucine. *Mar. Microb. Food webs* 6, 107–114.

Søreide, J. E., Leu, E. V. A., Berge, J., Graeve, M., and Falk-Petersen, S. (2010). Timing of blooms, algal food quality and *Calanus glacialis* reproduction and growth in a changing Arctic. *Global Change Biol.* 16, 3154–3163. doi: 10.1111/j.1365-2486.2010.02175.x

Spreen, G., Kaleschke, L., and Heygster, G. (2008). Sea ice remote sensing using AMSR-E 89 GHz channels. *J. Geophys. Res.* 113, C02S03. doi: 10.1029/2005JC003384

Stabeno, P. J., Kachel, N. B., Moore, S. E., Napp, J. M., Sigler, M., Yamaguchi, A., et al. (2012). Comparison of warm and cold years on the southeastern Bering Sea shelf and some implications for the ecosystem. *Deep Sea Res. Part II* 65, 31–45. doi: 10.1016/j.dsr2.2012.02.020

Steer, A., and Divine, D. (2023). *Sea ice concentrations in the northern Barents Sea and the area north of Svalbard at Nansen Legacy stations during 2017-2021* (Norwegian Polar Institute). doi: 10.21334/npolar.2023.24f2939c

Stige, L. C., Eriksen, E., Dalpadado, P., and Ono, K. (2019). Direct and indirect effects of sea ice cover on major zooplankton groups and planktivorous fishes in the Barents Sea. *ICES J. Mar. Sci.* 76, i24–i36. doi: 10.1093/icesjms/fsz063

Sundfjord, A., Assmann, K. M., Lundesgaard, Ø., Renner, A. H. H., Lind, S., and Ingvaldsen, R. B. (2020). Suggested water mass definitions for the central and northern Barents Sea, and the adjacent Nansen Basin. *NLRS*. doi: 10.7557/nlrs.2020.8

Svensen, C., Halvorsen, E., Vernet, M., Franzè, G., Dmoch, K., Lavrentyev, P. J., et al. (2019). Zooplankton communities associated with new and regenerated primary production in the Atlantic inflow north of Svalbard. *Front. Mar. Sci.* 6. doi: 10.3389/fmars.2019.00293

Svensen, C., and Kiørboe, T. (2000). Remote prey detection in *Oithona similis*: hydromechanical versus chemical cues. *J. Plankton Res.* 22, 1155–1166. doi: 10.1093/plankt/22.6.1155

Swalethorp, R., Kjellerup, S., Malanski, E., Munk, P., and Nielsen, T. G. (2014). Feeding opportunities of larval and juvenile cod (*Gadus morhua*) in a Greenlandic fjord: temporal and spatial linkages between cod and their preferred prey. *Mar. Biol.* 161, 2831–2846. doi: 10.1007/s00227-014-2549-9

Tarling, G. A., Freer, J. J., Banas, N. S., Belcher, A., Blackwell, M., Castellani, C., et al. (2022). Can a key boreal *Calanus* copepod species now complete its life-cycle in the Arctic? Evidence and implications for Arctic food-webs. *Ambio* 51, 333–344. doi: 10.1007/s13280-021-01667-y

The Nansen Legacy (2020). *Sampling Protocols* (NLRS). doi: 10.7557/nlrs.5719

Trudnowska, E., Gluchowska, M., Beszczynska-Möller, A., Blachowiak-Samolyk, K., and Kwasniewski, S. (2016). Plankton patchiness in the Polar Front region of the West Spitsbergen Shelf. *Mar. Ecol. Prog. Ser.* 560, 1–18. doi: 10.3354/meps11925

Turner, J. T. (2004). The importance of small planktonic copepods and their roles in pelagic marine food webs. *Zool. Stud.* 43, 255–266.

Unstad, K. H., and Tande, K. S. (1991). Depth distribution of *Calanus finmarchicus* and *C. glacialis* in relation to environmental conditions in the Barents Sea. *Polar Res.* 10, 409–420. doi: 10.1111/j.1751-8369.1991.tb00662.x

Utermöhl, H. (1958). Zur vervollkommnung der quantitativen phytoplankton-methodik: Mit 1 Tabelle und 15 abbildungen im Text und auf 1 Tafel. *Internationale Vereinigung für theoretische und angewandte Limnologie: Mitt.* 9, 1–38. doi: 10.1080/05384680.1958.11904091

Vader, A. (2022a). *Chlorophyll A and phaeopigments Nansen Legacy cruise 2019706*. doi: 10.21335/NMDC-1109067467

Vader, A. (2022b). *Chlorophyll A and phaeopigments Nansen Legacy cruise 2021708*. doi: 10.21335/NMDC-1248407516

Van Engeland, T., Bagøien, E., Wold, A., Cannaby, H. A., Majaneva, S., Vader, A., et al. (2023). Diversity and seasonal development of large zooplankton along physical gradients in the Arctic Barents Sea. *Progr. Oceanogr* 216, 103065. doi: 10.1016/j.pocean.2023.103065

Vihtakari, M. (2022). *ggOceanMaps: Plot data on oceanographic maps using "ggplot2". R package version 1*. doi: 10.5281/zenodo.4554714

Wassmann, P., and Reigstad, M. (2011). Future Arctic Ocean seasonal ice zones and implications for pelagic-benthic coupling. *Oceanogr.* 24, 220–231. doi: 10.5670/oceanog

Wold, A., Hop, H., Svensen, C., Søreide, J. E., Assmann, K. M., Ormanczyk, M., et al. (2023). Atlantification influences zooplankton communities seasonally in the northern Barents Sea and Arctic Ocean. *Prog. Oceanogr* 219, 103133. doi: 10.1016/j.pocean.2023.103133

Zamora-Terol, S., Nielsen, T. G., and Saiz, E. (2013). Plankton community structure and role of Oithona similis on the western coast of Greenland during the winter-spring transition. *Mar. Ecol. Prog. Ser.* 483, 85–102. doi: 10.3354/meps10288

frontiers | Frontiers in Marine Science

TYPE Original Research
PUBLISHED 22 April 2024
DOI 10.3389/fmars.2024.1351844



OPEN ACCESS

EDITED BY
Letterio Guglielmo,
Anton Dohrn Zoological Station Naples, Italy

REVIEWED BY
Matthew R. Baker,
North Pacific Research Board, United States
Svein Sundby,
Norwegian Institute of Marine Research (IMR), Norway

*CORRESPONDENCE
Hyoung Sul La
hsla@kopri.re.kr

RECEIVED 07 December 2023
ACCEPTED 22 March 2024
PUBLISHED 22 April 2024

CITATION
Kim SH, Son W, Yoo J, Cho K-H, Park T, Yang EJ, Kang S-H and La HS (2024) Patterns of summer ichthyoplankton distribution, including invasive species, in the Bering and Chukchi Seas. *Front. Mar. Sci.* 11:1351844. doi: 10.3389/fmars.2024.1351844



# Patterns of summer ichthyoplankton distribution, including invasive species, in the Bering and Chukchi Seas

Sung Hoon Kim[1], Wuju Son[1], Jaeill Yoo[1], Kyoung-Ho Cho[1], Taewook Park[1], Eun Jin Yang[1], Sung-Ho Kang[1] and Hyoung Sul La[1,2]*

[1]Division of Ocean and Atmosphere Sciences, Korea Polar Research Institute, Incheon, Republic of Korea, [2]Department of Polar Science, University of Science and Technology, Daejeon, Republic of Korea

A multidisciplinary survey was carried out in the Pacific Arctic and sub-Arctic regions of the North Pacific Ocean on the Korean icebreaking research vessel *Araon*. During this survey, ichthyoplankton fishes in the Pacific Arctic and sub-Arctic region ranged from the Bering Sea to the northern Chukchi Shelf in summer. The most dominant species was *Gadus chalcogrammus*, followed by *Pleuronectes quadrituberculatus* and *Boreogadus saida*. *Gadus chalcogrammus* and *P. quadrituberculatus* were particularly abundant near the Bering Sea and Bering Strait, whereas *B. saida* was dominant in the Chukchi Sea. Hierarchical cluster analysis revealed four distinct ichthyoplankton communities in Pacific Arctic and sub-Arctic regions based on geographical regions. However, *Eleginus gracilis*, which was previously known to be seen between latitudes 66.5°N and 69.5°N, was found above 70°N, suggesting that its distribution extends further north. Furthermore, we noticed that *Benthosema glaciale*, which is usually found in the Atlantic sector of Arctic Ocean, was observed in the northern Chukchi Sea. In addition to these unusual species distributions, several species that are mainly observed in coastal areas are observed in the Chukchi Sea region. The observed influx of various uncommon fish species into the Chukchi Sea can be attributed to multiple factors, including freshwater inflow from the East Siberian Sea and the intrusion of warm Atlantic and Pacific waters, which are strongly affected by global warming. Consequently, it is imperative to conduct rigorous monitoring of the Pacific Arctic region, with a particular focus on the Chukchi Sea, to better understand the implications of global warming.

KEYWORDS

**ichthyoplankton, community structure, Pacific Arctic Ocean, East Siberian Sea, Chukchi Sea, Bering Sea, Bering Strait**

# Introduction

The Pacific Arctic Ocean has been undergoing dramatic environmental change related to sea ice melting and increasing surface temperatures (Mueter and Litzow, 2008; Wang et al., 2018; Baker et al., 2020, 2023). Heat advected into the Arctic region resulted in a promoted decrease in sea ice coverage in the Arctic Ocean (Polyakov et al., 2017; Richards et al., 2022; Wang and Danilov, 2022). As a result, the minimum sea ice boundary in the western Arctic Ocean has gradually retreated northward, and the mean sea ice cover has been consistently below the mean sea ice cover over the last decade (Wood et al., 2015). Although the Bering Sea was excepted from these trends, increased warm southerly winds and air temperature influenced on the sea ice retreat in the Bering Sea, recently (Stabeno and Bell, 2019; Baker et al., 2020). Furthermore, more extended sea ice free periods are predicted in the Chuck Sea and Bering Sea under the global warming (Wang et al., 2018; Baker et al., 2023). This environmental change could affect the entire Arctic marine ecosystem, such as the community, behavior and phenology, growth and condition, abundance and demography, and range and regime shift (Wassmann et al., 2011; Wisz et al., 2015; Levine et al., 2023).

Ichthyoplankton are essential in Arctic pelagic ecosystems for evaluating ecosystem functions, assessing stocks, and investigating recruitment processes (Kendall and Duker, 1998; Kendall, 2000). They are also important sentinels to understand the consequences of Arctic climate change, as they rely on planktonic prey and lead to phase shifts in ecosystem dynamics. For this reason, many studies have been conducted in different regions of the Arctic Ocean, focusing on aspects of Arctic ichthyoplankton ecology. Oceanographic, geographic, and atmospheric features influence ichthyoplankton ecology, such as sea ice conditions (Bouchard and Fortier, 2008), water masses (Atwood et al., 2010; Busby et al., 2014; David et al., 2016; Randall et al., 2019), bathymetry (Doyle et al., 2002), currents (Siddon et al., 2011), precipitation (Boeing and Duffy-Anderson, 2008), freshwater input (Bouchard and Fortier, 2011), wind (Rodriguez et al., 2011), and air temperature (Genner et al., 2010). Furthermore, shifts in the assemblage of species, including the movement of sub-Arctic species into the Arctic region have been noted in recent years (Baker and Hollowed, 2014; Vestfals et al., 2019; Huntington et al., 2020; Marsh et al., 2020; Baker, 2021; Wildes et al., 2022).

Despite the ecological significance of ichthyoplankton, our knowledge of Arctic ichthyoplankton is insufficient in the high-latitude Arctic Ocean because of the harsh sea ice conditions that limit access. Few studies have been conducted around the East Siberian Shelf in the Pacific Arctic region, whereas most studies on ichthyoplankton have focused on the Pacific sub-Arctic and Arctic waters of the Bering, Chukchi, and Beaufort Seas (Benoit et al., 2008; Eisner et al., 2013; Falardeau et al., 2014; Randall et al., 2019; Stevenson and Lauth, 2019; Cooper et al., 2023; Levine et al., 2023).

Our aim of this study was to describe the community structures of ichthyoplankton and examine the relationship with environmental conditions in the Bering Sea and Bering Strait, Chukchi Shelf, northern Chukchi Shelf, and northern East Siberian Shelf in austral summer in 2020. This result can provide further knowledge to understand the variation in the species assemblages of larvae and juvenile fishes, as well as the ecology of adult fish in the Pacific Arctic Ocean.

# Materials and methods

## Study area background

The study area, including the Bering Sea, Bering Strait, and Chukchi Sea, is characterized by a broad, shallow, and continental shelf region (De Robertis et al., 2017). This region is the only pathway connecting the Pacific Arctic region and the northern Pacific Ocean that provides nutrients and heat as water currents (Woodgate et al., 2005; Stabeno et al., 2018). The features of the water masses that flow into the Chukchi Sea vary markedly according to the season (Jinping et al., 2006; Norcross et al., 2010; Eisner et al., 2013; Gong and Pickart, 2015). Although Pacific winter water, including cold water and relatively salty water, such as newly ventilated Pacific winter water (NVPWW), dominates in the winter and early spring, Pacific summer water has a warmer and fresher water inflow into the Chukchi Sea through the Bering Strait in the summer (Woodgate et al., 2005; Pickart et al., 2019). Two water masses flow into the Chukchi Sea through the Bering Strait in summer: Alaskan coastal water (ACW) and Bering Summer Water (BSW) (Lin et al., 2019). ACW consists of the warmest and freshest water flowing into the Chukchi Sea along the eastern coastline of the Bering Strait (Pickart et al., 2019). BSW is relatively colder and saltier than the ACW flow into the Chukchi Sea through the central and western coastlines of the Bering Strait (Lin et al., 2019; Pickart et al., 2019). These water masses discharge around the Barrow Canyon, transporting different pathways: ACW flows into the eastern Chukchi Sea, whereas BSW flows through the western and central Chukchi Sea (Gong and Pickart, 2015). Furthermore, the Siberian Coastal Current (SCC) has freshwater flow into the western Chukchi Sea along the Siberian coastline (Weingartner et al., 1999; Spall, 2007). Although the seasonal cycle of salinity in the Chukchi Sea is controlled by Pacific-originated water such as BSW, the SCC also often influences the western Chukchi Sea (Weingartner et al., 1999; Spall, 2007). Atlantic water (AW) also flows into the Pacific Arctic region along with the shelf break of the Eurasian basin (Karcher and Oberhuber, 2002; Li et al., 2022). In the northern Chukchi Sea, the AW occasionally upwells along the shelf-break region (Bourke and Paquette, 1976; Gong and Pickart, 2015). Different water masses flow into the Chukchi Sea, with northward AW and Pacific Water from the south, and eastward-flowing SCC.

## Data sampling and processing

A multidisciplinary survey around the Pacific Arctic and sub-Arctic was carried out on the Korean icebreaking research vessel (IBRV) *Araon* from 26 July to 26 August 2020. Ichthyoplankton were collected using a ring net (mesh size, 505 μm; mouth area, 1.77m$^2$) at 18 sampling stations (Figure 1). The net was obliquely hauled with a speed of 60 m min$^{-1}$, reaching a maximum depth of 344 m (Supplementary Table 1). In the shallow stations below 200-

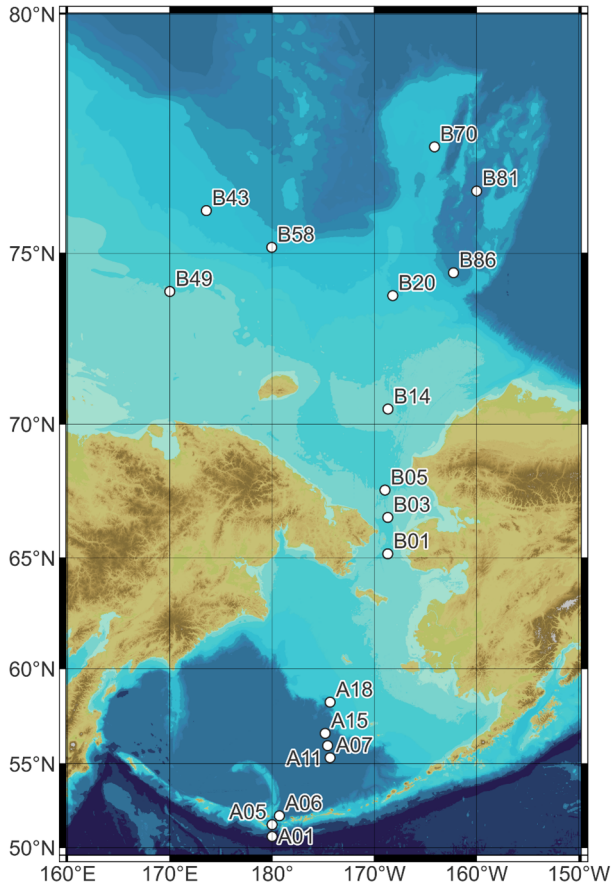


FIGURE 1
Map of the survey area showing the sampling stations in the Pacific Arctic and sub-Arctic regions from July to August 2020.

m depth, the net was towed from 5 m above the bottom to the surface. Tow speed and duration were about 1.5–2 knots and 20–30 min, respectively. The net depth was determined in association with the depth of sound scattering layers collected by a scientific echosounder (EK60). The collected samples were immediately subsampled using a Folsom plankton splitter, fixed in 4% filtered seawater formalin, and transported to the laboratory. Specimens were identified on the basis of morphological characteristics, such as habitus, preanus length, and melanophores, or ecological characteristics, such as habitats and spawning periods. Systematic accounts and morphology followed the methods by Matarese et al. (1989) and Okiyama (1989). The abundance was determined in individual numbers per cubic meter (ind./$m^3$), based on the volume filtered by the net, which was measured using the revolution count of a flow meter attached to the center of the net mouth. Total length of specimens was measured with a caliper.

Vertical profiles of seawater temperature (Temp), salinity (Sal), dissolved oxygen (DO), and fluorescence (Flu) were obtained using a conductivity-temperature-depth sampler (Sea-Bird, SBE 911 plus) with an oxygen sensor at each sampling station. For the following analyses, the surface, average, and bottom values were used for Temp, Sal, DO, and Flu. Classifications between surface, average, and bottom values are represented by subscripts (e.g., $Temp_{surface}$, $Temp_{average}$, and $Temp_{bottom}$). The "surface" values were determined from the 5-m to 10-m depth, the "average" value from the surface to the maximum hauled depth at each station, and the "bottom" value from the maximum hauled depth to 10 m above it at each station. The water column of the present study area was divided into five water masses, AW, ACW, BSW, meltwater/runoff (MW), and winter water (WW), according to Gong and Pickart (2015) and Pickart et al. (2019).

## Statistical analyses

All multivariate analyses were carried out using the PRIMER v7 package (Clarke et al., 2014; Clarke and Gorley, 2015) and PERMANOVA+ for PRIMER (Anderson et al., 2008). For the environmental analyses, draftsman plots were used on the basis of environmental data to apply an appropriate transformation (Valesini et al., 2014). As a result, $Sal_{surface}$, $Sal_{average}$, $Sal_{bottom}$, $DO_{surface}$, $DO_{average}$, and $DO_{bottom}$ were transformed by log (X+1) prior to analyses. All environmental values were normalized before the analyses. The spatial environmental status of the 18 sampling stations was described using CLUSTER based on Euclidean distance from the log-transformed and normalized environmental values. PERMANOVA was performed to confirm statistically significant ($P < 0.05$) differences between separated groups. Biological-environmental (BIOENV) analysis was applied to verify which environmental factors best explained the distinction between the ichthyoplankton communities.

For the biotic analyses, a square root transformation was applied to the data before the analyses. A resemblance matrix based on Bray–Curtis similarity was calculated to identify dissimilarities between sampling stations. Hierarchical cluster analyses (CLUSTER) were conducted on the basis of the Bray–Curtis similarities using group-average linking. Similarity profile (SIMPROF) permutation test was simultaneously conducted with CLUSTER to confirm whether the divided groups represent statistically significant ($P < 0.05$) differences. PERMANOVA was carried out to confirm whether ichthyoplankton communities had a significant ($P < 0.05$) distinction according to the divided groups. Similarity percentage (SIMPER) analyses were conducted to verify which species contributed to the differences between groups. Canonical analysis of principal coordinates (CAP) was carried out to visualize patterns in divided groups. The correlations between species and environmental values and stations were plotted using CAP.

# Results

## Spatial variation in physical and biological properties

The ranges of the environmental factors among the sampling stations are summarized in Table 1; Figure 2. The highest temperature was 10.88°C at the surface of station A11. The water temperature tended to increase southward. The salinity ranged from 25.14 to 34.80 PSU. The highest salinity was observed at

10.3389/fmars.2024.1351844

TABLE 1 Summary of the environmental values collected during the survey in the study area.

| | Min. | Max. | Av. | SD |
|---|---|---|---|---|
| $Temp_{surface}$ | −1.23 | 10.88 | 4.64 | 4.47 |
| $Temp_{average}$ | −1.22 | 5.21 | 2.27 | 2.61 |
| $Temp_{bottom}$ | −1.34 | 4.36 | 2.05 | 2.13 |
| $Sal_{surface}$ | 25.56 | 33.11 | 30.26 | 2.83 |
| $Sal_{average}$ | 28.96 | 33.58 | 32.67 | 1.08 |
| $Sal_{bottom}$ | 30.47 | 34.80 | 33.58 | 1.12 |
| $DO_{surface}$ | 95.40 | 390 | 246.56 | 136.59 |
| $DO_{average}$ | 65.61 | 392.62 | 206.55 | 116.46 |
| $DO_{bottom}$ | 14.30 | 397.16 | 169.29 | 126.7 |
| $Flu_{surface}$ | 0.08 | 24.61 | 5.89 | 7.76 |
| $Flu_{average}$ | 0.18 | 4.72 | 1.63 | 1.47 |
| $Flu_{bottom}$ | 0.16 | 2.67 | 0.74 | 0.62 |

Max, maximum; Min, minimum; Av, average; SD, standard deviation; Temp, temperature; Sal, salinity; DO, dissolved oxygen; Flu, fluorescence.

station B43, whereas the lowest salinity was observed at station B86. The reason for the large salinity gap between close stations was thought to be that the salinity values varied greatly according to the depth in this area. Additionally, the surface and average salinity decreased northward, but the bottom salinity showed a relatively even distribution pattern except for station 49. Although DO values were missing at stations B01, B03, B05, and B14, DO values were distinguished according to location. That is, the DO in the northern stations (>70°N) was much higher than the DO in the southern stations (<70°N), except for station B14. DO showed relatively low values in B14. Fluorescence indicated relatively high values at the surface of southern stations (A01, A05, A06, A07, A11, A15, and A18).

When the environmental values were analyzed using hierarchical cluster analysis, the stations were divided into five groups at three distance levels that were statistically significant (SIMPROF, $P < 0.05$, n = 999) (Figure 3A). At the 5.86 distance level, the stations were divided into two groups. One group included B20, B43, B49, B58, B70, B81, and B86. These stations were in the northern part of the survey region (>71°N). On the other hand, another group included southern stations (<71°N), A01, A05, A06, A07, A11, A15, A18, B01, B03, B05, and B14. In the first group, including northern stations, B49 separated from other stations, showing quite a high distance level. In the second group, including the southern station, B14 separated from other stations, representing quite a high distance level. The other stations were subdivided into two subgroups. One group included B01, B03, and B05, whereas another group is composed of A01, A05, A06, A07, A11, A15, and A18. As a result, the five groups could be distinguished from each other (Figure 3A). In the PERMANOVA, the null hypothesis that there was no difference in the environmental values between the five groups was rejected at a

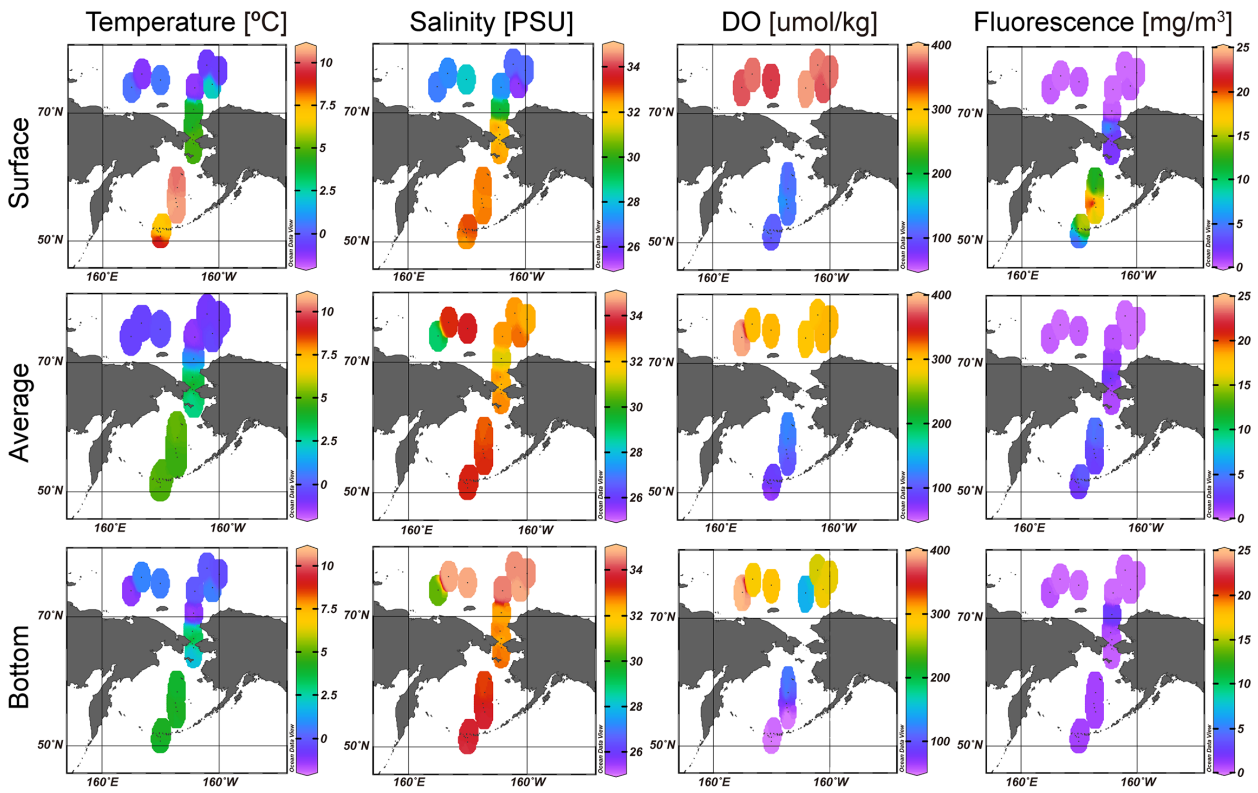


FIGURE 2
The spatial pattern of the environmental values among the sampling stations.

10.3389/fmars.2024.1351844

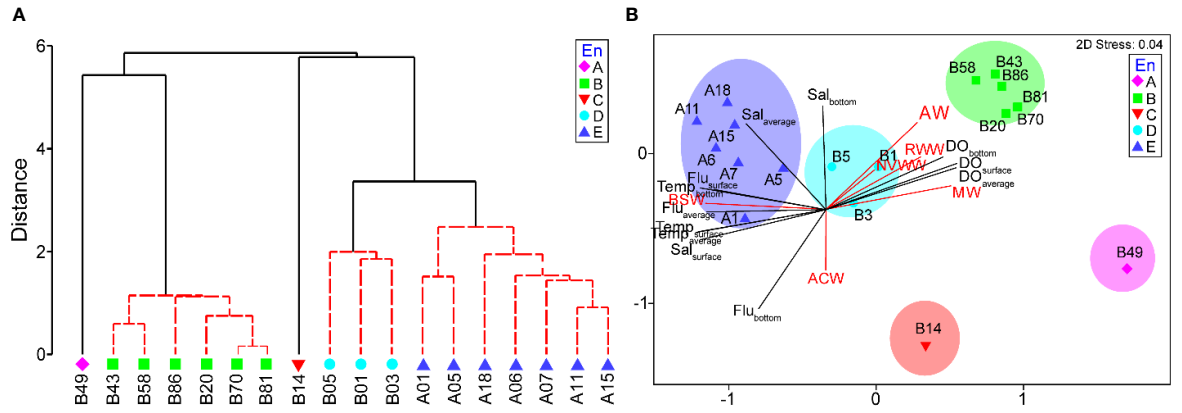


FIGURE 3
Dendrogram **(A)** and nonparametric multidimensional scaling (nMDS) plot **(B)** of the environmental values.

significance level of 5% (pseudo-F = 29.426, $P < 0.05$) (Table 2). However, in the pairwise tests, there were significant differences at a level of 5% only among three groups: B, D, and E (Table 2). Consequently, the environmental values could be distinguished according to the geographical distribution pattern, namely, north and south. In the southern stations, stations were subdivided into Bering Strait and Bering Sea.

Comparing the composition between the five water masses, AW, WW, ACW, BSW, and MW, according to the abovementioned groups, group A consisted of only MW. Group B was composed of subequal amounts of WW and MW, whereas some ACW and BSW were confirmed (Table 3; Figure 4). In group C, AW and WW dominated. The Pacific-originated water masses, ACW and BSW, dominated in groups D and E. Comparing water masses with the groups, AW, WW, and MW represented high correlations with group B, namely, northern stations, whereas ACW and BSW showed a positive correlation with groups C, D, and E, the southern stations (Figures 3B, 4B). Additionally, ACW only was confirmed at the B03 and B14. In the nMDS plot (stress, 0.04), the stations were closely grouped according to the cluster analysis grouping (Figure 3B). Temperature, salinity, and fluorescence showed a relatively high correlation with groups D and E. DO values positively correlated with group B. Groups A and C indicated negative correlation with the temperature and salinity.

TABLE 2 Results of the PERMANOVA test based on the environmental values according to groups and between (pairwise tests) groups from each group.

| Source | df | SS | MS | Pseudo-F | *P* |
|---|---|---|---|---|---|
| Groups | 4 | 181.28 | 45.319 | 29.426 | **0.001** |
| Residual | 13 | 20.021 | 1.5401 | | |
| Total | 17 | 201.3 | | | |
| Pairwise tests | df | t | P | | |
| Group A & B | 6.8154 | 0.157 | 5 | | |
| Group A & C | No test | | | | |
| Group A & D | 3.7554 | 0.266 | 2 | | |
| Group A & E | 4.9511 | 0.121 | 6 | | |
| Group B & C | 7.3028 | 0.152 | 5 | | |
| Group B & D | 6.1557 | **0.011** | 7 | | |
| Group B & E | 8.8073 | **0.001** | 11 | | |
| Group C & D | 3.1179 | 0.277 | 2 | | |
| Group C & E | 3.6952 | 0.135 | 6 | | |
| Group D & E | 2.9115 | **0.009** | 8 | | |

Significance differences ($P < 0.05$) were bolded.

## Spatial pattern of the ichthyoplankton community

The number of species and abundance is summarized in Table 4. In this study, 20 ichthyoplankton taxa were confirmed. Among the sorted specimens, the mean total length was 35.55 mm ranging from 6.11 mm (*Hippoglossoides dubius*) to 109.74 mm (*Chauliodus macouni*). The minimum abundance was indicated at station A07, whereas the maximum was represented at station B05. *Gadus chalcogrammus* was the most dominant taxon in the present study, followed by *Pleuronectes quadrituberculatus* and *Boreogadus saida*. *Gadus chalcogrammus* showed a relatively high abundance at station B05. *Pleuronectes quadrituberculatus* indicated high abundance at station B01. *Boreogadus saida* showed high abundance at station B43. Geographically, *G. chalcogrammus* and *P. quadrituberculatus* dominated near the Bering Strait, whereas *B. saida* dominated around the Chukchi Sea (Figure 5). These three species accounted for approximately 50% of the total abundance in the present study.

Through hierarchical cluster analysis, we divided the ichthyoplankton community into four groups (Figure 6). Group A included only station B14. Group B consisted of two stations (B58 and B70). Group C included five stations (B20, B43, B49, B81, and B86). Of the stations in group C, station 49 indicated relatively low similarity with the other stations. Group D was composed of ten stations (A01, A05, A06, A07, A11, A15, A18, B01, B03, and B05).

10.3389/fmars.2024.1351844

TABLE 3 Relative composition (%) of water masses of the divided groups.

| Water mass | Group A (%) | Group B (%) | Group C (%) | Group D (%) | Group E (%) |
|---|---|---|---|---|---|
| AW | 0.0 | 45.4 | 0.0 | 0.0 | 0.0 |
| WW | 0.0 | 38.4 | 46.7 | 0.0 | 0.0 |
| ACW | 0.0 | 0.0 | 6.7 | 10.6 | 0.0 |
| BSW | 0.0 | 3.4 | 6.7 | 89.4 | 100.0 |
| MW | 100.0 | 12.9 | 40.0 | 0.0 | 0.0 |

AW, Atlantic water; WW, winter water; ACW, Alaskan coastal water; BSW: Bering summer water; MW, meltwater/runoff.

The stations in group D showed a relatively low latitude distribution (< 70°N) (Figure 6B). The four groups were separated from each other at a similarity level of 0%. This result meant that the four groups had different species compositions. In the PERMANOVA, the null hypothesis that there were no significant differences in the ichthyoplankton community between the separated groups was rejected (pseudo-F = 3.6917, $P < 0.05$) (Table 5). However, pairwise comparisons represented no significant difference between the A & B, A & C, and A & D pairs of groups ($P > 0.05$), whereas the B & C, B & D, and C & D pairs of groups showed significant differences ($P < 0.05$) (Table 5). In the SIMPER analysis, the average similarity of group A was not determined because this group was composed of only one species (*Eleginus gracilis*) (Table 6). The average similarity of group B was 95.62%, showing that one species (*Benthosema glaciale*) contributed to the group similarity of 100%. Group C represented 58.11% of the average similarity with the 100% contribution of *B. saida*. This result meant that *B. saida* was the main species in group C. The average similarity of group D was 10.84%, and two species (*Stenobrachius leucopsarus* and *G. chalcogrammus*) contributed to the group similarity of the upper 70%. Considering the average similarity of group D, the community composition of group D was relatively more varied than that of the other groups. Comparing the group dissimilarity between the groups, the average dissimilarity between group A and the other groups was 100%, and *E. gracilis* commonly contributed to the group dissimilarity (Table 7). Additionally, *E. gracilis* was confirmed only in group A at station B14 (Table 4; Figure 5). The average dissimilarity of groups B and C was 100%, and two species (*B. saida* and *B. glaciale*) contributed to the group dissimilarity of the upper 70%. Among the two species, *B. saida* was confirmed only in group C, whereas *B. glaciale* was confirmed in only group B. The average dissimilarity of groups B and D was 100%, and five species (*B. glaciale*, *S. leucopsarus*, *G. chalcogrammus*, *P. quadrituberculatus*, and *Sebastes reedi*) contributed to the group dissimilarity of the upper 70%. Only *B. glaciale* was confirmed in group B, and the remaining species were confirmed in group D. Between groups C and D, the average dissimilarity was 100%. Seven species (*B. saida*, *G. chalcogrammus*, *S. leucopsarus*, *P. quadrituberculatus*, *S. reedi*, *Gymnocanthus tricuspis*, and *Stomiiformes* sp.) contributed to the group dissimilarity of the upper 70%. Among the seven species, *B. saida* and *G. tricuspis* were observed only in group C, whereas other species were confirmed only in group D.

## The relationship between the ichthyoplankton community and environmental variables

In the CAP analysis, the first two squared canonical correlations clearly discriminated the four groups that were separated by CLUSTER analysis (Figure 7). The first squared canonical axis with a large correlation ($\delta^2 = 0.9949$) separated ichthyoplankton

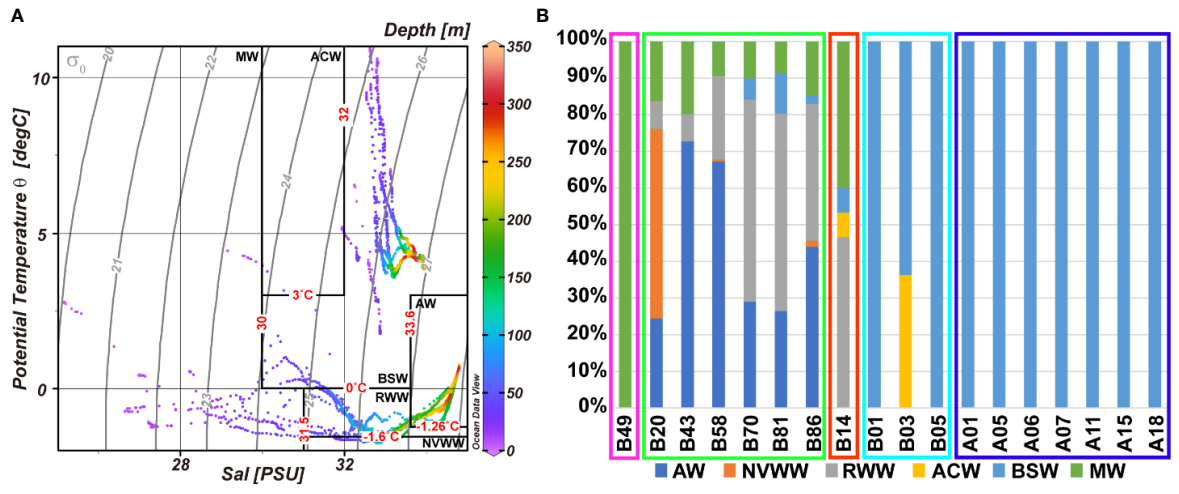


FIGURE 4
Potential temperature-salinity scatter plot (T-S diagram) for the sampling stations **(A)** and relative composition (%) of water masses **(B)**. ACW, Alaskan coastal water; AW, Atlantic water; BSW, Bering Sea water; MW, meltwater/runoff; NVWW, newly ventilated Pacific winter water; RWW, remnant Pacific winter water.

TABLE 4 Species composition and abundance (ind./$m^3$) of the ichthyoplankton community in the Pacific Arctic and sub-Arctic regions.

| Species | Group A | Group B | | Group C | | | | | Group D | | | | | | | | | | Total |
|---|---|---|---|---|---|---|---|---|---|---|---|---|---|---|---|---|---|---|---|
| | B14 | B58 | B70 | B20 | B43 | B49 | B81 | B86 | A1 | A5 | A6 | A7 | A11 | A15 | A18 | B1 | B3 | B5 | |
| *Albatrossia pectoralis* | | | | | | | | | | 0.66 | | | | | | | | | 0.66 |
| *Chauliodus macouni* | | | | | | | | | 0.57 | | | | | | | | | | 0.57 |
| *Gadus chalcogrammus* | | | | | | | | | | | | | | 7.42 | 1.88 | 4.84 | | 33.56 | 47.7 |
| *Sebastes polyspinis* | | | | | | | | | | 0.66 | | | | | | | | | 0.66 |
| *Sebastes reedi* | | | | | | | | | | 0.66 | 2.53 | | | | | | | | 3.19 |
| *Stenobrachius leucopsarus* | | | | | | | | | 2.83 | 0.66 | | | 3.72 | 1.85 | | | | | 9.06 |
| *Stenobrachius nannochir* | | | | | | | | | | 1.32 | | | | | | | | | 1.32 |
| *Zaprora silenus* | | | | | | | | | | | | | | | 5.65 | | | | 5.65 |
| *Stomiiformes* sp. | | | | | | | | | | | | 1.1 | | 0.93 | | | | | 2.03 |
| *Benthosema glaciale* | | 1.2 | 1.43 | | | | | | | | | | | | | | | | 2.63 |
| *Boreogadus saida* | | | | 2.71 | 3.31 | 8.3 | 2.54 | 2.53 | | | | | | | | | | | 19.39 |
| *Eleginus gracilis* | 6.66 | | | | | | | | | | | | | | | | | | 6.66 |
| *Gymnelus hemifasciatus* | | | | | | 8.3 | | | | | | | | | | | | | 8.3 |
| *Gymnocanthus tricuspis* | | | | | | | | 2.53 | | | | | | | | | | | 2.53 |
| *Hippoglossoides dubius* | | | | | | | | | | | | | | | | | | 8.39 | 8.39 |
| *Icelus spatula* | | | | | | 8.3 | | | | | | | | | | | | | 8.3 |
| *Liparis fabricii* | | | | | | 8.3 | | | | | | | | | | | | | 8.3 |
| *Pleuronectes quadrituberculatus* | | | | | | | | | | | | | | | | 14.52 | 6.99 | | 21.51 |
| *Hippoglossoides* sp. | | | | | | | | | | | | | | | | 4.84 | | | 4.84 |
| *Liparis* sp. | | | | | | | | | | | | | | | | 4.84 | | 8.39 | 13.23 |
| Total abundance | 6.66 | 1.2 | 1.43 | 2.71 | 3.31 | 33.2 | 2.54 | 5.06 | 3.4 | 3.96 | 2.53 | 1.1 | 3.72 | 10.2 | 7.53 | 29.04 | 6.99 | 50.34 | 174.92 |
| Total abundance by groups | 6.66 | 2.63 | | 46.82 | | | | | 118.81 | | | | | | | | | | |

communities in group B from other community groups. The second squared canonical axis with a large correlation ($\delta^2$ = 0.9949) discriminated the ichthyoplankton communities of the groups, although groups A and D were not clearly distinguished from each other. Among the species that contributed to group similarity and dissimilarity, *E. gracilis*, *G. chalcogrammus*, *P. quadrituberculatus*, *S. reedi*, *S. leucopsarus*, and *Stomiiformes* sp. showed a positive correlation with groups A and D. Two species (*B. saida* and *G. tricuspis*) indicated a positive relationship with group C. *Benthosema glaciale* represented a high positive correlation with group B (Figure 7A). Comparing the relationship between ichthyoplankton groups and environmental factors, temperature, salinity, and fluorescence had a positive relationship with groups A and D, although $Sal_{bottom}$ indicated a negative correlation with groups A and D. $Sal_{bottom}$ and DO showed a positive relationship with group C. Group B did not indicate any strong relationship with the environmental values (Figure 7B). In the BIOENV analysis, the ichthyoplankton community was best described by a combination of $Temp_{surface}$, $Temp_{average}$, $Sal_{surface}$, $Flu_{average}$, and $Flu_{bottom}$ ($\rho$ = 0.498, $P$ = 0.01) (Table 8).

# Discussion

## Physical properties of the Pacific Arctic and sub-Arctic regions in summer

For the environmental analyses, sampling stations could be divided into five groups. Geographically, groups A, B, and C were in the Chukchi Sea, whereas groups D and E were in the Bering Sea and Bering Strait, respectively. In other words, the former groups were included in the Pacific Arctic region, whereas the latter groups were in the Pacific sub-Arctic region. Group B included most of the Pacific Arctic region stations. Therefore, group B was considered to represent the summer physical properties of the Pacific Arctic region. However, group A was more closely grouped with group

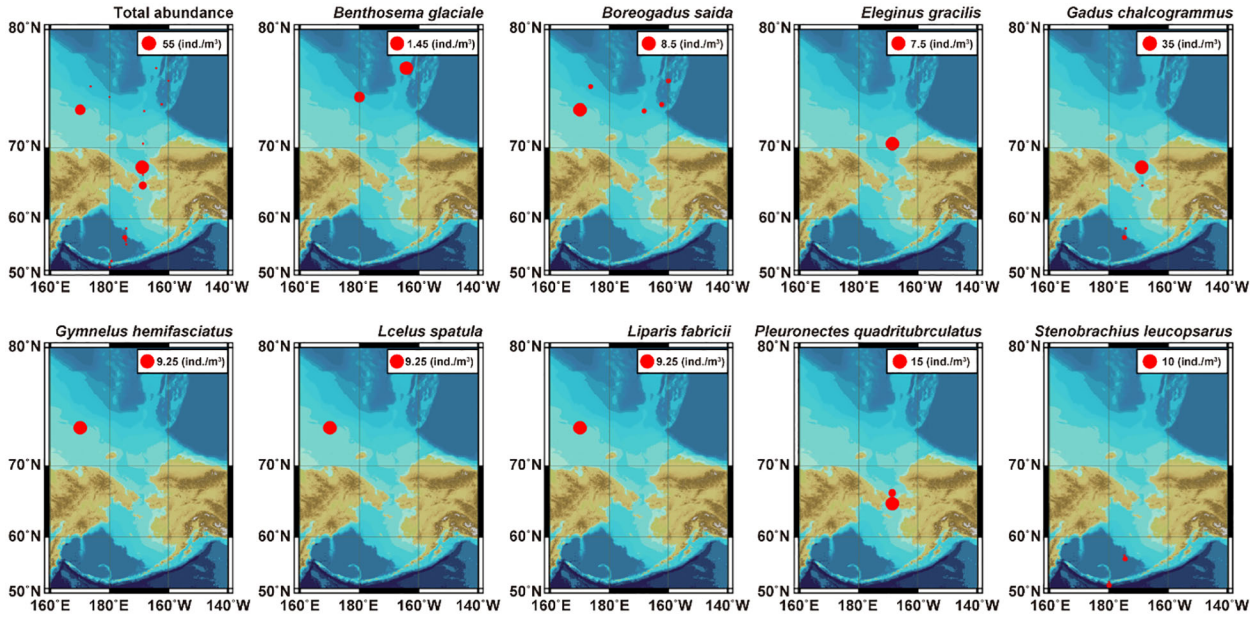


FIGURE 5
Comparison of the dominant species abundance (ind./$m^3$) at each survey station.

B than other groups, whereas group C was closer with groups D and E. Given that Pacific-originated water, ACW and BSW, have been confirmed in B14, the southern Chukchi Sea was influenced by the Pacific Ocean in this period. On the other hand, groups D and E were regarded as the typical Pacific sub-Arctic by including the stations located on the Bering Sea and Bering Strait. This clustering result corresponded well with the recent studies indicating that the Pacific Arctic and sub-Arctic biogeographic boundary now appears to the north of the Bering Strait (Baker et al., 2020, Baker et al., 2022). However, groups D and E can be subdivided into two groups according to the geographical region. Group D was composed of the Bering Sea station, whereas group E consisted of Bering Strait stations. In the nMDS analysis, the Pacific Arctic region stations, group B showed a positive correlation with the DO values. The Pacific sub-Arctic region stations, groups D and E, indicated a positive relationship with the water temperature, salinity, and fluorescence values. These results were derived from the effect of the warm surface water flow into the Chukchi Sea from the Pacific Ocean in summer (Jinping et al., 2006; Hu et al., 2019). This result well agreed with the future prediction that Arctic Ocean

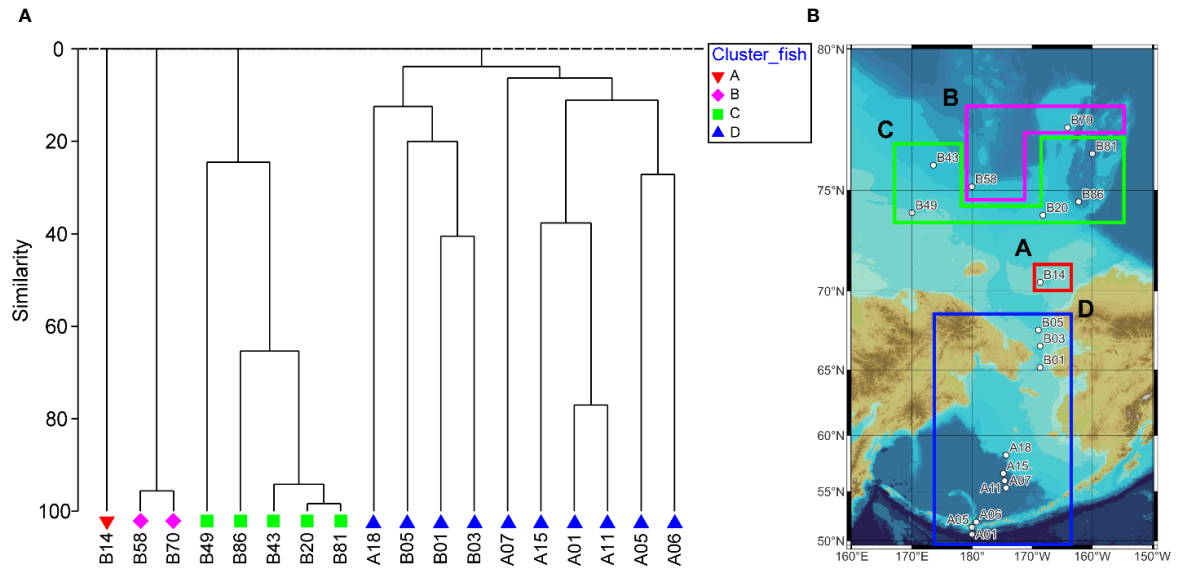


FIGURE 6
Dendrogram **(A)** indicating separated groups and map **(B)** representing divided groups according to the CLUSTER analysis.

TABLE 5 Results of the PERMANOVA test based on the ichthyoplankton abundance data according to groups and between (pairwise tests) groups.

| Source | df | SS | MS | Pseudo-F | *P* |
|---|---|---|---|---|---|
| Groups | 3 | 33559 | 11186 | 3.6917 | **0.001** |
| Residual | 14 | 42425 | 3030.4 | | |
| Total | 17 | 75984 | | | |
| Pairwise tests | df | t | P | | |
| Group A & B | 1 | 26.351 | 0.3388 | | |
| Group A & C | 4 | 2.3733 | 0.1676 | | |
| Group A & D | 9 | 1.1772 | 0.092 | | |
| Group B & C | 5 | 3.4701 | **0.0457** | | |
| Group B & D | 10 | 1.6793 | **0.0174** | | |
| Group C & D | 13 | 2.3114 | **0.0003** | | |

Significance differences (P < 0.05) were bolded.

temperatures will increase derived from higher heat fluxes through the sub-arctic region (Drinkwater et al., 2021). The higher fluorescence in the Pacific sub-Arctic region than in the Pacific Arctic region is believed to be caused by nutritional supplementation from the Pacific Ocean (Clement Kinney et al., 2022). Comparing the water masses between groups, group B was represented by the Pacific Arctic region composed of various water masses. That is, AW, WW, and MW were mixed, although the proportion differed according to the stations. Groups D and E, located in the Pacific sub-Arctic region, consisted of BSW, although B03 and B14 also included ACW. Of the Pacific Arctic groups, although the water mass composition of group C was similar to that of the other Pacific Arctic groups, Pacific-originated water masses, ACW and BSW, were also observed in group C. Therefore, it is thought that Pacific-originated summer water masses expanded to group A in this period. On the other hand, another Pacific Arctic group, group A, was composed only of the MW. Considering that meltwater could inflow from the SCC in the summer season (Weingartner et al., 1999; Semiletov et al., 2005; Spall, 2007) and freshened water is extending further east (Clement Kinney et al., 2022), group A could be affected by freshwater likely SCC containing relatively low salinity. Taken together, in the summer season, the survey region could be distinguished into the Pacific Arctic and sub-Arctic regions although climate changes such as warming and decreasing sea ice are changing water properties (Hirawake et al., 2021). The temperature increased southward as the warm surface water expanded from the Pacific Ocean (Jinping et al., 2006; Gong and Pickart, 2015; Pickart et al., 2019). The salinity decreased northward on the surface, although the average and bottom salinity were similar to each other. Considering that sea ice melt provides freshwater, the northwardly low surface salinity seems to be related to sea ice melting around the Arctic region (Gong and Pickart, 2015). DO was much higher in the Pacific Arctic region than in the Pacific sub-Arctic region. Given that winter water normally contains much oxygen supplied from the atmosphere, the high DO value in the Pacific Arctic region is related to the high winter water composition (Codispoti and Richards, 1971; Nishino et al., 2016). Considering water masses, although WW or MW dominated in the Pacific Arctic region, Pacific-originated summer water, such as ACW and BSW, flowed into the Pacific Arctic region in the southern Chukchi Sea (Pickart et al., 2019). The freshened MW that originated from the SCC flowed into the western Chukchi Sea from the East Siberian Sea (Semiletov et al., 2005; Spall, 2007).

TABLE 6 Result of the SIMPER analysis showing species that contribute to the group similarity of the divided groups.

| Group A (average similarity: -) | Av. Abund. | Av. sim. | Contrib.% | Cum.% |
|---|---|---|---|---|
| Less than 2 sample in group | | | | |
| Group B (average similarity: 95.62) | Av. Abund. | Av. sim. | Contrib.% | Cum.% |
| *Benthosema glaciale* | 1.15 | 95.62 | 100.0 | 100.0 |
| Group C (average similarity: 58.11) | Av. Abund. | Av. sim. | Contrib.% | Cum.% |
| *Boreogadus saida* | 1.91 | 58.11 | 100.0 | 100.0 |
| Group D (average similarity: 10.84) | Av. Abund. | Av. sim. | Contrib.% | Cum.% |
| *Stenobrachius leucopsarus* | 0.58 | 4.87 | 44.89 | 44.89 |
| *Gadus chalcogrammus* | 1.21 | 3.33 | 30.67 | 75.56 |

## Ichthyoplankton community structure

In this study, the ichthyoplankton community was distinguished according to geographical region. That is, the ichthyoplankton community was divided into two major groups, groups C and D. Group C consisted of the Pacific Arctic stations. The species that most contributed to the group similarity in the SIMPER analysis was *B. saida*, which is a typical dominant species in the Pacific Arctic region (Eisner et al., 2013; De Robertis et al., 2017; Vestfals et al., 2019; Axler et al., 2023). On the other hand, group D was composed of Pacific sub-Arctic stations. The species that contributed to the group similarity were *G. chalcogrammus* and *S. leucopsarus*, which commonly dominate in the Pacific sub-Arctic of the northern Pacific region (Pearcy et al., 1979; Beamish et al., 1999; Moku et al., 2000; Eisner et al., 2013; Majewski et al., 2017; Axler et al., 2023). Consequently, the two groups were thought to be made up of the typical ichthyoplankton community structure in each region. Groups A and B were distinguishable from groups C and D, respectively. *Eleginus gracilis* was the only species in group A. Considering a previous study, this species dominates between 66.5°N and 69.5°N (De Robertis et al., 2017). However, their distribution was confirmed above 70°N in 2019 (Levine et al., 2023). In this study, the distribution of *E. gracilis* was also confirmed above 70°N. These results agreed well with De Robertis

TABLE 7 Result of the SIMPER analysis, representing species that contribute to the group dissimilarity between the divided groups.

| Group A & B (average dissimilarity: 100.00) | A Av. Abund. | B Av. Abund. | Av. Diss. | Contrib.% | Cum.% |
|---|---|---|---|---|---|
| *Eleginus gracilis* | 2.58 | 0.00 | 69.27 | 69.27 | 69.27 |
| *Benthosema glaciale* | 0.00 | 1.15 | 30.73 | 30.73 | 100.0 |
| Group A & C (average dissimilarity: 100.00) | A Av. Abund. | C Av. Abund. | Av. Diss. | Contrib.% | Cum.% |
| *Eleginus gracilis* | 2.58 | 0.00 | 48.92 | 48.92 | 48.92 |
| *Boreogadus saida* | 0.00 | 1.91 | 33.30 | 33.30 | 82.22 |
| Group A & D (average dissimilarity: 100.00) | A Av. Abund. | D Av. Abund. | Av. Diss. | Contrib.% | Cum.% |
| *Eleginus gracilis* | 2.58 | 0.00 | 44.07 | 44.07 | 44.07 |
| *Gadus chalcogrammus* | 0.00 | 1.21 | 11.52 | 11.52 | 55.59 |
| *Stenobrachius leucopsarus* | 0.00 | 0.58 | 10.58 | 10.58 | 66.16 |
| *Pleuronectes quadrituberculatus* | 0.00 | 0.65 | 7.99 | 7.99 | 74.16 |
| Group B & C (average dissimilarity: 100.00) | B Av. Abund. | C Av. Abund. | Av. Diss. | Contrib.% | Cum.% |
| *Boreogadus saida* | 0.00 | 1.91 | 47.61 | 47.61 | 47.61 |
| *Benthosema glaciale* | 1.15 | 0.00 | 31.39 | 31.39 | 79.00 |
| Group B & D (average dissimilarity: 100.00) | B Av. Abund. | D Av. Abund. | Av. Diss. | Contrib.% | Cum.% |
| *Benthosema glaciale* | 1.15 | 0.00 | 27.49 | 27.49 | 27.49 |
| *Stenobrachius leucopsarus* | 0.00 | 0.58 | 14.63 | 14.63 | 42.12 |
| *Gadus chalcogrammus* | 0.00 | 1.21 | 13.65 | 13.65 | 55.78 |
| *Pleuronectes quadrituberculatus* | 0.00 | 0.65 | 10.28 | 10.28 | 66.05 |
| *Sebastes reedi* | 0.00 | 0.24 | 7.28 | 7.28 | 73.33 |
| Group C & D (average dissimilarity: 100.00) | C Av. Abund. | D Av. Abund. | Av. Diss. | Contrib.% | Cum.% |
| *Boreogadus saida* | 1.91 | 0.00 | 29.60 | 29.60 | 29.60 |
| *Gadus chalcogrammus* | 0.00 | 1.21 | 11.03 | 11.03 | 40.63 |
| *Stenobrachius leucopsarus* | 0.00 | 0.58 | 10.36 | 10.36 | 50.99 |
| *Pleuronectes quadrituberculatus* | 0.00 | 0.65 | 7.74 | 7.74 | 58.73 |
| *Sebastes reedi* | 0.00 | 0.24 | 4.94 | 4.94 | 63.67 |
| *Gymnocanthus tricuspis* | 0.32 | 0.00 | 4.87 | 4.87 | 68.54 |
| *Stomiiformes* sp. | 0.00 | 0.20 | 4.18 | 4.18 | 72.72 |

et al. (2017)'s argument that the distribution of *E. gracilis* is farther north than in earlier surveys (Vestfals et al., 2019; Marsh et al., 2020; Baker, 2021). Given that *E. gracilis* favors relatively high water temperatures, between 7°C and 9°C, and relatively low salinity, the inflow of relatively high temperature and low salinity water, such as the ACW, could influence the ichthyoplankton community of the Chukchi Sea (Gong and Pickart, 2015; De Robertis et al., 2017; Sigler et al., 2017; Lin et al., 2019; Pickart et al., 2019; Vestfals et al., 2019). This result agrees well with the present study that warm water and the ACW expanded to station B14 (Figures 2, 4B). *Benthosema glaciale* was the only species in group B. Considering that this species is mainly distributed in the Atlantic Arctic region, the observation of this species is unusual (Zhang et al., 2022). However, Zhang et al. (2022) confirmed the distribution of *B. glaciale* in the Chukchi Sea. These findings also correspond well with the present study. Considering that AW can flow into the Chukchi Sea through shelf-break upwelling along the continental slope (Lin et al., 2016; Corlett and Pickart, 2017; Jung et al., 2021; Wang and Danilov, 2022) and Atlantic species have been detected in the northern Chukchi Sea (Wildes et al., 2022), it is possible that this species was transported into the Chukchi Sea with shelf-break upwelling. The discovery of this species corresponds well with the

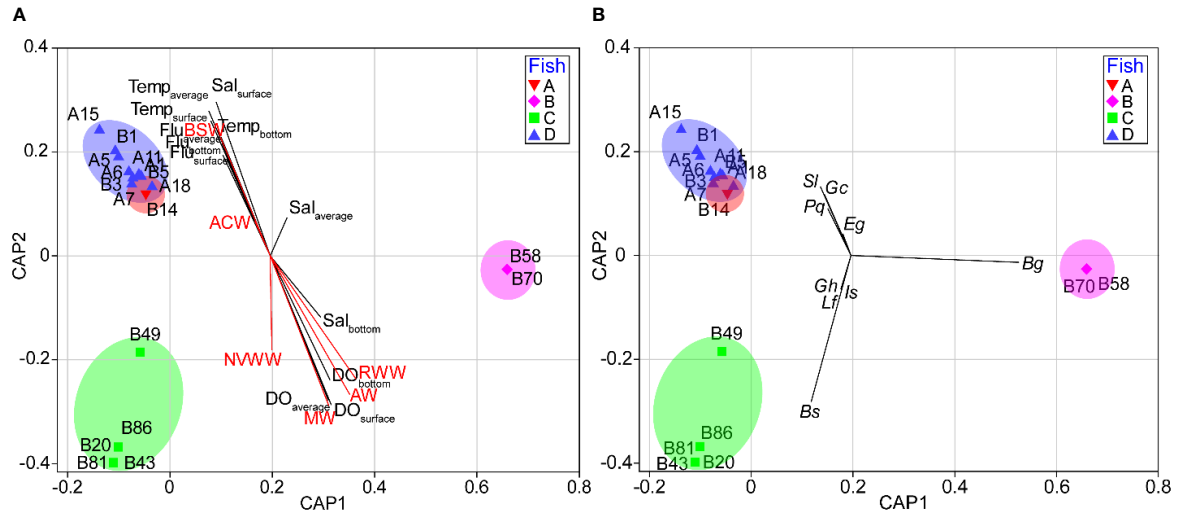


FIGURE 7
Canonical analysis of principal coordinates (CAP) plots based on log-transformed ichthyoplankton abundance data showing correlations with the dominant species **(A)** and environmental values **(B)**. Ba, *Benthosema glaciale*; Bs, *Boreogadus saida*; Eg, *Eleginus gracilis*; Gc, *Gadus chalcogrmmus*; Gh, *Gtmnelus hemifasciatus*; Is, *Icelus spatula*; Lf, *Liparis fabricii*; Pq, *Pleuronectes quadrituberculatus*; Sl, *Stenobrachius leucopsarus*.

route of the shelf-break jet (Corlett and Pickart, 2017; Zhang et al., 2022). Therefore, the invasion of Atlantic species is possible in the Chukchi Sea with AW upwelling. Additionally, although station 49 was classified within group C in the analysis of the ichthyoplankton community, it was separated from the other group C stations in the environmental analysis, indicating a relatively low similarity. Furthermore, the water mass composition of station 49 differed from that of the other Pacific Arctic region stations by consisting of only MW. In comparing the species composition of station 49, the three species, namely, *Gymnelus hemifasciatus*, *Icelus spatula*, and *Liparis fabricii*, were observed only at station 49 (Table 4). Of the three species, *I. spatula* and *L. fabricii* are mainly distributed along the coastline, showing that they favor fresh water (Tokranov and Orlov, 2005; Zorina and Chernova, 2022). Furthermore, although the two species show a wide distribution ranging from the Northern Pacific Ocean to the Atlantic Arctic region, considering that the spawning period of *Icelus spatula* occurs from late August in the Arctic region and after September in the sub-Arctic region, the larval specimens in this study likely originated from the eastern Siberian Sea (Tokranov and Orlov, 2005; Zorina and Chernova, 2022). *Liparis fabricii* is more abundant around the Atlantic Arctic region (Able, 1990; Walkusz et al., 2016; Smirnova et al., 2022). Currently, the record of this species has occasionally been reported in the East Siberian Sea and Chukchi Sea since Able (1990), whereas the abundance is low (Mecklenburg et al., 2007; Norcross et al., 2010; Smirnova et al., 2022). Considering that the SCC has freshwater inflow to the Chukchi Sea from the east, the two species at station 49 are thought to have invaded from the East Siberia Sea, whereas the MW expanded to the Chukchi Sea (Weingartner et al., 1999; Semiletov et al., 2005; Tokranov and Orlov, 2005; Spall, 2007).

TABLE 8 Summary of the results of the BIOENV analysis showing the best-matched combination between environmental values and the ichthyoplankton community.

| ρ | Best combination of environmental factors | *P* |
|---|---|---|
| 0.498 | $Temp_{surface}$, $Temp_{average}$, $Sal_{surface}$, $Flu_{average}$, $Flu_{bottom}$ | **0.01** |

ρ, Spearman correlation coefficient; *P*, statistical significance level.
Significance differences ($P < 0.05$) were bolded.

## Conclusions

In the Pacific Arctic, mainly in the Chukchi Sea, *B. saida* was the most dominant species, which is a typical Arctic fish (Eisner et al., 2013; Marsh et al., 2020; Baker et al., 2022; Axler et al., 2023; Cooper et al., 2023; Levine et al., 2023). In the Pacific sub-Arctic region, including the Bering Sea and Bering Strait, *G. chalcogrammus* and *P. quadrituberculatus* were the dominant and subdominant species, respectively (Eisner et al., 2013; Vestfals et al., 2019; Axler et al., 2023). Therefore, it is thought that the Bering Strait represented a more similar community structure to the Bering Sea than the Chukchi Sea in the summer season. This conclusion is supported by the biotic analyses of the close clustering of the stations around the Bering Strait with the Bering Sea. Additionally, the species composition was also well matched to typical species in the Pacific sub-Arctic region. Taken together, the typical ichthyoplankton communities in each region were confirmed in this survey. However, unusual community structures were also observed at several stations. At station B14, *E. gracilis* was observed. Considering a previous study, *E. gracilis* is more distributed northward than in previous reports because this species is mainly distributed between 66.5°N and 69.5°N (Vestfals et al., 2019; Baker, 2021; Levine et al., 2023). According to the previous studies, they are moving northward as the water temperature increases due to global warming (De Robertis et al., 2017; Baker et al., 2020; Axler et al., 2023; Levine et al., 2023). Furthermore, *B. glaciale*, typically

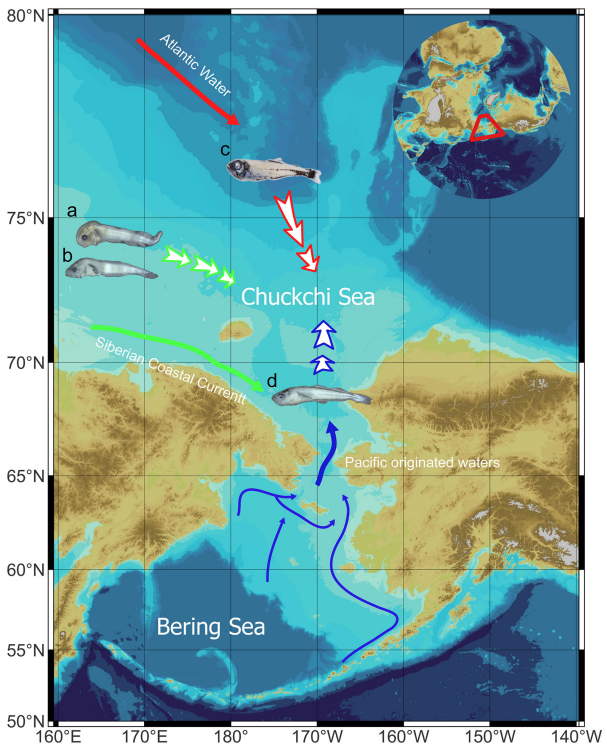


FIGURE 8
Diagram showing invasive species in the study area, the Chukchi Sea. **(A)**, *Liparis fabricii*; **(B)**, *Icelus spatula*; **(C)**, *Benthosema glaciale*; **(D)**, *Eleginus gracilis*.

distributed in the Atlantic Arctic region, was observed in the present study. Zhang et al. (2022) argued that this species is likely to invade the Pacific Arctic region through the expansion of warm AW because cold water restricts the expansion of *B. glaciale* to the North Pacific Arctic region (Zhang et al., 2022). This result is associated with "Atlantification, " which is triggered by the warm surface temperature and melting sea ice because sea ice melting leads to AW upwelling caused by the increased wind effect on the northern Chukchi Sea (Lin et al., 2016; Corlett and Pickart, 2017; Jung et al., 2021; Wang and Danilov, 2022). In addition to these unusual community compositions, several species, *I. spatula* and *L. fabricii*, moved to the Chukchi Sea region from the East Siberia Sea in this study as the SCC, including freshwater, expanded to the western Chukchi Sea. Considering that Siberian river discharge from permafrost thaw is increasing, water inflow from these rivers could often occur (Nummelin et al., 2016; Wang et al., 2021; Kanamori et al., 2023). All the abovementioned uncommon compositions are related to global warming, such as increased water temperature and sea ice melting (Richards et al., 2022; Wang and Danilov, 2022). That is, various fishes are transported into the Chukchi Sea as the water temperature increases and sea ice retreats. Species transportation from the Atlantic and East Siberian regions in this study is consistent with the findings of Wisz et al. (2015), who argued that transfers from the Atlantic to the Pacific Ocean would be primarily facilitated through the Northwest Passage. This phenomenon has been confirmed in various taxa (Beaugrand et al., 2002; Perry et al., 2005; Reid et al., 2007; Wisz et al., 2015; Kim et al., 2020, Kim et al., 2022). However, *Gadus macrocephalus*, another dominant species in the Pacific sub-Arctic regions, has not been observed in this survey although this species is also known as extending their distribution northward (Stevenson and Lauth, 2019; Baker, 2021; Cooper et al., 2023). Considering there have been various studies reported these days that record a dramatic shift in its geographical distribution, shift of the spatial distributions of the ichthyoplankton in the Pacific region (Mueter et al., 2017; Vestfals et al., 2019; Baker, 2021; Drinkwater et al., 2021). Further monitoring of the ichthyoplankton community in this region is required because of their commercial values (Stevenson and Lauth, 2019; Marsh et al., 2020; Baker, 2021). As the Chukchi Sea water masses are influenced by a variety of factors, including freshwater flow from the East Siberian Sea and warm water intrusion from the Pacific and Atlantic Oceans (Figure 8) (Grebmeier et al., 2006; Norcross et al., 2010), comprehensive monitoring of interbasin exchanges in the Chukchi Sea is critical in the context of global warming.

## Data availability statement

The original contributions presented in the study are included in the article/Supplementary Material. Further inquiries can be directed to the corresponding author.

## Author contributions

SK: Data curation, Formal analysis, Visualization, Writing – original draft, Writing – review & editing. WS: Writing – review & editing, Investigation, Methodology. JY: Data curation, Visualization, Software, Writing – review & editing. K-HC: Methodology, Formal analysis, Writing – review & editing. TP: Formal analysis, Methodology, Writing – review & editing, Resources. EY: Resources, Validation, Writing – review & editing. S-HK: Supervision, Conceptualization, Funding acquisition, Writing – review & editing. HL: Validation, Writing – review & editing, Conceptualization, Supervision.

## Funding

The author(s) declare financial support was received for the research, authorship, and/or publication of this article. This research was supported by the Ministry of Oceans and Fisheries projects, entitled "Korea-Arctic Ocean Warming and Response of Ecosystem (20210605)" and "Investigation and Prediction System Development of Marine Heat wave around the Korean Peninsula originated from the Sub-Arctic and Western Pacific (20230344)".

## Acknowledgments

The authors appreciate the careful assistance of the captain and crew of IBRV *Araon*. We express sincere gratitude to Professor Jinkoo Kim for the taxonomic identification of the ichthyoplankton species, which significantly contributed to this research.

## Conflict of interest

The authors declare that the research was conducted in the absence of any commercial or financial relationships that could be construed as a potential conflict of interest.

## Publisher's note

All claims expressed in this article are solely those of the authors and do not necessarily represent those of their affiliated organizations, or those of the publisher, the editors and the reviewers. Any product that may be evaluated in this article, or claim that may be made by its manufacturer, is not guaranteed or endorsed by the publisher.

## Supplementary material

The Supplementary Material for this article can be found online at: https://www.frontiersin.org/articles/10.3389/fmars.2024.1351844/full#supplementary-material

## References

Able, K. W. (1990). A revision of Arctic snailfishes of the genus Liparis (Scorpaeniformes: Cyclopteridae). *Copeia* 1990, 476–492. doi: 10.2307/1446352

Anderson, M. J., Gorley, R. N., and Clarke, K. R. (2008). *PERMANOVA+ for PRIMER: guide to software and statistical methods* (PRIMER-E: Plymouth).

Atwood, E., DUFFY-ANDERSON, J. T., Horne, J. K., and Ladd, C. (2010). Influence of mesoscale eddies on ichthyoplankton assemblages in the Gulf of Alaska. *Fisheries Oceanog.* 19, 493–507. doi: 10.1111/j.1365-2419.2010.00559.x

Axler, K. E., Goldstein, E. D., Nielsen, J. M., Deary, A. L., and Duffy-Anderson, J. T. (2023). Shifts in the composition and distribution of Pacific Arctic larval fish assemblages in response to rapid ecosystem change. *Global Change Biol.* 29, 4212–4233. doi: 10.1111/gcb.16721

Baker, M. R. (2021). Contrast of warm and cold phases in the Bering Sea to understand spatial distributions of Arctic and sub-Arctic gadids. *Polar Biol.* 44, 1083–1105. doi: 10.1007/s00300-021-02856-x

Baker, M. R., De Robertis, A., Levine, R. M., Cooper, D. W., and Farley, E. V. (2022). Spatial distribution of arctic sand lance in the Chukchi Sea related to the physical environment. *Deep Sea Res. Part II: Topical Stud. Oceanog.* 206, 105213. doi: 10.1016/j.dsr2.2022.105213

Baker, M. R., Farley, E. V., Danielson, S. L., Mordy, C., Stafford, K. M., and Dickson, D. M. (2023). Integrated research in the arctic-ecosystem linkages and shifts in the northern Bering Sea and eastern and western Chukchi Sea. *Deep Sea Res. Part II: Topical stud. Oceanog.* 208, 105251. doi: 10.1016/j.dsr2.2023.105251

Baker, M. R., and Hollowed, A. B. (2014). Delineating ecological regions in marine systems: Integrating physical structure and community composition to inform spatial management in the eastern Bering Sea. *Deep Sea Res. Part II: Topical Stud. Oceanog.* 109, 215–240. doi: 10.1016/j.dsr2.2014.03.001

Baker, M. R., Kivva, K. K., Pisareva, M. N., Watson, J. T., and Selivanova, J. (2020). Shifts in the physical environment in the Pacific Arctic and implications for ecological timing and conditions. *Deep Sea Res. Part II: Topical Stud. Oceanog.* 177, 104802. doi: 10.1016/j.dsr2.2020.104802

Beamish, R., Leask, K., Ivanov, O., Balanov, A., Orlov, A., and Sinclair, B. (1999). The ecology, distribution, and abundance of midwater fishes of the Subarctic Pacific gyres. *Prog. Oceanog.* 43, 399–442. doi: 10.1016/S0079-6611(99)00017-8

Beaugrand, G., Reid, P. C., Ibañez, F., Lindley, J. A., and Edwards, M. (2002). Reorganization of north atlantic marine copepod biodiversity and climate. *Science* 296, 1692–1694. doi: 10.1126/science.1071329

Benoit, D., Simard, Y., and Fortier, L. (2008). Hydroacoustic detection of large winter aggregations of Arctic cod (*Boreogadus saida*) at depth in ice-covered Franklin Bay (Beaufort Sea). *J. Geophys. Res.: Oceans* 113, C06S90. doi: 10.1029/2007jc004276

Boeing, W. J., and Duffy-Anderson, J. T. (2008). Ichthyoplankton dynamics and biodiversity in the Gulf of Alaska: responses to environmental change. *Ecol. Indic.* 8, 292–302. doi: 10.1016/j.ecolind.2007.03.002

Bouchard, C., and Fortier, L. (2008). Effects of polynyas on the hatching season, early growth and survival of polar cod Boreogadus saida in the Laptev Sea. *Mar. Ecol. Prog. Ser.* 355, 247–256. doi: 10.3354/meps07335

Bouchard, C., and Fortier, L. (2011). Circum-arctic comparison of the hatching season of polar cod Boreogadus saida: a test of the freshwater winter refuge hypothesis. *Prog. Oceanog.* 90, 105–116. doi: 10.1016/j.pocean.2011.02.008

Bourke, R. H., and Paquette, R. G. (1976). Atlantic water on the Chukchi shelf. *Geophys. Res. Lett.* 3, 629–632. doi: 10.1029/GL003i010p00629

Busby, M., Duffy-Anderson, J., Mier, K., and De Forest, L. (2014). Spatial and temporal patterns in summer ichthyoplankton assemblages on the eastern Bering Sea shelf 1996–2007. *Fisheries Oceanog.* 23, 270–287. doi: 10.1111/fog.12062

Clarke, K., and Gorley, R. (2015). *PRIMER v7: user manual/tutorial* (Plymouth: Primer-E Ltd).

Clarke, K. R., Gorley, R. N., Somerfield, P. J., and Warwick, R. M. (2014). *Change in marine communities: an approach to statistical analysis and interpretation. 3nd edition ed* (Plymouth: Primer-E Ltd).

Clement Kinney, J., Assmann, K. M., Maslowski, W., Björk, G., Jakobsson, M., Jutterström, S., et al. (2022). On the circulation, water mass distribution, and nutrient concentrations of the western Chukchi Sea. *Ocean Sci.* 18, 29–49. doi: 10.5194/os-18-29-2022

Codispoti, L., and Richards, F. (1971). Oxygen supersaturations in the Chukchi and East Siberian seas. *Deep Sea Res. Oceanograph. Abstracts*. 18, 341–351. doi: 10.1016/0011-7471(71)90039-8

Cooper, D. W., Cieciel, K., Copeman, L., Emelin, P. O., Logerwell, E., Ferm, N., et al. (2023). Pacific cod or tikhookeanskaya treska (Gadus macrocephalus) in the Chukchi Sea during recent warm years: Distribution by life stage and age-0 diet and condition. *Deep Sea Res. Part II: Topical Stud. Oceanog.* 208, 105241. doi: 10.1016/j.dsr2.2022.105241

Corlett, W. B., and Pickart, R. S. (2017). The Chukchi slope current. *Prog. Oceanog.* 153, 50–65. doi: 10.1016/j.pocean.2017.04.005

David, A. T., Simenstad, C. A., Cordell, J. R., Toft, J. D., Ellings, C. S., Gray, A., et al. (2016). Wetland loss, juvenile salmon foraging performance, and density dependence in Pacific Northwest estuaries. *Estuaries coasts* 39, 767–780. doi: 10.1007/s12237-015-0041-5

De Robertis, A., Taylor, K., Wilson, C. D., and Farley, E. V. (2017). Abundance and distribution of Arctic cod (*Boreogadus saida*) and other pelagic fishes over the US Continental Shelf of the Northern Bering and Chukchi Seas. *Deep Sea Res. Part II: Topical Stud. Oceanog.* 135, 51–65. doi: 10.1016/j.dsr2.2016.03.002

Doyle, M. J., Mier, K. L., Busby, M. S., and Brodeur, R. D. (2002). Regional variation in springtime ichthyoplankton assemblages in the northeast Pacific Ocean. *Prog. Oceanog.* 53, 247–281. doi: 10.1016/S0079-6611(02)00033-2

Drinkwater, K. F., Harada, N., Nishino, S., Chierici, M., Danielson, S. L., Ingvaldsen, R. B., et al. (2021). Possible future scenarios for two major Arctic Gateways connecting Subarctic and Arctic marine systems: I. Climate and physical–chemical oceanography. *ICES J. Mar. Sci.* 78, 3046–3065. doi: 10.1093/icesjms/fsab182

Eisner, L., Hillgruber, N., Martinson, E., and Maselko, J. (2013). Pelagic fish and zooplankton species assemblages in relation to water mass characteristics in the northern Bering and southeast Chukchi seas. *Polar Biol.* 36, 87–113. doi: 10.1007/s00300-012-1241-0

Falardeau, M., Robert, D., and Fortier, L. (2014). Could the planktonic stages of polar cod and Pacific sand lance compete for food in the warming Beaufort Sea? *ICES J. Mar. Sci.* 71, 1956–1965. doi: 10.1093/icesjms/fst221

Genner, M. J., Halliday, N. C., Simpson, S. D., Southward, A. J., Hawkins, S. J., and Sims, D. W. (2010). Temperature-driven phenological changes within a marine larval fish assemblage. *J. Plankton Res.* 32, 699–708. doi: 10.1093/plankt/fbp082

Gong, D., and Pickart, R. S. (2015). Summertime circulation in the eastern Chukchi Sea. *Deep Sea Res. Part II: Topical Stud. Oceanog.* 118, 18–31. doi: 10.1016/j.dsr2.2015.02.006

Grebmeier, J. M., Overland, J. E., Moore, S. E., Farley, E. V., Carmack, E. C., Cooper, L. W., et al. (2006). A major ecosystem shift in the northern Bering Sea. *Science* 311, 1461–1464. doi: 10.1126/science.1121365

Hirawake, T., Oida, J., Yamashita, Y., Waga, H., Abe, H., Nishioka, J., et al. (2021). Water mass distribution in the northern Bering and southern Chukchi seas using light absorption of chromophoric dissolved organic matter. *Prog. Oceanog.* 197, 102641. doi: 10.1016/j.pocean.2021.102641

Hu, X., Myers, P. G., and Lu, Y. (2019). Pacific Water pathway in the Arctic Ocean and Beaufort Gyre in two simulations with different horizontal resolutions. *J. Geophys. Res.: Oceans* 124, 6414–6432. doi: 10.1029/2019JC015111

Huntington, H. P., Danielson, S. L., Wiese, F. K., Baker, M., Boveng, P., Citta, J. J., et al. (2020). Evidence suggests potential transformation of the Pacific Arctic ecosystem is underway. *Nat. Climate Change* 10, 342–348. doi: 10.1038/s41558-020-0695-2

Jinping, Z., Jiuxin, S., Guoping, G., Yutian, J., and Hongxin, Z. (2006). Water mass of the northward throughflow in the Bering Strait in the summer of 2003. *Acta Oceanol. Sin.* 2), 25–32.

Jung, J., Cho, K. H., Park, T., Yoshizawa, E., Lee, Y., Yang, E. J., et al. (2021). Atlantic-origin cold saline water intrusion and shoaling of the nutricline in the Pacific Arctic. *Geophys. Res. Lett.* 48, e2020GL090907. doi: 10.1029/2020GL090907

Kanamori, H., Abe, M., Fujinami, H., and Hiyama, T. (2023). Impacts of global warming on summer precipitation trend over northeastern Eurasia during 1990–2010 using large-ensemble experiments. *Int. J. Climatol.* 43, 615–631. doi: 10.1002/joc.7798

Karcher, M. J., and Oberhuber, J. M. (2002). Pathways and modification of the upper and intermediate waters of the Arctic Ocean. *J. Geophys. Res.: Oceans* 107, 2–1-2-13. doi: 10.1029/2000jc000530

Kendall, A. W. (2000). An historical review of Seabastes taxonomy and systematics. *Mar. Fish. Rev.* 62, 1–24.

Kendall, A. W., and Duker, G. J. (1998). The development of recruitment fisheries oceanography in the United States. *Fisheries Oceanog.* 7, 69–88. doi: 10.1046/j.1365-2419.1998.00056.x

Kim, J.-H., Cho, K.-H., La, H. S., Choy, E. J., Matsuno, K., Kang, S.-H., et al. (2020). Mass occurrence of Pacific copepods in the Southern Chukchi Sea during summer: Implications of the high-temperature Bering summer water. *Front. Mar. Sci.* 7, 612. doi: 10.3389/fmars.2020.00612

Kim, J. H., La, H. S., Cho, K. H., Jung, J., Kang, S. H., Lee, K., et al. (2022). Spatial and interannual patterns of epipelagic summer mesozooplankton community structures in the western arctic ocean in 2016–2020. *J. Geophys. Res.: Oceans* 127, e2021JC018074. doi: 10.1029/2021jc018074

Levine, R. M., De Robertis, A., Grünbaum, D., Wildes, S., Farley, E. V., Stabeno, P. J., et al. (2023). Climate-driven shifts in pelagic fish distributions in a rapidly changing Pacific Arctic. *Deep Sea Res. Part II: Topical Stud. Oceanog.* 208, 105244. doi: 10.1016/j.dsr2.2022.105244

Li, S., Lin, P., Dou, T., Xiao, C., Itoh, M., Kikuchi, T., et al. (2022). Upwelling of atlantic water in barrow canyon, chukchi sea. *J. Geophys. Res.: Oceans* 127, e2021JC017839. doi: 10.1029/2021jc017839

Lin, P., Pickart, R. S., McRaven, L. T., Arrigo, K. R., Bahr, F., Lowry, K. E., et al. (2019). Water mass evolution and circulation of the northeastern Chukchi Sea in summer: Implications for nutrient distributions. *J. Geophys. Res.: Oceans* 124, 4416–4432. doi: 10.1029/2019jc015185

Lin, P., Pickart, R. S., Stafford, K. M., Moore, G., Torres, D. J., Bahr, F., et al. (2016). Seasonal variation of the B eaufort shelfbreak jet and its relationship to Arctic cetacean occurrence. *J. Geophys. Res.: Oceans* 121, 8434–8454. doi: 10.1002/jgrc.v121.12

Majewski, A. R., Atchison, S., MacPhee, S., Eert, J., Niemi, A., Michel, C., et al. (2017). Marine fish community structure and habitat associations on the Canadian Beaufort shelf and slope. *Deep Sea Res. Part I: Oceanograph. Res. Papers* 121, 169–182. doi: 10.1016/j.dsr.2017.01.009

Marsh, J. M., Mueter, F. J., and Quinn, T. J. (2020). Environmental and biological influences on the distribution and population dynamics of polar cod (Boreogadus saida) in the US Chukchi Sea. *Polar Biol.* 43, 1055–1072. doi: 10.1007/s00300-019-02561-w

Matarese, A. C., Kendall, A. W., Blood, J. D. M., and VInter, B. M. (1989). *Laboratory guide to early life history stages of northeast Pacific fishes* (Seattle: NOAA Technical Report NMFS).

Mecklenburg, C. W., Stein, D. L., Sheiko, B. A., Chernova, N. V., Mecklenburg, T. A., and Holladay, B. A. (2007). Russian–American long-term census of the Arctic: benthic fishes trawled in the Chukchi Sea and Bering Strait, August 2004. *Northwestern Nat.* 88, 168–187. doi: 10.1898/1051-1733(2007)88[168:RLCOTA]2.0.CO;2

Moku, M., Kawaguchi, K., Watanabe, H., and Ohno, A. (2000). Feeding habits of three dominant myctophid fishes, Diaphus theta, Stenobrachius leucopsarus and S. nannochir, in the subarctic and transitional waters of the western North Pacific. *Mar. Ecol. Prog. Ser.* 207, 129–140. doi: 10.3354/meps207129

Mueter, F. J., and Litzow, M. A. (2008). Sea ice retreat alters the biogeography of the Bering Sea continental shelf. *Ecol. Appl.* 18, 309–320. doi: 10.1890/07-0564.1

Mueter, F. J., Weems, J., Farley, E. V., and Sigler, M. F. (2017). Arctic ecosystem integrated survey (Arctic Eis): marine ecosystem dynamics in the rapidly changing Pacific Arctic Gateway. *Deep Sea Res II.* 135, 1–6. doi: 10.1016/j.dsr2.2016.11.005

Nishino, S., Kikuchi, T., Fujiwara, A., Hirawake, T., and Aoyama, M. (2016). Water mass characteristics and their temporal changes in a biological hotspot in the southern Chukchi Sea. *Biogeosciences* 13, 2563–2578. doi: 10.5194/bg-13-2563-2016

Norcross, B. L., Holladay, B. A., Busby, M. S., and Mier, K. L. (2010). Demersal and larval fish assemblages in the Chukchi Sea. *Deep Sea Res. Part II: Topical Stud. Oceanog.* 57, 57–70. doi: 10.1016/j.dsr2.2009.08.006

Nummelin, A., Ilicak, M., Li, C., and Smedsrud, L. H. (2016). Consequences of future increased Arctic runoff on Arctic Ocean stratification, circulation, and sea ice cover. *J. Geophys. Res.: Oceans* 121, 617–637. doi: 10.1002/2015JC011156

Okiyama, M. (1989). *An atlas of the early stage stage fishes in Japan* (Tokyo: Tokai University Press).

Pearcy, W. G., Nemoto, T., and Okiyama, M. (1979). Mesopelagic fishes of the Bering Sea and adjacent northern North Pacific Ocean. *J. Oceanograph. Soc. Japan* 35, 127–135. doi: 10.1007/BF02114305

Perry, A. L., Low, P. J., Ellis, J. R., and Reynolds, J. D. (2005). Climate change and distribution shifts in marine fishes. *Science* 308, 1912–1915. doi: 10.1126/science.1111322

Pickart, R. S., Nobre, C., Lin, P., Arrigo, K. R., Ashjian, C. J., Berchok, C., et al. (2019). Seasonal to mesoscale variability of water masses and atmospheric conditions in Barrow Canyon, Chukchi Sea. *Deep Sea Res. Part II: Topical Stud. Oceanog.* 162, 32–49. doi: 10.1016/j.dsr2.2019.02.003

Polyakov, I. V., Pnyushkov, A. V., Alkire, M. B., Ashik, I. M., Baumann, T. M., Carmack, E. C., et al. (2017). Greater role for Atlantic inflows on sea-ice loss in the Eurasian Basin of the Arctic Ocean. *Science* 356, 285–291. doi: 10.1126/science.aai8204

Randall, J. R., Busby, M. S., Spear, A. H., and Mier, K. L. (2019). Spatial and temporal variation of late summer ichthyoplankton assemblage structure in the eastern Chukchi Sea: 2010–2015. *Polar Biol.* 42, 1811–1824. doi: 10.1007/s00300-019-02555-8

Reid, P., Johns, D., Edwards, M., Starr, M., Poulin, M., and Snoeijs, P. (2007). A biological consequence of reducing Arctic ice cover: Arrival of the Pacific diatom Neodenticula seminae in the North Atlantic for the first time in 800000 years. *Global Change Biol.* 13, 1910–1921. doi: 10.1111/j.1365-2486.2007.01413.x

Richards, A. E., Johnson, H. L., and Lique, C. (2022). Spatial and temporal variability of Atlantic Water in the Arctic from 40 years of observations. *J. Geophys. Res.: Oceans* 127, e2021JC018358. doi: 10.1029/2021jc018358

Rodriguez, J., Gonzalez-Pola, C., Lopez-Urrutia, A., and Nogueira, E. (2011). Composition and daytime vertical distribution of the ichthyoplankton assemblage in the Central Cantabrian Sea shelf, during summer: An Eulerian study. *Continental Shelf Res.* 31, 1462–1473. doi: 10.1016/j.csr.2011.06.007

Semiletov, I., Dudarev, O., Luchin, V., Charkin, A., Shin, K. H., and Tanaka, N. (2005). The East Siberian Sea as a transition zone between Pacific-derived waters and Arctic shelf waters. *Geophys. Res. Lett.* 32, L10614. doi: 10.1029/2005GL022490

Siddon, E. C., Duffy-Anderson, J. T., and Mueter, F. J. (2011). Community-level response of fish larvae to environmental variability in the southeastern Bering Sea. *Mar. Ecol. Prog. Ser.* 426, 225–239. doi: 10.3354/meps09009

Sigler, M. F., Mueter, F. J., Bluhm, B. A., Busby, M. S., Cokelet, E. D., Danielson, S. L., et al. (2017). Late summer zoogeography of the northern Bering and Chukchi seas. *Deep Sea Res. Part II: Topical Stud. Oceanog.* 135, 168–189. doi: 10.1016/j.dsr2.2016.03.005

Smirnova, E., Chernova, N., and Karamushko, O. (2022). Species composition, abundance, distribution features and size characteristics of fish of the genus liparis (Cottiformes: liparidae) in the east-siberian and laptev seas. *J. Ichthyol.* 62, 850–862. doi: 10.1134/S0032945222050174

Spall, M. A. (2007). Circulation and water mass transformation in a model of the Chukchi Sea. *J. Geophys. Res.: Oceans* 112, C05025. doi: 10.1029/2005jc003364

Stabeno, P., Kachel, N., Ladd, C., and Woodgate, R. (2018). Flow patterns in the eastern Chukchi Sea: 2010–2015. *J. Geophys. Res.: Oceans* 123, 1177–1195. doi: 10.1002/2017jc013135

Stabeno, P. J., and Bell, S. W. (2019). Extreme conditions in the bering sea, (2017–2018): Record-breaking low sea-ice extent. *Geophys. Res. Lett.* 46, 8952–8959. doi: 10.1029/2019GL083816

Stevenson, D. E., and Lauth, R. R. (2019). Bottom trawl surveys in the northern Bering Sea indicate recent shifts in the distribution of marine species. *Polar Biol.* 42, 407–421. doi: 10.1007/s00300-018-2431-1

Tokranov, A., and Orlov, A. (2005). Some Features of the Biology of *Icelus spatula* (Cottidae) in Pacific Waters off the Northern Kuril Islands. *J. Ichthyol.* 45, 229–236.

Valesini, F., Tweedley, J., Clarke, K., and Potter, I. (2014). The importance of regional, system-wide and local spatial scales in structuring temperate estuarine fish communities. *Estuaries coasts* 37, 525–547. doi: 10.1007/s12237-013-9720-2

Vestfals, C. D., Mueter, F. J., Duffy-Anderson, J. T., Busby, M. S., and De Robertis, A. (2019). Spatio-temporal distribution of polar cod (Boreogadus saida) and saffron cod (Eleginus gracilis) early life stages in the Pacific Arctic. *Polar Biol.* 42, 969–990. doi: 10.1007/s00300-019-02494-4

Walkusz, W., Paulic, J. E., Wong, S., Kwasniewski, S., Papst, M. H., and Reist, J. D. (2016). Spatial distribution and diet of larval snailfishes (Liparis fabricii, Liparis gibbus, Liparis tunicatus) in the Canadian Beaufort Sea. *Oceanologia* 58, 117–123. doi: 10.1016/j.oceano.2015.12.001

Wang, M., Yang, Q., Overland, J. E., and Stabeno, P. (2018). Sea-ice cover timing in the Pacific Arctic: The present and projections to mid-century by selected CMIP5 models. *Deep Sea Res. Part II: Topical Stud. Oceanog.* 152, 22–34. doi: 10.1016/j.dsr2.2017.11.017

Wang, P., Huang, Q., Pozdniakov, S. P., Liu, S., Ma, N., Wang, T., et al. (2021). Potential role of permafrost thaw on increasing Siberian river discharge. *Environ. Res. Lett.* 16, 034046. doi: 10.1088/1748-9326/abe326

Wang, Q., and Danilov, S. (2022). A synthesis of the upper arctic ocean circulation during 2000-2019: understanding the roles of wind forcing and sea ice decline. *Front. Mar. Sci.* 9, 863204. doi: 10.3389/fmars.2022.863204

Wassmann, P., Duarte, C. M., Agusti, S., and Sejr, M. K. (2011). Footprints of climate change in the Arctic marine ecosystem. *Global Change Biol.* 17, 1235–1249. doi: 10.1111/j.1365-2486.2010.02311.x

Weingartner, T. J., Danielson, S., Sasaki, Y., Pavlov, V., and Kulakov, M. (1999). The Siberian Coastal Current: A wind-and buoyancy-forced Arctic coastal current. *J. Geophys. Res.: Oceans* 104, 29697–29713. doi: 10.1029/1999jc900161

Wildes, S., Whittle, J., Nguyen, H., Marsh, M., Karpan, K., D'Amelio, C., et al. (2022). Walleye Pollock breach the Bering Strait: a change of the cods in the arctic. *Deep Sea Res. Part II: Topical Stud. Oceanog.* 204, 105165. doi: 10.1016/j.dsr2.2022.105165

Wisz, M., Broennimann, O., Grønkjær, P., Møller, P. R., Olsen, S. M., Swingedouw, D., et al. (2015). Arctic warming will promote Atlantic–Pacific fish interchange. *Nat. Climate Change* 5, 261–265. doi: 10.1038/nclimate2500

Wood, K. R., Bond, N. A., Danielson, S. L., Overland, J. E., Salo, S. A., Stabeno, P. J., et al. (2015). A decade of environmental change in the Pacific Arctic region. *Prog. Oceanog.* 136, 12–31. doi: 10.1016/j.pocean.2015.05.005

Woodgate, R. A., Aagaard, K., and Weingartner, T. J. (2005). Monthly temperature, salinity, and transport variability of the Bering Strait through flow. *Geophys. Res. Lett.* 32, L04601. doi: 10.1029/2004GL021880

Zhang, R., Li, Y., Liu, Q., Song, P., Li, H., Wang, R., et al. (2022). Glacier lanternfish (Benthosema glaciale) first found on the continental slope of the Pacific Arctic. *Polar Biol.* 45, 1–6. doi: 10.1007/s00300-021-02988-0

Zorina, A., and Chernova, N. (2022). Morphological variability and diagnostics of two sculpins Icelus bicornis and I. spatula (Cottiformes: Cottidae) from the Arctic. *Proc. Zool. Institute RAS* 326, 86–101. doi: 10.31610/trudyzin

frontiers | Frontiers in Marine Science

TYPE Original Research
PUBLISHED 10 September 2024
DOI 10.3389/fmars.2024.1274582



OPEN ACCESS

EDITED BY
Jeff Shimeta,
RMIT University, Australia

REVIEWED BY
Rajani Kanta Mishra,
Ministry of Earth Sciences, India
Ajit Kumar Mohanty,
Indira Gandhi Centre for Atomic Research (IGCAR), India

*CORRESPONDENCE
Kerrie M. Swadling
k.swadling@utas.edu.au
Guang Yang
yangguang@qdio.ac.cn

RECEIVED 08 August 2023
ACCEPTED 22 July 2024
PUBLISHED 10 September 2024

CITATION
Liu Y, Wang Y, Sun Y, Yang G and Swadling KM (2024) Zooplankton vertical stratification in the East-pacific and Indian sectors of the Southern Ocean.
*Front. Mar. Sci.* 11:1274582.
doi: 10.3389/fmars.2024.1274582



# Zooplankton vertical stratification in the East-pacific and Indian sectors of the Southern Ocean

Yunzhe Liu[1,2], Yanqing Wang[1,3,4], Yongming Sun[5], Guang Yang[1,3,6,7]* and Kerrie M. Swadling[2,8]*

[1]Key Laboratory of Marine Ecology and Environmental Sciences, Institute of Oceanology, Chinese Academy of Sciences, Qingdao, China, [2]Institute for Marine and Antarctic Studies, University of Tasmania, Hobart, TAS, Australia, [3]Laboratory for Marine Ecology and Environmental Science, Qingdao National Laboratory for Marine Science and Technology, Qingdao, China, [4]Engineering and Technology Department, Institute of Oceanology, Chinese Academy of Sciences, Qingdao, China, [5]Key Laboratory of Physical Oceanography, College of Oceanic and Atmospheric Sciences, Ocean University of China, Qingdao, China, [6]Center for Ocean Mega-Science, Chinese Academy of Sciences, Qingdao, China, [7]College of Earth Science, University of Chinese Academy of Sciences, Beijing, China, [8]Australian Antarctic Program Partnership, Institute for Marine and Antarctic Studies, University of Tasmania, Hobart, TAS, Australia

**Introduction:** In the Southern Ocean, the large-scale distribution of zooplankton, including their abundance and community composition from the epipelagic to the upper bathypelagic layers, remains poorly understood. This gap in knowledge limits our comprehension of their ecological and biogeochemical roles.

**Methods:** To better understand their community structure, depth-stratified zooplankton samples were collected from 0 to 1500 m during four summers in the East-Pacific and Indian sectors of the Southern Ocean. In addition, analysis of environmental drivers including temperature, salinity, dissolved oxygen, and chlorophyll a concentration, as well as water masses was conducted.

**Results:** Our study indicates that zooplankton diversity may be similar between the two sectors, while zooplankton abundance was higher in the East-Pacific sector during different sampling months and years. Moreover, zooplankton abundance decreased with depth in both sectors. Based on cluster analysis, zooplankton communities were generally divided by either the epipelagic or the deeper layers' communities. In both sectors, the epipelagic layer was dominated by cyclopoid copepods, such as *Oithona similis* and *Oncaea curvata*, as well as calanoid copepods including *Calanoides acutus, Rhincalanus gigas*, and *Ctenocalanus citer*, while copepods and other taxa including Chaetognatha, Amphipoda, and Ostracoda, were important contributors to the deep layer communities.

**Discussion:** Our analysis revealed that water masses, combined with their physical characteristics such as specific temperature and salinity ranges and depth, along with biological factors such as chlorophyll a concentration, might be the most important drivers for structuring zooplankton communities from epipelagic to upper bathypelagic layer.

KEYWORDS

**mesozooplankton, vertical distribution, Antarctic Surface Water, Circumpolar Deep Water, Antarctic zooplankton survey, planktonic food webs**

# 1 Introduction

As one of the most important components in the marine ecosystems, zooplankton, which have a biomass in the millions of tons, maintain the structure and function of marine ecosystems and contribute to global biogeochemical cycles such as carbon cycle, particularly in the climatically important Southern Ocean (Robinson et al., 2010; Irigoien et al., 2014; Boyd et al., 2019; Johnston et al., 2022; Yang et al., 2022). The Southern Ocean, including the Antarctic Zone and the Southern Zone, has one of the most productive but dynamic ecosystems on the planet (Nicol et al., 2000; Constable, 2003; Arrigo et al., 2008; Yang et al., 2021). The Antarctic Zone between the Polar Front (PF) and the Southern Antarctic Circumpolar Current Front (SACCF) and the Southern Zone between the SACCF and the Southern Boundary Antarctic Circumpolar Current (SBACC) is characterized by seasonal sea ice (SSI) and the Antarctic Circumpolar Current (ACC) (Deacon, 1982; Carter et al., 2008; Talley et al., 2011). The SSI along with temperature and salinity dynamics regulates growth and reproduction of plankton (Arrigo and Thomas, 2004; Abelmann et al., 2015). The ACC, connecting to the Atlantic, Indian, and Pacific Ocean basins, exchanges salinity, heat, nutrients, and plankton with these three basins (Murphy et al., 2021). These exchanges are crucial for regulating global temperature and biogeochemical cycles, as well as zooplankton advection, dispersal, and distribution (Murphy et al., 2021). The Indian and East-Pacific sectors are connected by the same large-scale circulation (the ACC) and shared same water masses down to the bathypelagic layer, but display distinct regional oceanographic features, such as the Weddell Gyre and Ross Sea Gyre (Gouretski, 1999; Jacobs, 2004; Williams et al., 2010; Vernet et al., 2019). These two interconnected sectors, characterized by similar large-scale environmental conditions yet distinct mesoscale features, make these two sectors appropriate for conducting comparative analysis of zooplankton community structure and its environmental drivers.

Zooplankton distribution, which is reflected in their community structure and abundance, is shaped by a combination of abiotic factors such as physical oceanographic features, and biotic factors such as food availability (Atkinson, 1998a; Hunt and Hosie, 2005; McManus and Woodson, 2012). In the Southern Ocean, zooplankton with weak swimming capacity are driven by water masses, and large-scale ocean circulation such as the ACC (Johnston et al., 2022). To adapt to unique Antarctic environments, their distribution down to deep layer is affected by regional environmental factors such as seasonality, salinity and water temperature (Constable et al, 2014; Murphy et al., 2016; Boscolo-Galazzo et al., 2021; Johnston et al., 2022). As heterotrophs occupying lower levels of marine food webs, their abundance is also influenced by food availability such as chlorophyll-a (chl-a) concentration (bottom-up control), and other trophic interactions such as predation (top-down control), and competition (Swadling et al., 2010). Moreover, zooplankton perform ontogenetic, diel, and seasonal vertical migrations to complete their life cycles, and there is a balance between predation risk and foraging, which could potentially impact their vertical distribution (Swadling et al., 2010). Some of these critical physical factors, including temperature, salinity and depth, along with biological factors, such as chl-a concentration, can be combined and incorporated into physical and biological characteristics of water masses. However, how these characteristics of water masses could interactively influence the zooplankton communities from the epipelagic to the bathypelagic layers are uncertain.

To date, only a few studies have undertaken regional and local surveys of the vertical community structure of mesozooplankton down to the mesopelagic or upper bathypelagic layer in regions of the Southern Ocean including South Georgia, the Antarctic Peninsula, the Weddell Sea, the Lazarev Sea, the Scotia Sea, and Prydz Bay (Atkinson and Peck, 1988b; Hopkins and Torres, 1988; Atkinson and Sinclair, 2000; Flores et al., 2014; Ward et al., 2014a; Yang et al., 2017). These studies, which employed different sampling methods, sampling strata, and focused environmental drivers, have not yet provided a consistent overview of the large-scale vertical distribution patterns of zooplankton, nor their multiple environmental drivers in the Southern Ocean. Moreover, the difference and similarity of zooplankton communities between sectors are unclear. Consequently, the understanding of the community structure of zooplankton and its environmental drivers, particularly in the mesopelagic and upper bathypelagic layers, are limited in the Southern Ocean.

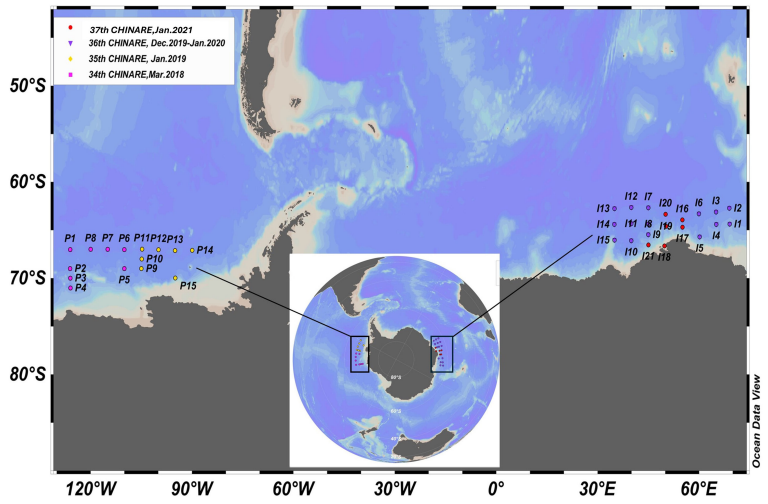


FIGURE 1
Sampling locations in the East-Pacific sector between 90 to 130 °W (station P1-P15) and the Indian sector between 30 to 70°E (station I1-I21).

To enhance our understanding of large-scale zooplankton distribution from the epipelagic to the upper bathypelagic layers in the Southern Ocean, therefore their ecological and biogeochemical roles, we analysed the fundamental aspects of zooplankton community, including their abundance, taxonomic diversity, and community composition, along with relevant environmental factors based on samples collected during the 34$^{th}$, 35$^{th}$, 36$^{th}$, and 37$^{th}$ Chinese National Antarctic Research Expeditions (CHINARE) from 2018 to 2021. We aim to provide valuable insights into the large-scale vertical distribution patterns of zooplankton and associated environmental drivers in the East-Pacific and Indian sectors.

# 2 Methods

## 2.1 Zooplankton samples and environmental data collection

During the 34$^{th}$ (Mar 2018), 35$^{th}$ (Jan 2019), 36$^{th}$ (Dec 2019-Jan 2020), and 37$^{th}$ (Jan 2021) CHINARE, zooplankton and environmental data were collected from a total of thirty-six stations in the East-Pacific sector (67-71 °S, 89-127 °W) and Indian sector (62-67 °S, 35-71 °E) of the Southern Ocean for four summers (Figure 1). The bathymetry at the stations ranged from 2101 m to 4993 m. This sampling was conducted onboard the Research Vessels Xue Long and Xue Long 2. All procedures and gears for collecting zooplankton samples and environmental data were the same on these four expeditions. The Hydro-Bios Multi-Net type Midi (mesh size of 200-µm, mouth of 0.25 m$^2$) was deployed vertically from 1500 m to 0 m upon the vessel's arrival at each station, irrespective of the time of day (Supplementary Table 1). Five sampling intervals were 0-100, 100-200, 200-500, 500-1000, and 1000-1500 m. After zooplankton sample collection, all samples were immediately preserved in a 5% neutral-buffered formaldehyde solution for later analysis. Environmental data, including temperature, salinity, and dissolved oxygen concentration from 0-1500 m, were measured using a Seabird 911plus Conductivity Temperature Depth (CTD) sensor with SBE 63 from stations. However, Seabird 911plus CTD sensor was lost during 36$^{th}$ CHINARE, so temperature, salinity and dissolved oxygen were not available from station I5 to I15. Therefore, mean values of temperature, salinity and dissolve oxygen and their correlations with zooplankton abundance for five sampling strata and three water layers including epipelagic (0-200 m), mesopelagic (200-1000 m) and upper bathypelagic layers (1000-1500 m) were only analysed at rest of 21 stations. For measuring *in situ* chl-a concentration above surface mixed layer where phytoplankton mainly grow, discrete water samples at each station were collected at depths of 25, 50, 75, 100, 150 and 200 m using 10-L Niskin bottles attached to a rosette of the Seabird 911 plus CTD. Moreover, the Phytoplankton cells from the 10 L water samples were collected using Whatman® Glass Microfiber Filters (0.7 mm nominal pore size) (Mock and Hoch, 2005). The concentrated cells containing chl-a pigments were then extracted in 90% acetone overnight at 4°C. Finally, a Turner Designs 10-AU field fluorometer, calibrated with a purified chl-a standard, was used to measure the chl-a concentration (Mock and Hoch, 2005).

## 2.2 Hydrography and water masses analysis

As potential physical drivers of zooplankton distribution, temperature, salinity, and dissolved oxygen patterns were exhibited by three-dimensional temperature, salinity and oxygen profiles by Python. Then, *in-situ* measurements of temperature and salinity were utilized to construct T-S diagrams and define water masses from 0-1500 m depth. AASW is characterized by temperatures ranging from −1.8 to 1.0 °C and salinity between 33.0 to 33.7 (Smith et al., 1999). Additionally, WW is located beneath AASW and can be identified by a temperature minimum of approximately −1.5 °C, with salinity between 33.8 to 34.0 (Smith et al., 1999). Circumpolar Deep Water (CDW) was defined by potential temperature lower than 1.5 °C and salinity between 34.5 to 34.75 thresholds, and modified CDW was identified as the water

mass with temperature lower than 1.5 °C and salinity lower than 34.7 (Zu et al., 2022). Furthermore, as physical characteristics of water masses, these temperature and salinity ranges will be used in subsequent steps to identify any correlation between zooplankton abundance and water masses.

## 2.3 Zooplankton identification and counts

In the laboratory, zooplankton specimens were identified to the lowest possible taxonomic level based on morphological features of species or groups and were counted using a Nikon SMZ 745T dissecting microscope. A compound microscope was used to examine closely the minute taxonomic characteristics. Various identification manuals and marine copepod websites were used to aid in identifying the specimens (Kirkwood, 1982; O'Sullivan, 1982a, O'Sullivan, 1982b, O'Sullivan, 1983, O'Sullivan, 1986; Razouls et al., 2023). Macro-zooplankton (>2 mm in body length) were counted in each complete sample. For meso-zooplankton (200 µm-2 mm), sub-splits of 1/2 to 1/32 (depending on the numerical density of individuals) of the complete sample were obtained using a Folsom plankton splitter, ensuring a minimum of 500 individuals per sample was counted. Additionally, four dominant calanoid copepod species (*Calanoides acutus*, *Calanus propinquus*, *Metridia gerlachei*, and *Rhincalanus gigas*) and Euphausiacea (in the genera *Euphausia* and *Thysanoessa*) were identified to adult, subadult, and copepodite stages. These different stages were totalled per species for analysing species abundance. Then, species abundance in each stratum was calculated by dividing counts of individuals by the volume of water filtered by each net. Finally, zooplankton average abundance in each stratum of each sector was calculated and visualized using Python.

## 2.4 Zooplankton cluster analysis

Zooplankton community structure was analysed using PRIMER version 6 and Python. To preprocess input data, zooplankton abundance data from 36 stations were fourth root-transformed to ensure influence from rarer species and down-weight the influence of abundant species (Quinn and Keough, 2002). The different life stages of the common copepods and Euphausiacea were analysed as separate components in the cluster analysis. To avoid potential effects caused by the diel vertical migration of zooplankton on community structure, all zooplankton samples in each sector were classified as daytime samples and nighttime samples based on local sunset and sunrise times (https://gml.noaa.gov/grad/solcalc/sunrise.html) in each sector and used three-way AMOSIM (sampling layers, sampling years and months, and sampling time) to test the effects of different sampling time (day or night). Subsequently, data from the East-Pacific sector and Indian sector were separately subjected to cluster, ANOSIM, and SIMPER (similarity percentage) analyses. To segregate the zooplankton into communities, the transformed data were used in a q-type cluster analysis based on the Bray-Curtis dissimilarity index and group-average linkage classification. Additionally, all cluster groups were visualized by PRIMER. Following this, ANOSIM was conducted to test for similarity within each resultant community (cluster), and identify the most significant sampling factors, such as water layer and sampling year and month. The cluster groups were treated to the SIMPER analysis to determine which species significantly contributed to the similarity within and between clusters. Finally, the proportion of the most abundance taxa that largely contribute to zooplankton clusters were illustrated by stacked bar chart using Python.

## 2.5 The environmental drivers on zooplankton abundance

To improve understanding of the environmental factors influencing zooplankton abundance, the relationships between temperature, salinity, oxygen, and zooplankton abundance were evaluated independently using Generalized Additive Models (GAMs) in R Studio (version 4.21). Average values of salinity, temperature, dissolved oxygen, and zooplankton abundance were calculated for each sampling stratum (0-100, 100-200, 200-500, 500-1000, 1000-1500 m) at fifteen stations in the East-Pacific sector and ten stations in the Indian sector. Data from other 11 stations (I5-I15) in the Indian sector were not analysed due to the lack of CTD data. To examine the relationships between zooplankton abundance and water masses further, we categorized zooplankton into three groups: 'highest abundance' (upper $90^{th}$ percentile), 'medium abundance' ($45^{th}$ to $55^{th}$ percentile), and 'lowest abundance' (lower $10^{th}$ percentile). GAMs were used to forecast the ranges of temperature, salinity, and dissolved oxygen corresponding to these three zooplankton abundance categories within each sector. We then tested whether these predicted temperature and salinity ranges correlated with specific water masses. For the analysis of chl-a concentration and zooplankton abundance, we used the average chl-a concentration at each station from the surface layer (0-200 m), where phytoplankton primarily grow, and the overall zooplankton abundance at each station from 0 to 1500 m for both sectors. We included deep layer zooplankton abundance into overall abundance because deep ocean zooplankton productivity is positively related to surface layer primary production in the global ocean (Hernández-León et al., 2020). Given the short turnover time of phytoplankton cells (chl-a concentration) and their rapid concentration changes, we also utilized monthly Aqua-MODIS satellite chl-a concentration data from NASA Ocean Color to verify phytoplankton phenology and changes during the sampling months (as shown in Supplementary Figures 1, 2). This approach aimed to mitigate the potential effects of different sampling years and months.

# 3 Results

## 3.1 Hydrographic features and water masses

Environmental conditions including temperature, salinity, and dissolved oxygen had similar ranges between stations in the two

10.3389/fmars.2024.1274582

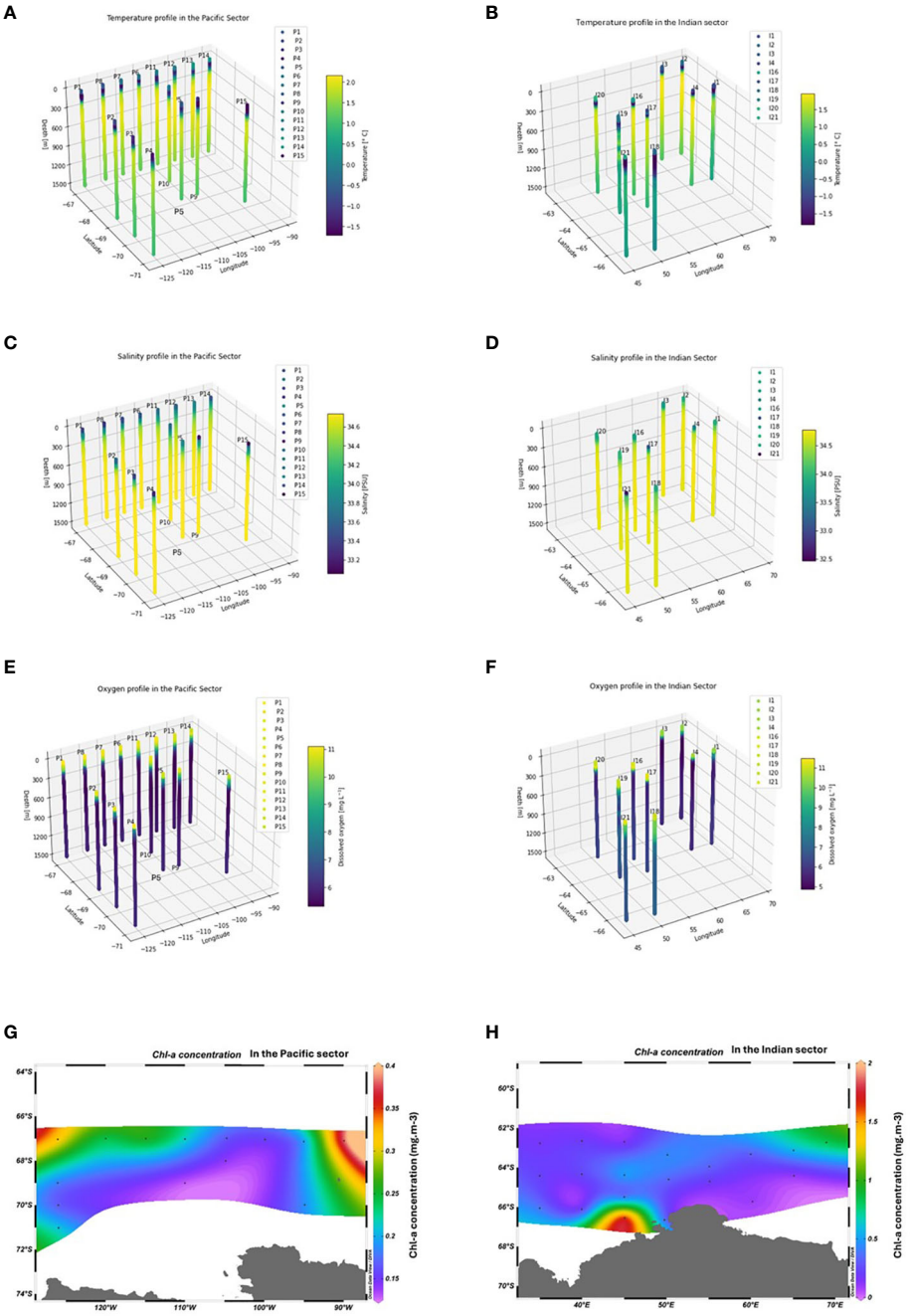


FIGURE 2
The three-dimensional temperature, salinity, dissolved oxygen profiles of each station from 0-1500m in the East-Pacific and Indian sectors of the Southern Ocean subplot **(A–F)**. The average phytoplankton concentration in each sector **(G, H)**.

sectors and exhibited similar patterns vertically from surface to 1500 m (Figure 2). Salinity ranged from 32.5 to 34.8 at different stations; additionally, it increased with depth and stabilized from around 500 to 1500 m (Figure 2). Dissolved oxygen levels generally decreased from the surface to depth ranging from 11 to 5 mg. $L^{-1}$. Ocean temperature, ranging from -1.7 to 2.1 °C at different stations, was low at around 0-200 m, peaked at approximately 500 m, and then slightly decreased from 500 to 1500 m (Figure 2). Chl-a, as a most important biotic variable, was primarily distributed in the top 200 m layer. The average depth-integrated chl-a concentration varied between stations, ranging from 0.12 to 1.87 mg. $m^{-3}$. The average chl-a concentrations in the 0-200 m layer in Mar 2018 and Jan 2019 in the East-Pacific sector (0.21 mg. $m^{-3}$) were lower than those in the Indian sector (0.39 mg. $m^{-3}$), measured in Dec 2019-Jan 2020 and Jan 2021.

The distribution of water masses was generally similar between the two sectors. In the East-Pacific sector (90-130 °W), three water masses were identified: AASW, WW, and CDW (Figure 3). AASW, with its relatively fresh water (salinity <33.8) and temperature, ranging from -1.5 to 0.5 °C, was found on the surface. WW

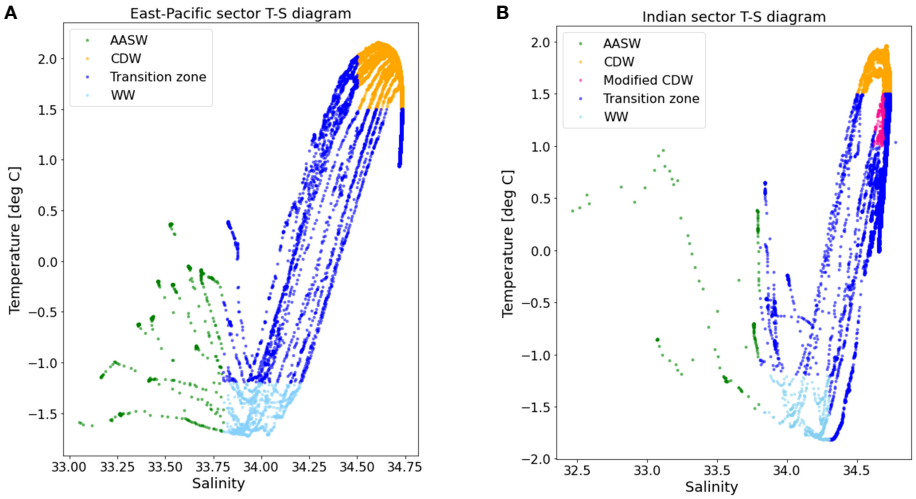


FIGURE 3
The T-S (Temperature to salinity) diagram showing distribution of the Antarctic Surface Water (ASW), Winter Water (WW), Circumpolar Deep Water (CDW), modified CDW and transition zone from 0 to 1500 m in the East-Pacific **(A)** and Indian sectors **(B)**. The temperature and salinity data in each sector were collected on different years and months. Data were collected in March 2018 and January 2019 in the East-Pacific sector and Dec 2019 to Jan 2020 and Jan 2021 in the Indian sector respectively.

**TABLE 1** Zooplankton diversity in the East-Pacific and Indian sectors, and three layers, as well as average zooplankton abundance for each species in the two sectors.

| Copepoda | Sector | Layer | Pacific | Indian |
|---|---|---|---|---|
| *Aetideopsis antarctica* (Wolfenden, 1908) | I | M | 0 | <0.01 |
| *Aetideopsis minor* (Wolfenden, 1911) | Both | All | <0.01 | 0.5 |
| *Bathycalanus bradyi* (Wolfenden, 1905) | I | All | 0 | 0.14 |
| *Bathycalanus richardi* Sars G.O., 1905 | P | All | 0.19 | 0 |
| *Calanoides acutus* (Giesbrecht, 1902) | Both | All | 3.42 | 2.26 |
| *Calanus propinquus* Brady, 1883 | Both | All | 1.15 | 0.2 |
| *Calanus simillimus* Giesbrecht, 1902 | I | M | 0 | <0.01 |
| *Candacia falcifera* Farran, 1929 | I | M | 0 | <0.01 |
| *Candacia maxima* Vervoort, 1957 | Both | All | 0.01 | 0.03 |
| *Clausocalanus brevipes* Frost & Fleminger, 1968 | I | E | 0 | <0.01 |
| *Clausocalanus laticeps* Farran, 1929 | Both | All | 0.64 | 0.03 |
| *Ctenocalanus citer* Heron & Bowman, 1971 | Both | All | 18.55 | 6.23 |
| *Farrania frigida* (Wolfenden, 1911) | P | E | <0.01 | 0 |
| *Haloptilus ocellatus* Wolfenden, 1905 | Both | All | 0.02 | 0.14 |
| *Heterorhabdus austrinus* Giesbrecht, 1902 | Both | All | 0.02 | 0.13 |
| *Megacalanus princeps* Wolfenden, 1904 | Both | All | 0.32 | 0.01 |
| *Metridia gerlachei* Giesbrecht, 1902 | Both | All | 0.94 | 0.77 |
| *Metridia lucens* Boeck, 1865 | I | E&M | 0 | <0.01 |
| *Microcalanus pygmaeus* (Sars G.O., 1900) | I | E&M | 0 | 0.01 |
| *Oithona frigida* Giesbrecht, 1902 | Both | All | 2.35 | 1.23 |

*(Continued)*

10.3389/fmars.2024.1274582

TABLE 1 Continued

| Copepoda | Sector | Layer | Pacific | Indian |
|---|---|---|---|---|
| *Oithona similis* Claus, 1866 | Both | All | 63.71 | 7.94 |
| *Oncaea curvata* Giesbrecht, 1902 | Both | All | 1.79 | 1.58 |
| *Paraeuchaeta antarctica* (Giesbrecht, 1902) | Both | All | 0.11 | 0.18 |
| *Paraeuchaeta* spp. | I | M&B | 0 | 0.05 |
| *Paragammaropsis prenes* Ren in Ren & Huang, 1991 | P | All | 0.02 | 0 |
| *Pleuromamma antarctica* Steuer, 1931 | Both | All | 0.01 | 0.05 |
| *Racovitzanus antarcticus* Giesbrecht, 1902 | I | All | 0 | 0.13 |
| *Rhincalanus gigas* Brady, 1883 | Both | All | 0.88 | 0.90 |
| *Scolecithricella minor* Brady, 1883 | Both | All | 0.56 | 0.07 |
| *Scaphocalanus farrni Park, 1982* | I | E&M | 0 | <0.01 |
| *Scolecithricella* spp. | I | M&B | 0 | 0.05 |
| *Stephos longipes* Giesbrecht, 1902 | I | E | 0 | 0.01 |
| *Triconia antarctica* (Heron, 1977) | Both | All | 1.77 | 0.80 |
| *Triconia conifera* (Giesbrecht, 1891) | I | All | 0 | <0.01 |
| Unknown Copepods | I | All | 0 | 1.06 |
| **Euphausiidae** | **Sector** | **Layer** | **Pacific** | **Indian** |
| *Euphausia crystallorophias* Holt & Tattersall, 1906 | I | E&M | 0 | 0.02 |
| *Euphausia superba* Dana, 1850 | Both | All | 0.12 | 0.02 |
| *Thysanoessa macrura* G.O. Sars, 1883 | Both | All | <0.01 | 0.14 |
| **Chaetognatha** | **Sector** | **Layer** | **Pacific** | **Indian** |
| *Eukrohnia hamata* (Möbius, 1875) | Both | All | 0.26 | 0.28 |
| *Pseudosagitta gazellae* (Ritter-Záhony, 1909) | Both | All | 0.15 | 0.02 |
| *Solidosagitta marri* (David, 1956) | I | All | 0 | 0.01 |
| Other Chaetognatha | I | All | 0 | 0.7 |
| **Polychaete** | **Sector** | **Layer** | **Pacific** | **Indian** |
| *Alciopidae* spp. | I | E&M | 0 | 0.01 |
| *Rhynchonereella petersii* (Langerhans, 1880) | Both | All | 0.01 | 0.01 |
| *Palabriaphoxus latifrons* (Ren in Ren & Huang, 1991) | P | All | 0.24 | 0 |
| *Tomopteris carpenteri* Quatrefages, 1866 | Both | All | 0.01 | 0.02 |
| *Travisiopsis coniceps* (Chamberlin, 1919) | P | All | <0.01 | <0.01 |
| *Travisiopsis levinseni Southern, 1910* | P | All | 0.01 | 0 |
| *Travisiopsis lobifera* Levinsen, 1885 | I | E | 0 | <0.01 |
| **Pteropoda** | **Sector** | **Layer** | **Pacific** | **Indian** |
| *Clione antarctica E. A. Smith, 1902* | Both | E&M | 2.77 | <0.01 |
| *Clione limacina E. A. Smith, 1902* | P | M | <0.01 | 0 |
| **Others** | **Sector** | **Layer** | **Pacific** | **Indian** |
| *Alacia* spp. | Both | All | 0.25 | 0.41 |

*(Continued)*

10.3389/fmars.2024.1274582

TABLE 1 Continued

| Others | Sector | Layer | Pacific | Indian |
|---|---|---|---|---|
| Cephalopoda | I | E&M | 0 | <0.01 |
| *Dimophyes arctica* (Chun 1897) | Both | E&M | <0.01 | <0.01 |
| *Diphyes antarctica* Moser, 1925 | Both | All | <0.01 | 0.02 |
| Fish Larvae | I | All | 0 | <0.01 |
| *Hyperia* spp. | Both | All | 0.028 | 0.01 |
| *Marrus antarcticus* Totton, 1954 | Both | All | <0.01 | <0.01 |
| *Muggiaea bargmannae* Totton, 1954 | Both | B | <0.01 | 0.01 |
| *Oikopleura* spp. | Both | E&M | 0.01 | 0.01 |
| *Rathkea* spp. | Both | All | 0.01 | 0.07 |
| *Salpa thompsoni* Foxton, 1961 | I | E&M | 0 | <0.01 |
| *Vibilia antarctica* Stebbing, 1988 | I | All | 0 | 0.04 |

P for East-Pacific sector, I for Indian sector, E for epipelagic layer, M for mesopelagic layer and B for upper bathypelagic layer.

characterized by higher salinity (33.8-34.3) and the lowest temperature (<-1 °C) lay beneath the AASW. CDW was found underneath WW, spanning approximately down to the upper bathypelagic layer, and had the highest temperature (1.5-2 °C) and highest salinity (34.4-34.75). In the Indian sector (30-70 °E), the same water masses as those in the East-Pacific sector, including AASW, WW, and CDW, were identified based on the T-S diagram shown in Figure 3. Modified CDW, characterized by lower temperature (<1.5 °C) and lower salinity (<34.7) than typical CDW, was found exclusively in the Indian sector (Figure 3).

## 3.2 Zooplankton diversity

Sixty-three taxa belonging to nine mesozooplankton groups were found in the two sectors (Table 1; Supplementary Table 2). These include Copepoda, Euphausiacea, Chaetognatha, Polychaeta, Amphipoda, Tunicata, Pteropoda, Ostracoda, and Cnidaria (Table 1). Taxonomic diversity was fifty-six taxa in the Indian sector and forty taxa in the East-Pacific sector across different years and months (Table 1). Copepods represented 53% of zooplankton diversity in the East-Pacific sector and 57% of zooplankton diversity in the Indian sector. Differences in species composition were largely attributed to variations among copepods. For instance, *Calanus simillimus*, *Microcalanus pygmaeus*, *Aetideopsis antarctica*, *Racovitzanus antarcticus*, *Stephos longipes* and *Bathycalanus bradyi* were only found in the Indian sector, whereas *Bathycalanus richardi*, and *Farrania frigida* were only collected in the East-Pacific sector, though these latter species were collected infrequently. For macro-zooplankton taxa (> 2 mm), *Euphausia superba* and *Thysanoessa macrura* were commonly found in both sectors but these species were likely underestimated due to avoidance of the Hydro-Bios multinet (Atkinson et al., 2012). Gelatinous taxa, such as salps, were absent in 28 out of 36 stations, and had low abundance in the samples. Chaetognaths such as *Eukrohnia hamata* and *Pseudosagitta gazellae* were abundant in the surface layer at some stations, although many specimens could only be identified to the phylum Chaetognatha due to damage to or disappearance of their lateral fins and heads, both of which are diagnostic features. For other common taxa, such as Polychaeta, Pteropoda, and Cnidaria, only a few specimens were found in the samples, and they were only infrequently observed.

Taxonomic diversity was higher in the 0-200 m layer, known as epipelagic layer, and the mesopelagic layer (500-1000 m) in the two sectors (Table 1). Additionally, diversity was lowest in the top 500 m of the bathypelagic layer, between 1000-1500 m (Table 1). The most common species could be found throughout the water column, down to 1500 m. In the epipelagic layer, fifty-five taxa were found, including a large proportion of common copepods such as *C. citer* and *O. similis*. In the 200-1000 m layer, as known as the mesopelagic layer, some copepods, such as *A. antarctica* (meso- to bathypelagic species), and *Scolecithricella* spp., which were absent from surface layers in the samples, were found. The upper bathypelagic layer had the lowest diversity (forty-four taxa). Species such as *Oikopleura* spp., *Salpa thompsoni*, *Clione antarctica*, and *Clione limacina* were rare or absent in deep layers, although they were abundant in the surface layers of a few stations.

## 3.3 Zooplankton abundance between layers in each sector

Zooplankton abundance was variable between water layers and sectors. Zooplankton abundance peaked in the epipelagic layer and subsequently declined with each successive water layer at each station (Figure 4). The average abundance was significantly higher in the East-Pacific sector (100 individual.m$^{-3}$) than in the Indian sector (27 individual.m$^{-3}$) (Figure 4). The elevated zooplankton abundance in the East-Pacific sector was predominantly due to a higher abundance of small common copepods such as *O. similis*, *O. frigida*, *O. curvata*, *T. antarctica*, and *C. citer* in the epi-pelagic layer. In our samples, these small copepods dominated numerically

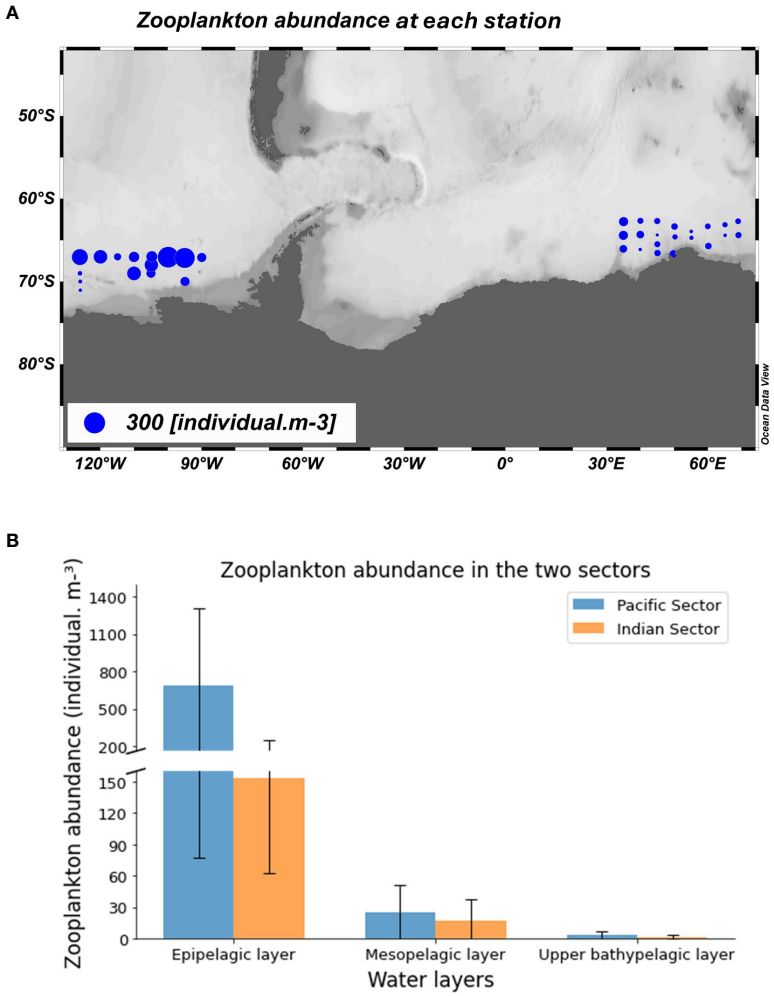


FIGURE 4
Average zooplankton abundance for each station subplot **(A)** and average zooplankton abundance in five continuous zooplankton sampling strata in the East-Pacific sector (Mar 2018 and Jan 2019) and the Indian sector (Dec 2019-Jan 2020 and Jan 2021) subplot **(B)**.

in most meso-zooplankton (0.2-20 mm) communities. Four large calanoids, including *C. acutus*, *C. propinquus*, *M. gerlachei*, and *R. gigas* were also abundant, including abundant copepodite stages of these calanoids were present in the surface layer.

## 3.4 The community structure of zooplankton

In the East-Pacific sector, five communities were identified by cluster analysis (Figure 5). Copepods numerically dominated all the meso-zooplankton communities, while communities in deeper layers had a higher proportion of non-copepod groups including Ostracoda, Chaetognatha and Amphipoda. Three larger communities (C, D, E) were broadly defined by ocean stratification, encompassing the epi-pelagic layer and deeper layers (200-1500m) (Figure 5). Cluster E consisted of zooplankton from the epipelagic layer, displaying a similarity of 50% (Figure 5). The epi-pelagic community (cluster E) was characterized by the highest average zooplankton abundance (796 individual. $m^{-3}$) and the highest composition of common copepod *Oithona similis* (66%) in total abundance (Figure 6). Pteropoda were the most abundant non-copepod group, representing 3% of total abundance. Other zooplankton taxonomic groups, including Chaetognatha, Amphipoda, Tunicata, and Cnidaria, contributed less than 1% of the total abundance. Cluster D, with a similarity of 54%, comprised zooplankton from the deeper layers between 200-1500 m, excluding samples P3(2), P4(2), and P15 (2) from the 100-200 m layer (Figure 6). In cluster D, copepods were also the most abundant group, making up 92% of total abundance (Figure 6). The *O. similis*, *C. citer*, *Oithona frigida* had more evenly distribution. Moreover, Chaetognatha, Ostracoda, and Amphipoda were the most abundant non-copepod taxa, constituting 3%, 2.4%, and 1.6% of the total abundance, respectively (Figure 6). Cluster C, with an average similarity of 51%, included the zooplankton communities mainly collected in the upper bathypelagic layer in May 2018. In cluster C, Amphipoda represented 11% of total abundance behind common copepods. The other two minor communities (A and B) mainly consisted of zooplankton from 500-

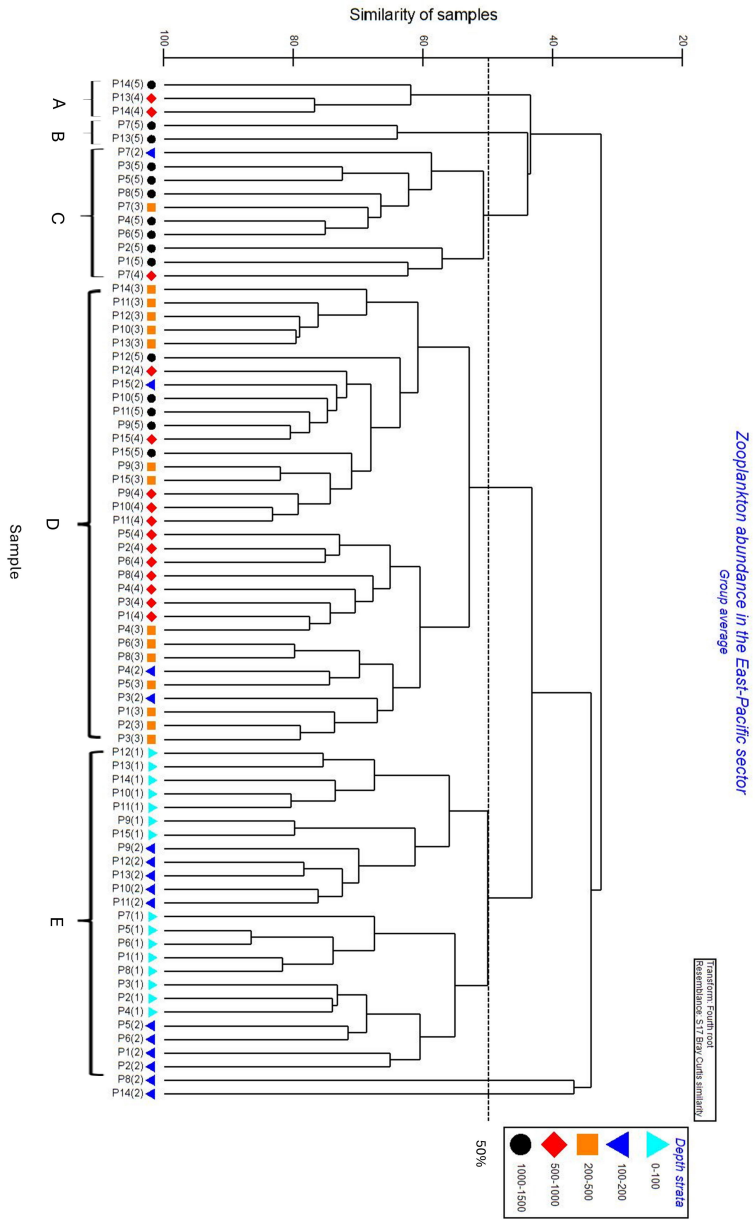


FIGURE 5
Cluster analysis of zooplankton assemblages in the East-Pacific sector between 90-130°W from 0-1500m with five continuous zooplankton sampling strata [0-100 m: (1), 100-200 m: (2), 200-500 m: (3), 500-1000 m: (4) and 1000-1500 m: (5)].

1500 m layers. Cluster A, with similarity of 62%, and cluster B, with similarity of 64%, mainly consisted of copepod. Moreover, the highest proportion of Chaetognatha (14%) and *Ctenocalanus citer* (33%) were recorded in cluster A and cluster B respectively.

In the Indian sector, four clusters were primarily distinguished based on water layers (Figure 7). Copepods dominated the mesozooplankton communities, representing 81% to 96% of total abundance (Figure 8). Cluster F, with an average similarity of 50%, comprised zooplankton from the epipelagic layer. In this epipelagic community, *O. similis* (40%) and *C. citer* (30%) were still numerically dominant. Non-copepods group including Chaetognatha (3.1%) made a small contribution to this community (Figure 8). Clusters G, with a similarity of 57% and H, with a similarity of approximately 50%, encompassed zooplankton collected in the 200-1500 m strata. These deeper layer communities had an increased proportion of non-copepods taxa such as Chaetognatha (14% and 6% respectively). Nonetheless, copepod taxa, especially *Paraeuchaeta* sp., were one of the most abundant species. Cluster I, with an average similarity of 60%, mainly included the zooplankton community in the 500-1500 m strata. In this community, four large calanoid copepods (*C. acutus*, *C. propinquus*, *M. gerlachei*, and *R. gigas*), and cyclopoids such as *O. frigida* (12%) and *O. curvata* (15%) made up a significant proportion; additionally, Ostracoda and Chaetognatha represented 5% and 7% of the total abundance (Figure 8).

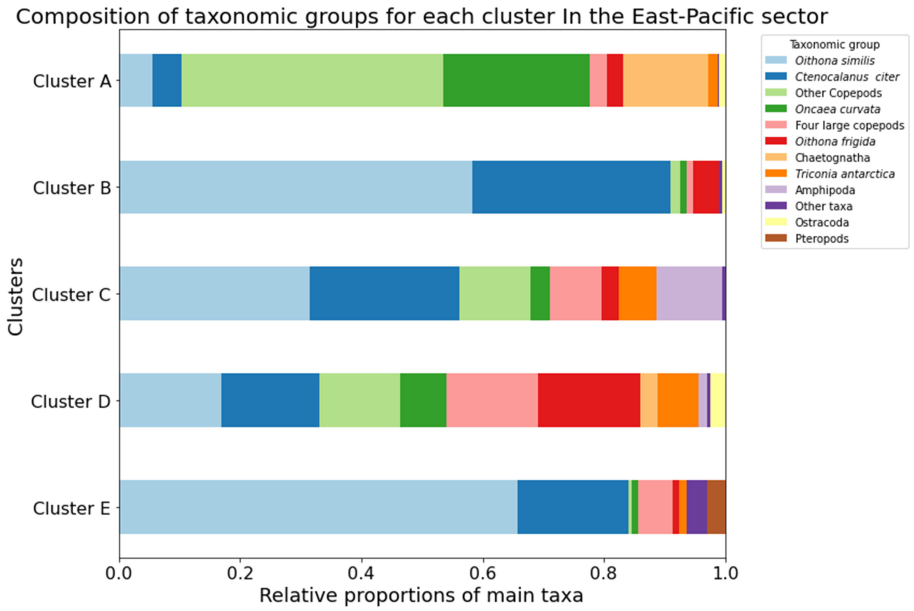


FIGURE 6
The proportion of most abundant meso-zooplankton taxa and species in zooplankton communities in the East-Pacific sector Cluster A–E.

## 3.5 Environmental drivers on zooplankton abundance and communities

Based on the two-ways ANOSIM, there was no significant difference between daytime and nighttime zooplankton data (R=0.2 for East-Pacific sector, and R=-0.1 for Indian sector), so the zooplankton abundance data was subsequently analysed regardless of the sampling time. The water layer is a more important factor than sampling year and month to define a community in both sectors. In the Indian sector, water layer (R=0.69) was identified as the main factor defining a zooplankton community, rather than the sampling year and month (R=0.17). In the East-Pacific sector, where zooplankton samples were collected in May 2018 and January 2019, the water layer (R=0.49) played a slightly more significant role than sampling year and month (R=0.47).

In both sectors, GAMs exhibit non-linear patterns between zooplankton abundance and temperature, salinity, and oxygen across all water strata (Figure 9, Table 2). Three zooplankton abundance categories were correlated with specific ranges of temperature and salinity, corresponding to particular water masses. In the East-Pacific sector, the highest zooplankton abundance was associated with specific ranges of temperature (-1 to -0.6 °C) and salinity (33.6 to 33.7). Notably, these specific temperature, salinity, and oxygen ranges overlapped with the physical properties of AASW observed in the Pacific sector, when comparing the water masses analysis in Figure 3 and GAMs results in Figure 9. Medium zooplankton abundance was associated with intermediate temperature (0.1 to 0.4 °C) and salinity (34.1 to 34.2), which did not correlate with any specific water mass but indicated a transition zone. The lowest zooplankton abundance was associated with higher temperatures (1.1 to 1.5°C) and salinities (34.5 to 34.6), corresponding to CDW (Figures 3, 9).

Similarly, in the Indian sector, the highest zooplankton abundance coincided with lower salinity (33.88 to 33.93) and the lowest temperatures (-1.8 to -1.4 °C), indicative of AASW (Figures 3, 9). Although the salinity range here is slightly higher than typical AASW (33.0 to 33.7), the salinity of AASW can measure up to 34.3 PSU (Carter et al., 2009). Medium zooplankton abundance was associated with intermediate temperature (-0.1 to 0.2 °C) and salinity (34.28 to 34.33), consistent with the transition zone's physical properties (Figures 3, 9). The lowest zooplankton abundance corresponded to the highest temperatures (1.3 to 1.7 °C) and salinities (34.63 to 34.68), overlapping with CDW in the Indian sector (Figures 3, 9). The results from GAM also revealed that chl-a concentration showed a positive relationship with zooplankton abundance in the East-Pacific sector but a non-significant relationship in the Indian sector (Figure 9, Table 2). Furthermore, the East-Pacific sector exhibited higher zooplankton abundance and lower chl-a concentrations in March 2018 and January 2019. In contrast, the Indian sector showed significantly higher chl-a concentration and lower zooplankton abundance in December-January of 2020 and January 2021.

# 4 Discussion

## 4.1 Comparing zooplankton diversity, abundance and communities between two sectors

All sixty-three taxa in our samples are commonly found in the Southern Ocean (Kirkwood, 1982; O'Sullivan, 1982a, O'Sullivan, 1982b, O'Sullivan, 1983, O'Sullivan, 1986; Ward et al., 2003, Ward et al., 2014a; Razouls et al., 2023). Zooplankton taxonomic diversity in our surveys is slightly lower compared to other observations

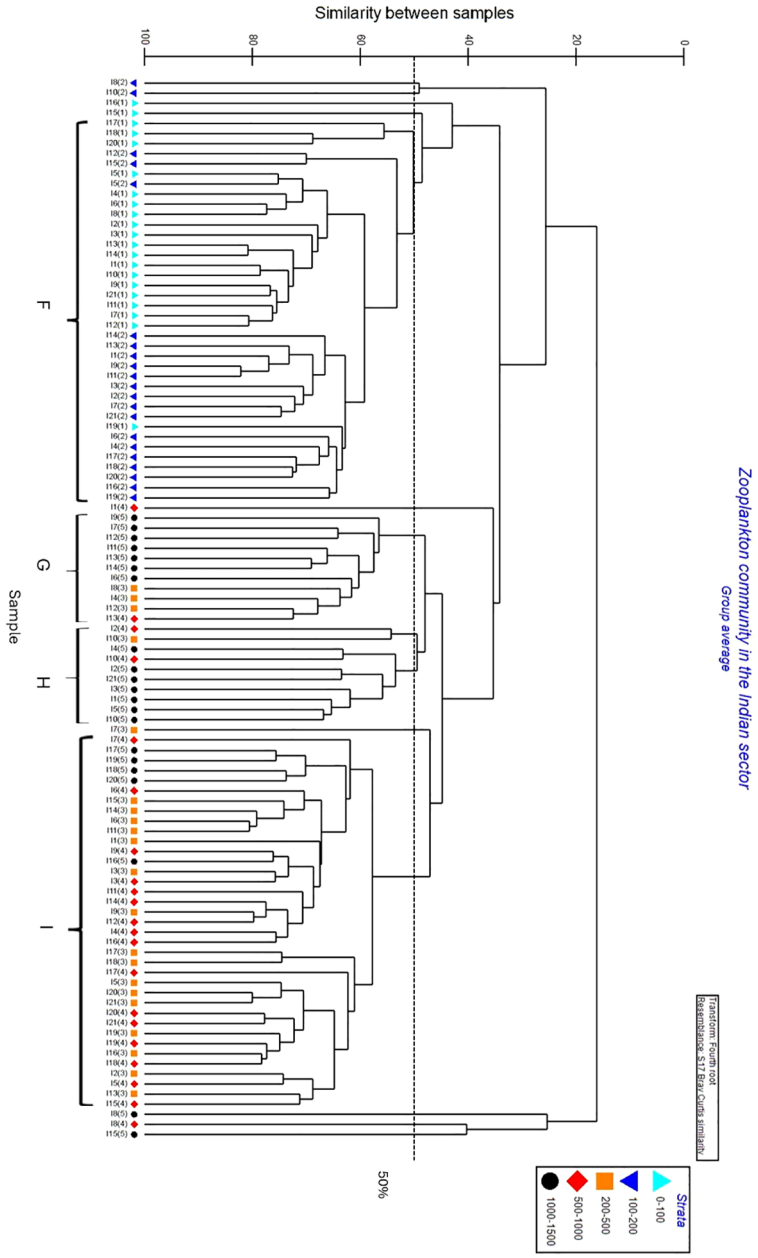


FIGURE 7
Cluster analysis of zooplankton assemblages in the Indian sector between 30-70°E from 0-1500m with five continuous zooplankton sampling strata.

(Atkinson and Sinclair, 2000; Nicol et al., 2010; Flores et al., 2014; Ward et al., 2014a; Yang et al., 2017). This is partly because of some fragmented or unknown jellyfish, Chaetognatha, copepod larvae and Cephalopoda being classified only as indetermined species or into Class level, which reduces the estimated species diversity. Some species, such as *C. brevipes, M. princeps*, and *Candacia falcifera*, that were only collected in the epipelagic layer or meso to bathypelagic layers, are restricted to these layers; however, others, including *C. simillimus* and *A. antarctica*, which were only collected in the mesopelagic layer, have a wider distribution from the epipelagic to mesopelagic layers (Razouls et al., 2023). For meso-zooplankton diversity in each sector, most species, including *M. pygmaeus, A. antarctica, R. antarcticus*, *S. longipes* and *B. bradyi* and *B. richardi*, that were only found in one sector by our survey are actually circumpolar species (Razouls et al., 2023). As a result, the *in-situ* diversity might be similar in the two sectors. The similarity in zooplankton diversity between the East-Pacific and Indian sectors aligns with previous findings of consistent taxonomic composition of Antarctic meso-zooplankton communities across the circumpolar region (Dubischar et al., 2002; Pinkerton et al., 2020; Takahashi and Hosie, 2020; Johnston et al., 2022).

Zooplankton abundance varies across sectors and layers (Wilson et al., 2015; Stevens et al., 2015; Pakhomov et al., 2020; Dietrich et al., 2021). Our results reveal that zooplankton

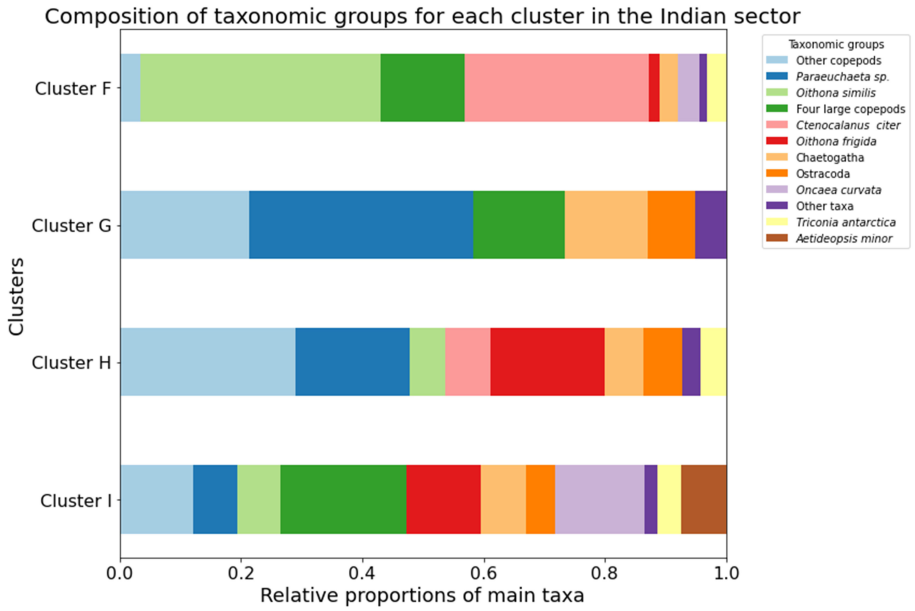


FIGURE 8
The proportion of most abundant meso-zooplankton taxa and species in zooplankton communities in the Indian sectors (Cluster F–I).

abundance in the deeper layers is generally an order of magnitude lower than the epi-pelagic assemblages. Moreover, the cluster analysis results revealed that zooplankton communities were generally divided by water layers. This finding is consistent with previous surveys in the various regions including Prydz Bay, the Scotia Sea, Drake Passage and the Polar Front (Atkinson and Sinclair, 2000; Ward et al., 2003; Flores et al., 2014; Ward et al., 2014a; Yang et al., 2017; Pinkerton et al., 2020). Our results also showed that zooplankton abundance was more than three times higher in the East-Pacific sector than in the Indian sector. There is little evidence showing significant higher zooplankton abundance between 90-130°W in the East-Pacific sector than between 30-70°E in the Indian sector by previous studies (Pakhomov and McQuaid, 1996; Atkinson et al., 2012; Venkataramana et al., 2020). As a result, this higher abundance may be partially influenced by variation in monthly and annual zooplankton population dynamics (Atkinson et al., 2012). Our ANOSIM analysis also highlighted the secondary roles of sampling years and months in regulating zooplankton communities. Previous studies have also found that the abundance of dominant calanoid copepods peaks in late summer in various regions of the Southern Ocean (Atkinson et al., 1997; Schnack-Schiel and Isla, 2005; Hunt and Hosie, 2006). Consequently, zooplankton abundance in the Indian sector may not have reached its peak between December to January, leading to underestimation (Takahashi and Hosie, 2020), when we were comparing zooplankton abundance between these two sectors.

Zooplankton community structure varied in each layer and sector, the dominant species in meso-zooplankton assemblages in the epipelagic and mesopelagic layers are consistently similar respectively in both sectors. These include calanoid species such as *C. acutus*, *C. propinquus*, *M. gerlachei*, *C. citer*, and *R. gigas* as well as smaller cyclopoid species including *O. similis* and *O. curvata*. These copepods account for more than 75% of total biomass in both our study and in previous observations (Atkinson et al., 2012). Other less abundant taxa, encompassing salps, Amphipoda, Polychaeta, and Chaetognatha, generally exhibit uneven proportions across different sectors in the Southern Ocean (Ward et al., 2003; Swadling et al., 2010; Pinkerton et al., 2020). As another dominant species in the Southern Ocean, Antarctic krill (Euphausia superba) may be underestimated by their net avoiding behaviour (Atkinson et al., 2012).

## 4.2 Influence of physical drivers especially water masses on zooplankton distribution in different layers and the two sectors

Water masses play a crucial role in regulating zooplankton communities across different regions of the Southern Ocean (Swadling et al., 2010; Marrari et al., 2011; Mańko et al., 2020). Our GAM model results showed that the most abundant zooplankton assemblages in both sectors were related to specific temperature and salinity ranges, aligning with the physical properties of the AASW, while the lowest zooplankton abundance corresponded to the physical properties of the CDW. These specific temperature and salinity ranges are best understood qualitatively rather than as precise predictors of zooplankton abundance. These results establish a correspondence between water masses and zooplankton abundance, highlighting the impacts of AASW and CDW on the highest and lowest zooplankton abundances, respectively. Comparing with previous studies, acoustic surveys have also demonstrated different zooplankton assemblages associated with AASW and upper CDW respectively in coastal regions of the Southern Ocean (Lawson et al., 2004; Marrari et al., 2011). This implies that not only

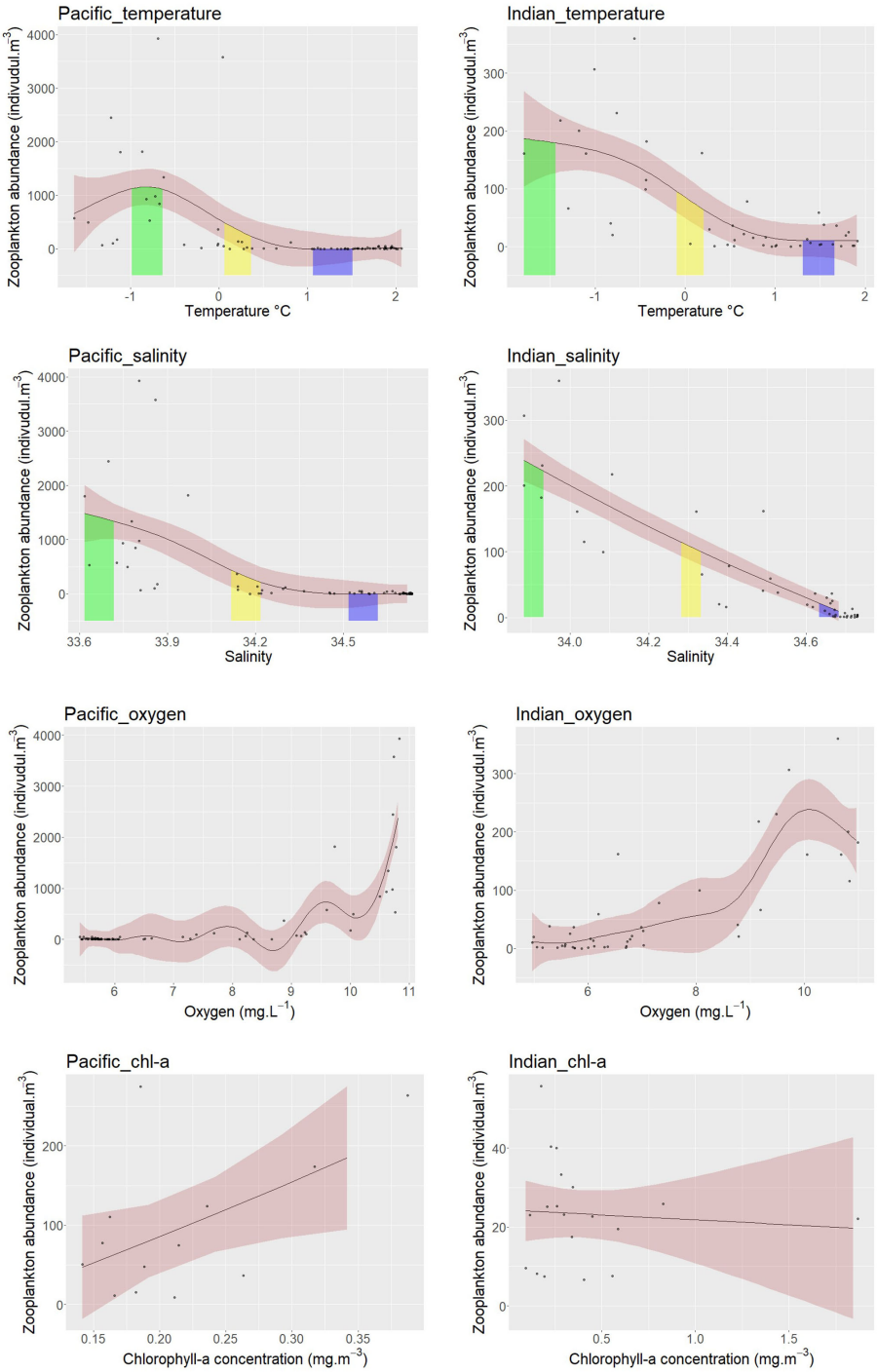


FIGURE 9
The relationships between salinity, temperature and dissolved oxygen and zooplankton abundance from five continuous sampling strata in the East-Pacific and Indian sectors, and the relationships between the chl-a concentration and zooplankton abundance for each station in the East-Pacific and Indian sector. Each curve represents the fitted relationship between zooplankton abundance and each parameter respectively. The pink shaded areas indicate the 95% confidence interval. The green, yellow, and purple shaded areas represent the upper 90$^{th}$, medium 45$^{th}$ to 55$^{th}$, and lower 10$^{th}$ percentiles of zooplankton abundance, along with their corresponding temperature, salinity, and oxygen ranges.

temperature, salinity, and oxygen themselves (Hunt et al., 2016), but also the combined physical and biological properties of AASW might have a critical effect on zooplankton abundance. Specifically, AASW, with its highest dissolved oxygen content and lower salinity and temperature, may provide a preferred environment for epipelagic zooplankton during the summer, although the thermal and salinity tolerances, as well as oxygen consumption of Antarctic zooplankton, are not well studied (Atkinson et al., 2012; Costa et al., 2021). Moreover, the highest concentration of food sources, such as phytoplankton cells, in the AASW tends to attract

TABLE 2 GAMs results including Effective degrees of freedom (edf), F, Reference Degree of Freedom (Ref.df) and P-value between temperature, salinity, oxygen, chl-a and zooplankton abundance for each sector.

| Sectors & variable | edf | F | Ref.df | P-value |
|---|---|---|---|---|
| Pacific_temperature | 3.9 | 7.7 | 4.8 | <2e-16 |
| Indian_temperature | 3 | 13.6 | 3.7 | <2e-16 |
| Pacific_salinity | 2.8 | 17 | 3.5 | <2e-16 |
| Indian_salinity | 1.5 | 96 | 1.8 | <2e-16 |
| Pacific_oxygen | 8.3 | 19.7 | 8.9 | <2e-16 |
| Indian_oxygen | 5.7 | 14.9 | 6.8 | <2e-16 |
| Pacific_chl-a | 1 | 4.4 | 1 | 0.05 |
| Indian_chl-a | 1 | 0.09 | 1 | 0.76 |

zooplankton and Euphausiacea swarms (Tarling and Fielding, 2016; Pauli et al., 2021). In deeper water masses, CDW with its lowest oxygen levels and food availability (Bindoff et al., 2000; Carter et al., 2008; Williams et al., 2010; Carter et al., 2012) could shape distinct zooplankton communities with lowest zooplankton abundance.

## 4.3 Biotic drivers including chl-a concentration on zooplankton community structure in both sectors

The difference in zooplankton abundance vertically could be affected by biotic factors such as chl-a concentration. As secondary producers, zooplankton abundance is also influenced by primary production, which is largely determined by chl-a concentration, a process known as bottom-up control (Hernández-León et al., 2020). Our observational data in the East-Pacific sector coincides with bottom-up control. However, the Indian sector showed non-significant relationship between zooplankton abundance and *in-situ* chl-a concentration. Moreover, the Indian sector had higher phytoplankton concentration but lower zooplankton abundance comparing with East-Pacific sector. These opposite results implicate the phenology of phytoplankton and zooplankton. For instance, *in-situ* chl-a concentration is generally higher in early summer between December to January, but zooplankton abundance reaches its peak in late summer in the high latitude of the Southern Ocean (Atkinson et al., 1997; Atkinson, 1988a; Schnack-Schiel and Isla, 2005; Hunt and Hosie, 2006; Wright et al., 2010; Takahashi and Hosie, 2020). NASA satellite data on chlorophyll-a (chl-a) concentrations supports our inference regarding phytoplankton phenology. In the East-Pacific sector, the average chl-a concentration decreased to 0.25 mg. $m^3$ in March 2018 (the sampling month during the 34th CHINARE) from higher values in early summer (0.43 mg.$m^3$ in December 2017 and 0.32 mg/$m^3$ in January 2018), as shown in Supplementary Figure 1. In the Indian sector, chl-a concentrations were higher in early summer, between December and January (our sampling months during the 36th and 37th CHINARE), compared to late summer, from February to March, as indicated in Supplementary Figure 2. For zooplankton abundance, small copepods including *O. similis*, *C. citer* and *O. curvata*, were important contributors to higher total abundance in the East-Pacific sector. However, many of these small herbivorous and omnivorous copepods reproduce during spring and early summer, but their early life stages are often too small to be effectively collected by nets with a mesh size of 200 μm during 36 and 37$^{th}$ CHINARE (Hagen, 1999; Ward and Hirst, 2007; Atkinson et al., 2012; Cornwell et al., 2020). Consequently, the chl-a concentration played important roles in regulating zooplankton abundance, but the underestimated contribution of small copepod larvae to total zooplankton abundance and peaked chl-a concentration in early summer may complicate the existing understanding of relationships between zooplankton abundance and chl-a concentration in the Indian sector.

The vertical distribution of zooplankton, including their abundance and community composition, is also consistent with their diet and food availability in each layer. In the surface layer, the proportion and abundance of copepods were highest than deeper layers. This coincides with the highest food availability, such as highest concentration of chl-a for grazers in the surface layer. For example, the most numerous taxa, including *O. similis*, *O. curvata*, *C. citer*, and *O. frigida*, as well as *C. acutus* and *C. propinquus* in the epipelagic layer in our sample, are either herbivorous or omnivorous (Kattner et al., 2003; Pond and Ward, 2011). Moreover, our observations and other studies have shown that the copepodite stages of calanoids, such as *C. acutus* and *C. propinquus*, concentrate in the epipelagic layer for ontogenetic development during summer (Conroy et al., 2020). In deeper layers, the reduction in phytoplankton cells but increases in sinking particles could benefit omnivores, scavengers, or predators such as Chaetognatha and Amphipoda (Nishikawa and Tsuda, 2001; Proud et al., 2017). In our samples, the relative proportions of the herbivorous and omnivorous copepods, including *O. similis*, *O. curvata*, *C. citer*, and *O. frigida*, *C. acutus* and *C. propinquus*, decreased in the deeper layers. However, the relative proportions of Amphipoda, Chaetognatha, and Ostracoda increased in the deeper layers in both sectors. Based on existing fatty acid and stable isotope analysis, these groups, including Hyperiidae, Gammaridae, *E. hamata*, *P. gazellae*, and *Alacia* spp. are generally considered to be either carnivores or omnivores (Øresland, 1990; Froneman and Pakhomov, 1998; Nelson et al., 2001; Kruse et al., 2010). The increased relative proportions of carnivores and omnivores in deeper layers align with previous observations that zooplankton trophic levels generally increase with depth (Hernández-León et al., 2020). When considering the combined effects of primary production, food availability and physical water mass properties on zooplankton abundance, the decrease in zooplankton abundance with increasing depth and water masses may be attributed to reduced food availability and unfavourable physical conditions, such as low oxygen levels, in deeper water masses.

Diel vertical migration of zooplankton between the surface and deeper layers potentially affects their vertical distribution. However, our samples were collected upon the vessel's arrival at each station, irrespective of the time of day, so these samples are not ideal and

designed for analysis vertical migration between layers. Moreover, this migratory behaviour was not clearly observed and recorded in our study, perhaps due to the shorter migration distances caused by longer photoperiods during the sampling periods and low predatory pressure from visual mesozooplankton predators in the high latitude of the Southern Ocean (Pinkerton et al., 2010; Saunders et al., 2019; Conroy et al., 2020; Cao et al., 2022; Li et al., 2022).

## 5 Conclusions

The mesozooplankton community composition and dominant taxa in each layer between the East-Pacific and Indian sectors were similar during Austral summer between 2018 to 2021. However, zooplankton abundance varies across different sectors and declines significantly with three water layers. Our study integrated the common environmental drivers, including temperature and salinity, and chl-a concentration, into physical and biological characteristics of different water masses, and demonstrated that water masses that combined all these characteristic play significant roles in regulating vertical distribution of zooplankton in terms of abundance and composition in both sectors. These multiple environmental drivers provide new insights for understanding large-scale zooplankton abundance and distribution in the Southern Ocean, thereby enhancing our ability to analyse and quantify their ecological and biogeochemical roles and the impacts of climate changes on zooplankton community (Fraser et al., 2018). However, the detailed mechanisms of how some physical properties and movement of water masses influence zooplankton physiology, advection, and dispersal, and therefore their distribution, remain beyond the scope of this paper. Future research might integrate water mass dynamics, physiological analysis of zooplankton, and acoustic zooplankton data to deepen our comprehension of the mechanisms driving large scale zooplankton distribution horizontally and vertically.

## Data availability statement

The original contributions presented in the study are included in the article/Supplementary Material. Further inquiries can be directed to the corresponding author.

## Ethics statement

The manuscript presents research on animals that do not require ethical approval for their study.

## Author contributions

YL: Conceptualization, Data curation, Formal analysis, Methodology, Software, Visualization, Writing – original draft, Writing – review & editing. YW: Data curation, Writing – review & editing. YS: Data curation, Writing – review & editing. GY: Conceptualization, Funding acquisition, Methodology, Project administration, Resources, Supervision, Writing – review & editing. KS: Methodology, Resources, Supervision, Writing – review & editing, Conceptualization.

## Funding

The author(s) declare financial support was received for the research, authorship, and/or publication of this article. This work was supported by the National Natural Science Foundation of China (42276238), Impact and Response of Antarctic Seas to Climate Change (IRASCC-01-02-01D) and the Tai Shan Scholars Program.

## Acknowledgments

We would like to thank the crew on R/V Xue long and Xue long 2 for their assistance with the plankton sampling and Polar Research Institute of China (https://www.pric.org.cn/) for providing temperature and salinity data.

## Conflict of interest

The authors declare that the research was conducted in the absence of any commercial or financial relationships that could be construed as a potential conflict of interest.

## Publisher's note



## Supplementary material

The Supplementary Material for this article can be found online at: https://www.frontiersin.org/articles/10.3389/fmars.2024.1274582/full#supplementary-material

# References


Abelmann, A., Gersonde, R., Knorr, G., Zhang, X., Chapligin, B., Maier, E., et al. (2015). The seasonal sea-ice zone in the glacial Southern Ocean as a carbon sink. *Nat. Commun.* 6, 8136. doi: 10.1038/ncomms9136

Arrigo, K. R., and Thomas, D. N. (2004). Large scale importance of sea ice biology in the Southern Ocean. *Antarct. Sci.* 16, 471–486. doi: 10.1017/S0954102004002263

Arrigo, K. R., van Dijken, G. L., and Bushinsky, S. (2008). Primary production in the Southern Ocean –2006. *J. Geophys. Res.* 113, C08004. doi: 10.1029/2007JC004551

Atkinson, A. (1998a). Life cycle strategies of epipelagic copepods in the Southern Ocean. *J. Mar. Syst.* 15, 289–311. doi: 10.1016/S0924-7963(97)00081-X

Atkinson, A., and Peck, J. M. (1988b). A summer-winter comparison of zooplankton in the oceanic area Around South Georgia. *Polar Biol.* 8, 463–473. doi: 10.1007/BF00264723

Atkinson, A., Schnack-Schiel, S., Ward, P., and Marin, V. (1997). Regional differences in the life cycle of Calanoides acutus (Copepoda: Calanoida) within the Atlantic sector of the Southern Ocean. *Mar. Ecol. Prog. Ser.* 150, 99–111. doi: 10.3354/meps150099

Atkinson, A., and Sinclair, J. D. (2000). Zonal distribution and seasonal vertical migration of copepod assemblages in the Scotia Sea. *Polar Biol.* 23, 46–58. doi: 10.1007/s003000050007

Atkinson, A., Ward, P., Cb, C., Hunt, B. P. V., Pakhomov, E. A., and Hosie, G. W. (2012). An overview of Southern Ocean zooplankton data: Abundance, biomass, feeding and functional relationships. *CCAMLAR Sci.* 9, 171–218.

Bindoff, N. L., Rosenberg, M. A., and Warner, M. J. (2000). On the circulation and water masses over the Antarctic continental slope and rise between 80 and 150°E. *Deep Sea Res. Part II Top. Stud. Oceanogr.* 47, 2299–2326. doi: 10.1016/S0967-0645(00)00038-2

Boscolo-Galazzo, F., Crichton, K. A., Ridgwell, A., Mawbey, E. M., Wade, B. S., and Pearson, P. N. (2021). Temperature controls carbon cycling and biological evolution in the ocean twilight zone. *Science* 371, 1148–1152. doi: 10.1126/science.abb6643

Boyd, P. W., Claustre, H., Levy, M., Siegel, D. A., and Weber, T. (2019). Multi-faceted particle pumps drive carbon sequestration in the ocean. *Nature* 568, 327–335. doi: 10.1038/s41586-019-1098-2

Cao, S., Li, Y., Miao, X., Zhang, R., Lin, L., and Li, H. (2022). DNA barcoding provides insights into Fish Diversity and Molecular Taxonomy of the Amundsen Sea. *Conserv. Genet. Resour.* 14, 281–289. doi: 10.1007/s12686-022-01273-4

Carter, L., McCave, I. N., and Williams, M. J. M. (2008). "Chapter 4 circulation and water masses of the southern ocean: A review," in *Developments in earth and environmental sciences* (Elsevier) 8, 85–114. doi: 10.1016/S1571-9197(08)00004-9

Carter, P., Vance, D., Hillenbrand, C. D., Smith, J. A., and Shoosmith, D. R. (2012). The neodymium isotopic composition of waters masses in the eastern Pacific sector of the Southern Ocean. *Geochim. Cosmochim. Acta* 79, 41–59. doi: 10.1016/j.gca.2011.11.034

Conroy, J. A., Steinberg, D. K., Thibodeau, P. S., and Schofield, O. (2020). Zooplankton diel vertical migration during Antarctic summer. *Deep Sea Res. Part Oceanogr. Res. Pap.* 162, 103324. doi: 10.1016/j.dsr.2020.103324

Constable, A. J. (2003). Southern Ocean productivity in relation to spatial and temporal variation in the physical environment. *J. Geophys. Res.* 108, 8079. doi: 10.1029/2001JC001270

Constable, A. J., Melbourne-Thomas, J., Corney, S. P., Arrigo, K. R., Barbraud, C., Barnes, D. K. A., et al. (2014). Climate change and Southern Ocean ecosystems I: how changes in physical habitats directly affect marine biota. *Glob. Change Biol.* 20, 3004–3025. doi: 10.1111/gcb.12623

Cornwell, L. E., Fileman, E. S., Bruun, J. T., Hirst, A. G., Tarran, G. A., Findlay, H. S., et al. (2020). Resilience of the copepod oithona similis to climatic variability: egg production, mortality, and vertical habitat partitioning. *Front. Mar. Sci.* 7. doi: 10.3389/fmars.2020.00029

Costa, R. R., Mendes, C. R. B., Ferreira, A., Tavano, V. M., Dotto, T. S., and Secchi, E. R. (2021). Large diatom bloom off the Antarctic Peninsula during cool conditions associated with the 2015/2016 El Niño. *Commun. Earth Environ.* 2, 252. doi: 10.1038/s43247-021-00322-4

Deacon, G. E. R. (1982). Physical and biological zonation in the Southern Ocean. *Deep Sea Res. Part Oceanogr. Res. Pap.* 29, 1–15. doi: 10.1016/0198-0149(82)90058-9

Dietrich, K. S., Santora, J. A., and Reiss, C. S. (2021). Winter and summer biogeography of macrozooplankton community structure in the northern Antarctic Peninsula ecosystem. *Prog. Oceanogr.* 196, 102610. doi: 10.1016/j.pocean.2021.102610

Dubischar, C. D., Lopes, R. M., and Bathmann, U. V. (2002). High summer abundances of small pelagic copepods at the Antarctic Polar Front—implications for ecosystem dynamics. *Deep Sea Res. Part II Top. Stud. Oceanogr.* 49, 3871–3887. doi: 10.1016/S0967-0645(02)00115-7

Flores, H., Hunt, B. P. V., Kruse, S., Pakhomov, E. A., Siegel, V., Van Franeker, J. A., et al. (2014). Seasonal changes in the vertical distribution and community structure of Antarctic macrozooplankton and micronekton. *Deep Sea Res. Part Oceanogr. Res. Pap.* 84, 127–141. doi: 10.1016/j.dsr.2013.11.001

Fraser, C. I., Morrison, A. K., Hogg, A. M., Macaya, E. C., Van Sebille, E., Ryan, P. G., et al. (2018). Antarctica's ecological isolation will be broken by storm-driven dispersal and warming. *Nat. Clim. Change* 8, 704–708. doi: 10.1038/s41558-018-0209-7

Froneman, P. W., and Pakhomov, E. A. (1998). Trophic importance of the chaetognaths Eukrohnia hamata and Sagitta gazellae in the pelagic system of the Prince Edward Islands (Southern Ocean). *Polar Biol.* 19, 242–249. doi: 10.1007/s003000050241

Gouretski, V. (1999). "The large-scale thermohaline structure of the ross gyre," in *Oceanography of the ross sea Antarctica*. Eds. G. Spezie and G. M. R. Manzella (Springer Milan, Milano), 77–100. doi: 10.1007/978-88-470-2250-8_6

Hagen, W. (1999). Reproductive strategies and energetic adaptations of polar zooplankton. *Invertebr. Reprod. Dev.* 36, 25–34. doi: 10.1080/07924259.1999.9652674

Hernández-León, S., Koppelmann, R., Fraile-Nuez, E., Bode, A., Mompeán, C., Irigoien, X., et al. (2020). Large deep-sea zooplankton biomass mirrors primary production in the global ocean. *Nat. Commun.* 11, 6048. doi: 10.1038/s41467-020-19875-7

Hopkins, T. L., and Torres, J. J. (1988). The zooplankton community in the vicinity of the ice edge, western Weddell Sea, March 1986. *Polar Biol.* 9, 79–87. doi: 10.1007/BF00442033

Hunt, B. P. V., and Hosie, G. W. (2005). Zonal structure of zooplankton communities in the Southern Ocean South of Australia: results from a 2150km continuous plankton recorder transect. *Deep Sea Res. Part Oceanogr. Res. Pap.* 52, 1241–1271. doi: 10.1016/j.dsr.2004.11.019

Hunt, B. P. V., and Hosie, G. W. (2006). The seasonal succession of zooplankton in the Southern Ocean south of Australia, part I: The seasonal ice zone. *Deep Sea Res. Part Oceanogr. Res. Pap.* 53, 1182–1202. doi: 10.1016/j.dsr.2006.05.001

Hunt, G. L., Drinkwater, K. F., Arrigo, K., Berge, J., Daly, K. L., Danielson, S., et al. (2016). Advection in polar and sub-polar environments: Impacts on high latitude marine ecosystems. *Prog. Oceanogr.* 149, 40–81. doi: 10.1016/j.pocean.2016.10.004

Irigoien, X., Klevjer, T., Røstad, A., Martinez, U., Boyra, G., Acuña, J. L., et al. (2014). Large mesopelagic fishes biomass and trophic efficiency in the open ocean. *Nat. Commun.* 5, 3271. doi: 10.1038/ncomms4271

Jacobs, S. S. (2004). Bottom water production and its links with the thermohaline circulation. *Antarct. Sci.* 16, 427–437. doi: 10.1017/S095410200400224X

Johnston, N. M., Murphy, E. J., Atkinson, A., Constable, A. J., Cotté, C., Cox, M., et al. (2022). Status, change, and futures of zooplankton in the southern ocean. *Front. Ecol. Evol.* 9. doi: 10.3389/fevo.2021.624692

Kattner, G., Albers, C., Graeve, M., and Schnack-Schiel, S. B. (2003). Fatty acid and alcohol composition of the small polar copepods, Oithona and Oncaea : indication on feeding modes. *Polar Biol.* 26, 666–671. doi: 10.1007/s00300-003-0540-x

Kirkwood, J. M. (1982). "A guide to the euphausiacea of the southern ocean," in *Kingston, tas: information services section* (Antarctic Division, Dept. of Science and Technology).

Kruse, S., Hagen, W., and Bathmann, U. (2010). Feeding ecology and energetics of the Antarctic chaetognaths Eukrohnia hamata, E. bathypelagica and E. bathyAntarctica. *Mar. Biol.* 157, 2289–2302. doi: 10.1007/s00227-010-1496-3

Lawson, G. L., Wiebe, P. H., Ashjian, C. J., Gallager, S. M., Davis, C. S., and Warren, J. D. (2004). Acoustically-inferred zooplankton distribution in relation to hydrography west of the Antarctic *Peninsula. Deep Sea Res. Part II Top. Stud. Oceanogr.* 51, 2041–2072. doi: 10.1016/j.dsr2.2004.07.022

Li, H., Cao, S., Li, Y., Song, P., Zhang, R., Wang, R., et al. (2022). Molecular assessment of demersal fish diversity in Prydz Bay using DNA taxonomy. *Deep Sea Res. Part II Top. Stud. Oceanogr.* 202, 105140. doi: 10.1016/j.dsr2.2022.105140

Mańko, M. K., Gluchowska, M., and Weydmann-Zwolicka, A. (2020). Footprints of Atlantification in the vertical distribution and diversity of gelatinous zooplankton in the Fram Strait (Arctic Ocean). *Prog. Oceanography.* 189, 102414.

Marrari, M., Daly, K. L., Timonin, A., and Semenova, T. (2011). The zooplankton of Marguerite Bay, western Antarctic Peninsula—Part II: Vertical distributions and habitat partitioning. *Deep Sea Res. Part II Top. Stud. Oceanogr.* 58, 1614–1629. doi: 10.1016/j.dsr2.2010.12.006

McManus, M. A., and Woodson, C. B. (2012). Plankton distribution and ocean dispersal. *J. Exp. Biol.* 215, 1008–1016. doi: 10.1242/jeb.059014

Mock, T., and Hoch, N. (2005). Long-term temperature acclimation of photosynthesis in steady-state cultures of the polar diatom fragilariopsis cylindrus. *Photosynth. Res.* 85, 307–317. doi: 10.1007/s11120-005-5668-9

Murphy, E. J., Cavanagh, R. D., Drinkwater, K. F., Grant, S. M., Heymans, J. J., Hofmann, E. E., et al. (2016). Understanding the structure and functioning of polar pelagic ecosystems to predict the impacts of change. *Proc. R. Soc B Biol. Sci.* 283, 20161646. doi: 10.1098/rspb.2016.1646

Murphy, E. J., Johnston, N. M., Hofmann, E. E., Phillips, R. A., Jackson, J. A., Constable, A. J., et al. (2021). Global connectivity of southern ocean ecosystems. *Front. Ecol. Evol.* 9. doi: 10.3389/fevo.2021.624451

Nelson, M. M., Mooney, B. D., Nichols, P. D., and Phleger, C. F. (2001). Lipids of Antarctic Ocean amphipods: food chain interactions and the occurrence of novel biomarkers. *Mar. Chem.* 73, 53–64. doi: 10.1016/S0304-4203(00)00072-4

Nicol, S., Meiners, K., and Raymond, B. (2010). BROKE-West, a large ecosystem survey of the South West Indian Ocean sector of the Southern Ocean, 30°E–80°E (CCAMLR Division 58.4.2). *Deep Sea Res. Part II Top. Stud. Oceanogr.* 57, 693–700. doi: 10.1016/j.dsr2.2009.11.002

Nicol, S., Pauly, T., Bindoff, N. L., Wright, S., Thiele, D., Hosie, G. W., et al. (2000). Ocean circulation off east Antarctica affects ecosystem structure and sea-ice extent. *Nature* 406, 504–507. doi: 10.1038/35020053

Nishikawa, J., and Tsuda, A. (2001). Diel vertical migration of the tunicate Salpa thompsoni in the Southern Ocean during summer. *Polar Biol.* 24, 299–302. doi: 10.1007/s003000100227

O'Sullivan, D. (1982a). *A guide to the chaetognaths of the southern ocean and adjacent waters* (Kingston, Australia: Department of Science and Technology, Antarctic Division).

O'Sullivan, D. (1982b). *A guide to the hydromedusae of the southern ocean and adjacent waters* (Kingston, Australia: Department of Science and Technology, Antarctic Division).

O'Sullivan, D. (1983). *A guide to the pelagic Tunicates of the Southern Ocean and adjacent waters* (Kingston, Tas., Australia: Antarctic Division, Dept. of Science).

O'Sullivan, D. (1986). *A guide to the Ctenophores of the Southern Ocean and adjacent waters* (Kingston, Tas., Australia: Antarctic Division, Dept. of Science).

Øresland, V. (1990). Feeding and predation impact of the chaetognath Eukrohnia hamata in Gerlache Strait, Antarctic Peninsula. *Mar. Ecol. Prog. Ser.* 63, 201–209. doi: 10.3354/meps063201

Pakhomov, E. A., and McQuaid, C. D. (1996). Distribution of surface zooplankton and seabirds across the Southern Ocean. *Polar Biol.* 16, 271–286.

Pakhomov, E. A., Pshenichnov, L. K., Krot, A., Paramonov, V., Slypko, I., and Zabroda, P. (2020). Zooplankton distribution and community structure in the Pacific and Atlantic Sectors of the Southern Ocean during austral summer 2017–18: A pilot study conducted from Ukrainian long-liners. *J. Mar. Sci Engineer.* 8 (7), 488.

Pauli, N.-C., Metfies, K., Pakhomov, E. A., Neuhaus, S., Graeve, M., Wenta, P., et al. (2021). Selective feeding in Southern Ocean key grazers—diet composition of Euphausiacea and salps. *Commun. Biol.* 4, 1061. doi: 10.1038/s42003-021-02581-5

Pinkerton, M. H., Décima, M., Kitchener, J. A., Takahashi, K. T., Robinson, K. V., Stewart, R., et al. (2020). Zooplankton in the Southern Ocean from the continuous plankton recorder: Distributions and long-term change. *Deep Sea Res. Part Oceanogr. Res. Pap.* 162, 103303. doi: 10.1016/j.dsr.2020.103303

Pinkerton, M. H., Smith, A. N. H., Raymond, B., Hosie, G. W., Sharp, B., Leathwick, J. R., et al. (2010). Spatial and seasonal distribution of adult Oithona similis in the Southern Ocean: Predictions using boosted regression trees. *Deep Sea Res. Part Oceanogr. Res. Pap.* 57, 469–485. doi: 10.1016/j.dsr.2009.12.010

Pond, D. W., and Ward, P. (2011). Importance of diatoms for Oithona in Antarctic waters. *J. Plankton Res.* 33, 105–118. doi: 10.1093/plankt/fbq089

Proud, R., Cox, M. J., and Brierley, A. S. (2017). Biogeography of the global ocean's mesopelagic zone. *Curr. Biol.* 27, 113–119. doi: 10.1016/j.cub.2016.11.003

Quinn, G. P., and Keough, M. J. (2002). *Experimental design and data analysis for biologists* (Cambridge: Cambridge University Press). doi: 10.1017/CBO9780511806384

Razouls, C., Desreumaux, N., Kouwenberg, J., and de Bovée, F. (2023). *Biodiversity of Marine Planktonic Copepods (morphology, geographical distribution and biological data)* (Sorbonne University, CNRS). Available online at: http://copepodes.obs-banyuls.fr/en (Accessed August 22, 2023).

Robinson, C., Steinberg, D. K., Anderson, T. R., Arístegui, J., Carlson, C. A., Frost, J. R., et al. (2010). Mesopelagic zone ecology and biogeochemistry – a synthesis. *Deep Sea Res. Part II Top. Stud. Oceanogr.* 57, 1504–1518. doi: 10.1016/j.dsr2.2010.02.018

Saunders, R. A., Hill, S. L., Tarling, G. A., and Murphy, E. J. (2019). Myctophid fish (Family myctophidae) are central consumers in the food web of the scotia sea (Southern ocean). *Front. Mar. Sci.* 6. doi: 10.3389/fmars.2019.00530

Schnack-Schiel, S. B., and Isla, E. (2005). The role of zooplankton in the pelagic-benthic coupling of the Southern Ocean. *Sci. Mar.* 69, 39–55. doi: 10.3989/scimar.2005.69s239

Smith, D. A., Hofmann, E. E., Klinck, J. M., and Lascara, C. M. (1999). Hydrography and circulation of the west antarctic peninsula continental shelf. *Deep Sea Res. Part Oceanogr. Res. Pap.* 46, 925–949. doi: 10.1016/S0967-0637(98)00103-4

Stevens, C. J., Pakhomov, E. A., Robinson, K. V., and Hall, J. A. (2015). Mesozooplankton biomass, abundance and community composition in the Ross Sea and the Pacific sector of the Southern Ocean. *Polar Biol.* 38, 275–286. doi: 10.1007/s00300-014-1583-x

Swadling, K. M., Kawaguchi, S., and Hosie, G. W. (2010). Antarctic mesozooplankton community structure during BROKE-West (30°E–80°E), January–February 2006. *Deep Sea Res. Part II Top. Stud. Oceanogr.* 57, 887–904. doi: 10.1016/j.dsr2.2008.10.041

Takahashi, E. K. T., and Hosie, G. W. (2020). *Report on the status and trends of southern ocean zooplankton based on the SCAR southern ocean continuous plankton recorder (SO-CPR) survey*. Available at: https://www.researchgate.net/publication/352895937.

Talley, L. D., Pickard, G. L., Emery, W. J., and Swift, J. H. (2011). *Descriptive physical oceanography: an introduction. 6. ed* (Amsterdam Heidelberg: Elsevier, AP).

Tarling, G. A., and Fielding, S. (2016). "Swarming and behaviour in antarctic euphausiacea Biology and ecology of antarctic euphausiacea," in *Advances in polar ecology*. Ed. V. Siegel (Springer, Cham). doi: 10.1007/978-3-319-29279-3_8

Venkataramana, V., Anilkumar, N., Swadling, K., Mishra, R. K., Tripathy, S. C., Sarkar, A., et al. (2020). Distribution of zooplankton in the Indian sector of the Southern Ocean. *Antarct. Sci.* 32, 168–179. doi: 10.1017/S0954102019000579

Vernet, M., Geibert, W., Hoppema, M., Brown, P. J., Haas, C., Hellmer, H. H., et al. (2019). The weddell gyre, southern ocean: present knowledge and future challenges. *Rev. Geophys.* 57, 623–708. doi: 10.1029/2018RG000604

Ward, B. A., Dutkiewicz, S., and Follows, M. J. (2014a). Modelling spatial and temporal patterns in size-structured marine plankton communities: top–down and bottom–up controls. *J. Plankton Res.* 36, 31–47. doi: 10.1093/plankt/fbt097

Ward, P., and Hirst, A. G. (2007). Oithona similis in a high latitude ecosystem: abundance, distribution and temperature limitation of fecundity rates in a sac spawning copepod. *Mar. Biol.* 151, 1099–1110. doi: 10.1007/s00227-006-0548-1

Ward, P., Whitehouse, M., Brandon, M., Shreeve, R., and Woodd-Walker, R. (2003). Mesozooplankton community structure across the Antarctic Circumpolar Current to the north of South Georgia: Southern Ocean. *Mar. Biol.* 143, 121–130. doi: 10.1007/s00227-003-1019-6

Williams, G. D., Nicol, S., Aoki, S., Meijers, A. J. S., Bindoff, N. L., Iijima, Y., et al. (2010). Surface oceanography of BROKE-West, along the Antarctic margin of the south-west Indian Ocean (30 – 80 ∘ E). *Deep Sea Res. Part II Top. Stud. Oceanogr.* 57, 738–757. doi: 10.1016/j.dsr2.2009.04.020

Wilson, S. E., Swalethorp, R., Kjellerup, S., Wolverton, M. A., Ducklow, H. W., Yager, P. L., et al. (2015). Meso-and macro-zooplankton community structure of the Amundsen Sea Polynya, Antarctica (Summer 2010–2011). *Elementa.* 3, 000033.

Wright, S. W., Van Den Enden, R. L., Pearce, I., Davidson, A. T., Scott, F. J., and Westwood, K. J. (2010). Phytoplankton community structure and stocks in the Southern Ocean (30–80°E) determined by CHEMTAX analysis of HPLC pigment signatures. *Deep Sea Res. Part II Top. Stud. Oceanogr.* 57, 758–778. doi: 10.1016/j.dsr2.2009.06.015

Yang, G., Atkinson, A., Hill, S. L., Guglielmo, L., Granata, A., and Li, C. (2021). Changing circumpolar distributions and isoscapes of Antarctic Euphausiacea: Indo-Pacific habitat refuges counter long-term degradation of the Atlantic sector. *Limnol. Oceanogr.* 66, 272–287. doi: 10.1002/lno.11603

Yang, G., Atkinson, A., Pakhomov, E. A., Hill, S. L., and Racault, M. (2022). Massive circumpolar biomass of Southern Ocean zooplankton: Implications for food web structure, carbon export, and marine spatial planning. *Limnol. Oceanogr.* 67, 2516–2530. doi: 10.1002/lno.12219

Yang, G., Li, C., Wang, Y., and Zhang, Y. (2017). Vertical profiles of zooplankton community structure in Prydz Bay, Antarctica, during the austral summer of 2012/2013. *Polar Biol.* 40, 1101–1114. doi: 10.1007/s00300-016-2037-4

Zu, Y., Gao, L., Guo, G., and Fang, Y. (2022). Changes of circumpolar deep water between 2006 and 2020 in the south-west Indian ocean, east Antarctica. *Deep Sea Res. Part II Top. Stud. Oceanogr.* 197, 105043. doi: 10.1016/j.dsr2.2022.105043

# Frontiers in Marine Science

**Explores ocean-based solutions for emerging global challenges**

The third most-cited marine and freshwater biology journal, advancing our understanding of marine systems and addressing global challenges including overfishing, pollution, and climate change.

---

## Discover the latest Research Topics

See more →

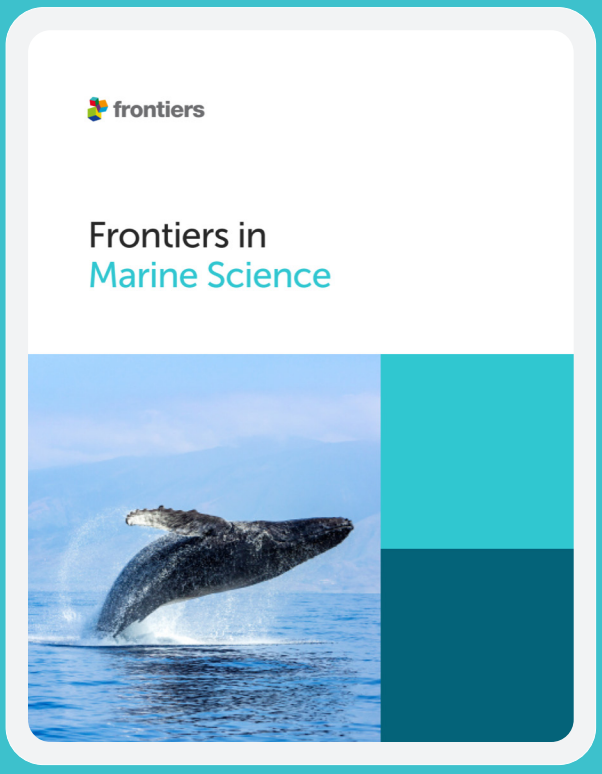


**Frontiers**

Avenue du Tribunal-Fédéral 34
1005 Lausanne, Switzerland
frontiersin.org

**Contact us**

+41 (0)21 510 17 00
frontiersin.org/about/contact